

# **Lipase catalyzed esterification of sugars with alkyl side chain containing amino acids**

A thesis submitted to the  
**University of Mysore**

for the award of  
*Doctor of Philosophy*  
in  
**BIOCHEMISTRY**

By  
**B. R. Somashekar M Sc.,**

Fermentation Technology and Bioengineering Department  
Central Food Technological Research Institute  
Mysore-570020, INDIA

**2007**

**B R Somashekar** M.Sc.,  
Senior Research Fellow  
Fermentation Technology and Bioengineering  
Central Food Technological Research Institute  
Mysore – 570 020, India

---

### **Declaration**

I hereby declare that the thesis entitled, “**Lipase catalyzed esterification of sugars with alkyl side chain containing amino acids**” submitted for the degree of **Doctor of Philosophy in Biochemistry** to the **University of Mysore** is the result of the work carried out by me under the guidance of **Dr. S. Divakar** in the Department of Fermentation Technology and Bioengineering, Central Food Technological Research Institute, Mysore, during the period 2004-2007.

I further declare that the results of this work have not been submitted for the award of any other degree or fellowship.

Date:  
Place: Mysore

(B.R Somashekar)



# CENTRAL FOOD TECHNOLOGICAL RESEARCH INSTITUTE

(COUNCIL OF SCIENTIFIC & INDUSTRIAL RESEARCH)

*cftri*

MYSORE - 570 020. INDIA.

Dr. S. Divakar  
Scientist 'F', Head  
Fermentation Technology and Bioengineering  
E-mail: [divakar643@gmail.com](mailto:divakar643@gmail.com)

## Certificate

I hereby declare that the thesis entitled, “**Lipase catalyzed esterification of sugars with alkyl side chain containing amino acids**” submitted by **Mr. B. R. Somashekar** for the degree of **Doctor of Philosophy** in **Biochemistry** to the **University of Mysore** is the result of the work carried out by him under my guidance in the Department of Fermentation Technology and Bioengineering, Central Food Technological Research Institute, Mysore during the period 2004-2007.

Date:  
Place: Mysore

(S. Divakar)  
Guide

..... *To My Beloved Parents  
and Brother*

## *Acknowledgements*

I express my deep sense of gratitude to **Dr. Soundar Divakar**, Head, Department of Fermentation Technology and Bioengineering, Central Food Technological Research Institute, Mysore for his guidance, highly constructive criticism and valuable guidance throughout the course of my Ph.D work.

I thank Director Dr. V. Prakash, for providing me an opportunity to carry out my research work at the Central Food Technological Research Institute, Mysore.

I would like to acknowledge my gratitude to Mr. B. Manohar, Scientist, Food Engineering Department, CFTRI for his kind help in my work.

I would like to acknowledge my gratitude to Dr. Muralidhara, Scientist, Biochemistry and Nutrition Department, CFTRI for his kind help in carrying out biological studies.

My gratitude to Dr. M.S. Thakur, Dr. S.G. Prafulla and all the other scientific and non-scientific staff of Fermentation Technology and Bioengineering Department for their support during the course of my research work.

I wish to express my deep sense of gratitude to former Heads of FTBE Dr. N. G. Karanth and Dr. M.C. Misra for their constant support and encouragement during my stay at the department.

I express my sincere thanks to my colleagues Mr. K. Lohith, Mr. G.R. Vijayakumar and Mr. R. Sivakumar for scientific inputs and being there for me whenever in need.

I am thankful to Mr. K.N. Chandrashekar, Mr. B.M. Thyagaraj, Mr. Ravikumar H and Ms. Shinomol from B&N, Mr. K.R. Santosh from PCT and all the friends of FTBE for their timely help during my course of work.

I express my sincere thanks to all the staff of Central Instrumentation Facilities and Service Departments for their technical help in analyzing my samples.

My sincere gratitude to NMR Research Centre, Indian Institute of Science, Bangalore and NMR facility centre, CFTRI for recording NMR spectra presented in this work.

My special thanks to all the scientific and non-scientific staff of CFTRI, Mysore and those who have directly or indirectly helped me in carrying out this work.

My special gratitude to my parents and brother for their constant encouragement and support.

Last but not least, I am grateful to the Department of Science and Technology for providing Junior Research fellowship and Council of Scientific and Industrial Research, India for providing the Senior Research fellowship.

*B. R. Somashekar*

## List of Patents and Publications

### Patents

1. K Lohith, **B R Somashekar**, B Manohar and S Divakar. An improved process for the preparation of amino acid esters of disaccharides. Indian Patent, 285/NF/2006, 2006.

### Publications

1. G R Vijayakumar, K Lohith, **B R Somashekar** and S Divakar. Lipase catalyzed synthesis of L-alanyl, L-leucyl and L-phenylalanyl esters of D-glucose using unprotected amino acids. **Biotechnology Letters** 2004; 26: 1323–1328.
2. Vasudeva Kamath, P S Rajani, K Lohith, **B R Somashekar** and S Divakar. Angiotensin Converting Enzyme inhibitory activity of amino acid esters of carbohydrates. **International Journal of Biological Macromolecules** 2006; 38: 89-93.
3. K. Lohith, G R Vijayakumar, **B R Somashekar**, R Sivakumar and S Divakar. Amino acyl esters of carbohydrates and glycosides as potent Angiotensin Converting Enzyme Inhibitors. **European Journal of Medicinal Chemistry** 2006; 41:1059-1072.
4. **B R Somashekar** and S Divakar. Lipase catalyzed synthesis of L-alanyl esters of carbohydrates. **Enzyme and Microbial Technology** 2007; 40: 299-309.
5. **B R Somashekar**, K. Lohith, B Manohar and S Divakar. Inhibition of *Rhizomucor miehei* and *Candida rugosa* lipases by D-glucose in the esterification reaction between L-alanine and D-glucose. **Journal of Bioscience and Bioengineering** 2007; 103: 122-128.
6. **B R Somashekar** and S Divakar. Synthesis of L-valyl, L-leucyl and L-isoleucyl esters of carbohydrates using lipase from *Candida rugosa*. 2007. Submitted for publication.

## **Abstract**

Amino acyl esters of carbohydrates are used as sweetening agents, surfactants, microcapsules in pharmaceutical preparations, active nucleoside amino acid esters, antibiotics and in the delivery of biological active agents. Chemical acylation of carbohydrates regio-selectively is complex due to the presence of multiple hydroxyl groups, which require protection and deprotection. However enzymatic reactions can overcome this drawback. Hitherto, very few references are available on the lipase catalyzed esterification of amino acyl esters of sugars. Most of the earlier workers used proteases and N-protected and carboxyl group activated amino acids for synthesizing aminoacyl esters of carbohydrates. All these reactions were conducted in shake flasks using lesser quantity of substrates and larger quantity of enzymes. The present work deals with lipases catalyzed preparation of amino acyl esters of carbohydrates using unprotected and unactivated amino acids and carbohydrates.

Chapter **ONE** deals with literature survey on mainly lipase catalyzed synthesis in organic media. Biotechnological applications of lipase catalysis in different food and pharmaceutical industries are discussed. A brief description on the lipase structure and catalytic mechanism on esterification is made. Parameters regulating lipase activity in organic media like nature of substrates, nature of solvents, effect of salt, thermal stability of lipases, water activity and immobilization are discussed. Diverse application of lipases like esterification using reverse micelles, supercritical carbon dioxide, micro oven, ionic liquids assisted reactions, kinetic studies and resolution of racemic mixture are presented. The chapter ends with a brief description on the scope of the present investigation.



Chapter **TWO** deals with materials and methods. Chemicals employed and their sources are listed. Methods of preparation of L-amino acyl esters of carbohydrates and the other related appropriate aspects of the same are discussed in detail.

Chapter **THREE** describes results from optimization of reaction parameters for the lipase catalyzed synthesis of L-alanyl **16a-e**, L-valyl **25a-e** and L-leucyl **34a-e** esters of D-glucose. Lipases from *Rhizomucor miehei* (RML), porcine pancreas (PPL) and *Candida rugosa* (CRL) were employed. The reaction conditions were optimized in terms of incubation period, solvent, enzyme concentrations, substrate concentrations, buffer (pH and concentration) and enzyme reusability. Under the experimental conditions employed, all the three lipases exhibited good esterification potentialities. Both RML and PPL showed maximum conversion yields of L-alanyl-D-glucose **16a-e** (30 % and 18 % respectively) at 40 % (w/w D-glucose) of enzyme, L-valyl-D-glucose **25a-e** (59 % and 62 % respectively) at 10 % (w/w D-glucose) of enzyme and L-leucyl-D-glucose **34a-e** (85 % and 18 % of respectively) at 40 % (w/w D-glucose) of enzyme employed. CRL showed a maximum conversion of 84 % of L-valyl-D-glucose **25a-e** at 30 % (w/w D-glucose) enzyme concentration. The present work showed enhanced activity of RML and CRL in presence of buffer salts. Optimum pH was found to be pH 4.0 for RML and pH 5.0 for PPL in case of L-alanyl-D-glucose, pH 7.0 for CRL in case of L-valyl-D-glucose and pH 5.0 for RML in case of L-leucyl-D-glucose reactions. Higher equivalents of D-glucose were found to inhibit RML in case of L-alanyl-D-glucose reaction. However, in case of L-valyl-D-glucose and L-leucyl-D-glucose reactions, free amino acids and D-glucose were not found to be inhibitors of RML and CRL. In the synthesis of L-alanyl-D-glucose **16a-e**, RML could be reused upto four cycles where as PPL could be used only upto two cycles.

Chapter **FOUR** describes the syntheses and characterization of L-alanyl **1**, L-valyl **2**, L-leucyl **3** and L-isoleucyl **4** esters of carbohydrates - D-glucose **5**, D-galactose **6**, D-mannose **7**, D-fructose **8**, D-arabinose **9**, D-ribose **10**, lactose **11**, maltose **12**, sucrose **13**, D-mannitol **14** and D-sorbitol **15**. Esterification was carried out by reacting 0.002 mol unprotected L-amino acid (**1-4**) and 0.001 mol of carbohydrate (**5-15**) along with 100 ml CH<sub>2</sub>Cl<sub>2</sub>: DMF (90:10 v/v, 40 °C) in presence of 40 % (w/w carbohydrate employed) of lipases under reflux for a period of three days. *Rhizomucor miehei* lipase (RML) in presence of 0.1 mM (0.1 ml of 0.1 M) of pH 4.0 acetate buffer, *Candida rugosa* lipase (CRL) in presence of 0.1 mM (0.1 ml of 0.1 M) of pH 7.0 phosphate buffer and crude porcine pancreas lipase in presence of 0.1 mM (0.1 ml of 0.1 M) of pH 5.0 acetate buffer were employed to impart 'pH tuning' to the enzyme. All the three lipases employed showed broad substrate specificity towards amino acids as well as carbohydrates. Esterification yields were obtained in the range of 3 – 78 %. Two dimensional HSQCT NMR confirmed the formation of 1-*O*-, 2-*O*-, 3-*O*-, 4-*O*-, 5-*O*-, 6-*O*- and 6'-*O*- mono esters and 1,6-di-*O*-, 2,5-di-*O*-, 2,6-di-*O*-, 3,5-di-*O*-, 3,6-di-*O*-, 4,6-di-*O*- and 6,6'-di-*O*- diesters to varying extents depending on the carbohydrate employed. Nature of the products clearly indicated that primary hydroxyl groups of the carbohydrates (1-*O*-, 5-*O*-, 6-*O*- and 6'-*O*-) esterified predominantly over the secondary hydroxyl groups (2-*O*-, 3-*O*- and 4-*O*-). Among the secondary hydroxyl groups, 4-*O*- ester was formed only in case of D-mannose (**18b**, **36b** and **46b**). Carbohydrates containing hydroxyl groups in axial position like C2 in D-mannose and D-ribose and C4 in D-galactose have not reacted, indicating that esterification with axial secondary hydroxyl groups are difficult, especially with alkyl amino acyl donors. In case of L-alanyl-D-glucose **16a-e**, only β-anomer of D-glucose reacted, the D-glucose employed being a 40: 60 mixture of α and β

anomers respectively. Lesser incubation periods gave rise to only monoesters. The anomeric hydroxyl groups of carbohydrate molecules did not react because of rapid glycosidic ring opening and closing process. Aldohexoses (D-glucose, D-mannose and D-galactose), ketohexose (D-fructose), pentose (D-ribose) and the disaccharides (maltose) showed better conversions with all the four amino acids. Least conversions were observed for carbohydrate alcohols and sucrose esters. L-Valyl esters (25 – 78 %) as well as L-leucyl esters (21 – 65 %) showed better conversion than L-alanyl esters (3 – 78 %) and L-isoleucyl esters (9 – 55 %). Among the lipases employed, *Candida rugosa* lipase and porcine pancreas lipase have shown better conversions than *Rhizomucor miehei* lipase. L-Alanine **1**, L-valine **2** and L-leucine **3** with D-glucose **5** and L-alanine **1** and L-isoleucine **4** with D-mannose **7** gave five diastereomeric esters. Both D-arabinose **9** and D-ribose **10** showed three diastereomeric esters with all the amino acids (**1-4**) employed. Lactose **11** did not react with L-valine and L-leucine and D-sorbitol **15** did not react with L-alanine, L-valine and L-isoleucine. L-Alanyl-sucrose **24**, L-valyl-D-mannose **27**, L-valyl-sucrose **32**, L-leucyl-maltose **40**, L-leucyl-sucrose **41** and L-isoleucyl-sucrose **52**, formed only 6-*O*- esters. Carbohydrates like lactose **11**, D-mannitol **14** and D-sorbitol **15** reacted selectively depending on the amino acid indicating that they may not be good nucleophiles, probably due to more hydrogen bonding propensity for D-mannitol and D-sorbitol and steric hindrance in case of lactose. About 99 L-amino acyl esters of carbohydrates were prepared out of which 97 esters have not been reported before. So far unreported esters are L-alanyl-D-glucose **16a,d,e**, L-alanyl-D-galactose **17a-c**, L-alanyl-D-mannose **18a-e**, L-alanyl-D-fructose **19a-c**, L-alanyl-D-arabinose **20a-c**, L-alanyl-D-ribose **21a-c**, L-alanyl-lactose **22a-c**, L-alanyl-maltose **23a-c**, L-alanyl-sucrose **24**, L-valyl-D-glucose **25a-e**, L-valyl-D-galactose **26a-c**, L-valyl-D-mannose **27**, L-valyl-D-fructose **28a-**

c, L-valyl-D-arabinose **29a-c**, L-valyl-D-ribose **30a-c**, L-valyl-maltose **31a,b**, L-valyl-sucrose **32**, L-valyl-D-mannitol **33**, L-leucyl-D-glucose **34a-e**, L-leucyl-D-galactose **35a,b**, L-leucyl-D-mannose **36a-c**, L-leucyl-D-fructose **37**, L-leucyl-D-arabinose **38a-c**, L-leucyl-D-ribose **39a-c**, L-leucyl-maltose **40**, L-leucyl-sucrose **41**, L-leucyl-D-mannitol **42a,b**, L-leucyl-D-sorbitol **43**, L-iso-leucyl-D-glucose **44a,b**, L-iso-leucyl-D-galactose **45a-c**, L-iso-leucyl-D-mannose **46a-e**, L-iso-leucyl-D-fructose **47a-c**, L-iso-leucyl-D-arabinose **48a-c**, L-iso-leucyl-D-ribose **49a-c**, L-iso-leucyl-lactose **50a-c**, L-iso-leucyl-maltose **51a-c**, L-iso-leucyl-sucrose **52** and L-leucyl-D-mannitol **53a,b**.

Chapter **FIVE** describes kinetic study on the esterification of D-glucose **5** with L-alanine **1** catalyzed by lipases from *Rhizomucor miehei* (RML) and *Candida rugosa* (CRL). A detailed investigation showed that both the lipases followed Ping-Pong Bi-Bi mechanism wherein L-alanine and D-glucose bind in subsequent steps releasing water and L-alanyl-D-glucose also in subsequent steps, with competitive substrate inhibition by D-glucose at higher concentrations leading to the formation of dead-end lipase-D-glucose complexes. An attempt to obtain the best fit of this kinetic model through curve fitting yielded in good approximation, the apparent values of four important kinetic parameters, RML:  $k_{cat} = 0.29 \pm 0.028 \times 10^{-3} \text{ M h}^{-1} \text{ mg}^{-1}$ ,  $K_m \text{ L-alanine} = 4.9 \pm 0.51 \times 10^{-3} \text{ M}$ ,  $K_m \text{ D-glucose} = 0.21 \pm 0.018 \times 10^{-3} \text{ M}$ ,  $K_i \text{ D-glucose} = 1.76 \pm 0.19 \times 10^{-3} \text{ M}$ ; CRL:  $k_{cat} = 0.75 \pm 0.08 \times 10^{-3} \text{ M h}^{-1} \text{ mg}^{-1}$ ,  $K_m \text{ L-alanine} = 56.2 \pm 5.7 \times 10^{-3} \text{ M}$ ,  $K_m \text{ D-glucose} = 16.2 \pm 1.8 \times 10^{-3} \text{ M}$ ,  $K_i \text{ D-glucose} = 21.0 \pm 1.9 \times 10^{-3} \text{ M}$ .

Chapter **SIX** describes potentiality of some of the amino acyl esters of carbohydrates as inhibitors towards Angiotensin Converting enzyme (ACE) activity. The esters tested are: L-alanyl-D-glucose **16a-e**, L-alanyl-lactose **22a-c**, L-valyl-D-glucose **25a-e**, L-valyl-D-fructose **28a-c**, L-valyl-D-arabinose **29a-c**, L-valyl-D-ribose **30a-c**, L-

valyl-maltose **31a,b**, L-valyl-D-mannitol **33**, L-leucyl-D-glucose **34a-e**, L-leucyl-D-fructose **37**, L-leucyl-D-ribose **39a-c**, L-leucyl-D-sorbitol **43**, L-isoleucyl-D-glucose **44a,b**, L-isoleucyl-D-fructose **47a-c**, L-isoleucyl-D-ribose **49a-c** and L-isoleucyl-maltose **51a-c**. Amino acyl esters of carbohydrates tested for ACE inhibition activity showed  $IC_{50}$  values for ACE inhibition in the 0.7 mM to 6.0 mM range. Among them, L-isoleucyl-D-glucose **44a,b** ( $IC_{50}$ :  $0.7 \pm 0.067$  mM), L-leucyl-D-fructose **37** ( $IC_{50}$ :  $0.9 \pm 0.08$  mM), L-isoleucyl-maltose **51a-c** ( $IC_{50}$ :  $0.9 \pm 0.09$  mM) and L-valyl-D-mannitol **33** ( $IC_{50}$ :  $1.0 \pm 0.092$  mM) showed the best ACE inhibitory activities.

The present investigation has thus demonstrated the potentiality of RML, PPL and CRL to synthesize biologically and nutritionally active amino acyl esters of carbohydrates (**16a-e** – **53a,b**) using unprotected and unactivated L-amino acids and carbohydrates.

CONTENTS	Page No.
<b>Chapter 1</b>	
<b>Introduction</b>	1
1.1. Enzymes in organic synthesis	1
1.2. Lipases	2
1.2.1. <i>Candida rugosa</i> lipase	4
1.2.2. Porcine pancreas lipase	5
1.2.3. <i>Rhizomucor miehei</i> lipase	6
1.3 Lipase specificity	7
1.4. Reactions catalyzed by lipases	8
1.4.1. Hydrolysis	9
1.4.2. Esterrification	9
1.4.3. Transesterification	9
1.5. Catalytic mechanism of lipase mediated esterification in organic media	10
1.6. Advantages of lipase catalysis over chemical catalysis	13
1.7. Important parameters regulating the lipase activity in organic solvents	27
1.7.1. Nature of substrate	27
1.7.2. Nature of solvent	29
1.7.3. Effect of salt	32
1.7.4. Thermal Stability	33
1.7.5. Significance of water in lipase catalysis	35
1.7.6. Immobilization	38
1.8. Diverse applications of lipases in reaction	41
1.8.1. Esterification in reverse micelles	41
1.8.2. Esterification in supercritical carbon dioxide	42
1.8.3. Esterification in micro wave assisted reactions	43
1.8.4. Esterification in ionic liquids	44
1.8.5. Kinetic studies of lipase catalyzed esterification reactions	46
1.8.6. Lipase catalyzed resolution of racemic esters	48
1.8. Scope of the present investigation	49
<b>Chapter 2</b>	
<b>Materials and methods</b>	
2.1. Materials	52
2.1.1. Lipases	52
2.1.2. L-Amino acids	52
2.1.3. Carbohydrates	53
2.1.4. Solvents	53
2.1.5. Other chemicals	53
2.2. Methods	54
2.2.1. Lipase activity	54
2.2.1.1. Hydrolytic activity	54
2.2.1.2. Esterification activity	55
2.2.2. Protein estimation	56
2.2.3. Preparation of buffers	58
2.2.4. Esterification procedure	58
2.2.5. High Performance Liquid Chromatography	59
2.2.6. Separation of L-amino acyl esters of carbohydrates	59

2.2.7. UV-Visible spectroscopy	60
2.2.8. Infra Red spectroscopy	60
2.2.9. Nuclear Magnetic Resonance spectroscopy	60
2.2.9.1. <sup>1</sup> H NMR	60
2.2.9.2. <sup>13</sup> C NMR	61
2.2.9.3. Two-dimensional HSQCT	61
2.2.10. Mass spectroscopy	61
2.2.11. Polarimetry	62
2.2.12. Determination of Critical micellar concentration (CMC)	62
2.2.13. Water activity	63
2.2.14. Preparation of N-Acetyl alanine	64
2.2.15. Extraction of Angiotensin Converting Enzyme (ACE) from porcine lung	64
2.2.16. Angiotensin Converting Enzyme (ACE) inhibition assay	65
2.2.17. Protease activity	66
2.2.18. Extraction of porcine pancreas lipase	67
2.2.19. Immobilization of porcine pancreas lipase	67
2.2.20. Identification of lipases and ACE by SDS-PAGE	68
<b>Chapter 3</b>	
<b>Optimization of reaction parameters for the syntheses of L-alanyl, L-valyl and L-leucyl esters of D-glucose</b>	
3.1. Introduction	71
3.2. Present work	73
3.2.1. Synthesis of L-alanyl-D-glucose	73
3.2.1.1. Esterification profile	74
3.2.1.2. Effect of lipase concentration	74
3.2.1.3. Effect of buffer salts	75
3.2.1.4. Effect of substrate concentration	77
3.2.1.5. Reusability of lipases	78
3.2.1.6. Synthesis of L-alanyl-D-glucose at gram scale using crude PPL and immobilized PPL	79
3.2.2. Synthesis of L-valyl-D-glucose	80
3.2.2.1. Esterification profile	80
3.2.2.2. Effect of buffer salts	81
3.2.2.3. Effect of lipase concentration	82
3.2.2.4. Effect of L-valine and D-glucose concentration	82
3.2.3. Synthesis of L-leucyl-D-glucose	83
3.2.3.1. Effect of <i>Rhizomucor miehei</i> lipase concentration	84
3.2.3.2. Effect of L-leucine concentration	84
3.2.3.3. Effect of buffer salts	85
3.2.4. Selectivity	86
3.2.5. Determination of Critical Micellar Concentration (CMC)	86
3.3. Products of L-alanyl, L-valyl and L-leucyl esters of D-glucose	87
3.3.1. Spectral data for L-alanyl, L-valyl and L-leucyl esters of D-glucose	88
3.3.1.1. L-alanyl-D-glucose <b>16a-e</b>	88
3.3.1.2. L-valyl-D-glucose <b>25a-e</b>	89

3.3.1.3. L-leucyl-D-glucose <b>34a-e</b>	89
3.4. Discussion	90
3.5. Experimental	95
3.5.1. Esterification procedure	95
3.5.2. High Performance Liquid Chromatography (HPLC)	96
3.5.3. Spectral characterization	96
3.5.4. Nuclear Magnetic Resonance Spectroscopy	97
3.5.4.1. <sup>1</sup> H NMR	97
3.5.4.2. <sup>13</sup> C NMR	97
3.5.4.3. Two-dimensional HSQCT	97
<b>Chapter 4</b>	
<b>Syntheses of carbohydrate esters of L-alanine, L-valine, L-leucine and L-isoleucine</b>	
4.1. Introduction	98
4.2. Present investigation	
Syntheses and characterization of L-alanyl, L-valyl, L-leucyl and L-isoleucyl esters of carbohydrates	99
4.2.1. Syntheses of L-alanyl esters of carbohydrates <b>16a-e to 24</b>	100
4.2.1.1. L-Alanyl-D-glucose ( <b>16a-e</b> )	105
4.2.1.2. L-Alanyl-D-galactose ( <b>17a-c</b> )	106
4.2.1.3. L-Alanyl-D-mannose ( <b>18a-e</b> )	107
4.2.1.4. L-Alanyl-D-fructose ( <b>19a-c</b> )	107
4.2.1.5. L-Alanyl-D-arabinose ( <b>20a-c</b> )	108
4.2.1.6. L-Alanyl-D-ribose ( <b>21a-c</b> )	108
4.2.1.7. L-Alanyl-lactose ( <b>22a-c</b> )	109
4.2.1.8. L-Alanyl-maltose ( <b>23a-c</b> )	109
4.2.1.9. L-Alanyl-sucrose ( <b>24</b> )	110
4.2.2. Syntheses of L-valyl esters of carbohydrates <b>25a-e to 33</b>	111
4.2.2.1. L-Valyl-D-glucose ( <b>25a-e</b> )	115
4.2.2.2. L-Valyl-D-galactose ( <b>26a-c</b> )	116
4.2.2.3. L-Valyl-D-mannose ( <b>27</b> )	117
4.2.2.4. L-Valyl-D-fructose ( <b>28a-c</b> )	117
4.2.2.5. L-Valyl-D-arabinose ( <b>29a-c</b> )	118
4.2.2.6. L-Valyl-D-ribose ( <b>30a-c</b> )	118
4.2.2.7. L-Valyl-maltose ( <b>31a,b</b> )	119
4.2.2.8. L-Valyl-sucrose ( <b>32</b> )	120
4.2.2.9. L-Valyl-D-mannitol ( <b>33</b> )	120
4.2.3. Syntheses of L-leucyl esters of carbohydrates <b>34a-e to 43</b>	120
4.2.3.1. L-Leucyl-D-glucose ( <b>34a-e</b> )	124
4.2.3.2. L-Leucyl-D-galactose ( <b>35a, b</b> )	125
4.2.3.3. L-Leucyl-D-mannose ( <b>36a-c</b> )	126
4.2.3.4. L-Leucyl-D-fructose ( <b>37</b> )	126
4.2.3.5. L-Leucyl-D-arabinose ( <b>38a-c</b> )	127
4.2.3.6. L-Leucyl-D-ribose ( <b>39a-c</b> )	127
4.2.3.7. L-Leucyl-maltose ( <b>40</b> )	128
4.2.3.8. L-Leucyl-sucrose ( <b>41</b> )	128
4.2.3.9. L-Leucyl-D-mannitol ( <b>42a, b</b> )	129
4.2.3.10. L-Leucyl-D-sorbitol ( <b>43</b> )	129



---

4.2.4. Syntheses of L-isoleucyl esters of carbohydrates <b>44a,b</b> to <b>53 a,b</b>	130
4.2.4.1. L-Isoleucyl-D-glucose ( <b>44a, b</b> )	134
4.2.4.2. L-Isoleucyl-D-galactose ( <b>45a-c</b> )	135
4.2.4.3. L-Isoleucyl-D-mannose ( <b>46a-e</b> )	136
4.2.4.4. L-Isoleucyl-D-fructose ( <b>47a-c</b> )	136
4.2.4.5. L-Isoleucyl-D-arabinose ( <b>48a-c</b> )	137
4.2.4.6. L-Isoleucyl-D-ribose ( <b>49a-c</b> )	137
4.2.4.7. L-Isoleucyl-lactose ( <b>50a-c</b> )	138
4.2.4.8. L-Isoleucyl-maltose ( <b>51a-c</b> )	139
4.2.4.9. L-Isoleucyl-sucrose ( <b>52</b> )	139
4.2.4.10. L-Isoleucyl-D-mannitol ( <b>53a, b</b> )	140
4.3. Spectral characterization of spectral data for L-alanyl, L-valyl, L-leucyl and L-isoleucyl esters of carbohydrates	141
4.3.1. L-Alanyl esters of carbohydrates <b>16a-e</b> to <b>24</b>	141
4.3.2. L-Valyl esters of carbohydrates <b>25a-e</b> to <b>33</b>	143
4.3.3. L-Leucyl esters of carbohydrates <b>34a-e</b> to <b>43</b>	144
4.3.4. L-Isoleucyl esters of carbohydrates <b>44a,b</b> to <b>53a,b</b>	145
4.4. Discussion	147
4.5. Experimental	151
4.5.1. Esterification procedure	151
4.5.2. High Performance Liquid Chromatography (HPLC)	152
4.5.3. Spectral characterization	152
4.5.4. Nuclear Magnetic Resonance Spectroscopy	152
4.5.4.1. <sup>1</sup> H NMR	152
4.5.4.2. <sup>13</sup> C NMR	153
4.5.4.3. Two-dimensional HSQCT	153
<b>Chapter 5</b>	
<b>Competitive inhibition by substrates in <i>Rhizomucor miehei</i> and <i>Candida rugosa</i> lipases catalysed esterification of D-glucose with L- alanine</b>	
5.1. Introduction	154
5.2. Present investigation	155
5.2.1. <i>Rhizomucor miehei</i> and <i>Candida rugosa</i> lipase catalysis	156
5.3. Discussion	162
5.4. Experimental	164
5.4.1. Kinetic experiments	164
5.4.2. High Performance Liquid Chromatography (HPLC)	165
<b>Chapter 6</b>	
<b>Angiotensin Converting Enzyme inhibition activity of L-alanyl, L- valyl, L-leucyl and L-isoleucyl esters of carbohydrates</b>	
6.1. Introduction	166
6.2. Present investigation	168
6.3. Discussion	172
6.4. Experimental	173
6.4.1. Extraction of ACE from pig lung	173
6.4.2. Esterification Procedure	174

---

---

6.4.3. Angiotensin Converting Enzyme inhibition assay	175
6.4.4. Protease and lipase assay	176
<b>Conclusion</b>	177
<b>Summary</b>	181
<b>References</b>	187
<b>Publications</b>	

---

## List of Figures

Number	Captions
Fig. 1.1	Overall structure of <i>Candida rugosa</i> lipase
Fig. 1.2	Schematic ribbon diagram of the porcine lipase-colipase structure.
Fig. 1.3	(A) The hydrogen-bonding network in the active site of the RML lipase. (B) A schematic drawing showing the packing within the $\beta$ - $\epsilon$ Ser- $\alpha$ -motif.
Fig. 2.1	Calibration curve for protein estimation by Lowry's method
Fig. 2.2	Calibration curve for hippuric acid estimation by spectrophotometric method
Fig. 2.3	Plot of $R_f$ values of molecular marker verses log molecular weight
Fig. 2.4	(A) SDS-PAGE for lipases (B) SDS-PAGE for Angiotensin Converting Enzyme
Fig. 3.1	HPLC chromatograph for the reaction mixture of L-alanine and D-glucose
Fig. 3.2	Reaction profile for L-alanyl-D-glucose synthesis
Fig. 3.3	Effect of substrate concentration on synthesis of L-alanyl-D-glucose.
Fig. 3.4	HPLC chromatograph for the reaction mixture of L-valine and L-valyl-D-glucose.
Fig. 3.5	Effect of incubation period on esterification of L-valyl-D-glucose.
Fig. 3.6	Effect of substrate concentration on synthesis of L-valyl-D-glucose.
Fig. 4.1	HPLC chromatogram: reaction mixture of L-alanine and D-fructose esterification catalyzed by RML.
Fig. 4.2	UV spectra for L-alanyl- $\beta$ -D-glucose <b>16a-e</b> from RML catalyzed reaction.
Fig. 4.3	A typical IR spectrum of L-alanyl- $\beta$ -D-glucose <b>16a-e</b> by RML catalyzed reaction.
Fig. 4.4	A typical mass spectrum of L-alanyl- $\beta$ -D-glucose <b>16a-e</b> .
Fig. 4.5	Two-dimensional HSQCT NMR spectrum for L-alanyl- $\beta$ -D-glucose <b>16a-e</b> of RML catalyzed reaction.
Fig. 4.6	Two-dimensional HSQCT NMR spectrum for L-alanyl-D-galactose <b>17a-c</b> of RML catalyzed reaction.
Fig. 4.7	$^{13}\text{C}$ NMR spectrum for L-alanyl-D-mannose <b>18a-e</b> catalyzed by RML.
Fig. 4.8	A typical mass spectrum of L-alanyl-D-fructose <b>19a-c</b> .
Fig. 4.9	UV spectra for L-alanyl-D-arabinose <b>20a-c</b> from RML catalyzed reaction.
Fig. 4.10	A typical mass spectrum for L-alanyl-D-arabinose <b>20a-c</b> .
Fig. 4.11	UV spectra for L-alanyl-D-ribose <b>21a-c</b> from RML catalyzed reaction.
Fig. 4.12	A typical mass spectrum for L-alanyl-D-ribose <b>21a-c</b> .
Fig. 4.13	A typical mass spectrum for L-alanyl-lactose <b>22a-c</b> .
Fig. 4.14	A typical IR spectrum of L-alanyl-D-maltose <b>23a-c</b> of RML catalyzed reaction.
Fig. 4.15	Two-dimensional HSQCT NMR spectrum for L-alanyl-maltose <b>23a-c</b> prepared through RML catalysis.
Fig. 4.16	Two-dimensional HSQCT NMR spectrum for L-alanyl-sucrose <b>24</b> of RML catalyzed reaction.
Fig. 4.17	HPLC chromatogram: reaction mixture of L-valine and D-mannose esterification catalyzed by RML.
Fig. 4.18	UV spectra for L-valyl-D-glucose <b>25a-e</b> from RML catalyzed reaction.

- 
- Fig. 4.19 A typical IR spectrum of L-valyl-D-glucose of CRL catalyzed reaction **25a-e**.
- Fig. 4.20 A typical mass spectrum for L-valyl-D-glucose **25a-e**.
- Fig. 4.21 UV spectra for L-valyl-D-galactose **26a-c** from CRL catalysed reaction.
- Fig. 4.22 Two-dimensional HSQCT NMR spectrum for L-valyl-D-galactose **26a-c** obtained through CRL catalysis.
- Fig. 4.23 A typical mass spectrum of L-valyl-D-mannose **27**.
- Fig. 4.24 UV spectra for L-valyl-D-fructose **28a-c** from CRL catalyzed reaction.
- Fig. 4.25 A typical mass spectrum of L-valyl-D-fructose **28a-c**.
- Fig. 4.26 UV spectra for L-valyl-D-arabinose **29a-c** from CRL catalyzed reaction
- Fig. 4.27 A typical mass spectrum of L-valyl-D-arabinose **29a-c**.
- Fig. 4.28 UV spectra for L-valyl-D-ribose **30a-c** from CRL catalyzed reaction
- Fig. 4.29 A typical mass spectrum of L-valyl-D-ribose **30a-c**.
- Fig. 4.30 Two-dimensional HSQCT NMR for L-valyl-maltose **31a,b** obtained through CRL catalysis.
- Fig. 4.31 Two-dimensional HSQCT NMR for L-valyl-sucrose **32** obtained through CRL catalysis.
- Fig. 4.32 Two-dimensional HSQCT NMR for L-valyl-D-mannitol **33** obtained through CRL catalysis.
- Fig. 4.33 HPLC chromatogram for reaction mixture of L-leucine and maltose esterification reaction catalyzed by CRL.
- Fig. 4.34 UV spectra for L-leucyl-D-glucose **34a-e** from CRL catalyzed reaction
- Fig. 4.35 A typical IR spectrum of L-leucyl-D-glucose **34a-e** of CRL catalyzed reaction.
- Fig. 4.36 A typical mass spectrum of L-leucyl-D-glucose **34a-e**.
- Fig. 4.37 Two-dimensional HSQCT NMR for L-leucyl- D-glucose **34a-e** obtained through CRL catalysis.
- Fig. 4.38 A typical IR spectrum of L-leucyl-D-galactose of RML catalyzed reaction **35a,b**.
- Fig. 4.39 A typical mass spectrum of L-leucyl-D-galactose. **35a,b**
- Fig. 4.40 UV spectra for L-leucyl-D-mannose **36a-c** from CRL catalyzed reaction
- Fig. 4.41 A typical mass spectrum of L-leucyl-D-mannose **36a-c**.
- Fig. 4.42 UV spectra for L-leucyl-D-fructose **37** from CRL catalyzed reaction.
- Fig. 4.43 A typical mass spectrum of L-leucyl-D-fructose **37**.
- Fig. 4.44 Two-dimensional HSQCT NMR for L-leucyl- D-arabinose **38a-c** obtained through CRL catalysis.
- Fig. 4.45 A typical mass spectrum of L-leucyl-D-ribose **39a-c**.
- Fig. 4.46 Two-dimensional HSQCT NMR for L-leucyl-maltose **40** obtained through CRL catalysis.
- Fig. 4.47 Two-dimensional HSQCT NMR for L-leucyl-sucrose **41** obtained through CRL catalysis.
- Fig. 4.48 A typical mass spectrum of L-leucyl-D-mannitol **42**.
- Fig. 4.49 Two-dimensional HSQCT NMR for L-leucyl-D-sorbitol **43** obtained through CRL catalysis.
- Fig. 4.50 HPLC chromatogram for reaction mixture of L-isoleucine and D-ribose esterification catalyzed by CRL.
- Fig. 4.51 UV spectra for L-isoleucyl-D-glucose **44a,b** from CRL catalyzed reaction.
-

- 
- Fig. 4.52 A typical IR spectrum of L-isooleucyl-D-glucose **44a,b** of CRL catalyzed reaction.
- Fig. 4.53 A typical mass spectrum of L-isooleucyl-D-glucose **44a,b**.
- Fig. 4.54 Two-dimensional HSQCT NMR for L-isooleucyl- D-glucose **44a,b** obtained through CRL catalysis.
- Fig. 4.55 A typical mass spectrum of L-isooleucyl-D-galactose **45a-c**.
- Fig. 4.56 UV spectra for L-isooleucyl-D-mannose **46a-e** from CRL catalyzed reaction
- Fig. 4.57 Two-dimensional HSQCT NMR for L-isooleucyl-D-mannose **46a-e** obtained through CRL catalysis.
- Fig. 4.58 Two-dimensional HSQCT NMR for L-isooleucyl-D-fructose **47a-c** obtained through CRL catalysis.
- Fig. 4.59 UV spectra for (A) L-isooleucine (B) L-isooleucyl-D-arabinose **48a-c**
- Fig. 4.60 Two-dimensional HSQCT NMR for L-isooleucyl- D-ribose **49a-c** obtained through CRL catalysis.
- Fig. 4.61 A typical mass spectrum of L-isooleucyl-lactose **50a-c**.
- Fig. 4.62 Two-dimensional HSQCT NMR for L-isooleucyl-lactose **50a-c** obtained through CRL catalysis.
- Fig. 4.63 UV spectra for L-isooleucyl-maltose **51a-c** from CRL catalyzed reaction
- Fig. 4.64 A typical mass spectrum of L-isooleucyl-maltose **51a-c**.
- Fig. 4.65 A typical mass spectrum of L-isooleucyl-sucrose **52**.
- Fig. 4.66 UV spectra for L-isooleucyl-D-mannitol **53a,b** from CRL catalyzed reaction
- Fig. 4.67 Two-dimensional HSQCT NMR for L-isooleucyl-D-mannitol **53a,b** obtained through CRL catalysis.
- Fig. 5.1 Time courses of esterification reactions – concentrations of L-alanyl-D-glucose versus incubation periods
- Fig. 5.2 Double reciprocal plots for RML-catalyzed L-alanyl-D-glucose reaction:  $1/v$  versus  $1/[D\text{-glucose}]$
- Fig. 5.3 Double reciprocal plots for RML-catalyzed L-alanyl-D-glucose reaction:  $1/v$  versus  $1/[L\text{-alanine}]$
- Fig. 5.4 Double reciprocal plots for CRL-catalyzed L-alanyl-D-glucose reaction:  $1/v$  versus  $1/[L\text{-alanine}]$  plots  $1/v$  versus  $1/[D\text{-glucose}]$
- Fig. 5.5 Double reciprocal plots for CRL-catalyzed L-alanyl-D-glucose reaction:  $1/v$  versus  $1/[L\text{-alanine}]$
- Fig. 5.6 Replot of slopes obtained from Fig. 5.3 versus  $[D\text{-glucose}]$  (RML).
- Fig. 5.7 Replot of slopes obtained from Fig. 5.5 versus  $[D\text{-glucose}]$  (CRL).
- Fig. 6.1 A typical ACE inhibition plot for captopril
- Fig. 6.2 ACE inhibition plots for L-alanyl esters of carbohydrates
- Fig. 6.3 ACE inhibition plots for L-valyl esters of carbohydrates
- Fig. 6.4 ACE inhibition plots for L-leucyl esters of carbohydrates
- Fig. 6.5 ACE inhibition plots for L-isooleucyl esters of carbohydrates
-

## List of Tables

Number	Title	Page No.
Table 1.1	Biotechnological applications of lipase	4
Table 1.2	Lists some of the commercially important esters synthesized by lipase mediated catalysis	15
Table 2.1	List of lipases and their sources	52
Table 2.2	List of chemicals and suppliers	53
Table 2.3	Esterification and hydrolytic activities of different lipases	56
Table 2.4	Protein content of different lipase preparations	57
Table 2.5	Water activities for different organic solvents by Karl-Fisher method	64
Table 3.1	Effect of lipase concentration on the synthesis of L-alanyl-D-glucose	75
Table 3.2	Effect of partially purified PPL concentration on the synthesis of L-alanyl-D-glucose	75
Table 3.3	Effect of buffer salts (pH and buffer concentration) on the synthesis of L-alanyl-D-glucose	77
Table 3.4	Reusability of lipase in presence and absence of buffer salt	79
Table 3.5	Effect of buffer salts (pH and buffer concentration) on the synthesis of L-valyl-D-glucose	81
Table 3.6	Effect of lipase concentration on the synthesis of L-valyl-D-glucose	82
Table 3.7	Effect of lipase concentration on the synthesis of L-leucyl-D-glucose	84
Table 3.8	Effect of L-leucine on the synthesis of L-leucyl-D-glucose	85
Table 3.9	Effect of buffer salts (pH and buffer concentration) on the synthesis of L-leucyl-D-glucose	86
Table 3.10	Synthesis of L-alanyl, L-valyl and L-leucyl esters of D-glucose	87
Table 4.1	Chemical shift values for free carbohydrates	102
Table 4.2	Syntheses of L-alanyl esters of carbohydrates	103
Table 4.3	Preparation of L-alanyl ester of carbohydrate using lipases from <i>Candida rugosa</i> and porcine pancreas	105
Table 4.4	Syntheses of L-valyl esters of carbohydrates	113
Table 4.5	Preparation of L-valyl esters of carbohydrates using crude porcine pancreas lipase	115
Table 4.6	Syntheses of L-leucyl esters of carbohydrates	122
Table 4.7	Preparation of L-leucyl esters of carbohydrates using crude porcine pancreas lipase	124
Table 4.8	Syntheses of L-isoleucyl esters of carbohydrates	132
Table 4.9	Preparation of L-isoleucyl esters of carbohydrates using crude porcine pancreas lipase	134
Table 4.10	Percentage yields and proportions of L-alanyl esters of carbohydrates from RML and L-valyl, L-leucyl and L-isoleucyl esters of carbohydrates CRL catalysed reactions	150
Table 5.1	Apparent values of kinetic parameters for RML and CRL-catalysed synthesis of L-alanyl-D-glucose	158

---

Table 5.2	Experimental and predicted initial rate values for the synthesis of L-alanyl-D-glucose by RML	160
Table 5.3	Experimental and predicted initial rate values for the synthesis of L-alanyl-D-glucose by CRL	161
Table 6.1	Protease inhibition assay for D-glucose ester	169
Table 6.2	IC <sub>50</sub> values for ACE inhibition by amino acyl esters of carbohydrates	170

---

## List of Schemes

Number	Title	Page No.
Scheme 1.1	Types of reactions catalyzed by lipases	10
Scheme 1.2	Catalytic mechanism of lipase mediated esterification in organic media	12
Scheme 1.3	Lipase catalyzed esterification at the microaqueous inter-phase	37
Scheme 3.1	Lipases catalyzed regioselective synthesis of L-alanyl-D-glucose esters in anhydrous organic media	73
Scheme 3.2	Lipases catalyzed synthesis of L-valyl-D-glucose esters in anhydrous organic media	80
Scheme 3.3	Lipases catalyzed synthesis of L-leucyl-D-glucose esters in anhydrous organic media	83
Scheme 4.1	Lipase catalyzed syntheses of L-alanyl esters of carbohydrates	102
Scheme 4.2	Lipase catalyzed syntheses of L-valyl esters of carbohydrates	112
Scheme 4.3	Lipase catalyzed syntheses of L-leucyl esters of carbohydrates	121
Scheme 4.4	Lipase catalyzed synthesis of L-isoleucyl esters of carbohydrates	131
Scheme 5.1	Ping-Pong Bi-Bi mechanism of RML- and CRL-catalyzed synthesis of L-alanyl-D-glucose showing inhibition by D-glucose.	157
Scheme 6.1	Role of angiotensin converting enzyme (ACE) in regulating blood pressure	166
Scheme 6.2	Hypothetical representation of ACE inhibition by captopril binding to the active sites	167
Scheme 6.3	Hypothetical representation of ACE active sites and binding of inhibitors	167



## List of abbreviations and symbols

---

A	Absorbance
$\alpha$	Alpha
ACE	Angiotensin Converting Enzyme
Å	Angstrom
$\beta$	Beta
BSA	Bovine serum albumin
CRL	<i>Candida rugosa</i> lipase
$^{13}\text{C}$	Carbon-13
J	Coupling constant
CMC	Critical Micellar Concentration
$k_{cat}$	Catalytic efficiency of the enzyme
$^{\circ}\text{C}$	Degree centigrade
$\delta$	Delta
DMSO- $d_6$	Deuteriated Dimethyl sulfoxide
$\text{CH}_2\text{Cl}_2$	Dichloromethane
DCF	Dichlorofluorecin
DMF	Dimethyl formamide
DMSO	Dimethyl sulfoxide
eV	Electron volt
EC	Enzyme commission
$\gamma$	Gamma
g	Gram
Hz	Hertz
HMQCT	Heteronuclear Multiple Quantum Coherence Transfer
HSQCT	Heteronuclear Single Quantum Coherence Transfer
HPLC	High Performance Liquid Chromatography
h	Hour
IR	Infra Red
$K_i$	Inhibitor constant
$v$	Initial velocity

---

---

KDa	Kilodalton
$K_{mA}$	Michelis-Menten constant for the lipase-L-alanine complex
$K_{mL\text{-alanine}}$	Michelis-Menten constant for the lipase-L-alanine complex
$K_{mB}$	Michelis-Menten constant for the lipase-D-glucose complex
$K_{mD\text{-glucose}}$	Michelis-Menten constant for the lipase-D-glucose complex
$K_i$	Dissociation constant for the lipase-inhibitor (D-glucose) complex
$K_{iD\text{-glucose}}$	Dissociation constant for the lipase-inhibitor (D-glucose) complex
MS	Mass Spectrometry
$V_{max}$	Maximum velocity
MHz	Mega hertz
$K_m$	Michelis Menton constant
$\mu\text{g}$	Microgram
$\mu\text{l}$	Microlitre
mg	Milligram
ml	Milliliter
mmol	Millimole
min	Minute
M	Molarity
mol	Mole
$\epsilon$	Molar extinction coefficient
$[\text{M}]^+$	Molecular ion
nm	Nanometer
N	Normality
nmol	Nano mole
NMR	Nuclear Magnetic Resonance
$[\alpha]$	Optical rotation
ppm	Parts per million
%	Percentage
$\pi$	Pi
PAGE	Polyacrylamide gel electrophoresis
PPL	Porcine pancreas lipase
KBr	Potassium bromide

---

---

$^1\text{H}$	Proton
$R_f$	Retention factor
R	Regression coefficient
$t_{ret}$	Retention time
RML	<i>Rhizomucor miehei</i> lipase
$\sigma$	Sigma
SDS	Sodium dodecyl sulfate
TEMED	N, N, N', N'-Tetramethylethylenediamine
TMS	Tetra methyl silane
TLC	Thin layer chromatography
2D	Two-Dimensional
UV	Ultra Violet
v/v	Volume by volume
$a_w$	Water activity
$\text{cm}^{-1}$	Wave per centimeter
w/w	Weight by weight

---

**Chapter 1**  
***Introduction***

## 1. Introduction

The enormous variety of biochemical reactions that takes place in living systems are all mediated by a series of enzymes (Michal, 1999). Of the estimated 25,000 enzymes present in nature, only about 2800 have been characterized and about 400 enzymes, mainly hydrolases, transferases and oxido-reductases have been identified as commercially potential ones. But only 50 different kinds of enzymes find application on an industrial scale (Winterhalter and Schreier, 1993; Schreier and Winterhalter, 1993; Berger, 1995). The enzymes of commercial importance in food industry are amylases, proteases, pectinases, cellulases, hemicellulases, lipases and lactases. About 75 % of the enzymes commercially used are hydrolytic enzymes. These enzymes are used as tools in hydrolysis, synthesis, analysis, biotransformation and affinity separation (Sharma *et al.*, 2001; Klivanov, 1986; Bosley and Calyton, 1994; Vulfson, 1993).

### 1.1. Enzymes in organic synthesis

Enzymes have given better solution for the problems encountered in chemical synthesis. Chemical approach in synthesis needs drastic conditions, like use of acids or alkaline media as catalysts, high temperature, hazardous chemicals, heavy metals, protection and deprotection of the reactants which in most cases lead to multi-step processes, high energy consumption, coloring of products, low regio and stereo selectivity, more number of byproducts, economically not so feasible conditions and results in environmental pollution. Some of the synthesized products are harmful in nature and require more purification. Hence, their use in food and pharmaceutical industry is very limited. However, enzymes are biocatalysts that catalyze reactions under mild conditions which do not require drastic conditions like high temperature, use of hazard chemicals and protection and deprotection of reactants. Using enzymes in non

aqueous media initiated by Alexander Klivanov resulted in wide applications in organic synthesis (Klivanov, 1986).

## 1.2. Lipases

Lipases (triacylglycerol acylhydrolases, E.C. 3.1.1.3) are ubiquitous enzymes of considerable physiological significance and industrial potential. Lipases are hydrolases which catalyze the hydrolysis of triacylglycerols to glycerol and free fatty acids. In eukaryotes, lipases are involved in various stages of lipid metabolism including fat digestion, absorption, reconstitution and lipoprotein metabolism. In plants, lipases are found in energy reserve tissues. They differ from esterases by their substrate specificity. While lipases acts on water insoluble long chain fatty acyl glycerides, esterases prefer water soluble short chain fatty acyl esters. Lipases contain a hydrophobic oligopeptide lid which is not present in esterases covering the entrance of its active site. It is this hydrophobic lid which requires interfacial activation at lipid-water interface (Martinelle *et al.*, 1995). In presence of hydrophobic interfaces, lipases undergo conformational change by acquiring an open structure in which the active site residues become accessible to substrates. However, in the absence of interfaces, lipase molecules exhibit a closed structure in which the lid covers the active site, making it inaccessible to substrates (Brzozowski *et al.*, 1990). The catalysis by lipase includes a steep substrate concentration gradient at the interface, better orientation of a scissile ester bond, reduction in the water shell around the substrate ester molecules and the conformational change of the enzyme (Derewenda and Sharp, 1993). Lipases can tolerate organic solvents in the reaction mixture. Therefore, lipases find promising position in organic chemical processing (Kiran and Divakar, 2001; Kiran *et al.*, 2001a; Therisod and Klivanov, 1986; Berglund and Hutt, 2000, Harikrishna and Karanth, 2001), detergent

formulations (Jaeger and Reetz, 1998), synthesis of biosurfactants (Plou *et al.* 1999; Sarney *et al.* 1996; 1995), oleochemical industry (Bornscheur, 2000; Undurraga *et al.*, 2001), dairy industry (Vulfson, 1994), paper manufacture (Jaeger and Reetz, 1998), nutrition (Pabai *et al.*, 1995a,b; Undurraga *et al.*, 2001) and cosmetics and pharmaceutical processing (Berglund and Hutt, 2000). Development of lipase-based technologies for the synthesis of novel compounds is rapidly expanding (Liese *et al.*, 2000). Other biotechnological applications of lipases are shown in Table 1.1. Lipases are employed to get poly unsaturated fatty acids (PUFAs) which are then used along with their mono- and diglycerides for the synthesis of nutraceuticals, pharmaceuticals like anti-cholesterolemics, anti-inflammatories and thrombolytics (Gill and Valivety, 1997; Belarbi *et al.*, 2000). *Candida rugosa* lipase is employed in the paper industry to remove the pitch from the pulp (Sharma *et al.*, 2001). The main reason for the use of lipases is the growing interest and demand for the products prepared through natural resource, which are environmentally compatible. Because of their versatility in application, lipases are regarded as enzymes with high commercial potential. Lipase catalyzed esterification in organic solvents offers synthetic challenges, which if dealt with successfully, can result in the generation of several useful compounds.

**Table 1.1 Biotechnological applications of lipases (Vulfson, 1994)**

<b>Industry</b>	<b>Action</b>	<b>Product or application</b>
Detergents	Hydrolysis of fats	Removal of oil stains from fabrics
Dairy	Hydrolysis of milk fat, cheese ripening, modification of butter fat	Development of flavoring agents in milk, cheese, and butter
Bakery	Flavor improvement and shelf-life elongation	Bakery products
Beverages	Improved aroma	Beverages
Food	Quality improvement, transesterification	Mayonnaise, dressings, and whippings, health foods
Meat and fish	Flavor development and removal of fats	Meat and fish products
Fats and oils	Transesterification, hydrolysis	Cocoa butter, margarine, fatty acids, glycerol, mono-, and diglycerides
Chemicals	Enantioselectivity, synthesis	Chiral building blocks and chemicals
Cosmetics	Synthesis	Emulsifiers, moisturizers
Leather	Hydrolysis	Leather products
Paper	Hydrolysis	Paper with improved quality by removing wax.
Cleaning	Synthesis and hydrolysis	Removal of cleaning agents like surfactants
Food dressing	Quality improvement	Mayoannaise, dressing and whipping
Pharmaceuticals	Transesterification, hydrolysis	Speciality lipids, digestive aids
Health food	Transesterification	Health foods

### 1.2.1. *Candida rugosa* lipase

*Candida rugosa* lipase (CRL) is the first example of a native interface-activatable lipase in ‘open’ form (Schrag *et al.*, 1996). CRL is a member of the  $\alpha/\beta$ -hydrolase fold family, which consists of a central hydrophobic eight-stranded  $\beta$ -sheet packed between two layers of amphiphilic  $\alpha$ -helices (Fig.1.1). CRL is made up of a single polypeptide chain with 534 amino acid residues with a molecular weight of 57 kDa. CRL appears in five isoforms, which have been cloned and sequenced (Kawaguchi *et al.*, 1989, Longhi *et*



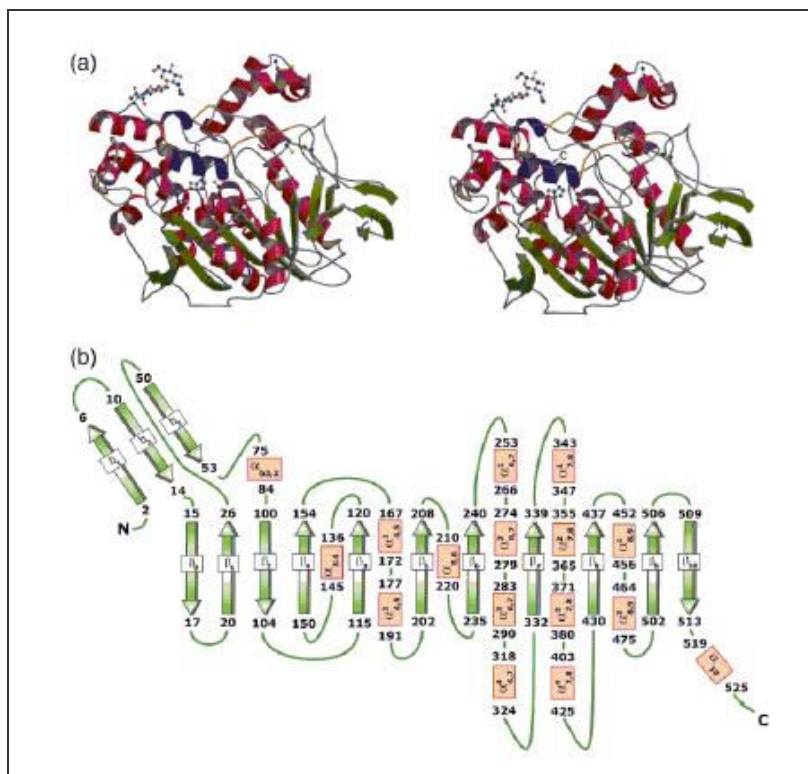


**Fig. 1.1.** Overall structure of *Candida rugosa* lipase. (a) Ribbon representation with  $\alpha$ -helices,  $\beta$ -strands and coils colored in red, green and gray, respectively. The helical and coil segments forming the flap region are shown in dark blue and orange, respectively. The catalytic triad residues (Ser-209, Glu-341 and His-449), the disulfide bridges and the Asn-attached N-acetyl-glucosamine moieties are shown in ball-and-stick representation. (b) A representation of the lipase 2 topology with the secondary structure elements identified ( $\beta$ , strands;  $\alpha$ , helix). (adopted from Mancheño *et al.*, 2003).

*al.*, 1992). In CRL, the active site triad consists of Ser-209, Glu-341 and His-449 and nearer to this active site and three surface loops (62-92, 122-129 and 294-305) are present which are very important for catalytic activity (Fig. 1.1). Ser-209 is embedded in a characteristic super secondary structure motif, found in all lipase. In the open conformation observed for CRL, the lid extends nearly perpendicular to the protein surface forming a large depression that surround the active site. The hydrophilic area consists of uncharged polar residues. The face of the flap facing the active site is hydrophobic in nature which is mainly composed of aliphatic side chain amino acid residues. The flap facing opposite the active site is hydrophilic in character. The geometry of loop 13 and 4 and the active site of CRL suggests that the oxyanion hole  $O_{\gamma}$  is formed by the backbone amide of Gly-123, Gly-124 and Ala-210, which are involved in hydrogen bond formation with the substrates (Fig. 1.1). Presence of two acyl binding ‘pockets’ in the active site of CRL depicts the substrate specificity for carbon chain lengths, a small pocket which can bind well with short chain acids and a bigger pocket which can bind well with longer chain acids (Parida and Dordick, 1993). Experimentally, this was proved by showing that the mechanism depends on the chain length of the acyl moiety and independent of the type of reaction catalysed and this behaviour is similar when the reaction was carried out in different solvent systems also.

### **1.2.2. Porcine pancreas lipase**

Pancreatic lipases are high active lipases where one molecule of lipase can cleave nearly 7000 ester bonds per second under optimal conditions (Scharpe *et al.*, 1997). Most of the work conducted with pancreatic lipase were from porcine pancreas. Porcine pancreas is the richest source for pancreatic lipases which was also the first purified lipase (Peschke, 1991). Pancreatic lipase is a single chain glycoprotein of 48 kDa

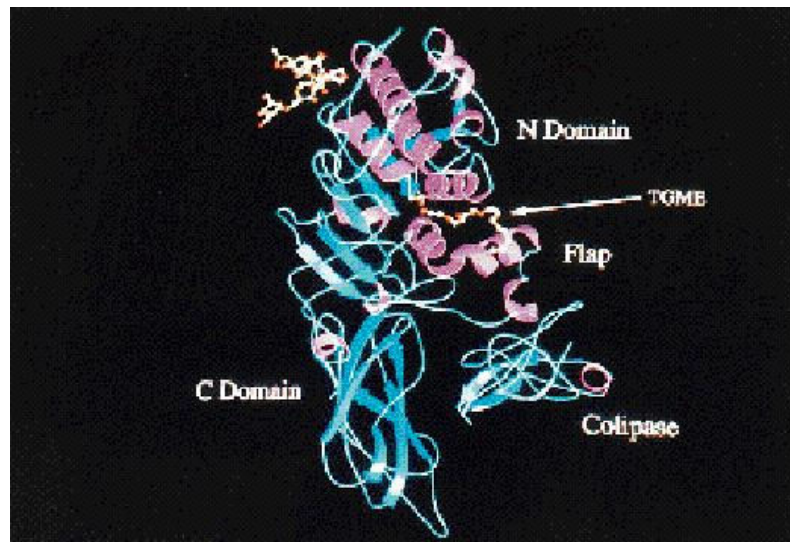


**Fig. 1.2.** Schematic ribbon diagram of the porcine lipase-colipase structure. The glycan chain, connected to the lipase N-terminal domain (N domain), is drawn as a stick model. One tetra ethylene glycol mono-octyl ether inhibitor molecule, located in the open active site, is represented by *balls* and *sticks*. Colipase interacts with the lipase C-terminal domain (C domain) and with the flap (adopted from Hermoso *et al.*, 1996).

molecular weight and it is a serine hydrolase (Winkler and Gubernator, 1994; Scharpe *et al.*, 1997). It consists of a central predominant parallel  $\beta$ -sheet having helical connection (van Tilbeurgh, 1992). From pH titration and photo-oxidation studies, histidine residue was found to be responsible for the catalytic activity (Winkler *et al.*, 1990), the catalytic triad consisting of Ser-152, His-263, and Asp-176. Donner (1976) purified and measured some of the physical parameters: molecular weight 52000, sedimentation coefficient (s degrees 20, w) 4.0 S, diffusion coefficient (D degrees 20, w)  $6.7 \times 10^{-7} \text{cm}^2 \text{s}^{-1}$ , Stokes' radius (r) 30.3 Å, partial specific volume (v)  $0.72 \text{cm}^3 \text{g}^{-1}$ , frictional ratio ( $f/f_0$ ) 1.23 and isoelectric point 5.18. Lipase was bound by prolipase at its edge with the plane of the prolipase roughly perpendicular to the C-terminal  $\beta$ -sheet domain of the lipase molecule (Fig. 1.2). Prolipase is a flattened molecule with dimension of about 33 Å x 24 Å x 16 Å consisting of mainly three finger shaped regions formed by residues between 26-39, 47-64 and 67-87 held together by disulfide bonds. It was found that majority of hydrophobic amino acids are found in the region opposite of the lipase binding site. The catalytic active site also contains a surface helix (residue 248-258) which is a part of the amphiphatic lid covering the active site (van Tilbeurgh, 1992).

### 1.2.3. *Rhizomucor miehei* lipase

*Rhizomucor miehei* lipase (RML) is made up of a single polypeptide chain with 269 amino acid residues with a molecular weight of 29 kDa (Brandy *et al.*, 1990, Brzozowski *et al.*, 1991). Brandy *et al.*, (1990) identified that RML is an  $\alpha/\beta$  type protein with a central eight-stranded mixed  $\beta$ -pleated sheet folded on to a highly amphiphatic N-terminal helix and a number of loops and helices including a semi-external, long kinked  $\alpha$ -helix, with three disulphide bonds which are responsible in stabilizing the two terminal strands. The catalytic triad is constituted by Ser-144, His-257

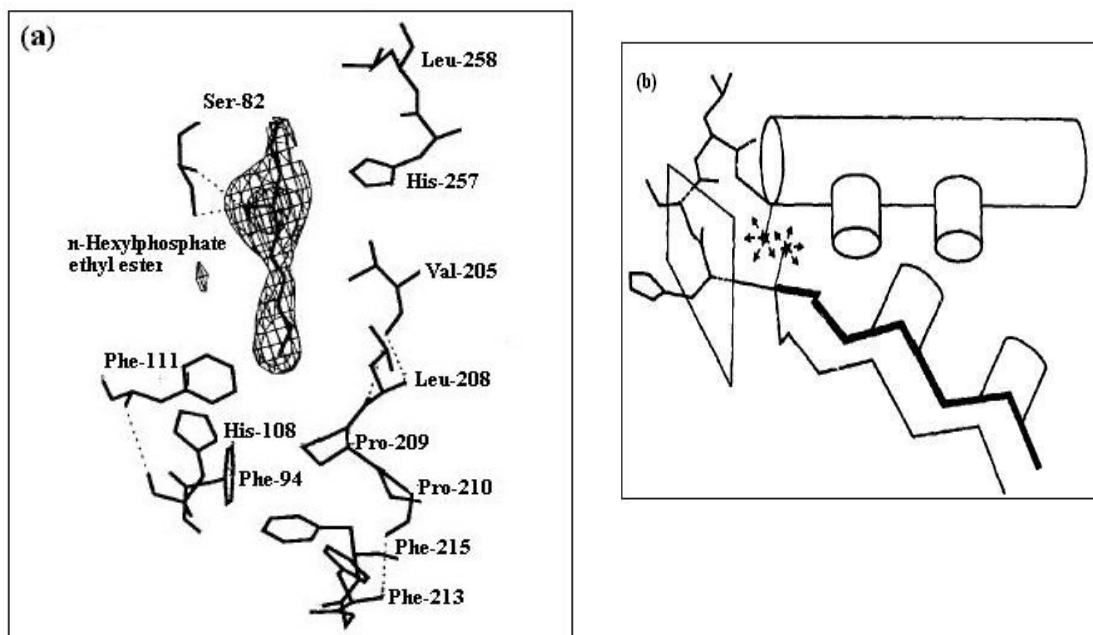


**Fig. 1.3** (a) The hydrogen-bonding network in the active site of the *Rhizomucor miehei* lipase. The crystal structure (at 3 Å resolution) of a complex of RML lipase with n-hexylphosphonate ethyl ester in which the enzyme's active site is exposed by the movement of the helical lid. The catalytic Ser-144 is immediately beneath the phosphorus atom of the inhibitor. His-257 is clearly displaced towards the ethyl oxygen consistent with the proposed orientation of the substrate and the mechanism of hydrolysis. Hydrogen bond contacts between O<sub>γ</sub> atom of Ser-82 and its amide NH are indicated (adopted from Brzozowski *et al.*, 1991)

(b) A schematic drawing showing the packing within the β-εSer-α-motif. The helix and strand pack against each other with four amino acids (tinted) forming the interface. The residues nearer the turn are in closer contact and therefore their side chains are restricted to those of smaller hydrophobic amino acids. The plane of the central peptide of the turn is perpendicular to the axis of the motif, which forces the catalytic Ser to adopt a strained ε conformation. The two stars show the positions that β-carbons of amino acids other than Gly would occupy if the two invariant Gly residues of the GX<sub>1</sub>SX<sub>2</sub>G pentapeptide were mutated (adopted from Derewenda *et al.*, 1993).

and Asp-203, which is buried under a single 17 residue long surface loop (82-96 residue) called lid, that occludes the active site in the native structure (Derewenda *et al.*, 1992). Brzozowski *et al.*, (1991) studying an atomic model of inhibitor-RML complex showed that a direct covalent bond formation between nucleophilic O<sub>γ</sub> of Ser-144 and substrate is formed (Fig. 1.3a). The sequence as Gly<sup>142</sup>-His<sup>143</sup>-Ser<sup>144</sup>-Leu<sup>145</sup>-Gly<sup>146</sup>, a pentapeptide corresponds to a tight turn between the fourth strand of the central β-sheet and a buried α-helix (Fig.1.3b). The catalytically active Ser found in the middle of the turn is in the rarely found ε-conformation ( $\phi=62$ ;  $\psi=121^\circ$ ). This structural motif consisting of a β-strand followed by a tight turn containing the active Ser and an α-helix was called as β-εSer-α-motif (Fig.1.3b; Derewenda *et al.*, 1993). Carbonyl oxygen of the substrate may be stabilized by the interaction of NH group of Leu-145 and Gly-146 and the hydroxyl of Ser-82 through hydrogen bonding and this Ser-82 possesses favorable conformation for the oxy-anion interaction (Brzozowski *et al.*, 199).

The inhibition study of lipase by serine protease inhibitors like di-isopropyl phosphofluoridate indicated that a Ser residue might be involved in the catalytic mechanism of the enzyme. All known amino acid sequence of neutral lipases share a consensus pentapeptide GX<sub>1</sub>SX<sub>2</sub>G (where X represents any amino acid, G represents glycine and S represents serine) which contain an essential Ser residue (Derewenda *et al.*, 1993).

### 1.3. Lipase specificity

One of the major advantage of enzymes is their ability to exhibit regioselectivity and stereospecificity in reactions catalyzed by them. Lipases show positional and substrate specificity. Based on positional specificity, lipases can be divided into five different classes (Camp *et al.*, 1998).

Lipases of first group catalyze hydrolysis of fatty acyl tri-glycerides independent of their type or position. Lipases from *Candida cylindraceae*, *Cornybacterium acnes*, *Staphylococcus aureus* come under this group (Camp *et al.*, 1998) which do not exhibit regioselectivity.

Lipases of second group are known as 1,3-specific lipases. Lipases from *Aspergillus niger*, *Rhizopus delemar*, *Rhizomucor miehei*, *Candida rugosa* and *porcine pancreas* catalyze reaction at *sn*-1 and *sn*-3 positions of triacyl glycerides (Macrea, 1985).

The third group of lipases cover lipases with different rates of hydrolysis of mono acyl, diacyl and triacyl glycerides. Some of these lipases are found in the tissues of rats and humans.

The fourth group of lipases catalyze the exchange of specific type of fatty acids. Extracellular lipases from the fungus *Geotrichium candidum* preferentially releases unsaturated *cis*-*n*-9 fatty acid groups (Macrea, 1985).

The fifth group of lipases contains special enzymes that show a faster rate of hydrolysis of fatty acids placed at the *sn*-1 position than the *sn*-3 position or vice versa. This is commonly referred as stereospecificity. Lipoprotein lipases from milk, adipose tissues and post heparin plasma preferentially cleave the ester bond in *sn*-1 and human and rat lingual lipases which react preferentially with the fatty acids at *sn*-3 position (Jensen *et al.*, 1983) are examples of this group.

#### **1.4. Reactions catalyzed by lipases**

The ranges of substrates with which lipases react and also the range of reactions they catalyze are probably far more than any other enzyme studied till date. Lipases catalyze three types of reactions (**Scheme 1.1**).

#### **1.4.1. Hydrolysis**

In aqueous media when there is large excess of water, ester hydrolysis is the dominant reaction.

#### **1.4.2. Esterification**

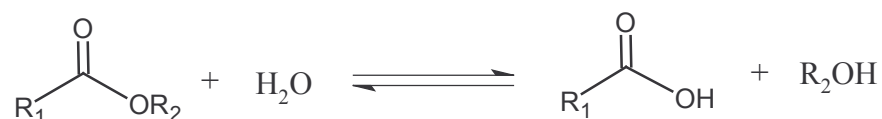
Under low water conditions such as in nearly anhydrous solvents, esterification can be achieved. If the water content of the medium is controlled, relatively better product yields can be obtained.

#### **1.4.3. Transesterification**

The acid moiety of an ester is exchanged with another one. If the acyl donor is a free acid, the reaction is called **acidolysis** and if the acyl donor is an ester, the reaction is called **interesterification**. In **alcoholysis**, the nucleophile alcohol acts as an acyl acceptor.



## 1. Hydrolysis

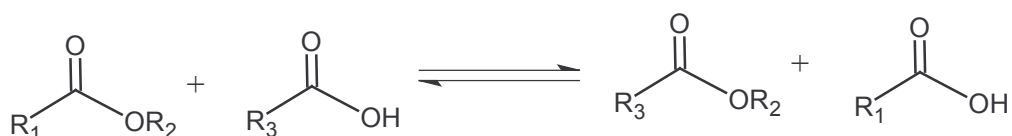


## 2. Esterification

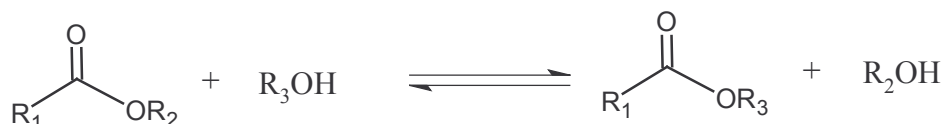


## 3. Transesterification

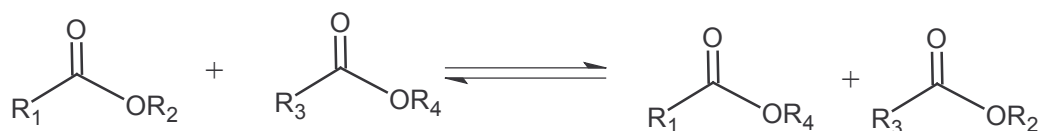
## a. Acidolysis



## b. Alcoholysis



## c. Interesterification



Scheme 1.1. Types of reactions catalyzed by lipases

## 1.5. Catalytic mechanism of lipase mediated esterification in organic media

Lipases show lipid splitting nature and the mechanism is same as that of serine proteases (Pleiss *et al.*, 1998). Catalytic triad in lipases is constituted by Ser, His and Asp / Glu residues. The serine residue in the active center is activated by histidine and aspartic / glutamic acid residues, together forming the catalytic triad. The substrate acid forms a tetrahedral acyl-enzyme intermediate by reaction with the OH group of the catalytic serine residue. The resulting excess negative charge that develops on the carbonyl oxygen atom is stabilized by the oxyanion hole (Brzozwski *et al.*, 1991). The

tetrahedral intermediate I, forms a serinate ester with elimination of water molecule. Subsequent nucleophilic attack of alcohol to the acyl-enzyme intermediate leads to tetrahedral intermediate II. Finally, the product ester is released and the enzyme is free for the next molecule to attack. Grochulski *et al.*, (1993), Cygler *et al.*, (1994) and Schrag and Cygler (1997) proposed a mechanism for the ester formation which is depicted in **Scheme 1.2**.

#### Step I. Acylation step

Initially serine hydroxyl group forms a tetrahedral intermediate complex I with acyl donor, the negative charge that is formed in the tetrahedral intermediate is stabilized by hydrogen bonding with the acid given which are responsible for the oxyanion hole formation.

#### Step II. Formation of acyl enzyme complex

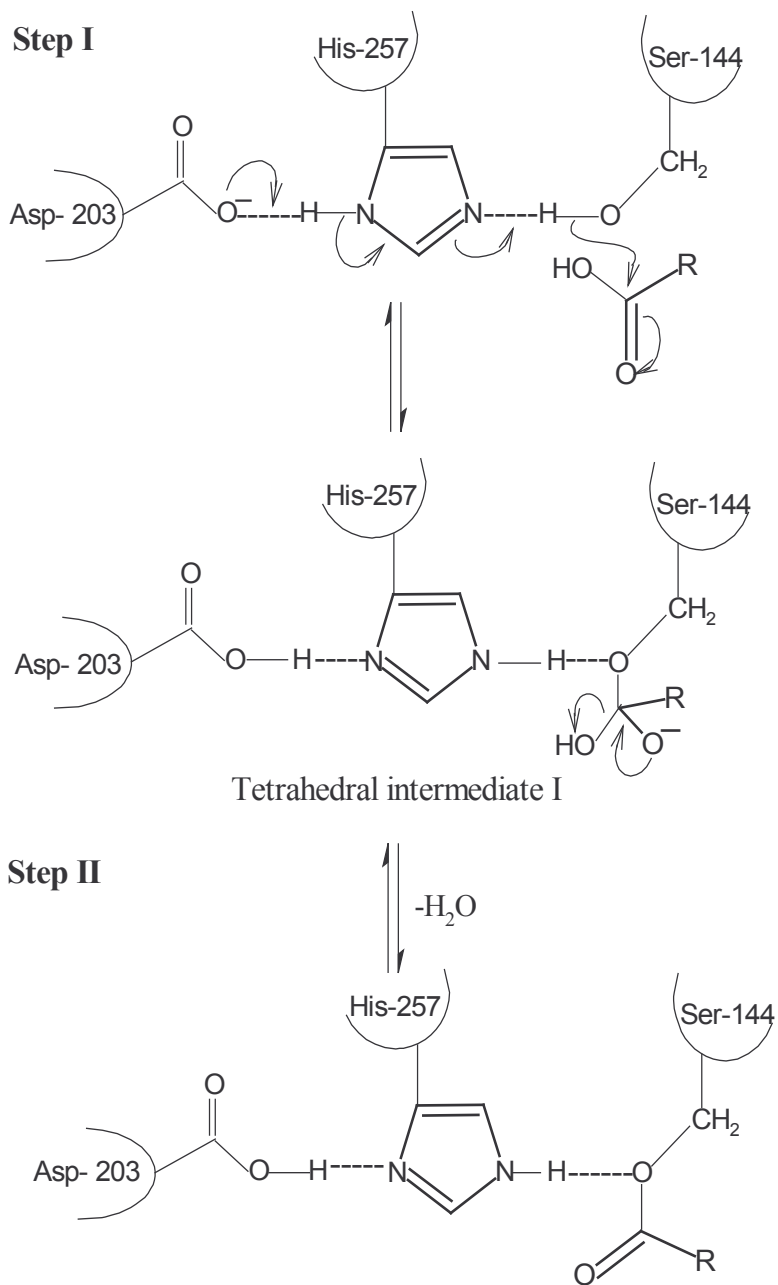
After the formation of the tetrahedral intermediate I, an acyl-enzyme complex is formed through covalent bond with Ser residue by losing one molecule of water.

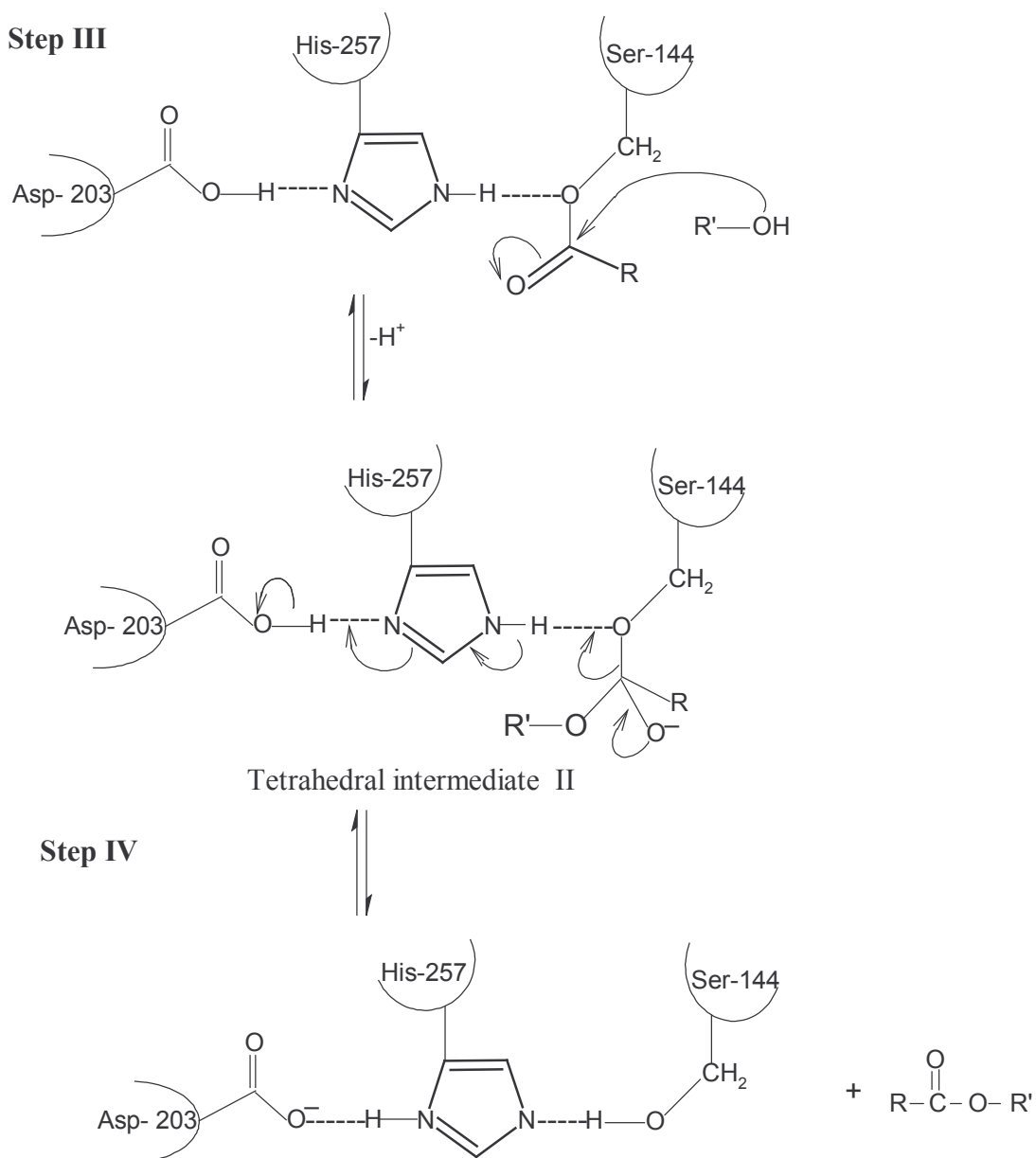
#### Step III. Nucleophilic attack by alcohol (Carbohydrate)

Nucleophile alcohol, attacks the carbonyl center of the tetrahedral intermediate forming a tetrahedral complex II forming an enzyme-acid-alcohol complex.

#### Step IV. Release of ester (L-amino acyl ester of carbohydrate)

Finally, the ester is released and the enzyme will be ready for the next molecule to attack.





**Scheme 1.2. Catalytic mechanism of lipase mediated esterification in organic media**

### 1.6. Advantages of lipase catalysis over chemical catalysis

Lipases are found to be advantageous over chemical synthesis. The following are the advantages of using lipases as biocatalysts.

1. Stereospecificity towards substrate.
2. Milder reaction conditions under which the synthetic process can be operated.
3. Non-generation of by-products associated with the use of several chemical

procedures.

4. Improved product-yield and better product quality.
5. Exploitation of the stereo and regio-specificities shown by lipases to produce high value chiral synthons.
6. Success in immobilization techniques that have enabled the reuse of lipases leading to economically viable processes.
7. Good conversion yields.
8. Lipases are highly thermostable, they exhibit activity even at 100 °C.
9. Use of non-polar solvents which impart stability to lipase rather than in water, renders insolubility of the enzyme, solubility of substrates and products in organic solvents resulting in homogenous reaction conditions, easy product workout procedures and easy removal of water formed as a by-product.

Table 1.2 lists some of the commercially important flavor, fragrance, surfactant and sweetener esters prepared through lipase mediated catalysis.



Table 1.2. Lists some of the commercially important esters synthesized by lipase mediated catalysis

Source of lipase	Name of the compound	the Applications	References
<b>1. Flavour esters</b>			
<i>Pseudomonas fluorescense</i>	Isoamyl acetate	Banana flavour	Takahashi <i>et al.</i> , 1988
<i>Candida antarctica</i>			Langrand <i>et al.</i> , 1990
<i>Rhizomucor miehei</i>			Rizzi <i>et al.</i> , 1992; Chulalaksananukul <i>et al.</i> , 1993; Razafindralambo <i>et al.</i> , 1994; Divakar <i>et al.</i> , 1999
<i>Rhizomucor miehei</i>			Harikrishna <i>et al.</i> , 2000; 2001
<i>Candida cylindraceae</i> , PPL,			Welsh <i>et al.</i> , 1990,
<i>Aspergillus niger</i>			Gubicza <i>et al.</i> , 2000
Novozyme 435			Afife Guvenc <i>et al.</i> , 2002
<i>Rhizomucor miehei</i> , <i>Candida antarctica</i>			Romero <i>et al.</i> , 2005a; 2005b; Kanwar and Goswami, 2002
<i>Pseudomonas pseudomallei</i>			Ngrek 1947

---

Porcine liver lipase				Kumar <i>et al.</i> , 2005
<i>Candida antarctica</i>	Isoamyl butyrate	Banana flavour		Langrand <i>et al.</i> , 1988; Langrand <i>et al.</i> , 1990
<i>Rhizomucor miehei</i>				Mestri and Pai, 1994b
<i>Candida cylindraceae</i> , PPL,				Welsh and Williams 1990
<i>Aspergillus niger</i>				
<i>Candida antarctica</i> ,				Gubicza <i>et al.</i> , 2000
<i>Geotrichum sp.</i> and <i>Rhizopus sp.</i>				Macedo <i>et al.</i> , 2004
<i>Candida antarctica</i>	Isoamyl propionate	Banana flavour		Langrand <i>et al.</i> , 1988
<i>Rhizomucor miehei</i>	Isoamyl isovalerate	Apple flavour		Chowdary <i>et al.</i> , 2002
<i>Rhizomucor miehei</i>	Isobutyl isobutyrate	Pineapple flavour		Hamsaveni <i>et al.</i> , 2001
<i>Rhizomucor miehei</i>	Methyl propionate	Fruity flavour		Perraud and Laboret, 1989
<i>Candida cylindracea</i>	Ethyl butyrate	Pineapple flavour		Gubicza <i>et al.</i> , 2000 Gillies <i>et al.</i> , 1987

---



---

<i>Candida cylindracea</i> , PPL and <i>Aspergillus niger</i>	Butyl isobutyrate	Sweet	fruity	Yadav and Lathi, 2003
<i>Rhizomucor miehei</i> , PPL	Protocatechuic aldehyde	odor		Welsh and Williams, 1990
<i>Staphylococcus warneri</i>	Short chain alcohol	Fruity odor		Divakar, 2003
<i>Staphylococcus xylosum</i>	esters of C <sub>2</sub> -C <sub>18</sub> acids			Talon <i>et al.</i> , 1996.
<i>Candida antarctica</i>	Short chain fatty acid esters	Fruity odor		Mestri and Pai, 1994a
	Long chain alcoholic esters of lactic acids	Flavor		Macedo <i>et al.</i> , 2003; Xu <i>et al.</i> , 2002
Novozym 435 <i>Rhizomucor miehei</i>				From <i>et al.</i> , 1997; Torres and Otero 1999;
<i>Candida rugosa</i>	Methyl benzoate	Exotic fruity		Parida and Dordick, 1991
		and berries		Bousquet <i>et al.</i> , 1999
		flavor		Leszczak and Minh, 1998

---

---

Novozym 435	Tetrahydrofurfuryl butyrate	Fruity favor	Yadav and Devi, 2004
<i>Rhizomucor miehei</i>	Cis-3-hexen-1-yl acetate	Fruity odor	Chiang <i>et al.</i> , 2003

---

**2. Fragrance esters**

<i>Rhizomucor miehei</i> ,	Tolyl esters	Honey note	Burdock, 1994
PPL			Suresh Babu <i>et al.</i> , 2002; Manohar and Divakar, 2002
<i>Candida cylindracea</i> ,	Anthranilic acid esters	Flowery odor	Kittleson and Pantaleone, 1994
PPL	of C <sub>2</sub> – C <sub>18</sub> alcohols.	of jasmine	Suresh Babu and Divakar, 2001 Manohar and Divakar, 2004a
PPL	4-t-Butylcyclohexyl acetate	Woody and intense flowery notes	Manohar and Divakar, 2004b

---

---

<i>Rhizomucor miehei</i> ,	Geranyl methacrylate	Floral fruity	Athawale <i>et al.</i> , 2002
PPL, <i>Pseudomonas cepacia</i>		odor	
<i>Candida antarctica</i> SP435	Citronellyl acetate	Fruity rose	Claon and Akoh, 1994b
<i>Pseudomonas fragi</i>	Citronellyl propionate	odor	Mishio <i>et al.</i> , 1987
	Citronellyl valerate		Marlot <i>et al.</i> , 1985
	Geranyl butyrate		
	Geranyl propionate		
	Geranyl valerate		
<i>Candida rugosa</i>	Farnesol butyrate	Fruity odor	Akoh <i>et al.</i> , 1992; Shieh <i>et al.</i> , 1996
	Farnesol propionate		
	Farnesol valerate		
	Phytol butyrate		
	Phytol propionate		
	Phytol valerate		

---

Novozym SP	Citronellyl laurate	Fruity,	Yadav and Lathi, 2004
<i>Rhizomucor miehei</i>	$\alpha$ -Terpinyl acetate	characteristic	Rao and Divakar, 2002
	$\alpha$ -Terpinyl propionate	lavendar and	
		bergamot-like	
		fragrance	
<i>Rhizomucor miehei</i>	$\alpha$ -Terpinyl esters of		Rao and Divakar, 2001
<i>Aspergillus niger, Rhizopus</i>	fatty acids		Iwai <i>et al.</i> , 1980
<i>delemar, Geotrichum candidum,</i>	$\alpha$ -Terpinyl esters of		Claon and Akoh, 1994a
<i>Pencillium cyclopium</i>	short chain acids		
	Terpinyl esters of		
	triglycerols		
<b>3. Surfactant esters</b>			
Novozym 435	Oleic acid esters of	Surfactants	Dorm <i>et al.</i> , 2004
	short chain alcohols		
<i>Rhizomucor miehei</i>	Butyl oleate	Surfactants	Knez <i>et al.</i> , 1990

---

<i>Rhizomucor miehei</i> , PPL	2-O- Alkanoyl lactic Surfactants	Kiran and Divakar, 2001a; Kiran <i>et al.</i> , 1998
	acid esters of C <sub>2</sub> -C <sub>18</sub>	
	alcohols	

---

**4. Surfactant and sweetener esters**

---

<i>Mucor javanicus</i> , <i>Pseudomonas cepacia</i> , Subtilisin,	N-Acetyl- L-leucyl -D-glucose	Surfactants	Maruyama <i>et al.</i> , 2002
	N-Acetyl-L-methionyl -D -glucose		
	N-Acetyl- L-tyrosinyl -D -glucose		
	N-Acetyl-L-tryptophanyl-D -glucose		
Subtilisin	N-Acetyl-L-phenylalanyl-D- glucose	Surfactants	Maruyama <i>et al.</i> , 2002;
	N-Acetyl-L-phenylalanyl-D -galactose		Riva <i>et al.</i> , 1988
	N-Acetyl-L-phenylalanyl-fructose		
	N-Acetyl-L-phenylalanyl - mannose		
	N-Acetyl-L-phenylalanyl - lactose		
	N-t-Boc-L-phenylalanyl - glucose		

---

---

	N-Acetyl-L-methionyl – methyl- $\beta$ -galactopyranoside		
Optimase M-440, Proleather, APG 380	N-t-Boc-L-phenylalanyl – galactose N-t-Boc-L-phenylalanyl – fructose N-t-Boc-L-phenylalanyl –methyl $\alpha$ -D- glucopyranoside	Surfactants	Park <i>et al.</i> , 1996
Optimase M-440	N-t-Boc-L-phenylalanyl – sorbitol N-t-Boc-L-phenylalanyl – sucrose N-t-Boc-L-phenylalanyl – cellobiose N-t-Boc-L-phenylalanyl – raffinose N-t-Boc-L-phenylalanyl – trehalose N-t-Boc-L-phenylalanyl – maltose N-t-Boc-L-phenylalanyl – lactose	Surfactants	Surfactants

---

---

Optimase M-440	N-t-Boc-L-leucyl – sucrose	Surfactants	Jeon <i>et al.</i> , 2001
	N-t-Boc-L-tyrosinyl – sucrose		
	N-t-Boc-L-methionyl – sucrose		
	N-t-Boc-L-aspartyl – sucrose		
	Di-N-t-Boc-L-lysyl – sucrose		
	N-t-Boc-L-phenylalanyl – xylitol		
	N-t-Boc-L-phenylalanyl – arabitol		
	N-t-Boc-L-phenylalanyl – mannitol		
	N-t-Boc-L-phenylalanyl–N-acetyl-D-glucosamine		
<i>Rhizomucor miehei</i> , PPL,	L-Alanyl, L-valyl, L-leucyl and L-isoleucyl	Surfactants,	Vijayakumar <i>et al.</i> , 2004;
<i>Candida rugosa</i>	ester of carbohydrates	Sweeteners	Somashekar and Divakar 2007

---

---

L-Prolyl, L-phenylalanyl, L-tryptophanyl and L-histidyl esters of carbohydrates 1- <i>O</i> -ester, 2- <i>O</i> -ester, 3- <i>O</i> -ester, 4- <i>O</i> - ester, 5- <i>O</i> -ester, 6- <i>O</i> -ester, 6'- <i>O</i> -ester, 2,5-di- <i>O</i> -ester, 3,5-di- <i>O</i> -ester, 2, 6-di- <i>O</i> -ester, 3, 6-di- <i>O</i> -ester, 6,6'-di- <i>O</i> -ester	Lohith <i>et al.</i> , 2003; Lohith and Divakar, 2005 ; 2007
Subtilisin <i>Rhodotorula lactosa</i>	Riva <i>et al.</i> , 1988 Suzuki <i>et al.</i> , 1991
N-Acetyl-L-alanyl -methyl- $\beta$ -D- galactopyranoside 2- <i>O</i> -ester, 3- <i>O</i> -ester, 4- <i>O</i> -ester, 6- <i>O</i> - ester	Surfactants, Sweeteners

---



---

	6- <i>O</i> -Butyl glucose	Surfactants	Therisod and Klibanov,
PPL			
Subtilisin	6- <i>O</i> - Acetyl glucose		1986
	6- <i>O</i> - Capryloyl glucose		Kirk <i>et al.</i> , 1992
	6- <i>O</i> - Acetyl galactose		Zaks and Dodds, 1997
	6- <i>O</i> - Acetyl maltose		Klibanov, 1986
	6- <i>O</i> - Acetyl fructose		Dordick, 1989
	1- <i>O</i> - Acetyl fructose		Schlotterbeck <i>et al.</i> , 1993
			Boyer <i>et al.</i> , 2001.
Lipozyme, <i>Rhizomucor miehei</i>	Fructose oleate	Surfactant	Khaled <i>et al.</i> , 1991
<i>Candida antarctica</i>	Fatty acid esters of glycosides		Adlerhorst <i>et al.</i> , 1990
<i>Candida rugosa</i>	Butyl oleate		Zaidi <i>et al.</i> , 2002
	Oleyl butyrate		
	Oleyl oleate		

---

---

<i>Humicola lanuginosa</i>	6- <i>O</i> -Lauroyl sucrose	Surfactants	Ferrer <i>et al.</i> , 1999;
<i>Candida antarctica</i> B	6- <i>O</i> -Lauroyl glucose		Ferrer <i>et al.</i> , 2005
	6- <i>O</i> -Lauroyl maltose		
	6- <i>O</i> -Palmitoyl maltose		
	1,6-di- <i>O</i> -Lauroyl sucrose		
	6,6-di- <i>O</i> -Lauroyl sucrose		
<i>Candida antarctica</i>	6'- <i>O</i> -Palmitoyl maltose		
	$\beta$ -Methylglucoside methacrylate / acrylate	Surfactants	Kim <i>et al.</i> , 2004

---

## 1.7. Important parameters regulating the lipase activity in organic solvents

### 1.7.1. Nature of substrate

Lipases display various degrees of selectivities towards the substrates with which they interact (Bloomer, 1992). Steric hindrance (branching, unsaturation and chain length) and electronic effects of the substrates are the two major forces that determine selectivity (Bevinakatti and Banerjee, 1988). In esterification reactions, many lipases display high selectivities on long and medium chain fatty acids than the short chain and branched ones (Alhir *et al.*, 1990). Most lipases display selectivities towards carboxylic acids. *Geotrichum candidum* lipase reacts only with fatty acids containing a *cis* bond at the 9th position (Schrag *et al.*, 1996). Generally alcohols like ethanol and geraniol have been reported to be inhibitory in esterification and transesterification reactions (Chulalaksananukul *et al.*, 1990 and 1992; Miller *et al.*, 1988). Molar ratio of the substrates plays an important role in esterification, which can be improved by increasing either alcohol or acid but in most of the cases, the alcohols may be inhibitory and acids may cause acidification of microaqueous interface resulting in inactivation of lipases (Dorm *et al.*, 2004; Guvenc *et al.*, 2002; Zaidi *et al.*, 2002). It is difficult to generalize the effect of chain length on esterification, because it depends on the lipase preparation and the specificity of the enzymes. Esterification increased with increase in chain length when the reaction was catalyzed by lipases from *Staphylococcus warneri* and *Staphylococcus xylosus* (Talon *et al.*, 1996). In case of Lipolase 100T, esterification decreased with increase in chain length and found to be independent of chain length when esterification was catalysed with Novozyme 435 (Kumar *et al.*, 2005). *Rhizomucor miehei* lipase exhibited fatty acid chain length optima towards C<sub>8</sub> and C<sub>12</sub> in an esterification reaction with glycerol and its diol analogues. However, *Candida antartica* B lipase exhibited fatty acid chain length optima only towards C<sub>8</sub>. Kirk *et al.*, (1992)

showed that *Candida antarctica* B lipase is not very selective in esterification reaction with *n*-octanol in hexane. Zhang *et al.*, (2005) found high specificity of pancreatic lipase towards butyric and valeric acids and a significantly lower esterification rate with lower (propionic) and higher (C<sub>6</sub>-C<sub>14</sub>) carbon number acids. The specificity increased in longer chain fatty acids (palmitic and stearic), but remained significantly lower than that observed for the best-suited substrates. For the same chain length, unsaturation leads to decrease in specificity as demonstrated for oleic acid compared to stearic acid (Zhang *et al.*, 2005).

Use of acetic acid as an acyl donor was attempted with little or no success (Takahashi *et al.*, 1988) in the preparation of acetates. Compared to its higher homologues (propionates, butyrates), acetic acid is a potent inhibitor (Segel, 1993) by preferentially reacting with the serine residue at the active site of lipase (Huang *et al.*, 1998). Iwai *et al.*, (1980) did not observe any reaction between acetic acid and geraniol using lipases from four different microorganisms. Langrand *et al.*, (1988) showed that acetic acid esters were difficult to synthesize in high yields due to lipase inactivation by acid. Although, few researchers have focused their attention on transesterification to obtain high yields of acetates (Langrand *et al.*, 1990; Rizzi *et al.*, 1992; Chulalaksananukul *et al.*, 1993), reports on maximizing acetate production by direct esterification are scanty. Also, low molecular weight substrates are more water-soluble and as such may react differently than do high molecular weight (less water soluble) substrates in non-aqueous systems.

In most cases, lipase showed enantio preference towards (*R*)-enantiomer than (*S*)-enantiomer (Cardenas *et al.*, 2001). There were also reports that lipase from *Fusarium oxysporum*, *Ophiostoma sulphureoohraceum*, *Staphylococcus halstedii* and *Fusarium*

*poae* displayed preference for the (*S*)-stereomer in the acylation of (*R*) and (*S*)-glycidol (Cardenas *et al.*, 2001).

### 1.7.2. Nature of solvent

Enzymes are known to be active and stable at physiological pH. Hence information regarding the rate of reaction, kinetics and catalytic mechanism of the enzyme has been derived from investigations conducted in aqueous buffer solutions (Dixon and Webb, 1979; Welsh and Williams, 1990). However, when enzymes are directly introduced in organic solvents, they display incredible changes in their properties (Klibanov, 1986). Organic solvents employed influence reaction rate, maximum velocity ( $V_{max}$ ) or specific activity ( $K_{cat}$ ), substrate affinity ( $K_m$ ), specificity constants ( $K_{cat}/K_m$ ) (Zaks and Klibanov, 1986), enantio-selectivity (Sakurai *et al.*, 1988), lipase stability (Kung and Rhee, 1989) and stereo and regio-selectivities (Parida and Dordick, 1991 and 1993; Nakamura *et al.*, 1991; Rubio *et al.*, 1991). Several efforts have also been made to rectify the kinetic affinity parameters for substrate-solvent interactions (Van Tol *et al.*, 1992; Reimann *et al.*, 1994). The enzyme activity in different solvents could be due to variable degree of enzyme hydration imposed by the solvents and not to their direct effect on the enzyme or substrates. Generally use of organic solvents in enzyme catalysed synthesis exhibit more advantages than in aqueous media (Klibanov, 1986).

1. Non polar / hydrophobic substrates can be employed for the reaction.
2. Enhances the reaction rate.
3. Shifting of thermodynamic equilibria towards synthesis of ester by maintaining

expensive and difficult.

5. Since enzymes are insoluble in organic solvents, can be easily recovered from the reaction mixture by simple filtration.
6. Water dependent reactions such as hydrolysis and racemization can be avoided.
7. Inhibition of enzymes by hydrophobic substrates or products is minimized due to dispersion in the organic solvents, which minimizes substrate concentration at enzyme surface.
8. Microbial contamination resulting in enzyme inhibition as well as degradation/  
minimization of desired products can be avoided.

*Introduction*

Investigations on quantification of solvent effects on enzyme catalysis were carried out (Brink and Tramper, 1985; Laane *et al.*, 1987). The efficiency of lipase was found to increase with log P value of solvent. Brink and Tramper (1985) tried to explain the influence of many water immiscible solvents on biocatalysis by employing the Hildebrand parameter,  $\delta$ , as a measure of solvent polarity. They concluded that enhanced reaction rates could be expected when the polarity of the organic solvents was low ( $\delta \approx 8$ ) and its molecular weight  $> 150$ . But later, it was demonstrated that  $\delta$  was a poor measure of solvent polarity. Laane *et al.*, (1987) quantified solvent polarity on the basis of log P values. The efficiency of lipase was found to increase with log P value of solvent. The log P value of a solvent could be defined as the logarithmic value of the partition coefficient of the solvent in *n*-octanol/water two-phase system. Generally, biocatalysis is low in solvents of log P  $< 2$ , is moderate in solvents with a log P value between 2 and 4 and high in non-polar solvents of log P  $> 4$ . *Rhizomucor miehei* lipase was shown to follow these rules when esterification reactions were conducted in different solvents (Laane *et al.*, 1987). The conversion of lipase in solvent improved

from tetrahydrofuran ( $\log P = 0.49$ ), toluene ( $\log P = 2.5$ ), hexane ( $\log P = 3.5$ ), *n*-heptane ( $\log P = 4.0$ ) and *n*-nonane ( $\log P = 5.1$ ). In general, enzymes are more stable when suspended in non-polar solvents that have low solubility for water than in polar solvents (Acros *et al.*, 2001). In presence of hydrophilic solvents ( $\log P < 2$ ) lipozyme showed no esterification. Hence, polar solvents may remove the essential water from the enzyme and disrupt the active confirmation (Gargouri *et al.*, 2002; Adachi and Kobayashi, 2005). They also probably form hydrogen bonding between solvent molecule and acids which are present on the surface of the enzyme. Solvents whose  $\log P$  values were  $>2$ , dissolve to a lesser degree in water, leaving the enzyme suitably hydrated in its active conformation and so were able to support product synthesis (Soo *et al.*, 2003). But a lipase which exhibits increasing activity with increased DMSO content (a polar solvent), has also been isolated (Bloomer, 1992). Effect of  $\log P$  values of organic solvents was studied by correlating with  $K_{cat}$  and  $K_m$ .  $K_{cat}$  showed strong correlation with  $\log P$  but not  $K_m$ .  $K_{cat}$  was not affected by different solvent composition with constant  $\log P$  whereas  $K_m$  was reported to change remarkably (Hirakawa *et al.*, 2005). Most of the lipases readily under go inactivation in presence of polar solvents, which is very much essential to dissolve certain substrates like sugars. Hence, the idea of solvent mixtures of non polar solvents with small amount of polar solvents was also employed in lipase catalysis (Ferrer *et al.*, 1999). Ongino *et al.*, 1999 screened solvent tolerant microorganism *Psuedomonas aeroginosa* which secretes LST-03 lipase which is much more stable in the presence of organic solvents than in its absence. While it is generally accepted that non-polar solvents are better than polar ones for lipase catalyzed esterification reactions, a clear consensus is yet to be reached regarding the issue of solvent effects on enzyme catalysis in general.

### 1.7.3 Effect of salt

Catalytic activity of the enzyme is based on protein ionization which is pH depend. Any change in pH is detrimental to 3D-structure of protein which in turn is detrimental to enzyme activity. It is well known that enzyme hydration play a crucial role in minimizing solvent-induced conformational rigidity (Patridge *et al.*, 1998) which is one of the cause for reducing catalytic activity in non-aqueous media (Klibanov, 1986). Along with the relevant factors such as degree of hydration and nature of solvent, ionization state of the enzyme also play a key role in overall reactions of the active conformation of the enzyme (Zacharis *et al.*, 1997). Use of buffers in the reaction mixture or lyophilizing enzyme from buffers of known pH can reset enzyme ionization state and ensure pH memory. (Valivety *et al.*, 1990; Xu and Klibanov, 1996). Quiros (2002) tuned *Candida antarctica* lipase B with solid state organic buffers like  $\text{ET}_3\text{N}$ , 3-[(1,1-dimethyl-2-hydroxyethyl)-amino]-2-hydroxypropane sulfonic acid and 3-[cyclohexyl-amino]-2-hydroxy-1-propane sulfonic acid and showed improved enantioselectivity and catalytic activity. Xu and Klibanov (1996) found the catalytic activity of substilisin Carlsberg lyophilized in buffers like phenylborate and *p*-toulene sulfonic acid and their corresponding sodium salt improved catalytic activity by 100 folds than without buffers in organic media. Fontes *et al.*, (2003) found that to achieve full activation of substilisin, the catalytic triad should be negatively charged which was achieved by replacing  $\text{H}^+$  by a counter  $\text{Na}^+$  adding salt hydrates of hydrogen phosphate, pyrophosphate and acetate. Addition of simple inorganic salts like KCl prior to lyophilization has dramatically enhanced  $V_{max}/K_m$  for several hydrolases in non-aqueous media (Lindsay *et al.*, 2002). This process was optimized by using numerous combinations of salt and lyophilization period (Ru *et al.*, 1999, 2000 and 2001).



Addition of salt hydrates to the reaction mixture accelerates the transfer of water between the salt hydrates pair and the enzyme by disturbing the ionic character of the enzyme microenvironment and thereby influencing catalytic activity (Fontes *et al.*, 2002)

Introduction

At least over a certain range of temperature, the reaction catalyzed by enzymes behave like ordinary chemical reactions - as the temperature is increased, the rate increases. The same will begin to suffer thermal inactivation at higher temperatures. The actual temperature at which an enzyme passes through its maximum activity as well as stability is also influenced by environmental factors such as purity of enzyme, substrate, presence of activators or inhibitors, pH, solvent and presence of metal ions. The thermostability of lipases varies considerably according to their origin: animal and plant lipase are less thermo stable than microbial extracellular lipase. Zhu *et al.*, (2001) reported that thermal stability of a lipase is obviously related to its structure. At least in some cases, thermal denaturation appears to occur through intermediate states of unfolding of the polypeptide (Zhu *et al.*, 2001). Of them, the two major ones are the nature of the organic medium employed and water content in the microenvironment of the enzyme (Halling, 1994). There are a few reports on the thermostability of lipases in aqueous media. Lipase from *Pseudomonas fluorescens* 33 was found to retain 10-20 % higher activity in the presence of casein and  $\text{Ca}^{2+}$  at higher temperatures (60 °C to 90 °C) at only 10 min of incubation (Kumura *et al.*, 1993). Novozym SP 435 is thermally stable at 60 °C (Yadav and Lathi, 2004). Thermostabilities of some serine esterases like chymotrypsin and lipase from *Candida rugosa* and *Rhizomucor miehei* have been studied as a function of hydration of the enzymes using differential scanning calorimetry (Turner *et al.*, 1995). It was found that the denaturation temperature ( $T_m$ )

was 30 °C to 50 °C higher in anhydrous environments than in aqueous solutions. Volkin *et al.*, (1991) reported that enzymes are more thermostable in hydrophobic solvents rather than in hydrophilic solvents. In hydrophilic solvents, stripping of water from the enzyme leads to denaturation. Porcine pancreas lipase was reported to retain higher esterification activity in dry organic environment (2 M heptanol solution in tributyrin) at a temperature of 100 °C when a low concentration of water (0.015 %) was maintained in the reaction system (Zaks and Klivanov, 1985). Half-life for the enzyme was found to be more than 12 h at 100 °C. However, when concentration of water was increased to 3 %, loss of activity was almost instantaneous (half life = 2 min). Porcine pancreas lipase (PPL) in non-aqueous media showed that longer periods of incubation of PPL at especially 80 °C did not affect the active conformation of PPL even after incubation for a period upto 10 days (Kiran *et al.*, 2001b) at very low water content. Immobilization of the enzyme and addition of salt hydrates are known to enhance the thermostability of lipases in organic media (Kvittengen *et al.*, 1992; Halling, 1992). Iso *et al.*, (2001) conducted experiments at a temperature range from 40 °C to 70 °C on both free and immobilised *Pseudomonas fluorescens* lipase where free lipase showed highest conversion at 60 °C and decreased activity at 70 °C. However, immobilized lipase showed increased activity at 70 °C and can be reused several times without much loss of activity. Immobilization shifts the temperature optima from 35 °C of the free lipase to 40 °C to 45 °C. It could be attributed to a low restriction in the diffusion of the substrates and products at higher temperature as well improved resistance of protein to thermal denaturation (Deng *et al.*, 2004). Storage stability of native and covalently immobilized lipase B from *Candida antarctica* was studied by Arrayo *et al.*, 1999 under wet conditions at 50 °C who found that immobilized lipases are thermally more stable than

native ones with half life values ranging from 0.5 to 14 h. Under the same conditions, native *Candida rugosa* lipase B is more stable than *Candida antartica* lipase as the former protein structure contains three disulfide bonds (Cys-22 to Cys-64, Cys-216 to Cys-258 and Cys-293 to Cys-311) and the latter contains only two (Cys-60 to Cys-97 and Cys-268 to Cys-277, Arroyo *et al.*, 1999). Thermal stability can also be improved by preparing a surfactant-lipase complex (Goto *et al.*, 2005; Maruyama *et al.*, 2002; Wu *et al.*, 2002). It is a common practice now to carry out lipase catalyzed esterification reactions at around 80 °C to 90 °C (Trani *et al.*, 1991). Noel and Combes (2003) conducted series of experiments at different temperatures to study the thermal effect of RML and concluded that thermal deactivation occurs due to the aggregation of enzymes of denatured proteins rather than protein unfolding.

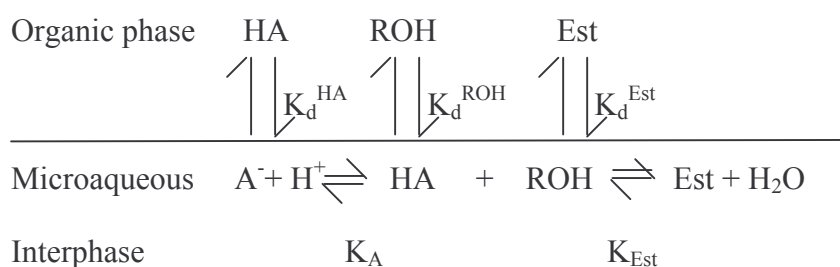
#### 3.1.1. Significance of water in lipase catalysis

Water plays a significant role in the reversible reaction catalyzed by lipase, involving hydrolysis and esterification (Hahn-Hägardal, 1986; Gayot *et al.*, 2003). While a critical amount of water is necessary for maintaining the active conformation of the enzyme, excess water facilitates hydrolysis (Halling, 1989 and 1994; Zaks and Klibanov, 1985 and 1988; Valivety *et al.*, 1993; Cameron *et al.*, 2002). The bound water structure is very essential in stabilizing the 3D-conformation of a lipase in non-aqueous media. There are 22 buried water molecules in case of *Rhizomucor miehei* lipase (Brady *et al.*, 1990) where water on the enzyme is bound to charged and polar residues on the surface as a monolayer (Tramper *et al.*, 1992; Kvittengen, 1994; Halling, 1994; Orrenius *et al.*, 1995; Vermue and Tramper, 1995; Zaks and Klibanov, 1988; Gorman and Dordick, 1992). Presence of excess water affects the catalytic activity from both kinetic and thermodynamic points of view (Chulalaksananukul *et al.*, 1990; Marty *et al.*, 1992). The

concentration of water in organic solvents is inversely proportional to the thermostability of lipases (Zaks and Klibanov, 1984). It was shown that for PPL, hydrophobic solvents served better than hydrophilic ones for catalysis (Zaks and Klibanov, 1988; Parida and Dordick, 1991). Substrate concentrations and water activity can control the product distribution. Hence, only monoester of ethylene glycol can be prepared by using either low water activity or employing higher concentrations of alcohols and *vice versa* for the diesters (Chand *et al.*, 1997). Presence of certain amount water (optimum water, 5%) with crude lipase from horse liver, enhanced the reaction rate by three fold and also stereoselectivity by 50% (Gutman and Shapira, 1991). Humeau, *et al.*, (1998) and Osorio *et al.*, (2001) reported that beyond the critical water concentration, esterification decreases because, the size of the water layer which is formed around the enzyme, retards the transfer of acyl donor to the active site of the enzyme. Yadav and Devi (2004) conducted experiments at various speed of agitation and found that there is no effect of speed of agitation (Guvenc *et al.*, 2002) on esterification. The water layer surrounding the enzyme makes the enzyme to be more flexible (act as molecular lubricant) by forming multiple hydrogen bonds and interacting with the organic solvent, causing denaturation. Organic substrates and products with poor solubility in aqueous medium diffuse with difficulty through the intra-particle water layer to the active centers of the enzyme. Thus the activity of the enzyme would depend on water-induced inactivation or partition of components between the bulk solvent and the microenvironment (Yadav and Devi, 2004; Yadav and Lathi, 2004). Almost all lipases are active at low water activity but there is large difference in optimal water activity between the lipases (Ma *et al.*, 2002; Gargouri *et al.*, 2002).

There are several techniques available to monitor the water activity like Karl-

Fischer titration (Halling, 1994) and specialized sensors (Blanco *et al.*, 1989). In esterification reactions, water formed, can be removed from the reaction mixture leading to higher yields (Bloomer *et al.*, 1992), by passing the reaction mixture through a bed of desiccants (Halling, 1990; Gubicza *et al.*, 2000). In a non-polar solvent, excess water adds to the already existing hydration shell on the enzyme constituting the microaqueous inter-phase. Partitioning of the acid, alcohol and product between microaqueous inter-phase and solvent phases plays a significant role in regulating esterification. The solubility of the acid and its dissociation result in a proton build-up at the inter-phase. In lipase catalyzed esterification, the various equilibria involved at the microaqueous inter-phase are shown in **Scheme 1.3** (Aires-Barros *et al.*, 1989).



**Scheme 1.3. Lipase catalyzed esterification at the microaqueous inter-phase**

where HA = acid, ROH = alcohol, Est = ester,  $K_d^{\text{HA}}$ ,  $K_d^{\text{ROH}}$  and  $K_d^{\text{Est}}$  = distribution coefficients of acid, alcohol and ester respectively;  $K_A$  = dissociation constant of acid,  $K_{\text{Est}}$  = equilibrium constant of esterification. Since water is present in micro-quantities and is inaccessible, direct measurement of microaqueous pH is not possible (Valivety *et al.*, 1990b). Attempts have been made to measure the pH in non-aqueous systems by Cambou and Klibanov (1984), who reported the use of an indicator, which changed colour with pH. A reliable method has been developed by Valivety *et al.*, (1990b) in which an hydrophobic indicator (fluorescein ester with 3,7,11- trimethyldodecanol) is used, which remains completely in the organic phase, but responds to pH changes in an

adjacent aqueous phase. Thermodynamic factors operating at the microaqueous enzyme-water-solvent phase in non-polar solvents were also investigated in terms of the water of reaction, partitioning of acid between the microaqueous phase and the organic solvent, dissolution and dissociation of the acid, the resultant number of  $H^+$  present in the microaqueous phase and the extent of esterification (Kiran *et al.*, 2002).

#### 1.7.6. Immobilization

The use of enzymes for analytical, clinical or any synthetic purposes has been limited because of certain disadvantages, such as their instability and lack of availability. Immobilization of enzymes on solid support renders both practical and economic advantages such as easy handling, enzyme recovery at any stage of the reaction and re-utilization. Immobilization of lipase facilitates large area of inter-phase for the reaction to occur. The advantages of immobilizing lipases are repetitive use of a given batch of enzymes, better process control, enhanced stability, enzyme - free products (Welsh and Williams, 1990; Rahman *et al.*, 2005), increased stability of polar substrates, shifting of thermodynamic equilibria to favour ester synthesis over hydrolysis, reduction in water dependent side reactions such as hydrolysis, elimination of microbial contamination and potential to be used directly within a chemical process. After immobilization, there are changes in activity, optimum pH, temperature, affinity towards substrate and stability of the enzyme, which are all depended upon the source of the enzyme as well as type of support material and immobilisation (Klinc *et al.*, 2006; Sato *et al.*, 1999). In presence of organic solvents, immobilized lipase showed enhanced activity (Ye *et al.*, 2005). Ye *et al.*, (2005) reported that at lesser water content, free lipase preparations showed increase in activity than the immobilized lipase preparation. With the increment of the amount of water added, conformational limitation on the enzyme as a result of covalent

bond formation between the enzyme and the matrix, led to increase in activity due to immobilization.

Immobilization of enzymes has been performed by variety of methods which has been broadly classified as physical where interaction between support and enzyme exists, and chemical where covalent bonds exist between support and enzyme. (Bullock 1995; Tischer and Wedekind, 1999). Physical immobilization method includes:

- (i) containment of an enzyme within a membrane reactor,
- (ii) adsorption (physical, ionic) on a water-insoluble matrix,
- (iii) inclusion (or gel entrapment),
- (iv) microencapsulation with a solid membrane,
- (v) microencapsulation with a liquid membrane, and
- (vi) formation of enzymatic Langmuir-Blodgett films

Chemical immobilization methods includes

- (i) covalent attachment to a water-insoluble matrix,
- (ii) crosslinking with use of a multifunctional, low molecular weight reagent, and
- (iii) co-crosslinking with other natural substances, e.g. proteins.

Introduction

In case of non-covalent immobilization, lipases can be adsorbed with very good activity to a weak anion exchange resin (Eigtved, 1989; Ison *et al.*, 1990). For covalent immobilization, usually, support matrices like silica beads are activated with glutaraldehyde (Ulbrich *et al.*, 1991). For non-covalent immobilization, both ionic and hydrophobic interactions between lipase and surface are important (Eigtved, 1989; Ison *et al.*, 1990; Malcata *et al.*, 1990). Polymers such as polyvinyl alcohol (PVA), carboxymethyl cellulose (CMC), poly ethylene oxide (PEO) and CMC-PVA blends can also be used for lipase immobilization (Vecchia *et al.*, 2005). Morphology of film

surfaces analyzed by scanning electron microscopy indicated that lipases were preferentially located on the polymer surface (Crespo *et al.*, 2005). Vecchia *et al.*, (2005) have immobilized 10 different lipases on polyvinyl alcohol, carboxymethyl cellulose and polyvinyl alcohol-carboxymethyl cellulose blends (50:50% m/m) and among them *Mucor javanicus* (MJL) and *Rhizopus oryzae* (ROL) exhibited highest activity. This immobilized enzyme can be reused at least 10 times for a span of 80 days. *Candida antarctica* B (Novozym 435) was immobilized on mesoporous silica with octyl triethoxysilane and it retained its activity even after 15 reaction cycles (Blanco *et al.*, 2004). Porcine pancreatic lipase immobilized on chitosans exhibited nearly twofold higher and that on chitins exhibited four-fold higher activity than that of the free enzyme. (Klnc, 2006). Porcine pancreas lipase and *Candida cylindracea* lipase immobilized on celite and amberlite IRA-938 showed activity at 7-10 °C and at acidic pH than that of free enzyme (Sagiroglu *et al.*, 2004). Calcium carbonate was found to be the most suitable adsorbent when crude *Rhizopus oryzae* lipase was immobilized on different supports and it exhibited long-chain fatty acid specificity (Ghamgui *et al.*, 2004). Lipase from *Pseudomonas cepacia* was gel-entrapped by polycondensation of hydrolyzed tetramethoxy silane and isobutyl trimethoxy silane and it was subjected to repeated use without losing much activity (Noureddini *et al.*, 2005). A major disadvantage of adsorption is the leaching of protein out of the carrier during on line utilization, which can be attributed to the relative weakness of binding forces. In presence of specific components such leaching will lead to loss of catalytic activity and to contamination of reaction products, especially at higher salt concentrations, unless the reaction mixture is hydrophobic and nonpolar in character (Paiva *et al.*, 2000). For covalent immobilization, usually, support matrices like silica beads are activated with glutaraldehyde (Ulbrich *et*



*al.*, 1991). Porcine pancreatic lipase immobilized by covalent attachment to C030F cellulose Nadir filtration membrane (of cut off value  $30 \text{ kg mol}^{-1}$ ) are found to be less active than the lipase adsorbed on a plain nylon surface. This may be due to modification of protein tertiary structure by covalent binding (Manjon *et al.*, 1991).

## **1.8. Diverse applications of lipases in reaction**

### **1.8.1. Esterification in reverse micelles**

Enzymatic reactions in water-in-oil microemulsions with reverse micelles offer many advantages over those in micelles (oil-in-water) or in organic solvents, like solubilization of lipases and both hydrophobic/hydrophilic substrates at higher concentrations, better control over water activity and large interfacial area leading to enhanced reaction rates in a thermodynamically stable single phase (Stamatis *et al.*, 1999). Various reactions like synthesis of flavour esters (Borzeix *et al.*, 1992), macrocyclic lactones (Rees *et al.*, 1995), and resolution of chiral alcohols (Rees and Robinson, 1995) have been attempted in reverse micelles. Krieger *et al.*, (2004) highlighted some of the recent developments on the use of lipases in reverse micelles. There have been some efforts to continuously recover the product as well as enzyme for reuse, which, are the major problems of enzyme catalysis in reverse micelles. Reverse micelles can exchange biocatalyst, water, substrates and products with the bulk organic solvent (Krieger *et al.*, 2004). Murakata *et al.*, (1996) have reported high esterification activity of entrapped lipases on lipophilic substrates. The effective diffusion coefficient of lauric acid varied with the lecithin microemulsion-based organogels (MBGs) composition, while that of butyl alcohol remained constant in the esterification of lauric acid with butyl alcohol catalyzed by *Candida rugosa* lipase (Nagayama *et al.*, 2002). High initial reaction rate was obtained in extremely low water content when the

esterification of oleic acid with octyl alcohol catalyzed by *Rhizopus delemar* lipase was investigated in reverse micellar system of sugar ester DK-F-110 (Naoe *et al.*, 2001). Kinetic studies were carried out to study the esterification of octanoic acid with 1-octanol, catalyzed by *Candida lipolytica* (CL) lipase, in water-in-oil microemulsions formed by water/ bis-(2-ethylhexyl) sulfosuccinate sodium (AOT)/isooctane (Zhou *et al.*, 2001). An esterification reaction of hexanol and hexanoic acid in the cyclohexane/dodecylbenzenesulfonic acid (DBSA)/water microemulsion system using *Candida cylindracea* lipase demonstrated that DBSA itself can act as a kind of acid catalyst (Han and Chu, 2005).

### **1.8.2. Esterification in supercritical carbon dioxide**

Use of super critical carbon dioxide (SCCO<sub>2</sub>) as a solvent and reaction medium is an emerging approach which is growing rapidly in recent years. Super critical carbon dioxide has several advantages over organic solvents: it is cheap, non-toxic, non-flammable, used at near ambient critical temperature (31.1 °C) and moderate critical pressure (Srivastava *et al.*, 2003). The solvent properties of SCCO<sub>2</sub> can be readily modified by adjusting the pressure and temperature, the diffusivity of solutes in CO<sub>2</sub>, which is higher than in organic solvents and easy recovery of CO<sub>2</sub> from the reaction products minimizing the need for costly downstream processing. When CO<sub>2</sub> is used along with organic solvents, it has an additional advantage of being an environment-friendly process (Clifford, 1994).

Fatty acid methyl esters were prepared from methanol and seed oils in flowing CO<sub>2</sub> by employing immobilized *Candida antartica* lipase (Holmberg *et al.*, 1989). Transesterification of soybean oil with glycerol, 1,2-propanediol and methanol by immobilized *Candida antartica* lipase for the synthesis of monoglycerides has also been

reported (Jackson and King, 1997). Isoamyl acetate was synthesized using lipases from *Candida antarctica* and *Rhizomucor miehei* in SCCO<sub>2</sub> where *Rhizomucor miehei* gave 100% esterification with acetic anhydride (Romero *et al.*, 2003). Enantioselective enzymatic hydrolysis of 3-hydroxy-5-phenyl-4-pentenoic acid ethyl ester in a biphasic buffer/SCCO<sub>2</sub>-system was also carried out (Hartmann *et al.*, 2001) where one ester enantiomer was preferably hydrolyzed, the other remained in the supercritical phase. *Candida cylindracea* lipase catalyzed enantioselective esterification of racemic 2-(6-methoxy-2-naphthyl) propionic acid in microaqueous isooctane showed that alcohol concentration influences enzyme performance, not because of stripping water from the enzyme (Wu and Liu, 2000). Production of ethyl esters from ethanol and cod liver oil by an immobilized lipase from *Candida antarctica*, in SCCO<sub>2</sub> has also been described (Gunnlaugsdottir *et al.*, 1998).

### 1.8.3. Esterification in micro oven assisted reactions

Recently, the use of microwave technology in organic synthesis is becoming an increasingly popular method because of short reaction time, enhanced selectivity, purity of the resulting products and enhancement of reaction yields (Loupy *et al.*, 1998). Adlerhorst *et al.*, 1990 synthesized monoesters of glucopyranosides in large scale using lipases from *Candida antarctica* and *Rhizomucor miehei* in dry media. Immobilised lipase from *Pseudomonas* and Novozyme SP 435 showed increased enantioselectivity in transesterification reaction of racemic sec-phenethyl alcohol with isopropenyl acetate with microwave activation than with conventional heating (Carrillo-Munoz *et al.*, 1996) Gelo-pujic *et al.*, (1996) investigated the esterification of methyl-D-glucopyranoside, D-glucose and  $\alpha,\alpha$ -trehalose with dodecanoic acid in dry media by employing immobilized *Candida antarctica* under focused microwave irradiation. Rajan and Abraham (2004)

studied *Thermomyces lanuginosa* lipase catalyzed esterification of starch from maize and cassava with lauric acid using microwave heating and found a substitution percentage of 53 % with a degree of substitution of 1.55 in case of maize starch and a substitution percentage 39 % with a degree of substitution of 1.1 in the case of cassava starch. Parker *et al.*, 1996 found that an irradiated hydrated cutinase in organic media using microwaves enhanced the reaction rate 2-3 folds over classical heating. A selective esterification of  $\gamma$ -linolenic acid in a mixture of free fatty acids with *n*-butanol was reported with lipase from *Rhizomucor miehei* under microwave irradiation (Vacek *et al.*, 2000). Lipase from porcine pancreas is demonstrated to catalyze acylation reactions in organic media under microwave irradiation. Reaction rates and enantioselectivities are significantly enhanced 1-14 and 3-9 folds, respectively. It was found that micro wave assisted reactions enhanced enzyme selectivity and retained its activity without much loss.

#### **1.8.4. Esterification in ionic liquids**

Biocatalytic transformations in ionic liquids have also become the subject of intense research. Different combinations of cationic and anionic solvents made possible to dissolve enzymes and carbohydrates that would not dissolve adequately in organic solvent directly in ionic liquids (Park and Kazlauskas 2001; Swatloski *et al.*, 2002; Patel *et al.*, 2002). Different enzymes such as hydrolases (proteases and lipases) and oxidoreductases (peroxidases and dehydrogenases) retained their activity in ionic liquids. Transesterification reaction of ethyl butanoate with butan-1-ol catalysed by immobilised *Candida antartica* lipase B gave good yields and enantio selectivity in 1-butyl-3-methylimidazolium tetrafluoroborate, [bmim][BF<sub>4</sub>] and 1-butyl-3-methylimidazolium hexafluorophosphate, [bmim][PF<sub>6</sub>] than in *tert*-butanol and *n*-butanol which were better

than native lipase (Lau *et al.*, 2000). The same was observed with *Pseudomonas cepacia* lipase (Kim *et al.*, 2001). The native *Pseudomonas cepacia* lipase showed a high initial rate in [bmim][PF<sub>6</sub>] as compared to [bmim][BF<sub>4</sub>] and dichloromethane and the difference in activity in the two ionic liquids was attributed to their hydrophobicity (Nara *et al.*, 2002). Relatively hydrophobic solvents are capable of removing the essential water from the enzyme surface, leading to insufficient hydration of the enzyme, which may, in some cases, exert a strong influence on the enzyme and decrease its activity (Yang and Russel, 1996). The ionic liquids with the enzyme were recycled for five consecutive runs without any substantial diminution in the lipase activity. Enantioselective esterification of (±)-menthol with propionic anhydride using *Candida rugosa* lipase in ionic liquids ([bmim][PF<sub>6</sub>] and [bmim][PF<sub>4</sub>]) showed 2.5 times higher activity and enantioselectivity in recycling application than in hexane (Yuan *et al.*, 2006). Nara (2004) studied lipase-mediated regioselective biotransformations involving hydrolysis and alcoholysis of 3,4,6-tri-*O*-acetyl-D-glucal in tetrahydrofuran (THF) and two different ionic liquids, namely [bmim]PF<sub>6</sub> and [bmim]BF<sub>4</sub> showing marked regioselectivity towards the formation of 4,6-di-*O*-acetyl-D-glucal in [bmim]PF<sub>6</sub> with 84% product formation after 6 h with 98% selectivity in hydrolysis and 48% after 8 h with 98% selectivity in alcoholysis (Nara *et al.*, 2004). The main limitation of usage of ionic liquid in organic synthesis is recovery of reaction products. To separate products one should use solvents that are immiscible with ionic liquids which give biphasic systems. However even that extract will contain small amount of ionic liquid as well as catalysts (Gordon, 2001). Also, the partitioning of the solute between the phases limits the extent of solute

### 1.8.5. Kinetic studies of lipase catalyzed esterification reactions

Kinetic study of enzyme reactions help in determining the rate of a reaction and how this rate changes in response to different conditions which can be intimately related to the path followed by the reaction and is therefore indicative of its reaction mechanism. It also describes the intricate details of enzyme inhibition and how the rate of enzymatic reactions vary with enzyme and concentration, incubation period, pH, solvent and temperature. When lipases were used in organic solvents, it was found that they followed a complex two-substrate Ping-Pong Bi-Bi mechanism (Zaks and Klibanov, 1986). A Ping-Pong Bi-Bi mechanism, which stands for two-substrate two-product reaction, is a sequential one where both substrates do not bind to the enzyme simultaneously before the product is formed. The amount of lipase available and the rate of breakdown of the enzyme-substrate complex govern the overall rate of reaction. If the organic acid employed is inhibitory in nature, then it remains bound to the enzyme strongly and no acyl transfer occurs. In some cases, even if the acyl transfer occurs, product formed may remain bound to the enzyme resulting in inhibition.

Lipase-catalyzed esterification between oleic acid and ethanol (Chulalaksananukul *et al.*, 1990) and transesterification between geraniol and propyl acetate (Chulalaksananukul *et al.*, 1992) were found to follow Ping-Pong Bi-Bi mechanism where both ethanol and geraniol were found to be inhibitory. Similar Ping-Pong Bi-Bi mechanism was found to be followed in the kinetics of esterification of lauric acid by (-)-menthol catalyzed by lipase from *Penicillium simplicissium* with (-) menthol being inhibitory (Stamatis *et al.*, 1993). In a transesterification reaction between isoamyl alcohol and ethyl acetate catalyzed by Lipozyme IM20, the substrates, ethyl acetate and isoamyl alcohol and one of the products (ethanol) were found to be inhibitory. Of the

others. *n*-Octanol is inhibitory to RML and CRL in the transesterification between vinyl acetate and *n*-octanol (Yadav and Trivedi, 2003) following the Ternary Complex Bi-Bi mechanism, in which *n*-octanol binds twice or once to lipase to yield a dead-end lipase-*n*-octanol complex and a second molecule of *n*-octanol binds to give another dead-end lipase-*n*-octanol complex. For citronellyl laurate synthesis, RML follows the Ordered Bi-Bi mechanism wherein  $\beta$ -citronellol binds to the enzyme to yield the  $\beta$ -citronellol-enzyme complex, which again binds to lauric acid to form the ternary enzyme- $\beta$ -citronellol-lauric acid complex. Finally, the complex decomposes to give  $\beta$ -citronellyl laurate and water as products in this process (Yadav and Lathi, 2004). A series of dead-end RML-lauric acid complexes were also reported in this process.

A kinetic model has also been proposed, taking into account, the effect of solvent ( $\gamma_s$  – substrate solvation) and  $a_w$ , which are thermodynamic parameters. In this model, the hydration state of the enzyme molecule was examined and equilibrium kinetic constants were expressed in terms of thermodynamic activity. Predictions based on this model were found to be in good agreement with experimental observations (Lee, 1995; Janssen *et al.*, 1999). Mathematical analyses of experimentally observed initial rates yielded various parameters,  $K_{m(\text{lactic acid})} = 0.059 \text{ M}$ ,  $K_{m(\text{stearic acid})} = 0.04 \text{ M}$ ,  $V_{\max(\text{lactic acid-stearic acid})} = 0.00163 \text{ M/h}$  and  $K_{i(\text{lactic acid})} = 0.079 \text{ M}^{-1}$  in the kinetic study of the reaction between stearic acid and lactic acid (Kiran and Divakar, 2002). Thus, with improved kinetic models being proposed, one can predict the enzyme behaviour in a more efficient manner.

### 1.8.6. Lipase catalyzed resolution of racemic esters

There is an increasing demand for preparing optically active pure compounds in pharmaceutical industry. Various methods are available to synthesize the optically active compounds and among them enzymatic methods are more attractive (Sheldon, 1996). Lipases have also been extensively used in the resolution of racemic alcohols and carboxylic acids through asymmetric hydrolysis of the corresponding esters (Cambou and Klibanov, 1984b). Chirally pure hydroxyalkanoic acids which find wide applications as drug intermediates have been obtained from racemic ( $\pm$ )-hydroxyalkanoic esters (Scilimati *et al.*, 1988; Feichte *et al.*, 1989; Engel *et al.*, 1991). Molecular modelling studies have revealed that enzyme behaviour towards racemic substrates can be predicted (Hult and Norin, 1993). Rantwijk and Sheldon (2004) critically reviewed resolution of chiral amines through enantioselective acylation by three different serine hydrolases - lipases, subtilisin and *Penicillin* acylase and recommended *Candida antartica* lipase because of its high enantioselectivity and stability. Resolution of some enantiomeric alcohols like (*R,S*)-2-octanol, (*R,S*)-2-(4-chlorophenoxy) propionic and (*R,S*)-2-bromo hexanoic acids were carried out using lipases from *Candida rugosa* and *Pseudomonas* species where *R*-alcohol was obtained with an enantiometric excess of about 98% (Crespo *et al.*, 2005). Optically active (*S*)- $\alpha$ -cyano-3-phenoxybenzyl (CPB) acetate was obtained from racemic cyanohydrins by transesterification using lipase from *Alcaligenes* sp. in organic media (Zhang *et al.*, 2005). Lipase isolated from porcine pancreas immobilized in DEAE-Sepharose gave pure (*S*)-(-) glycidol from (*R*)-(-)-glycidyl butyrate when the reaction was carried out in pH 7.0 and 10 % dioxane at 25 °C (Palomo *et al.*, 2003). Bocola *et al.*, 2003 reported that in kinetic resolution of (*R*)- and (*S*)-1-phenylethylamine using *Candida antartica* lipase B preacylated with an ethoxyacetyl group. The reaction showed a remarkable stereo discrimination with an enantiomeric



ratio  $E > 1000$  in favour of (*R*)-1-phenylethylamide. The differential activation free energy showed that the fast-reacting (*R*)-amine is discriminated with respect to the slow-reacting (*S*)-amine by a free energy difference of 19.4 kJ/mol (Bocola *et al.*, 2003). From molecule crystal structure analysis, it was found that fast reacting (*R*)-phospho-transition state analogue appears to exhibit perfect surface and shape complementarity to the *Candida antartica* lipase B binding pocket (Bocola *et al.*, 2003).

### 1.9. Scope of the present investigation

The above described features have clearly established that, as one of the most thoroughly studied hydrolyzing enzymes in synthetic reactions, lipases have come a long way in establishing themselves as an important synthetic tool in bio-organic reactions. The main scope of the present work described in this thesis is to use the lipases in esterification reactions to prepare commercially important esters. Amino acyl esters of carbohydrates, find use in a wide variety of applications. They are used in industry as detergents, microcapsules in pharmaceutical preparations, in the delivery of biologically active agents, antibiotics, sweetening agents, emulsifying agents, active nucleoside amino acid esters, antitumor agents, plant growth inhibitors and peptide prodrugs (Kirk *et al.*, 1992; Zaks & Dodds, 1997; Glinskii and Guennadi, 1998; Jeric-Horvat, 2001; Perng *et al.*, 1998). Hence, the present work deals with the syntheses of the amino acyl esters of carbohydrates and that too, involving amino acids with alkyl side chain like L-alanine, L-valine, L-leucine and L-isoleucine.

Literature survey indicates that lipase catalysed synthesis of amino acyl esters of carbohydrates are very few (Park *et al.*, 1999; 1996; Boyer *et al.*, 2001; Maruyama *et al.*, 2002; Vijayakumar *et al.*, 2004; Lohith and Divakar, 2004). The available literature deals with N-protected and carboxyl group activated amino acids and carbohydrates. The

reported protocols exhibit some severe limitations. Most of researchers have employed proteases for their work (Boyer *et al.*, 2001; Park *et al.*, 1999; 1996; Riva *et al.*, 1988). Reactions were carried out with health hazardous solvents like dimethyl sulphoxide, pyridine and dimethylformamide. Most of the reports are from experiments carried out in shake flask levels with large amount of enzyme being employed in such reactions (Riva *et al.*, 1988). Lipases have been reported to give insignificant results in preparing amino acyl esters of carbohydrates (Park *et al.*, 1996).

The experimental protocols developed in the present work described in this thesis have efficiently dealt with the above mentioned disadvantages. Commercially available lipases, which are also economically viable, were employed in the present work. Use of unprotected and unactivated amino acids and carbohydrates have been employed for the reactions, which effectively reduce the number of acylation and deacylation steps. Low boiling solvents were employed for the reactions such that solvents can be easily recovered. The work out procedures are easy and the product recovery involved very few unit operations. Smaller amounts of enzyme and larger amounts substrates were employed to obtain high yields than the reported. All the reactions were carried out in presence of solvent mixtures using an experimental set up, which maintained a very low water activity, very much essential for high enzyme activity and for carrying out reactions in a large-scale level as well.

Thus, the present work describes synthesis of L-alanyl, L-valyl, L-leucyl and L-isoleucyl esters of aldohexoses (D-glucose, D-galactose and D-mannose), ketohexose (D-fructose), pentoses (D-arabinose and D-ribose), disaccharides (lactose, maltose and sucrose) and sugar alcohols (D-sorbitol and D-mannitol) using lipases from *Rhizomucor miehei*, *Candida rugosa* and porcine pancreas in organic solvents. The effects of various

parameters such as enzyme, substrate, buffer pH, concentrations, enzyme reusability, kinetics and stereo selectivity were investigated. The isolated product esters were also tested for probable pharmaceutical and biological activities as well. Thus the full potentialities of lipases are brought out in this study which describes the synthesis of several of the above mentioned amino acyl esters of carbohydrates for the first time.

*Chapter 2*  
*Materials and Methods*

## 2.1. Materials

### 2.1.1. Lipases

In the present work, three different lipases were employed - two from fungal sources, *Rhizomucor miehei* lipase (RML) and *Candida rugosa* lipase (CRL) and one from animal source, porcine pancreatic lipase (PPL).

**Table 2.1. List of lipases and their sources**

Lipase	Source	Employed for
Porcine pancreas lipase (Type II, Steapsin, crude preparation)	Sigma Chemical Co., St. Louis. MO, USA.	Preparation of L-alanyl and L-valyl esters of D-glucose
<i>Rhizomucor miehei</i> lipase (Lipozyme IM20 immobilized on weak anion exchange resin)	Novo-Nordisk, Bagsvaerd, Denmark and Boehringer Mannheim, Germany.	Preparation of L-alanyl, L-valyl, L-leucyl and L-isoleucyl esters of D-glucose, D-galactose, D-mannose, D-fructose, D-arabinose, D-ribose, lactose, maltose, sucrose, D-mannitol and D-sorbitol and esterification kinetics.
<i>Candida rugosa</i> lipase	Sigma Chemical. Co. MO, USA.	Preparation of L-alanyl, L-valyl, L-leucyl and L-isoleucyl esters of D-glucose, D-mannose, D-galactose, D-arabinose, D-ribose, lactose, maltose, sucrose, D-mannitol and D-sorbitol and esterification kinetics.

### 2.1.2. L-Amino acids

L-Alanine, L-valine, L-leucine and L-isoleucine from Hi-Media Ind. Ltd. were employed as such.

### 2.1.3. Carbohydrates

D-Glucose and sucrose from SD fine chemicals (Ind.) Ltd.; D-galactose and D-fructose from Hi-Media Ind. Ltd.; D-mannose, D-arabinose, D-ribose and D-mannitol from LOBA Chemie Pvt. Ltd. India; maltose from Sigma Chemical. Co. MO, USA; lactose from SISCO Research Laboratories Pvt. Ltd. India and D-sorbitol from Rolex Laboratory Reagent India Ltd. were procured and employed as such.

### 2.1.4. Solvents

Solvents such as chloroform, dichloromethane, *n*-hexane, *n*-heptane, pyridine, dimethylformamide, *n*-butanol, acetic acid, butyric acid, acetone and diethyl ether purchased from SD fine Chemicals (Ind.) Ltd. were employed after distilling once. Acetonitrile and methanol of HPLC grade were obtained from Qualigens fine chemicals (Ind) Ltd. and were used as such. Deuterium oxide and dimethyl sulfoxide- $d_6$  from Aldrich Chemicals limited were used for preparing samples for Nuclear Magnetic Resonance Spectroscopy.

### 2.1.5. Other chemicals

**Table 2.2 List of chemicals and suppliers**

Chemicals	Manufacturer
Sodium acetate ( $\text{CH}_3\text{COONa}$ ), Sodium dihydrogen phosphate ( $\text{Na}_2\text{HPO}_4$ )	Ranbaxy Laboratories Ltd. India,
Di-sodium tetraborate ( $\text{Na}_2\text{B}_4\text{O}_7 \cdot 10\text{H}_2\text{O}$ ), sodium hydroxide, potassium dihydrogen phosphate, acetic acid, hydrochloric acid, sulphuric acid, iodine (resublimed), molecular sieves 4Å, copper sulphate, silica gel and sodium potassium tartarate.	SD fine Chemicals (Ind.) Ltd.
Ninhydrin, sodium benzoate, sodium dodecyl sulfate, 1-naphthol, hippuric acid, gum acacia and triton x-100	LOBA Chemie Pvt. Ltd. India.

---

Hippuryl-L-histidyl-L-leucine tetrahydrate, bovine serum albumin, tributyrin, hemoglobin from bovine serum, Sephadex G-10 and Sephadex G-25	Sigma Chemical. Co. MO, USA
Bio Gel P-2	Bio-Rad Laboratories, USA.
Potassium bromide, Folin-Cicolteau reagent and HEPES buffer (N-[2-hydroxyethyl]-piperazine-N'-[2-Ethane sulphonic acid])	SISCO Research Laboratories Pvt. Ltd. India
Karl Fischer Reagent	Qualigens Fine Chemicals Ltd. India

---

## 2.2. Methods

### 2.2.1. Lipase activity

Both esterification as well as hydrolytic activities of the lipases were determined.

#### 2.2.1.1. Hydrolytic activity

Hydrolytic activities of different lipases were determined by the tributyrin method (Vorderwulbecke *et al.*, 1993). Hydrolytic activity of lipase is defined as  $\mu\text{mol}$  of butyric acid released from tributyrin per min with one mg of immobilized lipase preparation. The specific activity is expressed as  $\mu\text{mol}$  of butyric acid released per min per mg of protein present in the lipase (Table 2.3).

A stock solution was prepared consisting of 10 ml of tributyrin, 90 ml of 0.01 M sodium phosphate buffer (pH 7.0), 0.2 g sodium benzoate, 0.5 g of gum acacia and 50  $\mu\text{l}$  10% SDS. It was emulsified by stirring and the pH was adjusted to 7.0 with concentrated NaOH. From this stock solution, 4 ml was pipetted out into stoppered conical flasks (S), containing 8 ml, 0.01 M sodium phosphate buffer (pH 7.0) to obtain a solution with a final concentration of 0.113 M tributyrin. Known quantities of lipases (5 –20 mg) were added to this solution and incubated at 37 °C in a Heto-Holten shaker water bath for

different intervals of time. After incubation, the reaction mixture in the flask was titrated with 0.04 N NaOH until a pH of 9.5 was reached. A blank (B) was also performed without adding the enzyme. The hydrolytic activity was determined by using the following equation.

$$\text{Hydrolytic activity} = \frac{(\text{S}-\text{B}) \times \text{N}}{1000 \times \text{E} \times \text{T}} \quad \mu\text{mol}/(\text{min} \cdot \text{mg of lipase preparation or protein})$$

(S-B) = difference in volume of NaOH in ml between sample (S) and blank (B),

N= normality of NaOH,

E = amount of lipase preparation or protein in mg and

T= incubation period in min.

#### 2.2.1.2. Esterification activity

Esterification activities of four different lipases from porcine pancreas, *Rhizomucor miehei*, *Candida rugosa* and Chirozyme were determined by butyl butyrate method (Kiran *et al.*, 2000). Esterification activity of lipase is defined as  $\mu\text{mol}$  of butyl butyrate formed from *n*-butanol and butyric acid per min with one mg of immobilized lipase preparation. The specific activity is expressed as  $\mu\text{mol}$  of butyric acid released per min per mg of protein present in the lipase (Table 2.3).

A stock solution containing 0.33 M *n*-butanol and 0.16 M butyric acid was prepared. In a 25 ml stoppered conical flask, 3 ml of the stock solution was dispersed in 5 ml of *n*-heptane. The reaction mixtures were incubated with known quantities of lipases for different intervals (30, 60, 90 and 120 min) in a Heto-Holten shaker water bath at 50 °C. After incubation, the contents of the flasks were titrated with standard 0.02 N NaOH. A blank (without the enzyme) was also performed. Table 2.3 shows the esterification



activities of four different lipases. The esterification activity was evaluated by using the following equation.

$$\text{Esterification activity} = \frac{(B-S) \times N}{1000 \times E \times T} \text{ } \mu\text{mol}/(\text{min.mg of lipase preparation or protein})$$

(B-S) = difference in volume of NaOH in ml between blank (B) and sample (S),

N= normality of NaOH,

E= actual amount of the lipase preparation or protein in mg and

T= incubation period in min.

**Table 2.3. Esterification and hydrolytic activities of different lipases <sup>a</sup>.**

Lipase	Esterification activity <sup>b</sup>		Hydrolytic activity <sup>c</sup>	
	Activity $\mu\text{mol}/(\text{min.mg}$ of lipase preparation)	Specific activity $\mu\text{mol}/(\text{min.mg}$ of enzyme protein)	Activity $\mu\text{mol}/(\text{min.mg}$ of lipase preparation)	Specific activity $\mu\text{mol}/(\text{min.mg}$ of enzyme protein)
Porcine pancreas	0.06	0.17	0.32	0.97
<i>Rhizomucor miehei</i>	0.46	7.27	0.10	1.59
<i>Candida rugosa</i>	0.03	7.64	-	-
Chirozyme	0.35	0.32	-	-
Porcine pancreas (partially purified)	0.02	0.2	0.02	2.45

<sup>a</sup> For each enzyme the activity results were obtained from an average of three individual experiments for different time intervals. Error in activity measurements were within  $\pm 10\%$ .

<sup>b</sup> Butyl butyrate method, lipase employed : 5, 10 and 15 mg, Incubation temperature : 50 °C.

<sup>c</sup> Tributyrin method, lipase employed : 5, 10, 15 and 20 mg, Incubation temperature : 37 °C.

### 2.2.2. Protein estimation

Protein content of all the above mentioned five lipases were determined by using Lowry's method (Lowry *et al.*, 1951). In order to leach out the protein from the

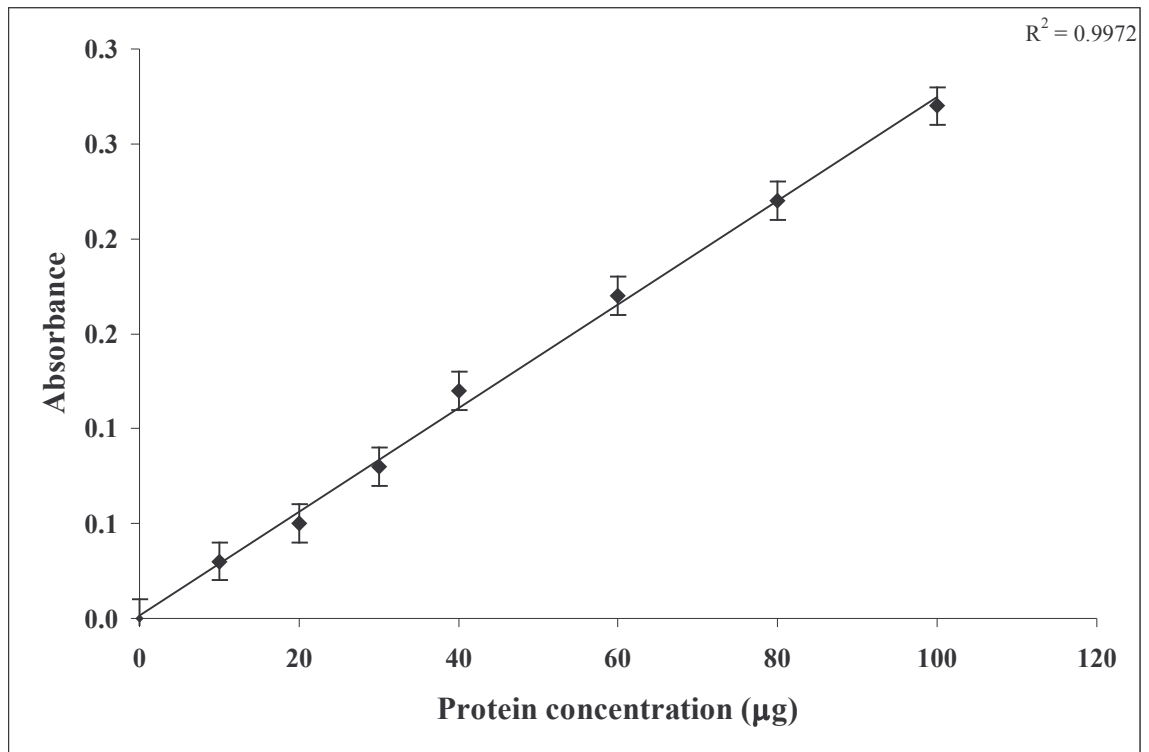


**Fig. 2.1.** Calibration curve for protein estimation by Lowry's method. A stock solution of 300 µg of 3 ml BSA solution was prepared. From the stock solution 0.2, 0.3, 0.4, 0.6, 0.8, 1.0 ml solutions were pipetted out and the total volume was made upto 1 ml with distilled water after treatment with solutions as described in the text (Section 2.2.2) Absorbance was measured at 750 nm.

immobilized matrix or carrier, 20 mg lipase preparations were stirred in 50 ml of 0.5 M NaCl at 4 °C for 12 h and from this, known volumes of the samples were taken for protein estimation.

Solution **A** – 1 % of copper sulphate in water, solution **B** – 1 % of sodium potassium tartarate in water and solution **C** – 2 % of sodium carbonate solution in 0.1 N NaOH were prepared. Lowry's working solution **I** was prepared by mixing one part each of solution **A** and **B** and 98 parts of **C**. A 1:1 diluted solution of commercially available Folin-Cicolteau reagent with distilled water served as working solution **II**. To the protein sample in 1 ml water, 5 ml of Lowry's working solution **I** was added and incubated for 10 min at room temperature. A 0.5 ml of working solution **II** was then added followed by incubation at room temperature for 30 min and absorbance was measured at 750 nm using a Shimadzu UV – 1601 spectrophotometer. Calibration curve for protein concentrations was prepared by employing bovine serum albumin (BSA) in the concentration range 0 - 100 µg in 6.5 ml of the sample (Fig. 2.1). Using this calibration plot protein content of four different lipases were determined and values are shown in Table 2.4.

**Table 2.4. Protein content of different lipase preparations <sup>a</sup>**

<b>Lipase</b>	<b>Protein content (%)</b>
Porcine pancreas	32.8
<i>Rhizomucor miehei</i>	6.3
<i>Candida rugosa</i>	35.3
Chirazyme	3.2
Porcine pancreas (partially purified)	8.3

<sup>a</sup> Lowry's method, Lipase employed - 20 mg in 50 ml 0.5 M NaCl, Absorbance measured at 750 nm. Values are an average of three different concentrations of lipases. Errors in measurement will be within ± 5%.

### 2.2.3. Preparation of buffers

Decimolar concentrations of CH<sub>3</sub>COONa buffer for pH 4.0 and 5.0, Na<sub>2</sub>HPO<sub>4</sub> for pH 6.0 and 7.0 and Na<sub>2</sub>B<sub>4</sub>O<sub>7</sub>·10H<sub>2</sub>O for pH 8.0 buffers were prepared by dissolving appropriate amounts of respective salts in distilled water and the pH was adjusted with dilute HCl or NaOH using Controlled dynamics pH meter, model – APX175 E/C, India.

### 2.2.4. Esterification procedure

Preparation of L-amino acyl esters of carbohydrates was carried out by adopting a bench-scale level procedure (Divakar *et al.*, 1999). Esterification was carried out in presence of 0.018 – 0.225 g of lipases (expressed in terms of % w/w based on the carbohydrate employed). Unprotected L-amino acids (0.001 - 0.005 mol) and carbohydrates (0.001 – 0.005 mol) in 100 ml of organic media containing CH<sub>2</sub>Cl<sub>2</sub>: DMF (v/v 90:10) or hexane: CHCl<sub>3</sub>:DMF (v/v/v 45:45:10) were taken in a flat bottomed two necked flask and refluxed for a period of 3 - 120 h. The enzymes were ‘pH tuned’ in some experiments by adding known volumes of 0.1 M buffer solutions of specified pH value to 100 ml (solvent) of the reaction mixture. The condensed vapours of solvent which formed an azeotrope with water during reflux was passed through a desiccant (sodium aluminosilicate molecular sieves of 4Å) before being returned into the reaction mixture, thereby facilitating complete removal of water of reaction (Lohith and Divakar, 2005). This set up maintained a very low water activity of  $a_w = 0.0054$  throughout the reaction period which was determined by Karl Fischer titration of the reaction mixture using Karl Fischer reagent by examining the aliquots of the reaction mixture for the water content during the course of the reaction. The reaction mixture after distilling off the solvent was then added to 20 - 30 ml of water, stirred and filtered to remove the lipase. The filtrate was evaporated on a water bath to get the unreacted carbohydrate,

unreacted L-amino acids and the product esters which were then analyzed by HPLC. The amino acids employed were L-alanine **1**, L-valine **2**, L-leucine **3** and L-isoleucine **4** and the carbohydrates employed were D-glucose **5**, D-mannose **6**, D-galactose **7**, D-fructose **8**, D-arabinose **9**, D- ribose **10**, lactose **11**, maltose **12**, sucrose **13**, D-mannitol **14** and D-sorbitol **15**.

### **2.2.5. High Performance Liquid Chromatography**

The reaction mixture was monitored by employing a Shimadzu LC10AT high-performance liquid chromatography instrument (Kyoto, Japan) connected to a  $\mu$ -Bondapak aminopropyl column (10  $\mu$ m particle size, 3.9 x 300 mm length) with acetonitrile:water (v/v 80:20) as mobile phase at a flow rate of 1 ml/min and refractive index detector. Also, a LiChrosorb RP-18 column (5  $\mu$ m particle size, 4.6 x 150 mm length) with acetonitrile:water (v/v 20:80) as a mobile phase at a flow rate of 1 ml/min and UV detector at 210 nm was employed. Since different equivalents of L-amino acids were employed, the conversion yields were determined based on the peak areas of L-amino acid and L-amino acid ester of the carbohydrate and expressed in mmol as well as in percentage values with respect to the L-amino acid concentration employed. The error in HPLC yields will be within  $\pm 10$  %.

### **2.2.6. Separation of L-amino acyl esters of carbohydrates**

The esters formed were separated by size exclusion chromatography using Sephadex G-10/Sephadex G-25/Bio Gel P-2 in a column of size 100 cm x 1.0 cm. About 30 g of gel (bed volume of 70-80 ml) was packed and 150 mg of the reaction mixture was dissolved in distilled water and loaded onto these columns and eluted with water at a flow rate of 1 ml/h. Separation was observed by performing thin layer chromatography by spotting individual fractions on silica plate. Silica plates were prepared by dissolving

8 g of silica gel (mesh 60-120) in 20 ml of water which were spreaded uniformly over 20 x 20 cm glass plate. After air and oven drying, chromatography was performed using *n*-butanol: acetic acid: water (v/v/v 70:20:10) as mobile phase. The spots were identified by spraying ninhydrin (for NH<sub>2</sub> group detection) and 1-naphthol (for reducing sugar detection) and kept in hot air oven at 100 °C for 20 minutes to obtain colored spots. Ninhydrin reagent was prepared by dissolving 400 mg of ninhydrin in absolute alcohol. Sugar spray was prepared by dissolving 1.46 g of 1-naphthol in 41 ml of ethanol and then to that was added 3.4 ml of water and 5.6 ml of concentrated sulfuric acid. The fraction containing product esters were evaporated on a water bath and subjected to spectral characterization.

#### **2.2.7. UV-Visible spectroscopy**

A Shimadzu UV-1601 spectrophotometer (Kyoto, Japan) was used for UV characterization of the isolated esters. Samples were prepared in water at 0.1 - 2.0 mM range.

#### **2.2.8. Infra Red spectroscopy**

A Nicolet 5700 FTIR instrument (Madison, USA) was used for recording IR spectra for the isolated esters. A 2.0 to 3.0 mg of ester sample was prepared as KBr pellet and the IR spectrum was recorded.

#### **2.2.9. Nuclear Magnetic Resonance Spectroscopy**

##### **2.2.9.1. <sup>1</sup>H NMR**

A Brüker DRX-500 MHz spectrometer (Fallanden, Switzerland) operating at 500.13 MHz was used to record <sup>1</sup>H NMR spectra in DMSO-*d*<sub>6</sub> with 40 mg of the sample dissolved in 0.5 ml of solvent. About 50-200 scans were accumulated with a recycle period of 2-3 seconds to obtain good spectra. The spectra were recorded at 35 °C with TMS as internal standard for measuring the chemical shift values to within ± 0.01 ppm.

A region from 0 –10 ppm was scanned for all the samples.

#### **2.2.9.2. $^{13}\text{C}$ NMR**

A Bruker DRX-500 MHz spectrometer (Fallanden, Switzerland) operating at 125 MHz was used to record  $^{13}\text{C}$  NMR. Samples were dissolved in 0.5 ml of DMSO- $d_6$  and recorded at 35 °C. A region from 0-200 ppm was scanned and about 500-6000 scans were accumulated for each spectrum. TMS was taken as the internal standard.

#### **2.2.9.3. Two-dimensional HSQCT**

Two dimensional Heteronuclear Multiple Quantum Coherence Transfer spectra (2-D HMQCT) and Heteronuclear Single Quantum Coherence Transfer spectra (2-D HSQCT) were recorded at 500 MHz on a Bruker DRX-500 MHz spectrometer (500.13 MHz for  $^1\text{H}$  and 125 MHz for  $^{13}\text{C}$ ). Proton and carbon  $90^\circ$  pulse widths were 12.25 and 10.5  $\mu\text{s}$  respectively. Chemical shift values were expressed in ppm relative to internal tetramethylsilane standard. About 40 mg of the sample dissolved in DMSO- $d_6$  was used for recording the spectra in magnitude mode with sinusoidal shaped z-gradients of strength 25.7, 15.42 and 20.56 G/cm with a gradient recovery delay of 100  $\mu\text{s}$  to defocus unwanted coherences. The  $t_1$  was incremented in 256 steps with a computer memory size of 4K. The spectra were processed using unshifted and  $\pi/4$  shifted sine bell window function in  $F_1$  and  $F_2$  dimensions respectively.

#### **2.2.10. Mass spectrometry**

Mass spectra of the isolated esters were recorded on a Q-TOF Waters Ultima instrument (No.Q-Tof GAA 082, Waters corporation, Manchester, UK) fitted with an electron spray ionization (ESI) source. Version 4.0 data acquisition software was used. The spectra were recorded in positive ion mode using spray voltage at 3.5 kV and a source temperature of 80 °C. Mass spectra were recorded under electron impact

ionization at 70 eV electron energy. Samples were prepared in the concentration range of 0.5 - 1.0 mg/ml in distilled water and injected by flow injection analysis at a flow rate of 10 µl/min. The recorded mass of the sample was in the range of 100-1000.

### 2.2.11. Polarimetry

Optical rotations of the isolated esters were measured at 20 °C using Perkin-Elmer 243 polarimeter (Überlingen, Germany). A 0.2 – 1.5 % solutions of the ester in distilled water was employed for the measurements. Optical rotations were determined from

$$[\alpha]_{\text{D}}^{20\text{ }^{\circ}\text{C}} = \frac{[\alpha]_{\text{obs}} \times 100}{C \times l}$$

$[\alpha]_{\text{D}}$  = specific rotation in degrees in sodium lamp at 590 nm

$[\alpha]_{\text{obs}}$  = observed rotation,

C= concentration of the esters in g/100 ml and

l = path length in dm.

### 2.2.12. Determination of Critical micellar concentration (CMC)

Critical micellar concentration for L-alanyl-β-D-glucose was determined by using Coomassie Brilliant Blue G 250 reagent (Rosenthal and Koussale, 1983) by dissolving 100 mg of the dye in 50 ml of 95 % ethanol. To this solution, 100 ml of 85 % (w/w) phosphoric acid was added and the resulting solution was diluted to a final volume of 1L using distilled water. Thus, final concentrations were 0.01 % (w/v) Coomassie Brilliant Blue G 250, 4.7 % (w/v) ethanol and 8.5 % (w/v) phosphoric acid.

Aliquots of sample concentrations in the range of 0 - 15 mM were prepared and made up to 1 ml by adding Coomassie brilliant blue G 250 reagent. The reaction mixture was shaken well and the absorption was measured at 470 nm. A plot of concentrations of



the sample versus absorption was constructed, from which CMC was determined as the concentration of the ester corresponding to a change in the slope of the absorption versus concentration plot.

### **2.2.13. Water activity**

Water activity of the reaction media was measured using Mettler Toledo DL-50 auto titrator (Vogel, 1961; Grünke, 2003). Known amount of the solvents were titrated against the Karl-Fischer reagent. Karl-Fischer reagent contains mixture of pyridine, iodine and sulfur dioxide dissolved in methanol. The main reaction can be described in two steps. In the first step, formation of an intermediate 'pyridine sulfurtrioxide' takes place and this is later converted into 'pyridine-N-sulfuric acid' by the action of pyridine, sulfur dioxide and methanol. In the second step, pyridine-N-sulfuric acid is oxidized by iodine in presence of water.

The Karl-Fischer titrator contains a polarizing double platinum electrode and the voltage between the electrodes is measured against added titrant (Karl-Fischer reagent). As long as traces of water is present in the titration cell, all iodine molecules are immediately reduced to iodide by the KF reagent. The electrical resistance of the solution stays at a high level. After titrating all the water molecules, a small excess of iodine leads to a strong decrease in the resistance which is considered as the end point. The stoichiometry in the reaction is 1:1  $I_2:H_2O$  where one molecule of iodine is equivalent to one molecule of water. A 5.0 g of Karl-Fischer reagent can react with 1.0 g of water. Amount of water was determined by the amount of Karl-Fischer reagent consumed by the solvent. Table 2.5 shows the water activities of some organic solvents.

**Table 2.5. Water activities for different organic solvents by Karl-Fisher method**

Solvent <sup>a</sup>	Water activity ( $a_w$ )
Acetone	0.008
Benzene	0.142
Chloroform	0.028
Dichloromethane	0.054
Heptane	≈0
Hexane	0.183
Methyl isobutyl ketone	0.043

a – volume of solvent taken – 40 ml, Errors in measurement were within  $\pm 10\%$ .

#### 2.2.14. Preparation of N-Acetyl alanine

A 5.0 g (56 mmol) of L-alanine was dissolved in 15 ml (186 mmol) of pyridine in 100 ml round bottomed flask. The reaction mixture was allowed to stir for 10 min. To this stirring solution 26.5 ml (280 mmol) of acetic anhydride was added drop wise. The reaction mixture was allowed to react for 24 h at room temperature and then the whole reaction mixture was poured into ice. Unreacted pyridine and acetic anhydride were removed by evaporation using a flash evaporator. N-Acetyl alanine was then extracted by using 4-methyl penta-2-one repeatedly for three times and then recrystallized using dry acetone. 4.0 g of N-acetyl alanine was obtained, yield (54 %); Mpt: 127 °C; specific rotation:  $-4.44^\circ$ .

#### 2.2.15. Extraction of Angiotensin Converting Enzyme (ACE) from porcine lung

ACE was partially purified from porcine lung by following the method of Andujar-Sanchez *et al.*, (2003). A 100 g of porcine lung was minced and homogenized using a blender with 10 mM HEPES buffer (pH 7.0) containing 0.4 M NaCl at a volume ratio of 5:1 (v/w of pig lung) at 4 °C. The homogenate was centrifuged at 9000 g for 60 min. The supernatant was discarded and the precipitate was washed twice with 200 ml of

10 mM HEPES buffer (pH 7.0) containing 0.4 M NaCl. The final precipitate was resuspended in 200 ml of 10 mM HEPES buffer (pH 7.0) containing 0.4 M NaCl, 10  $\mu$ M ZnCl<sub>2</sub> and 0.5 % (w/v) triton-X-100 and stirred over night. The solution was centrifuged to remove the pellets. The supernatant was dialyzed against water using a dialysis bag of molecular weight cut off of 10 kD and later lyophilized. A yield of 2.3 g crude ACE was obtained. The protein content determined by Lowry method (Section 2.2.2) was found to be 8.3 %. The specific activity of the enzyme was found to be 0.243  $\mu$ mol/min/mg of enzyme protein.

#### **2.2.16. Angiotensin Converting Enzyme (ACE) inhibition assay**

ACE inhibition assay for the esters prepared were performed by following Cushman and Cheung (1971) method. Aliquots of ester solutions in the concentration range 0.2 to 2.5 mM (0.1 ml to 1.0 ml of 5.0 mM stock solution) were taken and to this 0.1 ml of ACE solution (0.1% in 0.1 M phosphate buffer, pH 8.3 containing 300 mM NaCl) was added. To this solution, 0.1 ml of 5.0 mM hippuryl-L-histidyl-L-leucine (HHL) was also added and the total volume was made upto 1.25 ml by adding phosphate buffer (1.05 ml to 0.15 ml of 0.1 M phosphate buffer, pH 8.3 containing 300 mM NaCl). The solution was incubated on a Heto-Holten shaking water bath for 30 min at 37 °C. Blanks were performed without the enzyme by taking only the ester solution (0.1 to 1.0 ml) along with 0.1 ml of 5.0 mM HHL. The total volume was made upto to 1.25 ml by adding the same buffer (1.15 ml to 0.25 ml). The reaction was terminated by adding 0.25 ml of 1 M HCl. Hippuric acid formed in the reaction was extracted with 1.5 ml of ethyl acetate. One ml of ethyl acetate layer was evaporated to dryness and treated with equal amount of distilled water and the absorbance was measured at 228 nm for hippuric acid. The hippuric acid formed in 1.5 ml of ethyl acetate was determined from a calibration

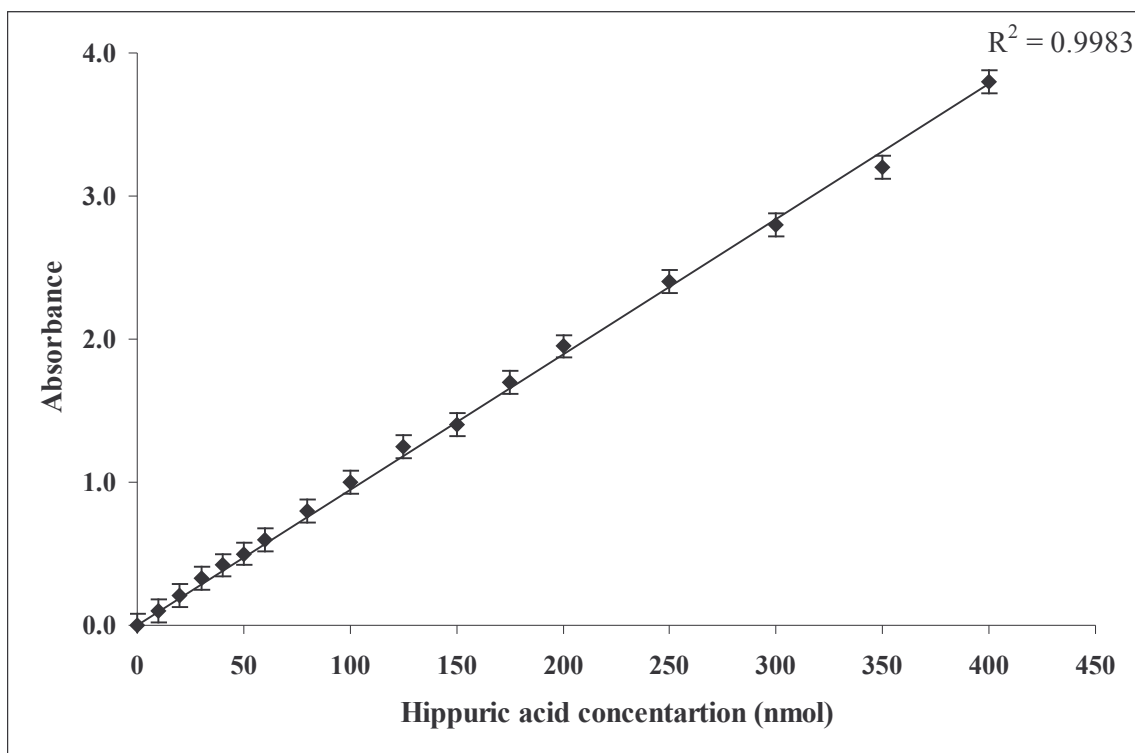


**Fig. 2.2.** Calibration curve for hippuric acid estimation by spectrophotometric method. A stock solution of 44.8 mg hippuric acid in 25 ml water was prepared, from which different aliquots of concentrations 0 to 350 nmol were pipetted out and made up to 1 ml. Absorbance was measured at 228 nm after following the procedure described in the text (Section 2.2.16).

curve prepared using a standard hippuric acid solutions of 0 – 400 nmol in 1 ml of distilled water (Fig. 2.2). Specific activity was expressed as  $\mu\text{mol}$  of hippuric acid formed per min per mg of enzyme protein.

$$\text{Specific activity} = \frac{A_{\text{ts}} - A_{\text{blank}}}{T \times S \times E}$$

$A_{\text{ts}}$  = absorbance of test solution,

$A_{\text{blank}}$  = absorbance of blank solution,

T = incubation period in min,

S = slope value of the calibration plot ( $1.006 \times 10^{-2}$  Abs units/nmol of hippuric acid),

E = amount of enzyme in mg of protein.

#### 2.2.17. Protease activity

The hydrolyzing activity of the protease (in ACE) was determined using bovine hemoglobin as substrate (Dubey and Jagannadham, 2003). To 0.5 ml of ACE enzyme solution, 0.5 ml of 0.6 % (w/v) bovine hemoglobin solution was added and the reaction was allowed to proceed for 30 min at 37 °C. The reaction was terminated by the addition of 0.5 ml of 10 % trichloro acetic acid and allowed to stand for 10 min. The resulted precipitate was removed by centrifugation at 20000 g for 15 min. A 0.5 ml of supernatant was taken and mixed with equal volume of 0.5 M NaOH and the color developed was measured by absorbance at 440 nm. A control assay without the enzyme was carried out and used as reference (blank). Protease inhibition activity to compare with ACE inhibition activity was tested by adding 0.5 ml of the amino acyl esters of carbohydrates solution to 0.5 ml of ACE enzyme solution. To this was added, 0.5 ml of hemoglobin solution and incubated at 37 °C for 30 min. The specific activity of protease in crude ACE preparation was found to be 0.0436 unit/min/mg of enzyme protein.

One unit of enzyme activity was expressed as the amount of enzyme under given assay conditions that gives rise to an increase in one unit of absorbance at 440 nm per min of digestion. Number of units of activity per mg of protein was taken as the specific activity of the enzyme.

$$\text{Specific activity} = \frac{A_{\text{sample}} - A_{\text{blank}}}{T \times E}$$

$A_{\text{sample}}$  = Sample absorbance at 440 nm

$A_{\text{blank}}$  = Blank absorbance at 440 nm

T = Time in min

E = amount of enzyme in mg of protein.

#### **2.2.18. Extraction of porcine pancreas lipase**

The crude PPL was extracted by adopting the procedure of Verger *et al.* (1969). Porcine pancreas bought from local slaughter house was minced into small pieces. About 100 g pancreas was homogenized with 300 ml of chloroform:butanol mixture in the ratio of 9:1 (v/v) at 25 °C. The solvent was decanted and washed with 200 ml of a fresh solvent mixture of 4:1 (v/v) chloroform:butanol mixture and drained completely. The lipid free pellets were then washed with 200 ml of cold acetone and finally with 150 ml diethyl ether to get a fine powder which was then lyophilized. A yield of 11 g crude PPL was obtained. The protein content determined by Lowry method (Section 2.2.2) was found to be 8.3 %. The specific hydrolytic activity and esterification activity of the PPL were found to be 2.45 and 0.2  $\mu\text{mol}/\text{min}/\text{mg}$  of enzyme protein respectively.

#### **2.2.19. Immobilization of porcine pancreas lipases**

Immobilization of the isolated porcine pancreas lipase was carried out according

to the method described by Won *et al.*, (2005) by entrapping lipase on calcium-alginate beads. A 200 ml of 1 g PPL solution was mixed with 800 ml of 1 % sodium alginate. The mixture was stirred thoroughly to ensure complete mixing. The mixed solution was drawn with a syringe into 1 L of 50 mM CaCl<sub>2</sub> solution through a needle of 0.5 mm diameter. The beads formed were allowed to harden for 30 minutes. The CaCl<sub>2</sub> solution was separated from beads by filtration. They were then washed twice with 50 mM Tris-HCl buffer (pH 7.2). The calcium alginate beads obtained were then lyophilized. A yield of 3.54 g immobilized PPL was obtained. The protein content determined by Lowry method (Section 2.2.2) was found to be 0.64 %. The hydrolytic activity and specific hydrolytic activity of the immobilized PPL were found to be 6.67 nmol/min/mg of enzyme protein and 1.04 μmol/min/mg of enzyme protein respectively. The esterification activity and specific esterification activity of the immobilized PPL were found to be 0.74 nmol/min/mg of enzyme protein and 0.115 μmol/min/mg of enzyme protein respectively.

#### **2.2.20. Identification of lipases and ACE by SDS-PAGE**

Sodium dodecyl sulphate-polyacrylamide gel electrophoresis (SDS-PAGE) was carried out to check the purity of lipases according to the method described by Laemmli (1970) in a discontinuous buffer system.

The following reagents were prepared.

- A. Acrylamide (29.2 g) and bis-acrylamide (0.8 g) were dissolved in 100 ml water (30 % solution) filtered and stored in a dark brown bottle at 4 °C.
- B. Separating gel buffer (18.1 g) was dissolved in water and the pH of the solution adjusted to 8.8 with HCl. Then the solution was made upto 100 ml and stored at 4 °C.
- C. Stocking gel buffer – Tris-HCl (3.0 g) was dissolved in water, pH of the solution adjusted to 6.8 with HCl (6.0 N) and made upto 100 ml in water.

- D. Sodium dodecyl sulphate (SDS), 10 g was dissolved in 100 ml water
- E. Ammonium persulphate was freshly prepared by dissolving 50 mg in 0.5 ml of distilled water.
- F. Tank buffer – Tris-HCl (0.3 g), glycine (1.44 g) and SDS (0.15 g) were dissolved in 150 ml of water.
- G. Staining solution – A 0.2 g of Coomassie brilliant blue R 250 was dissolved in a mixture of methanol:acetic acid:water (v/v/v 25:15:60). The reagent was filtered and stored in room temperature.
- H. Destaining solution – Methanol:acetic acid:water (v/v/v 25:15:60).
- I. Sample buffer was prepared in solution C diluted to 1:4 containing SDS (w/v 4 %),  $\beta$ -mercaptoethanol (v/v 10 %), glycerol (v/v 20 %) and bromophenol blue (w/v 0.1 %).

Preparation of separating gel – A 3.2 ml of A, 0.92 ml of B, 2.71 ml of distilled water, 0.05 ml of D and 0.03 ml of solution E were mixed and then degassed which was then poured between the assembled glass plates sealed with agar (w/v 2 %). The gels were layered with 0.5 ml of distilled water and allowed to polymerize at room temperature for 30 min.

A stock solution was prepared by mixing the solutions of 0.66 ml of A, 1.0 ml of C, 2.25 ml of distilled water, 0.05 ml of D, 0.01 ml of TEMED and 0.03 ml of E and poured above the polymerized gel. The gel thus prepared was of the size 10.5 x 9.0 cm and thickness 0.8 mm.

Lipase and ACE samples were prepared by dissolving 25  $\mu$ g of protein in solution 'I' (50  $\mu$ L). The samples were heated in a boiling water bath for 10 min, then samples were loaded into the wells immersed in solution F (tank buffer) and were run at



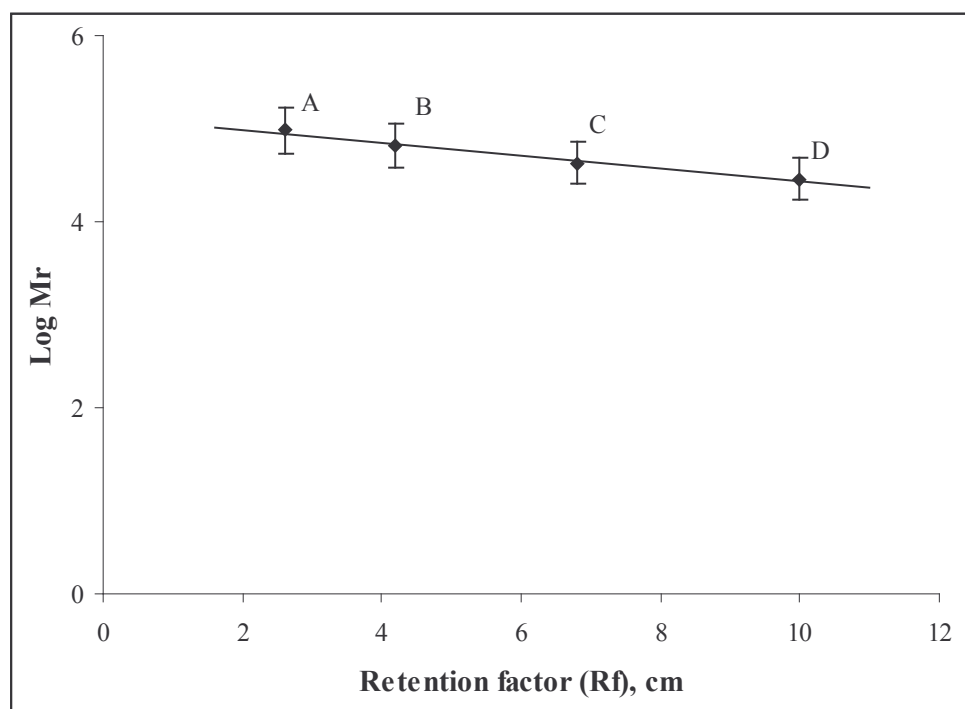


**Fig. 2.3** Log  $M_r$  versus  $R_f$  plot. (A) Phosphorylase (97.4 kDa), (B) BSA (66.3 kDa), (C) Ovalbumin (43.0 kDa), (D) Carbonic anhydrase (29.0 kDa).

a constant voltage of 40 Volts until the tracking dye, bromophenol blue was just (0.5 cm) above the lower end of the gel. Medium range protein markers phosphorylase (97.4 kDa), bovine serum albumin (66.3 kDa), ovalbumin (43.0 kDa), carbonic anhydrase (29.0 kDa) and soyabean trypsin inhibitor (20.0 kDa) were used as a solution having each protein at a concentration of 0.5 to 0.8 mg/ml. The markers were 1:1 diluted with solution I and boiled prior to use. Later the gel was stained for protein with reagent 'G' for 6 h at room temperature followed by destaining in reagent H.

A plot was constructed by taking  $R_f$  values of the molecular marker on X-axis and  $\log M_r$  values of each molecular marker on Y-axis (Fig 2.3). From this plot molecular weight of the unknown protein was determined. Lipases from *Rhizomucor miehei*, porcine pancreas and *Candida rugosa* and molecular weight markers were subjected to SDS-PAGE and stained with Coomassie brilliant blue R 250 (Fig. 2.4A). Lane 1 is the crude porcine pancreas extracted from pig lung, showing large number of bands and one band corresponding to a molecular mass of 54.9 kDa along with other protein contaminants of different molecular masses. Lane 2 is a commercial PPL showing a major band of molecular mass 54.9 kDa, also containing some protease of molecular masses less than 50 kDa. Lane 3 representing *Candida rugosa* lipase, showed a band corresponding to a molecular mass of 57.5 kDa. The band with a molecular mass of 30.2 kDa was obtained for *Rhizomucor miehei* lipase in lane 4. Molecular masses of the all the three lipases showed good correspondence to literature reports (Pernas *et al.*, 2002; Brady *et al.*, 1990; Winkler and Gubernator, 1994).

Angiotensin Converting Enzyme (ACE) showed a molecular mass of 152 kDa (along with the other protein contaminations, Fig. 2.4B, Lane 1) and this band showed a good correspondence to the reported molecular mass of 147 kDa by Hopper *et al.*, (1987).

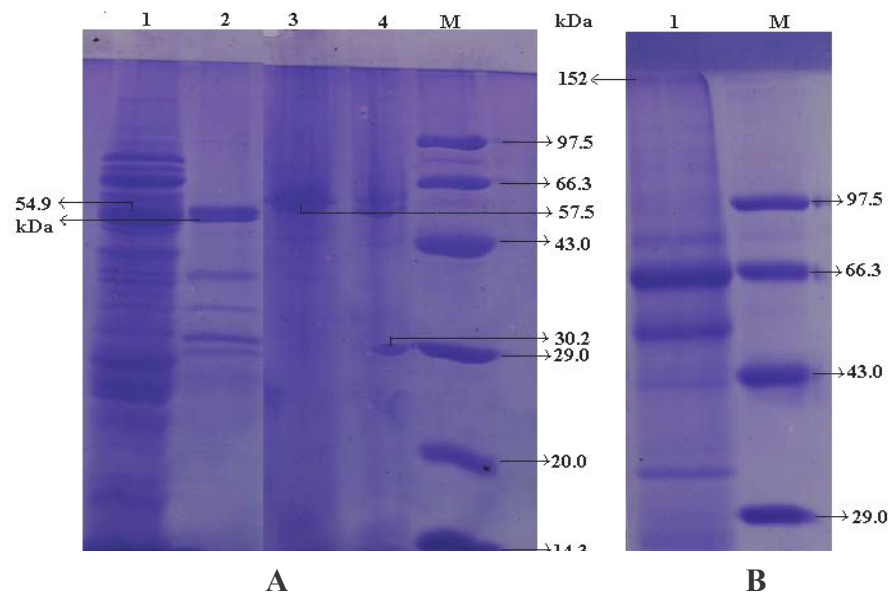


**Fig. 2.4.** SDS-PAGE for (A) lipases; Lane 1 –crude PPL isolated from porcine pancreas; Lane 2 – PPL from Sigma; Lane 3- CRL from Sigma; Lane 4 –RML from Novo-Nordisk; Lane M for  $M_r$  standard proteins: Phosphorylase (97.4 kDa), BSA (66.3 kDa), Ovalbumin (43.0 kDa), Carbonic anhydrase (29.0 kDa) and soyabean trypsin inhibitor (20.0 kDa). (B) Lane 1 for ACE isolated from pig lung.

**Chapter 3**  
***Optimization of reaction parameters for the  
synthesis of L-alanyl, L-valyl and L-leucyl  
esters of D-glucose***

### 3.1 Introduction

Amino acyl esters of carbohydrates are used as sweetening agents, surfactants, microcapsules in pharmaceutical preparations, active nucleoside amino acid esters, antibiotics and in the delivery of biological active agents (Dordick, 1989; Tamura *et al.*, 1985; Kirk *et al.*, 1992; Zaks and Dodds, 1997; Vulfson *et al.*, 1993). Chemical acylation of carbohydrates regio-selectively is complex due to the presence of multiple hydroxyl groups, which require protection and deprotection (Tamura *et al.*, 1985; Haines, 1981). When enzymes are used in organic media, they exhibit specificity (Wescott and Klibanov, 1994), thermostability (Ayala *et al.*, 1986; Wheeler and Croteau, 1986), molecular memory (Stahl *et al.*, 1991; Dabulis and Klibanov, 1993) and capacity to catalyze reverse reactions (Kuhl *et al.*, 1990; West *et al.*, 1990).

Hitherto, very few references are available on the lipase catalyzed esterification of amino acyl esters of sugars. Most of the earlier workers used proteases and N-protected and carboxyl group activated amino acids for synthesizing aminoacyl esters of carbohydrates (Riva *et al.*, 1988; Park *et al.*, 1996, 1999; Jeon *et al.*, 2001). Therisod and Klibanov (1986) used subtilisin to acylate carbohydrates with activated carboxylic acids in anhydrous organic solvents. Riva *et al.*, (1998) carried out subtilisin catalyzed synthesis of N-acetyl-L-alanyl-methyl- $\beta$ -D-galactopyranoside in anhydrous DMF, with an yield of 70% (4-O- 16 % and 6-O- 84 %) and N-acetyl-D-alanyl-methyl- $\beta$ -D-galactopyranoside with an yield of 35 % (2-O- 10 %, 3-O- 10 %, 4-O- 12 % and 6-O- 68 %). Suzuki *et al.*, (1998) synthesized L-alanyl-D-glucose by using D-glucose, methyl-L-alaninate hydrochloride and intact cells of *Rhodotorula lactosa*. There are no reports on the synthesis of L-valyl-D-glucose esters enzymatically. There are some reports on the chemical synthesis of methyl 2-O-[N-*t*-boc]-L-valyl-D-glucose, methyl-2,3-di-O-L-leucyl- $\alpha$ -D-glucose and methyl-3-O-[N-*t*-boc]-L-valyl-glucose and diesters such as ethyl-

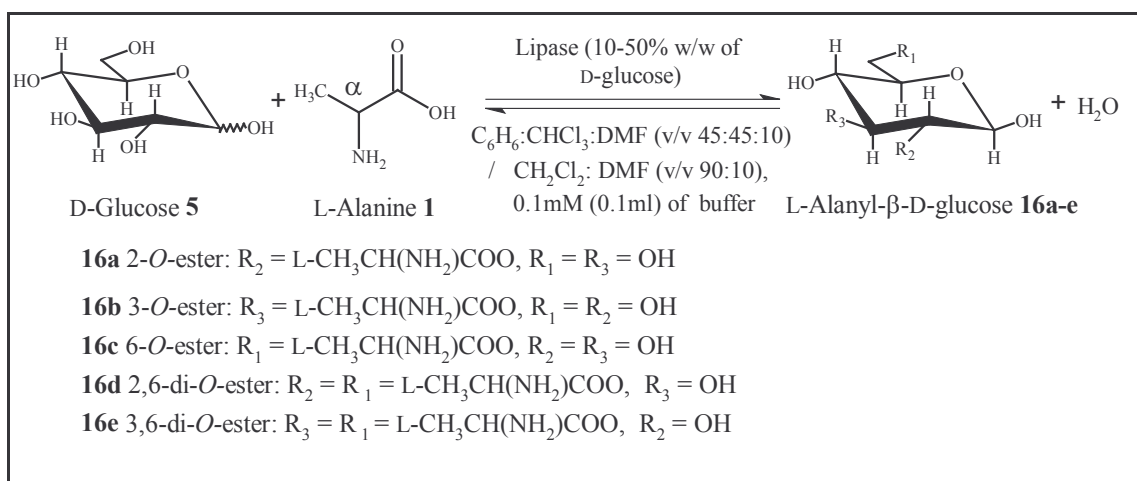
2,3-di-*O*-[*N*-*t*-*boc*]-L-valyl-D-glucose, methyl-2,3-di-*O*-L-valyl-D-glucose, methyl-4,6-di-*O*-L-valyl-D-glucose and methyl-2,3-di-*O*-L-isoleucyl- $\alpha$ -D-glucose (Tamura *et al.*, 1985) whose synthesis involved protection and deprotection. Park *et al.*, (1999) has carried out transesterification with Optimase M 440 to synthesize *t*-*boc*-leucyl-sucrose by using tert-butoxy-carbonyl-L-leucyl-cyanomethyl ester / tert-butoxy-carbonyl-L-leucyl-trifluoroethyl ester and sucrose. Maruyama *et al.*, (2002) have investigated the synthesis of N-acetyl-L-leucyl-D-glucose in *t*-butanol containing 10 % dimethyl sulfoxide by transesterification between N-acetyl-L-leucyl-cyanomethyl ester and D-glucose. Park *et al.*, (1999) reported that lipase from porcine pancreas and Lipozyme IM20 gave very low yields (< 2 %), compared to proteases which gave conversion yields ranging from 15 – 98 % when N-protected and carboxyl group activated amino acid was used for the acylation of D-glucose in pyridine. All these reactions were conducted in shake flasks using lesser quantity of substrates and larger quantity of enzymes.

In the present work, optimization of reaction parameters for the lipase catalyzed synthesis of L-alanyl, L-valyl and L-leucyl esters of D-glucose is described. Attempts to synthesize the same using N-acetyl-L-alanine resulted in very little conversion with the above mentioned enzymes. Hence, unprotected and unactivated L-amino acids and carbohydrates were employed to synthesize L-alanyl, L-valyl and L-leucyl acyl esters of carbohydrates using lipases from *Rhizomucor miehei* (RML), *Candida rugosa* (CRL) and porcine pancreas (PPL) as biocatalysts.

## 3.2. Present work

### 3.2.1. Synthesis of L-alanyl-D-glucose

Esterification was carried out in presence of lipase by incubating D-glucose and L-alanine in an organic media (**Scheme 3.1**). Lipases from *Rhizomucor miehei* (RML) and porcine pancreas (PPL) were employed for the reaction. The extent of esterification was monitored by HPLC (Fig. 3.1).



**Scheme 3.1** Lipases catalyzed regioselective synthesis of L-alanyl-D-glucose esters in anhydrous organic media

Since different equivalents of L-alanine were employed, the conversion yields were determined based on the peak areas of L-alanine and L-alanyl esters of carbohydrates and were expressed relative to the L-alanine concentration employed (Fig. 3.1). The error in HPLC yields were within 10 %. The esters formed were separated by size exclusion chromatography using Sephadex G-10/Bio Gel P-2 as column materials and eluted with water and subjected to spectral characterization by UV, IR, optical activity, MS and NMR (shown in detail in Section 3.3.1.1). The esterification reaction between unprotected and unactivated L-alanine and D-glucose was studied in detail using RML and PPL in terms of incubation period, lipase concentrations, substrate concentrations, buffer (pH and concentration) and enzyme reusability. The esterification reactions described in present work did not occur without the use of enzymes.

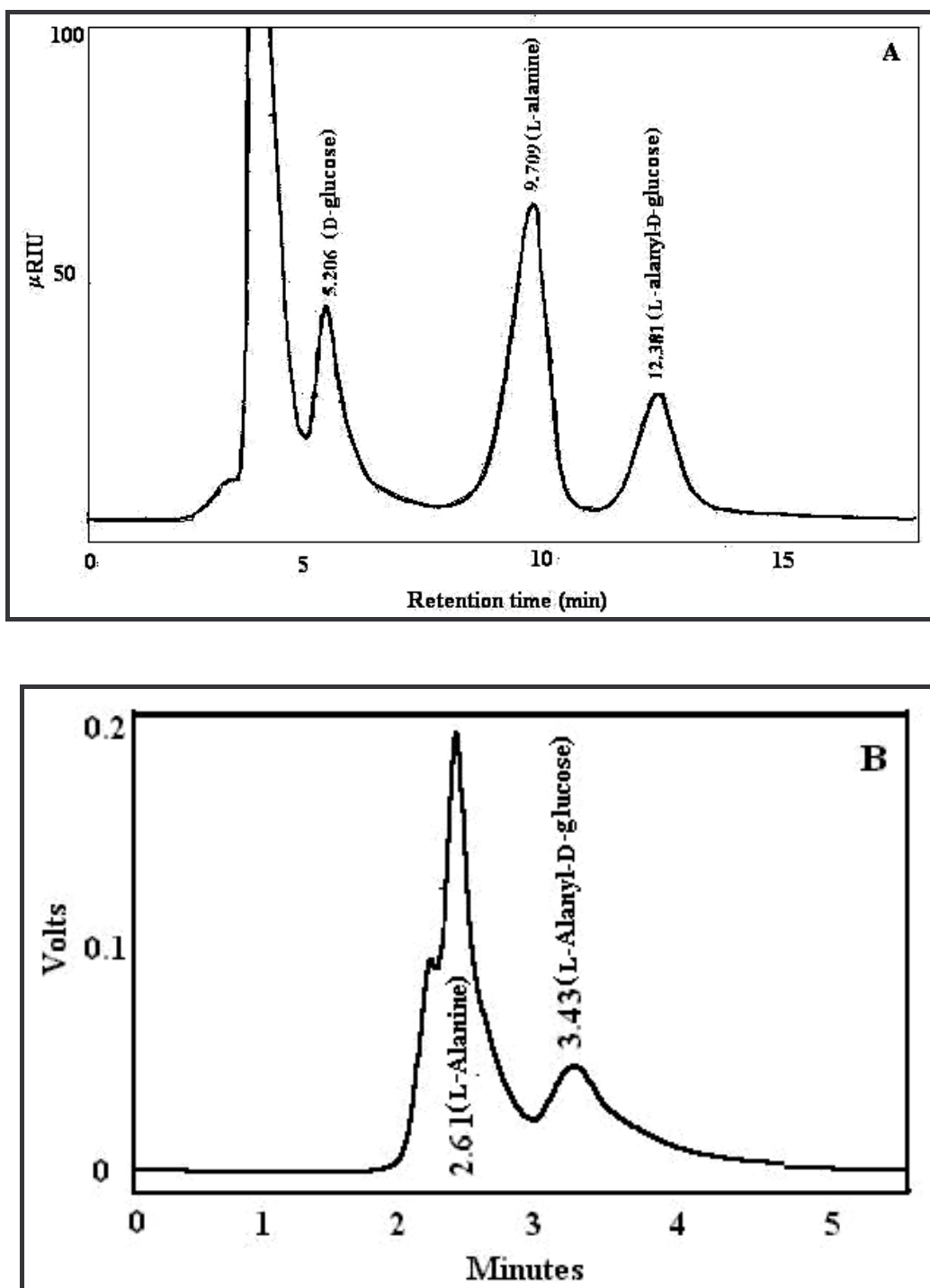


**Fig. 3.1.** HPLC chromatograph for the reaction mixture of L-alanine and D-glucose. (A) Column – aminopropyl, mobile phase – acetonitrile: water (80:20 v/v), flow rate - 1 ml/min, detector – Refractive Index. (B) Column – C-18, mobile phase – acetonitrile: water (v/v 20:80), flow rate- 1 ml/min, detector – UV at 210 nm. Errors in yields are within  $\pm 10\%$ .



### **3.2.1.1. Esterification profile**

In presence of RML (30 % w/w D-glucose), the conversion yields showed an increase in esterification from 5 % at 3 h to 26 % at 72h and thereafter remained constant up to 120 h at 26 % (Fig. 3.2). From the initial slope value of the plot, the rate of esterification was found to be 0.004 mmol h<sup>-1</sup>.

### **3.2.1.2. Effect of lipase concentration**

In case of RML (Table 3.1), maximum esterification (18 %) was achieved at 50 % w/w D-glucose (1 mmol D-glucose and 2 mmol L-alanine for incubation up to 72h). In case of PPL (Table 3.1), maximum yield of 18 % was achieved at 40 % w/w D-glucose (1 mmol D-glucose and 2 mmol L-alanine for an incubation period of 72 h). In presence of 0.1 mM (0.1 ml of 0.1 M) acetate buffer (pH 4.0), RML at 40 % w/w D-glucose showed (Table 3.1) a maximum esterification of 30 % (for 1 mmol D-glucose and 2 mmol L-alanine for incubation up to 72 h). While lesser amounts of enzymes ( $\leq 20$  % RML and PPL employed) could be inhibited by L-alanine (2 mmol) and D-glucose (1 mmol),  $>30$  % RML and PPL could favour better conversion as the enzyme/substrate ratio is enhanced.

Lipase from porcine pancreas purified partially (Section 2.2.18) was also employed in the range of 100 mg to 500 mg (Table 3.2) in presence of 0.1 mM (0.1 ml of 0.1 M) acetate buffer (pH 5.0). Esterification increased from 100 mg (41 %) to 200 mg (78 %) and thereafter decreased upto 500 mg (39 %).

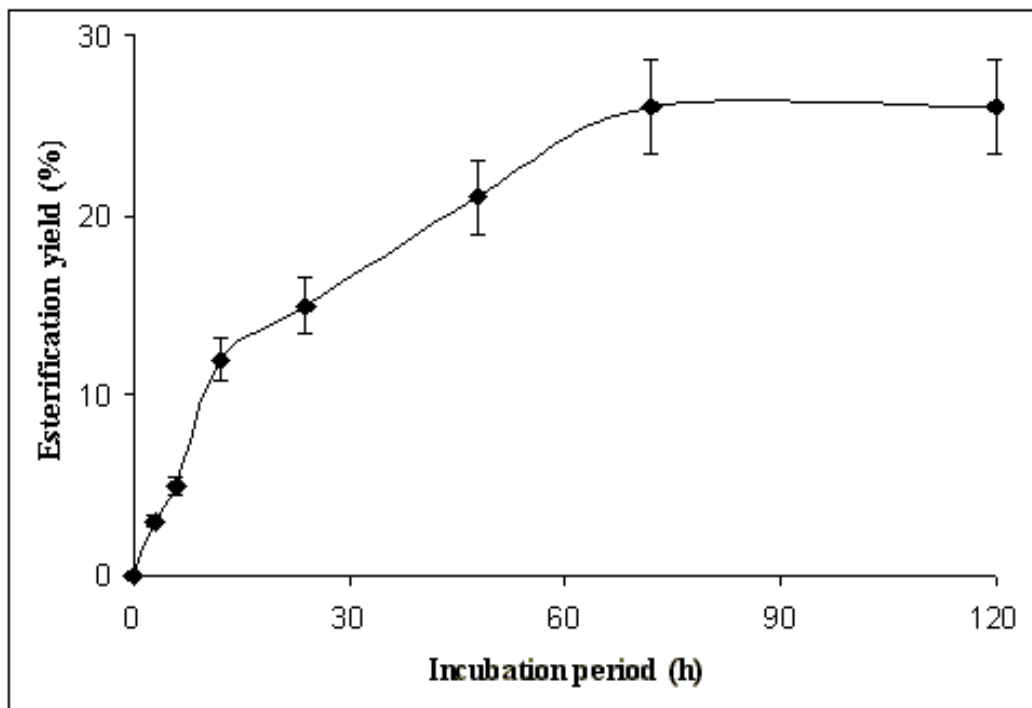


**Fig. 3.2.** Reaction profile for L-alanyl-D-glucose synthesis. Reaction conditions:  $\text{CH}_2\text{Cl}_2$ :DMF (v/v 90:10), RML -54 mg (30 % w/w D-glucose), L-alanine - 2 mmol, D-glucose - 1.0 mmol, Buffer - 0.1 mM (0.1 ml of 0.1M) acetate buffer (pH 4.0).

**Table 3.1 Effect of lipase concentration on the synthesis of L-alanyl-D-glucose <sup>a</sup>**

Lipase concentration (% w/w D-glucose)	<i>Rhizomucor miehei</i> lipase (RML) <sup>b</sup> Yield % (mmol)	Porcine pancreas lipase (PPL) <sup>c</sup> Yield % (mmol)	<i>Rhizomucor miehei</i> lipase (RML) <sup>d</sup> Yield % (mmol)
10	2 (0.04)	14 (0.27)	7 (0.14)
20	1 (0.02)	15 (0.29)	10 (0.21)
30	3 (0.05)	17 (0.35)	26 (0.53)
40	9 (0.17)	18 (0.36)	30 (0.60)
50	18 (0.37)	15 (0.29)	22 (0.44)

<sup>a</sup> D-glucose-1 mmol and L-alanine - 2 mmol. Conversion yields from HPLC determined with respect to L-alanine. Error in yield measurements will be  $\pm 10 - 15$  %. This applies to all the yields given in the subsequent tables also.

<sup>b</sup> Solvent - CHCl<sub>3</sub>:hexane:DMF - (v/v/v 45:45:10) at 60 °C.

<sup>c</sup> Solvent - CH<sub>2</sub>Cl<sub>2</sub>:DMF - (v/v 90:10) at 40 °C.

<sup>d</sup> Carried out in presence of buffer with 100 ml of solvent system b containing 0.1 mM (0.1 ml of 0.1M) acetate buffer (pH 4.0) .

**Table 3.2 Effect of partially purified PPL concentration on the synthesis of L-alanyl-D-glucose <sup>a</sup>**

Partially purified PPL concentration (% w/w of D-glucose)	Yield % (mmol)
55.6	41 (0.41)
111.1	78 (0.78)
166.7	64 (0.68)
222.2	50 (0.50)
277.8	39 (0.39)

<sup>a</sup> D-glucose - 1 mmol and L-alanine - 1 mmol; Solvent CH<sub>2</sub>Cl<sub>2</sub>:DMF - (v/v 90:10) at 40 °C. Carried out in presence of buffer with 100 ml of solvent system b containing 0.2 mM (0.2 ml of 0.1 M) acetate buffer (pH 5.0).

### 3.2.1.3. Effect of buffer salts

While earlier workers have not studied the effect of buffer salts on this esterification reaction, the present study investigated the same, in connection with both the stabilization of the enzyme in non-polar solvents and also the use of zwitter ionic amino acid in the reaction. Carrying out this esterification reaction in presence of buffers

of certain pH not only imparted 'pH memory' or 'pH tuning' to the enzyme, but also provided the optimum water activity necessary for better performance of the enzyme. Besides, addition of buffer salts of certain concentration also affected the ionic activities of especially the micro-aqueous layer around the enzyme, where the buffer salts are concentrated during the course of the reaction. All these have been found to be operative in these esterification reactions.

In presence of buffer salts, conversion yield increased in case of RML. In presence of 0.1 mM (0.1 ml of 0.1 M) pH 4.0 buffer, RML showed maximum esterification of 26 % (at 1 mmol D-glucose and 2 mmol L-alanine for a period of 72 h, Table 3.3). However, PPL, in presence of 0.1 mM (0.1 ml of 0.1 M) pH 5.0 buffer showed maximum esterification of 17 % only (Table 3.3), similar to the conversion yield obtained in the absence of buffer salts.

The effect of buffer salt concentration was studied by using different concentrations (0.05 mM to 0.5 mM) of pH 4.0 buffer in case of RML and pH 5.0 buffer in case of PPL. In case of RML, the maximum conversion yield of 26 % (at 1 mmol D-glucose and 2 mmol L-alanine for 72 h) was obtained when 0.1 mM (0.1 ml) pH 4.0 buffer was employed (Table 3.3). In case of PPL, 0.5 mM (0.5 ml) pH 5.0 buffer showed the maximum conversion yield (Table 3.3) of 17 % (at 1 mmol D-glucose and 2 mmol L-alanine for 72 h incubation).

**Table 3.3 Effect of buffer salts (pH and buffer concentration) on the synthesis of L-alanyl-D-glucose<sup>a</sup>**

RML				PPL			
pH <sup>b</sup>	Yield % (mmol)	pH 4.0 <sup>c</sup> concn mM	Yield % (mmol)	pH <sup>d</sup>	Yield % (mmol)	pH 5.0 <sup>e</sup> concn mM	Yield % (mmol)
4.0	26 (0.53)	0.05	25 (0.49)	4.0	9 (0.18)	0.05	13 (0.25)
5.0	7 (0.13)	0.1	26 (0.53)	5.0	17 (0.33)	0.1	17 (0.33)
6.0	20 (0.39)	0.2	8 (0.16)	6.0	15 (0.31)	0.2	11 (0.23)
7.0	8 (0.16)	0.3	7 (0.15)	7.0	11 (0.23)	0.3	10 (0.21)
8.0	10 (0.19)	0.4	17 (0.34)	8.0	No yield	0.4	12 (0.24)
-	-	0.5	18 (0.35)	-	-	0.5	17 (0.34)

<sup>a</sup> D-glucose - 1 mmol and L-alanine - 2 mmol; Incubation period - 72 h; RML – 30 % (w/w D-glucose). 100 ml of the solvent containing specified volumes, concentration and pH of the buffer

<sup>b</sup> Solvent – 100 ml CHCl<sub>3</sub>:hexane:DMF (v/v/v 45:45:10) at 60 °C; Buffer - 0.1 mM (0.1 ml of 0.1 M) appropriate pH buffer

<sup>c</sup> Solvent – 100 ml CH<sub>2</sub>Cl<sub>2</sub>:DMF (v/v 90:10) at 40 °C; Buffer – 0.05 ml to 0.5 ml of 0.1 M acetate (pH 4.0).

<sup>d</sup> Same solvent system as c. Buffer - 0.1 mM (0.1 ml of 0.1 M) appropriate pH.

<sup>e</sup> Solvent – Same solvent system as c. 0.05 ml to 0.5 ml of 0.1 M acetate (pH 5.0).

#### 3.2.1.4. Effect of substrate concentration

When L-alanine was varied from 1 mmol to 5 mmol at a constant 1 mmol D-glucose, there was in general, an increase in esterification (Fig. 3.3) from 0.68 mmol (68 % with respect to 1 mmol L-alanine - 0.54 mmol monoesters and 0.14 mmol diesters) to 1.12 mmol (28 % with respect to 4 mmol L-alanine – 0.88 mmol monoesters and 0.24 mmol diesters) in presence of 30 % (w/w D-glucose) RML, 0.1 mM (0.1 ml of 0.1 M) acetate buffer (pH 4.0) for 72 h incubation. The yields were determined with respect to L-alanine concentrations which were usually greater than that of D-glucose (1 mmol). In terms of D-glucose, one D-glucose molecule forms mono as well as diesters with L-alanine. Hence, in presence of higher equivalents of L-alanine, yields >1 mmol (D-glucose concentration) are reported.

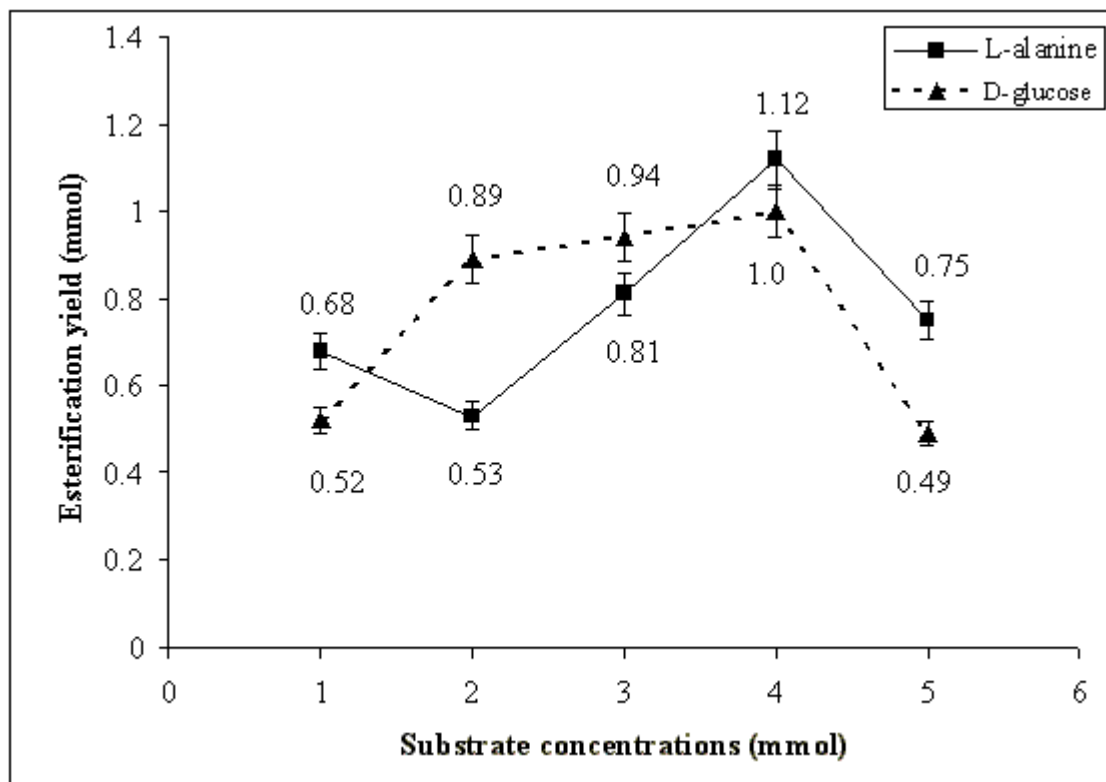


**Fig 3.3.** Effect of substrate concentration on synthesis of L-alanyl-D-glucose. RML – 30 % (w/w D-glucose); Solvent -  $\text{CH}_2\text{Cl}_2$ :DMF - (v/v 90:10) at 40 °C; Buffer – 0.1 mM (0.1 ml of 0.1 M) acetate buffer (pH 4.0). L-alanine (■) – 1 – 5 mmol at 1 mmol D-glucose; D-glucose (▲) – 1 – 5 mmol at 1 mmol L-alanine and a constant enzyme concentration of 54 mg.

Similarly, when D-glucose was varied from 1 mmol to 5 mmol, at a constant 1 mmol L-alanine, there was a steep increase in esterification from 52 % (0.52 mmol - 0.41 mmol monoesters and 0.11 mmol diesters) at 1mmol D-glucose to > 99 % (> 0.99 mmol - 0.78 mmol monoesters and 0.21 mmol diesters) at 4 mmol D-glucose. In both the cases, esterification decreased after 4 equivalents which could be due to inhibition at higher concentrations of L-alanine and D-glucose.

### **3.2.1.5. Reusability of lipases**

Reusability of both RML and PPL employed were studied at optimized conditions. After completion of each reaction (cycle, 72 h), the enzyme was separated from the reaction mixture by filtration, air dried and reused in the next reaction. After each cycle, total esterification activity ( $\mu\text{mol}/\text{min}$ ) of the enzyme was determined. In case of RML, there was a steady loss of 15 % to 22 % of enzyme concentration after each cycle (Table 3.4) both in presence as well as absence of 0.2 mM (0.2 ml of 0.1 M) acetate buffer (pH 4.0). In the absence of buffer salts, the esterification activity decreased from 24 % (1<sup>st</sup> cycle: total enzyme activity - 99.4  $\mu\text{mol}/\text{min}$ ) to 8 % (4<sup>th</sup> cycle- total enzyme activity - 23.5  $\mu\text{mol}/\text{min}$ ). The yields in 2<sup>nd</sup> and 3<sup>rd</sup> cycles were 17 % (total enzyme activity - 66.4  $\mu\text{mol}/\text{min}$ ) and 10 % (total enzyme activity - 43.1  $\mu\text{mol}/\text{min}$ ) respectively. In presence of buffer salts (pH 4.0), the esterification activity decreased from 17 % (1<sup>st</sup> cycle: total enzyme activity - 99.4  $\mu\text{mol}/\text{min}$ ) to 5 % (4<sup>th</sup> cycle - enzyme activity of 23  $\mu\text{mol}/\text{min}$ ). The yields in 2<sup>nd</sup> and 3<sup>rd</sup> cycles were 11 % (total enzyme activity - 66.9  $\mu\text{mol}/\text{min}$ ) and 8 % (total enzyme activity - 42.2  $\mu\text{mol}/\text{min}$ ) respectively.

However, in case of PPL, there was a drastic loss of enzyme concentration from 20 % to 60 % after each cycle, as PPL was partially soluble in water and the reaction was stopped after the 2<sup>nd</sup> cycle due to reduction in enzyme (Table 3.4). In the absence of

buffer salts, esterification activity of the PPL decreased from 19 % (1<sup>st</sup> cycle- total enzyme activity - 15  $\mu\text{mol}/\text{min}$ ) to 3 % (4<sup>th</sup> cycle-total enzyme activity - 0.7  $\mu\text{mol}/\text{min}$ ). The 2<sup>nd</sup> and 3<sup>rd</sup> cycle yields were 12 % (total enzyme activity - 5.6  $\mu\text{mol}/\text{min}$ ) and 10 % (total enzyme activity - 3.3  $\mu\text{mol}/\text{min}$ ) respectively. However, in presence of buffer salts (pH 5.0), the esterification activity decreased slightly from 11 % (1<sup>st</sup> cycle- total enzyme activity - 15  $\mu\text{mol}/\text{min}$ ) to 6 % (2<sup>nd</sup> cycle-total enzyme activity - 4.1  $\mu\text{mol}/\text{min}$ ). **Table**

### 3.4 Reusability of lipase in presence and absence of buffer salts <sup>a</sup>

No. of reactions (cycles)	RML		PPL	
	% Yield (Total enzyme activity, $\mu\text{mol}/\text{min}$ )	% Yield <sup>b</sup> (Total enzyme activity, $\mu\text{mol}/\text{min}$ )	% Yield (Total enzyme activity, $\mu\text{mol}/\text{min}$ )	% Yield <sup>c</sup> (Total enzyme activity, $\mu\text{mol}/\text{min}$ )
1	24 (99.4)	17 (99.4)	19 (15)	11 (15)
2	17 (66.4)	11 (66.9)	12 (5.6)	6 (4.1)
3	10 (43.1)	8 (42.2)	10 (3.3)	-
4	8 (23.5)	5 (24.6)	3 (0.7)	-

<sup>a</sup> D-glucose - 4 mmol and L-alanine - 8 mmol; Incubation period -72 h; Solvent - 100 ml  $\text{CH}_2\text{Cl}_2:\text{DMF}$  - (v/v 90:10) at 40 °C. Total enzyme activity of the recovered enzyme employed for the reaction. Percentage yields are an average from two independent experiments.

<sup>b</sup> in presence of 0.2 mM (0.2 ml of 0.1M) acetate buffer (pH 4.0) in each cycle.

<sup>c</sup> in presence of 0.2 mM (0.2 ml of 0.1 M) acetate buffer (pH 5.0) in each cycle.

#### 3.2.1.6. Synthesis of L-alanyl-D-glucose at gram scale using crude PPL and immobilized PPL

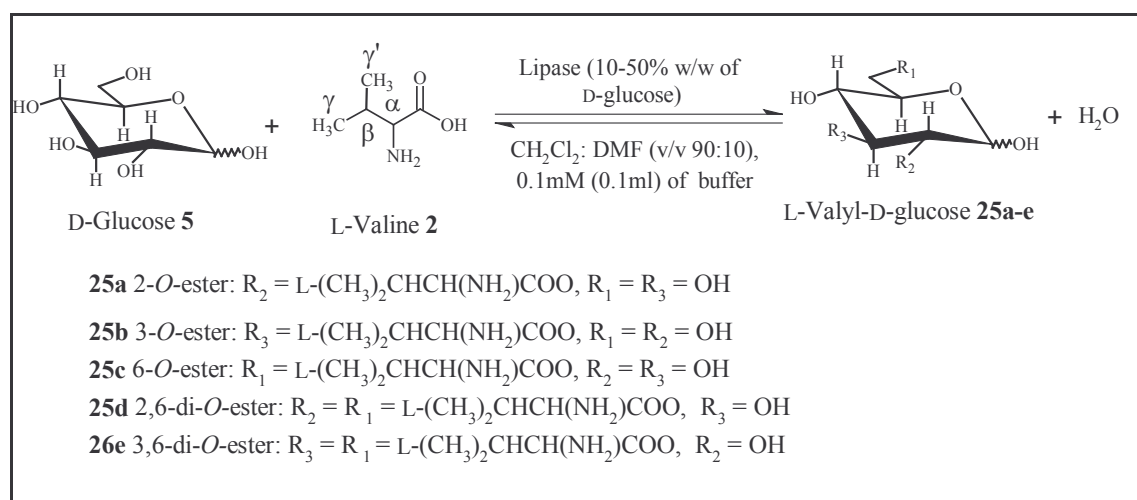
Synthesis of L-alanyl-D-glucose was carried out at large scale by employing 1 g L-alanine, 2 g D-glucose in 200 ml of  $\text{CH}_2\text{Cl}_2:\text{DMF}$  (v/v 90:10) in presence of 1 g of crude PPL (50 % w/w D-glucose, described in Section 2.2.18) / 1.5 g of immobilized PPL (described in Section 2.2.19) and 1.15 mM (2.3 ml of 0.1 M) acetate buffer (pH 5.0) for a period of 72 h. Conversion yield of 47 % with crude PPL and 58 % with immobilized PPL were obtained.



### 3.2.2. Synthesis of L-valyl-D-glucose

Esterification was carried out in presence of lipase by incubating D-glucose and L-valine in an organic media (**Scheme 3.2**). Lipases from *Rhizomucor miehei* (RML) and porcine pancreas (PPL) were employed for the reaction. The extent of esterification was monitored by HPLC (Fig. 3.4). The esters formed were separated by size exclusion chromatography using Sephadex G-10/Bio Gel P-2 as column materials and eluted with water and subjected to spectral characterization by UV, IR, optical activity, MS and NMR (shown in detail in Section 3.3.1.2).

The esterification reaction between unprotected and unactivated L-valine and D-glucose was studied in detail using RML and PPL in terms of incubation period, lipase concentrations, buffer (pH and concentration) and substrate concentrations.



**Scheme 3.2 Lipases catalysed synthesis of L-valyl-D-glucose esters in anhydrous organic media**

#### 3.2.2.1. Esterification profile

For CRL (40 % w/w D-glucose) catalyzed esterification of L-valine with D-glucose (1 mmol each) in presence of 0.1 mM (0.1 ml of 0.1 M) phosphate buffer (pH 7.0), it was found that there was a linear increase in esterification upto 72 h and thereafter decreased at 120h (Fig. 3.5). Esterification yield obtained after each incubation period was: 52 % (0.52 mmol) at 6 h, 56 % (0.56 mmol) at 12 h, 57 % (0.57 mmol) at 24 h, 61 % (0.61

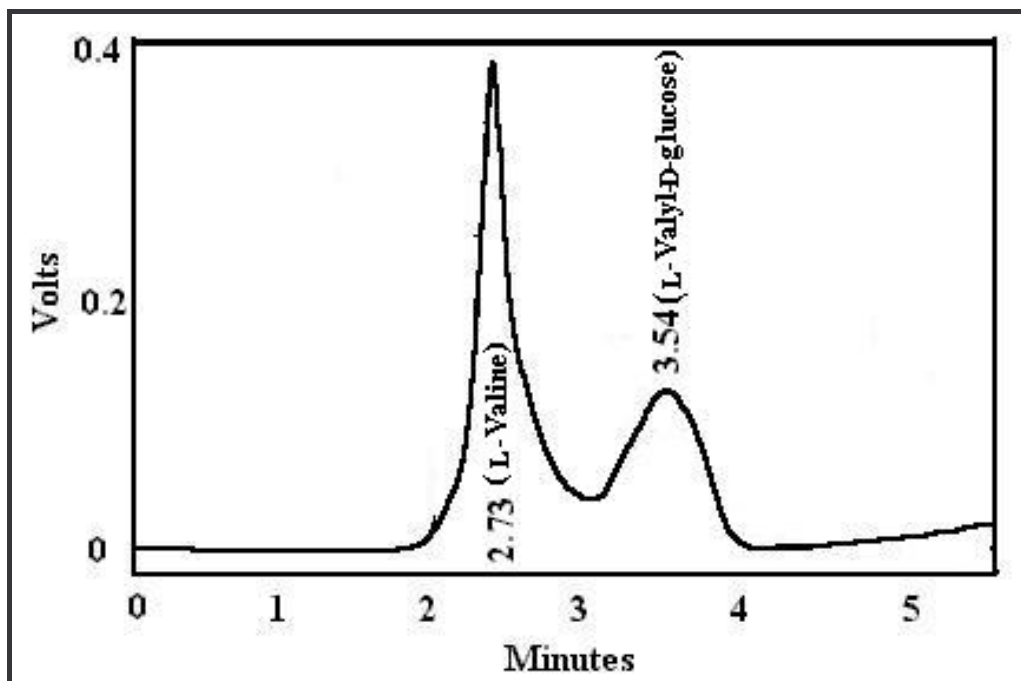


**Fig. 3.4.** HPLC chromatograph for the reaction mixture of L-valine and L-valyl-D-glucose. Column – C-18, mobile phase – acetonitrile: water (v/v 20:80), flow rate- 1 ml/min, detector – UV at 210nm. Errors in yields are within  $\pm 10\%$ .

mmol) at 48 h, 68 % (0.68 mmol) at 72 h, 52 % (0.52 mmol) at 96 h and 47 % (0.47 mmol) at 120 h. From the initial slope value, the initial rate of esterification was found to be 0.0425 mmol h<sup>-1</sup>

### 3.2.2.2. Effect of buffer salts

Treatment of buffer salts stabilizes three-dimensional structure of enzymes against denaturation in organic solvents by dissolving in the micro aqueous layer thereby imparting effective ‘pH memory’ or ‘pH tuning’ to the enzyme. A buffer of known pH and concentration was treated to the reaction mixture to study the effect of imparting ‘pH tuning’ to the enzyme on esterification.

Effect of buffer salts at a fixed CRL concentration of 40 % (w/w of D-glucose) and 1:1 millimolar equivalent of D-glucose and L-valine on the synthesis of L-valyl-D-glucose showed that CRL in presence of 0.1 mM (0.1 ml of 0.1 M) phosphate buffer (pH 7.0) showed the highest yield of 68 % (0.68 mmol) which was 48 % higher than in its absence (Table 3.5). With increase in buffer concentration above 0.1 mM (0.1 ml) there was a steady decrease in esterification. It was found that 0.1 mM (0.1 ml of 0.1 M) phosphate buffer (pH 7.0) showed the highest yield of 68 % (0.68 mmol).

**Table 3.5 Effect of buffer salts (pH and buffer concentration) on the synthesis of L-valyl-D-glucose<sup>a</sup>**

pH <sup>b</sup>	Yield % (mmol)	pH 7.0 <sup>c</sup> concn mM	Yield % (mmol)
4.0	47 (0.47)	0.05	58 (0.58)
5.0	43 (0.43)	0.1	68 (0.68)
6.0	59 (0.59)	0.2	48 (0.48)
7.0	64 (0.64)	0.3	49 (0.49)
8.0	54 (0.54)	0.4	44 (0.44)
-	-	0.5	43 (0.43)

<sup>a</sup> D-glucose - 1mmol and L-valine - 1 mmol; Incubation period - 72h; CRL – 40 % (w/w D-glucose); 100 ml of the solvent containing specified volumes, concentration and pH of the buffer. <sup>b</sup> Solvent - 100 ml CH<sub>2</sub>Cl<sub>2</sub>:DMF (v/v 90:10) at 40 °C . Buffer - 0.1 mM (0.1 ml of 0.1 M) appropriate pH buffer.

<sup>c</sup> Solvent – 100 ml. Buffer - 0.05 ml to 0.5 ml of 0.1 M phosphate (pH 7.0).

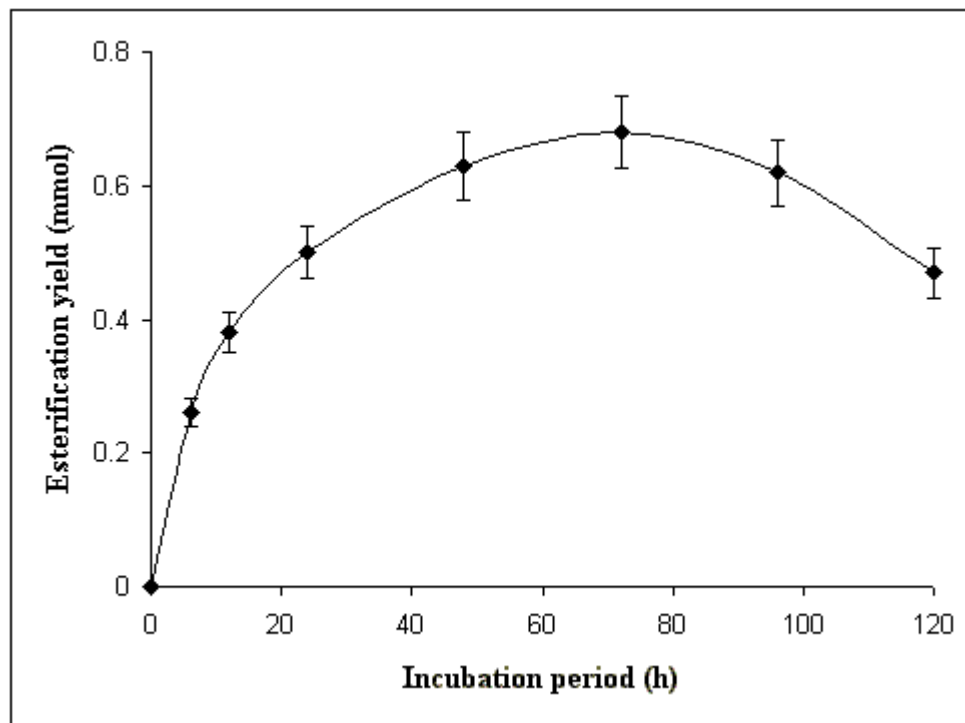


**Fig. 3.5.** Effect of incubation period on esterification of L-valyl-D-glucose. CRL – 40 % (w/w D-glucose); D-glucose - 1 mmol and L-valine - 1 mmol; Solvent - CH<sub>2</sub>Cl<sub>2</sub>:DMF - (v/v 90:10) at 40 °C. Buffer - 100 ml of solvent containing 0.1 mM (0.1 ml of 0.1 M) phosphate buffer (pH 7.0).

### 3.2.2.3. Effect of lipase concentration

With increase in CRL concentration, in the lipase range 10 % to 50 % (w/w D-glucose) at 1 mmol of both D-glucose and L-valine, there was a steady increase in esterification upto 40 % enzyme concentration in the absence of the buffer, with a maximum yield of 0.19 mmol (Table 3.6). However, in presence of 0.1 mM (0.1 ml of 0.1 M) phosphate buffer (pH 7.0), with the increase in CRL concentration, there was a steady increase in esterification upto 30 % enzyme concentration (84 %, 0.84 mmol) which decreased thereafter upto 50 % of lipase concentration (Table 3.6). Both 10 % (w/w D-glucose) RML and PPL in presence of 0.1 mM (0.1 ml of 0.1 M) acetate buffer (pH 5.0) showed a maximum yield of 59 % (0.59 mmol) and 62 % (0.62 mmol) respectively which thereafter decreased upto 50 % of lipase concentration (Table 3.6).

**Table 3.6** Effect of lipase concentration on the synthesis of L-valyl-D-glucose <sup>a</sup>

Lipase concentration (% w/w D-glucose)	<i>Candida rugosa</i> lipase (CRL) Yield % (mmol)	<i>Candida rugosa</i> lipase (CRL) <sup>b</sup> Yield % (mmol)	<i>Rhizomucor miehei</i> lipase (RML) <sup>c</sup> Yield % (mmol)	Porcine pancreas lipase (PPL) <sup>c</sup> Yield % (mmol)
10	2 (0.02)	73 (0.73)	59 (0.59)	62 (0.62)
20	6 (0.06)	77 (0.77)	41 (0.41)	45 (0.45)
30	14 (0.14)	84 (0.84)	31(0.31)	33 (0.33)
40	25 (0.25)	68 (0.68)	24 (0.24)	27 (0.27)
50	10 (0.10)	65 (0.65)	25 (0.25)	36 (0.36)

<sup>a</sup> D-glucose - 1 mmol and L-valine - 1 mmol; Solvent - CH<sub>2</sub>Cl<sub>2</sub>:DMF - (v/v 90:10) at 40 °C.

<sup>b</sup> Carried out in presence of buffer with 100 ml of solvent containing 0.1 mM (0.1 ml of 0.1 M) phosphate buffer (pH 7.0).

<sup>c</sup> Carried out in presence of buffer with 100 ml of solvent containing 0.1 mM (0.1 ml of 0.1 M) acetate buffer (pH 5.0).

### 3.2.2.4. Effect of L-valine and D-glucose concentration

Effect of L-valine and D-glucose concentrations at a fixed CRL concentration of 40 % (w/w D-glucose) on the synthesis of L-valyl-D-glucose was investigated (Fig. 3.6). When L-valine concentrations were varied in the range 1 to 5 mmol at a fixed 1 mmol of

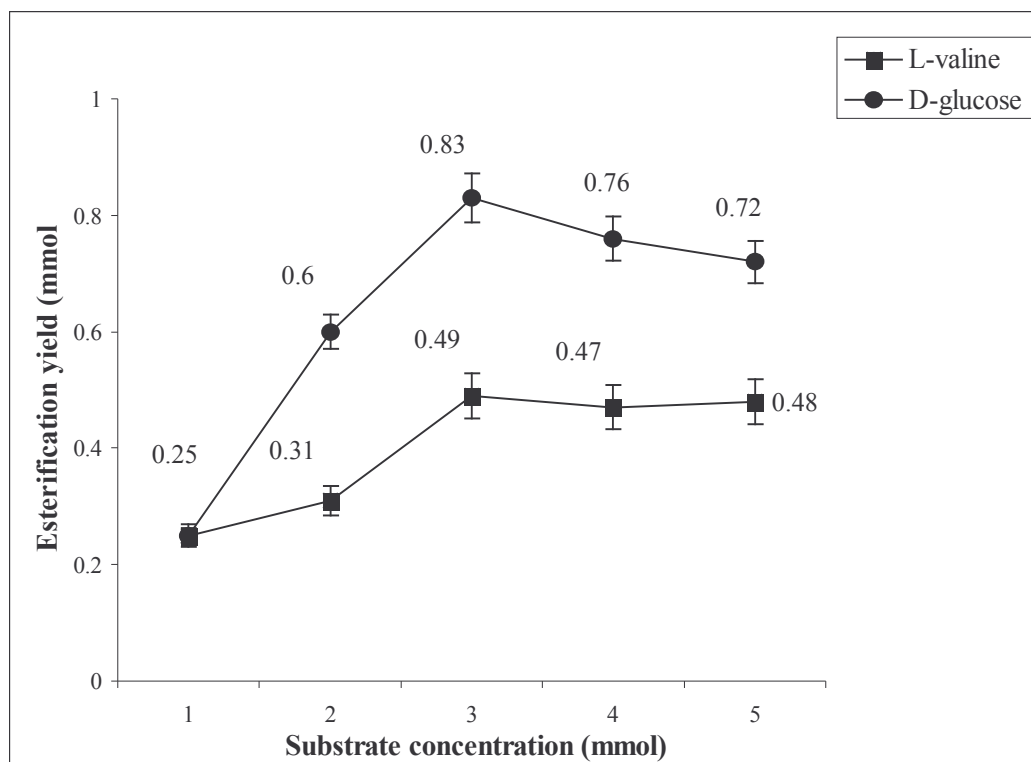
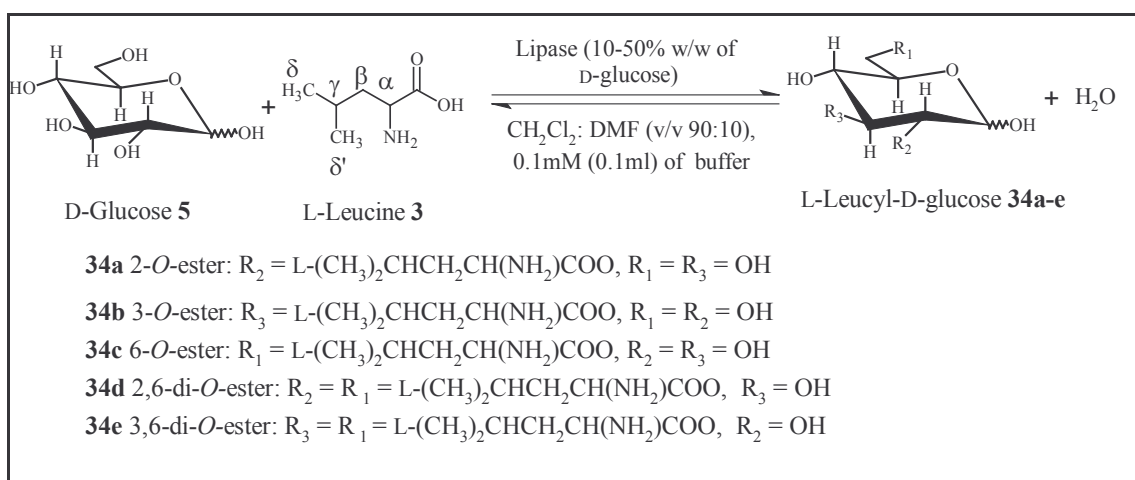


**Fig. 3.6.** Effect of substrate concentration on synthesis of L-valyl-D-glucose. CRL – 40 % (w/w D-glucose); Solvent -  $\text{CH}_2\text{Cl}_2$ :DMF - (v/v 90:10) at 40 °C. L-Valine (■) – 1 – 5 mmol at 1 mmol D-glucose; D-glucose (●) – 1 – 5 mmol at 1 mmol L-valine and a constant enzyme concentration of 72 mg.

D-glucose, there was an increase in esterification from 1 mmol L-valine (yield - 0.25 mmol) to 3 mmol L-valine (yield - 0.49 mmol) and thereafter remained constant upto 5 mmol L-valine. Similarly, when D-glucose was varied from 1 mmol to 5 mmol at a fixed 1 mmol of L-valine, there was a steep increase in esterification from 1 mmol D-glucose (yield - 0.25 mmol) to 3 mmol D-glucose (yield - 0.83 mmol) and thereafter decreased upto 5 mmol D-glucose (yield - 0.72 mmol). In both the cases, esterification increased upto 3 equivalents, indicating that L-valine and D-glucose are not inhibitors to CRL.

### 3.2.3. Synthesis of L-leucyl-D-glucose

Esterification was carried out in presence of lipase from *Rhizomucor miehei* (RML) and porcine pancreas (PPL) by incubating D-glucose and L-alanine in an organic media (**Scheme 3.3**). The extent of esterification was monitored by HPLC. The esters formed were separated by size exclusion chromatography using Sephadex G-10 / Bio Gel P-2 as column materials and eluted with water and subjected to spectral characterization by UV, IR, optical activity, MS and NMR (shown in detail in Section 3.3.1.3). The esterification reaction between unprotected and unactivated L-leucine and D-glucose was studied in detail using RML and PPL in terms of lipase concentrations, buffer (pH and concentration) and substrate concentrations.



**Scheme 3.3. Lipases catalyzed synthesis of L-leucyl-D-glucose esters in anhydrous organic media**

### 3.2.3.1. Effect of *Rhizomucor miehei* lipase concentration

Effect of increasing lipase concentration on the synthesis of L-leucyl-D-glucose ester was studied by employing various RML concentrations ranging from 10 % to 50 % (w/w D-glucose, Table 3.7). The results showed that the yields obtained were very low. The enzyme showed the highest yield of 10.8 % (0.22 mmol) at 20 % enzyme concentration. With the increase in enzyme concentration from 10 % (yield - 0.11 mmol, 5.7 %) to 20 % (yield - 0.22 mmol, 10.8 %) there was an increase in esterification and beyond 30 % there was decrease (30 % - 0.04 mmol, 0.2 % yield; 50 % - 0.03 mmol, 0.3 % yield) in esterification probably due to hydrolysis of the esters formed.

**Table 3.7 Effect of lipase concentration on the synthesis of L-leucyl-D-glucose<sup>a</sup>**

RML concentration (% w/w D-glucose)	<i>Rhizomucor miehei</i> lipase (RML) Yield % (mmol)
10	5.7 (0.11)
20	10.8 (0.22)
30	0.2 (0.04)
50	0.3 (0.06)

<sup>a</sup> D-glucose - 1 mmol and L-leucine - 2 mmol. Conversion yields from HPLC determined with respect to L-leucine. Error in yield measurements will be  $\pm 10 - 15$  %. Solvent - CH<sub>2</sub>Cl<sub>2</sub>:DMF (v/v 90:10) at 40 °C. Buffer - 100 ml of solvent containing 0.1 mM (0.1 ml of 0.1 M) acetate buffer (pH 4.0).

### 3.2.3.2. Effect of L-leucine concentration

Effect of L-leucine concentrations at fixed RML and PPL concentrations of 30 % (w/w D-glucose) on the synthesis of L-leucyl-D-glucose ester was studied by increasing the L-leucine concentration from 1 to 5 molar equivalent (Table 3.8). The results showed that better conversions could be achieved with both the enzymes at 5 equivalents of L-leucine.



**Table 3.8** Effect of L-leucine on the synthesis of L-leucyl-D-glucose <sup>a</sup>

L-Leucine (mmol)	Yield % (mmol)	
	RML	PPL
1	0.2 (0.04)	18 (0.31)
2	7 (0.14)	4 (0.8)
3	6 (0.12)	9 (0.18)
4	8 (0.16)	6 (0.12)
5	36 (0.72)	24 (0.48)

<sup>a</sup> Lipase – 40 % (w/w D-glucose); L-leucine – 1 – 5 mmol at 1 mmol D-glucose; Solvent – CH<sub>2</sub>Cl<sub>2</sub>:DMF - (v/v 90:10) at 40 °C.

### 3.2.3.3. Effect of buffer salts

Depending on the method of preparation, the enzyme always possesses a micro-aqueous layer around it. Buffer salts dissolve in such a micro aqueous layer and stabilize the enzyme structure against denaturation and subsequent loss of activity in non-polar solvents. A buffer of known pH and volume was added to the reaction mixture and their effect on imparting ‘pH memory’ or ‘pH tuning’ to the enzyme was studied. This reaction also gave better yields in presence of buffer salts than in their absence. Effect of buffer salts in terms of pH in the range 4.0 to 8.0 with RML at 40 % (w/w D-glucose) on the synthesis of L-leucyl-D-glucose ester at 1:2 molar equivalent of D-glucose and L-leucine (Table 3.9) showed that 0.2 mM (0.1 ml of 0.1 M) acetate buffer (pH 5.0) gave the highest yield of 63 % (0.63 mmol). The yields were: 16 % (0.31 mmol) at pH 4.0, 16 % (0.33 mmol) at pH 6.0, 14 % (0.27 mmol) at pH 7.0 and 7 % (0.14 mmol) at pH 8.0. The effect of various buffer volumes in the range 0.05 mM (0.05 ml) to 0.6 mM (0.6 ml) of phosphate buffer (pH 7.0) showed that the esterification yields increased with increase in the buffer concentration from 0.05 mM (0.05 ml) to 0.6 mM (0.6 ml) with 0.6 mM (0.6 ml) phosphate buffer (pH 7.0) showing the highest yield of 85 % (1.7 mmol).

**Table 3.9 Effect of buffer salts (pH and buffer concentration) on the synthesis of L-leucyl-D-glucose<sup>a</sup>**

pH <sup>b</sup>	Yield % (mmol)	pH 7.0 <sup>c</sup> concn mM	Yield % (mmol)
4.0	16 (0.31)	0.05	5 (0.1)
5.0	63 (1.26)	0.1	21 (0.42)
6.0	16 (0.33)	0.2	14 (0.28)
7.0	14 (0.27)	0.4	32 (0.64)
8.0	7 (0.14)	0.6	85 (1.70)

<sup>a</sup> D-glucose – 1 mmol and L-leucine - 2 mmol; Incubation period - 72 h; RML – 40 % (w/w D-glucose) 100 ml of the solvent containing specified volumes, concentration and pH of the buffer

<sup>b</sup> Solvent – 100 ml C<sub>6</sub>H<sub>6</sub>:CHCl<sub>3</sub>:DMF (v/v/v 45:45:10) at 60 °C. Buffer - 0.2 mM (0.2 ml of 0.1 M) appropriate pH buffer.

<sup>c</sup> Solvent – 100 ml. Buffer - 0.05 ml to 0.6 ml of 0.1 M phosphate (pH 7.0).

### 3.2.4. Selectivity:

An attempt to improve the selectivity of ester formation was also made by reducing the incubation period in case of L-alanyl-D-glucose synthesis using RML (at 1 mmol D-glucose and 2 mmol L-alanine, RML – 40 % w/w D-glucose, incubation period - 12 h, solvent CH<sub>2</sub>Cl<sub>2</sub>:DMF - (v/v 90:10) at 40 °C buffer – 100 ml of solvent containing 0.1 mM acetate buffer, pH 4.0). A conversion yield of 15 % was obtained. From two-dimensional HSQCT NMR the formation of three monoesters (6-*O*- 42 %, 3-*O*- 33 % and 2-*O*- 25 %) with only β-anomer of D-glucose were found, the D-glucose employed being a 40:60 mixture of α and β anomers respectively.

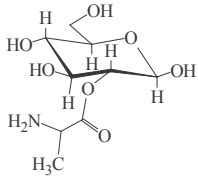
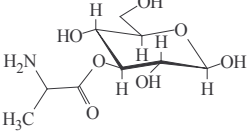
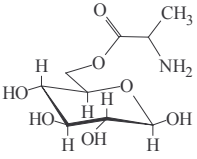
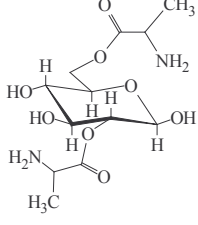
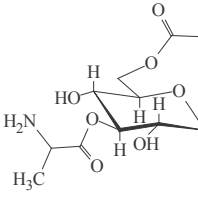
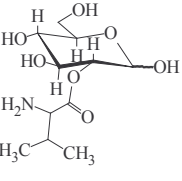
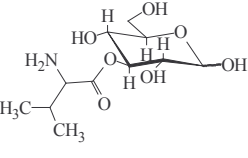
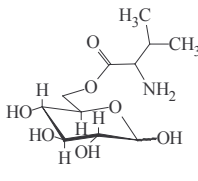
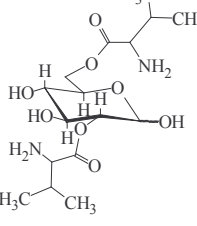
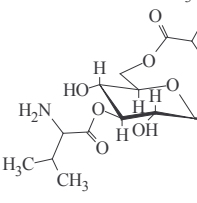
### 3.2.5. Determination of Critical Micellar Concentration (CMC)

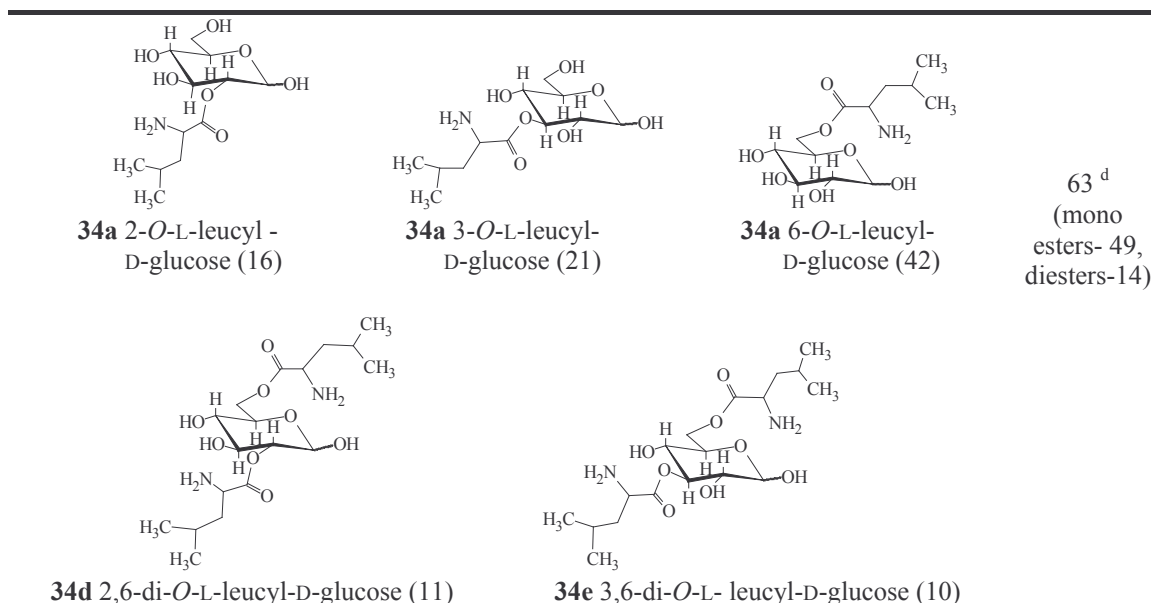
Surfactant property of the amino acyl esters of carbohydrate was evaluated by determining the critical micellar concentration (CMC) value for L-alanyl-β-D-glucose spectroscopically at 470 nm (Rosenthal and Koussale, 1983) by following the method explained in Section 2.2.12. The CMC of L-alanyl-β-D-glucose was found to be 2.25 mM (0.056 %).

### 3.3. Products of L-alanyl, L-valyl and L-leucyl esters of D-glucose

The isolated esters were subjected to UV, IR, MS and 2-D HSQCT NMR characterization (Section 3.3.1.1 – 3.3.1.3). Table 3.10 shows the ester yields from HPLC, types of esters formed and percentage proportions of the individual esters yields from HPLC by both RML and CRL.

**Table 3.10 Synthesis of L-alanyl, L-valyl and L-leucyl esters of D-glucose<sup>a</sup>**

L-amino acyl esters of D-glucose (% proportions <sup>c</sup> )			Yield (%)
			30 <sup>b</sup> (mono esters- 24, diesters-6)
<b>16a</b> 2- <i>O</i> -L-alanyl- $\beta$ -D-glucose (20)	<b>16b</b> 3- <i>O</i> -L-alanyl- $\beta$ -D-glucose (12)	<b>16c</b> 6- <i>O</i> -L-alanyl- $\beta$ -D-glucose (47)	
			
<b>16d</b> 2,6-di- <i>O</i> -L-alanyl- $\beta$ -D-glucose (15)	<b>16e</b> 3,6-di- <i>O</i> -L-alanyl- $\beta$ -D-glucose (6)		
			68 <sup>c</sup> (mono esters- 36, di esters-32)
<b>25a</b> 2- <i>O</i> -L-valyl-D-glucose (10)	<b>25b</b> 3- <i>O</i> -L-valyl-D-glucose (12)	<b>25c</b> 6- <i>O</i> -L-valyl-D-glucose (31)	
			
<b>25d</b> 2,6-di- <i>O</i> -L-valyl-D-glucose (23)	<b>25e</b> 3,6-di- <i>O</i> -L-valyl-D-glucose (24)		



<sup>a</sup> L-Amino acid – 2 mmol and D-glucose – 1 mmol. Conversion yields were from HPLC with respect to L-amino acid concentration. Solvent – 100 ml of CH<sub>2</sub>Cl<sub>2</sub>:DMF (v/v 90:10) at 40 °C, incubation period – 72 h.

<sup>b</sup> RML – 40 % (w/w carbohydrate), buffer – 0.1 mM (0.1 ml of 0.1 M) acetate buffer pH 4.0.

<sup>c</sup> CRL – 40 % (w/w carbohydrate), buffer – 0.1 mM (0.1 ml of 0.1 M) phosphate buffer pH 7.0,

<sup>d</sup> RML – 40 % (w/w carbohydrate), buffer – 0.1 mM (0.1 ml of 0.1 M) acetate buffer pH5.0.

<sup>e</sup> Percentage proportions of individual esters were determined from the peak areas or from their cross peaks of the Carbon-13 C6 signals in the 2D HSQCT spectrum.

### 3.3.1. Spectral data for L-alanyl, L-valyl and L-leucyl esters of D-glucose

**3.3.1.1. L-Alanyl-D-glucose (16a-e):** Solid; HPLC  $t_{ret}$ : 3.4 min;  $R_f$ : 0.22; UV (H<sub>2</sub>O,  $\lambda_{max}$ ): 227.0nm ( $\sigma \rightarrow \sigma^*$   $\epsilon_{227.0} - 1150.8 \text{ M}^{-1}$ ), 294.0nm ( $n \rightarrow \pi^*$   $\epsilon_{294.0} - 763.8 \text{ M}^{-1}$ ); IR (KBr, stretching frequency): 3371cm<sup>-1</sup> (NH), 3410cm<sup>-1</sup> (OH), 2297 cm<sup>-1</sup> (CH), 1653 cm<sup>-1</sup> (CO); MS ( $m/z$ ): 274 [M+Na]<sup>+</sup>.

2D HSQCT (DMSO-*d*<sub>6</sub>) **2-O- ester (16a)** : <sup>1</sup>H NMR  $\delta$  (500.13 MHz) : 2.95 ( $\alpha$ CH), 1.07 ( $\beta$ CH<sub>3</sub>), 3.62 (H-2 $\beta$ ), 3.83 (H-3 $\beta$ ), 3.67 (H-4 $\beta$ ), 3.44 (H-6) ppm; <sup>13</sup>C NMR  $\delta$  (125 MHz) : 52.1 ( $\alpha$ CH), 15.7 ( $\beta$ CH<sub>3</sub>), 102.8 (C1 $\beta$ ), 82.6 (C2 $\beta$ ), 77.9 (C3 $\beta$ ), 68.8 (C4 $\beta$ ), 60.5 (C6 $\beta$ ) ppm; **3-O- ester (16b)** : <sup>1</sup>H NMR  $\delta$  : 2.87 ( $\alpha$ CH), 3.93 (H-3 $\beta$ ), 3.58 (H-4 $\beta$ ), 3.36 (H-6) ppm; <sup>13</sup>C NMR  $\delta$  (125 MHz) : 51.4 ( $\alpha$ CH), 83.3 (C3 $\beta$ ), 69.3 (C4 $\beta$ ), 57.3 (C6 $\beta$ ) ppm; **6-O- ester (16c)** : <sup>1</sup>H NMR  $\delta$  : 2.95 ( $\alpha$ CH), 1.30 ( $\beta$ CH<sub>3</sub>), 3.86 (H-2 $\beta$ ), 3.76 (H-5 $\beta$ ), 3.82 (H-6) ppm; <sup>13</sup>C NMR  $\delta$  : 50.2 ( $\alpha$ CH), 15.1 ( $\beta$ CH<sub>3</sub>), 171.4 (CO), 101.8 (C1 $\beta$ ), 75.0 (C2 $\beta$ ),

70.1 (C5 $\beta$ ), 63.5 (C6 $\beta$ ) ppm; **2,6-di-O- ester (16d)** :  $^1\text{H}$  NMR  $\delta$  : 3.36 ( $\alpha\text{CH}$ ), 1.30 ( $\beta\text{CH}_3$ ), 3.78 (H-2 $\beta$ ), 3.47 (H-6) ppm;  $^{13}\text{C}$  NMR  $\delta$  : 49.5 ( $\alpha\text{CH}$ ), 16.4 ( $\beta\text{CH}_3$ ), 100.8 (C1 $\beta$ ), 76.5 (C2 $\beta$ ), 62.7 (C6 $\beta$ ) ppm; **3,6-di-O- ester (16e)** :  $^1\text{H}$  NMR  $\delta$ : 1.30 ( $\beta\text{CH}_3$ ), 3.78 (H-3 $\beta$ ), 3.82 (H-6) ppm;  $^{13}\text{C}$  NMR  $\delta$  : 51.4 ( $\alpha\text{CH}$ ), 16.7 ( $\beta\text{CH}_3$ ), 81.6 (C3 $\beta$ ), 63.1 (C6 $\beta$ ) ppm.

**3.3.1.2. L-Valyl-D-glucose (25a-e)**: Solid; HPLC  $t_{\text{ret}}$ : 3.5 min;  $R_f$ : 0.22; UV ( $\text{H}_2\text{O}$ ,  $\lambda_{\text{max}}$ ): 200.0 nm ( $\sigma \rightarrow \sigma^*$   $\epsilon_{200.0} - 2630 \text{ M}^{-1}$ ), 295.0 nm ( $n \rightarrow \pi^*$   $\epsilon_{295.0} - 2089 \text{ M}^{-1}$ ); IR (KBr, stretching frequency): 2971  $\text{cm}^{-1}$  (NH), 3407  $\text{cm}^{-1}$  (OH), 2950  $\text{cm}^{-1}$  (CH), 1622  $\text{cm}^{-1}$  (CO); MS ( $m/z$ ) : 302  $[\text{M}+\text{Na}]^+$ .

2D-HSQCT (DMSO- $d_6$ ) : **2-O- ester (25a)**:  $^1\text{H}$  NMR  $\delta$  (500.13 MHz) : 3.08 ( $\alpha\text{CH}$ ), 1.35 ( $\gamma\text{CH}_3$ ), 3.75 (H-2 $\alpha$ ), 3.67 (H-3 $\alpha$ ), 3.78 (H-4 $\alpha$ ), 4.22 (H-5 $\alpha$ ), 3.50 (H-6) ppm;  $^{13}\text{C}$  NMR  $\delta$  (125 MHz): 51.5 ( $\alpha\text{CH}$ ), 19.4 ( $\gamma\text{CH}_3$ ), 77.4 (C2 $\alpha$ ), 74.6 (C3 $\alpha$ ), 71.3 (C4 $\alpha$ ), 71.3 (C5 $\alpha$ ), 60.0 (C6 $\alpha$ ) ppm; **3-O- ester (25b)** :  $^1\text{H}$  NMR  $\delta$ : 3.10 ( $\alpha\text{CH}$ ), 1.15 ( $\beta\text{CH}_3$ ), 3.85 (H-2 $\alpha$ ), 3.90 (H-3 $\alpha$ ), 4.01 (H-3 $\beta$ ), 3.34 (H-6) ppm;  $^{13}\text{C}$  NMR  $\delta$  : 52.3 ( $\alpha\text{CH}$ ), 18.3 ( $\gamma\text{CH}_3$ ), 71.3 (C2 $\alpha$ ), 82.6 (C3 $\alpha$ ), 83.1 (C3 $\beta$ ), 60.4 (C6 $\alpha$ ) ppm; **6-O- ester (25c)**:  $^1\text{H}$  NMR  $\delta$  : 3.20 ( $\alpha\text{CH}$ ), 3.35 ( $\beta\text{CH}$ ), 1.55 ( $\gamma\text{CH}_3$ ), 4.95 (H-1 $\alpha$ ), 4.24 (H-1 $\beta$ ), 3.90 (H-3 $\alpha$ ), 3.74 (H-4 $\alpha$ ), 3.41 (H-5 $\alpha$ ), 3.15 (H-6) ppm;  $^{13}\text{C}$  NMR  $\delta$  : 53.4 ( $\alpha\text{CH}$ ), 29.9 ( $\beta\text{CH}$ ), 19.8 ( $\gamma\text{CH}_3$ ), 94.9 (C1 $\alpha$ ), 103.4 (C1 $\beta$ ), 76.2 (C3 $\alpha$ ), 69.5 (C4 $\alpha$ ), 69.0 (C5 $\beta$ ), 63.4 (C6 $\alpha$ ) ppm; **2,6-di-O- ester (15d)**:  $^1\text{H}$  NMR  $\delta$  : 3.20 ( $\alpha\text{CH}$ ), 3.85 (H-2 $\alpha$ ), 3.56 (H-6) ppm;  $^{13}\text{C}$  NMR  $\delta$ : 51.4 ( $\alpha\text{CH}$ ), 76.4 (C2 $\alpha$ ), 61.5 (C6 $\alpha$ ) ppm ; **3,6-di-O-ester (25e)**:  $^1\text{H}$  NMR  $\delta$  : 3.15 ( $\alpha\text{CH}$ ), 1.45 ( $\gamma\text{CH}_3$ ), 3.70 (H-3 $\alpha$ ), 3.52 (H-6) ppm;  $^{13}\text{C}$  NMR  $\delta$  : 53.4 ( $\alpha\text{CH}$ ), 19.5 ( $\gamma\text{CH}_3$ ), 82.4 (C3 $\alpha$ ), 61.8 (C6 $\alpha$ ) ppm.

**3.3.1.3. L-Leucyl-D-glucose (34a-e)**: Solid; HPLC  $t_{\text{ret}}$ : 3.5 min;  $R_f$ : 0.22; UV ( $\text{H}_2\text{O}$ ,  $\lambda_{\text{max}}$ ): 230.0 nm ( $\sigma \rightarrow \sigma^*$   $\epsilon_{230.0} - 724 \text{ M}^{-1}$ ), 297.0 nm ( $n \rightarrow \pi^*$   $\epsilon_{297.0} - 363 \text{ M}^{-1}$ ); IR (KBr,

stretching frequency): 3383  $\text{cm}^{-1}$  (NH), 3360  $\text{cm}^{-1}$  (OH), 2240  $\text{cm}^{-1}$  (CH), 1657  $\text{cm}^{-1}$  (CO); MS ( $m/z$ ): 316  $[\text{M}+\text{Na}]^+$ .

2D-HSQCCT (DMSO- $d_6$ ): **2-O-ester (34a)**:  $^1\text{H}$  NMR  $\delta$  (500.13 MHz): 3.85 (H-2 $\alpha$ ) ppm;  $^{13}\text{C}$   $\delta$  (125 MHz): 75.5 (C2 $\alpha$ ) ppm; **3-O-ester (34b)**:  $^1\text{H}$  NMR  $\delta$ : 3.15 ( $\alpha\text{CH}$ ), 3.85 (H-3 $\alpha$ ), 3.96 (H-3 $\beta$ ) ppm;  $^{13}\text{C}$  NMR  $\delta$ : 50.0 ( $\alpha\text{CH}$ ), 83.5 (C3 $\alpha$ ), 83.6 (C3 $\beta$ ) ppm; **6-O-ester (24c)**:  $^1\text{H}$  NMR  $\delta$ : 3.10 ( $\alpha\text{CH}$ ), 1.56 ( $\beta\text{CH}_2$ ), 1.82 ( $\gamma\text{CH}$ ), 0.82 ( $\delta$ ,  $\delta'$   $\text{CH}_3$ ), 4.99 (H-1 $\alpha$ ), 3.81 (H-2 $\alpha$ ), 3.45 (H-3 $\alpha$ ), 3.68 (H-4 $\alpha$ ), 3.55 (H-5 $\alpha$ ), 3.80 (H-6) ppm;  $^{13}\text{C}$  NMR  $\delta$ : 53.2 ( $\alpha\text{CH}$ ), 40.5 ( $\beta\text{CH}_2$ ), 23.5 ( $\gamma\text{CH}$ ), 25.0 ( $\delta$ ,  $\delta'$   $\text{CH}_3$ ), 173.6 (CO), 92.5 (C1 $\alpha$ ), 70.3 (C2 $\alpha$ ), 75.8 (C3 $\alpha$ ), 70.2 (C4 $\alpha$ ), 71.0 (C5 $\alpha$ ), 65.0 (C6 $\alpha$ ) ppm; **2,6-di-O-ester (34d)**:  $^1\text{H}$  NMR  $\delta$ : 3.21 (H-2 $\alpha$ ), 3.59 (H-6) ppm;  $^{13}\text{C}$  NMR  $\delta$ : 76.3 (C2 $\alpha$ ), 65.0 (C6 $\alpha$ ) ppm. **3,6-di-O-ester (34e)**:  $^1\text{H}$  NMR  $\delta$ : 3.68 (H-3 $\alpha$ ), 3.59 (H-6) ppm;  $^{13}\text{C}$   $\delta$ : 81.5 (C3 $\alpha$ ), 65.0 (C6 $\alpha$ ) ppm.

### 3.4. Discussion

The optimum conditions determined for these esterification reactions by studying the effect of variables like incubation period, enzyme and substrate concentrations, pH and buffer concentration clearly explain the behaviour of the lipases. Most of the parameters show that esterification increases upto a certain point, and thereafter they remain as such or decrease a little. This complex esterification reaction is not controlled by kinetic factors or thermodynamic factors or water activity alone.

Use of lower enzyme concentrations did not result in thermodynamic yields. The thermodynamic binding equilibria regulate the concentrations of the unbound substrates at different enzyme and substrate concentrations and thereby conversion as the reaction proceeds with time. At lesser enzyme concentrations, for a given amount of substrates (enzyme/substrate ratio low), rapid exchange between bound and unbound forms of both

the substrates with the enzyme (on a weighted average based on binding constant values of both the substrates) leaves substantial number of unbound substrate molecules at the start of the reaction which decrease progressively as conversion takes place (Romero *et al.*, 2005a; Marty *et al.*, 1992). This becomes more so, if one of them binds more firmly to the enzyme than the other (higher binding constant value) as the respective enzyme/substrate ratios change (during the course of the reaction) unevenly till the conversion stops due to total predominant binding (inhibition). At intermediary enzyme concentrations, such a competitive binding results in a favorable proportions of bound and unbound substrates to effect quite a good conversion. At higher enzyme concentrations, most of the substrates would be in the bound form leading to inhibition and lesser conversion (higher enzyme/substrate ratios). Also, the esterification reaction requires larger amount of enzyme compared to hydrolysis. While this leads to lesser selectivity, they also give rise to varying bound and unbound substrate concentrations till the conversion ends. For a given amount of enzyme and substrates there is no increase in conversion beyond 72 h to 120 h. Longer incubation periods of especially lesser enzyme concentrations could also result in partial enzyme inactivation. However, not all the enzymes are inactivated before the end of the reaction.

By imparting 'pH memory' or 'pH tuning', the catalytic activity of the lyophilized subtilisin Carlsberg in the pH range 5.0 - 11.0, in organic solvents like acetonitrile and 3-pentanone was reported to be enhanced (Xu and Klivanov, 1996). The enzymatic activity of subtilisin cross linked crystals in anhydrous 3-pentanone was accelerated by the addition of organic soluble (a mixture of a suitable acid and sodium salt) buffers (Xu and Klivanov, 1996). The enantio selectivity of *Candida antarctica* lipase B in organic media was increased by 'pH tuning' of the enzyme by the addition of

certain buffer salts which altered the protonation state of the enzyme and selectively tuned enantioselectivity and catalytic activity (Quiros et al., 2002). Similarly, the present work also showed enhanced activity of RML and CRL in presence of buffer salts. However, buffer salts did not enhance esterification with PPL.

Besides imparting 'pH memory' or 'pH tuning', added water is essential for the integrity of the three-dimensional structure of the enzyme molecule and therefore its activity (Dordick, 1989). Zaks and Klivanov (1988) reported that at low water activities, lower the solvent polarity, the higher the enzyme activity. Beyond the critical water concentration, esterification decreases because the size of the water layer formed around the enzyme retards the transfer of acyl donor to the active site of the enzyme (Humeau *et al.*, 1998, Camacho-Paez *et al.*, 2003) and also the water layer surrounding the enzymes makes enzyme to be more flexible by forming multiple hydrogen bonds and interacting with organic solvent causing denaturation (Valiveti *et al.*, 1991). Increase in buffer volume affected this esterification reaction significantly. It could increase the water activity of the system in the initial stages by increasing the thickness of the microaqueous layer around the enzyme. Higher volumes of the buffer in the microaqueous layer could also cause slight inactivation of the enzyme due to increase in salt concentration beyond a critical point. Patridge *et al.*, (2001) reported that when an enzyme is suspended in a low-water organic solvent, the counter ions are in closer contact with the opposite charges on the enzyme because of the lower dielectric constant of the medium. Thus, protonation of the ionizable groups on the enzyme could be controlled by the type and availability of these ions as well as hydrogen ions resulting in a 'pH memory' or 'pH tuning'. The third factor is the increase in ionic strength which could play a favourable role in esterification. Optimum pH were found to be pH 4.0 for



RML and pH 5.0 for PPL in case of L-alanyl-D-glucose, pH 7.0 for CRL in case of L-valyl-D-glucose and pH 5.0 for RML in case of L-leucyl-D-glucose reactions clearly indicate a slight unfavorable conformational change in the enzyme at about pH 4.0 to 6.0 leading to lesser conversion beyond pH 4.0 and 5.0 for RML, 5.0 for PPL and 7.0 for CRL.

The experimental setup employed in the present work is such that it maintained a low water activity ( $a_w = 0.0054$ ) due to azeotropic distillation and recycling the solvent back into the reaction system after passing through a bed of desiccant. Even the water of reaction formed could also be used to constitute the microaqueous layer around the enzyme and the excess water could be removed by azeotropic distillation. The same could occur even with the addition of added enzyme (with little water content) and buffer volume. The added carbohydrate molecule could also reduce the water content of the reaction mixture. Adachi and Kobayashi (2005) have reported that the hexose which is more hydrated decreased the water activity in the system and shifts the equilibrium towards synthesis. All these factors lead to maintenance of an equilibrium concentration of water around the enzyme all the time. Hence, thermodynamic binding equilibria interplayed by inactivation and inhibition along with maintenance of an optimum water activity could be governing this reaction as reflected by the extent of conversion under different reaction conditions of added buffer, enzyme and substrate concentrations.

As monosaccharides contain five hydroxyl groups, 31 diastereomeric esters (mono, di, tri, tetra and penta) are possible for both the anomers. In case of L-alanyl, L-valyl and L-leucyl esters of D-glucose (Section 3.3.1.1, 3.3.1.2 and 3.3.1.3), only 6-*O*- was the major ester produced (47 %, 31 % and 42 % respectively, Table 3.10). The anomeric composition of D-glucose employed for the reaction was 40:60 ( $\alpha$ : $\beta$ ) and the

equal peak areas of anomeric H-1 chemical shift values observed at 4.24 and 4.0 ppm indicated that either both the anomers have reacted to equal extent (1:1) or D-glucose had undergone mutarotation in case of L-valyl and L-leucyl esters of D-glucose. In case of L-alanyl-D-glucose, only  $\beta$ -anomer of D-glucose was found to react, the D-glucose employed being a 40:60 mixture of  $\alpha$  and  $\beta$  anomers respectively. Only monoesters were formed with only  $\beta$ -anomer of D-glucose, when an attempt was made to improve the selectivity of ester formation by decreasing the incubation period in case of L-alanyl-D-glucose synthesis using RML.

Commercial crude PPL preparations contain variety of estero/lipo lytic enzymes with low PPL concentrations (Segura *et al.*, 2006, Birner-Grunberger *et al.*, 2004) which could also perform facile esterification. Hence, a small amount of esters formed from esterases along with those of lipases in the present reaction cannot be ruled out. Since the reactions were carried out at a low temperature of 40 – 60 °C, the formation of peptide was less than 3 %, even though unprotected L-amino acid was used for the reaction. NMR data clearly indicated that no Maillard reaction occurred. Under these reaction conditions, formation of Maillard reaction products are quite likely. For instance, Maillard and Pictet Spengler phenolic condensation products were reported in the reaction between phenolic amino acids and D-glucose in phosphate buffer at different pH from 5.0 to 9.0 at 90 °C (Manini *et al.*, 2005). Similarly Maillard products from the reaction between D-glucose and N-t-boc-L-lysine incubated with aminoguanidine in phosphate buffer (pH 7.4) at 70 °C was also reported (Reihl *et al.*, 2004). No such Maillard reaction type products were detected by mass as well as NMR in the present investigation. RML, CRL and PPL showed significant esterification (up to 84 %) when unprotected L-amino acid was used. When N-acetyl-L-alanine was used in the present

work, both RML and PPL gave < 5 % yield. Riva *et al.*, (1988) have reported two monoesters (4-*O*- and 6-*O*- ester) and no diester for L-alanine, using subtilisin, a protease. Our present study has shown that comparable esterification yields to others could be achieved by employing PPL, CRL and RML instead of protease. Thus, our study clearly indicates that unprotected L-amino acid could be used for esterification of carbohydrates.

### **3.5. Experimental**

#### **3.5.1. Esterification procedure**

Preparation of L-alanyl, L-valyl and L-leucyl esters of D-glucose was carried out by adopting a bench-scale level procedure (Divakar *et al.*, 1999). Esterification was carried out in presence of 0.018 – 0.090 g of lipases (expressed in terms of % w/w D-glucose employed). Unprotected L-amino acids (L-alanine **1**, L-valine **2** and L-leucine **3**, 0.001- 0.005 mol) and D-glucose **5** (0.001 – 0.005 mol) in 100 ml of organic media containing CH<sub>2</sub>Cl<sub>2</sub>:DMF (v/v 90:10) or hexane:CHCl<sub>3</sub>:DMF (v/v/v 45:45:10) were taken in a flat bottomed two necked flask and refluxed for a period of 3 - 120 h. The enzymes were imparted with or ‘pH memory’ or ‘pH tuning’ in some experiments by adding known volumes of 0.1 M buffer solutions of specified pH value to 100 ml (solvent) of the reaction mixture. The condensed vapors of solvent which formed an azeotrope with water during reflux was passed through a desiccant (sodium aluminosilicate molecular sieves of 4 Å) before being returned into the reaction mixture, thereby facilitating complete removal of water of reaction (Lohith and Divakar, 2005). This set up maintained a very low water activity of  $a_w = 0.0054$  throughout the reaction period which was determined by Karl Fischer titration of the reaction mixture using Karl Fischer reagent by examining aliquots for the water content during the course of the reaction.

The reaction mixture after distilling off the solvent was then treated with 20-50 ml of water, stirred and filtered to remove the lipase. The filtrate was evaporated on a water bath to get the unreacted D-glucose, unreacted L-amino acids and the product esters which were then analyzed by HPLC. The conversion yields were determined with respect to peak areas of the L-amino and that of the esters. The esters formed were separated by size exclusion chromatography using Sephadex G-10/Bio-Gel P-2 as column materials and eluted with water. The product esters separated were subjected to spectral characterization by UV, IR, mass, specific rotation and 2D-NMR (Sections 3.3.1.1, 3.3.1.2 and 3.3.1.3). Although, the esters were separated from unreacted amino acids and D-glucose by this procedure, the individual esters in the mixture of esters formed could not be separated. This could be due to the similar polarity of the ester molecules.

### **3.5.2. High Performance Liquid Chromatography (HPLC)**

A Shimadzu LC 10AT HPLC instrument connected to a  $\mu$ -Bondapak aminopropyl column (10  $\mu$ m particle size, 3.9 x 300 mm length) was employed for analyzing the reaction mixture. Acetonitrile:water (80:20 v/v) as a mobile phase at a flow rate of 1ml/min was used with Refractive Index detector. Also LiChrosorb RP-18 column (5  $\mu$ m particle size, 4.6 x 150 mm length) was employed with an UV detector at 210 nm using acetonitrile: water (v/v 20:80) as a mobile phase at a flow rate of 1 ml/min.

### **3.5.3. Spectral characterization**

A Shimadzu UV – 1601 spectrophotometer (Kyoto, Japan) was used for recording UV spectra of the isolated esters in water at 0.1 - 2.0 mM concentrations. A Nicolet 5700 FTIR instrument (Madison, USA) was used for recording the IR spectra with a 1.0 - 3.0 mg of ester sample as KBr pellet. Specific rotation of the isolated esters

were measured at 25 °C using Perkin-Elmer 243 polarimeter (Überlingen, Germany) with a 0.2 – 1.5 % solution of the esters in water. Mass spectra of the isolated esters were recorded using a Q-TOF Waters Ultima instrument (No.Q-Tof GAA 082, Waters corporation, Manchester, UK) fitted with an electron spray ionization (ESI) source.

### **3.5.4. Nuclear Magnetic Resonance Spectroscopy**

#### **3.5.4.1. <sup>1</sup>H NMR**

A Brüker DRX-500 MHz spectrometer (Fallanden, Switzerland) operating at 500.13 MHz was used to record <sup>1</sup>H NMR. A 40 mg of sample was dissolved in 0.5 ml of DMSO-*d*<sub>6</sub> solvent. About 50 - 200 scans were accumulated with a recycle period of 2 - 3 seconds to obtain good spectra. The spectra were recorded at 35 °C with TMS as internal standard for measuring the chemical shift values to within ± 0.001 ppm. A region from 0 – 10 ppm was scanned for all the samples.

#### **3.5.4.2. <sup>13</sup>C NMR**

A Brüker DRX-500 MHz spectrometer (Fallanden, Switzerland) operating at 125 MHz was used to record <sup>13</sup>C NMR. Samples were dissolved in 0.5 ml of DMSO-*d*<sub>6</sub> and recorded at 35 °C. A region from 0 - 200 ppm region was scanned and about 500 – 6000 scans were accumulated for each spectrum to get good spectrum. TMS was taken as an internal standard.

#### **3.5.4.3. Two-dimensional HSQCT**

Two dimensional Heteronuclear Multiple Quantum Coherence Transfer spectra (2-D HMQCT) and Heteronuclear Single Quantum Coherence Transfer spectra (2-D HSQCT) (Fallanden, Switzerland) were recorded at 500 MHz on a Brüker DRX-500 MHz spectrometer (500.13 MHz for <sup>1</sup>H and 125 MHz for <sup>13</sup>C). Chemical shift values were expressed in ppm relative to internal tetramethylsilane standard. About 40 mg of the sample dissolved in DMSO-*d*<sub>6</sub> was used for recording the spectra.

*Chapter 4*  
*Syntheses of carbohydrate esters of L-alanine, L-*  
*valine, L-leucine and L-isoleucine*

## 4.1 Introduction

Carbohydrates are biologically interesting molecules whose modification can bestow useful additional functionality to sugar moiety. Introduction of an amino acid into the carbohydrate moiety results in an additional functionality like an amino group besides converting an hydroxyl group into an ester. Addition of amino acids to sugar moiety can also improve the bioavailability of amino acids in biological systems. Presence of hydroxyl as well as amino groups in the molecule help in the polycondensation reactions (Park *et al.*, 1999). Recently Shiraki *et al.*, (2004) reported that amino acid esters prevent thermal inactivation and aggregation of lysozyme. Besides these uses, other applications of amino acyl esters of carbohydrates have been mentioned in previous chapters.

Hitherto, very few references are available on the lipase catalyzed acylation of amino acids with carbohydrates, most of which have been described in Section 3.1.

A comprehensive investigation has been carried out on the lipase catalyzed syntheses of L-amino acid esters of eleven carbohydrate molecules. In the present investigation, lipases from *Candida rugosa* (CRL), *Rhizomucor miehei* (RML) and porcine pancreas (PPL) were employed towards syntheses of L-alanyl, L-valyl, L-leucyl and L-isoleucyl esters of carbohydrates. Aldohexoses (D-glucose, D-galactose and D-mannose), ketohexose (D-fructose), pentoses (D-arabinose and D-ribose), disaccharides (lactose, maltose and sucrose) and sugar alcohols (D-mannitol and D-sorbitol) are the carbohydrate molecules employed. Attempts to synthesize the same using N-acetyl derivatives of these amino acids resulted in a very low conversion with the above mentioned enzymes. Hence, unprotected and unactivated L-amino acids and carbohydrates were employed. The results are presented below.

## 4.2. Present investigation

### Syntheses and characterization of L-alanyl, L-valyl, L-leucyl and L-isoleucyl esters of carbohydrates

Syntheses of L-amino acid esters of different carbohydrates were carried out between different amino acids (L-alanine **1**, L-valine **2**, L-leucine **3** and L-isoleucine **4**) and carbohydrates (D-glucose **5**, D-galactose **6**, D-mannose **7**, D-fructose **8**, D-arabinose **9**, D-ribose **10**, lactose **11**, maltose **12**, sucrose **13**, D-mannitol **14**, D-sorbitol **15**) using *Rhizomucor miehei* lipase (RML), *Candida rugosa* lipase (CRL) and porcine pancreas lipase (PPL) in presence of organic solvent. A 0.1 mM (0.1 ml of 0.1M) acetate buffer (pH 4.0) in case of RML, 0.1 mM (0.1 ml of 0.1 M) phosphate buffer (pH 7.0) in case of CRL and 0.1 mM (0.1 ml of 0.1 M) acetate buffer (pH 5.0) in case of PPL were employed in the reaction mixture to impart the 'pH memory' or 'pH tuning' to the lipase. The reaction mixture containing L-amino acid **1-4** (1-2 mmol), carbohydrate **5-15** (1 mmol), lipase (40 % in case of RML and CRL w/w based on respective carbohydrate and 111 % in case of PPL) and the solvent were refluxed for a period of 72 h (experimental procedure is described in Section 2.2.4). The esterification reaction described in this present work did not occur without the use of enzymes. Extent of esterification was analyzed by HPLC and the esters were isolated by passing through Sephadex G-10/Bio Gel P2 and eluting with water. The isolated esters were then subjected to characterization by UV, IR, Mass, optical rotation and 2D-HSQCT NMR spectroscopy. NMR assignments of amino acids as well as carbohydrates and esters were made according to literature reports (Suzuki *et al.*, 1991; Riva *et al.*, 1988; Park *et al.*, 1996, 1999). Some of the assignments, especially  $^{13}\text{C}$  signals mentioned in the sections 4.2.1.1 – 4.2.1.9 for L-alanyl esters, 4.2.2.1 – 4.2.2.9 for L-valyl esters, 4.2.3.1 – 4.2.3.10 for L-leucyl esters and 4.2.4.1 - 4.2.4.10 for L-isoleucyl esters are interchangeable. Only resolvable signals are

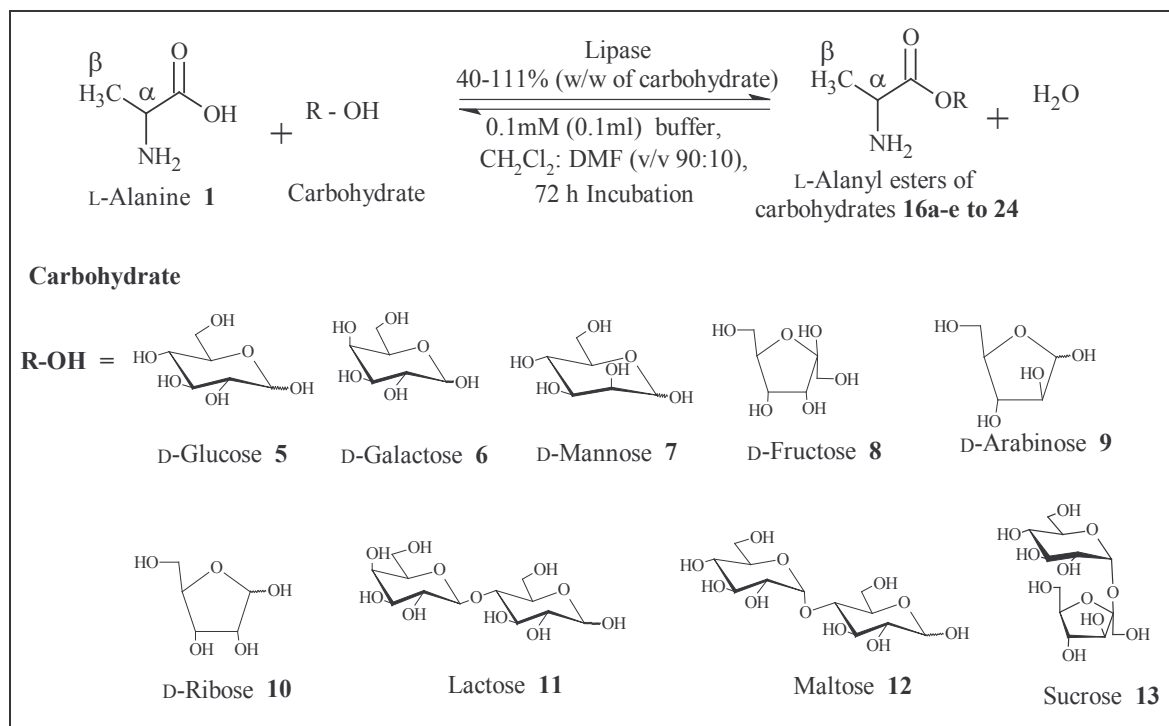


shown. Non-reducing end carbohydrate signals in disaccharides are primed. Since, the esters are surfactant molecules, they appear to aggregate in the solvent and usually give broad signals, thus, making it difficult to resolve the coupling constant values in the  $^1\text{H}$  NMR spectra accurately. Mass data for the monoesters are shown. However, although NMR data clearly indicated the presence of di-*O*- esters, they were not detected in the mass spectra, which could be due to instantaneous decomposition. The percentage proportions of the individual esters formed were determined by considering the peak areas of the C6, C5 (in case of pentoses) of  $^{13}\text{C}$  signals or cross peaks from 2D-NMR. Although column chromatography using Sephadex G-10/Bio Gel P2 separated unreacted amino acids and carbohydrates from the esters, the individual esters could not be separated in many cases due to similar polarity of the ester molecules. However, NMR data from individual esters could be detected unequivocally.

#### **4.2.1. Syntheses of L-alanyl esters of carbohydrates 16a-e to 24**

L-Alanine is a polar and a non-essential amino acid containing methyl group as a side chain. Esterification of L-alanine with carbohydrates was carried out using CRL, RML and crude PPL under optimal conditions (Section 2.2.4, **Scheme 4.1**). The reaction mixture consists of 1-2 mmol L-alanine **1** and 1 mmol carbohydrates (D-glucose **5**, D-galactose **6**, D-mannose **7**, D-fructose **8**, D-arabinose **9**, D-ribose **10**, lactose **11**, maltose **12**, sucrose **13**, D-mannitol **14**, D-sorbitol **15**) along with 40 % RML (w/w carbohydrate) / 40 % CRL (w/w carbohydrate) / 111 % PPL (w/w carbohydrate) and incubated in 100 ml of  $\text{CH}_2\text{Cl}_2$  and DMF (v/v 90:10, 40 °C) containing 0.1 mM (0.1 ml of 0.1 M) of acetate buffer, pH 4.0 (RML) or 0.1 mM (0.1 ml of 0.1 M) of phosphate buffer, pH 7.0 (CRL) or 0.2 mM (0.2 ml of 0.1 M) of acetate buffer, pH 5.0 (crude PPL). The reaction mixture was analyzed by HPLC using a C-18 column with acetonitrile:water (v/v 20:80) mobile phase and detected at 210 nm using a UV detector (Fig. 4.1). Ester formation was

also monitored by TLC and spots were detected by spraying ninhydrin (for NH<sub>2</sub> group detection) and 1-naphthol (for reducing sugar detection). The retention times ( $t_{ret}$ ) by HPLC and retention factor ( $R_f$ ) values by TLC are mentioned in sections 4.2.1.1 – 4.2.1.9.



**Scheme 4.1 Lipase catalyzed syntheses of L-alanyl esters of carbohydrates**

The isolated esters were subjected to UV, IR, MS, optical rotation and 2D-HSQCT NMR characterization (Sections 4.2.1.1 – 4.2.1.9). The spectral data for the isolated esters are shown in Sections 4.2.1.1 – 4.2.1.9. Table 4.1 shows chemical shift values for free carbohydrates. Table 4.2 shows the ester yields from HPLC, types of esters formed and percentage proportions of the individual esters by RML and Table 4.3 shows the ester yields from HPLC by both CRL and PPL.

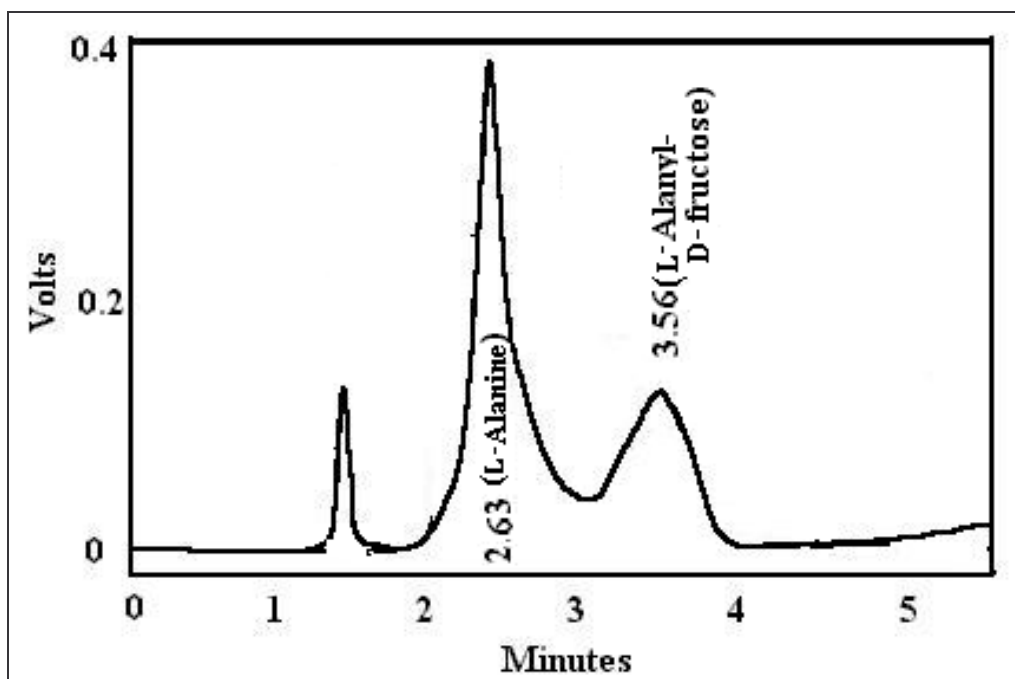


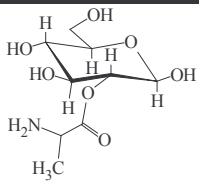
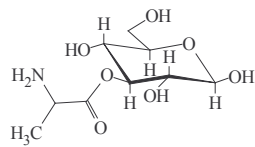
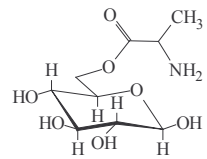
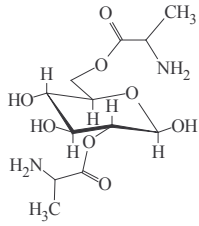
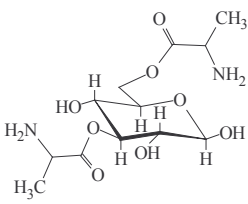
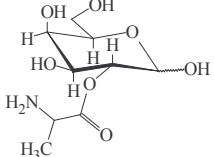
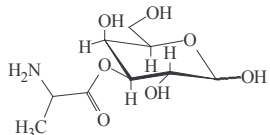
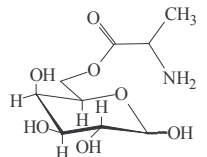
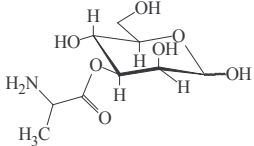
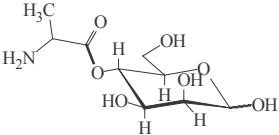
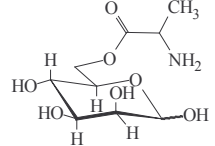
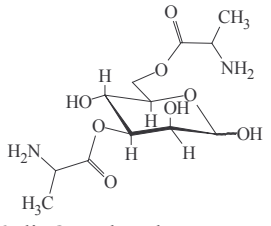
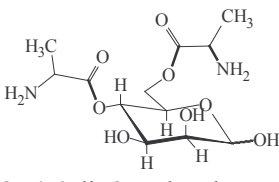
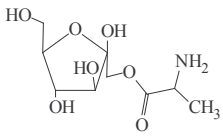
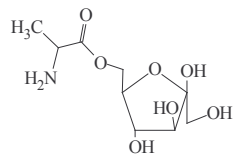
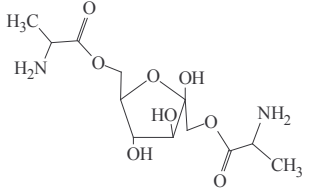
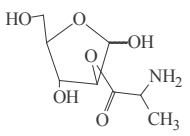
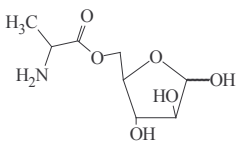
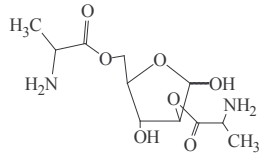
**Fig. 4.1.** HPLC chromatogram: reaction mixture of L-alanine and D-fructose esterification catalyzed by RML. Column – C-18; mobile phase – acetonitrile: water (v/v 20:80); flow rate- 1 ml /min; detector – UV at 210 nm; errors in conversion yields are within  $\pm 10\%$ .

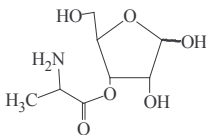
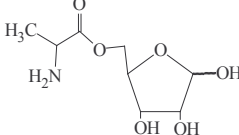
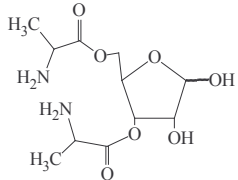
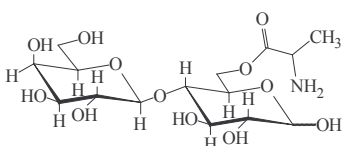
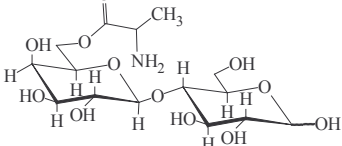
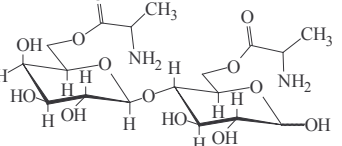
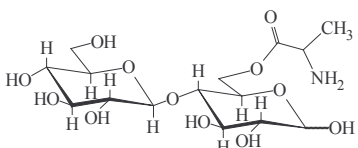
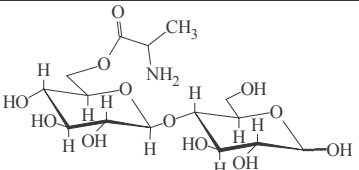
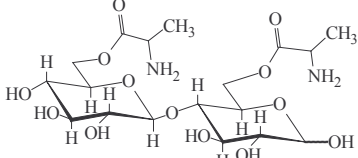
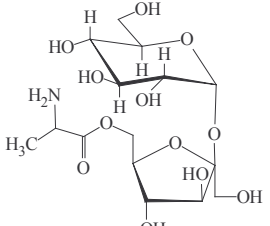
**Table 4.1 Chemical shift values for free carbohydrates<sup>a</sup>**

Carbohydrate	Chemical shift values in ppm (J Hz)																										
	<sup>1</sup> H H-1	<sup>13</sup> C C1	<sup>1</sup> H H-2	<sup>13</sup> C C2	<sup>1</sup> H H-3	<sup>13</sup> C C3	<sup>1</sup> H H-4	<sup>13</sup> C C4	<sup>1</sup> H H-5	<sup>13</sup> C C5	<sup>1</sup> H H-6	<sup>13</sup> C C6	<sup>1</sup> H H-1'	<sup>13</sup> C C1'	<sup>1</sup> H H-2'	<sup>13</sup> C C2'	<sup>1</sup> H H-3'	<sup>13</sup> C C3'	<sup>1</sup> H H-4'	<sup>13</sup> C C4'	<sup>1</sup> H H-5'	<sup>13</sup> C C5'	<sup>1</sup> H H-6'	<sup>13</sup> C C6'			
D-Glucose	α	4.95	92.3	3.14	72.5	3.44	72.0	3.07	70.7	3.58	72.0	3.53	61.4														
	β	4.30	97.0	2.92	75.0	3.06	76.9	-	-	3.45	76.9	3.62	61.6														
D-Galactose	α	4.14	92.7	3.50	68.4	3.59	69.0	3.70	70.0	3.35	70.5	3.31	60.7														
	β	4.83	97.6	--	--	3.15	73.7	3.10	72.3	3.25	74.8	3.32	60.8														
D-Mannose	α	4.89	94.0	3.54	71.3	3.55	70.0	3.36	67.4	3.50	73.0	3.63	61.5														
	β	4.54	93.9	3.32	71.5	3.26	73.7	3.37	67.0	3.02	77.0	3.46	61.4														
D-Fructose	β	3.80	63.9	-	97.5	3.56	67.9	3.64	69.9	3.57	68.7	3.50	62.6														
	α	4.75	93.2	3.23	70.6	3.33	68.8	3.71	66.7	3.51	62.8																
D-Ribose	α	4.31	94.0	3.31	71.5	3.38	68.0	3.54	67.5	3.29	62.8																
	β	4.92	92.3	4.32	-	4.6	-	4.08	-	3.73	60.4																
D-Arabinose	α	4.33	96.2	3.65	69.1	4.02	68.9	3.37	67.1	3.64	60.7																
	β	4.5		4.5	7.2	7.2	4.0	4.0	2.4	2.4	12.0																
Lactose	α	4.90	91.9	3.70	69.8	3.54	71.4	3.27	80.8	3.55	72.1	3.64	60.5														
	β	4.34	96.3	3.31	74.2	3.53	74.7	3.28	81.1	3.44	74.9	3.72	60.6														
Maltose	α	4.80	92.0	2.85	73.9	3.29	76.4	3.15	79.7	3.30	73.3	3.50	60.8														
	β	4.20	96.9	3.10	74.3	3.31	76.0	3.19	79.4	3.38	76.4	3.34	60.9														
Sucrose	Glc α																										
	Fru β	3.41	62.0	-	103.9	3.78	77.1	3.88	74.1	3.41	82.4	3.55	62.0														
D-Sorbitol	α	3.41	62.5	3.54	73.6	3.68	68.9	3.39	72.2	3.48	71.4	3.56	63.3														
	β	3.40	63.7	3.47	71.2	3.54	69.6	3.54	69.6	3.47	71.2	3.61	63.7														
D-mannitol	α	4.20	96.9	3.10	74.3	3.31	76.0	3.19	79.4	3.38	76.4	3.34	60.9														
	β	4.20	96.9	3.10	74.3	3.31	76.0	3.19	79.4	3.38	76.4	3.34	60.9														

<sup>a</sup> 40 mg of carbohydrate in 0.5 ml of DMSO-*d*<sub>6</sub> (Bock and Pedersen 1983; Bock *et al.* 1984)

Table 4.2 Syntheses of L-alanyl esters of carbohydrates <sup>a</sup>

L-Alanyl esters of carbohydrates (% proportions <sup>b</sup> )			Yield (%)
			30 (mono esters- 24, diesters-6)
<b>16a</b> 2- <i>O</i> -L-alanyl- $\beta$ -D-glucose (20)	<b>16b</b> 3- <i>O</i> -L-alanyl- $\beta$ -D-glucose (12)	<b>16c</b> 6- <i>O</i> -L-alanyl- $\beta$ -D-glucose (47)	
			
<b>16d</b> 2,6-di- <i>O</i> -L-alanyl- $\beta$ -D-glucose (15)	<b>16e</b> 3,6-di- <i>O</i> -L-alanyl- $\beta$ -D-glucose (6)		
			21 (only mono esters)
<b>17a</b> 2- <i>O</i> -L-alanyl-D-galactose (33)	<b>17b</b> 3- <i>O</i> -L-alanyl-D-galactose (32)	<b>17c</b> 6- <i>O</i> -L-alanyl-D-galactose (35)	
			49 (mono esters-39, diesters-10)
<b>18a</b> 3- <i>O</i> -L-alanyl-D-mannose (25)	<b>18b</b> 4- <i>O</i> -L-alanyl-D-mannose (25)	<b>18c</b> 6- <i>O</i> -L-alanyl-D-mannose (30)	
			
<b>18d</b> 3,6-di- <i>O</i> -L-alanyl-D-mannose (9)	<b>18e</b> 4,6-di- <i>O</i> -L-alanyl-D-mannose (11)		
			52 (mono esters-35, diester-17)
<b>19a</b> 1- <i>O</i> -L-alanyl-D-fructose (34)	<b>19b</b> 6- <i>O</i> -L-alanyl-D-fructose (34)	<b>19c</b> 1,6-di- <i>O</i> -L-alanyl-D-fructose (32)	
			9 <sup>c</sup> (mono esters-6, diester-3)
<b>20a</b> 2- <i>O</i> -L-alanyl-D-arabinose (33)	<b>20b</b> 5- <i>O</i> -L-alanyl-D-arabinose(34)	<b>20c</b> 2,5-di- <i>O</i> -L-alanyl-D-arabinose (33)	

			48 <sup>c</sup> (mono esters-23, diester-25)
<b>21a</b> 3- <i>O</i> -L-alanyl-D-ribose (16)	<b>21b</b> 5- <i>O</i> -L-alanyl-D-ribose (32)	<b>21c</b> 3,5-di- <i>O</i> -L-alanyl-D-ribose (52)	
			20 (mono esters-14, diester-6)
<b>22a</b> 6- <i>O</i> -L-alanyl-lactose (34)	<b>22b</b> 6'- <i>O</i> -L-alanyl-lactose (34)	<b>22c</b> 6,6'-di- <i>O</i> -L-alanyl-lactose (32)	
			56 (mono esters-38, diester-18)
<b>23a</b> 6- <i>O</i> -L-alanyl-maltose (34)	<b>23b</b> 6'- <i>O</i> -L-alanyl-maltose (34)		
			
<b>23c</b> 6,6'-di- <i>O</i> -L-alanyl-maltose (32)			
			8 (only mono ester)
<b>24</b> 6- <i>O</i> -L-alanyl-sucrose			

<sup>a</sup> L-Alanine – 2 mmol, carbohydrates – 1 mmol, RML – 40 % (w/w carbohydrate), buffer – 0.1 mM (0.1 ml of 0.1 M) acetate buffer (pH 4.0), CH<sub>2</sub>Cl<sub>2</sub>:DMF (v/v 90:10) at 40 °C, Incubation period – 72 h. Conversion yields were from HPLC with respect to L-alanine concentration.

<sup>b</sup> Percentage proportions of individual esters were determined from the peak areas or from their cross peaks of the Carbon-13 C6 and C5 (in case of pentoses) signals in the 2D HSQCT spectrum.

<sup>c</sup> Several cross peaks, due to opening and/or degradation of the five membered ring during esterification.

**Table 4.3 Preparation of L-alanyl ester of carbohydrate using lipases from *Candida rugosa* and porcine pancreas**

L-Alanyl ester of carbohydrate	CRL <sup>a</sup> %Yield (mmol)	Crude PPL <sup>b</sup> %Yield (mmol)
L-Alanyl-D-glucose <b>16a-e</b>	25 (0.50)	78 (0.78)
L-Alanyl-D-galactose <b>17a-c</b>	22 (0.44)	72 (0.72)
L-Alanyl-D-mannose <b>18a-e</b>	33 (0.66)	10 (0.10)
L-Alanyl-D-fructose <b>19a-c</b>	12 (0.24)	67 (0.67)
L-Alanyl-D-arabinose <b>20a-c</b>	3 (0.06)	27 (0.27)
L-Alanyl-D-ribose <b>21a-c</b>	12 (0.24)	38 (0.38)
L-Alanyl- lactose <b>22a-c</b>	27 (0.54)	58 (0.58)
L-Alanyl- maltose <b>23a-c</b>	17 (0.34)	28 (0.28)
L-Alanyl- sucrose <b>24</b>	8 (0.16)	8 (0.83)

<sup>a</sup> L-Alanine – 2 mmol, carbohydrates – 1 mmol, CRL – 40 % (w/w carbohydrate), buffer – 0.1 mM (0.1 ml of 0.1 M) phosphate buffer pH 7.0, CH<sub>2</sub>Cl<sub>2</sub>:DMF (v/v 90:10) at 40 °C, Incubation period – 72 h. Conversion yields were from HPLC with respect to L-alanine concentration.

<sup>b</sup> L-Alanine – 1 mmol, carbohydrates – 1 mmol, crude PPL – 111% (w/w carbohydrate), buffer – 0.2 mM (0.2 ml of 0.1 M) acetate buffer pH 5.0, CH<sub>2</sub>Cl<sub>2</sub>: DMF (v/v 90:10) at 40°C, Incubation period – 72 h.

**Spectral data for L-Alanine (1):** Solid; Mpt: 258 °C; HPLC  $t_{ret}$ : 2.6 min;  $R_f$ : 0.30; UV (H<sub>2</sub>O,  $\lambda_{max}$ ): 190.0 nm ( $\sigma \rightarrow \sigma^*$   $\epsilon_{190.0} = 111.9 \text{ M}^{-1}$ ), IR (KBr, stretching frequency): 3415 cm<sup>-1</sup> (OH), 2945 cm<sup>-1</sup> (CH), 1715 cm<sup>-1</sup> (CO); optical rotation ( $c$  1.0, H<sub>2</sub>O):  $[\alpha]_D$  at 25°C = +3.33°.

2D HSQCT (DMSO- $d_6$ ): <sup>1</sup>H NMR  $\delta$  (500.13 MHz) : 3.35 ( $\alpha$ CH), 1.25 ( $\beta$ CH<sub>3</sub>) ppm; <sup>13</sup>C NMR  $\delta$  (125 MHz) : 53.0 ( $\alpha$ CH), 15.5 ( $\beta$ CH<sub>3</sub>), 170.5 (CO) ppm.

**4.2.1.1. L-Alanyl-D-glucose (16a-e):** Solid; HPLC  $t_{ret}$ : 3.4 min;  $R_f$ : 0.22; UV (H<sub>2</sub>O,  $\lambda_{max}$ ): 227.0nm ( $\sigma \rightarrow \sigma^*$   $\epsilon_{227.0} = 1150.8 \text{ M}^{-1}$ ), 294.0nm ( $n \rightarrow \pi^*$   $\epsilon_{294.0} = 763.8 \text{ M}^{-1}$ ); IR (KBr, stretching frequency): 3371cm<sup>-1</sup> (NH), 3410 cm<sup>-1</sup> (OH), 2297 cm<sup>-1</sup> (CH), 1653 cm<sup>-1</sup> (CO); MS ( $m/z$ ) : 274 [M+Na]<sup>+</sup>.

2D HSQCT (DMSO- $d_6$ ) **2-O- ester (16a)** : <sup>1</sup>H NMR  $\delta$  (500.13 MHz) : 2.95 ( $\alpha$ CH), 1.07 ( $\beta$ CH<sub>3</sub>), 3.62 (H-2 $\beta$ ), 3.83 (H-3 $\beta$ ), 3.67 (H-4 $\beta$ ), 3.44 (H-6) ppm; <sup>13</sup>C NMR  $\delta$  (125 MHz)

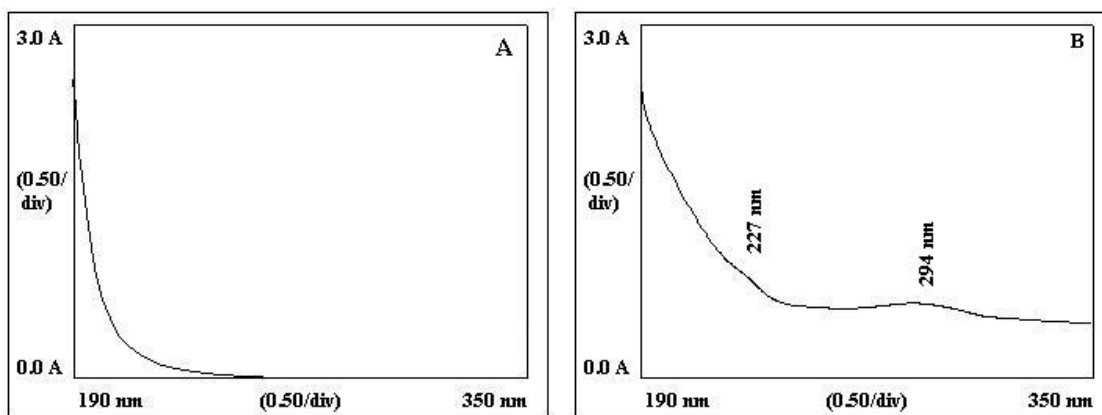


Fig. 4.2. UV spectra for L-alanyl- $\beta$ -D-glucose **16a-e** from RML catalyzed reaction. (A) L-alanine (B) L-alanyl-D-glucose

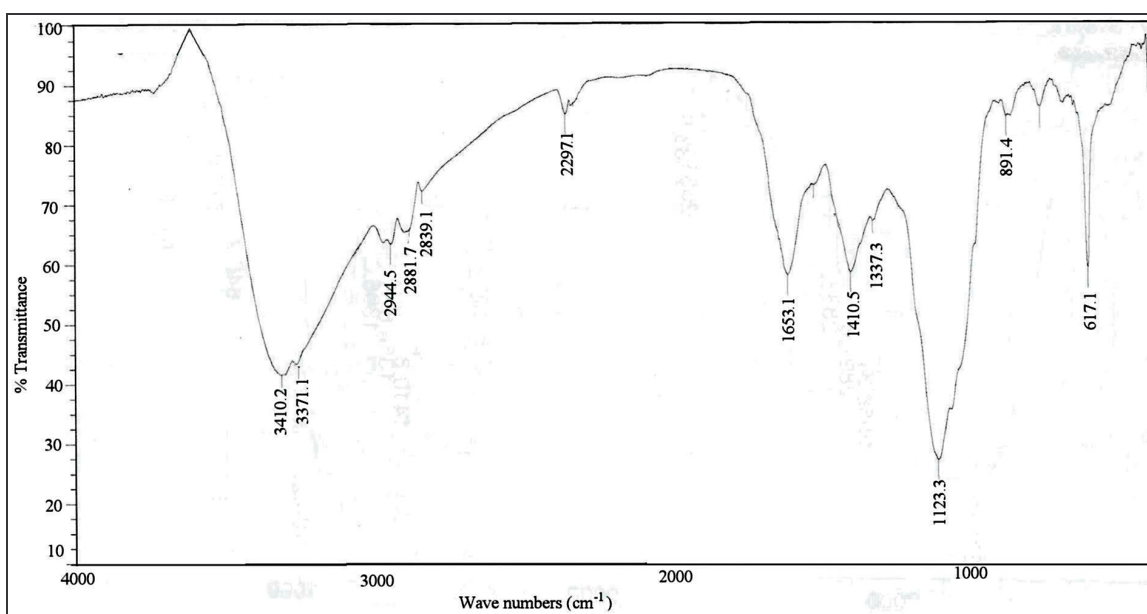


Fig. 4.3. A typical IR spectrum of L-alanyl- $\beta$ -D-glucose **16a-e** by RML catalyzed reaction. A 2.0 mg of ester sample was prepared as KBr pellet and used.

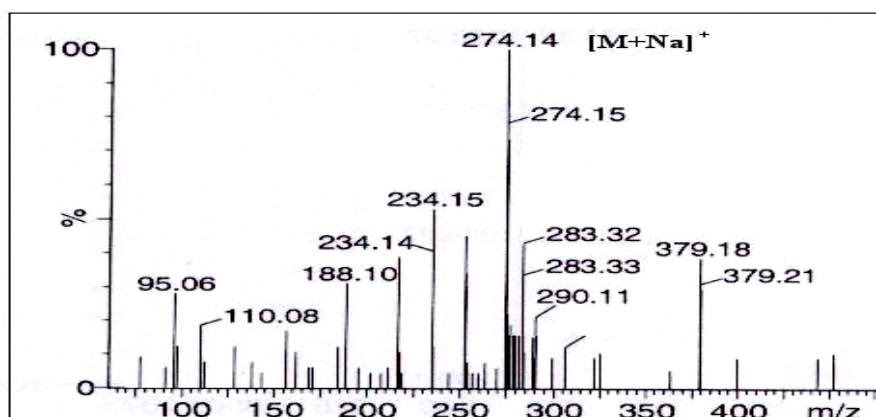


Fig. 4.4. A typical mass spectrum of L-alanyl- $\beta$ -D-glucose **16a-e**



: 52.1 ( $\alpha$ CH), 15.7 ( $\beta$ CH<sub>3</sub>), 102.8 (C1 $\beta$ ), 82.6 (C2 $\beta$ ), 77.9 (C3 $\beta$ ), 68.8 (C4 $\beta$ ), 60.5 (C6 $\beta$ ) ppm; **3-O- ester (16b)** : <sup>1</sup>H NMR  $\delta$ : 2.87 ( $\alpha$ CH), 3.93 (H-3 $\beta$ ), 3.58 (H-4 $\beta$ ), 3.36 (H-6) ppm; <sup>13</sup>C NMR  $\delta$  (125 MHz) : 51.4 ( $\alpha$ CH), 83.3 (C3 $\beta$ ), 69.3 (C4 $\beta$ ), 57.3 (C6 $\beta$ ) ppm; **6-O- ester (16c)** : <sup>1</sup>H NMR  $\delta$  : 2.95 ( $\alpha$ CH), 1.30 ( $\beta$ CH<sub>3</sub>), 3.86 (H-2 $\beta$ ), 3.76 (H-5 $\beta$ ), 3.82 (H-6) ppm; <sup>13</sup>C NMR  $\delta$  : 50.2 ( $\alpha$ CH), 15.1 ( $\beta$ CH<sub>3</sub>), 171.4 (CO), 101.8 (C1 $\beta$ ), 75.0 (C2 $\beta$ ), 70.1 (C5 $\beta$ ), 63.5 (C6 $\beta$ ) ppm; **2,6-di-O- ester (16d)** : <sup>1</sup>H NMR  $\delta$  : 3.36 ( $\alpha$ CH), 1.30 ( $\beta$ CH<sub>3</sub>), 3.78 (H-2 $\beta$ ), 3.47 (H-6) ppm; <sup>13</sup>C NMR  $\delta$  : 49.5 ( $\alpha$ CH), 16.4 ( $\beta$ CH<sub>3</sub>), 100.8 (C1 $\beta$ ), 76.5 (C2 $\beta$ ), 62.7 (C6 $\beta$ ) ppm; **3,6-di-O- ester (16e)** : <sup>1</sup>H NMR  $\delta$ : 1.30 ( $\beta$ CH<sub>3</sub>), 3.78 (H-3 $\beta$ ), 3.82 (H-6) ppm; <sup>13</sup>C NMR  $\delta$  : 51.4 ( $\alpha$ CH), 16.7 ( $\beta$ CH<sub>3</sub>), 81.6 (C3 $\beta$ ), 63.1 (C6 $\beta$ ) ppm.

A typical UV, IR, mass and 2D-HSQCT NMR spectra for L-alanyl-D-glucose **16a-e** are shown in Figures 4.2, 4.3, 4.4 and 4.5 respectively.

**4.2.1.2. L-Alanyl-D-galactose (17a-c)**: Solid; HPLC  $t_{ret}$ : 3.4 min;  $R_f$ : 0.19; UV (H<sub>2</sub>O,  $\lambda_{max}$ ): 200.0 nm ( $\sigma \rightarrow \sigma^*$   $\epsilon_{200.0} - 2630.3 \text{ M}^{-1}$ ), 295.0 nm ( $n \rightarrow \pi^*$   $\epsilon_{295.0} - 2089.3 \text{ M}^{-1}$ ); IR (KBr, stretching frequency): 2889  $\text{cm}^{-1}$  (NH), 3407  $\text{cm}^{-1}$  (OH), 2950  $\text{cm}^{-1}$  (CH), 1622  $\text{cm}^{-1}$  (CO); MS ( $m/z$ ) : 274 [M+Na]<sup>+</sup>.

2D HSQCT (DMSO-*d*<sub>6</sub>) **2-O- ester (17a)** : <sup>1</sup>H NMR  $\delta$  (500.13 MHz) : 2.95 ( $\alpha$ CH), 3.38 (H-2 $\alpha$ ), 3.36 (H-2 $\beta$ ), 3.55 (H-6) ppm; <sup>13</sup>C NMR  $\delta$  (125 MHz) : 51.5 ( $\alpha$ CH), 76.4(C2 $\alpha$ ), 76.5 (C2 $\beta$ ), 60.7(C6 $\beta$ ) ppm; **3-O- ester (17b)** : <sup>1</sup>H NMR  $\delta$  : 3.75 (H-3 $\alpha$ ), 3.60 (H-3 $\beta$ ), 3.35 (H-6) ppm; <sup>13</sup>C NMR  $\delta$  : 81.6 (C3 $\alpha$ ), 82.6 (C3 $\beta$ ), 60.7 (C6 $\alpha$ ) ppm; **6-O- ester (17c)** : <sup>1</sup>H NMR  $\delta$  : 3.05 ( $\alpha$ CH), 4.90 (H-1 $\alpha$ ), 4.85 (H-1 $\beta$ ), 3.85 (H-3 $\alpha$ ), 3.30 (H-6) ppm; <sup>13</sup>C NMR  $\delta$  : 52.0 ( $\alpha$ CH), 175.0 (CO), 95.4 (C1 $\alpha$ ), 101.8 (C1 $\beta$ ), 70.8 (C3 $\alpha$ ), 63.1 (C6 $\alpha$ ) ppm.

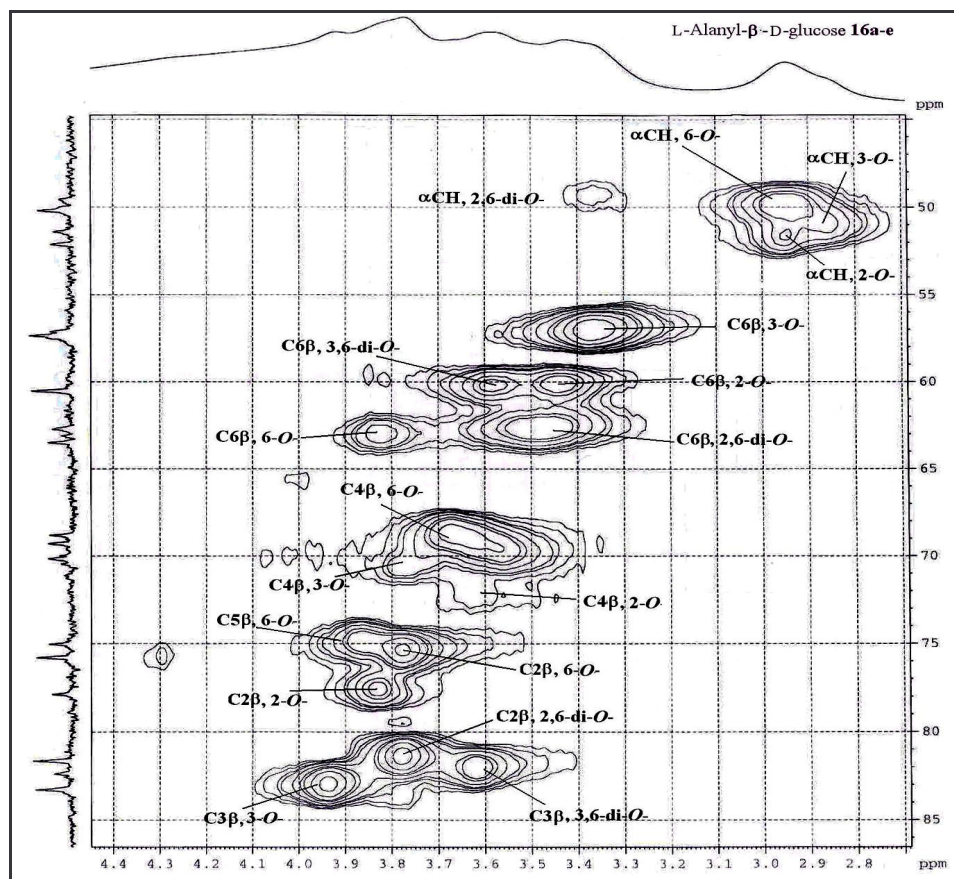


**Fig. 4.5.** Two-dimensional HSQCT NMR spectrum for L-alanyl-β-D-glucose **16a-e** of RML catalyzed reaction. Isolated through repeated HPLC injections in an aminopropyl column eluted with acetonitrile:water (v/v 80:20) as mobile phase and detected by Refractive Index detector.

A typical 2D-HSQCT NMR spectrum for L-alanyl-D-galactose **17a-c** is shown in Figure 4.6.

**4.2.1.3. L-Alanyl-D-mannose (18a-e)** : Solid; HPLC  $t_{ret}$ : 3.4 min;  $R_f$ : 0.19; UV(H<sub>2</sub>O,  $\lambda_{max}$ ): 194.0 nm ( $\sigma \rightarrow \sigma^*$   $\epsilon_{194.0} - 2630.3 \text{ M}^{-1}$ ), 295.0 nm ( $n \rightarrow \pi^*$   $\epsilon_{295.0} - 1047.1 \text{ M}^{-1}$ ); IR (KBr, stretching frequency): 2887  $\text{cm}^{-1}$  (NH), 3387  $\text{cm}^{-1}$  (OH), 2816  $\text{cm}^{-1}$  (CH), 1626  $\text{cm}^{-1}$  (CO); MS ( $m/z$ ) : 274 [M+Na]<sup>+</sup>.

2D HSQCT (DMSO- $d_6$ ) **3-O- ester (18a)**: <sup>13</sup>C NMR  $\delta$  (125 MHz) : 51.5 ( $\alpha$ CH), 15.2 ( $\beta$ CH<sub>3</sub>), 74.0 (C2 $\alpha$ ), 89.2 (C3 $\alpha$ ), 60.1 (C6 $\alpha$ ) ppm; **4-O- ester (18b)** : <sup>13</sup>C NMR  $\delta$  : 49.7 ( $\alpha$ CH), 14.7 ( $\beta$ CH<sub>3</sub>), 75.32 (C4 $\beta$ ), 60.1 (C6 $\alpha$ ) ppm; **6-O- ester (18c)** : <sup>13</sup>C NMR  $\delta$  : 52.1 ( $\alpha$ CH), 15.9 ( $\beta$ CH<sub>3</sub>), 172.0 (CO), 95.5 (C1 $\alpha$ ), 101.5 (C1 $\beta$ ), 69.7 (C2 $\alpha$ ), 69.0 (C3 $\alpha$ ), 68.4 (C4 $\alpha$ ), 74.9 (C5 $\alpha$ ), 63.1 (C6 $\alpha$ ) ppm; **3,6-di-O- ester (18d)** : <sup>13</sup>C NMR  $\delta$  : 82.0 (C3 $\alpha$ ), 82.9 (C3 $\beta$ ), 62.8 (C6 $\alpha$ ) ppm; **4,6-di-O- ester (18e)** : <sup>13</sup>C NMR  $\delta$  : 77.2 (C4 $\alpha$ ), 62.5 (C6 $\alpha$ ) ppm.

A typical <sup>13</sup>C NMR spectrum for L-alanyl-D-mannose **18a-e** is shown in Figure 4.7.

**4.2.1.4. L-Alanyl-D-fructose (19a-c)** : Solid; HPLC  $t_{ret}$ : 3.5 min;  $R_f$ : 0.19; UV (H<sub>2</sub>O,  $\lambda_{max}$ ): 200.0 nm ( $\sigma \rightarrow \sigma^*$   $\epsilon_{200.0} - 2630.3 \text{ M}^{-1}$ ), 295.0 nm ( $n \rightarrow \pi^*$   $\epsilon_{295.0} - 2089.3 \text{ M}^{-1}$ ); IR (KBr, stretching frequency): 2889  $\text{cm}^{-1}$  (NH), 3407  $\text{cm}^{-1}$  (OH), 2950  $\text{cm}^{-1}$  (CH), 1622  $\text{cm}^{-1}$  (CO); MS ( $m/z$ ) : 274 [M+Na]<sup>+</sup>.

2D HSQCT (DMSO- $d_6$ ) **1-O- ester (19a)** : <sup>1</sup>H NMR  $\delta$  (500.13 MHz) : 3.05 ( $\alpha$ CH), 3.40 (H-1 $\alpha$ ), 4.85 (H-2 $\beta$ ), 3.85 (H-3 $\alpha$ ), 3.30 (H-6) ppm; <sup>13</sup>C NMR  $\delta$  (125 MHz) : 52.0 ( $\alpha$ CH), 175.0 (CO), 63.5 (C1 $\alpha$ ), 102.4 (C2 $\beta$ ), 70.8 (C3 $\alpha$ ), 62.8 (C6 $\alpha$ ) ppm; **6-O- ester (19b)** : <sup>1</sup>H NMR  $\delta$  : 3.75 (H-3 $\alpha$ ), 3.60 (H-3 $\beta$ ), 3.30 (H-6) ppm; <sup>13</sup>C NMR  $\delta$  : 81.6 (C3 $\alpha$ ), 82.6 (C3 $\beta$ ), 63.6 (C6 $\alpha$ ) ppm; **1,6-di-O- ester (19c)** : <sup>1</sup>H NMR  $\delta$  : 2.95 ( $\alpha$ CH), 3.12 (H-

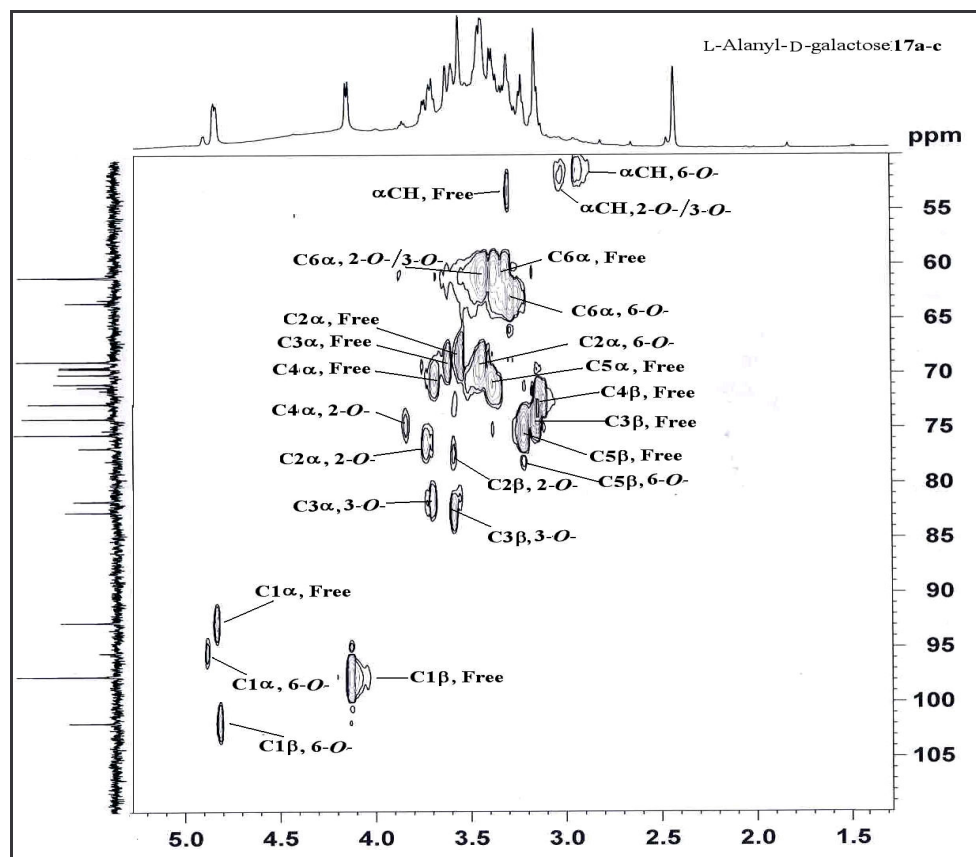


Fig. 4.6. Two-dimensional HSQCT NMR spectrum for L-alanyl-D-galactose **17a-c** of RML catalyzed reaction.

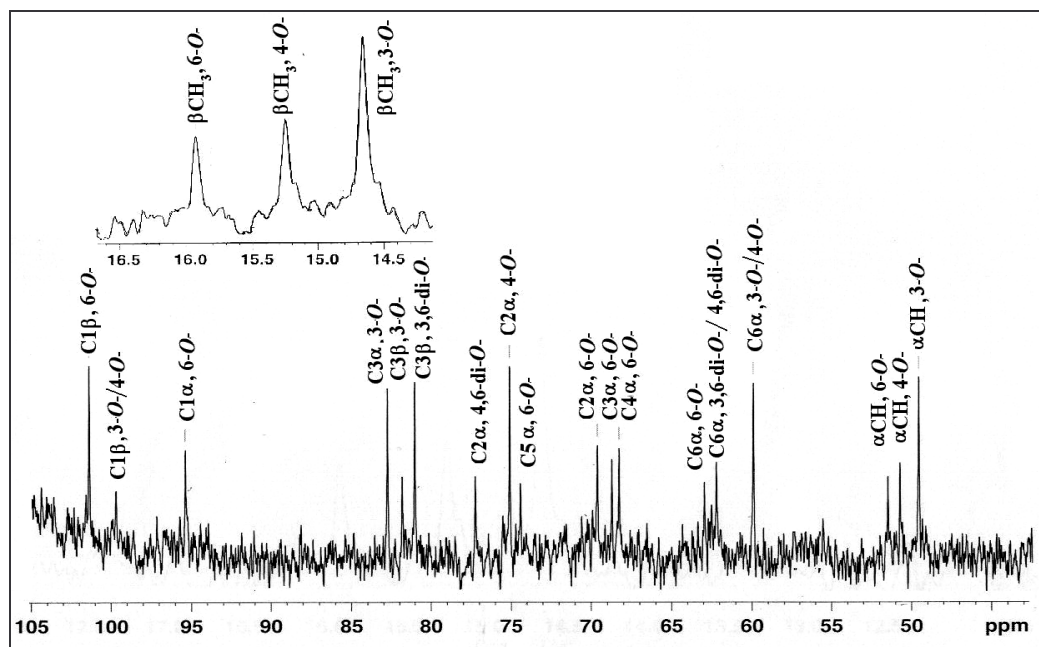


Fig. 4.7.  $^{13}\text{C}$  NMR spectrum for L-alanyl-D-mannose **18a-e** catalyzed by RML. Isolated through Sephadex G-10 using water as eluant.

1 $\alpha$ ), 3.38 (H-2 $\alpha$ ), 3.36 (H-2 $\beta$ ), 3.55 (H-6) ppm;  $^{13}\text{C}$  NMR  $\delta$  : 51.5 ( $\alpha\text{CH}$ ), 63.6 (C1 $\alpha$ ), 76.4 (C2 $\alpha$ ), 76.5 (C2 $\beta$ ) ppm.

A typical mass spectrum for L-alanyl-D-fructose **19a-c** is shown in Figure 4.8.

**4.2.1.5. L-Alanyl-D-arabinose (20a-c):** Solid; HPLC  $t_{ret}$ : 3.2 min;  $R_f$ : 0.23; UV ( $\text{H}_2\text{O}$ ,  $\lambda_{max}$ ): 200.0 nm ( $\sigma \rightarrow \sigma^*$   $\epsilon_{200.0} - 1584.9 \text{ M}^{-1}$ ), 276.0 nm ( $n \rightarrow \pi^*$   $\epsilon_{276.0} - 933.3 \text{ M}^{-1}$ ); IR (KBr, stretching frequency): 3397  $\text{cm}^{-1}$  (NH), 3443  $\text{cm}^{-1}$  (OH), 2940  $\text{cm}^{-1}$  (CH), 1629  $\text{cm}^{-1}$  (CO); MS ( $m/z$ ) : 219 [M-2] $^+$  and 293 [M+1] $^+$ .

2D HSQCT (DMSO- $d_6$ ) **2-O- ester (20a)** :  $^1\text{H}$  NMR  $\delta$  (500.13 MHz) : 3.15 ( $\alpha\text{CH}$ ), 1.22 ( $\beta\text{CH}_3$ ), 5.0 (H-1 $\alpha$ ), 4.93 (H-1 $\beta$ ), 3.60 (H-2 $\alpha$ ), 3.15 (H-3 $\alpha$ ), 3.35 (H-5) ppm;  $^{13}\text{C}$  NMR  $\delta$  (125 MHz) : 48.2 ( $\alpha\text{CH}$ ), 17.2 ( $\beta\text{CH}_3$ ), 172.5 (CO), 96.0 (C1 $\alpha$ ), 102.0 (C1 $\beta$ ), 77.8(C2 $\alpha$ ), 72.0 (C3 $\alpha$ ), 63.5 (C5 $\alpha$ ) ppm; **5-O- ester (20b)** :  $^1\text{H}$  NMR  $\delta$  (500.13 MHz) 3.92 ( $\alpha\text{CH}$ ), 1.20 ( $\beta\text{CH}_3$ ), 4.30 (H-1 $\alpha$ ), 4.18 (H-1 $\beta$ ), 3.35 (H-2 $\alpha$ ), 3.25 (H-3 $\alpha$ ), 3.60 (H-4 $\alpha$ ), 3.60 (H-5) ppm;  $^{13}\text{C}$  NMR  $\delta$  : 48.2 ( $\alpha\text{CH}$ ), 16.0 ( $\beta\text{CH}_3$ ), 97.1 (C1 $\alpha$ ), 104.0 (C1 $\beta$ ), 72.9 (C2 $\alpha$ ), 72.0 (C3 $\alpha$ ), 67.8 (C4 $\alpha$ ), 65.1 (C5 $\alpha$ ) ppm; **2,5-di-O- ester (20c)** :  $^1\text{H}$  NMR  $\delta$  : 1.30 ( $\beta\text{CH}_3$ ), 3.45 (H-2 $\alpha$ ), 3.30 (H-5) ppm;  $^{13}\text{C}$  NMR  $\delta$  : 17.2 ( $\beta\text{CH}_3$ ), 76.9 (C2 $\alpha$ ), 65.1 (C5 $\alpha$ ) ppm.

A typical UV and mass spectra for L-alanyl-D-arabinose **20a-c** are shown in Figures 4.9 and 4.10 respectively

**4.2.1.6. L-Alanyl-D-ribose (21a-c):** Solid; HPLC  $t_{ret}$ : 3.2 min;  $R_f$ : 0.22; UV ( $\text{H}_2\text{O}$ ,  $\lambda_{max}$ ): 224.0 nm ( $\sigma \rightarrow \sigma^*$   $\epsilon_{224.0} - 3801.9 \text{ M}^{-1}$ ), 294.0 nm ( $n \rightarrow \pi^*$   $\epsilon_{294.0} - 1288.2 \text{ M}^{-1}$ ); IR (KBr, stretching frequency): 3402  $\text{cm}^{-1}$  (NH), 3242  $\text{cm}^{-1}$  (OH), 2887  $\text{cm}^{-1}$  (CH), 1625  $\text{cm}^{-1}$  (CO); MS ( $m/z$ ): 221 [M] $^+$ .

2D HSQCT (DMSO- $d_6$ ) **3-O- ester (21a)**:  $^1\text{H}$  NMR  $\delta$  (500.13 MHz): 1.25 ( $\alpha\text{CH}$ ), 3.12 ( $\beta\text{CH}_3$ ), 3.50 (H-2 $\alpha$ ), 3.67 (H-3 $\alpha$ ), 3.63 (H-4 $\alpha$ ), 3.64 (H-5) ppm;  $^{13}\text{C}$  NMR  $\delta$  (125

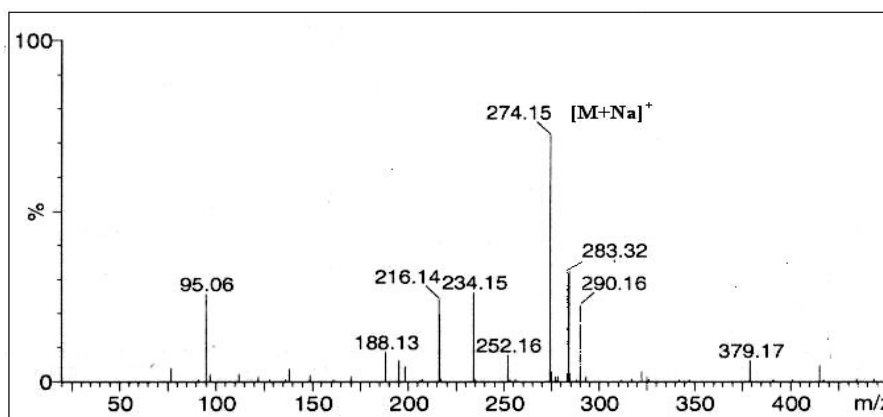


Fig. 4.8. A typical mass spectrum of L-alanyl-D-fructose **19a-c**.

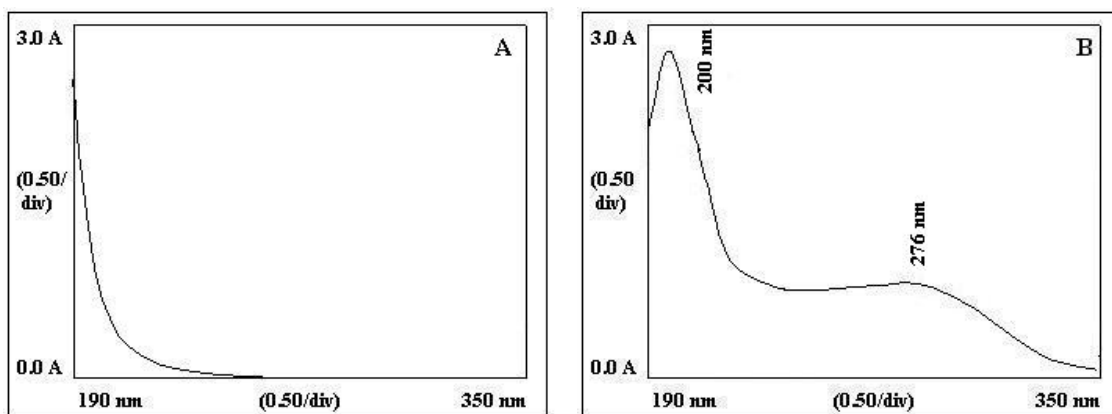


Fig. 4.9. UV spectra for L-alanyl-D-arabinose **20a-c** from RML catalyzed reaction. (A) L-alanine. (B) L-alanyl-D-arabinose.

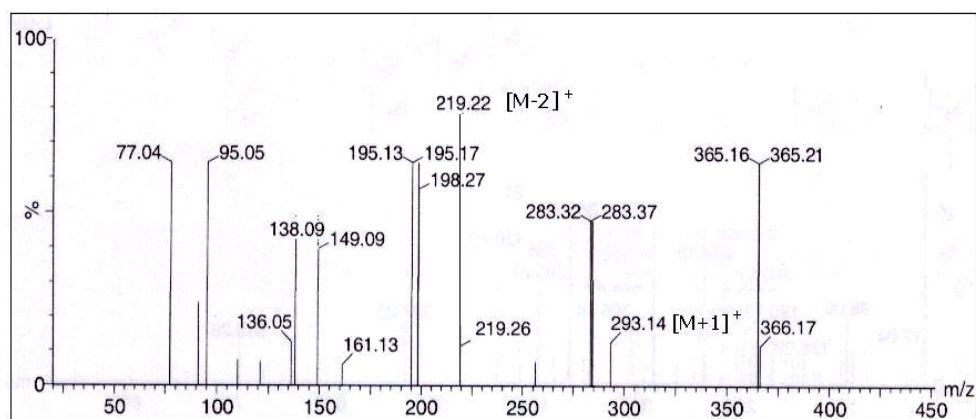


Fig. 4.10. A typical mass spectrum for L-alanyl-D-arabinose **20a-c**.

MHz): 48.2 ( $\alpha\text{CH}$ ), 15.9 ( $\beta\text{CH}_3$ ), 67.2 ( $\text{C}2\alpha$ ), 75.7 ( $\text{C}3\alpha$ ), 68.1 ( $\text{C}4\alpha$ ), 60.6 ( $\text{C}5\alpha$ ) ppm; **5-O- ester (21b)** :  $^1\text{H}$  NMR  $\delta$  : 3.39 ( $\alpha\text{CH}$ ), 1.25 ( $\beta\text{CH}_3$ ), 4.95 (H-1 $\alpha$ ), 4.20 (H-1 $\beta$ ), 3.27 (H-3 $\alpha$ ), 3.88 (H-4 $\alpha$ ), 3.61(H-5) ppm;  $^{13}\text{C}$  NMR  $\delta$  : 53.0 ( $\alpha\text{CH}$ ), 18.5 ( $\beta\text{CH}_3$ ), 173.5 (CO), 101.6 (C1 $\alpha$ ), 103.9 (C1 $\beta$ ), 75.0 (C3 $\alpha$ ), 71.0 (C4 $\alpha$ ), 63.4 (C5 $\alpha$ ) ppm; **3,5-di-O- ester (21c)** :  $^1\text{H}$  NMR  $\delta$  : 1.20 ( $\beta\text{CH}_3$ ), 3.45 (H-3 $\alpha$ ), 3.79 (H-4 $\alpha$ ), 3.52 (H-5) ppm;  $^{13}\text{C}$  NMR  $\delta$  : 18.5 ( $\beta\text{CH}_3$ ), 74.9 (C3 $\alpha$ ), 63.4 (C5 $\alpha$ ) ppm.

A typical UV and mass spectra for L-alanyl-D-ribose **22a-c** are shown in Figures 4.11 and 4.12 respectively.

**4.2.1.7. L-Alanyl-lactose (22a-c)**: Solid; HPLC  $t_{\text{ret}}$ : 3.3 min;  $R_f$ : 0.10; UV ( $\text{H}_2\text{O}$ ,  $\lambda_{\text{max}}$ ): 220.0 nm ( $\sigma \rightarrow \sigma^*$   $\epsilon_{220.0} = 436.5 \text{ M}^{-1}$ ), 294.0 nm ( $n \rightarrow \pi^*$   $\epsilon_{294.0} = 239.9 \text{ M}^{-1}$ ); IR (KBr, stretching frequency): 3378  $\text{cm}^{-1}$  (NH), 3378  $\text{cm}^{-1}$  (OH), 2946  $\text{cm}^{-1}$  (CH), 1624  $\text{cm}^{-1}$  (CO); MS ( $m/z$ ) : 436 [ $\text{M}+\text{Na}$ ] $^+$ .

2D HSQCT ( $\text{DMSO}-d_6$ ) **6-O- ester (22a)** :  $^1\text{H}$  NMR  $\delta$  (500.13 MHz) : 3.55 ( $\alpha\text{CH}$ ), 1.25 ( $\beta\text{CH}_3$ ), 4.78 (H-1 $\alpha$ ), 4.82 (H-1 $\beta$ ), 2.95 (H-2 $\alpha$ ), 3.25 (H-2 $\beta$ ), 2.95 (H-3 $\alpha$ ), 4.05 (H-4 $\alpha,\beta$ ), 3.15 (H-5 $\alpha$ ), 3.35 (H-5 $\beta$ ), 3.80 (H-6), 4.90 (H'-1 $\beta$ ), 3.90 (H'-2), 2.85 (H'-3), 3.70 (H'-4), 3.60 (H'-5), 3.40 (H'-6) ppm;  $^{13}\text{C}$  NMR  $\delta$  (125 MHz) : 51.0 ( $\alpha\text{CH}$ ), 15.5 ( $\beta\text{CH}_3$ ), 173.0 (CO), 98.0 (C1 $\alpha$ ), 100.2 (C1 $\beta$ ), 70.3 (C2 $\alpha$ ), 72.4 (C2 $\beta$ ), 74.3 (C3 $\alpha$ ), 81.0 (C4 $\alpha,\beta$ ), 73.3 (C5 $\alpha$ ), 73.4 (C5 $\beta$ ), 61.2 (C6 $\alpha,\beta$ ), 100.2 (C'1 $\beta$ ), 76.5 (C'2), 75.1 (C'3), 68.5 (C'4), 78.5 (C'5), 60.6 (C'6) ppm; **6'-O- ester (22b)**:  $^1\text{H}$  NMR  $\delta$  : 3.35 ( $\alpha\text{CH}$ ), 3.85 (H-4 $\alpha$ ), 3.70 (H'-6) ppm;  $^{13}\text{C}$  NMR  $\delta$  : 53.5 ( $\alpha\text{CH}$ ), 81.5 (C4 $\alpha$ ), 64.0 (C'6) ppm. **6,6'-di-O- ester (22c)** :  $^1\text{H}$  NMR  $\delta$  : 3.85 (H'-6) ppm;  $^{13}\text{C}$  NMR  $\delta$  : 67.5 (C'6) ppm.

A typical mass spectrum for L-alanyl-lactose **22a-c** is shown in Figure 4.13.

**4.2.1.8. L-Alanyl-maltose (23a-c)** : Solid; HPLC  $t_{\text{ret}}$ : 3.3 min;  $R_f$ : 0.11; UV ( $\text{H}_2\text{O}$ ,  $\lambda_{\text{max}}$ ): 228.0 nm ( $\sigma \rightarrow \sigma^*$   $\epsilon_{228.0} = 114.8 \text{ M}^{-1}$ ), 294.0 nm ( $n \rightarrow \pi^*$   $\epsilon_{294.0} = 56.2 \text{ M}^{-1}$ ); IR (KBr,

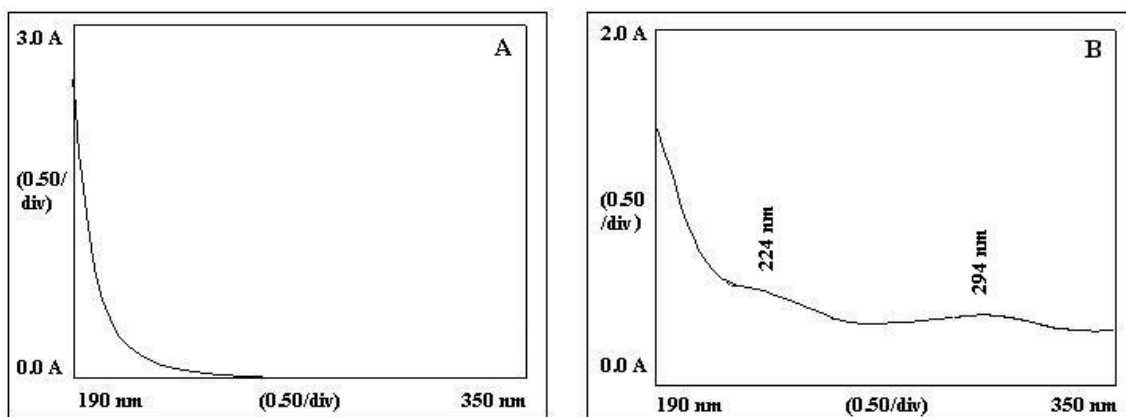


Fig. 4.11. UV spectra for L-alanyl-D-ribose **21a-c** from RML catalyzed reaction. (A) L-alanine. (B) L-alanyl-D-ribose.

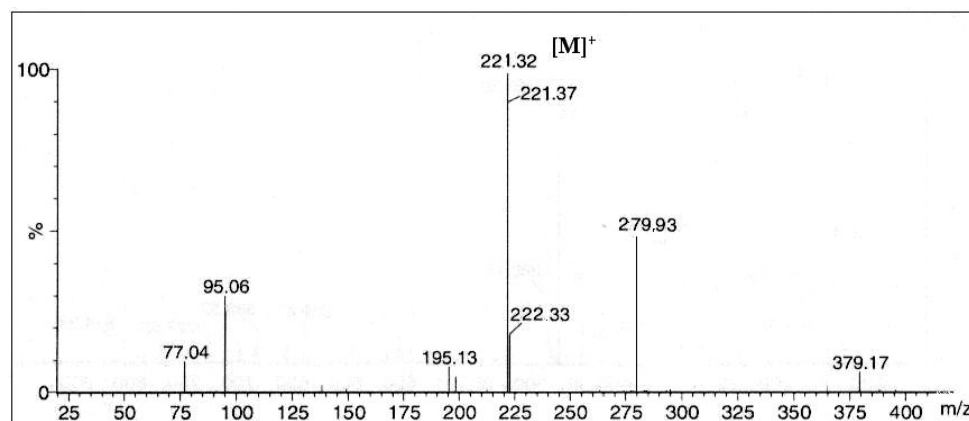


Fig. 4.12. A typical mass spectrum for L-alanyl-D-ribose **21a-c**.

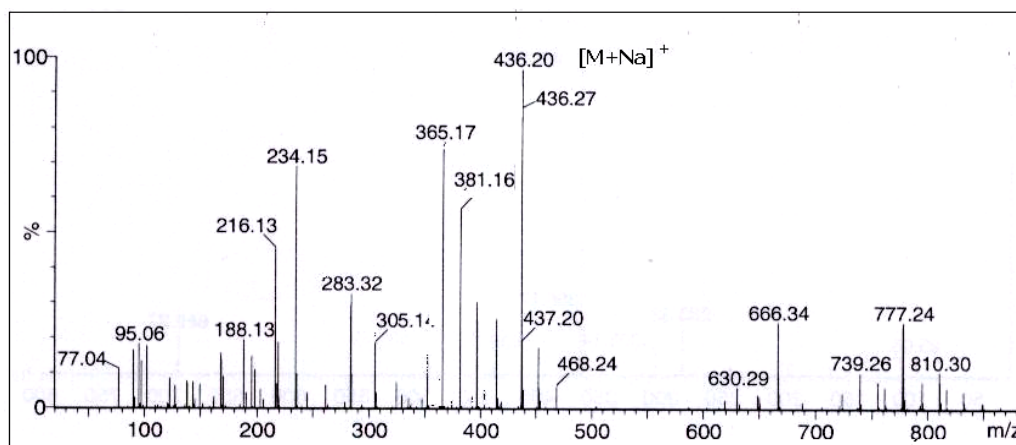


Fig. 4.13. A typical mass spectrum for L-alanyl-lactose **22a-c**.



stretching frequency): 3283  $\text{cm}^{-1}$  (NH), 3380  $\text{cm}^{-1}$  (OH), 2937  $\text{cm}^{-1}$  (CH), 1626  $\text{cm}^{-1}$  (CO); MS ( $m/z$ ): 436  $[\text{M}+\text{Na}]^+$ .

2D HSQCT (DMSO- $d_6$ ) **6-O- ester (23a)**:  $^1\text{H}$  NMR  $\delta$  (500.13 MHz): 3.55 ( $\alpha\text{CH}$ ), 1.25 ( $\beta\text{CH}_3$ ), 4.80 (H-1 $\alpha$ ), 4.20 (H-1 $\beta$ ), 4.05 (H-2 $\alpha,\beta$ ), 3.30 (H-3 $\alpha$ ), 3.85 (H-4 $\alpha,\beta$ ), 3.65 (H-5 $\alpha,\beta$ ), 3.50 (H-6), 4.90 (H'-1 $\alpha$ ), 2.95 (H'-2), 3.10 (H'-3), 3.50 (H'-4), 3.60 (H'-5), 3.60 (H'-6) ppm;  $^{13}\text{C}$  NMR  $\delta$  (125 MHz): 50.0 ( $\alpha\text{CH}$ ), 175.5 (CO), 92.0 (C1 $\alpha$ ), 96.7 (C1 $\beta$ ), 79.7 (C2 $\alpha,\beta$ ), 76.4 (C3 $\alpha$ ), 81.5 (C4 $\alpha,\beta$ ), 77.2 (C5 $\alpha,\beta$ ), 67.5 (C6 $\alpha,\beta$ ), 100.7 (C'1 $\alpha$ ), 70.3 (C'2), 71.8 (C'3), 69.9 (C'4'), 72.4 (C'5), 60.6 (C'6) ppm; **6'-O- ester (23b)**:  $^1\text{H}$  NMR  $\delta$  : 3.35 ( $\alpha\text{CH}$ ), 3.95 (H'-6) ppm;  $^{13}\text{C}$  NMR  $\delta$  : 53.0 ( $\alpha\text{CH}$ ), 67.0 (C'6 $\alpha$ ) ppm; **6,6'-di-O- ester (23c)**:  $^1\text{H}$  NMR  $\delta$  : 3.75 (H'-6) ppm;  $^{13}\text{C}$  NMR  $\delta$ : 63.0 (C'6) ppm.

A typical IR and 2D-HSQCT NMR spectra for L-alanyl-maltose **23a-c** are shown in Figures 4.14 and 4.15 respectively.

**4.2.1.9. L-Alanyl-sucrose (24)**: Solid; Mpt : 155  $^\circ\text{C}$ ; HPLC  $t_{\text{ret}}$ : 3.3 min;  $R_f$ : 0.13; UV ( $\text{H}_2\text{O}$ ,  $\lambda_{\text{max}}$ ): 224.0 nm ( $\sigma \rightarrow \sigma^*$   $\epsilon_{224.0} - 2344.2 \text{ M}^{-1}$ ), 294.0 nm ( $n \rightarrow \pi^*$   $\epsilon_{294.0} - 1288.2 \text{ M}^{-1}$ ); IR (KBr, stretching frequency): 3100  $\text{cm}^{-1}$  (NH), 3319  $\text{cm}^{-1}$  (OH), 2958  $\text{cm}^{-1}$  (CH), 1625  $\text{cm}^{-1}$  (CO); optical rotation ( $c$  0.5,  $\text{H}_2\text{O}$ ) :  $[\alpha]_{\text{D}}$  at 25  $^\circ\text{C} = -17.4^\circ$ ; MS ( $m/z$ ): 436  $[\text{M}+\text{Na}]^+$ .

2D HSQCT (DMSO- $d_6$ ) **6-O- ester (24)**:  $^1\text{H}$  NMR  $\delta$  (500.13 MHz): 3.59 ( $\alpha\text{CH}$ ), 1.30 ( $\beta\text{CH}_3$ ), 3.41 (H-1 $\beta$ ), 3.79 (H-3 $\beta$ ), 3.54 (H-4 $\beta$ ), 3.47 (H-5 $\beta$ ), 3.67 (H-6), 4.35 (H'-1 $\alpha$ ), 3.31 (H'-2), 3.45 (H'-3), 3.31 (H'-4), 3.58 (H'-5), 3.54 (H'-6) ppm;  $^{13}\text{C}$  NMR  $\delta$  (125 MHz): 49.5 ( $\alpha\text{CH}$ ), 18.0 ( $\beta\text{CH}_3$ ), 172.0 (CO), 64.0 (C1 $\beta$ ), 104.2 (C2 $\beta$ ), 77.33 (C3 $\beta$ ), 82.71 (C4 $\beta$ ), 74.5 (C5 $\beta$ ), 67.0 (C6 $\beta$ ), 96.0 (C'1 $\alpha$ ), 71.0 (C'2), 75.5 (C'3), 71.0 (C'4'), 74.0 (C'5), 60.71 (C'6) ppm.

A typical 2D-HSQCT NMR spectrum for L-alanyl-sucrose **24** is shown in Figures 4.16.

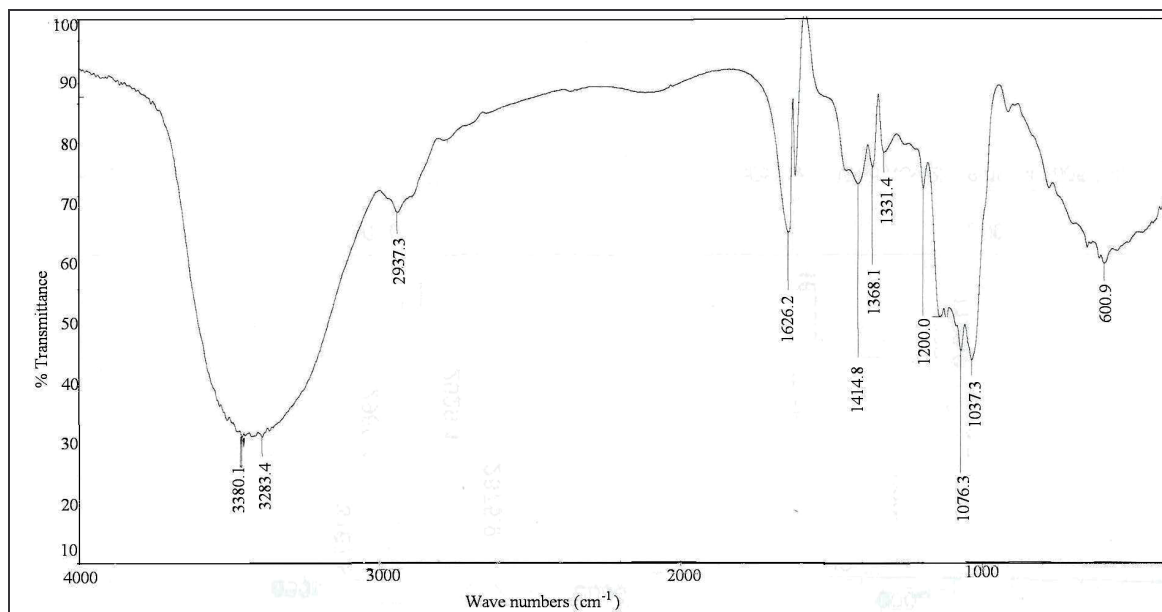


Fig. 4.14. A typical IR spectrum of L-alanyl-D-maltose **23a-c** of CRL catalyzed reaction.

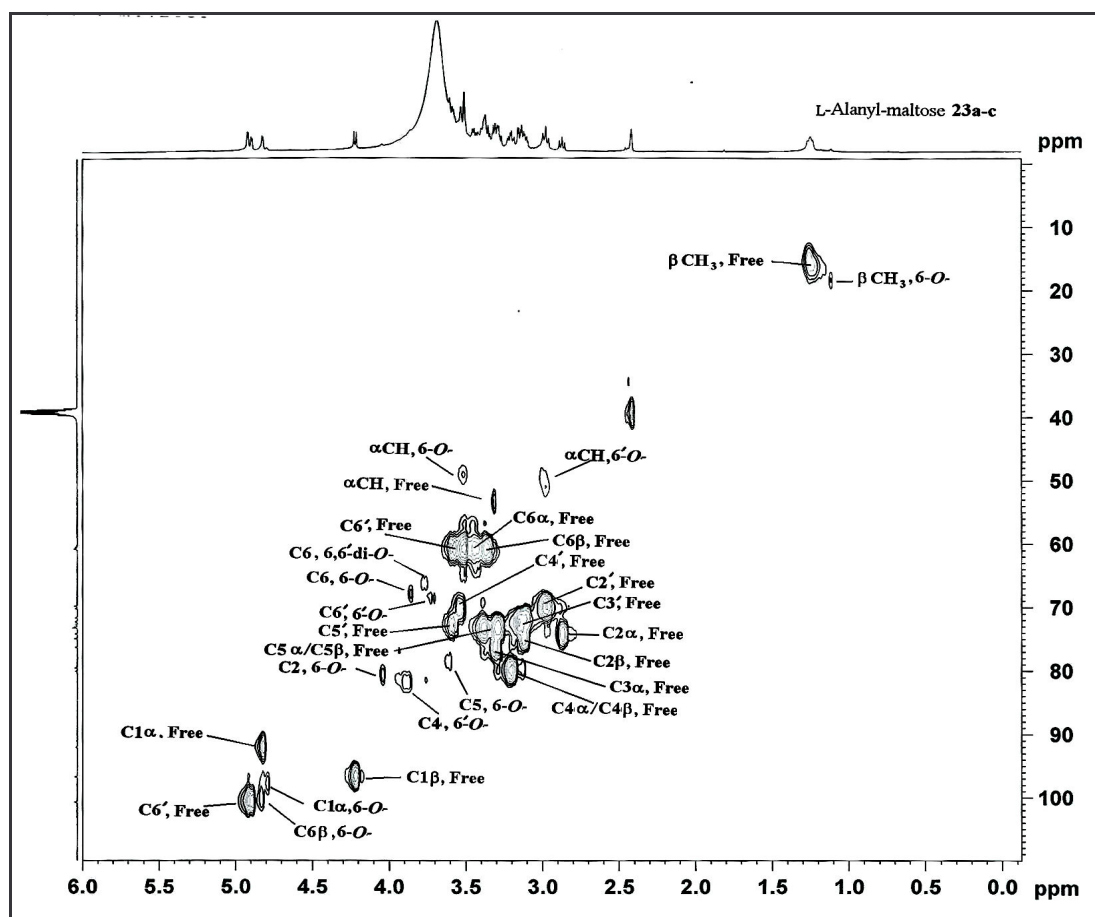
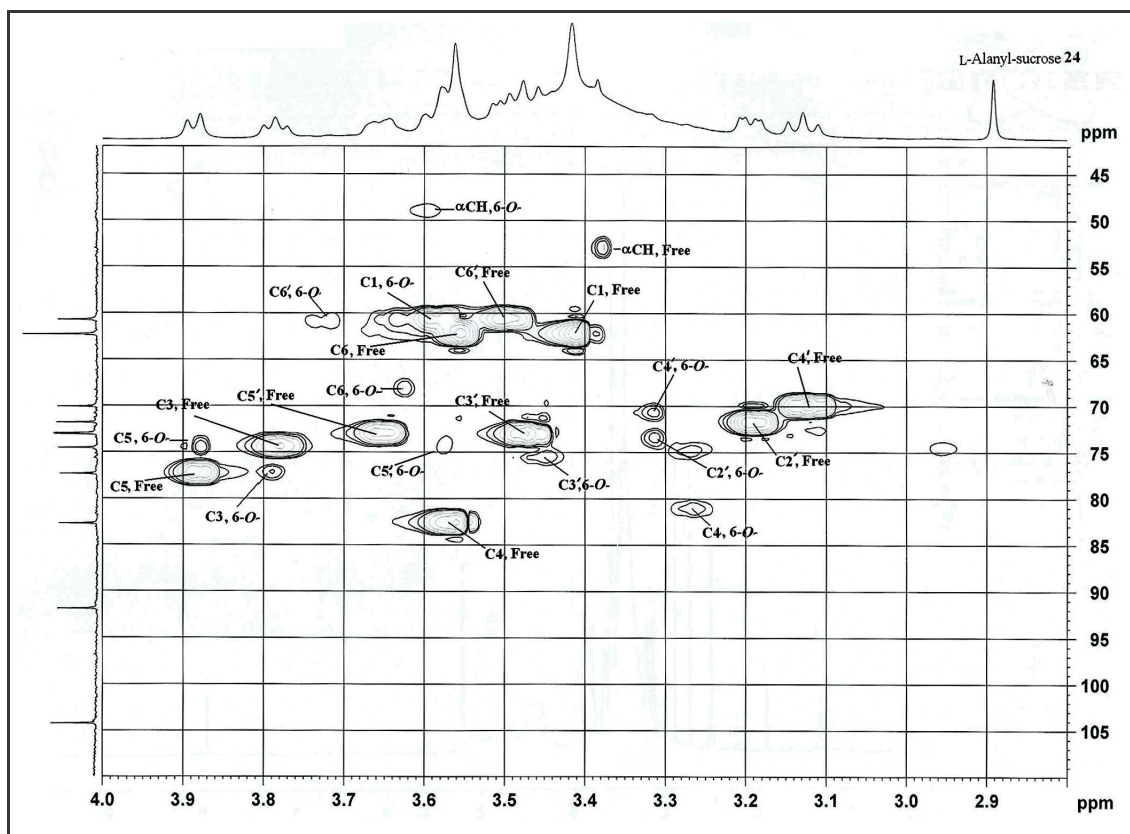


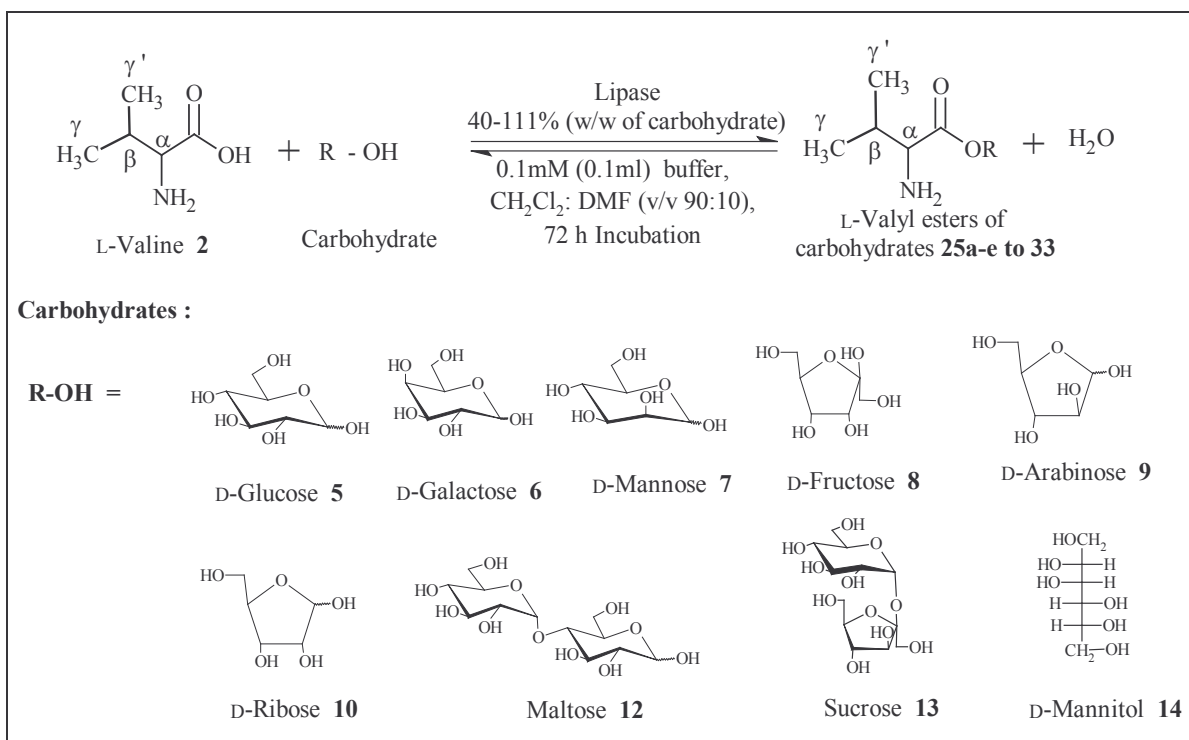
Fig. 4.15. Two-dimensional HSQCT NMR spectrum for L-alanyl-maltose **23a-c** prepared through RML catalysis.



**Fig. 4.16.** Two-dimensional HSQCT NMR spectrum for L-alanyl-sucrose **24** of RML catalyzed reaction.

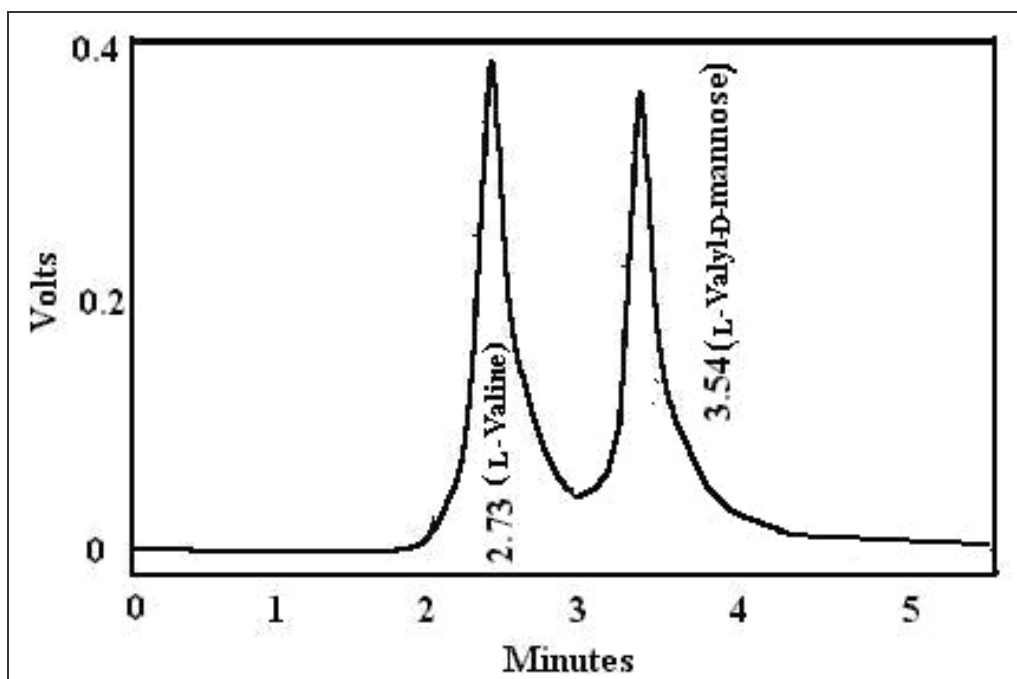
#### 4.2.2. Syntheses of L-valyl esters of carbohydrates 25a-e to 33

L-Valine (L-2-amino-3-methyl butanoic acid) is a polar and an essential dietary amino acid containing isopropyl group as a side chain. Using optimum conditions, an attempt was made to prepare L-valyl esters of different carbohydrates (**Scheme 4.2**). Esterification of L-valine with carbohydrates was carried out using CRL and crude PPL under optimal conditions (Section 2.2.4). The reaction mixture consists of 1-2 mmol L-valine **2** and 1 mmol carbohydrates (D-glucose **5**, D-galactose **6**, D-mannose **7**, D-fructose **8**, D-arabinose **9**, D-ribose **10**, lactose **11**, maltose **12**, sucrose **13**, D-mannitol **14**, D-sorbitol **15**) along with 40 % CRL (w/w carbohydrate) / 111 % of crude PPL (w/w carbohydrate) and incubated in 100 ml of CH<sub>2</sub>Cl<sub>2</sub> and DMF (v/v 90:10, 40 °C) containing 0.1 mM (0.1 ml of 0.1M) of phosphate buffer, pH 7.0 (CRL) or 0.2 mM (0.2 ml of 0.1M) of acetate buffer, pH 5.0 (crude PPL). The reaction mixture was analyzed by HPLC using C-18 column with acetonitrile:water (v/v 20:80) as mobile phase and detected at 210 nm (Fig. 4.17). Ester formation was also monitored by TLC and spots were detected by spraying ninhydrin (for NH<sub>2</sub> group detection) and 1-naphthol (for reducing sugar detection). The retention times ( $t_{ret}$ ) by HPLC and retention factor ( $R_f$ ) values by TLC are mentioned in sections 4.2.2.1 – 4.2.2.9.



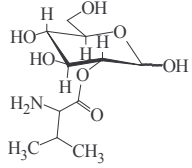
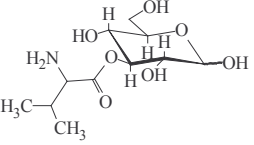
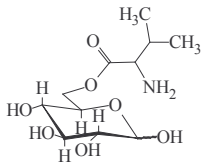
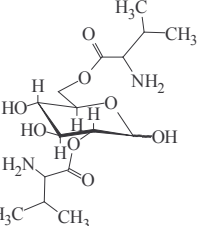
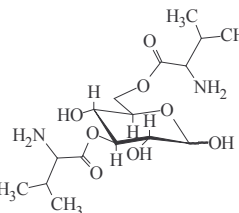
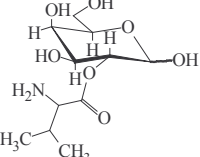
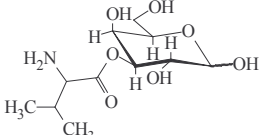
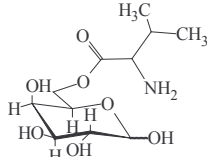
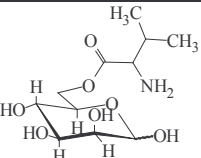
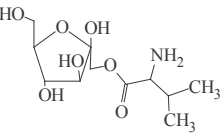
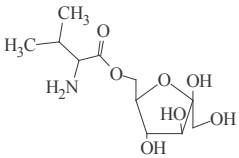
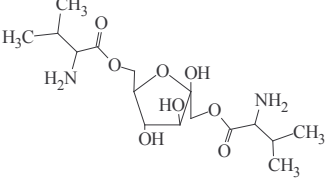
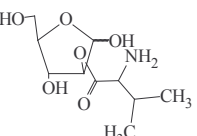
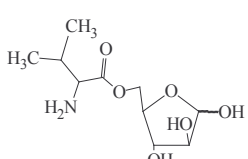
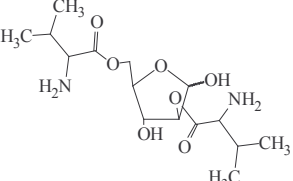
**Scheme 4.2 Lipase catalyzed syntheses of L-valyl esters of carbohydrates**

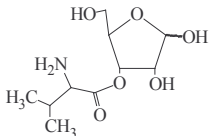
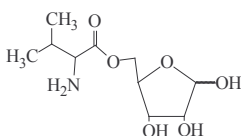
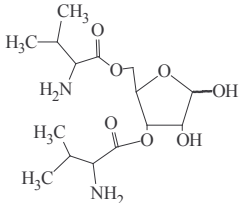
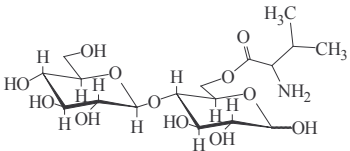
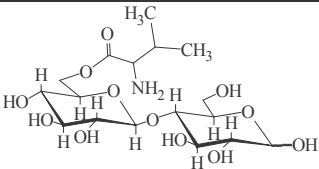
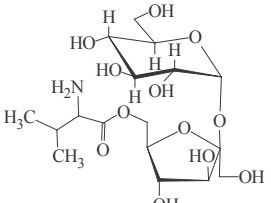
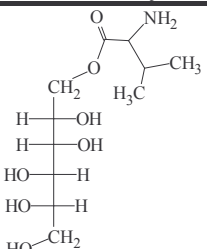
The isolated esters were subjected to UV, IR, MS, optical rotation and 2D- NMR characterization (Sections 4.2.2.1 – 4.2.2.9). The spectral data for the isolated esters are shown in Sections 4.2.2.1 – 4.2.2.9. Table 4.4 shows the HPLC ester yields, types of esters formed and percentage proportions of the individual esters from CRL catalyzed reaction and Table 4.5 shows the HPLC ester yields obtained through crude PPL catalysis.



**Fig. 4.17.** HPLC chromatogram: reaction mixture of L-valine and D-mannose esterification catalysed by CRL. Column – C-18; mobile phase – acetonitrile:water (v/v 20:80); flow rate - 1 ml/min; detector – UV at 210 nm; errors in conversion yields are within  $\pm 10\%$ .

Table 4.4. Syntheses of L-valyl esters of carbohydrates <sup>a</sup>

L-Valyl esters of carbohydrates (% proportions <sup>b</sup> )			Yield (%)
			68 (mono esters- 36, di esters- 32)
25a 2- <i>O</i> -L-valyl-D-glucose (10)	25b 3- <i>O</i> -L-valyl-D-glucose (12)	25c 6- <i>O</i> -L-valyl-D-glucose (31)	
			
25d 2,6-di- <i>O</i> -L-valyl-D-glucose (23)	25e 3,6-di- <i>O</i> -L-valyl-D-glucose (24)		
			30 (only mono esters)
26a 2- <i>O</i> -L-valyl-D-galactose (48)	26b 3- <i>O</i> -L-valyl-D-galactose (26)	26c 6- <i>O</i> -L-valyl-D-galactose (26)	
			
27 6- <i>O</i> -L-valyl-D-mannose			
			34 (mono esters-21, diester-13)
28a 1- <i>O</i> -L-valyl-D-fructose (29)	28b 6- <i>O</i> -L-valyl-D-fructose (34)	28c 1,6-di- <i>O</i> -L-valyl-D-fructose (37)	
			
29a 2- <i>O</i> -L-valyl-D-arabinose (32)	29b 5- <i>O</i> -L-valyl-D-arabinose (25)	29c 2,5-di- <i>O</i> -L-valyl-D-arabinose (43)	

			33 <sup>c</sup> (mono esters-17, diester-16)
<b>30a</b> 3- <i>O</i> -L-valyl-D-ribose (26)	<b>30b</b> 5- <i>O</i> -L-valyl-D-ribose (26)	<b>30c</b> 3,5-di- <i>O</i> -L-valyl-D-ribose (48)	
			47 (only mono esters)
<b>31a</b> 6- <i>O</i> -L-valyl-maltose (49)	<b>31b</b> 6'- <i>O</i> -L-valyl-maltose (51)		
			60 (only mono ester)
<b>32</b> 6- <i>O</i> -L-valyl- sucrose			
			52 (only mono ester)
<b>33</b> 1- <i>O</i> -L-valyl-D-mannitol			

<sup>a</sup> L-Valine – 2 mmol, carbohydrates – 1 mmol, CRL – 40 % (w/w carbohydrate), buffer – 0.1 mM (0.1 ml of 0.1M) phosphate buffer pH 7.0, CH<sub>2</sub>Cl<sub>2</sub>:DMF (v/v, 90:10) at 40 °C, incubation period – 72 h. Conversion yields were from HPLC with respect to L-valine concentration.

<sup>b</sup> Percentage proportions of individual esters were determined from the peak areas or from their cross peaks of the Carbon-13 C6 and C5 (in case of pentoses) signals in the 2D HSQCT spectrum.

<sup>c</sup> Several cross peaks, due to opening and/or degradation of the five membered ring during esterification



**Table 4.5 Preparation of L-valyl esters of carbohydrates using crude porcine pancreas lipase <sup>a</sup>**

L-Valyl ester of carbohydrate	%Yield (mmol)
L- Valyl-D-glucose <b>25a-e</b>	31 (0.31)
L- Valyl-D-galactose <b>26a-c</b>	26 (0.26)
L- Valyl-D-mannose <b>27</b>	43 (0.43)
L- Valyl-D-fructose <b>28a-c</b>	47 (0.47)
L- Valyl-D-arabinose <b>29a-c</b>	31 (0.31)
L- Valyl-D-ribose <b>30a-c</b>	53 (0.53)
L- Valyl-maltose <b>31a,b</b>	79 (0.79)
L- Valyl-sucrose <b>32</b>	58 (0.58)
L- Valyl-D-mannitol <b>33</b>	52 (0.52)

<sup>a</sup> L-Valine – 1 mmol, carbohydrates – 1 mmol, Crude PPL – 111 % (w/w carbohydrate), buffer – 0.2 mM (0.2 ml of 0.1 M) acetate buffer pH 5.0, CH<sub>2</sub>Cl<sub>2</sub>:DMF (v/v 90:10) at 40 °C, Incubation period – 72 h. Conversion yields were from HPLC with respect to L-valine concentration.

**Spectral data for L-Valine (2):** Solid; Mpt : 298 °C; HPLC  $t_{ret}$ : 2.7 min;  $R_f$ : 0.32; UV (H<sub>2</sub>O,  $\lambda_{max}$ ): 195.0 nm ( $\sigma \rightarrow \sigma^*$   $\epsilon_{195.0} - 116 \text{ M}^{-1}$ ); IR (KBr, stretching frequency): 3415 cm<sup>-1</sup> (OH), 2945 cm<sup>-1</sup> (CH), 1605 cm<sup>-1</sup> (CO); optical rotation ( $c$  1.0, H<sub>2</sub>O) :  $[\alpha]_D$  at 25 °C = +3.33 °.

2D-HSQCT (DMSO- $d_6$ ) : <sup>1</sup>H NMR  $\delta$  (500.13 MHz) : 3.30 ( $\alpha$ CH), 1.90 ( $\beta$ CH), 0.98 ( $\gamma$ ,  $\gamma'$ CH<sub>3</sub>) ppm; <sup>13</sup>C NMR  $\delta$  (125 MHz) : 53.2 ( $\alpha$ CH), 29.2( $\beta$ CH), 18.1 ( $\gamma$ ,  $\gamma'$ CH<sub>3</sub>), 170.5 (CO) ppm.

**4.2.2.1. L-Valyl-D-glucose (25a-e):** Solid; HPLC  $t_{ret}$ : 3.5 min;  $R_f$ : 0.22; UV (H<sub>2</sub>O,  $\lambda_{max}$ ): 200.0 nm ( $\sigma \rightarrow \sigma^*$   $\epsilon_{200.0} - 2630 \text{ M}^{-1}$ ), 295.0 nm ( $n \rightarrow \pi^*$   $\epsilon_{295.0} - 2089 \text{ M}^{-1}$ ); IR (KBr, stretching frequency): 2971 cm<sup>-1</sup> (NH), 3407 cm<sup>-1</sup> (OH), 2950 cm<sup>-1</sup> (CH), 1622 cm<sup>-1</sup> (CO); MS ( $m/z$ ) : 302 [M+Na]<sup>+</sup>.

2D-HSQCT (DMSO- $d_6$ ) : **2-O- ester (25a):** <sup>1</sup>H NMR  $\delta$  (500.13 MHz) : 3.08 ( $\alpha$ CH), 1.35 ( $\gamma$ CH<sub>3</sub>), 3.75 (H-2 $\alpha$ ), 3.67 (H-3 $\alpha$ ), 3.78 (H-4 $\alpha$ ), 4.22 (H-5 $\alpha$ ), 3.50 (H-6) ppm; <sup>13</sup>C NMR

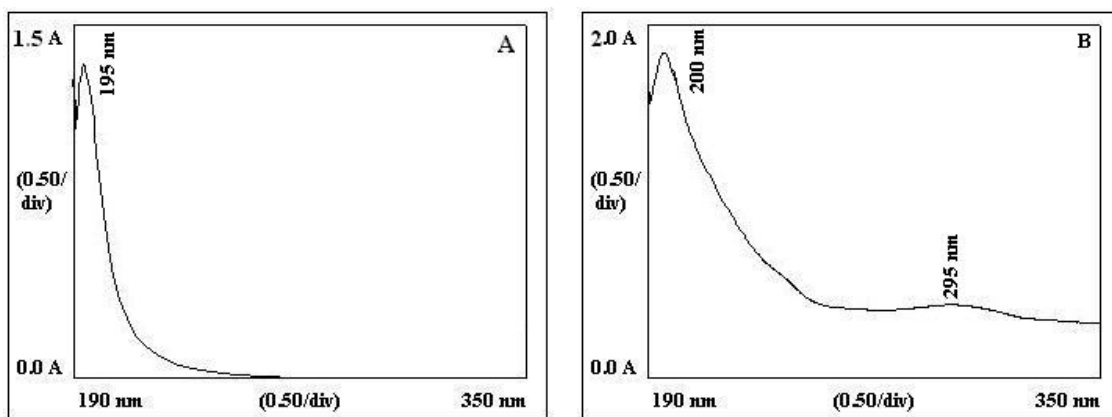


Fig. 4.18. UV spectra for L-valyl-D-glucose **25a-e** from CRL catalyzed reaction. (A) L-valine (B) L-valyl-D-glucose.

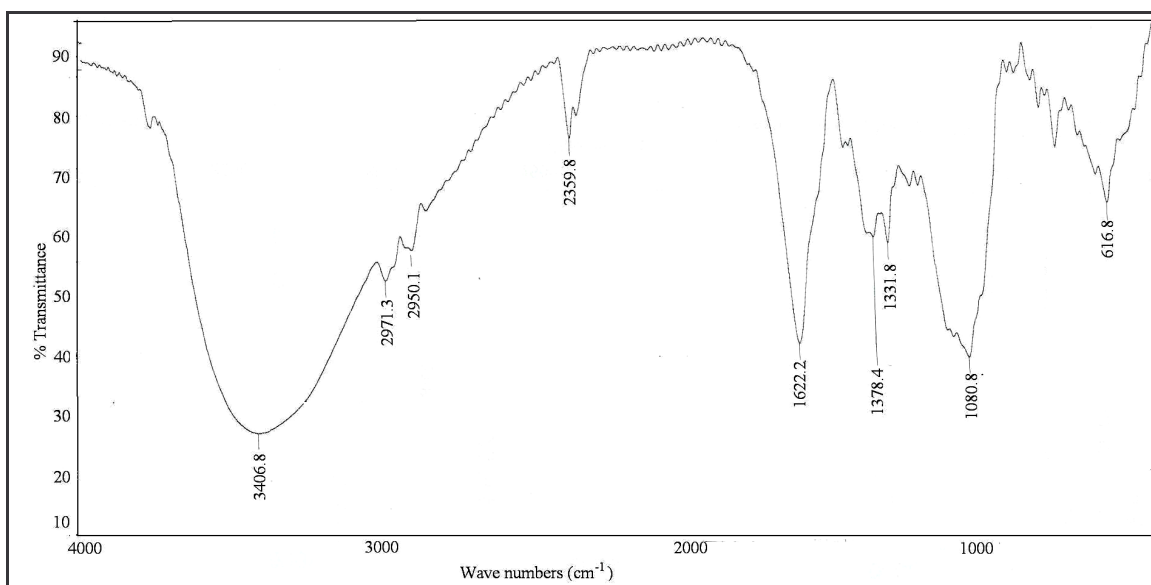


Fig. 4.19. A typical IR spectrum of L-valyl-D-glucose of CRL catalysed reaction **25a-e**.

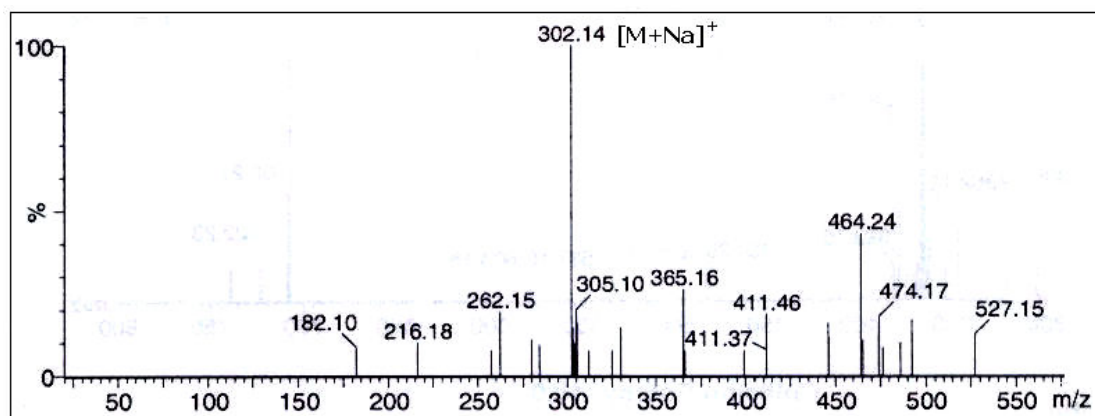


Fig. 4.20. A typical mass spectrum for L-valyl-D-glucose **25a-e**.

$\delta$  (125 MHz): 51.5 ( $\alpha$ CH), 19.4 ( $\gamma$ CH<sub>3</sub>), 77.4 (C2 $\alpha$ ), 74.6 (C3 $\alpha$ ), 71.3 (C4 $\alpha$ ), 71.3 (C5 $\alpha$ ), 60.0 (C6 $\alpha$ ) ppm; **3-O- ester (25b)**: <sup>1</sup>H NMR  $\delta$ : 3.10 ( $\alpha$ CH), 1.15 ( $\beta$ CH<sub>3</sub>), 3.85 (H-2 $\alpha$ ), 3.90 (H-3 $\alpha$ ), 4.01 (H-3 $\beta$ ), 3.34 (H-6) ppm; <sup>13</sup>C NMR  $\delta$ : 52.3 ( $\alpha$ CH), 18.3 ( $\gamma$ CH<sub>3</sub>), 71.3 (C2 $\alpha$ ), 82.6 (C3 $\alpha$ ), 83.1 (C3 $\beta$ ), 60.4 (C6 $\alpha$ ) ppm; **6-O- ester (25c)**: <sup>1</sup>H NMR  $\delta$ : 3.20 ( $\alpha$ CH), 3.35 ( $\beta$ CH), 1.55 ( $\gamma$ CH<sub>3</sub>), 4.95 (H-1 $\alpha$ ), 4.24 (H-1 $\beta$ ), 3.90 (H-3 $\alpha$ ), 3.74 (H-4 $\alpha$ ), 3.41 (H-5 $\alpha$ ), 3.15 (H-6) ppm; <sup>13</sup>C NMR  $\delta$ : 53.4 ( $\alpha$ CH), 29.9 ( $\beta$ CH), 19.8 ( $\gamma$ CH<sub>3</sub>), 94.9 (C1 $\alpha$ ), 103.4 (C1 $\beta$ ), 76.2 (C3 $\alpha$ ), 69.5 (C4 $\alpha$ ), 69.0 (C5 $\beta$ ), 63.4 (C6 $\alpha$ ) ppm; **2,6-di-O- ester (15d)**: <sup>1</sup>H NMR  $\delta$ : 3.20 ( $\alpha$ CH), 3.85 (H-2 $\alpha$ ), 3.56 (H-6) ppm; <sup>13</sup>C NMR  $\delta$ : 51.4 ( $\alpha$ CH), 76.4 (C2 $\alpha$ ), 61.5 (C6 $\alpha$ ) ppm; **3,6-di-O-ester (25e)**: <sup>1</sup>H NMR  $\delta$ : 3.15 ( $\alpha$ CH), 1.45 ( $\gamma$ CH<sub>3</sub>), 3.70 (H-3 $\alpha$ ), 3.52 (H-6) ppm; <sup>13</sup>C NMR  $\delta$ : 53.4 ( $\alpha$ CH), 19.5 ( $\gamma$ CH<sub>3</sub>), 82.4 (C3 $\alpha$ ), 61.8 (C6 $\alpha$ ) ppm.

A typical UV, IR and mass spectra for L-valyl-D-glucose **25a-e** are shown in Figures 4.18, 4.19, and 4.20 respectively.

**4.2.2.2. L-Valyl-D-galactose (26a-c)**: Solid; HPLC  $t_{ret}$ : 3.5 min;  $R_f$ : 0.21; UV (H<sub>2</sub>O,  $\lambda_{max}$ ): 225.0 nm ( $\sigma \rightarrow \sigma^*$   $\epsilon_{225.0} - 871 \text{ M}^{-1}$ ), 295.0 nm ( $n \rightarrow \pi^*$   $\epsilon_{295.0} - 407 \text{ M}^{-1}$ ), IR (KBr, stretching frequency): 3309 cm<sup>-1</sup> (NH), 2944 cm<sup>-1</sup> (CH) and 1621 cm<sup>-1</sup> (CO); MS ( $m/z$ ): 302 [M+ Na]<sup>+</sup>.

2D-HSQCCT (DMSO- $d_6$ ): **2-O- ester (26a)**: <sup>1</sup>H NMR  $\delta$  (500.13 MHz): 3.30 ( $\alpha$ CH), 1.90 ( $\beta$ CH), 0.98 ( $\gamma$ ,  $\gamma'$ CH<sub>3</sub>), 3.83 (H-2 $\alpha$ ), 3.65 (H-2 $\beta$ ), 3.54 (H-6) ppm; <sup>13</sup>C NMR  $\delta$  (125 MHz): 53.2 ( $\alpha$ CH), 29.2 ( $\beta$ CH), 18.1 ( $\gamma$ ,  $\gamma'$ CH<sub>3</sub>), 171.2 (CO), 76.4 (C2 $\alpha$ ), 77.6 (C2 $\beta$ ), 60.6 (C6 $\alpha$ ) ppm; **3-O- ester (26b)**: <sup>1</sup>H NMR  $\delta$ : 3.80 (H-3 $\alpha$ ), 3.67 (H-3 $\beta$ ), 3.54 (H-6) ppm; <sup>13</sup>C NMR  $\delta$ : 81.6 (C3 $\alpha$ ), 82.7 (C3 $\beta$ ), 60.6 (C6 $\alpha$ ) ppm; **6-O- ester (26c)**: <sup>1</sup>H NMR  $\delta$ : 4.98 (H-1 $\alpha$ ), 4.89 (H-1 $\beta$ ), 3.56 (H-2 $\alpha$ ), 3.71 (H-3 $\alpha$ ), 3.31 (H-3 $\beta$ ), 3.78 (H-4 $\alpha$ ), 3.23

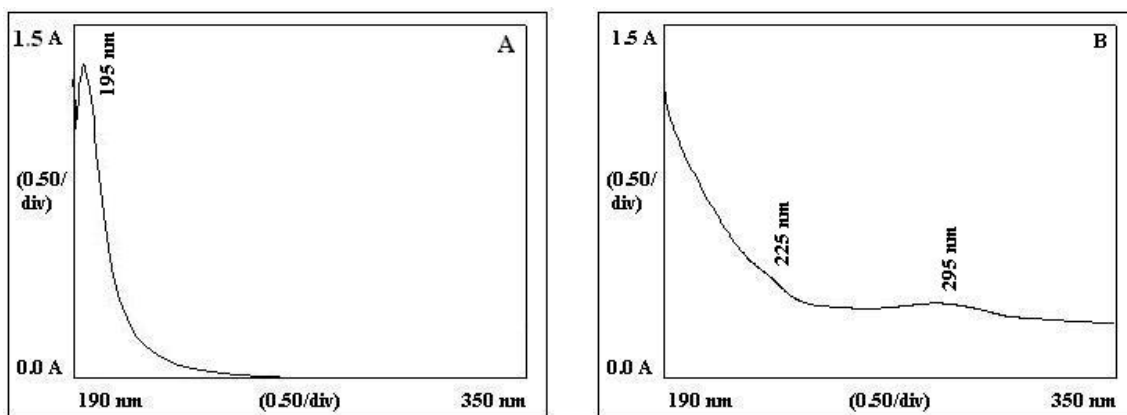


Fig. 4.21. UV spectra for L-valyl-D-galactose **26a-c** from CRL catalysed reaction. (A) L-valine; (B) L-valyl-D-galactose.

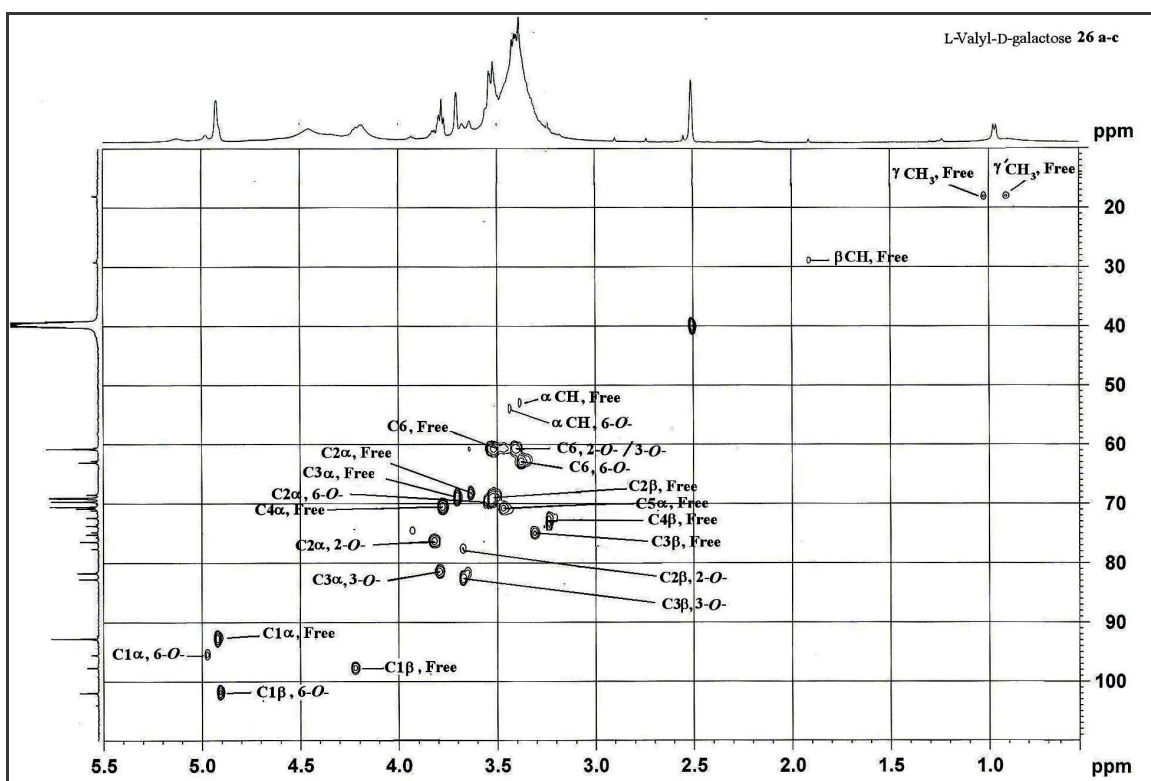


Fig. 4.22. Two-dimensional HSQCT NMR spectrum for L-valyl-D-galactose **26a-c** obtained through CRL catalysis.

(H-4 $\beta$ ), 3.44 (H-5 $\alpha$ ), 3.35 (H-6) ppm;  $^{13}\text{C}$  NMR  $\delta$  : 95.5 (C1 $\alpha$ ), 101.9 (C1 $\beta$ ), 69.6 (C2 $\alpha$ ), 69.1 (C3 $\alpha$ ), 73.7 (C3 $\beta$ ), 70.5 (C4 $\alpha$ ), 72.3 (C4 $\beta$ ), 70.5 (C5 $\alpha$ ), 63.1 (C6 $\alpha$ ) ppm.

A typical UV and 2D-HSQCT NMR spectra for L-valyl-D-galactose **26a-c** are shown in Figures 4.21 and 4.22 respectively.

**4.2.2.3. L-Valyl-D-mannose (27):** Solid; Mpt : 98 °C; HPLC  $t_{ret}$ : 2.0 min;  $R_f$ : 0.59; UV ( $\text{H}_2\text{O}$ ,  $\lambda_{max}$ ): 227.0 nm ( $\sigma \rightarrow \sigma^*$   $\epsilon_{227.0} - 447 \text{ M}^{-1}$ ), 290.0 nm ( $n \rightarrow \pi^*$   $\epsilon_{290.0} - 603 \text{ M}^{-1}$ ); IR (KBr, stretching frequency): 3410  $\text{cm}^{-1}$  (NH), 3354  $\text{cm}^{-1}$  (OH), 2932  $\text{cm}^{-1}$  (CH), 1644  $\text{cm}^{-1}$  (CO); optical rotation ( $c$  0.5,  $\text{H}_2\text{O}$ ) :  $[\alpha]_D$  at 25 °C = -20 ° ; MS ( $m/z$ ) : 302  $[\text{M}+\text{Na}]^+$ .

2D-HSQCT ( $\text{DMSO}-d_6$ ) : **6-O- ester (27)** :  $^1\text{H}$  NMR  $\delta$  (500.13 MHz): 3.90 ( $\alpha\text{CH}$ ), 2.16 ( $\beta\text{CH}$ ), 1.02 ( $\gamma$ ,  $\gamma'\text{CH}_3$ ), 4.31 (H-1 $\alpha$ ), 3.63 (H-2 $\alpha$ ), 3.32 (H-3 $\alpha$ ), 3.51 (H-4 $\alpha$ ), 3.45 (H-5 $\alpha$ ), 3.63 (H-6) ppm;  $^{13}\text{C}$  NMR  $\delta$  (125 MHz): 53.0 ( $\alpha\text{CH}$ ), 29.2 ( $\beta\text{CH}$ ), 18.2 ( $\gamma$ ,  $\gamma'\text{CH}_3$ ), 171.0 (CO), 96.8 (C1 $\alpha$ ), 67.5 (C2 $\alpha$ ), 73.5 (C3 $\alpha$ ), 67.5 (C4 $\alpha$ ), 75.5 (C5 $\alpha$ ), 63.5 (C6 $\alpha$ ) ppm.

A typical mass spectrum for L-valyl-D-mannose **29** is shown in Figure 4.23.

**4.2.2.4. L-Valyl-D-fructose (28a-c):** Solid; HPLC  $t_{ret}$ : 3.5 min;  $R_f$ : 0.20; UV ( $\text{H}_2\text{O}$ ,  $\lambda_{max}$ ): 223.0 nm ( $\sigma \rightarrow \sigma^*$   $\lambda_{223.0} - 53 \text{ M}^{-1}$ ), 288.0 nm ( $n \rightarrow \pi^*$   $\epsilon_{288.0} - 23 \text{ M}^{-1}$ ); IR (KBr, stretching frequency): 3352  $\text{cm}^{-1}$  (NH), 3290  $\text{cm}^{-1}$  (OH), 2946  $\text{cm}^{-1}$  (CH), 1623  $\text{cm}^{-1}$  (CO); MS ( $m/z$ ) : 304  $[\text{M}^{+2}+\text{Na}]^+$ ;

2D-HSQCT ( $\text{DMSO}-d_6$ ) : **1-O-ester (28a)**:  $^1\text{H}$  NMR  $\delta$  (500.13 MHz) : 3.38 ( $\alpha\text{CH}$ ), 2.14 ( $\beta\text{CH}$ ), 1.06 ( $\gamma$ ,  $\gamma'\text{CH}_3$ ), 3.78 (H-1 $\alpha$ ), 3.32 (H-3 $\alpha$ ), 3.55 (H-3 $\beta$ ), 3.78 (H-4 $\alpha$ ), 3.45 (H-4 $\beta$ ), 3.22 (H-5 $\alpha$ ), 3.32 (H-6) ppm;  $^{13}\text{C}$  NMR  $\delta$  (125 MHz) : 52.5 ( $\alpha\text{CH}$ ), 29.2 ( $\beta\text{CH}$ ), 18.4 ( $\gamma$ ,  $\gamma'\text{CH}_3$ ), 171.2 (CO), 64.1 (C1 $\alpha$ ), 104.3 (C2 $\beta$ ), 70.8 (C3 $\alpha$ ), 83.9 (C3 $\beta$ ), 72.5 (C4 $\alpha$ ), 76.0 (C4 $\beta$ ), 73.2 (C5 $\alpha$ ), 64.0 (C6 $\alpha$ ) ppm; **6-O-ester (28b)** :  $^1\text{H}$  NMR  $\delta$  : 3.63 (H-

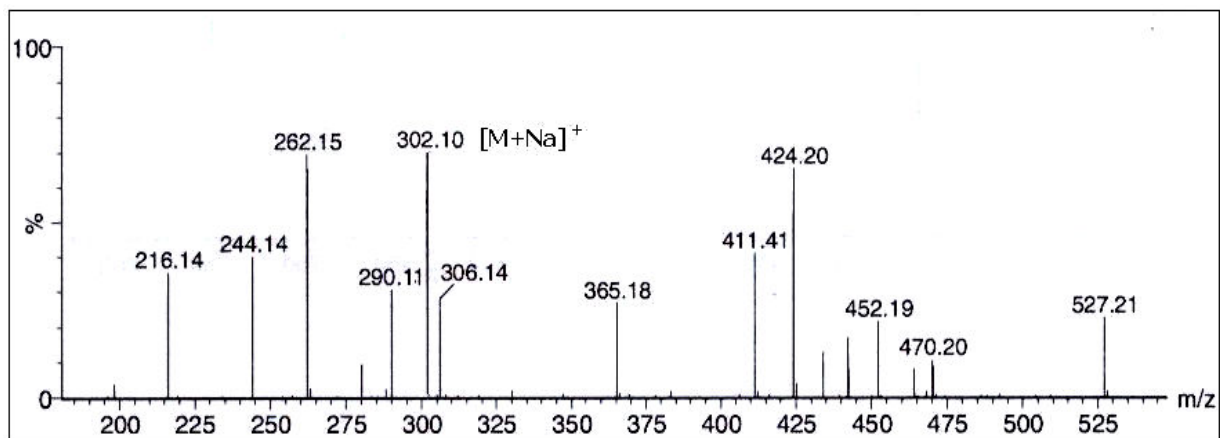


Fig. 4.23. A typical mass spectrum of L-valyl-D-mannose **27**.

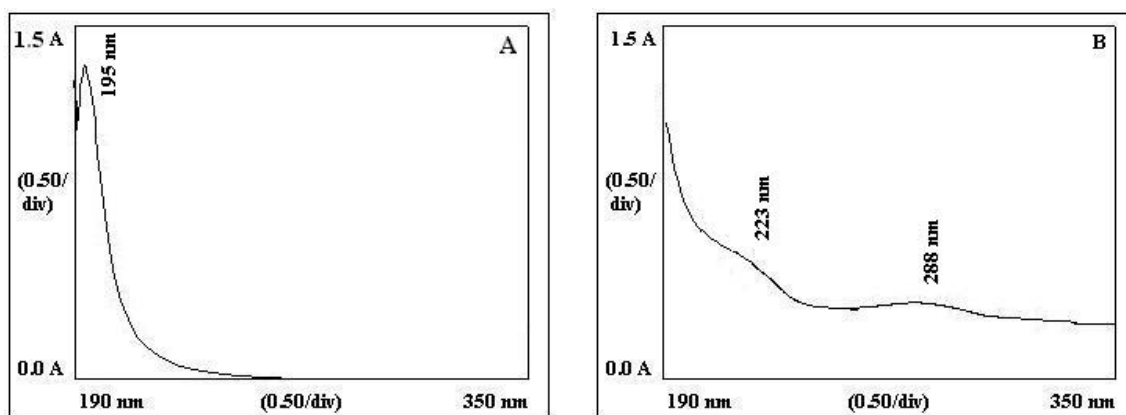


Fig. 4.24. UV spectra for L-valyl-D-fructose **28a-c** from CRL catalyzed reaction (A), L-valine; (B) L-valyl-D-fructose.

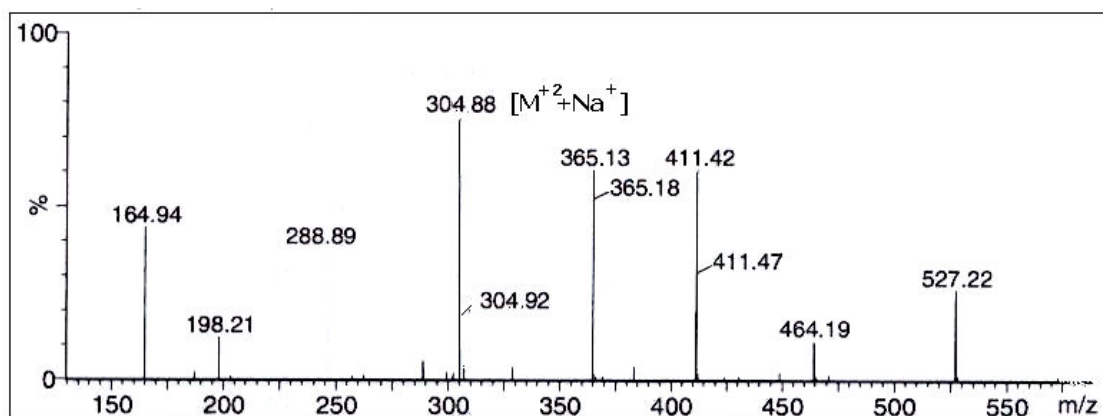


Fig. 4.25. A typical mass spectrum of L-valyl-D-fructose **28a-c**.

1 $\alpha$ ), 3.73 (H-4 $\beta$ ), 3.72 (H-5 $\beta$ ), 3.18 (H-6) ppm;  $^{13}\text{C}$  NMR  $\delta$  : 63.0 (C1 $\alpha$ ), 75.9 (C4 $\beta$ ), 81.2 (C5 $\beta$ ), 64.0 (C6 $\alpha$ ) ppm; **1,6-di-O-ester (28c)**:  $^1\text{H}$  NMR  $\delta$  : 3.83 (H-4 $\beta$ ), 3.28 (H-6 $\alpha$ ) ppm;  $^{13}\text{C}$  NMR  $\delta$  : 76.1 (C4 $\beta$ ), 63.4 (C6 $\alpha$ ) ppm.

A typical UV and mass spectra for L-valyl-D-fructose **28a-c** are shown in Figures 4.24 and 4.25 respectively.

**4.2.2.5. L-Valyl-D-arabinose (29a-c)**: Solid; HPLC  $t_{\text{ret}}$ : 3.3 min;  $R_f$ : 0.23; UV ( $\text{H}_2\text{O}$ ,  $\lambda_{\text{max}}$ ): 224.0 nm ( $\sigma \rightarrow \sigma^*$   $\epsilon_{224.0}$  - 1585  $\text{M}^{-1}$ ), 281.0 nm ( $n \rightarrow \pi^*$   $\epsilon_{281.0}$  - 933  $\text{M}^{-1}$ ); IR (KBr, stretching frequency): 3339  $\text{cm}^{-1}$  (NH), 3290  $\text{cm}^{-1}$  (OH), 2963  $\text{cm}^{-1}$  (CH), 1598  $\text{cm}^{-1}$  (CO); MS ( $m/z$ ) : 273 [ $\text{M}^+ + \text{Na}$ ] $^+$ .

2D-HSQCT ( $\text{DMSO}-d_6$ ) : **2-O-ester (29a)** :  $^1\text{H}$  NMR  $\delta$  (500.13 MHz): 1.05 ( $\alpha\text{CH}$ ), 4.99 (H-1 $\alpha$ ), 4.91 (H-1 $\beta$ ), 3.65 (H-2 $\alpha$ ), 3.19 (H-3 $\alpha$ ), 3.72 (H-5) ppm;  $^{13}\text{C}$  NMR  $\delta$  (125 MHz): 15.5 ( $\alpha\text{CH}$ ), 95.9 (C1 $\alpha$ ), 102.1 (C1 $\beta$ ), 77.0 (C2 $\alpha$ ), 71.9 (C3 $\alpha$ ), 60.5 (C5 $\alpha$ ) ppm; **5-O-ester (29b)**:  $^1\text{H}$  NMR  $\delta$  : 3.39 ( $\alpha\text{CH}$ ), 2.08 ( $\beta\text{CH}$ ), 1.02 ( $\gamma$ ,  $\gamma'\text{CH}_3$ ), 4.32 (H-1 $\alpha$ ), 4.21 (H-1 $\beta$ ); 3.28 (H-2 $\alpha$ ), 3.33 (H-3 $\alpha$ ), 3.69 (H-4 $\alpha$ ), 3.64 (H-5) ppm;  $^{13}\text{C}$  NMR  $\delta$ : 53.0 ( $\alpha\text{CH}$ ), 29.5 ( $\beta\text{CH}$ ), 19.3 ( $\gamma$ ,  $\gamma'\text{CH}_3$ ), 172.0 (CO), 96.8 (C1 $\alpha$ ), 103.9 (C1 $\beta$ ), 74.8 (C2 $\alpha$ ), 70.8 (C3 $\alpha$ ), 67.6 (C4 $\alpha$ ), 65.0 (C5 $\alpha$ ) ppm; **2,5-di-O-ester (29c)**:  $^1\text{H}$  NMR  $\delta$  : 3.45 (H-2 $\alpha$ ), 3.26 (H-3 $\alpha$ ), 3.68 (H-5 $\alpha$ ), 3.35 (H-5 $\beta$ ) ppm;  $^{13}\text{C}$  NMR  $\delta$  : 75.6 (C2 $\alpha$ ), 73.4 (C3 $\alpha$ ), 63.3 (C5 $\alpha$ ), 65.0 (C5 $\beta$ ) ppm.

A typical UV and mass spectra for L-valyl-D-arabinose **29a-c** are shown in Figures 4.26 and 4.27 respectively.

**4.2.2.6. L-Valyl-D-ribose (30a-c)**: Solid; HPLC  $t_{\text{ret}}$ : 3.4 min;  $R_f$ : 0.22; UV ( $\text{H}_2\text{O}$ ,  $\lambda_{\text{max}}$ ): 230.0 nm ( $\sigma \rightarrow \sigma^*$   $\epsilon_{230.0}$  - 1412  $\text{M}^{-1}$ ), 297.0 nm ( $n \rightarrow \pi^*$   $\epsilon_{297.0}$ -1072  $\text{M}^{-1}$ ); IR (KBr, stretching frequency): 3349  $\text{cm}^{-1}$  (NH), 3137  $\text{cm}^{-1}$  (OH), 2934  $\text{cm}^{-1}$  (CH), 1588  $\text{cm}^{-1}$  (CO); MS ( $m/z$ ) : 273 [ $\text{M}^+ + \text{Na}$ ] $^+$ .

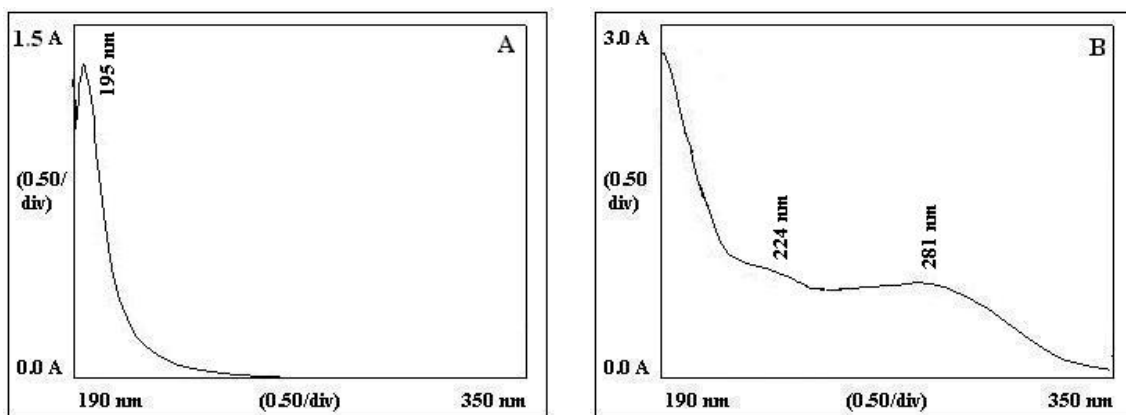


Fig. 4.26. UV spectra for L-valyl-D-arabinose **29a-c** from CRL catalyzed reaction (A) L-valine; (B) L-valyl-D-arabinose.

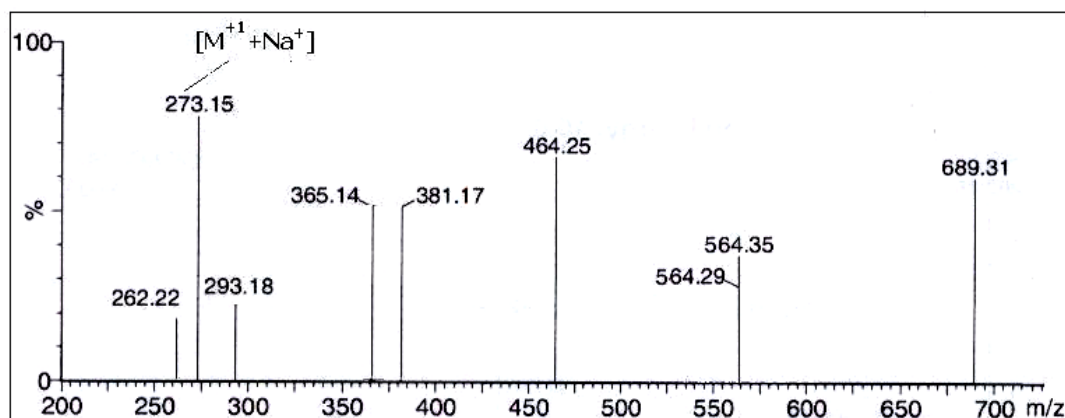


Fig. 4.27. A typical mass spectrum of L-valyl-D-arabinose **29a-c**.

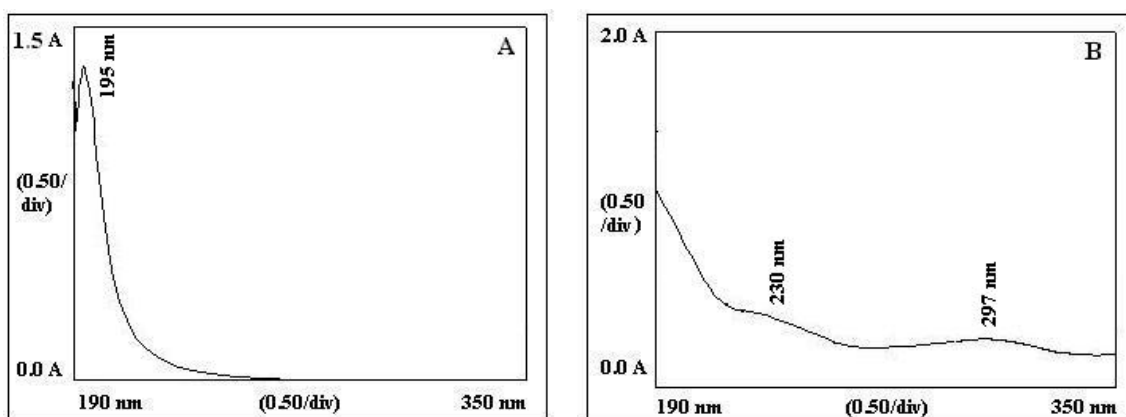


Fig. 4.28. UV spectra for L-valyl-D-ribose **30a-c** from CRL catalyzed reaction (A) L-valine; (B) L-valyl-D-ribose.



2D-HSQCT (DMSO- $d_6$ ) : **3-O-ester (30a)**:  $^1\text{H NMR } \delta$  (500.13 MHz) : 3.38 ( $\alpha\text{CH}$ ), 1.82 ( $\beta\text{CH}$ ), 0.68 ( $\gamma$ ,  $\gamma'\text{CH}_3$ ), 3.98 (H-3 $\alpha$ ), 3.72 (H-5) ppm;  $^{13}\text{C NMR } \delta$  (125 MHz): 53.2 ( $\alpha\text{CH}$ ), 30.5 ( $\beta\text{CH}$ ), 18.4 ( $\gamma$ ,  $\gamma'\text{CH}_3$ ), 174.3 (CO), 77.1 (C3 $\alpha$ ), 61.2 (C5 $\alpha$ ) ppm; **5-O-ester (30b)**:  $^1\text{H NMR } \delta$  : 2.08 ( $\beta\text{CH}$ ), 1.03 ( $\gamma\text{CH}_3$ ), 4.20 (H-1 $\alpha$ ), 4.93 (H-1 $\beta$ ), 3.22 (H-2 $\alpha$ ), 3.31 (H-2 $\beta$ ), 3.31 (H-3 $\alpha$ ), 3.54 (H-3 $\beta$ ), 3.81 (H-4 $\alpha$ ), 3.62 (H-5) ppm;  $^{13}\text{C NMR } \delta$  : 29.7 ( $\alpha\text{CH}$ ), 18.3 ( $\gamma\text{CH}_3$ ), 173.5 (CO), 101.5 (C1 $\alpha$ ), 93.8 (C1 $\beta$ ), 72.1 (C2 $\alpha$ ), 73.4 (C2 $\beta$ ), 70.4 (C3 $\alpha$ ), 68.6 (C3 $\beta$ ), 65.1 (C4 $\alpha$ ), 63.9 (C5 $\alpha$ ) ppm; **3,5-di-O-ester (30c)**:  $^1\text{H NMR } \delta$ : 4.42 (H-1 $\alpha$ ), 4.62 (H-1 $\beta$ ), 3.67 (H-3 $\alpha$ ), 3.34 (H-5) ppm;  $^{13}\text{C NMR } \delta$  : 97.0 (C1 $\alpha$ ), 94.0 (C1 $\beta$ ), 74.6 (C3 $\alpha$ ), 65.4 (C5 $\alpha$ ) ppm.

A typical UV and mass spectra for L-valyl-D-ribose **30a-c** are shown in Figures 4.28 and 4.29 respectively.

**4.2.2.7. L-Valyl-maltose (31a,b)**: Solid; HPLC  $t_{ret}$ : 3.5 min;  $R_f$ : 0.13; UV ( $\text{H}_2\text{O}$ ,  $\lambda_{max}$ ): 221.0 nm ( $\sigma \rightarrow \sigma^*$   $\epsilon_{221.0} - 1622 \text{ M}^{-1}$ ), 291.0 nm ( $n \rightarrow \pi^*$   $\epsilon_{291.0} - 776 \text{ M}^{-1}$ ); IR (KBr, stretching frequency): 3419  $\text{cm}^{-1}$  (NH), 3267  $\text{cm}^{-1}$  (OH), 2936  $\text{cm}^{-1}$  (CH), 1634  $\text{cm}^{-1}$  (CO); MS ( $m/z$ ) : 464  $[\text{M}+\text{Na}]^+$ .

2D-HSQCT (DMSO- $d_6$ ) : **6-O-ester (31a)**:  $^1\text{H NMR } \delta$  (500.13 MHz) : 3.12 ( $\alpha\text{CH}$ ), 2.25 ( $\beta\text{CH}$ ), 1.05 ( $\gamma$ ,  $\gamma'\text{CH}_3$ ), 4.92 (H-1 $\alpha$ ), 5.0 (H-1 $\beta$ ), 3.32 (H-2 $\alpha$ ), 3.41 (H-3 $\alpha$ ), 4.14 (H-4 $\alpha$ ), 3.39 (H-5 $\alpha$ ), 3.93 (H-6), 4.90 (H-1' $\alpha$ ), 3.27 (H-2'), 3.35 (H-3'), 3.63 (H-4'), 3.68 (H-5'), 3.67 (H-6') ppm;  $^{13}\text{C NMR } \delta$  (125 MHz) : 51.0 ( $\alpha\text{CH}$ ), 31.1 ( $\beta\text{CH}$ ), 18.8 ( $\gamma\text{CH}_3$ ), 175.5 (CO), 97.0 (C1 $\alpha$ ), 100.5 (C1 $\beta$ ), 73.0 (C2 $\alpha$ ), 76.3 (C3 $\alpha$ ), 80.5 (C4 $\alpha$ ), 78.8 (C5 $\alpha$ ), 66.5 (C6), 100.7 (C1' $\alpha$ ), 67.5 (C2'), 67.0 (C3'), 70.2 (C4'), 72.3 (C5'), 60.5 (C6') ppm; **6'-O-ester (31b)**:  $^1\text{H NMR } \delta$  : 2.90 ( $\alpha\text{CH}$ ), 3.98 (H-4 $\alpha$ ), 3.07 (H-2'), 3.32 (H-3'), 3.83 (H-6') ppm;  $^{13}\text{C NMR } \delta$  : 52.0 ( $\alpha\text{CH}$ ), 80.6 (C4 $\alpha$ ), 71.5 (C2'), 70.5 (C3'), 68.0 (C6') ppm.

A typical 2D-HSQCT NMR spectrum for L-valyl-maltose **31a,b** is shown in Figure 4.30.

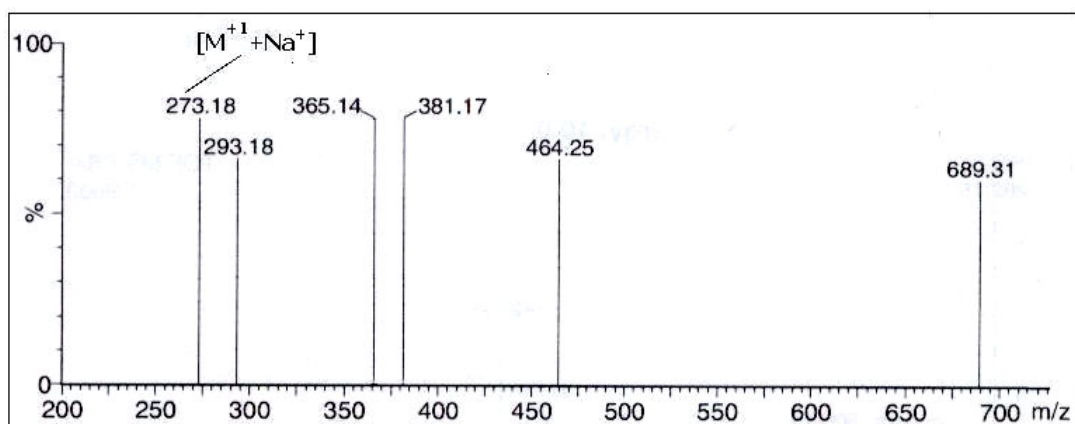


Fig. 4.29. A typical mass spectrum of L-valyl-D-ribose **30a-c**.

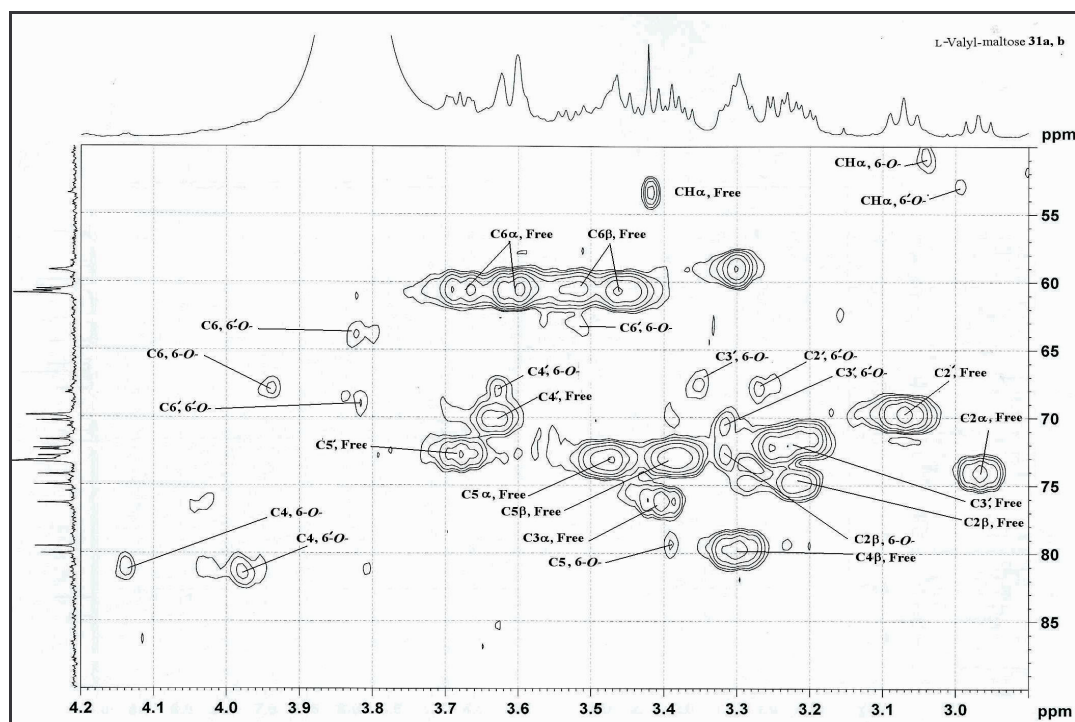
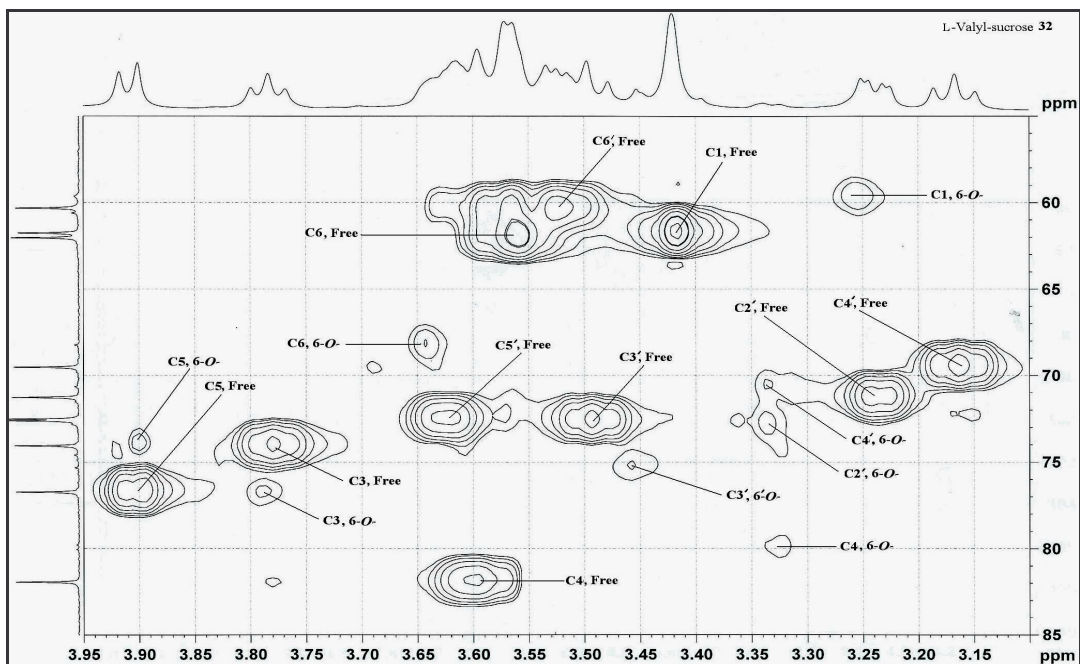
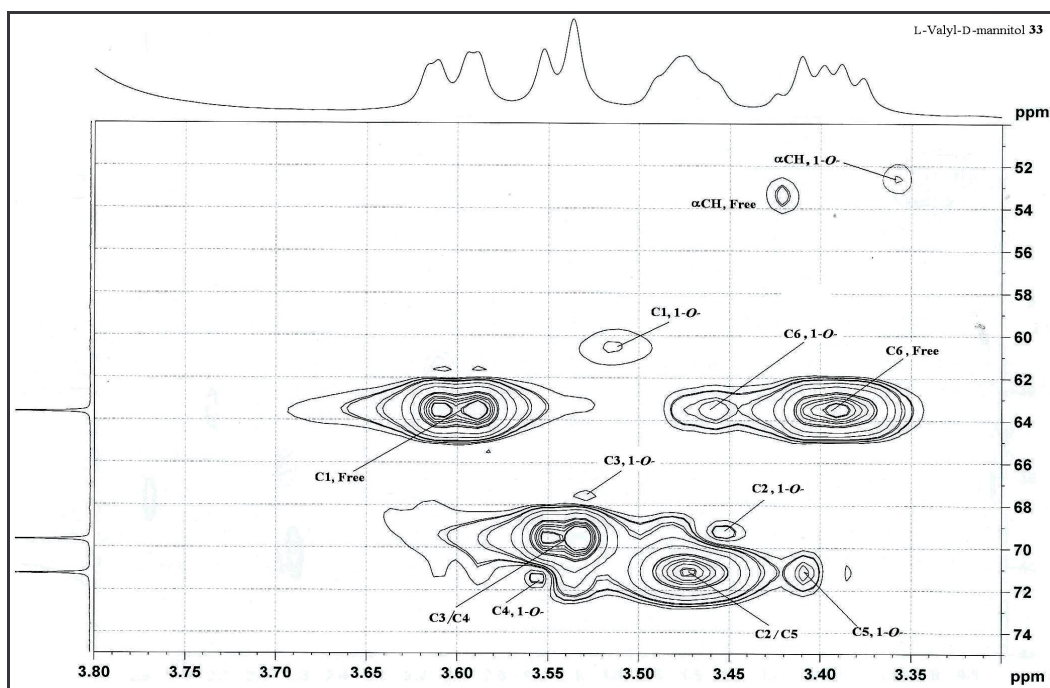


Fig. 4.30. Two-dimensional HSQCT NMR for L-valyl-maltose **31a,b** obtained through CRL catalysis.



**Fig. 4.31.** Two-dimensional HSQCT NMR for L-valyl-sucrose **32** obtained through CRL catalysis.



**Fig. 4.32.** Two-dimensional HSQCT NMR for L-valyl-D-mannitol **33** obtained through CRL catalysis.

**4.2.2.8. L-Valyl-sucrose (32):** Solid; Mpt: 184 °C; HPLC  $t_{ret}$ : 3.4 min;  $R_f$ : 0.13; UV (H<sub>2</sub>O,  $\lambda_{max}$ ): 225.0 nm ( $\sigma \rightarrow \sigma^*$   $\epsilon_{225.0} - 195 \text{ M}^{-1}$ ), 275.0 nm ( $n \rightarrow \pi^*$   $\epsilon_{275.0} - 91 \text{ M}^{-1}$ ); IR (KBr, stretching frequency): 3520  $\text{cm}^{-1}$  (NH), 3411  $\text{cm}^{-1}$  (OH), 2940  $\text{cm}^{-1}$  (CH), 1588  $\text{cm}^{-1}$  (CO); optical rotation ( $c$  0.5, H<sub>2</sub>O) :  $[\alpha]_D$  at 25 °C = +36 °; MS ( $m/z$ ) : 464  $[\text{M}+\text{Na}]^+$ .

2D-HSQCT (DMSO- $d_6$ ) : **6-O-ester (32):** <sup>1</sup>H NMR  $\delta$  (500.13 MHz) : 3.13 ( $\alpha\text{CH}$ ), 2.42 ( $\beta\text{CH}$ ), 1.05 ( $\gamma$ ,  $\gamma'\text{CH}_3$ ), 3.26 (H-1 $\alpha$ ), 3.79 (H-3 $\beta$ ), 3.33 (H-4 $\beta$ ), 3.90 (H-5 $\beta$ ), 3.64 (H-6), 4.92 (H-1' $\alpha$ ), 3.34 (H-2'), 3.46 (H-3'), 3.34 (H-4'), 3.62 (H-5'), 3.52 (H-6') ppm; <sup>13</sup>C NMR  $\delta$  (125 MHz) : 53.5 ( $\alpha\text{CH}$ ), 28.8 ( $\beta\text{CH}$ ), 18.5 ( $\gamma$ ,  $\gamma'\text{CH}_3$ ), 172.0 (CO), 59.5 (C1 $\beta$ ), 103.3 (C2 $\beta$ ), 74.1 (C3 $\beta$ ), 80.0 (C4 $\beta$ ), 74.3 (C5 $\beta$ ), 68.2 (C6 $\beta$ ), 91.8 (C1' $\alpha$ ), 72.9 (C2'), 75.2 (C3'), 70.6 (C4'), 72.6 (C5'), 60.3 (C6') ppm .

A typical 2D-HSQCT NMR spectrum for L-valyl-sucrose **32** is shown in Figure 4.31.

**4.2.2.9. L-Valyl-D-mannitol (33):** Solid; Mpt: 132 °C; HPLC  $t_{ret}$ : 3.5 min;  $R_f$ : 0.22; UV (H<sub>2</sub>O,  $\lambda_{max}$ ): 225.0 nm ( $\sigma \rightarrow \sigma^*$   $\epsilon_{225.0} - 372 \text{ M}^{-1}$ ), 270.0 nm ( $n \rightarrow \pi^*$   $\epsilon_{270.0} - 178 \text{ M}^{-1}$ ); IR (KBr, stretching frequency): 3294  $\text{cm}^{-1}$  (OH), 2957  $\text{cm}^{-1}$  (CH), 1630  $\text{cm}^{-1}$  (CO); optical rotation ( $c$  0.5, H<sub>2</sub>O) :  $[\alpha]_D$  at 25 °C = +6.6 °; MS ( $m/z$ ) : 304  $[\text{M}+\text{Na}]^+$ .

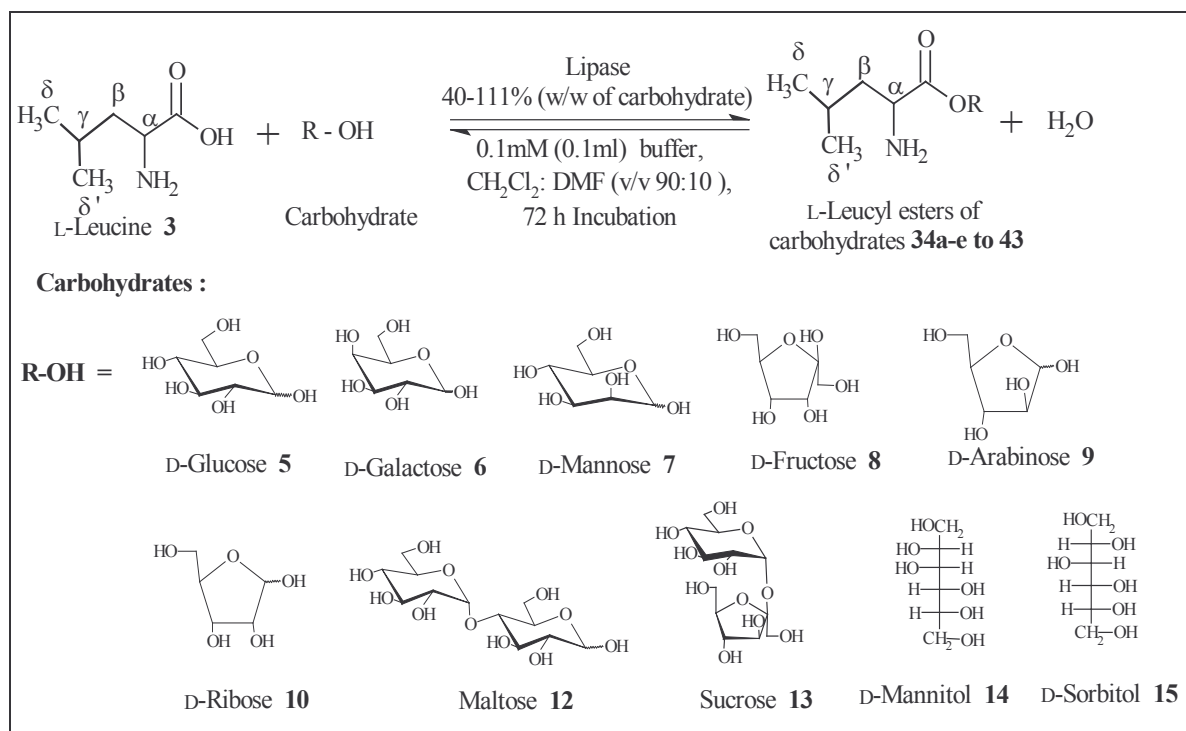
2D-HSQCT (DMSO- $d_6$ ): **1-O-ester (33):** <sup>1</sup>H NMR  $\delta$  (500.13 MHz): 3.12 ( $\alpha\text{CH}$ ), 2.05 ( $\beta\text{CH}$ ), 0.92 ( $\gamma$ ,  $\gamma'\text{CH}_3$ ), 3.53 (H-1), 3.46 (H-2), 3.53 (H-3), 3.56 (H-4), 3.41 (H-5), 3.46 (H-6) ppm; <sup>13</sup>C NMR  $\delta$  (125 MHz): 55.8 ( $\alpha\text{CH}$ ), 29.8 ( $\beta\text{CH}_2$ ), 19.1 ( $\gamma, \gamma'\text{CH}_3$ ), 60.6 (C1), 69.5 (C2), 67.5 (C3), 71.2 (C4), 71.0 (C5) 63.6 (C6) ppm.

A typical 2D-HSQCT NMR spectrum for L-valyl-D-mannitol **33** is shown in Figure 4.32.

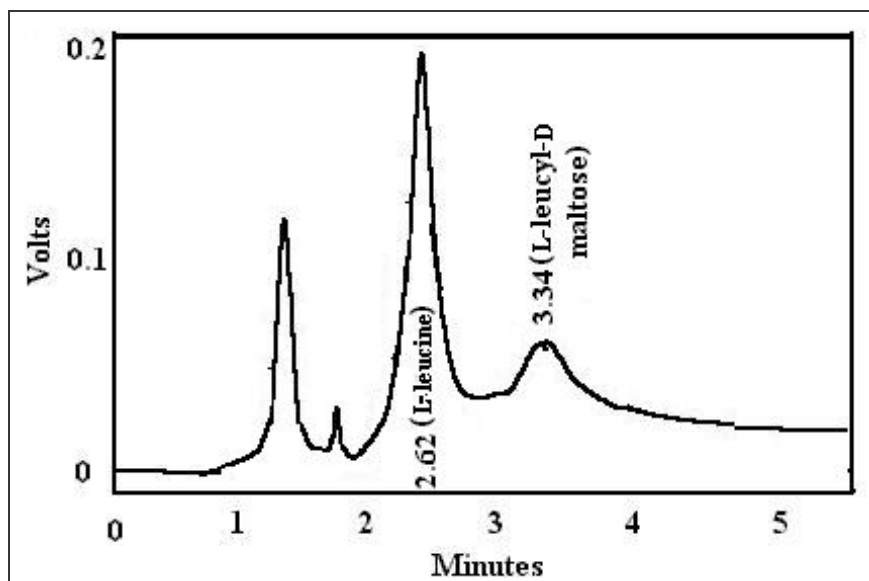
#### 4.2.3. Syntheses of L-leucyl esters of carbohydrates 34a-e to 43

L-Leucine (L-2-amino-4-methyl pentanoic acid) is a polar and an essential dietary amino acid containing 2-methyl propyl group as a side chain. Compared to L-alanine (solubility 127.3 g/l at 25 °C) and L-valine (solubility 88.5 g/l at 25 °C), the solubility of

L-leucine in water is low (24.26 g/l at 25 °C). However, the carbohydrate esters can be expected to exhibit higher solubility in water. Using optimum conditions, L-leucyl esters of different carbohydrates (**Scheme 4.3**) were prepared using CRL and crude PPL (Section 2.2.5). The reaction mixture consists of 1 – 2 mmol L-leucine and 1 mmol carbohydrates (D-glucose **5**, D-galactose **6**, D-mannose **7**, D-fructose **8**, D-arabinose **9**, D-ribose **10**, lactose **11**, maltose **12**, sucrose **13**, D-mannitol **14**, D-sorbitol **15**) along with 40% CRL (w/w carbohydrate)/111% of crude PPL (w/w carbohydrate) incubated in 100 ml of CH<sub>2</sub>Cl<sub>2</sub> and DMF (v/v 90:10, 40 °C) containing 0.1 mM (0.1 ml of 0.1 M) of phosphate buffer, pH 7.0 (CRL) or 0.2 mM (0.2 ml of 0.1 M) of acetate buffer, pH 5.0 (crude PPL). The reaction mixture was analyzed by HPLC using a C-18 column with acetonitrile:water (v/v 20:80) as a mobile phase and detected at 210 nm (Fig. 4.33). Ester formation was also monitored by TLC as described in Section 4.2.2. The retention times ( $t_{ret}$ ) by HPLC and retention factor ( $R_f$ ) values by TLC are mentioned in sections 4.2.3.1 – 4.2.3.10.



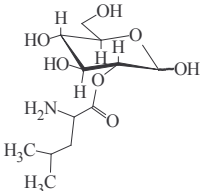
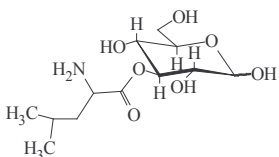
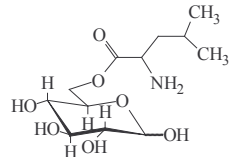
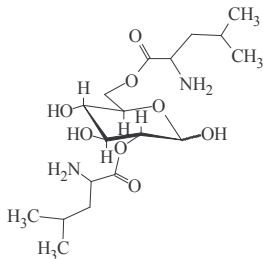
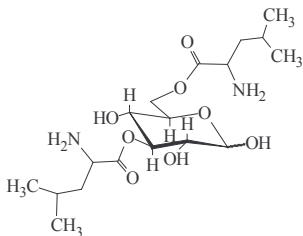
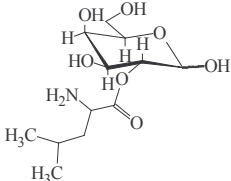
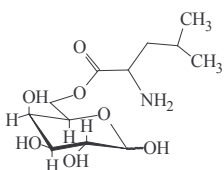
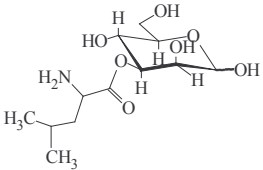
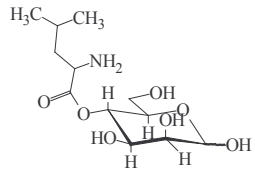
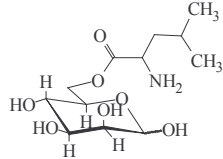
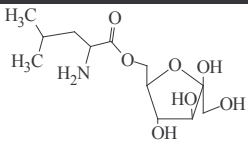
**Scheme 4.3** Lipase catalyzed syntheses of L-leucyl esters of carbohydrates



**Fig. 4.33.** HPLC chromatogram for reaction mixture of L-leucine and maltose esterification reaction catalysed by CRL. Column – C-18; mobile phase – acetonitrile:water (v/v 20:80); flow rate - 1 ml/min; detector – UV at 210 nm; errors in conversion yields are within  $\pm 10\%$ .

The isolated esters were subjected to UV, IR, MS, optical rotation and 2D- NMR characterization (Sections 4.2.3.1 – 4.2.3.10). The spectral data for the isolated esters were shown in Sections 4.2.3.1 – 4.2.3.10. Table 4.6 shows the HPLC ester yields, types of esters formed and percentage proportions of the individual esters from CRL catalysis and Table 4.7 shows the HPLC ester yields from crude PPL catalysis.

**Table 4.6 Syntheses of L-leucyl esters of carbohydrates<sup>a</sup>**

L-Leucyl esters of carbohydrates (% proportions <sup>b</sup> )			Yield (%)
			43 (mono esters- 34, diesters-9)
<b>34a 2-O-L-leucyl -D-glucose (17)</b>	<b>34a 3-O-L-leucyl-D-glucose (20)</b>	<b>34a 6-O-L-leucyl-D-glucose (42)</b>	
			
<b>34d 2,6-di-O-L-leucyl-D-glucose (10)</b>	<b>34e 3,6-di-O-L-leucyl-D-glucose (11)</b>		
			21 (only mono esters)
<b>35a 2-O-L-leucyl-D-galactose (48)</b>	<b>35b 6-O-L-leucyl-D-galactose (52)</b>		
			31 (only mono esters)
<b>36a 3-O-L-leucyl-D-mannose (28)</b>	<b>36b 4-O-L-leucyl-D-mannose (30)</b>	<b>36b 6-O-L-leucyl-D-mannose (42)</b>	
			48 (only mono ester)
<b>37 6-O-L-leucyl-D-fructose</b>			

			42 <sup>c</sup> (mono esters-24, diester-18)
<b>38a</b> 2- <i>O</i> -L-leucyl-D-arabinose (24)	<b>38b</b> 5- <i>O</i> -L-leucyl-D-arabinose (33)	<b>38c</b> 2,5-di- <i>O</i> -L-leucyl-D-arabinose (43)	
			38 <sup>c</sup> (mono esters-18, diester-20)
<b>39a</b> 3- <i>O</i> -L-leucyl-D-ribose (16)	<b>39b</b> 5- <i>O</i> -L-leucyl-D-ribose (32)	<b>39c</b> 3,5-di- <i>O</i> -L-leucyl-D-ribose (52)	
			44 (only mono ester)
<b>40</b> 6- <i>O</i> -L-leucyl-maltose			
			38 (only mono ester)
<b>41</b> 6- <i>O</i> -L-leucyl-sucrose			
			45 (mono ester-25, diester-20)
<b>42a</b> 1- <i>O</i> -L-leucyl-D-mannitol (56)	<b>42b</b> 1,6-di- <i>O</i> -L-leucyl-D-mannitol (44)		
			25 (only mono ester)
<b>43</b> 1- <i>O</i> -L-leucyl-D-sorbitol			

<sup>a</sup> L-Leucine – 2 mmol, carbohydrates – 1 mmol, CRL – 40 % (w/w carbohydrate), buffer – 0.1 mM (0.1 ml of 0.1M) phosphate buffer (pH 7.0), CH<sub>2</sub>Cl<sub>2</sub>:DMF (v/v 90:10) at 40 °C, incubation period – 72 h. Conversion yields were from HPLC with respect to L-leucine concentration.

<sup>b</sup> Percentage proportions of individual esters were determined from the peak areas or from their cross peaks of the Carbon-13 C6 and C5 (in case of pentoses) signals in the 2D HSQCT spectrum.

<sup>c</sup> Several cross peaks, due to opening and/or degradation of the five membered ring during esterification.



**Table 4.7 Preparation of L-leucyl esters of carbohydrates using crude porcine pancreas lipase <sup>a</sup>**

L-Leucyl ester of carbohydrate	%Yield (mmol)
L- Leucyl-D-glucose <b>34a-e</b>	58 (0.58)
L- Leucyl-D-galactose <b>35a,b</b>	46 (0.46)
L- Leucyl-D-mannose <b>36a-c</b>	44 (0.44)
L- Leucyl-D-fructose <b>37</b>	52 (0.52)
L- Leucyl-D-arabinose <b>38a-c</b>	39 (0.39)
L-Leucyl-D-ribose <b>39a-c</b>	57 (0.57)
L- Leucyl-maltose <b>40</b>	64 (0.64)
L- Leucyl-sucrose <b>41</b>	65 (0.65)
L- Leucyl-D-mannitol <b>42a,b</b>	50 (0.50)
L- Leucyl-D-sorbitol <b>43</b>	54 (0.54)

<sup>a</sup> L-Leucine – 1 mmol, carbohydrates – 1 mmol, Crude PPL – 111 % (w/w carbohydrate), buffer – 0.2 mM (0.2 ml of 0.1 M) acetate buffer (pH 5.0), CH<sub>2</sub>Cl<sub>2</sub>: DMF (v/v 90: 10) at 40 °C, Incubation period – 72 h. Conversion yields were from HPLC with respect to L-leucine concentration.

**Spectral data for L-leucine (3):** Solid; Mpt: 293-295 °C; HPLC  $t_{ret}$ : 2.6 min;  $R_f$ : 0.32; UV (H<sub>2</sub>O,  $\lambda_{max}$ ): 190.0 nm ( $\sigma \rightarrow \sigma^*$   $\epsilon_{190.0}$  - 132 M<sup>-1</sup>), IR (KBr, stretching frequency): 3415 cm<sup>-1</sup> (OH), 2945 cm<sup>-1</sup> (CH), 1595 cm<sup>-1</sup> (CO); optical rotation ( $c$  1.0, H<sub>2</sub>O):  $[\alpha]_D$  at 25 °C = -15.2 °.

2D-HSQCT (DMSO-*d*<sub>6</sub>) : <sup>1</sup>H NMR  $\delta$  (500.13 MHz) : 3.41 ( $\alpha$ CH), 1.56 ( $\beta$ CH<sub>2</sub>), 1.64 ( $\gamma$ CH), 0.85 ( $\delta$ ,  $\delta'$  CH<sub>3</sub>) ppm; <sup>13</sup>C NMR  $\delta$  (125 MHz) : 53.2 ( $\alpha$ CH), 39.4 ( $\beta$ CH<sub>2</sub>), 24.0 ( $\gamma$ CH), 21.8 ( $\delta$ ,  $\delta'$  CH<sub>3</sub>), 173.0 (CO) ppm.

**4.2.3.1. L-Leucyl-D-glucose (34a-e):** Solid; HPLC  $t_{ret}$ : 3.5 min;  $R_f$ : 0.22; UV (H<sub>2</sub>O,  $\lambda_{max}$ ): 230.0 nm ( $\sigma \rightarrow \sigma^*$   $\epsilon_{230.0}$  - 724 M<sup>-1</sup>), 297.0 nm ( $n \rightarrow \pi^*$   $\epsilon_{297.0}$  - 363 M<sup>-1</sup>); IR (KBr, stretching frequency): 3383 cm<sup>-1</sup> (NH), 3360 cm<sup>-1</sup> (OH), 2240 cm<sup>-1</sup> (CH), 1657 cm<sup>-1</sup> (CO); MS ( $m/z$ ) : 316 [M+Na]<sup>+</sup>.

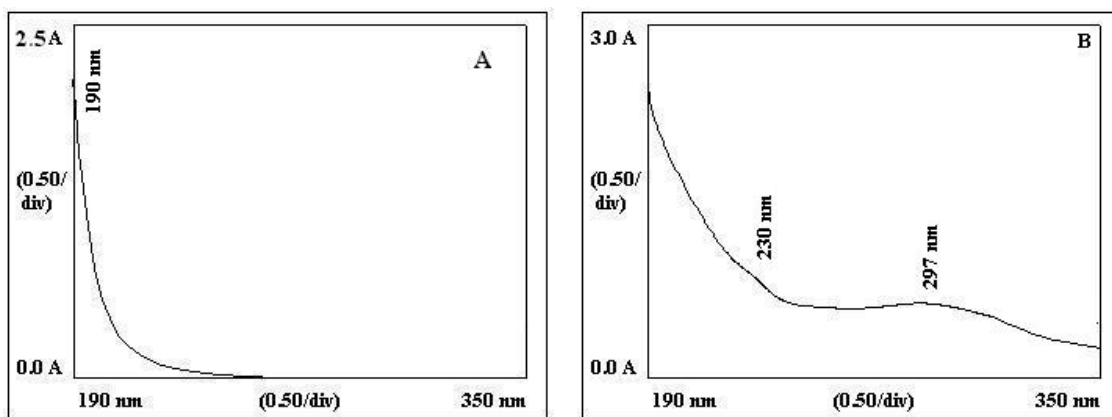


Fig. 4.34. UV spectra for L-leucyl-D-glucose **34a-e** from CRL catalyzed reaction (A) L-leucine; (B) L-leucyl-D-glucose.

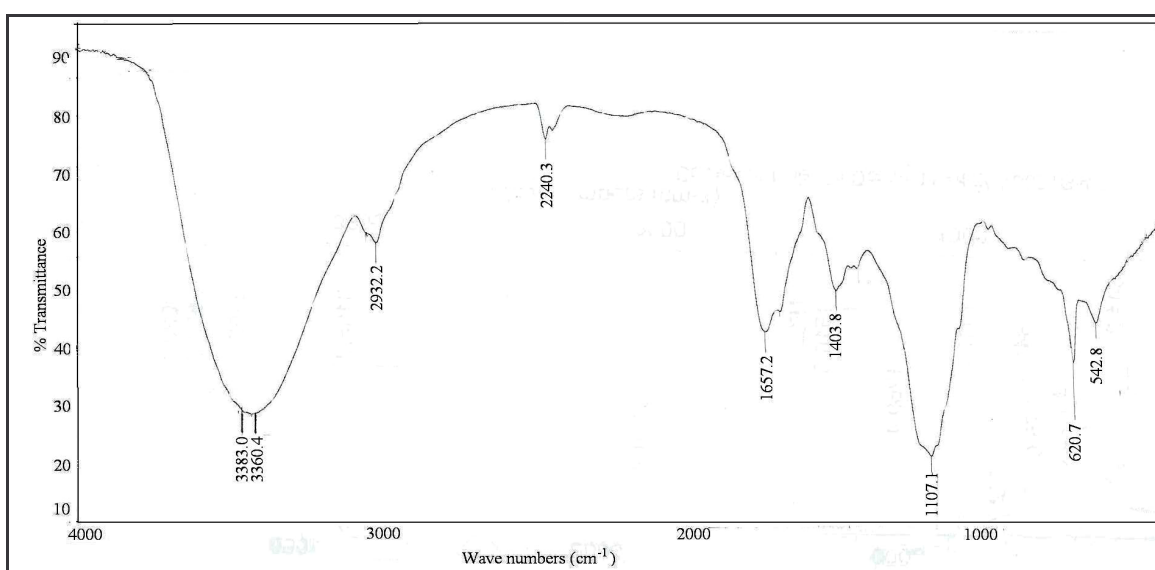


Fig. 4.35. A typical IR spectrum of L-leucyl-D-glucose **34a-e** of CRL catalysed reaction. A 2.5 mg of ester sample was prepared as KBr pellet.

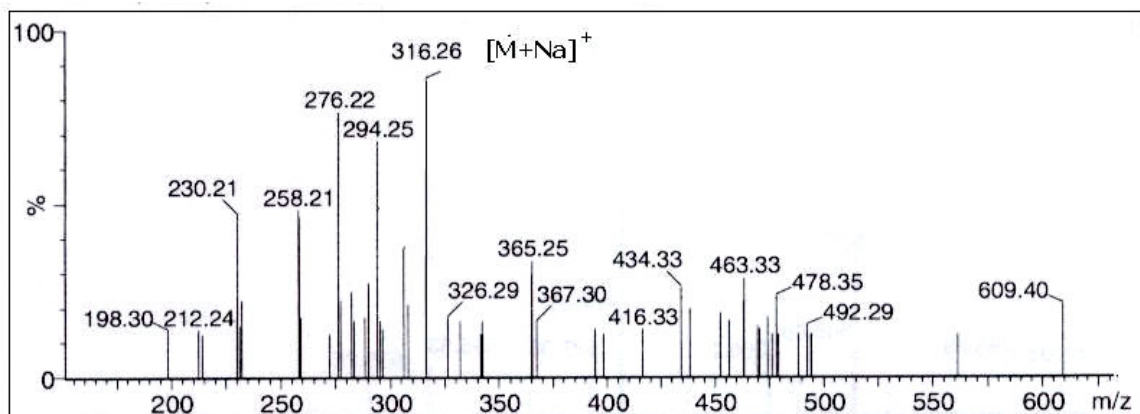


Fig. 4.36. A typical mass spectrum of L-leucyl-D-glucose **34a-e**.

2D-HSQCT (DMSO- $d_6$ ) : **2-O-ester (34a)**:  $^1\text{H}$  NMR  $\delta$  (500.13 MHz): 3.85 (H-2 $\alpha$ ) ppm;  $^{13}\text{C}$   $\delta$  (125 MHz): 75.5 (C2 $\alpha$ ) ppm; **3-O-ester (34b)**:  $^1\text{H}$  NMR  $\delta$  : 3.15 ( $\alpha\text{CH}$ ), 3.85 (H-3 $\alpha$ ), 3.96 (H-3 $\beta$ ) ppm;  $^{13}\text{C}$  NMR  $\delta$  : 50.0 ( $\alpha\text{CH}$ ), 83.5 (C3 $\alpha$ ), 83.6 (C3 $\beta$ ) ppm; **6-O-ester (24c)**:  $^1\text{H}$  NMR  $\delta$  : 3.10 ( $\alpha\text{CH}$ ), 1.56 ( $\beta\text{CH}_2$ ), 1.82 ( $\gamma\text{CH}$ ), 0.82 ( $\delta$ ,  $\delta'$   $\text{CH}_3$ ), 4.99 (H-1 $\alpha$ ), 3.81 (H-2 $\alpha$ ), 3.45 (H-3 $\alpha$ ), 3.68 (H-4 $\alpha$ ), 3.55 (H-5 $\alpha$ ), 3.80 (H-6) ppm ;  $^{13}\text{C}$  NMR  $\delta$ : 53.2 ( $\alpha\text{CH}$ ), 40.5 ( $\beta\text{CH}_2$ ), 23.5 ( $\gamma\text{CH}$ ), 25.0 ( $\delta$ ,  $\delta'$   $\text{CH}_3$ ), 173.6 (CO), 92.5 (C1 $\alpha$ ), 70.3 (C2 $\alpha$ ), 75.8 (C3 $\alpha$ ), 70.2 (C4 $\alpha$ ), 71.0 (C5 $\alpha$ ), 65.0 (C6 $\alpha$ ) ppm; **2,6-di-O-ester (34d)**:  $^1\text{H}$  NMR  $\delta$  : 3.21 (H-2 $\alpha$ ), 3.59 (H-6) ppm;  $^{13}\text{C}$  NMR  $\delta$  : 76.3 (C2 $\alpha$ ), 65.0 (C6 $\alpha$ ) ppm. **3,6-di-O-ester (34e)**:  $^1\text{H}$  NMR  $\delta$ : 3.68 (H-3 $\alpha$ ), 3.59 (H-6) ppm;  $^{13}\text{C}$  NMR  $\delta$ : 81.5 (C3 $\alpha$ ), 65.0 (C6 $\alpha$ ) ppm.

A typical UV, IR, mass and 2D-HSQCT NMR spectra for L-leucyl-D-glucose **34a-e** are shown in Figures 4.34, 4.35, 4.36 and 4.37 respectively.

**4.2.3.2. L-Leucyl-D-galactose (35a,b)**: Solid; HPLC  $t_{\text{ret}}$ : 3.5 min;  $R_f$ : 0.22; UV ( $\text{H}_2\text{O}$ ,  $\lambda_{\text{max}}$ ): 226.0 nm ( $\sigma \rightarrow \sigma^*$   $\epsilon_{226.0} - 2291 \text{ M}^{-1}$ ), 295.0 nm ( $n \rightarrow \pi^*$   $\epsilon_{295.0} - 1349 \text{ M}^{-1}$ ); IR (KBr, stretching frequency): 3426  $\text{cm}^{-1}$  (NH), 3317  $\text{cm}^{-1}$  (OH), 2815  $\text{cm}^{-1}$  (CH), 1589  $\text{cm}^{-1}$  (CO); MS ( $m/z$ ) : 316  $[\text{M}+\text{Na}]^+$ .

2D-HSQCT (DMSO- $d_6$ ) : **2-O-ester (35a)**:  $^1\text{H}$  NMR  $\delta$  (500.13 MHz) : 3.74 (H-2 $\alpha$ ), 3.70 (H-6) ppm;  $^{13}\text{C}$  NMR (125 MHz)  $\delta$  : 171.4 (CO), 72.5 (C2 $\alpha$ ), 59.5 (C6 $\alpha$ ) ppm; **6-O-ester (35b)**:  $^1\text{H}$  NMR  $\delta$  : 3.50 ( $\alpha\text{CH}$ ), 1.54 ( $\beta\text{CH}_2$ ), 1.44 ( $\gamma\text{CH}$ ), 0.95 ( $\delta$ ,  $\delta'$   $\text{CH}_3$ ), 5.0 (H-1 $\alpha$ ), 4.49 (H-1 $\beta$ ), 3.66 (H-2 $\alpha$ ), 3.68 (H-3 $\alpha$ ), 3.74 (H-4 $\alpha$ ), 3.42 (H-4 $\beta$ ), 3.62 (H-5 $\alpha$ ), 3.48 (H-5 $\beta$ ), 3.65 (H-6) ppm;  $^{13}\text{C}$  NMR  $\delta$ : 54.0 ( $\alpha\text{CH}$ ), 39.2 ( $\beta\text{CH}_2$ ), 24.0 ( $\gamma\text{CH}$ ), 21.6 ( $\delta$ ,  $\delta'$   $\text{CH}_3$ ), 172.1 (CO), 92.0 (C1 $\alpha$ ), 96.1 (C1 $\beta$ ), 62.5 (C2 $\alpha$ ), 68.0 (C3 $\alpha$ ), 68.2 (C4 $\alpha$ ), 72.5 (C4 $\beta$ ), 70.0 (C5 $\alpha$ ), 74.5 (C5 $\beta$ ), 62.5 (C6 $\alpha$ ) ppm.

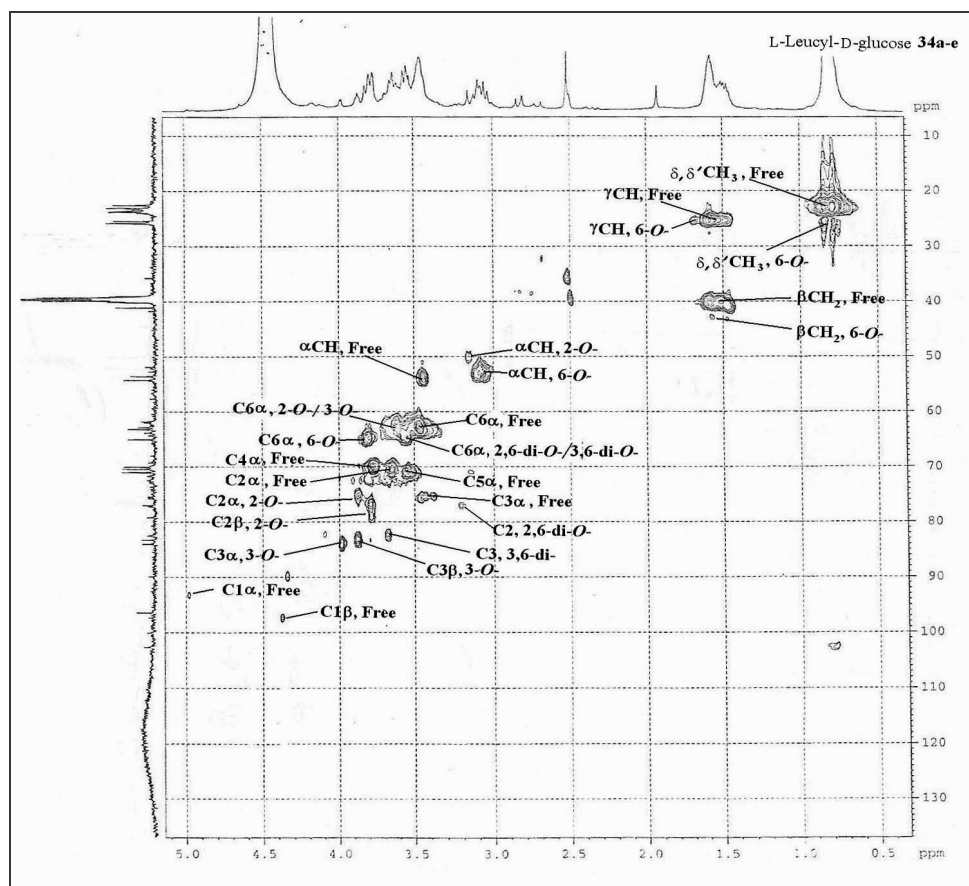


Fig. 4.37. Two-dimensional HSQCT NMR for L-leucyl-D-glucose **34a-e** obtained through CRL catalysis.

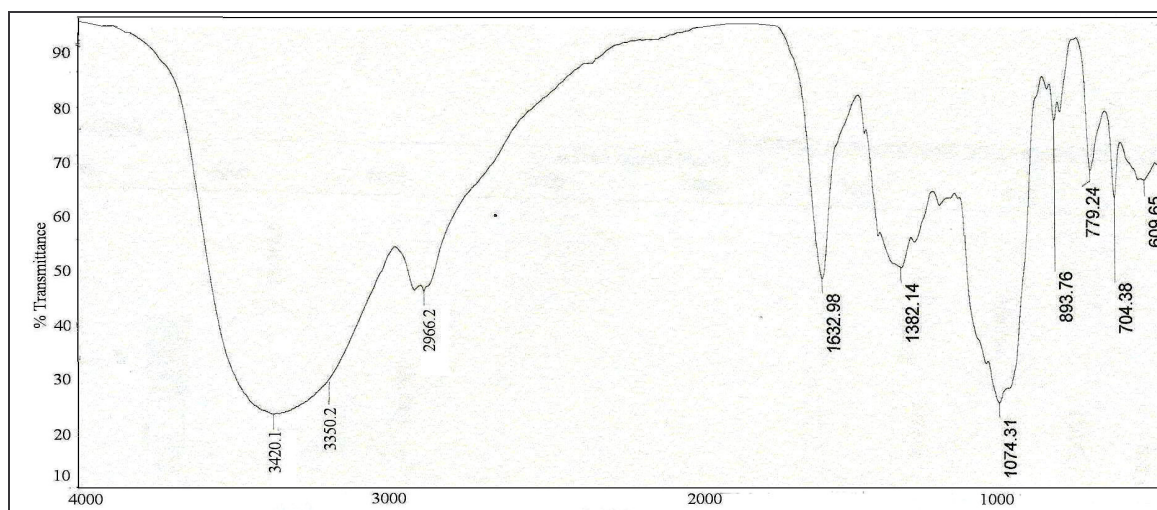


Fig. 4.38. A typical IR spectrum of L-leucyl-D-galactose of RML catalyzed reaction **35a,b**.

A typical IR and mass spectra for L-leucyl-D-galactose **35a,b** are shown in Figures 4.38 and 4.39 respectively.

**4.2.3.3. L-Leucyl-D-mannose (36a-c):** Solid; HPLC  $t_{ret}$ : 3.5 min;  $R_f$ : 0.22; UV ( $H_2O$ ,  $\lambda_{max}$ ): 230.0 nm ( $\sigma \rightarrow \sigma^*$   $\epsilon_{230.0} - 1122 M^{-1}$ ), 292.0 nm ( $n \rightarrow \pi^*$   $\epsilon_{292.0} - 120.2 M^{-1}$ ); IR (KBr, stretching frequency): 3425  $cm^{-1}$  (NH), 3329  $cm^{-1}$  (OH), 2950  $cm^{-1}$  (CH), 1591  $cm^{-1}$  (CO); MS ( $m/z$ ): 316  $[M+Na]^+$ .

2D-HSQCT (DMSO- $d_6$ ) **3-O-ester (36a)**:  $^1H$  NMR  $\delta$  (500.13 MHz): 3.05 ( $\alpha CH$ ), 3.86 (H-3 $\alpha$ ), 3.97 (H-3 $\beta$ ), 3.55 (H-6) ppm;  $^{13}C$  NMR  $\delta$  (125 MHz) : 51.5 ( $\alpha CH$ ), 81.4 (C3 $\alpha$ ), 82.5 (C3 $\beta$ ), 61.7 (C6 $\alpha$ ) ppm; **4-O-ester (36b)** :  $^1H$  NMR  $\delta$  : 3.86 (H-4 $\alpha$ ), 3.78 (H-4 $\beta$ ), 3.61 (H-6) ppm;  $^{13}C$  NMR  $\delta$ : 73.8 (C4 $\alpha$ ), 75.0 (C4 $\beta$ ), 61.6 (C6 $\alpha$ ) ppm; **6-O-ester (36c)**:  $^1H$  NMR  $\delta$ : 3.47 ( $\alpha CH$ ), 1.59 ( $\beta CH_2$ ), 1.64 ( $\gamma CH$ ), 1.0 ( $\delta$ ,  $\delta' CH_3$ ), 4.91 (H-1 $\alpha$ ), 4.75 (H-2 $\alpha$ ), 3.65 (H-3 $\alpha$ ), 3.43 (H-4 $\alpha$ ), 3.63 (H-5 $\alpha$ ), 3.80 (H-6) ppm;  $^{13}C$  NMR  $\delta$  : 53.9 ( $\alpha CH$ ), 39.4 ( $\beta CH_2$ ), 24.0 ( $\gamma CH$ ), 21.1 ( $\delta$ ,  $\delta' CH_3$ ), 172.6 (CO), 95.3 (C1 $\alpha$ ), 68.0 (C2 $\alpha$ ), 68.1 (C3 $\alpha$ ), 66.3 (C4 $\alpha$ ), 72.3 (C4 $\beta$ ), 70.5 (C5 $\alpha$ ), 63.2 (C6 $\alpha$ ) ppm.

A typical UV and mass spectra for L-leucyl-D-mannose **36a-c** are shown in Figures 4.40 and 4.41 respectively.

**4.2.3.4. L-Leucyl-D-fructose (37):** Solid; Mpt: 128 °C; HPLC  $t_{ret}$ : 3.5 min;  $R_f$ : 0.22; UV ( $H_2O$ ,  $\lambda_{max}$ ): 223.0 nm ( $\sigma \rightarrow \sigma^*$   $\epsilon_{223.0} - 1023 M^{-1}$ ), 284.0 nm ( $n \rightarrow \pi^*$   $\epsilon_{284.0} - 489.8 M^{-1}$ ); IR (KBr, stretching frequency): 3266  $cm^{-1}$  (NH), 3219  $cm^{-1}$  (OH), 2951  $cm^{-1}$  (CH), 1630  $cm^{-1}$  (CO); optical rotation ( $c$  0.5,  $H_2O$ ):  $[\alpha]_D$  at 25 °C = -6.7 °; MS ( $m/z$ ): 332  $[M+K]^+$ .

2D-HSQCT (DMSO- $d_6$ ): **6-O-ester (37)**:  $^1H$  NMR  $\delta$  (500.13 MHz) : 3.47 ( $\alpha CH$ ), 1.56 ( $\beta CH_2$ ), 1.64 ( $\gamma CH$ ), 1.0 ( $\delta$ ,  $\delta' CH_3$ ), 3.58 (H-1 $\alpha$ ), 3.61 (H-3 $\alpha$ ), 3.87 (H-3 $\beta$ ), 3.77 (H-4 $\beta$ ), 3.65 (H-5 $\alpha$ ), 3.83 (H-6) ppm;  $^{13}C$  NMR  $\delta$  (125 MHz) : 52.8 ( $\alpha CH$ ), 39.4 ( $\beta CH_2$ ), 24.0

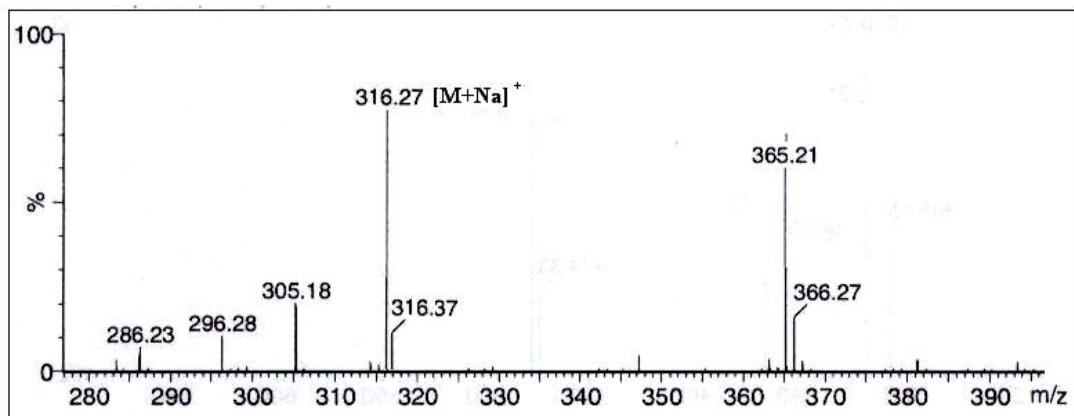


Fig. 4.39. A typical mass spectrum of L-leucyl-D-galactose. **35a,b**

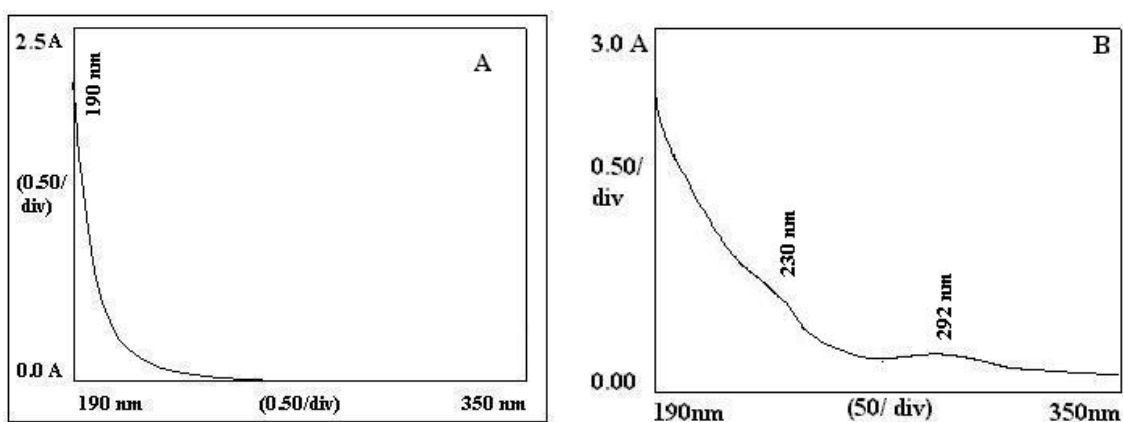


Fig. 4.40 UV spectra for L-leucyl-D-mannose **36a-c** from CRL catalyzed reaction (A) L-leucine; (B) L-leucyl-D-mannose.

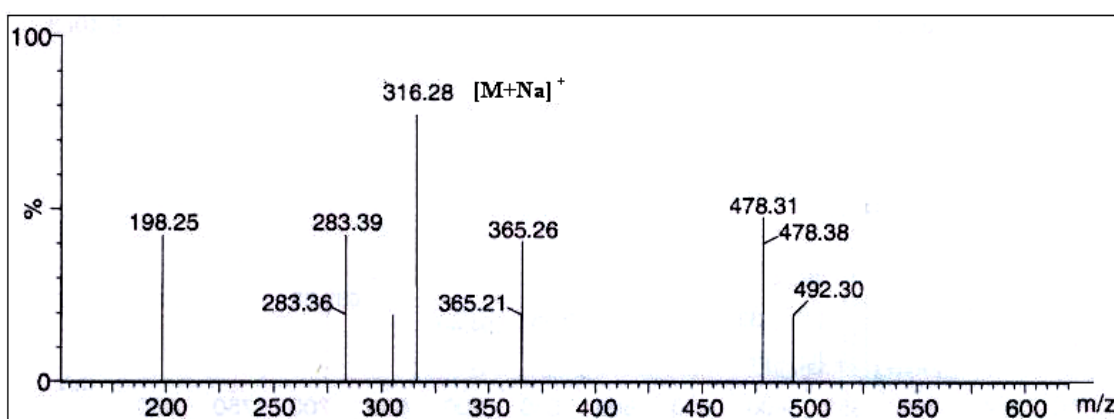


Fig. 4.41. A typical mass spectrum of L-leucyl-D-mannose **36a-c**.

( $\gamma$ CH), 22.2 ( $\delta$ ,  $\delta'$ CH<sub>3</sub>), 173.1 (CO), 61.5 (C1 $\alpha$ ), 104.2 (C2 $\alpha$ ), 69.0 (C3 $\alpha$ ), 82.0 (C3 $\beta$ ), 75.4 (C4 $\beta$ ), 66.8 (C5 $\alpha$ ), 63.5 (C6 $\alpha$ ) ppm.

A typical UV and mass spectra for L-leucyl-D-fructose **37** are shown in Figures 4.42 and 4.43 respectively.

**4.2.3.5. L-Leucyl-D-arabinose (38a-c):** Solid; HPLC  $t_{ret}$ : 3.3 min;  $R_f$ : 0.24; UV (H<sub>2</sub>O,  $\lambda_{max}$ ): 210.0 nm ( $\sigma \rightarrow \sigma^*$   $\epsilon_{210.0}$  - 7080 M<sup>-1</sup>), 295.0 nm ( $n \rightarrow \pi^*$   $\epsilon_{295.0}$  - 3236 M<sup>-1</sup>); IR (KBr, stretching frequency): 3275 cm<sup>-1</sup> (NH), 3094 cm<sup>-1</sup> (OH), 2958 cm<sup>-1</sup> (CH), 1609 cm<sup>-1</sup> (CO); MS ( $m/z$ ): 287 [M<sup>+</sup>+Na]<sup>+</sup>.

2D-HSQCT (DMSO- $d_6$ ) : **2-O-ester (38a)** : <sup>1</sup>H NMR  $\delta$  (500.13 MHz): 3.41( $\alpha$ CH), 2.51 ( $\beta$ CH<sub>2</sub>), 1.64 ( $\gamma$ CH), 0.85 ( $\delta$ ,  $\delta'$  CH<sub>3</sub>), 4.32 (H-1 $\alpha$ ), 4.89 (H-1 $\beta$ ), 3.76 (H-2 $\alpha$ ), 3.45 (H-2 $\beta$ ), 3.70 (H-3 $\alpha$ ), 3.68 (H-5) ppm; <sup>13</sup>C NMR  $\delta$  (125 MHz): 53.0 ( $\alpha$ CH), 39.4 ( $\beta$ CH<sub>2</sub>), 24.0 ( $\gamma$ CH), 22.2 ( $\delta$ ,  $\delta'$  CH<sub>3</sub>), 173.0 (CO), 96.6 (C1 $\alpha$ ), 92.0 (C1 $\beta$ ), 75.0 (C2 $\alpha$ ), 75.2 (C2 $\beta$ ), 69.5 (C3 $\alpha$ ), 62.6 (C5 $\alpha$ ) ppm; **5-O-ester (38b)**: <sup>1</sup>H NMR  $\delta$  : 4.91 (H-1 $\alpha$ ), 4.99 (H-1 $\beta$ ), 3.47 (H-2 $\alpha$ ), 3.60 (H-3 $\alpha$ ), 3.67 (H-4 $\alpha$ ), 3.64 (H-5) ppm; <sup>13</sup>C NMR  $\delta$ : 101.6 (C1 $\alpha$ ), 94.2 (C1 $\beta$ ), 74.2 (C2 $\alpha$ ), 69.5 (C3 $\alpha$ ), 67.3 (C4 $\alpha$ ), 64.8 (C5 $\alpha$ ) ppm; **2,5-di-O-ester (38c)**: <sup>1</sup>H NMR  $\delta$  : 4.18 (H-1 $\alpha$ ), 3.66 (H-2 $\alpha$ ), 2.96 (H-3 $\alpha$ ), 3.35 (H-5) ppm; <sup>13</sup>C NMR  $\delta$  : 103.5 (C1 $\alpha$ ), 77.2 (C2 $\alpha$ ), 74.2 (C3 $\alpha$ ), 64.8 (C5 $\alpha$ ) ppm.

A typical 2D-HSQCT NMR spectrum for L-leucyl-D-arabinose **38a-c** is shown in Figure 4.44.

**4.2.3.6. L-Leucyl-D-ribose (39a-c):** Solid; HPLC  $t_{ret}$ : 3.3 min;  $R_f$ : 0.23; UV (H<sub>2</sub>O,  $\lambda_{max}$ ): 226.0 nm ( $\sigma \rightarrow \sigma^*$   $\epsilon_{226.0}$  - 170 M<sup>-1</sup>), 295.0 nm ( $n \rightarrow \pi^*$   $\epsilon_{295.0}$  - 891 M<sup>-1</sup>); IR (KBr, stretching frequency): 3332 cm<sup>-1</sup> (NH), 3120 cm<sup>-1</sup> (OH), 2960 cm<sup>-1</sup> (CH), 1585 cm<sup>-1</sup> (CO); MS ( $m/z$ ) : 286 [M+Na]<sup>+</sup> and 400 (diester) [M<sup>+</sup>+Na]<sup>+</sup>.

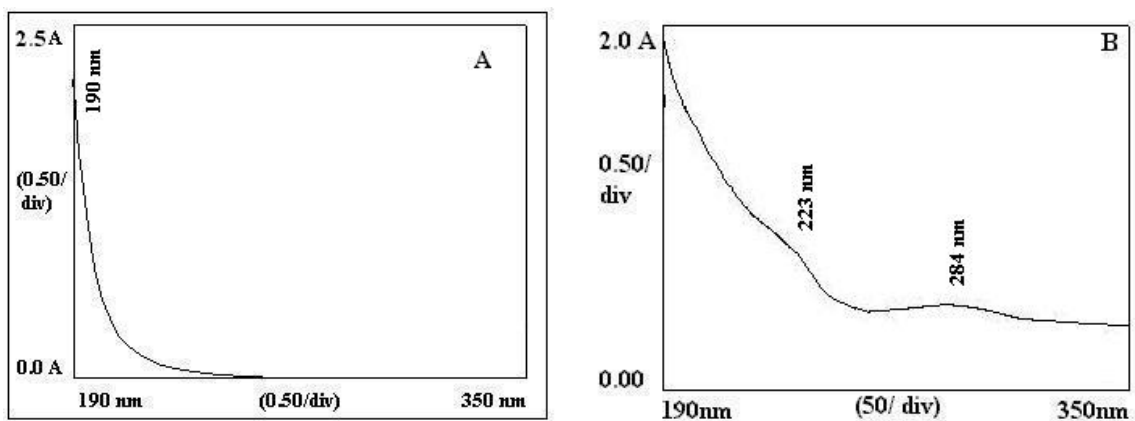


Fig. 4.42 UV spectra for L-leucyl-D-fructose **37** from CRL catalyzed reaction (A) L-leucine; (B) L-leucyl-D-fructose.

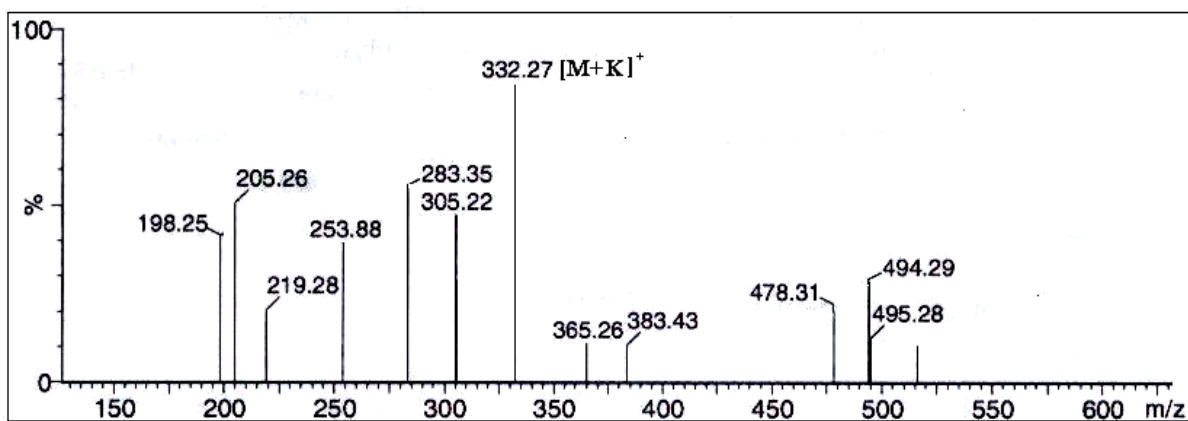


Fig. 4.43. A typical mass spectrum of L-leucyl-D-fructose **37**.



2D-HSQCT (DMSO- $d_6$ ) : **3-O-ester (39a)** :  $^1\text{H}$  NMR  $\delta$  (500.13 MHz): 3.41( $\alpha\text{CH}$ ), 1.56 ( $\beta\text{CH}_2$ ), 1.64 ( $\gamma\text{CH}$ ), 0.85 ( $\delta$ ,  $\delta'\text{CH}_3$ ), 4.89 (H-1 $\alpha$ ), 4.85 (H-1 $\beta$ ), 3.18 (H-2 $\alpha$ ), 3.60 (H-3 $\alpha$ ), 3.68 (H-4 $\alpha$ ), 3.64 (H-5) ppm;  $^{13}\text{C}$  NMR  $\delta$  (125 MHz): 53.0 ( $\alpha\text{CH}$ ), 39.4 ( $\beta\text{CH}_2$ ), 24.0 ( $\gamma\text{CH}$ ), 22.2 ( $\delta$ ,  $\delta'\text{CH}_3$ ), 173.0 (CO), 92.3 (C1 $\alpha$ ), 92.6 (C1 $\beta$ ), 71.8 (C2 $\alpha$ ), 76.0 (C3 $\alpha$ ), 67.2 (C4 $\alpha$ ), 60.8 (C5 $\alpha$ ) ppm; **5-O-ester (39b)**:  $^1\text{H}$  NMR  $\delta$  : 4.92 (H-1 $\alpha$ ), 4.22 (H-1 $\beta$ ), 3.45 (H-2 $\alpha$ ), 3.48 (H-3 $\alpha$ ), 3.72 (H-4 $\alpha$ ), 3.59 (H-5a) and 3.68 (H-5b) ppm;  $^{13}\text{C}$  NMR  $\delta$  : 101.5 (C1 $\alpha$ ), 97.0 (C1 $\beta$ ), 75.8 (C2 $\alpha$ ), 69.0 (C3 $\alpha$ ), 70.8 (C4 $\alpha$ ), 63.0 (C5 $\alpha$ ) ppm; **3,5-di-O-ester (39c)**:  $^1\text{H}$  NMR  $\delta$ : 3.27 (H-2 $\alpha$ ), 3.77 (H-3 $\alpha$ ), 3.77 (H-4 $\alpha$ ), 3.34 (H-5a) and 3.37 (H-5b) ppm;  $^{13}\text{C}$  NMR  $\delta$  : 74.7 (C2 $\alpha$ ), 76.2 (C3 $\alpha$ ), 71.0 (C4 $\alpha$ ), 64.8 (C5 $\alpha$ ) ppm.

A typical mass spectrum for L-leucyl-D-ribose **39a-c** is shown in Figure 4.45.

**4.2.3.7. L-Leucyl-maltose (40)**: Solid; Mpt : 157 °C; HPLC  $t_{ret}$ : 3.3 min;  $R_f$ : 0.13; UV ( $\text{H}_2\text{O}$ ,  $\lambda_{max}$ ): 224.0 nm ( $\sigma \rightarrow \sigma^*_{224.0} - 617 \text{ M}^{-1}$ ), 281.0 nm ( $n \rightarrow \pi^*_{281.0} - 191 \text{ M}^{-1}$ ); IR (KBr, stretching frequency): 3419  $\text{cm}^{-1}$  (NH), 3300  $\text{cm}^{-1}$  (OH), 2956  $\text{cm}^{-1}$  (CH), 1642  $\text{cm}^{-1}$  (CO); optical rotation ( $c$  0.5,  $\text{H}_2\text{O}$ ):  $[\alpha]_D$  at 25 °C = +54.6 °; MS ( $m/z$ ) : 478  $[\text{M}+\text{Na}]^+$ .

2D-HSQCT (DMSO- $d_6$ ) : **6-O-ester (40)** :  $^1\text{H}$  NMR  $\delta$  (500.13 MHz): 3.60 ( $\alpha\text{CH}$ ), 1.58 ( $\beta\text{CH}_2$ ), 1.69 ( $\gamma\text{CH}$ ), 0.87 ( $\delta$ ,  $\delta'\text{CH}_3$ ), 4.91 (H-1 $\alpha$ ), 4.19 (H-1 $\beta$ ), 2.97 (H-2 $\alpha$ ), 3.23 (H-2 $\beta$ ), 3.40 (H-3 $\alpha$ ), 3.23 (H-4 $\beta$ ), 3.32 (H-5 $\alpha$ ), 3.33 (H-6), 5.0 (H-1' $\alpha$ ), 3.06 (H-2'), 3.23 (H-3'), 3.63 (H-4'), 3.67 (H-5'), 3.59 (H-6') ppm;  $^{13}\text{C}$  NMR  $\delta$  (125 MHz) : 51.0 ( $\alpha\text{CH}$ ), 39.5 ( $\beta\text{CH}_2$ ), 24.0 ( $\gamma\text{CH}$ ), 22.4 ( $\delta$ ,  $\delta' \text{CH}_3$ ), 173.5 (CO), 94.0 (C1 $\alpha$ ), 103.5 (C1 $\beta$ ), 73.2 (C2 $\alpha$ ), 75.4 (C2 $\beta$ ), 76.3 (C3 $\alpha$ ), 79.9 (C4 $\beta$ ), 70.5 (C5 $\alpha$ ), 62.9 (C6 $\alpha$ ), 102.2 (C1' $\alpha$ ), 70.2 (C2'), 71.3 (C3'), 69.8 (C4'), 72.3 (C5'), 62.5 (C6') ppm.

A 2D-HSQCT NMR spectrum for L-leucyl-maltose **40** is shown in Figure 4.46.

**4.2.3.8. L-Leucyl-sucrose (41)** Solid; Mpt: 125 °C; HPLC  $t_{ret}$ : 3.3 min;  $R_f$ : 0.13; UV ( $\text{H}_2\text{O}$ ,  $\lambda_{max}$ ): 223.0 nm ( $\sigma \rightarrow \sigma^* \epsilon_{223.0} - 324 \text{ M}^{-1}$ ), 275.0 nm ( $n \rightarrow \pi^* \epsilon_{275.0} - 174 \text{ M}^{-1}$ ); IR

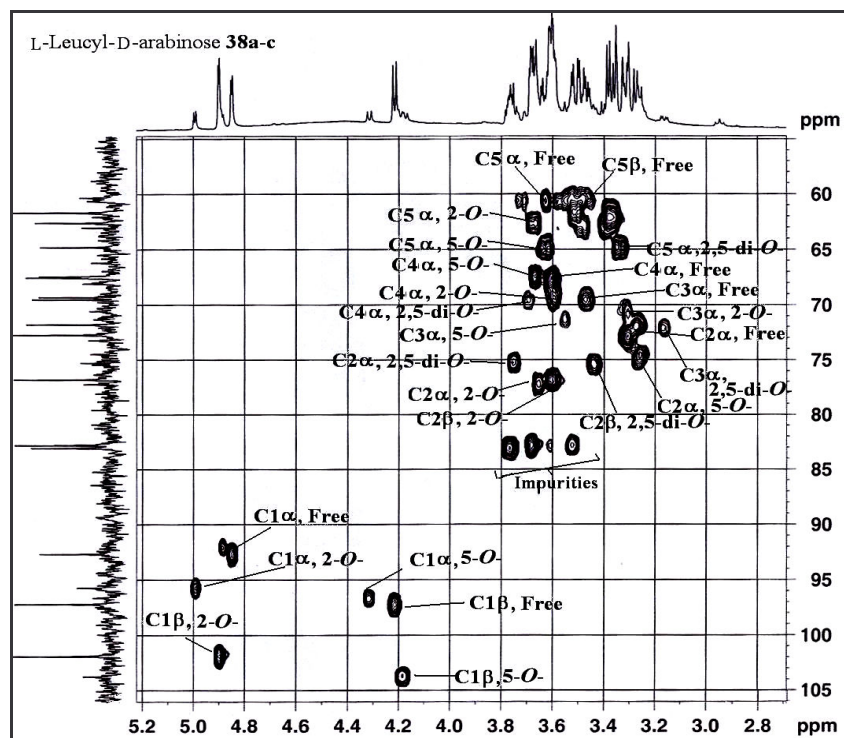


Fig. 4.44. Two-dimensional HSQCT NMR for L-leucyl-D-arabinose **38a-c** obtained through CRL catalysis.

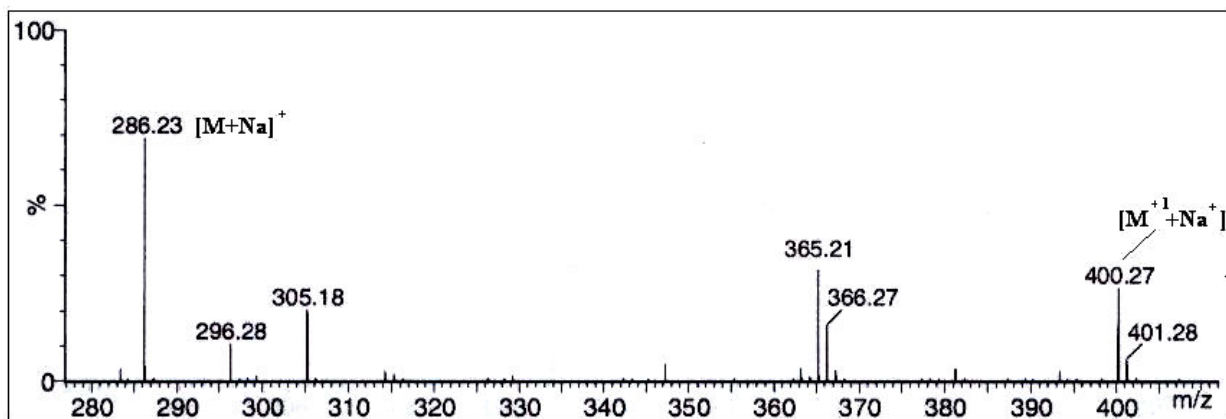


Fig. 4.45. A typical mass spectrum of L-leucyl-D-ribose **39a-c**.

(KBr, stretching frequency): 3598  $\text{cm}^{-1}$  (NH), 3455  $\text{cm}^{-1}$  (OH), 3105  $\text{cm}^{-1}$  (CH), 1616  $\text{cm}^{-1}$  (CO); optical rotation ( $c$  0.5,  $\text{H}_2\text{O}$ ):  $[\alpha]_{\text{D}}$  at 25  $^{\circ}\text{C}$  = -27.1  $^{\circ}$ ; MS ( $m/z$ ): 478  $[\text{M}+\text{Na}]^+$ .

2D-HSQCT (DMSO- $d_6$ ) : **6-O-ester (41)**:  $^1\text{H}$  NMR  $\delta$  (500.13 MHz) :3.45 ( $\alpha\text{CH}$ ), 1.55 ( $\beta\text{CH}_2$ ), 1.68 ( $\gamma\text{CH}$ ), 0.50 ( $\delta$ ,  $\delta'$   $\text{CH}_3$ ), 3.39 (H-1 $\beta$ ), 3.76 (H-3 $\beta$ ), 3.58 (H-4 $\beta$ ), 3.89 (H-5 $\beta$ ), 3.64 (H-6), 5.16 (H-1' $\alpha$ ), 3.23 (H-2'), 3.41 (H-3'), 3.49 (H-4'), 3.59 (H-5'), 3.51 (H-6') ppm;  $^{13}\text{C}$  NMR  $\delta$  (125 MHz) : 53.0 ( $\alpha\text{CH}$ ), 39.5 ( $\beta\text{CH}_2$ ), 24.1 ( $\gamma\text{CH}$ ), 22.0 ( $\delta$ ,  $\delta'\text{CH}_3$ ), 172.0 (CO), 64.5 (C1 $\beta$ ), 103.4 (C2 $\beta$ ), 74.0 (C3 $\beta$ ), 84.1 (C4 $\beta$ ), 79.0 (C5 $\beta$ ), 68.2 (C6 $\beta$ ), 92.1 (C1' $\alpha$ ), 71.3 (C2'), 71.6 (C3'), 74.5 (C4'), 72.8 (C5'), 64.5 (C6') ppm.

A typical 2D-HSQCT NMR spectrum for L-leucyl-sucrose **41** is shown in Figure 4.47.

**4.2.3.9. L-Leucyl-D-mannitol (42a,b)** Solid; HPLC  $t_{\text{ret}}$ : 3.3 min;  $R_f$ : 0.19; UV ( $\text{H}_2\text{O}$ ,  $\lambda_{\text{max}}$ ): 224.0 nm ( $\sigma \rightarrow \sigma^*$   $\epsilon_{224.0}$  - 2344  $\text{M}^{-1}$ ), 294.0 nm ( $n \rightarrow \pi^*$   $\epsilon_{294.0}$  - 1288  $\text{M}^{-1}$ ); IR (KBr, stretching frequency): 3294  $\text{cm}^{-1}$  (NH), 3068  $\text{cm}^{-1}$  (OH), 2957  $\text{cm}^{-1}$  (CH), 1630  $\text{cm}^{-1}$  (CO); MS ( $m/z$ ) : 320  $[\text{M}^{+2}+\text{Na}]^+$ .

2D-HSQCT (DMSO- $d_6$ ) : **1-O-ester (42a)**:  $^1\text{H}$  NMR  $\delta$  (500.13 MHz) : 3.58 ( $\alpha\text{CH}$ ), 1.57( $\beta\text{CH}_2$ ), 1.67 ( $\gamma\text{CH}$ ), 0.71 ( $\delta$ ,  $\delta'\text{CH}_3$ ), 3.51 (H-1), 3.45 (H-2), 3.54 (H-3), 3.56 (H-4), 3.39 (H-5), 3.46 (H-6) ppm;  $^{13}\text{C}$  NMR  $\delta$  (125 MHz) : 51.5 ( $\alpha\text{CH}$ ), 39.5 ( $\beta\text{CH}_2$ ), 24.0 ( $\gamma\text{CH}$ ), 21.8 ( $\delta, \delta'$   $\text{CH}_3$ ), 171.5 (CO), 60.4 (C1), 75.4 (C2), 72.6 (C3), 71.3 (C4), 71.2(C5), 63.5 (C6) ppm; **1,6-di-O-ester (42b)**:  $^1\text{H}$  NMR  $\delta$  : 1.02 ( $\delta, \delta'$   $\text{CH}_3$ ), 3.61 (H-1), 3.32 (H-2), 3.32 (H-5), 3.64 (H-6) ppm;  $^{13}\text{C}$  NMR  $\delta$  : 21.8 ( $\delta, \delta'$   $\text{CH}_3$ ), 60.4 (C1), 72.8 (C2), 70.5 (C5), 68.2 (C6) ppm.

A typical mass spectrum for L-leucyl-D-mannitol **42a,b** is shown in Figure 4.48.

**4.2.3.10. L-Leucyl-D-sorbitol (43)**: Solid; Mpt : 155  $^{\circ}\text{C}$ ; HPLC  $t_{\text{ret}}$ : 3.3 min;  $R_f$ : 0.19; UV ( $\text{H}_2\text{O}$ ,  $\lambda_{\text{max}}$ ): 203.0 nm ( $\sigma \rightarrow \sigma$   $\epsilon_{203.0}$  - 4677  $\text{M}^{-1}$ ), 285.0 nm ( $n \rightarrow \pi^*$   $\epsilon_{285.0}$  - 182  $\text{M}^{-1}$ );

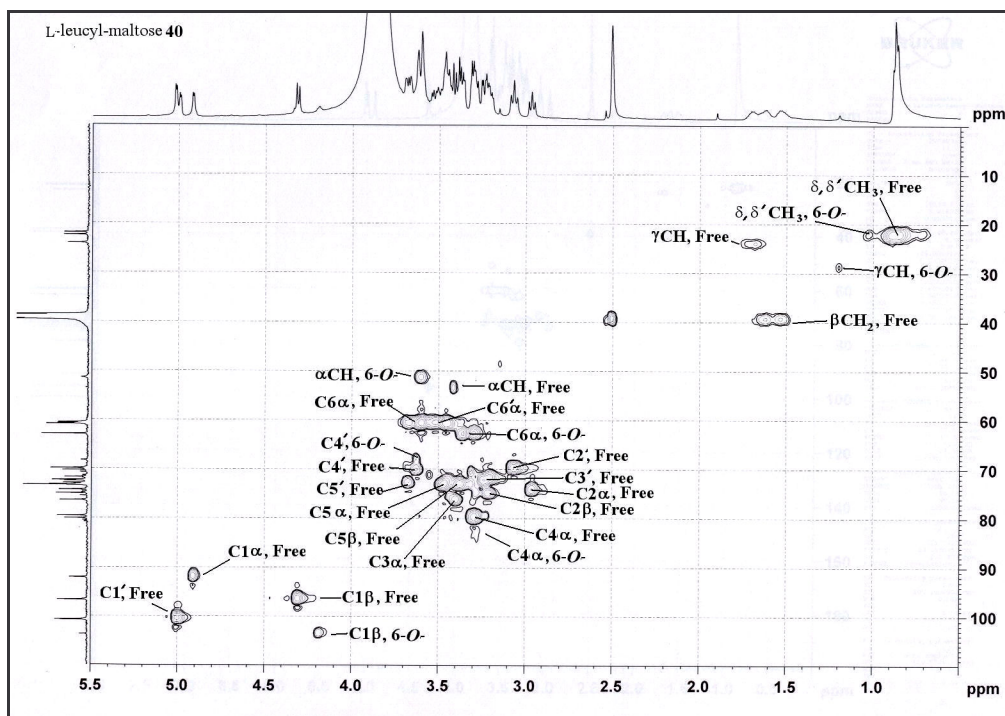


Fig. 4.46. Two-dimensional HSQCT NMR for L-leucyl-maltose **40** obtained through CRL catalysis.

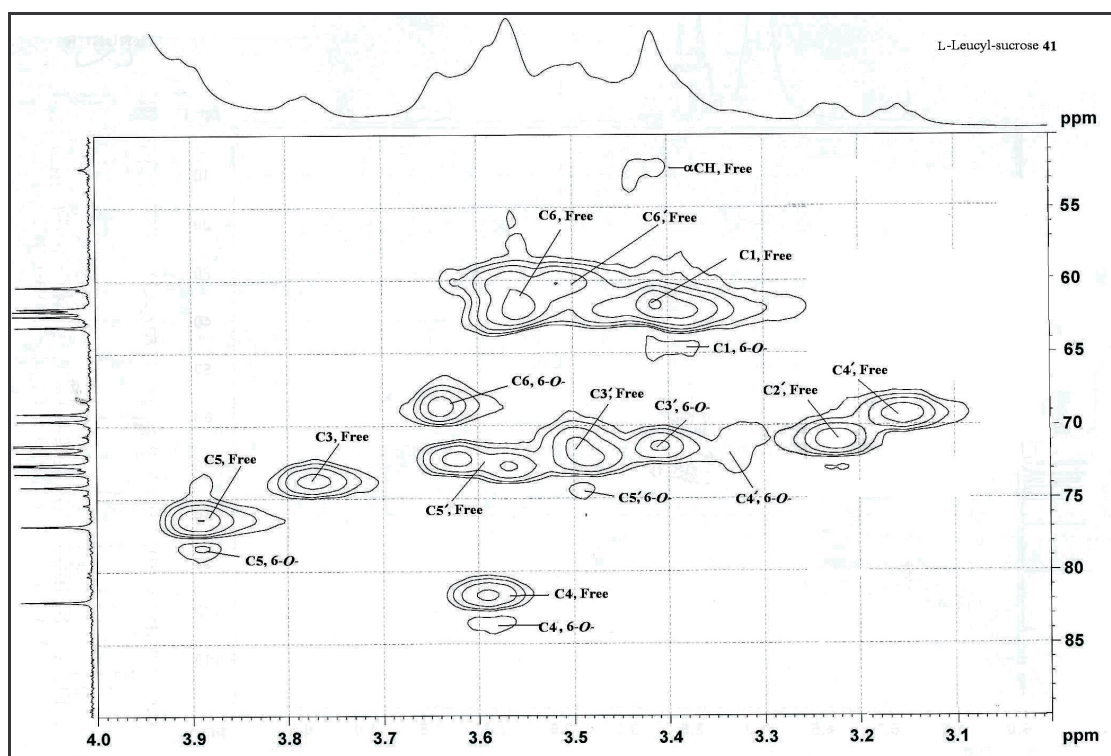


Fig. 4.47. Two-dimensional HSQCT NMR for L-leucyl-sucrose **41** obtained through CRL catalysis.

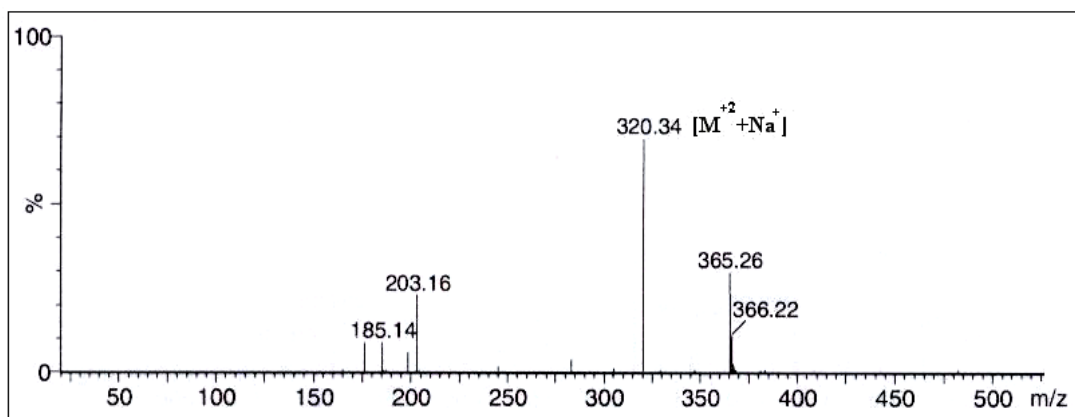


Fig. 4.48. A typical mass spectrum of L-leucyl-D-mannitol 42

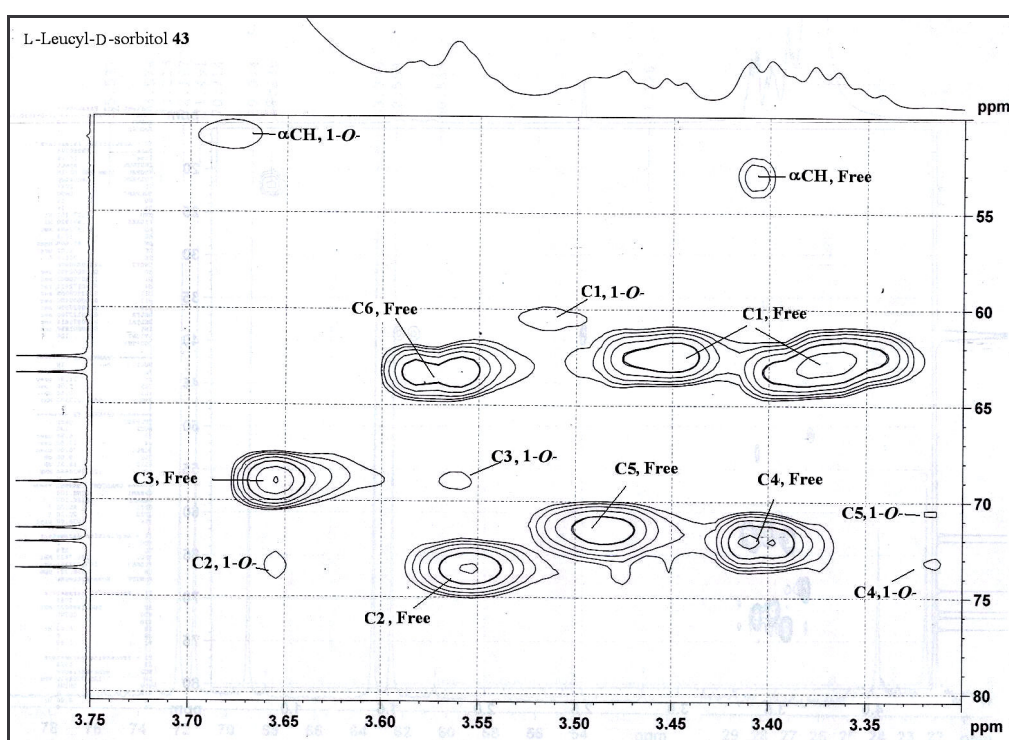


Fig. 4.49. Two-dimensional HSQCT NMR for L-leucyl-D-sorbitol 43 obtained through CRL catalysis.

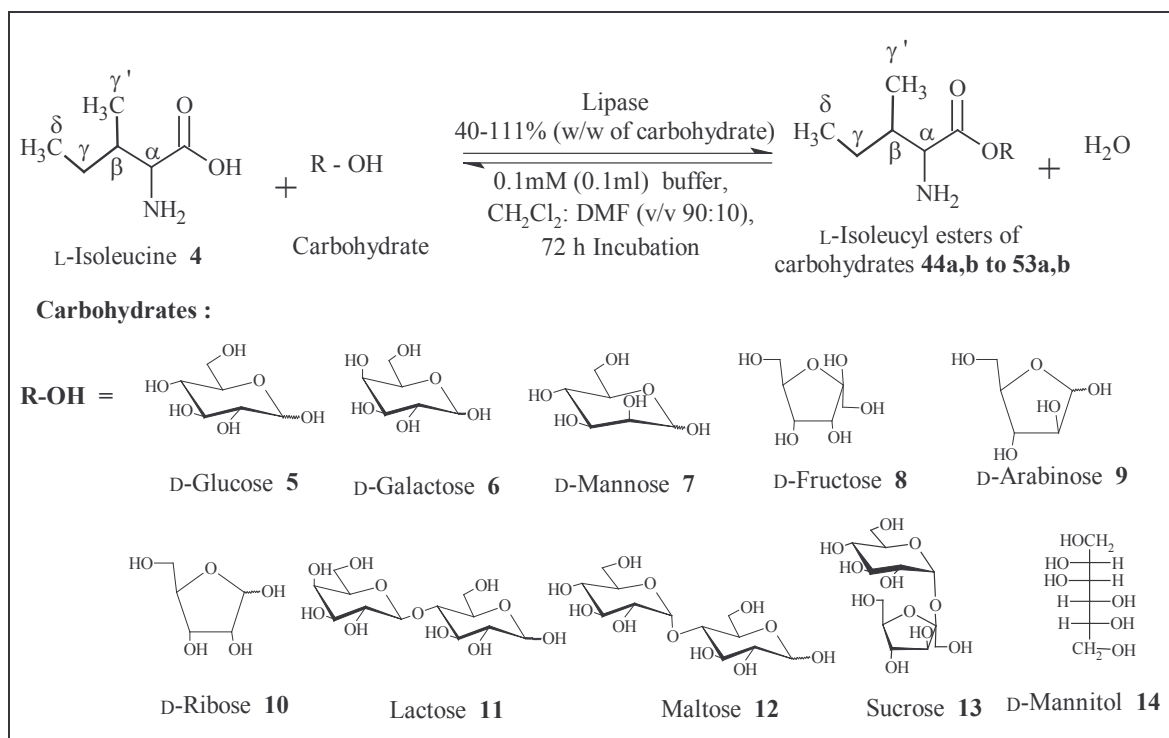
IR (KBr, stretching frequency): 3250  $\text{cm}^{-1}$  (NH), 3150  $\text{cm}^{-1}$  (OH), 2917  $\text{cm}^{-1}$  (CH), 1606  $\text{cm}^{-1}$  (CO); optical rotation ( $c$  0.5,  $\text{H}_2\text{O}$ ) :  $[\alpha]_{\text{D}}$  at 25 °C = -5.3 °; MS ( $m/z$ ): 316  $[\text{M}^{-2} + \text{Na}]^+$ .

2D-HSQCT (DMSO- $d_6$ ) **1-O-ester (43)**:  $^1\text{H}$  NMR  $\delta$  (500.13 MHz): 3.68 ( $\alpha\text{CH}$ ), 1.59 ( $\beta\text{CH}_2$ ), 1.72 ( $\gamma\text{CH}$ ), 1.04 ( $\delta, \delta'\text{CH}_3$ ), 3.51 (H-1), 3.66 (H-2), 3.56 (H-3), 3.32 (H-4), 3.32 (H-5), 3.57 (H-6) ppm;  $^{13}\text{C}$  NMR  $\delta$  (125 MHz) : 51.3 ( $\alpha\text{CH}$ ), 35.9 ( $\beta\text{CH}_2$ ), 24.0 ( $\gamma\text{CH}$ ), 22.0 ( $\delta, \delta'\text{CH}_3$ ), 171.6 (CO), 60.5 (C1), 73.8 (C2), 68.8 (C3), 74.2 (C4), 70.5 (C5), 63.4 (C6) ppm.

A typical 2D-HSQCT NMR spectrum for L-leucyl-D-sorbitol **43** is shown in Figure 4.49.

#### 4.2.4. Syntheses of L-isoleucyl esters of carbohydrates **44a,b** to **53a, b**

L-Isoleucine (L-2-amino-3-methyl pentanoic acid) is a polar and an essential dietary amino acid containing 3-methyl propyl group as a side chain. Here also, the solubility of L-isoleucine is low (41.2 g/L at 25 °C) like of that of L-leucine. Using optimum conditions, L-isoleucyl esters of different carbohydrates were prepared using CRL and crude PPL (Section 2.2.4, **Scheme 4.4**). The reaction mixture consists of 1 – 2 mmol L-isoleucine **4** and 1 mmol carbohydrates (D-glucose **5**, D-galactose **6**, D-mannose **7**, D-fructose **8**, D-arabinose **9**, D-ribose **10**, lactose **11**, maltose **12**, sucrose **13**, D-mannitol **14**, D-sorbitol **15**) along with 40 % CRL (w/w carbohydrate) / 111% of crude PPL (w/w carbohydrate) incubated with 100 ml of  $\text{CH}_2\text{Cl}_2$  and DMF (v/v 90:10, 40 °C) containing 0.1 mM (0.1 ml of 0.1M) of phosphate buffer, pH 7.0 (CRL) or 0.2 mM (0.2 ml of 0.1M) of acetate buffer, pH 5.0 (crude PPL). The reaction mixture was analyzed by HPLC with C-18 column using acetonitrile:water (v/v 20:80) as a mobile phase and detected at 210 nm (Fig. 4.50). Ester formation was also monitored by TLC as described in Section 4.2.1. The retention times ( $t_{\text{ret}}$ ) by HPLC and retention factor ( $R_f$ ) values by TLC are mentioned in sections 4.2.4.1 – 4.2.4.10



**Scheme 4.4 Lipase catalyzed synthesis of L-isoleucyl esters of carbohydrates**

The isolated esters were subjected to UV, IR, MS, optical rotation and 2D- NMR characterization (Sections 4.2.4.1 – 4.2.4.10). The spectral data for the isolated esters were shown in Sections 4.2.4.1 – 4.2.4.10. Table 4.8 shows the HPLC ester yields, types of esters formed and percentage proportions of the individual esters from CRL catalyzed reaction and Table 4.9 shows the HPLC ester yields from crude PPL catalyzed reaction.

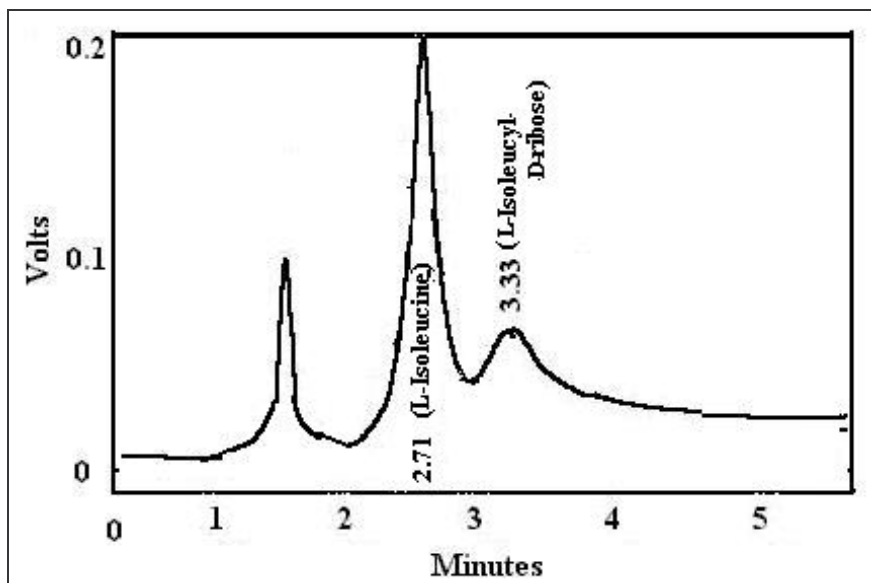


**Fig. 4.50.** HPLC chromatogram for reaction mixture of L-isoleucine and D-ribose esterification catalyzed by CRL. Column – C-18; mobile phase – acetonitrile: water (v/v 20:80); flow rate - 1 ml/min; detector – UV at 210 nm; errors in conversion yields are within  $\pm 10\%$ .



Table 4.8 Syntheses of L-isoleucyl esters of carbohydrates<sup>a</sup>

L-Isoleucyl esters of carbohydrates (% proportions <sup>b</sup> )			Yield (%)
			47 (only mono esters)
<b>44a</b> 3- <i>O</i> -L-isoleucyl-D-glucose (42)	<b>44b</b> 6- <i>O</i> -L-isoleucyl-D-glucose (58)		
			46 (only mono esters)
<b>45a</b> 2- <i>O</i> -L-isoleucyl-D-galactose(78)	<b>45b</b> 3- <i>O</i> -L-isoleucyl-D-galactose(10)	<b>45c</b> 6- <i>O</i> -L-isoleucyl-D-galactose(12)	
			55 (mono esters-25, diesters-30)
<b>46a</b> 3- <i>O</i> -L-isoleucyl-D-mannose (19)	<b>46b</b> 4- <i>O</i> -L-isoleucyl-D-mannose (13)	<b>46c</b> 6- <i>O</i> -L-isoleucyl-D-mannose (13)	
<b>46d</b> 3,6-di- <i>O</i> -L-isoleucyl-D-mannose (27)	<b>46e</b> 4,6-di- <i>O</i> -L-isoleucyl-D-mannose (28)		
			43 (mono esters-28, diester-15)
<b>47a</b> 1- <i>O</i> -L-isoleucyl-D-fructose (36)	<b>47b</b> 6- <i>O</i> -L-isoleucyl-D-fructose (30)	<b>47c</b> 1,6-di- <i>O</i> -L-isoleucyl-D-fructose (34)	
			55 <sup>c</sup> (mono esters-31, diester-24)
<b>48a</b> 2- <i>O</i> -L-isoleucyl-D-arabinose (24)	<b>48b</b> 5- <i>O</i> -L-isoleucyl-D-arabinose (33)	<b>48c</b> 2,5-di- <i>O</i> -L-isoleucyl-D-arabinose (43)	

			53 <sup>c</sup> (mono esters-38, diester-15)
<b>49a</b> 3- <i>O</i> -L-isoleucyl-D-ribose (52) <b>49b</b> 5- <i>O</i> -L-isoleucyl-D-ribose (20) <b>49c</b> 3,5-di- <i>O</i> -L-isoleucyl-D-ribose (28)			
			45 (only mono esters)
<b>50a</b> 2- <i>O</i> -L-isoleucyl -lactose (39) <b>50b</b> 6- <i>O</i> -L-isoleucyl-lactose (40) <b>50c</b> 6'- <i>O</i> -L-isoleucyl-lactose (21)			
			54 (only mono esters)
<b>51a</b> 2- <i>O</i> -L-isoleucyl-maltose (38) <b>51b</b> 6- <i>O</i> -L-isoleucyl-maltose (40) <b>51c</b> 6'- <i>O</i> -L-isoleucyl-maltose (22)			
			22 (only mono ester)
<b>52</b> 6- <i>O</i> -L-isoleucyl – sucrose			
			52 (mono esters-32, diester-20)
<b>53a</b> 1- <i>O</i> -L-isoleucyl -D-mannitol (62) <b>53b</b> 1,6-di- <i>O</i> -L-isoleucyl-D-mannitol (38)			

<sup>a</sup> L-Isoleucine – 2 mmol, carbohydrates – 1 mmol, CRL – 40 % (w/w carbohydrate), buffer – 0.1 mM (0.1 ml of 0.1 M) phosphate buffer (pH 7.0), CH<sub>2</sub>Cl<sub>2</sub>:DMF (v/v 90:10) at 40 °C, incubation period – 72 h. Conversion yields were from HPLC with respect to L-isoleucine concentration.

<sup>b</sup> Percentage proportions of individual esters were determined from the peak areas or from their cross peaks of the Carbon-13 C6 and C5 (in case of pentoses) signals in the 2D HSQCT spectrum.

<sup>c</sup> Several cross peaks, due to opening and/or degradation of the five membered ring during esterification.

**Table 4.9 Preparation of L-isoleucyl esters of carbohydrates using crude porcine pancreas lipase <sup>a</sup>**

L-Isoleucyl ester of carbohydrate	%Yield (mmol)
L-Isoleucyl-D-glucose <b>44a,b</b>	30 (0.30)
L-Isoleucyl-D-galactose <b>45a-c</b>	21 (0.21)
L-Isoleucyl-D-mannose <b>46a-e</b>	22 (0.22)
L-Isoleucyl-D-fructose <b>47a-c</b>	25 (0.25)
L-Isoleucyl-D-arabinose <b>48a-c</b>	9 (0.09)
L-Isoleucyl-D-ribose <b>49a-c</b>	--
L-Isoleucyl-lactose <b>50a-c</b>	39 (0.39)
L-Isoleucyl-maltose <b>51a-c</b>	32 (0.32)
L-Isoleucyl-sucrose <b>52</b>	17 (0.17)
L-Isoleucyl-D-mannitol <b>53a,b</b>	28 (0.28)

<sup>a</sup> L-Isoleucine – 1 mmol, carbohydrates – 1 mmol, Crude PPL – 111% (w/w carbohydrate), buffer – 0.2 mM (0.2 ml of 0.1 M) acetate buffer pH 5.0, CH<sub>2</sub>Cl<sub>2</sub>:DMF (v/v 90:10) at 40 °C, Incubation period – 72 h. Conversion yields were from HPLC with respect to L-isoleucine concentration.

**Spectral data for L-isoleucine (4)** : Solid; Mpt : 284 °C; HPLC *t<sub>ret</sub>*: 2.7 min; *R<sub>f</sub>*: 0.33;

UV (H<sub>2</sub>O, λ<sub>max</sub>): 195.0 nm (σ→σ\* ε<sub>195.0</sub> - 126 M<sup>-1</sup>), IR (KBr, stretching frequency): 3415 cm<sup>-1</sup> (OH), 2945 cm<sup>-1</sup> (CH), 1584 cm<sup>-1</sup> (CO); optical rotation (*c* 1.0, H<sub>2</sub>O) : [α]<sub>D</sub> at 25 °C = +8.6 °.

2D-HSQCT (DMSO-*d*<sub>6</sub>) : <sup>1</sup>H NMR δ (500.13 MHz) : 3.03 (αCH), 1.72 (βCH), 0.84 (γCH<sub>2</sub>), 1.38 (γ'CH<sub>3</sub>), 0.84 (δCH<sub>3</sub>) ppm; <sup>13</sup>C NMR δ (125 MHz): 52.5 (αCH), 36.8 (βCH), 15.1 (γCH<sub>2</sub>), 25.0 (γ'CH<sub>3</sub>), 11.2 (δCH<sub>3</sub>), 171.4 (CO) ppm.

**4.2.4.1. L-Isoleucyl-D-glucose (44a, b)**: Solid; HPLC *t<sub>ret</sub>*: 3.5 min; *R<sub>f</sub>*: 0.23; UV (H<sub>2</sub>O, λ<sub>max</sub>): 227.0 nm (σ→σ\* ε<sub>227.0</sub> - 1862 M<sup>-1</sup>), 278.0 nm (n→π\* ε<sub>278.0</sub> - 1047 M<sup>-1</sup>); IR (KBr, stretching frequency): 3420 cm<sup>-1</sup> (NH), 3350 cm<sup>-1</sup> (OH), 2966 cm<sup>-1</sup> (CH), 1631 cm<sup>-1</sup> (CO); MS (*m/z*) : 316 [M+Na]<sup>+</sup>.

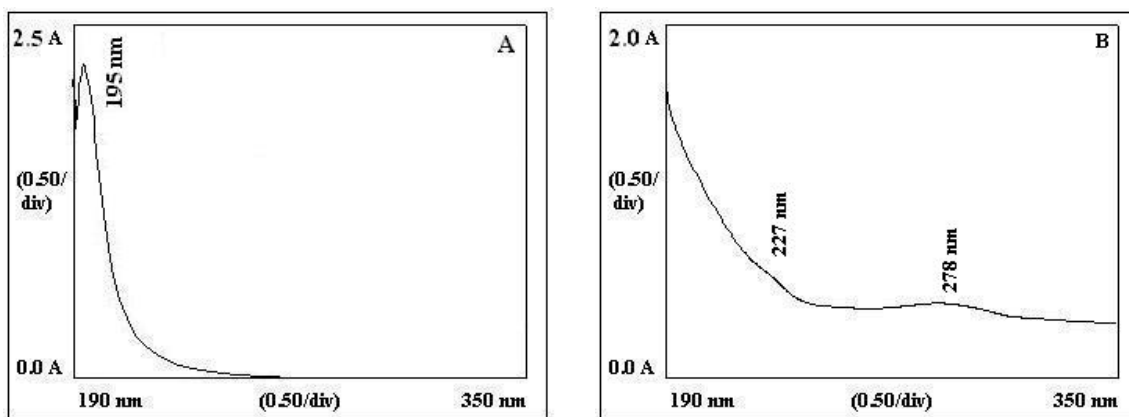


Fig. 4.51 UV spectra for L-isoleucyl-D-glucose 44a,b from CRL catalyzed reaction (A) L-isoleucine; (B) L-isoleucyl-D-glucose.

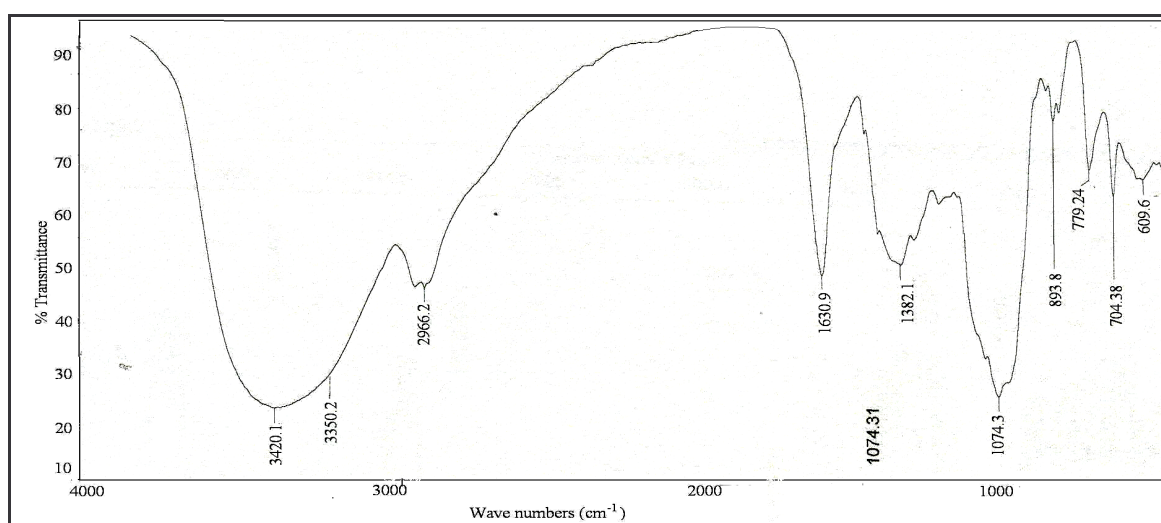


Fig. 4.52. A typical IR spectrum of L-isoleucyl-D-glucose 44a,b of CRL catalyzed reaction. A 1.5 mg of ester sample was prepared as KBr pellet and used.

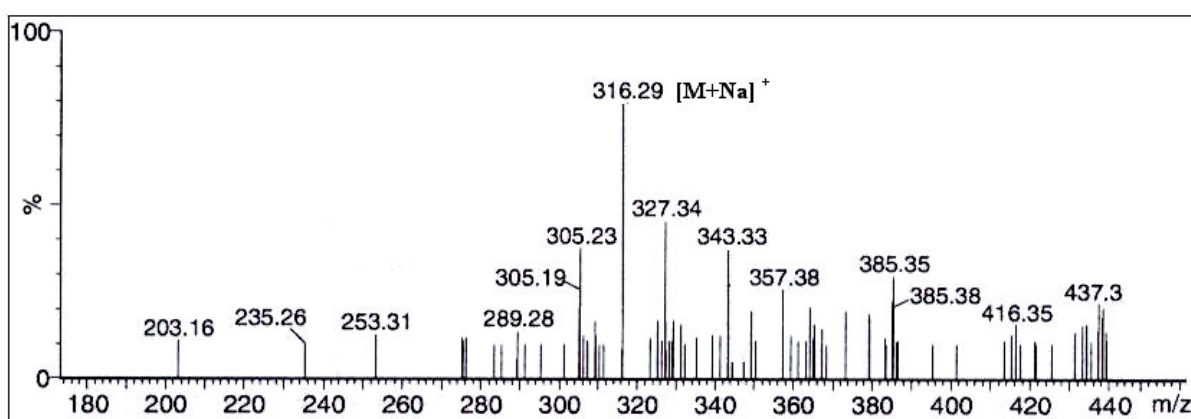


Fig. 4.53. A typical mass spectrum of L-isoleucyl-D-glucose 44a,b.

2D-HSQCT (DMSO- $d_6$ ) : **3-O-ester (44a)**:  $^1\text{H NMR } \delta$  (500.13 MHz) : 3.13 ( $\alpha\text{CH}$ ), 1.61 ( $\beta\text{CH}$ ), 0.61 ( $\gamma\text{CH}_2$ ), 1.08 ( $\gamma'\text{CH}_3$ ), 0.59 ( $\delta\text{CH}_3$ ), 5.0 (H-1 $\alpha$ ), 4.4 (H-1 $\beta$ ), 4.01 (H-3 $\alpha$ ), 3.88 (H-3 $\beta$ ), 3.46 (H-4 $\alpha$ ), 3.58 (H-6) ppm;  $^{13}\text{C NMR } \delta$  (125 MHz): 51.0 ( $\alpha\text{CH}$ ), 35.3 ( $\beta\text{CH}$ ), 14.0 ( $\gamma\text{CH}_2$ ), 25.6 ( $\gamma'\text{CH}_3$ ), 11.2 ( $\delta\text{CH}_3$ ), 171.4 (CO), 91.8 (C1 $\alpha$ ), 95.8 (C1 $\beta$ ), 82.0 (C3 $\alpha$ ), 81.9 (C3 $\beta$ ), 67.5 (C4 $\alpha$ ), 63.0 (C6 $\alpha$ ) ppm; **6-O-ester (44b)**:  $^1\text{H NMR } \delta$  : 3.11 ( $\alpha\text{CH}$ ), 1.61 ( $\beta\text{CH}$ ), 1.08 ( $\gamma'\text{CH}_3$ ), 0.61 ( $\gamma\text{CH}_2$ ), 0.59 ( $\delta\text{CH}_3$ ), 5.0 (H-1 $\alpha$ ), 4.4 (H-1 $\beta$ ), 3.59 (H-2 $\alpha$ ), 3.48 (H-3 $\alpha$ ), 3.64 (H-4 $\alpha$ ), 3.63 (H-5 $\alpha$ ), 3.82 (H-6) ppm;  $^{13}\text{C NMR } \delta$  : 53.1 ( $\alpha\text{CH}$ ), 35.3 ( $\beta\text{CH}$ ), 25.2 ( $\gamma'\text{CH}_3$ ), 14.0 ( $\gamma\text{CH}_2$ ), 11.2 ( $\delta\text{CH}_3$ ), 91.8 (C1 $\alpha$ ), 95.8 (C1 $\beta$ ), 70.0 (C2 $\alpha$ ), 72.2 (C3 $\alpha$ ), 69.0 (C4 $\alpha$ ), 69.2 (C4 $\beta$ ), 63.6 (C6 $\alpha$ ) ppm.

A typical UV, IR, mass and 2D-HSQCT NMR spectra for L-isoleucyl-D-glucose **44a,b** are shown in Figures 4.51, 4.52, 4.53 and 4.54 respectively.

**4.2.4.2. L-Isoleucyl-D-galactose (45a-c)**: Solid; HPLC  $t_{\text{ret}}$ : 3.5 min;  $R_f$ : 0.23; UV (H<sub>2</sub>O,  $\lambda_{\text{max}}$ ): 224.0 nm ( $\sigma \rightarrow \sigma^*$   $\epsilon_{224.0} - 1622 \text{ M}^{-1}$ ), 290.0 nm ( $n \rightarrow \pi^*$   $\epsilon_{290.0} - 776 \text{ M}^{-1}$ ), IR (KBr, stretching frequency): 3309  $\text{cm}^{-1}$  (NH), 2944  $\text{cm}^{-1}$  (CH), 1621  $\text{cm}^{-1}$  (CO); MS ( $m/z$ ) : 316  $[\text{M}+\text{Na}]^+$ .

2D-HSQCT (DMSO- $d_6$ ) : **2-O-ester (45a)**:  $^1\text{H NMR } \delta$  (500.13 MHz): 3.81 (H-2 $\alpha$ ), 3.45 (H-5 $\alpha$ ), 3.40 (H-6) ppm;  $^{13}\text{C NMR } \delta$  (125 MHz): 76.2 (C2 $\alpha$ ), 70.5 (C5 $\alpha$ ), 60.4 (C6 $\alpha$ ) ppm; **3-O-ester (45b)**:  $^1\text{H NMR } \delta$  : 3.58 (H-3 $\alpha$ ), 3.58 (H-3 $\beta$ ), 3.66 (H-3 $\beta$ ), 3.64 (H-6) ppm;  $^{13}\text{C NMR } \delta$  : 66.3 (C2 $\alpha$ ), 81.3 (C3 $\alpha$ ), 82.2 (C3 $\beta$ ), 60.4 (C6 $\alpha$ ) ppm; **6-O-ester (45c)**:  $^1\text{H NMR } \delta$  : 2.79 ( $\alpha\text{CH}$ ), 1.78 ( $\alpha\text{CH}$ ), 0.94 ( $\gamma\text{CH}_2$ ), 1.35 ( $\gamma'\text{CH}_3$ ), 0.93 ( $\delta\text{CH}_3$ ), 4.97 (H-1 $\alpha$ ), 4.87 (H-1 $\beta$ ), 3.51 (H-2 $\alpha$ ), 3.69 (H-3 $\alpha$ ), 3.76 (H-4 $\alpha$ ), 3.22 (H-4 $\beta$ ), 3.59 (H-5 $\alpha$ ), 3.30 (H-5 $\beta$ ), 3.40 (H-6) ppm;  $^{13}\text{C NMR } \delta$  : 53.5 ( $\alpha\text{CH}$ ), 36.5 ( $\beta\text{CH}$ ), 15.2 ( $\gamma\text{CH}_2$ ), 25.0 ( $\gamma'\text{CH}_3$ ), 11.2 ( $\delta\text{CH}_3$ ), 95.0 (C1 $\alpha$ ), 101.6 (C1 $\beta$ ), 68.8 (C2 $\alpha$ ), 68.5 (C3 $\alpha$ ), 70.5 (C4 $\alpha$ ), 72.6 (C4 $\beta$ ), 75.0 (C5 $\alpha$ ), 62.8 (C6 $\alpha$ ) ppm.

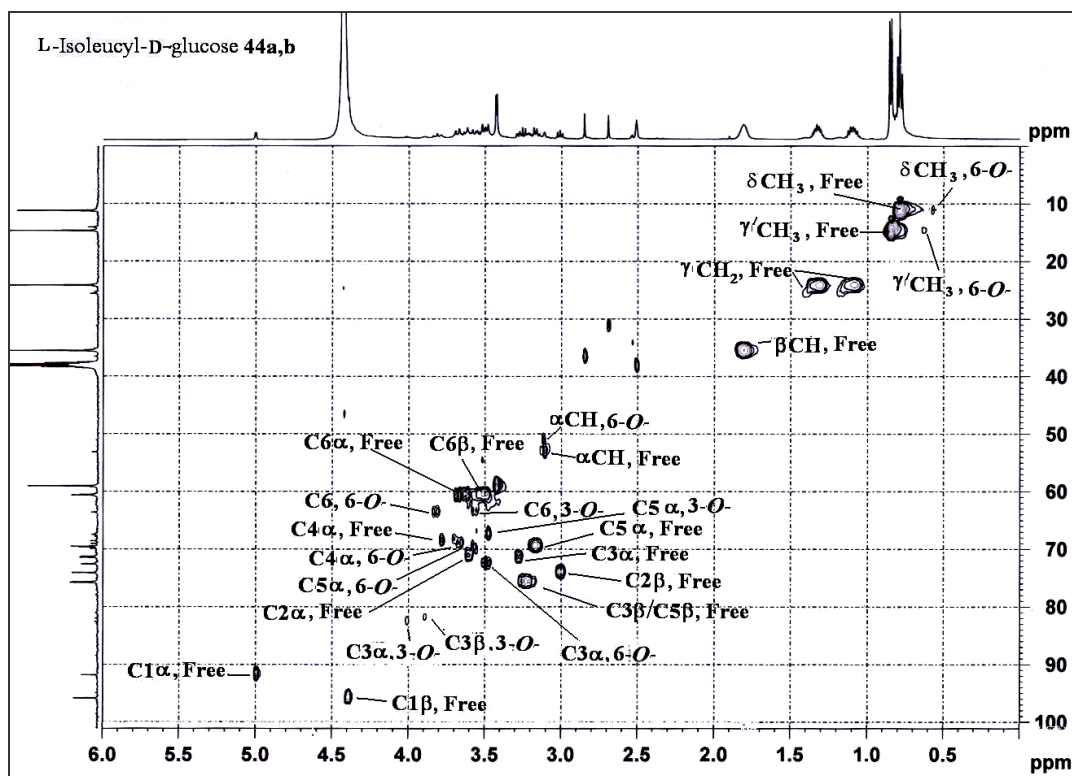


Fig. 4.54. Two-dimensional HSQCT NMR for L-isoleucyl- D-glucose **44a,b** obtained through CRL catalysis.

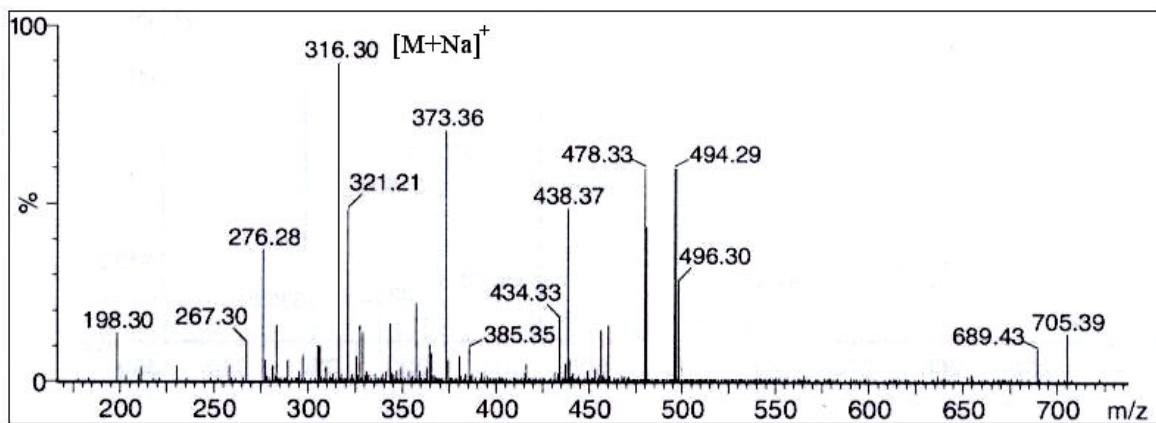


Fig. 4.55. A typical mass spectrum of L-isoleucyl-D-galactose **45a-c**.

A typical mass spectrum for L-isoleucyl-D-galactose **45a-c** is shown in Figure 4.55.

**4.2.4.3. L-Isoleucyl-D-mannose (46a-e)**: Solid; HPLC  $t_{ret}$ : 3.5 min;  $R_f$ : 0.23; UV ( $H_2O$ ,  $\lambda_{max}$ ): 226.0 nm ( $\sigma \rightarrow \sigma^*$   $\epsilon_{226.0} - 1737.8 M^{-1}$ ), 281.0 nm ( $n \rightarrow \pi^*$   $\epsilon_{281.0} - 891 M^{-1}$ ); IR (KBr, stretching frequency): 3385  $cm^{-1}$  (NH), 3267  $cm^{-1}$  (OH), 2966  $cm^{-1}$  (CH), 1641  $cm^{-1}$  (CO); MS ( $m/z$ ): 316  $[M+Na]^+$ .

2D-HSQCT (DMSO- $d_6$ ) : **3-O- Ester (46a)**:  $^1H$  NMR  $\delta$  (500.13 MHz) : 3.72 (H-3 $\alpha$ ), 3.85 (H-3 $\beta$ ), 2.92 (H-4 $\alpha$ ), 3.41 (H-6) ppm;  $^{13}C$  NMR  $\delta$  (125 MHz): 80.5 (C3 $\alpha$ ), 83.1 (C3 $\beta$ ), 65.9 (C4 $\alpha$ ), 60.5 (C6 $\alpha$ ) ppm; **4-O-ester (46b)**:  $^1H$  NMR  $\delta$  : 2.72 ( $\alpha$ CH), 3.80 (H-4 $\alpha$ ), 3.90 (H-4 $\beta$ ), 3.41 (H-6) ppm;  $^{13}C$  NMR  $\delta$  : 52.7 ( $\alpha$ CH), 75.0 (C4 $\alpha$ ), 77.1 (C4 $\beta$ ), 60.5 (C6 $\alpha$ ) ppm; **6-O-ester (46c)**:  $^1H$  NMR  $\delta$  : 2.68 ( $\alpha$ CH), 1.72 ( $\beta$ CH), 0.77 ( $\gamma$ CH $_2$ ), 1.38 ( $\gamma'$ CH $_3$ ), 0.79 ( $\delta$ CH $_3$ ), 4.31 (H-1 $\alpha$ ), 3.64 (H-2 $\alpha$ ), 3.58 (H-3 $\alpha$ ), 3.06 (H-4 $\alpha$ ), 3.58 (H-5 $\alpha$ ), 3.79 (H-6) ppm;  $^{13}C$  NMR  $\delta$  : 52.4 ( $\alpha$ CH), 36.8 ( $\alpha$ CH), 25.0 ( $\gamma'$ CH $_3$ ), 15.0 ( $\gamma$ CH $_2$ ), 11.3 ( $\delta$ CH $_3$ ), 103.0 (C1 $\alpha$ ), 69.0 (C2 $\alpha$ ), 69.8 (C3 $\alpha$ ), 65.8 (C4 $\alpha$ ), 69.9 (C5 $\alpha$ ), 63.1 (C6 $\alpha$ ) ppm; **3,6-di-O-ester (46d)**:  $^1H$  NMR  $\delta$  : 3.55 (H-3 $\alpha$ ), 3.41 (H-6) ppm;  $^{13}C$  NMR  $\delta$  : 82.1 (C3 $\alpha$ ), 62.9 (C6 $\alpha$ ) ppm; **4,6-di-O-ester (46e)**:  $^1H$  NMR  $\delta$  : 3.75 (H-4 $\alpha$ ), 3.52 (H-6) ppm;  $^{13}C$  NMR  $\delta$  : 76.0 (C4 $\alpha$ ), 62.9 (C6 $\alpha$ ) ppm.

A typical UV and 2D-HSQCT NMR spectra for L-isoleucyl-D-mannose **46a-e** are shown in Figures 4.56 and 4.57 respectively.

**4.2.4.4. L-Isoleucyl-D-fructose (47a-c)**: Solid; HPLC  $t_{ret}$ : 3.5 min;  $R_f$ : 0.23; UV ( $H_2O$ ,  $\lambda_{max}$ ): 226.0nm ( $\sigma \rightarrow \sigma^*$   $\epsilon_{226.0} - 309 M^{-1}$ ), 302.0 nm ( $n \rightarrow \pi^*$   $\epsilon_{302.0} - 110 M^{-1}$ ); IR (KBr, stretching frequency): 3378  $cm^{-1}$  (NH), 3217  $cm^{-1}$  (OH), 2900  $cm^{-1}$  (CH), 1632  $cm^{-1}$  (CO); MS ( $m/z$ ): 316  $[M+Na]^+$ .

2D-HSQCT (DMSO- $d_6$ ) : **1-O-ester (47a)**:  $^1H$  NMR  $\delta$  (500.13 MHz): 3.15 ( $\alpha$ CH), 1.65 ( $\beta$ CH), 0.87 ( $\gamma$ CH $_2$ ), 1.35 ( $\gamma'$ CH $_3$ ), 0.83 ( $\delta$ CH $_3$ ), 3.25 (H-1 $\alpha$ ), 3.32 (H-3 $\alpha$ ), 3.32 (H-4 $\alpha$ ),

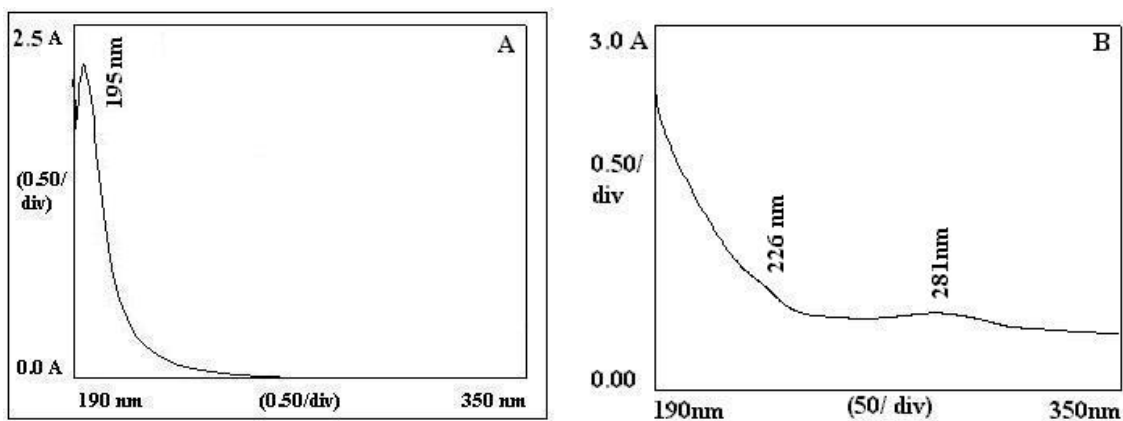


Fig. 4.56 UV spectra for L-isoleucyl-D-mannose **46a-e** from CRL catalyzed reaction (A) L-isoleucine; (B) L-isoleucyl-D-mannose.

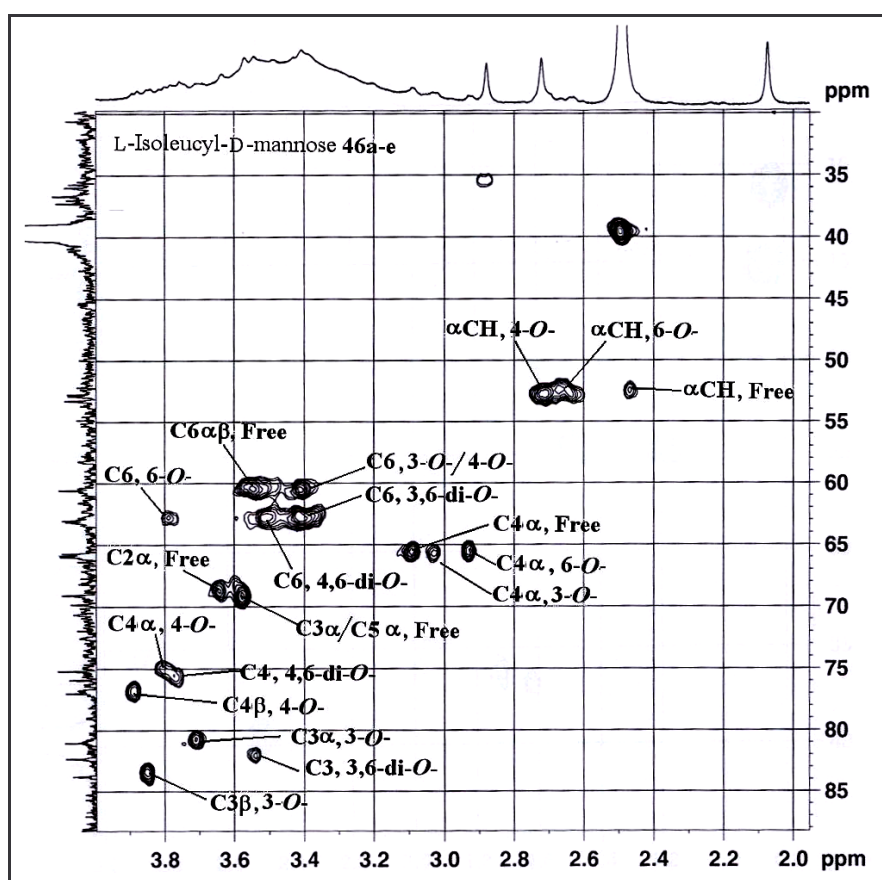


Fig. 4.57. Two-dimensional HSQC NMR for L-isoleucyl-D-mannose **46a-e** obtained through CRL catalysis.



3.73 (H-4 $\beta$ ), 3.72 (H-5 $\beta$ ), 3.50 (H-6) ppm;  $^{13}\text{C}$  NMR  $\delta$  (125 MHz): 57.0 ( $\alpha\text{CH}$ ), 36.9 ( $\beta\text{CH}$ ), 14.8 ( $\gamma\text{CH}_2$ ), 24.8 ( $\gamma'\text{CH}_3$ ), 11.4 ( $\delta\text{CH}_3$ ), 63.7 (C1 $\alpha$ ), 104.0 (C2 $\alpha$ ), 72.8 (C3 $\alpha$ ), 70.5 (C4 $\alpha$ ), 75.8 (C4 $\beta$ ), 81.0 (C5 $\beta$ ), 62.4 (C6 $\alpha$ ) ppm; **6-O-ester (47b)**:  $^1\text{H}$  NMR  $\delta$  : 3.77 (H-5 $\alpha$ ), 3.78 (H-6) ppm;  $^{13}\text{C}$  NMR  $\delta$  : 71.5 (C5 $\alpha$ ), 63.1 (C6) ppm; **1,6-di-O-ester (47c)**:  $^1\text{H}$  NMR  $\delta$  : 3.28 (H-1 $\alpha$ ) ppm;  $^{13}\text{C}$  NMR  $\delta$ : 64.4 (C1 $\alpha$ ) ppm.

A typical 2D-HSQCT NMR spectrum for L-isoleucyl-D-fructose **47a-c** is shown in Figure 4.58.

**4.2.4.5. L-Isoleucyl-D-arabinose (48a-c)**: Solid; HPLC  $t_{\text{ret}}$ : 3.3 min;  $R_f$ : 0.21; UV ( $\text{H}_2\text{O}$ ,  $\lambda_{\text{max}}$ ): 225.0 nm ( $\sigma \rightarrow \sigma^*$   $\epsilon_{225.0} - 661 \text{ M}^{-1}$ ), 297.0 nm ( $n \rightarrow \pi^*$   $\epsilon_{297.0} - 363.1 \text{ M}^{-1}$ ); IR (KBr, stretching frequency): 3320  $\text{cm}^{-1}$  (NH), 3168  $\text{cm}^{-1}$  (OH), 2929  $\text{cm}^{-1}$  (CH), 1629  $\text{cm}^{-1}$  (CO);

2D-HSQCT (DMSO- $d_6$ ) : **2-O-ester (48a)**:  $^1\text{H}$  NMR  $\delta$  (500.13 MHz) : 3.70 ( $\alpha\text{CH}$ ), 1.65 ( $\beta\text{CH}$ ), 1.35 ( $\gamma\text{CH}_2$ ), 0.87 ( $\gamma'\text{CH}_3$ ), 0.83 ( $\delta\text{CH}_3$ ), 4.32 (H-1 $\alpha$ ), 4.89 (H-1 $\beta$ ), 3.76 (H-2 $\alpha$ ), 3.45 (H-2 $\beta$ ), 3.70 (H-3 $\alpha$ ), 3.68 (H-5) ppm;  $^{13}\text{C}$  NMR  $\delta$  (125 MHz): 54.8 ( $\alpha\text{CH}$ ), 36.5 ( $\beta\text{CH}$ ), 14.8 ( $\gamma\text{CH}_2$ ), 24.8 ( $\gamma'\text{CH}_3$ ), 11.4 ( $\delta\text{CH}_3$ ), 96.6 (C1 $\alpha$ ), 92.0 (C1 $\beta$ ), 75.0 (C2 $\alpha$ ), 75.2 (C2 $\beta$ ), 69.5 (C3 $\alpha$ ), 62.6 (C5 $\alpha$ ) ppm;. **5-O-ester (48b)**:  $^1\text{H}$  NMR  $\delta$  : 4.91 (H-1 $\alpha$ ), 4.99 (H-1 $\beta$ ), 3.27 (H-2 $\alpha$ ), 3.60 (H-3 $\alpha$ ), 3.67 (H-4 $\alpha$ ), 3.64 (H-5) ppm;  $^{13}\text{C}$  NMR  $\delta$ : 101.6 (C1 $\alpha$ ), 94.2 (C1 $\beta$ ), 74.2 (C2 $\alpha$ ), 69.5 (C3 $\alpha$ ), 67.3 (C4 $\alpha$ ), 64.8 (C5 $\alpha$ ) ppm; **2,5-di-O-ester (48c)**:  $^1\text{H}$  NMR  $\delta$  : 4.18 (H-1 $\alpha$ ), 3.66 (H-2 $\alpha$ ), 2.96 (H-3 $\alpha$ ), 3.35 (H-5) ppm;  $^{13}\text{C}$  NMR  $\delta$  : 103.5 (C1 $\alpha$ ), 77.2 (C2 $\alpha$ ), 74.2 (C3 $\alpha$ ), 64.8 (C5 $\alpha$ ) ppm.

A typical UV spectrum for L-isoleucyl-D-arabinose **48a-c** is shown in Figure 4.59.

**4.2.4.6. L-Isoleucyl-D-ribose (49a-c)**: Solid; HPLC  $t_{\text{ret}}$ : 3.3 min;  $R_f$ : 0.21; UV ( $\text{H}_2\text{O}$ ,  $\lambda_{\text{max}}$ ): 225.0 nm ( $\sigma \rightarrow \sigma^*$   $\lambda_{225.0} - 1585 \text{ M}^{-1}$ ), 284.0 nm ( $n \rightarrow \pi^*$   $\lambda_{284.0} - 871 \text{ M}^{-1}$ ); IR (KBr,

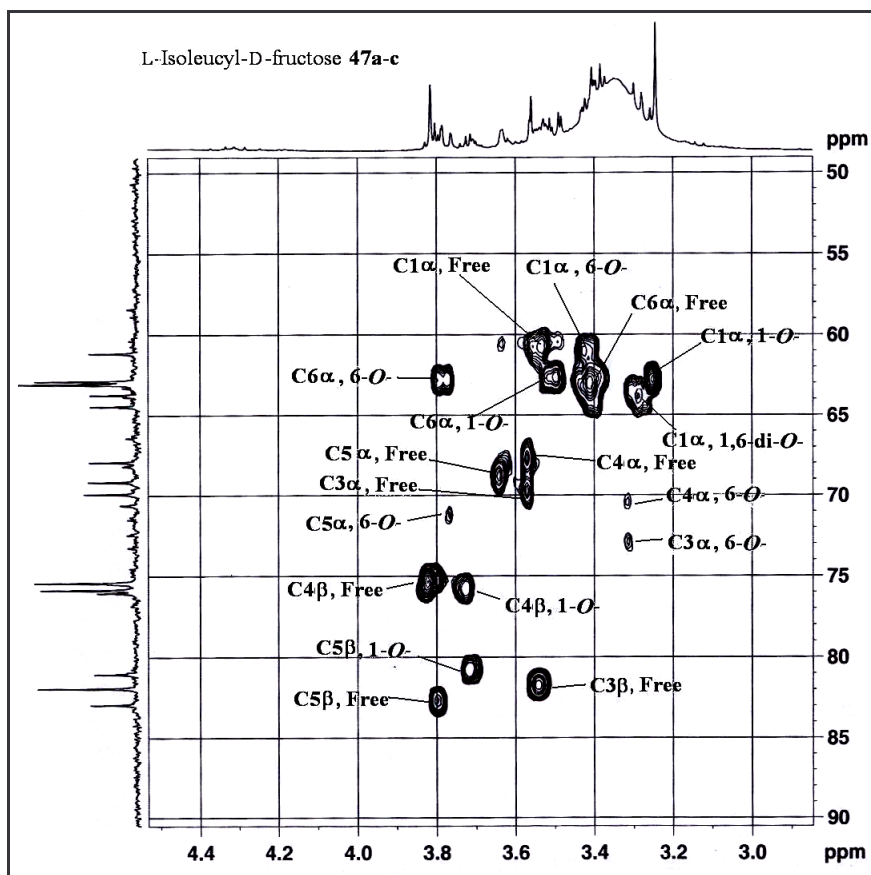


Fig. 4.58. Two-dimensional HSQC NMR for L-isoleucyl-D-fructose 47a-c obtained through CRL catalysis.

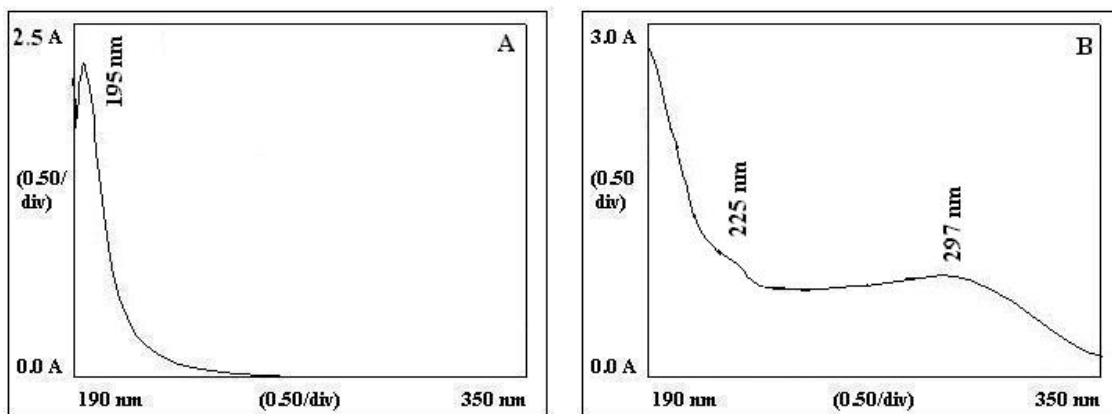


Fig. 4.59. UV spectra for (A) L-isoleucine (B) L-isoleucyl-D-arabinose 48a-c, CRL catalyzed reaction; concentration – 2.6 mM.

stretching frequency): 3384  $\text{cm}^{-1}$  (NH), 3233  $\text{cm}^{-1}$  (OH), 2936  $\text{cm}^{-1}$  (CH), 1631  $\text{cm}^{-1}$  (CO); MS ( $m/z$ ): 283 [ $\text{M}^2+\text{Na}$ ] $^+$ .

2D-HSQCT (DMSO- $d_6$ ) : **3-O- ester (49a)**:  $^1\text{H}$  NMR  $\delta$  (500.13 MHz) : 2.86 ( $\alpha\text{CH}$ ), 1.65 ( $\beta\text{CH}$ ), 0.87 ( $\gamma\text{CH}_2$ ), 1.35 ( $\gamma'\text{CH}_3$ ), 0.83 ( $\delta\text{CH}_3$ ), 4.90 (H-1 $\beta$ ), 3.98 (H-3 $\alpha$ ), 3.92 (H-3 $\beta$ ), 3.64 (H-5) ppm;  $^{13}\text{C}$  NMR  $\delta$  (125 MHz): 51.1 ( $\alpha\text{CH}$ ), 36.5 ( $\beta\text{CH}$ ), 14.8 ( $\gamma\text{CH}_2$ ), 24.8 ( $\gamma'\text{CH}_3$ ), 11.4 ( $\delta\text{CH}_3$ ), 91.9 (C1 $\alpha$ ), 76.5 (C3 $\alpha$ ), 77.7 (C3 $\beta$ ), 60.4 (C5 $\alpha$ ) ppm; **5-O-ester (49b)**:  $^1\text{H}$  NMR  $\delta$ : 5.05 (H-1 $\alpha$ ), 3.65 (H-2 $\alpha$ ), 3.50 (H-3 $\beta$ ), 3.87 (H-4 $\alpha$ ), 3.72 (H-4 $\beta$ ), 3.58 (H-5) ppm;  $^{13}\text{C}$  NMR  $\delta$  : 95.9 (C1 $\alpha$ ), 73.1 (C2 $\alpha$ ), 66.5 (C3 $\beta$ ), 70.5 (C4 $\alpha$ ), 70.7 (C4 $\beta$ ), 63.2 (C5 $\alpha$ ) ppm; **3,5-di-O-ester (49c)**:  $^1\text{H}$  NMR  $\delta$ : 4.64 (H-1 $\alpha$ ), 3.60 (H-3 $\alpha$ ), 3.76 (H-4 $\alpha$ ), 3.52 (H-5) ppm;  $^{13}\text{C}$  NMR  $\delta$  : 93.5 (C1 $\alpha$ ), 75.5 (C3 $\alpha$ ), 70.3 (C4 $\alpha$ ), 63.3 (C5 $\alpha$ ) ppm.

A 2D-HSQCT NMR spectrum for L-isoleucyl-D-ribose **49a-c** is shown in Figure 4.60.

**4.2.4.7. L-Isoleucyl-lactose (50a-c)**: Solid; HPLC  $t_{\text{ret}}$ : 3.4 min;  $R_f$ : 0.12; UV ( $\text{H}_2\text{O}$ ,  $\lambda_{\text{max}}$ ): 227.0 nm ( $\sigma\rightarrow\sigma^*$   $\epsilon_{227.0} - 81\text{ M}^{-1}$ ), 279.0 nm ( $n\rightarrow\pi^*$   $\epsilon_{279.0} - 37\text{ M}^{-1}$ ); IR (KBr, stretching frequency): 3520  $\text{cm}^{-1}$  (NH), 3344  $\text{cm}^{-1}$  (OH), 2900  $\text{cm}^{-1}$  (CH), 1640  $\text{cm}^{-1}$  (CO); MS ( $m/z$ ): 478 [ $\text{M}+\text{Na}$ ] $^+$ .

2D-HSQCT (DMSO- $d_6$ ) : **2-O-ester (50a)**:  $^1\text{H}$  NMR  $\delta$  (500.13 MHz) : 4.28 ( $\alpha\text{CH}$ ), 1.78 ( $\beta\text{CH}$ ), 0.84 ( $\gamma\text{CH}_2$ ), 1.30 ( $\gamma'\text{CH}_3$ ), 0.81 ( $\delta\text{CH}_3$ ), 4.96 (H-1 $\alpha$ ), 4.32 (H-1 $\beta$ ), 4.0 (H-2 $\alpha$ ), 3.82 (H-2 $\beta$ ), 3.56 (H-3 $\alpha$ ), 2.96 (H-3 $\beta$ ), 3.27 (H-4 $\alpha$ ), 3.17 (H-5 $\alpha$ ), 3.28 (H-5 $\beta$ ), 3.49 (H-6), 5.0 (H-1' $\alpha$ ), 3.06 (H-2'), 3.23 (H-3'), 3.63 (H-4'), 3.67 (H-5'), 3.64 (H-6') ppm;  $^{13}\text{C}$  NMR  $\delta$  (125 MHz) : 53.8 ( $\alpha\text{CH}$ ), 36.5 ( $\beta\text{CH}$ ), 15.3 ( $\gamma\text{CH}_2$ ), 24.5 ( $\gamma'\text{CH}_3$ ), 11.2 ( $\delta\text{CH}_3$ ), 172.5 (CO), 92.0 (C1 $\alpha$ ), 96.5 (C1 $\beta$ ), 84.5 (C2 $\alpha$ ), 85.0 (C2 $\beta$ ), 71.5 (C3 $\alpha$ ), 74.8 (C3 $\beta$ ), 81.4 (C4 $\alpha$ ), 81.1 (C4 $\beta$ ), 72.3 (C5 $\alpha$ ), 75.1 (C5 $\beta$ ), 63.0 (C6 $\alpha$ ), 100.7 (C1' $\alpha$ ), 70.3 (C2'), 71.8 (C3'), 69.9 (C4'), 72.4 (C5'), 60.6 (C6') ppm; **6-O-ester (50b)**:  $^1\text{H}$  NMR  $\delta$ : 3.85 (H-6), 3.50 (H-6') ppm;  $^{13}\text{C}$  NMR  $\delta$ : 66.5 (C6 $\alpha$ ), 68.0 (C6') ppm; **6'-O-ester (50c)**:  $^1\text{H}$  NMR

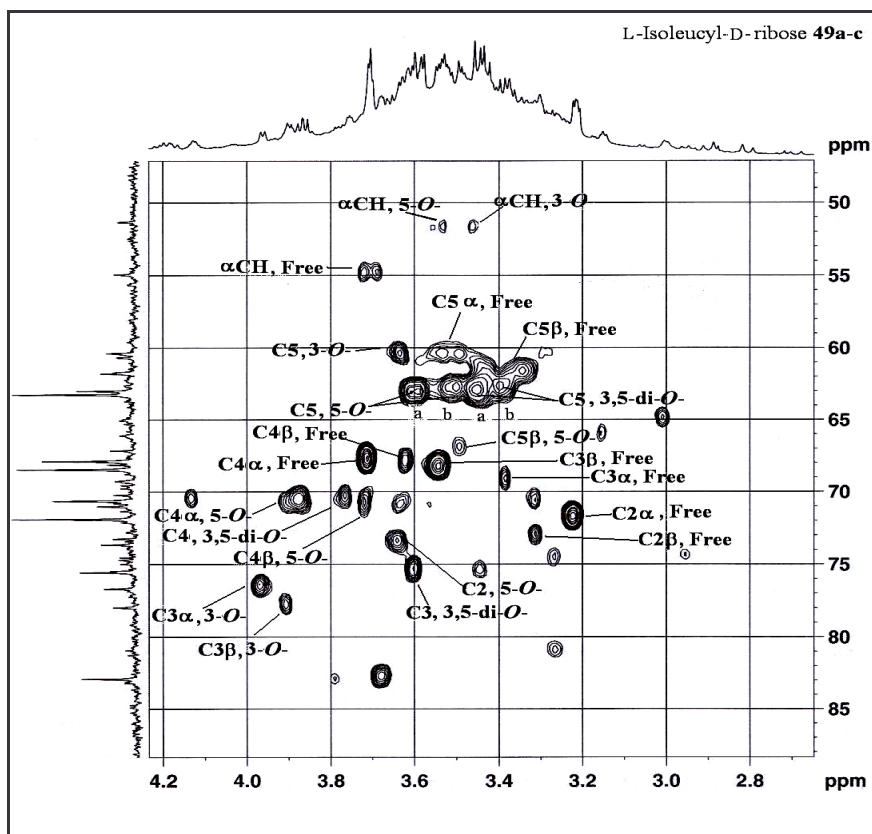


Fig. 4.60. Two-dimensional HSQCT NMR for L-isoleucyl- D-ribose **49a-c** obtained through CRL catalysis.

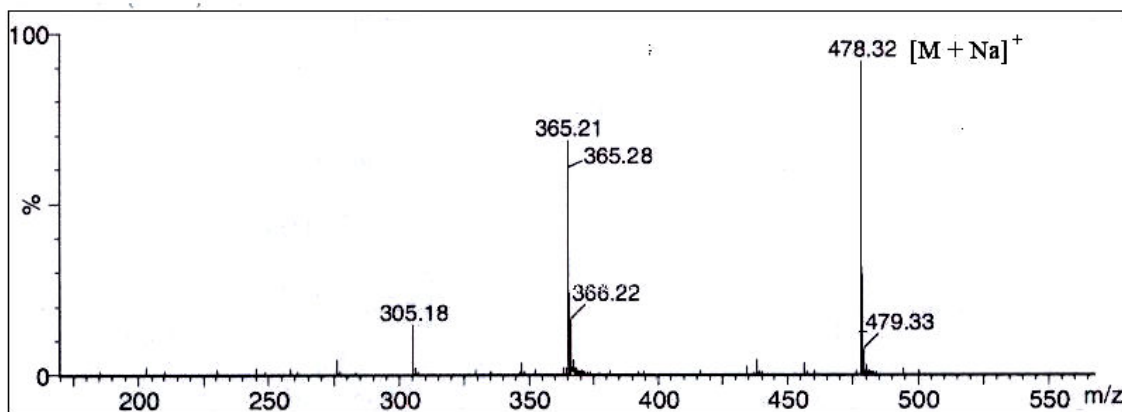


Fig. 4.61. A typical mass spectrum of L-isoleucyl-lactose **50a-c**.

$\delta$  : 3.50 (H-6), 3.54 (H-4'), 3.85 (H-6') ppm;  $^{13}\text{C}$  NMR  $\delta$  (125 MHz) : 61.5 (C6 $\alpha$ ), 70.0 (C4'), 66.9 (C6') ppm.

A typical mass and 2D-HSQCT NMR spectra for L-isooleucyl-lactose **50a-c** are shown in Figures 4.61 and 4.62 respectively.

**4.2.4.8. L-Isoleucyl-maltose (51a-c):** Solid; Mpt. 122 °C; HPLC  $t_{ret}$ : 3.4 min;  $R_f$ : 0.12; UV (H<sub>2</sub>O,  $\lambda_{max}$ ): 224.0 nm ( $\sigma \rightarrow \sigma^*$   $\epsilon_{224.0} - 525 \text{ M}^{-1}$ ), 276.0 nm ( $n \rightarrow \pi^*$   $\epsilon_{276.0} - 234.4 \text{ M}^{-1}$ ); IR (KBr, stretching frequency) : 3450  $\text{cm}^{-1}$  (NH), 3386  $\text{cm}^{-1}$  (OH), 2937  $\text{cm}^{-1}$  (CH), 1646  $\text{cm}^{-1}$  (CO); MS ( $m/z$ ) : 478 [M+Na]<sup>+</sup>.

2D-HSQCT (DMSO- $d_6$ ) : **2-O-ester (51a)**:  $^1\text{H}$  NMR  $\delta$  (500.13 MHz) : 4.25 ( $\alpha\text{CH}$ ), 1.78 ( $\beta\text{CH}$ ), 0.84 ( $\gamma\text{CH}_2$ ), 1.30 ( $\gamma'\text{CH}_3$ ), 0.81 ( $\delta\text{CH}_3$ ), 4.91 (H-1 $\alpha$ ), 4.32 (H-1 $\beta$ ), 4.05 (H-2 $\alpha$ ), 3.96 (H-2 $\beta$ ), 3.40 (H-3 $\alpha$ ), 3.29 (H-4 $\beta$ ), 3.42 (H-5 $\alpha$ ), 3.38 (H-5 $\beta$ ), 3.48 (H-6), 5.0 (H-1' $\alpha$ ), 3.06 (H-2'), 3.23 (H-3'), 3.63 (H-4'), 3.67 (H-5'), 3.64 (H-6') ppm;  $^{13}\text{C}$  NMR  $\delta$  (125 MHz) : 53.8 ( $\alpha\text{CH}$ ), 36.5 ( $\beta\text{CH}$ ), 15.3 ( $\gamma\text{CH}_2$ ), 24.5 ( $\gamma'\text{CH}_3$ ), 11.2 ( $\delta\text{CH}_3$ ), 172.5 (CO), 92.0 (C1 $\alpha$ ), 96.5 (C1 $\beta$ ), 81.2 (C2 $\alpha$ ), 81.4 (C2 $\beta$ ), 76.3 (C3 $\alpha$ ), 79.9 (C4 $\beta$ ), 72.4 (C5 $\alpha$ ), 72.8 (C5 $\beta$ ), 63.0 (C6 $\alpha$ ), 100.7 (C1' $\alpha$ ), 70.3 (C2'), 71.8 (C3'), 69.9 (C4'), 72.4 (C5'), 60.6 (C6') ppm; **6-O-ester (51b)**:  $^1\text{H}$  NMR  $\delta$  : 3.21 (H-4 $\beta$ ), 3.32 (H-5 $\alpha$ ), 3.62 (H-6), 3.70 (H-4') ppm;  $^{13}\text{C}$  NMR  $\delta$  : 79.5 (C4 $\beta$ ), 70.5 (C5 $\alpha$ ), 68.0 (C6 $\alpha$ ), 69.5 (C4') ppm; **6'-O-ester (51c)**:  $^1\text{H}$  NMR  $\delta$  : 3.55 (H-6), 3.62 (H-6') ppm;  $^{13}\text{C}$  NMR  $\delta$  (125 MHz) : 63.0 (C6 $\alpha$ ), 67.2 (C6') ppm.

A typical UV and mass spectra for L-isooleucyl-maltose **51a-c** are shown in Figures 4.63 and 4.64 respectively.

**4.2.4.9. L-Isoleucyl-sucrose (52):** Solid; Mpt. 162 °C; HPLC  $t_{ret}$ : 3.4 min;  $R_f$ : 0.12; UV (H<sub>2</sub>O,  $\lambda_{max}$ ): 226.0 nm ( $\sigma \rightarrow \sigma^*$   $\epsilon_{226.0} - 324 \text{ M}^{-1}$ ), 275.0 nm ( $n \rightarrow \pi^*$   $\epsilon_{275.0} - 174 \text{ M}^{-1}$ ); IR (KBr, stretching frequency): 3598  $\text{cm}^{-1}$  (NH), 3455  $\text{cm}^{-1}$  (OH), 3105  $\text{cm}^{-1}$  (CH), 1616

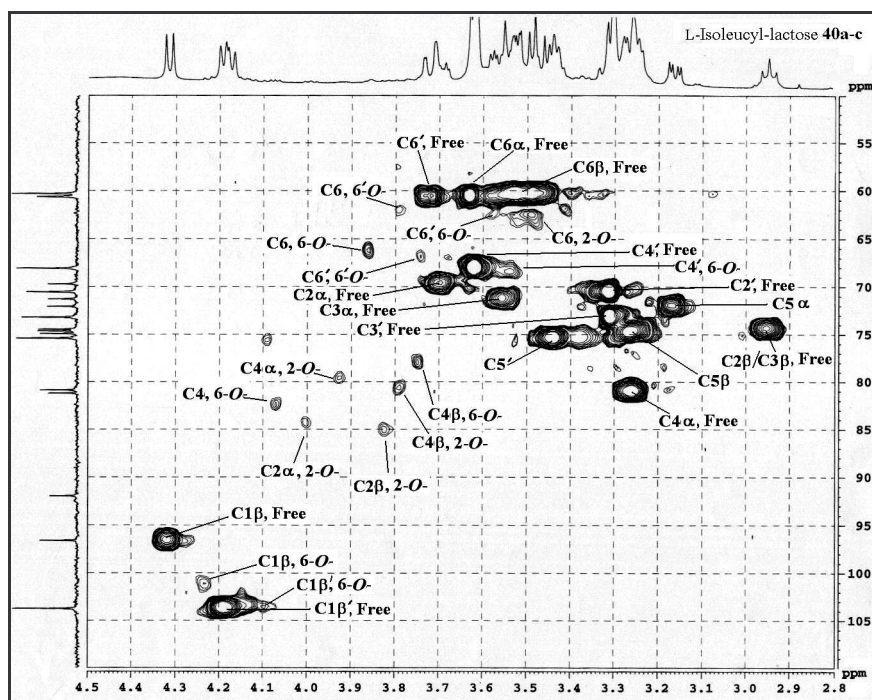


Fig. 4.62. Two-dimensional HSQCT NMR for L-isoleucyl-lactose 50a-c obtained through CRL catalysis.

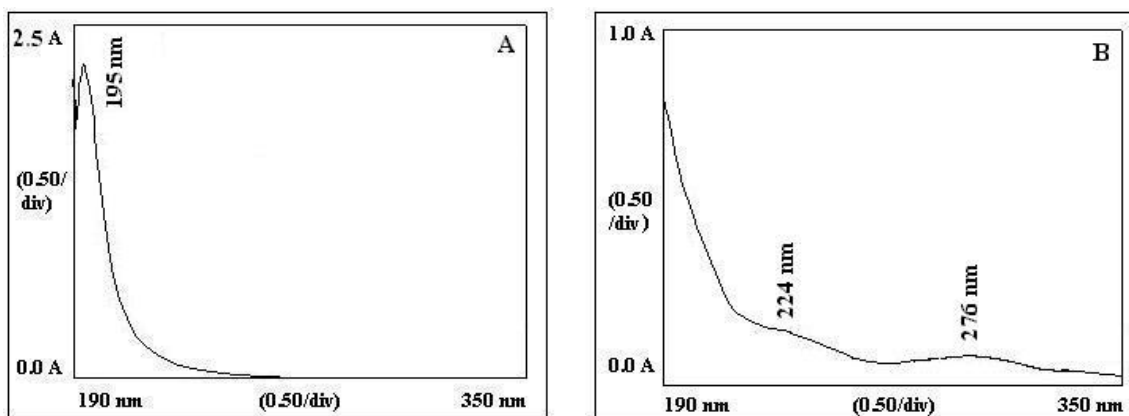


Fig. 4.63 UV spectra for L-isoleucyl-maltose 51a-c from CRL catalyzed reaction. (A) L-isoleucine (B) L-isoleucyl-maltose.

$\text{cm}^{-1}$  (CO); optical rotation ( $c$  0.5,  $\text{H}_2\text{O}$ ):  $[\alpha]_{\text{D}}$  at  $25\text{ }^\circ\text{C} = -28.3\text{ }^\circ$ ; MS ( $m/z$ ) : 478  $[\text{M}+\text{Na}]^+$ .

2D-HSQCT (DMSO- $d_6$ ) : **6-O- ester (52)**:  $^1\text{H}$  NMR  $\delta$  (500.13 MHz): 4.25 ( $\alpha\text{CH}$ ), 1.78 ( $\beta\text{CH}$ ), 0.84 ( $\gamma\text{CH}_2$ ), 1.30 ( $\gamma'\text{CH}_3$ ), 0.81 ( $\delta\text{CH}_3$ ), 3.41 (H-1 $\beta$ ), 3.31 (H-3 $\beta$ ), 3.27 (H-4 $\beta$ ), 3.87 (H-5 $\beta$ ), 3.63 (H-6), 4.89 (H-1' $\alpha$ ), 3.19 (H-2'), 3.44 (H-3'), 3.32 (H-4'), 3.70 (H-5'), 3.63 (H-6'a) and 3.71 (H-6'b) ppm;  $^{13}\text{C}$  NMR  $\delta$  (125 MHz) : 54.8 ( $\alpha\text{CH}$ ), 36.9 ( $\beta\text{CH}$ ), 24.5 ( $\gamma\text{CH}_2$ ), 15.3 ( $\gamma'\text{CH}_3$ ), 11.2 ( $\delta\text{CH}_3$ ), 172.5 (CO), 62.3 (C1 $\beta$ ), 103.5 (C2 $\beta$ ), 73.0 (C3 $\beta$ ), 81.0 (C4 $\beta$ ), 74.5 (C5 $\beta$ ), 67.2 (C6), 92.0 (C1' $\alpha$ ), 71.8 (C2'), 75.0 (C3'), 70.5 (C4'), 69.5 (C5'), 60.7 (C6') ppm.

A typical mass spectrum for L-isoleucyl-sucrose **52** is shown in Figure 4.65.

**4.2.4.10. L-Isoleucyl-D-mannitol (53a, b)**: Solid; HPLC  $t_{\text{ret}}$ : 3.3 min;  $R_f$ : 0.15; UV ( $\text{H}_2\text{O}$ ,  $\lambda_{\text{max}}$ ): 214.0 nm ( $\sigma \rightarrow \sigma^*$   $\epsilon_{214.0} - 87\text{ M}^{-1}$ ), 281.0 nm ( $n \rightarrow \pi^*$   $\epsilon_{281.0} - 22\text{ M}^{-1}$ ); IR (KBr, stretching frequency): 3425  $\text{cm}^{-1}$  (NH), 3068  $\text{cm}^{-1}$  (OH), 2957  $\text{cm}^{-1}$  (CH), 1630  $\text{cm}^{-1}$  (CO); MS ( $m/z$ ) : 319  $[\text{M}^{+1}+\text{Na}]^+$ .

2D-HSQCT (DMSO- $d_6$ ) : **1-O-ester (53a)**:  $^1\text{H}$  NMR  $\delta$  (500.13 MHz) : 3.15 ( $\alpha\text{CH}$ ), 1.78 ( $\beta\text{CH}$ ), 1.30 ( $\gamma\text{CH}_2$ ), 0.84 ( $\gamma'\text{CH}_3$ ), 0.81 ( $\delta\text{CH}_3$ ), 3.49 (H-1a), 3.53 (H-1b), 3.41 (H-2), 3.48 (H-3), 3.54 (H-4), 3.32 (H-5), 3.45 (H-6) ppm;  $^{13}\text{C}$  NMR  $\delta$  (125 MHz) : 58.2 ( $\alpha\text{CH}$ ), 39.5 ( $\beta\text{CH}$ ), 24.5 ( $\gamma\text{CH}_2$ ), 15.3 ( $\delta'\text{CH}_3$ ), 11.2 ( $\delta\text{CH}_3$ ), 172.5 (CO), 60.8 (C1), 71.2 (C2), 69.0 (C3), 71.0 (C4), 70.8 (C5), 63.8 (C6) ppm; **1,6-di-O- ester (53b)**:  $^1\text{H}$  NMR  $\delta$  : 3.63 (H-1), 3.45 (H-2), 3.63 (H-3), 3.32 (H-5), 3.29 (H-6) ppm;  $^{13}\text{C}$  NMR  $\delta$  : 60.8 (C1), 75.2 (C2), 68.0 (C3), 73.0 (C5), 63.5 (C6) ppm.

A typical UV and 2D-HSQCT NMR spectra for L-isoleucyl-D-mannitol **53a,b** are shown in Figures 4.66 and 4.67 respectively.

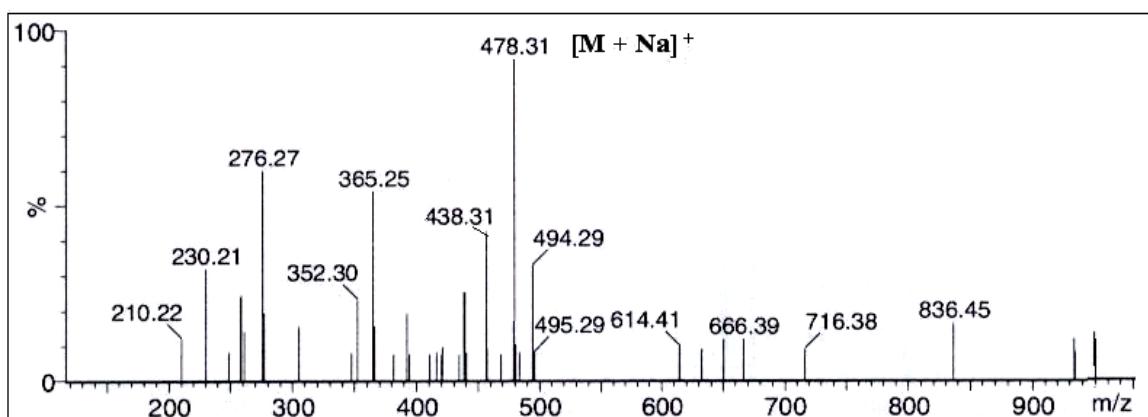


Fig. 4.64. A typical mass spectrum of L-isoleucyl-maltose **51a-c**.

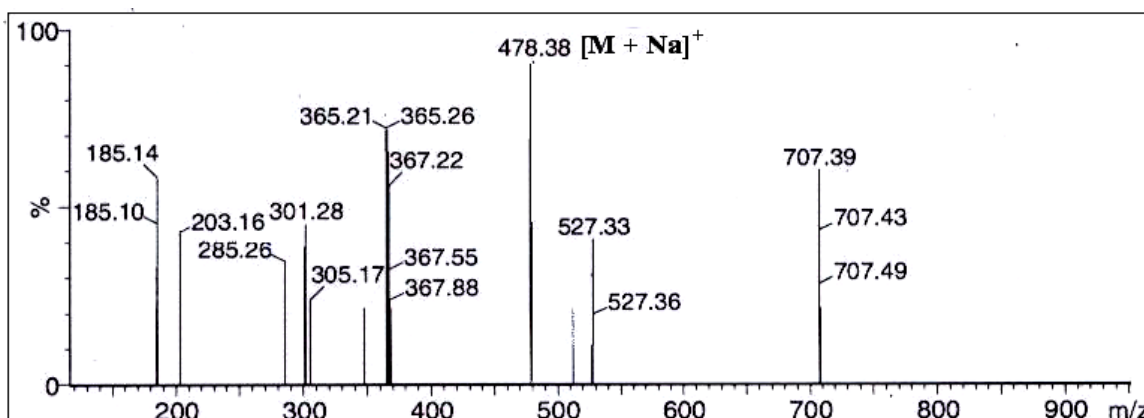


Fig. 4.65. A typical mass spectrum of L-isoleucyl-sucrose **52**.

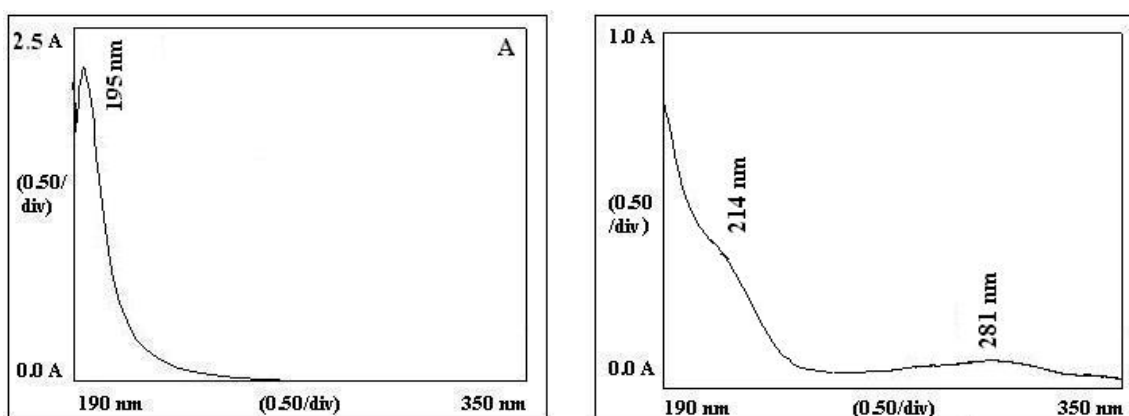


Fig. 4.66 UV spectra for L-isoleucyl-D-mannitol **53a,b** from CRL catalyzed reaction (A) L-isoleucine; (B) for L-isoleucyl-D-mannitol.



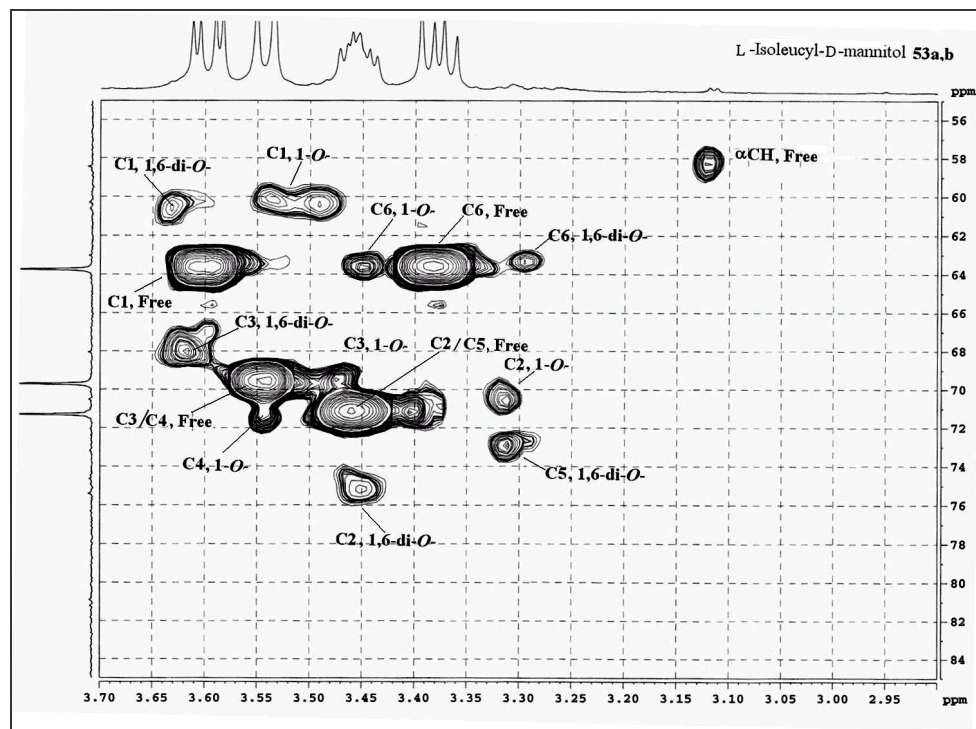


Fig. 4.67. Two-dimensional HSQCT NMR for L-isoleucyl-D-mannitol **53a,b** obtained through CRL catalysis.

### 4.3. Spectral characterization of L-alanyl, L-valyl, L-leucyl and L-isoleucyl esters of carbohydrates

Two-dimensional HSQCT NMR spectroscopy of all the four amino acyl esters of carbohydrates gave good information on the nature and proportion of the esters formed (Table 4.10). Two-dimensional HSQCT NMR data showed that upfield chemical shift values for  $\alpha$ -CH from L-alanyl and  $\beta$ -CH<sub>2</sub> from L-valyl, L-leucyl and L-isoleucyl units indicated that the respective amino acids reacted with the carbohydrates and multiple cross peaks indicated that the reaction occurred at more than one hydroxyl group of the carbohydrate molecules employed.

#### 4.3.1. L-Alanyl esters of carbohydrates 16a-e to 24

UV spectra of L-alanyl esters of carbohydrates showed shifts in the  $\sigma \rightarrow \sigma^*$  band in the 194-228 nm range (190 nm for L-alanine **1**) and IR carbonyl stretching frequencies in the 1606 – 1653 cm<sup>-1</sup> range (1715 cm<sup>-1</sup> for L-alanine **1**) indicating that L-amino acid carboxylic group had been converted into their corresponding carbohydrate esters. In the 2D HSQCT spectra of the L-alanyl esters of carbohydrates, the following ester formation were confirmed from their respective chemical shift values: from D-glucose (**5**), 2-*O*-ester **16a** to C2 $\beta$  at 82.6 ppm and the corresponding H-2 $\beta$  cross peak at 3.62 ppm, 3-*O*-ester **16b** to C3 $\beta$  at 83.3 ppm (H-3 $\beta$  at 3.93 ppm), 6-*O*- ester **16c** to C6 $\beta$  at 63.5 ppm (H-6 at 3.82 ppm), 2,6-di-*O*- ester **16d** to C6 $\beta$  at 62.7 ppm (H-6 at 3.47 ppm) and C2 $\beta$  at 76.5 ppm (H-2 $\beta$  at 3.78 ppm) and 3,6-di-*O*- ester **16e** to C6 $\beta$  at 63.1 ppm (H-6 at 3.82 ppm) and C3 $\beta$  at 81.6 ppm (H-3 $\beta$  at 3.78 ppm); from D-galactose (**6**), 2-*O*- ester **17a** to C2 $\alpha$  at 76.4 ppm (H-2 $\alpha$  at 3.38 ppm) and C2 $\beta$  at 76.5 ppm (H-2 $\beta$  at 3.36 ppm), 3-*O*- ester **17b** to C3 $\alpha$  at 81.6 ppm (H-3 $\alpha$  at 3.75 ppm) and C3 $\beta$  at 82.6 ppm (H-3 $\beta$  at 3.60 ppm) and 6-*O*- ester **17c** to C6 $\alpha$  at 63.1 ppm (H-6 at 3.30 ppm); from D-mannose (**7**), 3-

*O*- ester **18a** to C3 $\alpha$  at 89.2 ppm, 4-*O*-ester **18b** to C-4 $\beta$  at 75.3 ppm, 6-*O*- ester **18c** to C6 $\alpha$  at 63.1 ppm, 3,6-di-*O*- ester **18d** to C6 $\alpha$  at 62.8 ppm and C3 $\alpha$  at 82.9 ppm and 4,6-di-*O*- ester **18e** to C6 $\alpha$  at 62.5 ppm and C4 $\alpha$  at 77.2 ppm; from D-fructose (**8**), 1-*O*- ester **19a** to C1 $\alpha$  at 63.1 ppm (H-1 $\alpha$  at 3.40 ppm), 6-*O*- ester **19b** to C6 $\alpha$  at 63.6 ppm (H-6 at 3.30 ppm) and 1,6-di-*O*- ester **19c** to C1 and C6 at around 63.6 ppm (H-1 and H-6 at around 3.12 ppm); from D-arabinose (**9**), 2-*O*- ester **20a** to C2 $\alpha$  at 77.8 ppm (H-2 $\alpha$  at 3.60 ppm), 5-*O*- ester **20b** to C5 $\alpha$  at 65.1 ppm (H-5 at 3.60 ppm) and 2,5-di-*O*- ester **20c** to C2 $\alpha$  at 76.9 ppm (H-2 $\alpha$  at 3.45 ppm) and C5 $\alpha$  at 65.1 ppm (H-5 at 3.30 ppm); from D-ribose (**10**), 3-*O*- ester **21a** to C3 $\alpha$  at 75.7 ppm (H-3 $\alpha$  at 3.67 ppm), 5-*O*- ester **21b** to C5 $\alpha$  at 63.4 ppm (H-5 at 3.61 ppm) and 3,5-di-*O*- ester **21c** to C3 $\alpha$  at 74.9 ppm (H-3 $\alpha$  at 3.45 ppm) and C5 $\alpha$  at 63.4 ppm (H-5 at 3.52 ppm); from lactose (**11**), 6-*O*- ester **22a** to C6 at 61.2 ppm (H-6 at 3.80 ppm) of glucose moiety, 6'-*O*- ester **22b** to C-6' at 64.0 ppm (H-6' at 3.70 ppm) of galactose moiety and 6,6'-di-*O*- ester **22c** to C6 and C6' at around 67.5 ppm (H-6 and H-6' at around 3.85 ppm); from maltose (**12**), 6-*O*- ester **23a** to C6 at 67.5 ppm (H-6 at 3.50 ppm) of reducing end glucose moiety, 6'-*O*- ester **23b** to C6' at 67.0 ppm (H-6' at 3.95 ppm) of the non reducing end glucose moiety and 6,6'-di-*O*- ester **23c** to C6 and C6' at around 63.0 ppm (H-6 and H-6' at around 3.75 ppm); and from sucrose (**13**), 6-*O*-ester **24** to C6 $\beta$  at 67.0 ppm (H-6 $\beta$  at 3.67 ppm) of the fructose moiety. In D-glucose, only  $\beta$ -D-glucose esterified as observed from C1 at 102.6 (2-*O*-ester), 101.8 (6-*O*-ester) and 100.8 (2,6-di-*O*-ester) from a 40:60, mixture of  $\alpha$  and  $\beta$  anomers of the D-glucose employed. Mass spectra also confirmed the formation of the above mentioned esters.

### 4.3.2. L-Valyl esters of carbohydrates **25a-e** to **33**

UV spectra of L-valyl esters of carbohydrates showed shifts in the  $\sigma \rightarrow \sigma^*$  band in the 200-230 nm range (195 nm for L-valine **2**) and IR carbonyl stretching frequencies in the 1588 -1644  $\text{cm}^{-1}$  range (1605  $\text{cm}^{-1}$  for L-valine **2**) indicating that L-amino acid carboxylic group had been converted into their corresponding carbohydrate esters. In the 2D HSQCT spectra of the L-valyl esters of carbohydrates, the following ester formation were confirmed from their respective chemical shift values: from D-glucose (**5**), 2-*O*-ester **25a** to C2 $\alpha$  at 77.4 ppm and the corresponding H-2 $\alpha$  cross peak at 3.75 ppm, 3-*O*-ester **25b** to C3 $\alpha$  at 82.6 ppm (H-3 $\alpha$  at 3.96 ppm) and C3 $\beta$  at 83.1 ppm (H-3 $\beta$  at 4.01 ppm), 6-*O*-ester **25c** to C6 at 63.4 ppm (H-6 at 3.15 ppm), 2,6-di-*O*-ester **25d** to C6 $\alpha$  at 61.5 ppm (H-6 at 3.56 ppm) and C2 $\alpha$  at 76.4 ppm (H-2 $\alpha$  at 3.85 ppm) and 3,6-di-*O*-ester **25e** to C6 $\alpha$  at 61.8 ppm (H-6 at 3.52 ppm) and C3 $\alpha$  at 82.4 ppm (H-3 $\alpha$  at 3.70 ppm); from D-galactose (**6**), 2-*O*-ester **26a** to C2 $\alpha$  at 76.4 ppm (H-2 $\alpha$  at 3.83 ppm) and C2 $\beta$  at 77.6 ppm (H-2 $\beta$  at 3.65 ppm), 3-*O*-ester **26b** to C3 $\alpha$  at 81.6 ppm (H-3 $\alpha$  at 3.80 ppm) and C3 $\beta$  at 82.7 ppm (H-3 $\beta$  at 3.67 ppm) and 6-*O*-ester **26c** to C6 $\alpha$  at 63.1 ppm (H-6 at 3.35 ppm); from D-mannose (**7**), 6-*O*-ester **27** to C6 $\alpha$  at 63.5 ppm (H-6 at 3.63 ppm); from D-fructose (**8**), 1-*O*-ester **28a** to C1 $\alpha$  at 64.1 ppm (H-1 $\alpha$  at 3.78 ppm), 6-*O*-ester **28b** to C6 $\alpha$  at 64.0 ppm (H-6 at 3.18 ppm) and 1,6-di-*O*-ester **28c** to C1 and C6 $\alpha$  at around 63.4 ppm (H-1 and H-6 at around 3.28 ppm); from D-arabinose (**9**), 2-*O*-ester **29a** to C2 $\alpha$  at 77.0 ppm (H-2 $\alpha$  at 3.65 ppm), 5-*O*-ester **29b** to C5 $\alpha$  at 65.0 ppm (H-5 at 3.64 ppm) and 2,5-di-*O*-ester **29c** to C2 $\alpha$  at 75.6 ppm (H-2 $\alpha$  at 3.45 ppm) and C5 $\alpha$  and C5 $\beta$  at 63.3 ppm and 65.0 ppm (H-5 $\alpha$  at 3.35 ppm and H-5 $\beta$  at 3.35 ppm) respectively; from D-ribose (**10**), 3-*O*-ester **30a** to C3 $\alpha$  at 77.1 ppm (H-3 $\alpha$  at 3.98 ppm), 5-*O*-ester **30b** to C5 $\alpha$  at 63.9 ppm (H-5 at 3.62 ppm) and 3,5-di-*O*-ester **30c** to C3 $\alpha$  at 74.6 ppm

(H-3 $\alpha$  at 3.67 ppm) and C5 $\alpha$  at 65.4 ppm (H-5 at 3.34 ppm); from maltose (**12**), 6-*O*-ester **31a** to C6 $\alpha,\beta$  at 66.5 ppm (H-6 at 3.93 ppm) of reducing end glucose moiety, 6'-*O*-ester **31b** to C6' at 68.0 ppm (H-6' at 3.83 ppm) of the non reducing end glucose moiety; from sucrose (**13**), 6-*O*-ester **32** to C6 $\beta$  at 68.2 ppm (H-6 $\beta$  at 3.64 ppm) of the fructose moiety; and from D-mannitol (**14**), 1-*O*- ester **33** to C1 at 60.6 ppm and the corresponding H-1 cross peak at 3.53 ppm. Mass spectra also confirmed the formation of the above mentioned esters.

#### 4.3.3. L-Leucyl esters of carbohydrates **34a-e** to **43**

UV spectra of L-leucyl esters of carbohydrates showed shifts in the  $\sigma \rightarrow \sigma^*$  band in the 203-230 nm range (190 nm for L-leucine **3**) and IR carbonyl stretching frequencies in the 1580 -1657  $\text{cm}^{-1}$  range (1605  $\text{cm}^{-1}$  for L-leucine **3**) indicating that L-amino acid carboxylic group had been converted into their corresponding carbohydrate esters. In the 2D HSQCT spectra of the L-leucyl esters of carbohydrates, the following ester formation were confirmed from their respective chemical shift values: from D-glucose (**5**), 2-*O*-ester **34a** to C2 $\alpha$  at 75.5 ppm and the corresponding H-2 $\alpha$  cross peak at 3.85 ppm, 3-*O*-ester **34b** to C3 $\alpha$  at 83.5 ppm (H-3 $\alpha$  at 3.85 ppm) and C3 $\beta$  at 83.6 ppm (H-3 $\beta$  at 3.96 ppm), 6-*O*- ester **34c** to C6 $\alpha$  at 65.0 ppm (H-6 at 3.80 ppm), 2,6-di-*O*- ester **34d** to C6 $\alpha$  at 65.0 ppm (H-6 at 3.59 ppm) and C2 $\alpha$  at 76.3 ppm (H-2 $\alpha$  at 3.21 ppm) and 3,6-di-*O*-ester **34e** to C6 $\alpha$  at 65.0 ppm (H-6 at 3.59 ppm) and C3 $\alpha$  at 81.5 ppm (H-3 $\alpha$  at 3.68 ppm); from D-galactose (**6**), 2-*O*- ester **35a** to C2 $\alpha$  at 72.5 ppm (H-2 $\alpha$  at 3.74 ppm), 6-*O*- ester **35b** to C6 $\alpha$  at 62.5 ppm (H-6 at 3.65 ppm); from D-mannose (**7**), 3-*O*- ester **36a** to C3 $\alpha$  at 81.4 ppm (H-3 $\alpha$  at 3.86 ppm) and C3 $\beta$  at 82.5 ppm (H-3 $\beta$  at 3.97 ppm), 4-*O*-ester **36b** to C4 $\alpha$  at 73.8 ppm (H-4 $\alpha$  at 3.86 ppm) and C4 $\beta$  at 75.0 ppm (H-4 $\beta$  at 3.78 ppm) and 6-*O*- ester **36c** to C6 $\alpha$  at 63.2 ppm (H-6 at 3.80 ppm); from D-fructose (**8**), 6-

*O*- ester **37** to C1 $\alpha$  at 63.5 ppm (H-1 $\alpha$  at 3.83 ppm); from D-arabinose (**9**), 2-*O*- ester **38a** to C2 $\alpha$  at 75.0 ppm (H-2 $\alpha$  at 3.76 ppm) C2 $\beta$  at 75.2 ppm (H-2 $\beta$  at 3.45 ppm) and 5-*O*- ester **38b** to C5 $\alpha$  at 64.8 ppm (H-5 at 3.64 ppm), 2,5-di-*O*- ester **38c** to C2 $\alpha$  at 77.2 ppm (H-2 $\alpha$  at 3.66 ppm) and C5 $\alpha$  at 64.8 ppm (H-5 at 3.35); from D-ribose (**10**), 3-*O*- ester **39a** to C3 $\alpha$  at 76.0 ppm (H-3 $\alpha$  at 3.60 ppm), 5-*O*- ester **39b** to C5 $\alpha$  at 63.0 ppm (H-5a at 3.59 ppm and H-5b at 3.68 ppm), 3,5-di-*O*- ester **39c** to C3 $\alpha$  at 76.2 ppm (H-3 $\alpha$  at 3.77 ppm) and C5 $\alpha$  at 64.8 ppm (H-5a at 3.34 ppm and H-5b at 3.37 ppm); from maltose (**12**), 6-*O*- ester **40** to C6 at 62.9 ppm (H-6 at 3.33 ppm) of reducing end glucose moiety; from sucrose (**13**), 6-*O*-ester **41** to C6 $\beta$  at 68.2 ppm (H-6 at 3.64 ppm) of the fructose moiety; from D-mannitol (**14**), 1-*O*- ester **42a** to C1 at 60.4 ppm (H-1 at 3.51 ppm), 1,6-di-*O*- ester **42b** to C1 at 60.4 ppm (H-1 at 3.61 ppm) and C6 at 68.2 ppm (H-6 at 3.64 ppm); and from D-sorbitol (**15**), 1-*O*- ester **43** to C1 at 60.5 ppm (H-1 at 3.51 ppm). Mass spectra also confirmed the formation of the above mentioned esters.

#### **4.3.4. L-Isoleucyl esters of carbohydrates 44a-e to 53a, b**

UV spectra of L-leucyl esters of carbohydrates showed shifts in the  $\sigma \rightarrow \sigma^*$  band in the 214-227 nm range (195 nm for L-isoleucine **4**) and IR carbonyl stretching frequencies in the 1616 -1646  $\text{cm}^{-1}$  range (1584  $\text{cm}^{-1}$  for L-isoleucine **4**) indicating that L-amino acid carboxylic group had been converted into their corresponding carbohydrate esters. In the 2D HSQCT spectra of the L-isoleucyl esters of carbohydrates, the following ester formation were confirmed from their respective chemical shift values: from D-glucose (**5**), 3-*O*- ester **44a** to C3 $\alpha$  at 82.0 ppm (H-3 $\alpha$  at 4.01 ppm) and C3 $\beta$  at 81.9 ppm (H-3 $\beta$  at 3.88 ppm), 6-*O*- ester **44b** to C6 $\alpha$  at 63.6 ppm (H-6 at 3.82 ppm); from D-galactose (**6**), 2-*O*- ester **45a** to C2 $\alpha$  at 76.2 ppm (H-2 $\alpha$  at 3.81 ppm), 3-*O*- ester **45b** to C3 $\alpha$  at 81.3 ppm (H-3 $\alpha$  at 3.58 ppm) and C3 $\beta$  at 82.2 ppm (H-3 $\beta$  at 3.66 ppm), 6-*O*-

ester **45c** to C6 $\alpha$  at 62.8 ppm (H-6 at 3.40 ppm); from D-mannose (**7**), 3-*O*- ester **46a** to C3 $\alpha$  at 80.5 ppm (H-3 $\alpha$  at 3.72 ppm) and C3 $\beta$  at 83.1 ppm (H-3 $\beta$  at 3.85 ppm), 4-*O*- ester **46b** to C4 $\alpha$  at 75.0 ppm (H-4 $\alpha$  at 3.80 ppm) and C4 $\beta$  at 77.1 ppm (H-4 $\beta$  at 3.90 ppm), 6-*O*- ester **46c** to C6 $\alpha$  at 63.1 ppm (H-6 at 3.79 ppm), 3,6-di-*O*- ester **46d** to C6 $\alpha$  at 62.9 ppm (H-6 at 3.41 ppm) and C3 $\alpha$  at 82.1 ppm (H-3 $\alpha$  at 3.55 ppm) and 4,6-di-*O*- ester **46e** to C6 $\alpha$  at 62.9 ppm (H-6 at 3.52 ppm) and C4 $\alpha$  at 76.0 ppm (H-4 $\alpha$  at 3.75 ppm); from D-fructose (**8**), 1-*O*- ester **47a** to C1 $\alpha$  at 63.7 ppm (H-1 $\alpha$  at 3.25 ppm), 6-*O*- ester **47b** to C6 $\alpha$  at 63.1 ppm (H-6 at 3.78 ppm) and 1,6-di-*O*- ester **47c** to C1 $\alpha$  and C6 $\alpha$  at around 64.4 ppm (H-1 and H-6 at around 3.28 ppm); from D-arabinose (**9**), 2-*O*- ester **48a** to C2 $\alpha$  at 75.0 ppm (H-2 $\alpha$  at 3.76 ppm) and C2 $\beta$  at 75.2 ppm (H-2 $\beta$  at 3.45 ppm), 5-*O*- ester **48b** to C5 $\alpha$  at 64.8 ppm (H-5 at 3.64 ppm) and 2,5-di-*O*- ester **48c** to C2 $\alpha$  at 77.2 ppm (H-2 $\alpha$  at 3.66 ppm) and C5 $\alpha$  at 64.8 ppm (H-5 at 3.35 ppm); from D-ribose (**10**), 3-*O*- ester **49a** to C3 $\alpha$  at 76.5 ppm (H-3 $\alpha$  at 3.98 ppm) and C3 $\beta$  at 77.7 ppm (H-3 $\beta$  at 3.92 ppm), 5-*O*- ester **49b** to C5 $\alpha$  at 63.2 ppm (H-5 at 3.58 ppm) and 3,5-di-*O*- ester **49c** to C3 $\alpha$  at 75.5 ppm (H-3 $\alpha$  at 3.60 ppm) and C5 $\alpha$  at 63.3 ppm (H-5 at 3.52 ppm); from lactose (**11**), 2-*O*- ester **50a** to C2 $\alpha$  at 84.5 ppm (H-2 $\alpha$  at 3.40 ppm), C2 $\beta$  at 85.0 ppm (H-2 $\beta$  at 3.82 ppm) of glucose moiety, 6-*O*- ester **50b** to C6 at 66.5 ppm (H-6 at 3.85 ppm) of glucose moiety and 6'-*O*- ester **50c** to C-6' at 66.9 ppm (H-6' at 3.85 ppm) of galactose moiety; from maltose (**12**), 2-*O*- ester **51a** to C2 $\alpha$  at 81.2 ppm (H-2 $\alpha$  at 4.05 ppm) C2 $\beta$  at 81.4 ppm (H-2 $\beta$  at 3.96 ppm) of reducing end glucose moiety, 6-*O*- ester **51b** to C6 at 68.0 ppm (H-6 at 3.62 ppm) of reducing end glucose moiety and 6'-*O*- ester **51c** to C6' at 67.2 ppm (H-6' at 3.62 ppm) of the non reducing end glucose moiety; from sucrose (**13**), 6-*O*- ester **52** to C6 $\beta$  at 67.2 ppm (H-6 at 3.63 ppm) of the fructose moiety; and from D-mannitol (**14**), 1-*O*- ester **53a** to C1 at 60.8 ppm (H-1 at 3.51 ppm) and 1,6-

di-*O*- ester **53b** to C1 at 60.8 ppm (H-1 at 3.63 ppm) and C6 at 63.5 ppm (H-6 at 3.29 ppm). Here also, mass spectra also confirmed the formation of the above mentioned esters.

#### 4.4. Discussion

Two dimensional HSQCT NMR confirmed the formation of 1-*O*-, 2-*O*-, 3-*O*-, 4-*O*-, 5-*O*-, 6-*O*- and 6'-*O*- mono esters and 1,6-di-*O*-, 2,5-di-*O*-, 2,6-di-*O*-, 3,5-di-*O*-, 3,6-di-*O*-, 4,6-di-*O*- and 6,6'-di-*O*- diesters to varying extents depending on the carbohydrate employed (Table 4.2, 4.4, 4.6, 4.8 and 4.10). Lipases from *Candida rugosa*, *Rhizomucor miehei* and porcine pancreas showed broad substrate specificity towards amino acids as well as carbohydrates. The present work describes preparation of 99 L-amino acyl esters of carbohydrates of which 97 esters have not been reported before. So far unreported esters are L-alanyl-D-glucose **16a,d,e**, L-alanyl-D-galactose **17a-c**, L-alanyl-D-mannose **18a-e**, L-alanyl-D-fructose **19a-c**, L-alanyl-D-arabinose **20a-c**, L-alanyl-D-ribose **21a-c**, L-alanyl-lactose **22a-c**, L-alanyl-maltose **23a-c**, L-alanyl-sucrose **24**, L-valyl-D-glucose **25a-e**, L-valyl-D-galactose **26a-c**, L-valyl-D-mannose **27**, L-valyl-D-fructose **28a-c**, L-valyl-D-arabinose **29a-c**, L-valyl-D-ribose **30a-c**, L-valyl-maltose **31a,b**, L-valyl-sucrose **32**, L-valyl-D-mannitol **33**, L-leucyl-D-glucose **34a-e**, L-leucyl-D-galactose **35a,b**, L-leucyl-D-mannose **36a-c**, L-leucyl-D-fructose **37**, L-leucyl-D-arabinose **38a-c**, L-leucyl-D-ribose **39a-c**, L-leucyl-maltose **40**, L-leucyl-sucrose **41**, L-leucyl-D-mannitol **42a,b**, L-leucyl-D-sorbitol **43**, L-isoleucyl-D-glucose **44a,b**, L-isoleucyl-D-galactose **45a-c**, L-isoleucyl-D-mannose **46a-e**, L-isoleucyl-D-fructose **47a-c**, L-isoleucyl-D-arabinose **48a-c**, L-isoleucyl-D-ribose **49a-c**, L-isoleucyl-lactose **50a-c**, L-isoleucyl-maltose **51a-c**, L-isoleucyl-sucrose **52**, L-isoleucyl-D-mannitol **53a,b**.

D-Glucose **5**, D-galactose **6** and D-mannose **7**, D-fructose **8** and maltose **12** showed better conversions with all the four amino acids. Least conversions were



observed for carbohydrate alcohols and sucrose esters. Among the four amino acids investigated, L-alanine showed lesser conversion (3 – 78 %) to esters compared to the other three amino acids (9 – 78 %). L-Alanine being smaller compared to the other amino acids employed would not be binding firmly to the active site. L-Valyl esters (25 - 78 %) as well as L-leucyl esters (21 – 65 %) showed better conversion followed by L-isoleucyl esters (9 – 55 %, Tables 4.4 - 4.9). Among the lipases employed, *Candida rugosa* lipase and porcine pancreas lipase have shown better conversion than *Rhizomucor miehei* lipase

Except lactose **11** and D-sorbitol **15**, all the carbohydrates employed have reacted with all the three amino acids (**1-4**). L-Alanine **1**, L-valine **2** and L-leucine **3** with D-glucose **5** and L-alanine **1** and L-isoleucine **4** with D-mannose **7** gave five diastereomeric esters. Both D-arabinose **9** and D-ribose **10** have shown three diastereomeric esters with all the amino acids (**1-4**) employed. Lactose with L-valine and L-leucine and D-sorbitol with L-alanine and L-valine and L-isoleucine did not undergo any reaction. L-Alanyl-sucrose **24**, L-valyl-D-mannose **27**, L-valyl-sucrose **32**, L-leucyl-maltose **40**, L-leucyl-sucrose **41** and L-isoleucyl-sucrose **52** formed only 6-*O*- ester.

Nature of the products clearly indicated that primary hydroxyl groups of the carbohydrates (1-*O*-, 5-*O*-, 6-*O*- and 6'-*O*-) esterified predominantly over the secondary hydroxyl groups (2-*O*-, 3-*O*- and 4-*O*-). Among the secondary hydroxyl groups, 4-*O*- ester was formed only in case of D-mannose (**18b**, **36b** and **46b**). Carbohydrates containing axial hydroxyl groups in axial position like C2 in D-mannose and D-ribose and C4 in D-galactose, have not reacted indicating that esterification with axial secondary hydroxyl groups are difficult, especially with alkyl amino acyl donors.

The anomeric hydroxyl groups of carbohydrate molecules did not react because of rapid glycosidic ring opening and closing process. Loss of specificity could be due to

use of larger amount of enzymes (about 40% w/w carbohydrate), which gave a large number of esters.

Carbohydrates like lactose, D-mannitol and D-sorbitol reacted selectively depending on the amino acid indicated that they may not be good nucleophiles. This could be due to more hydrogen bonding propensity for D-mannitol and D-sorbitol and steric hindrance in case of lactose. In case of aldopentoses (D-arabinose and D-ribose), NMR spectrum clearly indicated degradation and/or ring opening during the reaction. In case of L-alanyl-D-ribose and L-valyl-D-ribose, opening of the five membered ring during esterification was noticed by observation of a large number of signals in the 3.0 - 5.0 ppm ( $^1\text{H}$ ) and 63 - 75 ppm ( $^{13}\text{C}$ ) region which could be due to excess strain on the ring due to introduction of bulky amino acid groups to D-ribose OH groups.

Since the reactions were carried out at a low temperature of 40-60 °C, the formation of peptide was less than 3 %, even though unprotected L-alanine was used for the reaction. NMR data clearly indicated that no Maillard reaction occurred. RML and PPL showed significant esterification (up to 68 %) when unprotected L-alanine was used. When N-protected amino acid N-acetyl-L-alanine, was used in the present work, both RML and PPL gave < 5 % yield. Our present study has shown that comparable esterification yields to others could be achieved by employing PPL, CRL and RML instead of protease.

Thus this study has shown that unprotected and unactivated amino acids containing hydrophobic alkyl side chain can serve as good acyl donors in the esterification reaction catalyzed by lipases from *Candida rugosa*, *Rhizomucor miehei* and porcine pancreas.

**Table 4.10. Percentage yields and proportions of L-alanyl esters of carbohydrates from RML and L-valyl, L-leucyl and L-isoleucyl esters of carbohydrates CRL catalyzed reactions<sup>a</sup>**

Carbohydrate	L-Alanyl		L-Valyl		L-Leucyl		L-Isoleucyl					
	Yield <sup>a</sup>	% Proportions	Yield <sup>b</sup>	% Proportions	Yield <sup>b</sup>	% Proportions	Yield <sup>b</sup>	% Proportions				
D-glucose	30	16a: 2- <i>O</i> -Ester (20) 16b: 3- <i>O</i> -Ester (12) 16c: 6- <i>O</i> -Ester (47) 16d: 2,6-di- <i>O</i> -Ester (15) 16e: 3,6-di- <i>O</i> -Ester (6)	68	25a: 2- <i>O</i> -Ester (10) 25b: 3- <i>O</i> -Ester (12) 25c: 6- <i>O</i> -Ester (31) 25d: 2,6-di- <i>O</i> -Ester (23) 25e: 3,6-di- <i>O</i> -Ester (24)	43	34a: 2- <i>O</i> -Ester (17) 34b: 3- <i>O</i> -Ester (20) 34c: 6- <i>O</i> -Ester (42) 34d: 2,6-di- <i>O</i> -Ester (10) 34e: 3,6-di- <i>O</i> -Ester (12)	47	44a: 3- <i>O</i> -Ester (42) 44b: 6- <i>O</i> -Ester (58)				
	D-galactose	21	17a: 2- <i>O</i> -Ester (33) 17b: 3- <i>O</i> -Ester (32) 17c: 6- <i>O</i> -Ester (35)	30	26a: 2- <i>O</i> -Ester (48) 26b: 3- <i>O</i> -Ester (26) 26c: 6- <i>O</i> -Ester (26) 27: 6- <i>O</i> -Ester	21	35a: 2- <i>O</i> -Ester (48) 35b: 6- <i>O</i> -Ester (52)	46	45a: 2- <i>O</i> -Ester (78) 45b: 3- <i>O</i> -Ester (10) 45c: 6- <i>O</i> -Ester (12)			
		D-mannose	49	18a: 3- <i>O</i> -Ester (25) 18b: 4- <i>O</i> -Ester (25) 18c: 6- <i>O</i> -Ester (30) 18d: 3,6-di- <i>O</i> -Ester (9) 18e: 4,6-di- <i>O</i> -Ester (11)	51	27: 6- <i>O</i> -Ester	31	36a: 3- <i>O</i> -Ester (28) 36b: 4- <i>O</i> -Ester (30) 36c: 6- <i>O</i> -Ester (42)	55	46a: 3- <i>O</i> -Ester (19) 46b: 4- <i>O</i> -Ester (13) 46c: 6- <i>O</i> -Ester (13) 46d: 3,6-di- <i>O</i> -Ester (27) 46e: 4,6-di- <i>O</i> -Ester (28)		
			D-fructose	52	19c: 1- <i>O</i> -Ester (34) 19b: 6- <i>O</i> -Ester (34) 19c: 1,6-di- <i>O</i> -Ester (32)	34	28a: 1- <i>O</i> -Ester (29) 28b: 6- <i>O</i> -Ester (34) 28c: 1,6-di- <i>O</i> -Ester (37)	48	37: 6- <i>O</i> -Ester	43	47a: 1- <i>O</i> -Ester (36) 47b: 6- <i>O</i> -Ester (30) 47c: 1,6-di- <i>O</i> -Ester (34)	
				D-arabinose	9	20a: 2- <i>O</i> -Ester (33) 20b: 5- <i>O</i> -Ester (34) 20c: 2,5-di- <i>O</i> -Ester (33)	25	29a: 2- <i>O</i> -Ester (32) 29b: 5- <i>O</i> -Ester (25) 29c: 2,5-di- <i>O</i> -Ester (43)	42	38a: 2- <i>O</i> -Ester (24) 38b: 5- <i>O</i> -Ester (33) 38c: 2,5-di- <i>O</i> -Ester (43)	55	48a: 2- <i>O</i> -Ester (24) 48b: 5- <i>O</i> -Ester (33) 48c: 2,5-di- <i>O</i> -Ester (43)
					D-ribose	48	21a: 3- <i>O</i> -Ester (16) 21b: 5- <i>O</i> -Ester (32) 21c: 3,5-di- <i>O</i> -Ester (52)	33	30a: 3- <i>O</i> -Ester (26) 30b: 5- <i>O</i> -Ester (26) 30c: 3,5-di- <i>O</i> -Ester (48)	38	39a: 3- <i>O</i> -Ester (16) 39b: 5- <i>O</i> -Ester (32) 39c: 3,5-di- <i>O</i> -Ester (52)	53
lactose	20	22a: 6- <i>O</i> -Ester (34) 22b: 6'- <i>O</i> -Ester (34) 22c: 6,6'-di- <i>O</i> -Ester (32)				--	--	--	45	50a: 2- <i>O</i> -Ester (39) 50b: 6- <i>O</i> -Ester (40) 50c: 6'- <i>O</i> -Ester (21)		
	maltose	56	23a: 6- <i>O</i> -Ester (34) 23b: 6'- <i>O</i> -Ester (34) 23c: 6,6'-di- <i>O</i> -Ester (32)			47	31a: 6- <i>O</i> -Ester (49) 31b: 6'- <i>O</i> -Ester (51)	44	40: 6- <i>O</i> -Ester	54	51a: 2- <i>O</i> -Ester (38) 51b: 6- <i>O</i> -Ester (40) 51c: 6'- <i>O</i> -Ester (22)	
		sucrose	8	24: 6- <i>O</i> -Ester		60	32: 6- <i>O</i> -Ester	38	41: 6- <i>O</i> -Ester	22	52: 6- <i>O</i> -Ester	
D-mannitol			--		52	33: 1- <i>O</i> -Ester	45	42a: 1- <i>O</i> -Ester (56) 42b: 1,6-di- <i>O</i> -Ester (44)	52	53a: 1- <i>O</i> -Ester (62) 53b: 1,6-di- <i>O</i> -Ester (38)		
	D-sorbitol	--	--	--	--	25	43: 1- <i>O</i> -Ester	--	--			

<sup>a</sup> Confirmation of esters and their percentage proportions were determined by 2D-HSQCT NMR. Conversion yields are an average from two experiments. <sup>b</sup> Yields from HPLC. Errors in yield measurements will be within  $\pm 10\%$

## 4.5. Experimental

### 4.5.1. Esterification procedure

Esterification was carried out in a flat bottom two necked flask by reacting 0.002 mol unprotected L-amino acid (L-alanine **1**, L-valine **2**, L-leucine **3** and L- isoleucine **4**) and 0.001 mol of carbohydrate (D-glucose **5**, D-galactose **6**, D-mannose **7**, D-fructose **8**, D-arabinose **9**, D-ribose **10**, lactose **11**, maltose **12**, sucrose **13**, D-sorbitol **14** and D-mannitol **15**) along with 100 ml CH<sub>2</sub>Cl<sub>2</sub>:DMF (90:10 v/v, 40 °C) in presence of 0.75 - 0.18 g (50 % w/w carbohydrate employed) of lipases under reflux for a period of three days. *Rhizomucor miehei* lipase (RML) in presence of 0.1 mM (0.1 ml of 0.1M) of acetate buffer (pH 4.0), *Candida rugosa* lipase (CRL) in presence of 0.1 mM (0.1 ml of 0.1M) of phosphate buffer (pH 7.0) and crude porcine pancreas lipase in presence of 0.2 mM (0.2 ml of 0.1 M) of acetate buffer (pH 5.0) were employed to impart 'pH memory' or 'pH tuning' to the enzyme. The condensed vapour of solvents which formed an azeotrope with water was passed through a desiccant (molecular sieves of 4Å made up of sodium aluminosilicate were used as desiccants) before being returned into the reaction mixture, thereby facilitating complete removal of water of reaction (Lohith and Divakar 2005). This set up maintained a very low water activity of  $a_w = 0.0054$  throughout the reaction period. After completion of the reaction, the solvent was distilled off and 20- 30 ml of warm water was added, stirred and filtered to remove the lipase. The filtrate was evaporated to get a mixture of the unreacted carbohydrate, unreacted L-amino acids and the product esters, which were then analyzed by HPLC. The conversion yields were determined with respect to peak areas of the L-amino acid and that of the esters. The esters formed were separated by size exclusion chromatography using Sephadex G-10 and Bio Gel P-2 as column materials and eluted with water. Although, the esters were separated from unreacted amino acids and carbohydrates by this procedure, the

individual esters in the mixture of esters formed could not be separated. This could be due to the similar polarity of the ester molecules. The product esters separated were subjected to spectral characterization by UV, IR, mass, specific rotation and 2D-NMR.

#### **4.5.2. High Performance Liquid Chromatography**

A Shimadzu LC 10AT HPLC (Kyoto, Japan) connected to LiChrosorb RP-18 column (5  $\mu\text{m}$  particle size, 4.6 x 150 mm length) with acetonitrile:water (v/v 20:80) as a mobile phase at a flow rate of 1 ml/ min was employed using an UV detector at 210 nm.

#### **4.5.3. Spectral characterization**

A Shimadzu UV – 1601 spectrophotometer (Kyoto, Japan) was used for recording UV spectra of the isolated esters in water at 0.1 - 2.0 mM concentrations. A Nicolet 5700 FTIR instrument (Madison, USA) was used for recording the IR spectra with a 1.0 - 3.0 mg of ester sample as KBr pellet. Specific rotation of the isolated esters were measured at 25 °C using Perkin-Elmer 243 polarimeter (Überlingen, Germany) with a 0.2 – 1.5 % solution of the esters in water. Mass spectra of the isolated esters were recorded using a Q-TOF Waters Ultima instrument (No.Q-Tof GAA 082, Waters corporation, Manchester, UK) fitted with an electron spray ionization (ESI) source.

#### **4.5.4. Nuclear Magnetic Resonance Spectroscopy**

##### **4.5.4.1. $^1\text{H}$ NMR**

A Brüker DRX-500 MHz spectrometer (Fallanden, Switzerland) operating at 500.13 MHz was used for recording  $^1\text{H}$  NMR. A 40 mg of sample dissolved in 0.5 ml of DMSO- $d_6$  solvent was employed. About 50-200 scans were accumulated with a recycle period of 2-3 seconds to obtain good spectra. The spectra were recorded at 35 °C with TMS as internal standard for measuring the chemical shift values to within  $\pm 0.001$  ppm. A region from 0 – 10 ppm was scanned for all the samples.

#### **4.5.4.2. $^{13}\text{C}$ NMR**

A Brüker DRX-500 MHz spectrometer (Fallanden, Switzerland) operating at 125 MHz was used to record the  $^{13}\text{C}$  NMR. Samples were dissolved in 0.5 ml of  $\text{DMSO-}d_6$  and recorded at 35 °C. A region from 0-200 ppm region was scanned and about 500 – 6000 scans were accumulated for each spectrum to get a good spectrum. TMS was taken as an internal standard.

#### **4.5.4.3. Two-dimensional HSQCT**

Two dimensional Heteronuclear Multiple Quantum Coherence Transfer spectra (2-D HMQCT) and Heteronuclear Single Quantum Coherence Transfer spectra (2-D HSQCT) (Fallanden, Switzerland) were recorded at 500 MHz on a Brüker DRX-500 MHz spectrometer (500.13 MHz for  $^1\text{H}$  and 125 for MHz  $^{13}\text{C}$ ). Chemical shift values were expressed in ppm relative to internal tetramethylsilane standard. About 40mg of the sample dissolved in  $\text{DMSO-}d_6$  was used for recording the spectra.

## *Chapter 5*

*Competitive inhibition by D-glucose in Rhizomucor miehei and Candida rugosa lipases in the esterification reaction between L-alanine and D-glucose*

## 5.1. Introduction

Lipase is a single-domain molecule that belongs to the family of  $\alpha/\beta$ -hydrolase proteins (Derewenda *et al.*, 1992; Grochulski *et al.*, 1993). Most of the lipases reported contain Ser-His-Asp/Glu catalytic triads in their active site (Grochulski *et al.*, 1993) with the exception of esterases from *Streptomyces scabies*, which contain only Ser-144 and His-283 (Wei *et al.*, 1995).

Kinetic studies of esterification (Yadav and Trivedi, 2003; Kiran and Divakar, 2002; Janssen *et al.*, 1999; Lortie *et al.*, 1993; Rizzi *et al.*, 1992), racemization (Duan *et al.*, 1997) and hydrolysis (Van-Tol *et al.*, 1992) using lipases have been performed. In some esterifications, lipases follow the Ping-Pong Bi-Bi mechanism (Kiran and Divakar, 2002; Zhang *et al.*, 2005; Zaidi *et al.*, 2002; Yadav and Lathi, 2004). This mechanism involves binding acid with alcohol in successive steps, which is followed by the release of water and the ester products in succession. The kinetic behavior of CRL in the esterification of long-chain fatty acids with alcohols (Zaidi *et al.*, 2002) and tetrahydrofurfuryl alcohol with butyric acid (Yadav and Devi, 2004) follows the Ping-Pong Bi-Bi mechanism, in which the binding of an acid leads to an acyl enzyme complex followed by the release of water molecules. The subsequent binding of an alcohol leads to the transfer of the acyl group to the alcohol, which results in ester formation. Thereafter, an ester product is released. *n*-Octanol is inhibitory to RML and CRL in the transesterification between vinyl acetate and *n*-octanol (Yadav and Trivedi, 2003) following the Ternary Complex Bi-Bi mechanism, in which *n*-octanol binds twice or once to lipase yield a dead-end lipase-*n*-octanol complex and a second molecule of *n*-octanol that binds to this dead-end lipase-*n*-octanol complex to give another dead-end lipase-*n*-octanol complex.



In citronellyl laurate synthesis, RML follows the Ordered Bi-Bi mechanism wherein  $\beta$ -citronellol binds to the enzyme to yield the  $\beta$ -citronellol-enzyme complex, which again binds to lauric acid to form the ternary enzyme- $\beta$ -citronellol-lauric acid complex. Finally, it decomposes to give  $\beta$ -citronellyl laurate and water as products in this process (Yadav and Lathi, 2004). A series of dead-end RML-lauric acid complexes were also reported in this process.

In this chapter, kinetics of esterification between L-alanine and D-glucose to form L-alanyl-D-glucose with RML and CRL is carried out and the results from these investigations are described below.

## 5.2. Present investigation

To graphically evaluate the apparent values of the kinetic parameters, initial rate (specific reaction rate) was determined from the concentration of L-alanyl-D-glucose at different incubation periods, and typical time courses of RML and CRL- catalyzed reactions are shown in Fig. 5.1.

For the concentrations of D-glucose and L-alanine, individual experiments in duplicate (30 x 2 lipases) were performed for incubation periods of 3 h, 6 h, 12 h, 24 h and 36 h. Initial rate (specific reaction rate,  $v$ ) was determined from the initial slope of the plot of the amount of esters formed (M) versus incubation period (h) and expressed as  $M h^{-1} (mg \text{ protein})^{-1}$ .  $R^2$  obtained from least-squares analysis for the initial rate in each cases was found to be within 0.88 - 0.95. Each plot shown in this work was constructed from all experimentally determined values; a few initial rates were obtained by curve-fitting.

The initial rates ( $v$ ) for RML were found to be in the range of  $15\text{-}176 \times 10^{-6} M h^{-1} (mg \text{ protein})^{-1}$ . CRL experiments showed the initial rates to be in the range of  $20\text{-}460 \times$

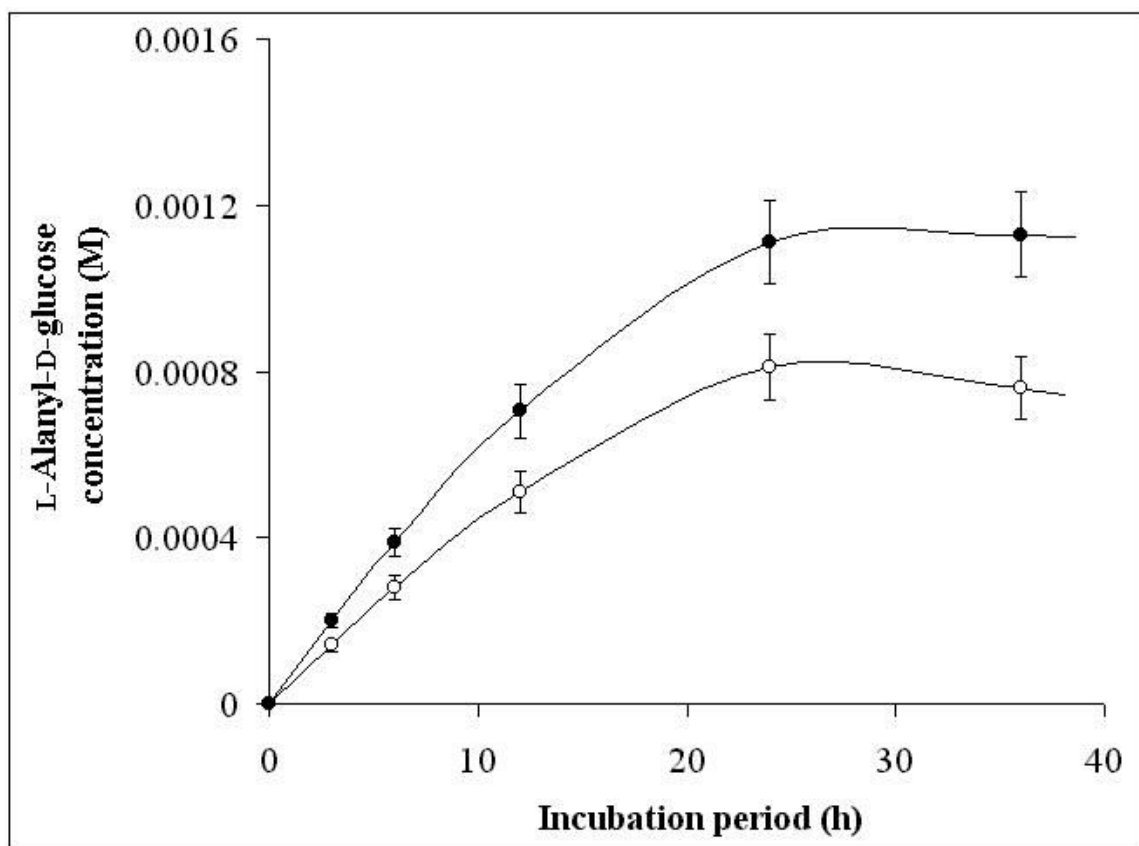


**Fig.5.1.** Time courses of esterification reactions – concentrations of L-alanyl-D-glucose versus incubation periods; RML (90 mg) or CRL (90 mg) was allowed to react with 0.005 M L-alanine and 0.020 M D-glucose in 100 ml of mixture of dichloromethane /dimethylformamide (v/v 90:10) mixed with 0.1 mM (0.1 ml of 0.1 M) sodium acetate buffer (pH 4.0) for RML or 0.1 mM (0.1 ml of 0.1 M) sodium phosphate buffer (pH 7.0) for CRL.

$10^{-6} \text{ M h}^{-1}(\text{mg protein})^{-1}$ . At the initial periods of incubation, the reaction is relatively fast owing to the shift in equilibrium towards esterification. The process slows down at incubation periods longer than 24 h, resulting in a stable steady-state equilibrium. The effects of external mass transfer phenomena - internal and external diffusions (Yadav and Devi, 2004; Marty *et al.*, 1992), if any, on the RML and CRL enzymes employed were not tested in this work.

### 5.2.1. *Rhizomucor miehei* and *Candida rugosa* lipase catalysis

Using initial rates, double reciprocal plots were constructed to graphically evaluate the apparent values of  $k_{cat}$ ,  $K_m$  *L-alanine*,  $K_m$  *D-glucose* and  $K_i$ : RML – Fig. 5.2 ( $1/v$  versus  $1/[\text{D-glucose}]$ ) and Fig. 5.3 ( $1/v$  versus  $1/[\text{L-alanine}]$ ); CRL – Fig. 5.4 ( $1/v$  versus  $1/[\text{D-glucose}]$ ) and Fig. 5.5 ( $1/v$  versus  $1/[\text{L-alanine}]$ ). Figure 5.6 shows a replot of the slopes from Fig. 5.3 (RML), and Fig. 5.7 shows the replot of the slopes from Fig. 5.5 (CRL). Figure 5.2 from RML reactions and Fig. 5.4 from CRL reactions show a series of curves obtained for different fixed concentrations of L-alanine for varying D-glucose concentration, in which slight increases in initial rate are observed at lower D-glucose concentrations. At higher D-glucose concentrations, the rates markedly decrease. Also, increasing L-alanine concentration increases the initial rates at all D-glucose concentrations. Figure 5.3 from RML reactions and Fig. 5.5 from CRL reactions show a series of parallel lines for different fixed low D-glucose concentrations at varying L-alanine concentration. These change to lines with different slopes at higher D-glucose concentrations.

The plots in Figs. 5.2, 5.3, 5.4 and 5.5 show that the kinetics could be best described by Ping-Pong Bi-Bi model in which L-alanine and D-glucose bind in

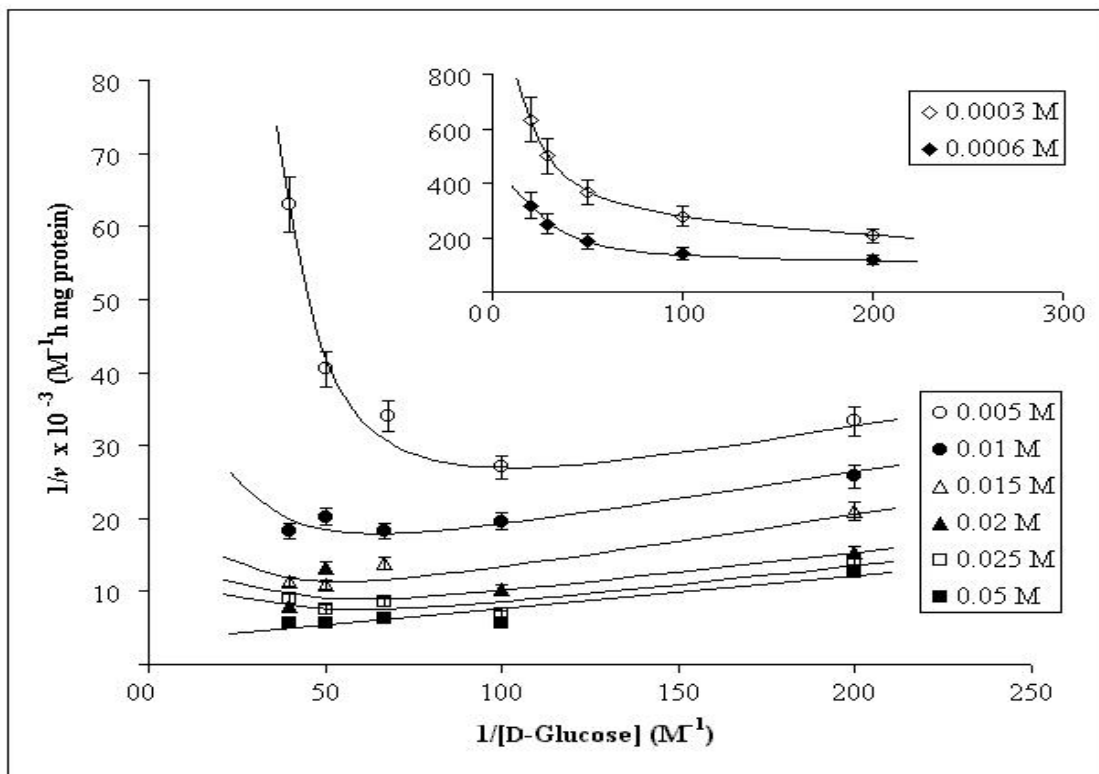
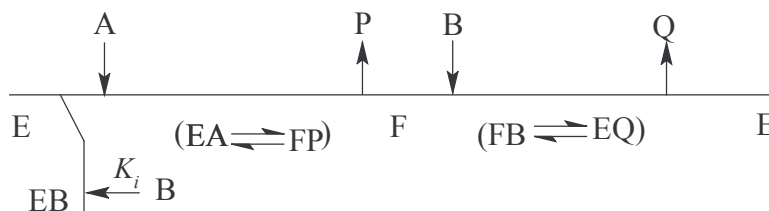


**Fig. 5.2.** Double reciprocal plots for RML-catalyzed L-alanyl-D-glucose reaction:  $1/v$  versus  $1/[D\text{-glucose}]$  plots; a series of curves show the effect of varying D-glucose concentration at different fixed L-alanine concentrations in the range of 0.005 - 0.05 M. The inset shows plots obtained by the computer simulation for 0.0003 M and 0.0006 M L-alanine concentrations

subsequent steps releasing water and L-alanyl-D-glucose. This also happens in subsequent steps, (Scheme 5.1) with competitive substrate inhibition that lead to dead-end inhibition (Segel, 1993). Both RML and CRL were found to be inhibited by D-glucose.



A = L-alanine, P = H<sub>2</sub>O, B = D-glucose, E = Lipase -*Rhizomucor miehei* lipase/ *Candida rugosa* lipase, F = lipase-L-alanyl complex, EA = lipase-L-alanine complex, FP = lipase-L-alanyl-water complex, EB = lipase-D-glucose complex,  $K_i$  = dissociation constant of lipase-D-glucose complex, FB = L-alanyl-lipase-D-glucose complex, EQ = lipase-L-alanyl-D-glucose complex, Q = L-alanyl-D-glucose.

**Scheme 5.1. Ping-Pong Bi-Bi mechanism of RML and CRL-catalysed synthesis of L-alanyl-D-glucose showing inhibition by D-glucose.**

This model could be described by the following rate equation,

$$\frac{v}{V_{max}} = \frac{[A][B]}{K_{mA}[B](1+[B]/K_i) + K_{mB}[A] + [A][B]} \quad \dots\dots\dots (5.1)$$

where  $v$  is initial rate,  $V_{max}$  is maximum velocity,  $[A]$  is L-alanine concentration,  $[B]$  is D-glucose concentration,  $K_{mA}$  is Michaelis-Menten constant for the lipase-L-alanine complex,  $K_i$  is dissociation constant for the lipase-inhibitor (D-glucose) complex and  $K_{mB}$  is Michaelis-Menten constant for the lipase-D-glucose complex. Because the initial rates are in  $M h^{-1} (mg \text{ protein})^{-1}$ ,  $V_{max}$  is expressed as  $k_{cat} = V_{max}/\text{enzyme concentration}$ .

The apparent values of the four important kinetic parameters  $K_{i \text{ D-glucose}}$ ,  $K_{m \text{ L-alanine}}$ ,  $K_{m \text{ D-glucose}}$  and  $k_{cat}$  were graphically evaluated. The intercepts of the positive slopes of the curves in Fig. 5.2 and Fig. 5.4 on the Y-axis, particularly, at the highest L-alanine

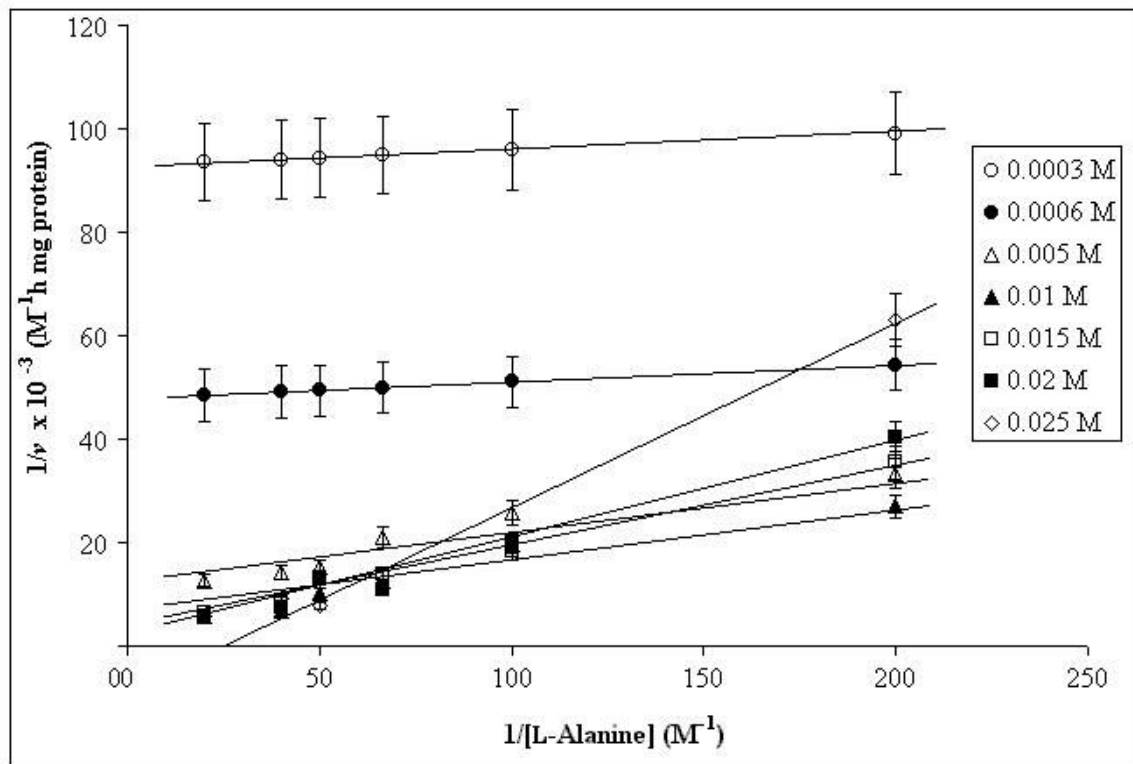


**Fig. 5.3.** Double reciprocal plots for RML-catalyzed L-alanyl-D-glucose reaction:  $1/v$  versus  $1/[L\text{-alanine}]$  plots; a series of plots shows the effects of varying L-alanine concentration at different fixed D-glucose concentrations in the range of 0.005 - 0.025 M, plots shown for 0.0003 and 0.0006 M D-glucose concentrations are from computer simulation.

concentration (0.05 M / 0.1 M) employed, gave  $1/k_{cat}$  for RML and CRL (Table 5.1). Figure 5.6 (RML) and Fig. 5.7 (CRL) shows a replot of the slopes from Fig. 5.3 and Fig. 5.5 versus [D-glucose], respectively, for which slope =  $K_{m\text{-}L\text{-}alanine}/(k_{cat} K_i)$ , Y intercept =  $K_{m\text{-}L\text{-}alanine}/k_{cat}$  and X intercept =  $-K_i$ , where  $K_i$  represents the dissociation constant for the lipase-D-glucose complex.  $K_{m\text{-}D\text{-}glucose}$  was obtained using equation 5.2 derived by rearranging equation 5.1,

$$K_{mB} = \frac{k_{cat} [B]}{v} - \frac{K_{mA} [B]}{[A]} - \frac{K_{mA} [B]^2}{[A] K_i} \dots\dots\dots (5.2)$$

where,  $K_{mB}$  = Michelis-Menten constant for the lipase-D-glucose complex.

**Table 5.1. Apparent values of kinetic parameters for RML and CRL-catalysed synthesis of L-alanyl-D-glucose.**

Name of the lipase		$k_{cat} \times 10^3$ (M h <sup>-1</sup> mg <sup>-1</sup> )	$K_{mA} \times 10^3$ (M)	$K_{mB} \times 10^3$ (M)	$K_i \times 10^3$ (M)
RML	a	0.29 ± 0.028	4.9 ± 0.51	0.21 ± 0.018	1.76 ± 0.19
	b	0.4 ± 0.038	11.2 ± 1.23	10.0 ± 0.96	5.5 ± 0.59
CRL	a	0.75 ± 0.08	56.2 ± 5.7	16.2 ± 1.8	21.0 ± 1.9
	b	1.0 ± 0.11	56.2 ± 5.4	16.1 ± 1.5	21.0 ± 2.3

A = L-alanine, B = D-glucose, a=graphical method, b=curve-fitted values.

To confirm that the kinetics of the RML- and CRL- catalyzed syntheses of L-alanyl-D-glucose follow the above-mentioned model, the apparent values of the four important kinetic parameters  $k_{cat}$ ,  $K_i$ ,  $K_{mA}$  and  $K_{mB}$  were also estimated through curve fitting using equation 5.1.

The range of values tested for these parameters and the constraints employed for the iteration procedure are as follows:  $k_{cat} < 1 \text{ M h}^{-1} \text{ mg}^{-1}$ ,  $K_{i\text{-}D\text{-}glucose} > K_{m\text{-}D\text{-}glucose}$ ,  $K_{m\text{-}D\text{-}glucose} < K_{m\text{-}L\text{-}alanine}$ , and  $K_{m\text{-}L\text{-}alanine} < 10 \text{ M}$ .

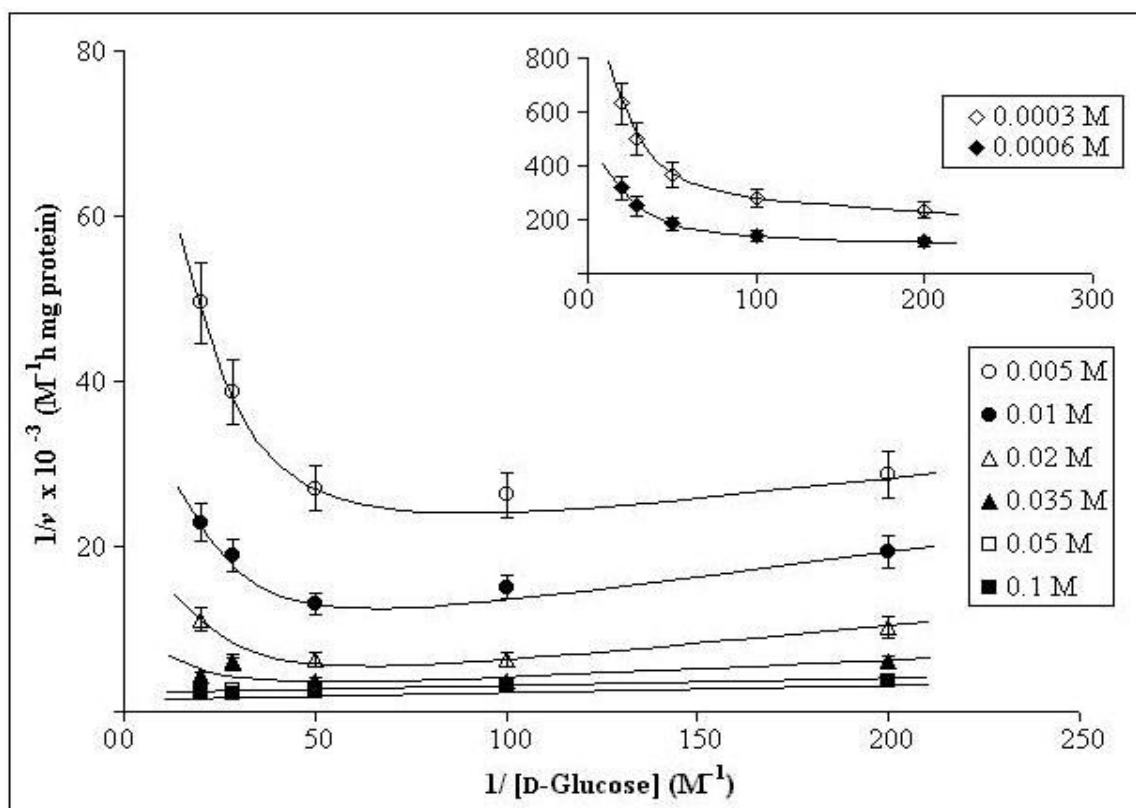


**Fig. 5.4.** Double reciprocal plots for CRL-catalyzed L-alanyl-D-glucose reaction:  $1/v$  versus  $1/[L\text{-alanine}]$  plots  $1/v$  versus  $1/[D\text{-glucose}]$  plots; a series of plots show the effect of varying D-glucose concentration at different fixed L-alanine concentrations in the range of 0.005 - 0.1 M, the plots shown for 0.0003 M and 0.0006 M L-alanine concentrations are from computer simulation.



The iteration procedure for the curve-fitting method involved non-linear optimization through minimizing the sum of squares of deviations between  $v_{exptl}$  and  $v_{pred}$ , such that values for the four kinetic parameters mentioned above correspond to the best fit achieved.

Table 5.1 lists graphical as well as the curve-fitted values for comparison. Table 5.2 and Table 5.3 show the comparison between experimental and predictive initial rate obtained under different reaction conditions. Although computer simulated  $v_{pred}$  values showed  $R^2$  values of 0.84 for RML and 0.86 for CRL, the discrepancy between  $v_{exptl}$  and  $v_{pred}$  appeared to be significant at several substrate concentrations. This could be due to (i) the constraints employed in the iteration procedure (curve fitting method), which limits the flexibility required to examine the real system in solution (ii) the error in the experimental graphical methods based on HPLC measurements, which itself could involve errors of the order of  $\pm 10\%$  and (iii) the heterogeneous experimental conditions employed involving undissolved carbohydrate and enzyme, on one hand, and, partly due to dissolved amino acid, on the other, in the mixture of dichloromethane and dimethylformamide.

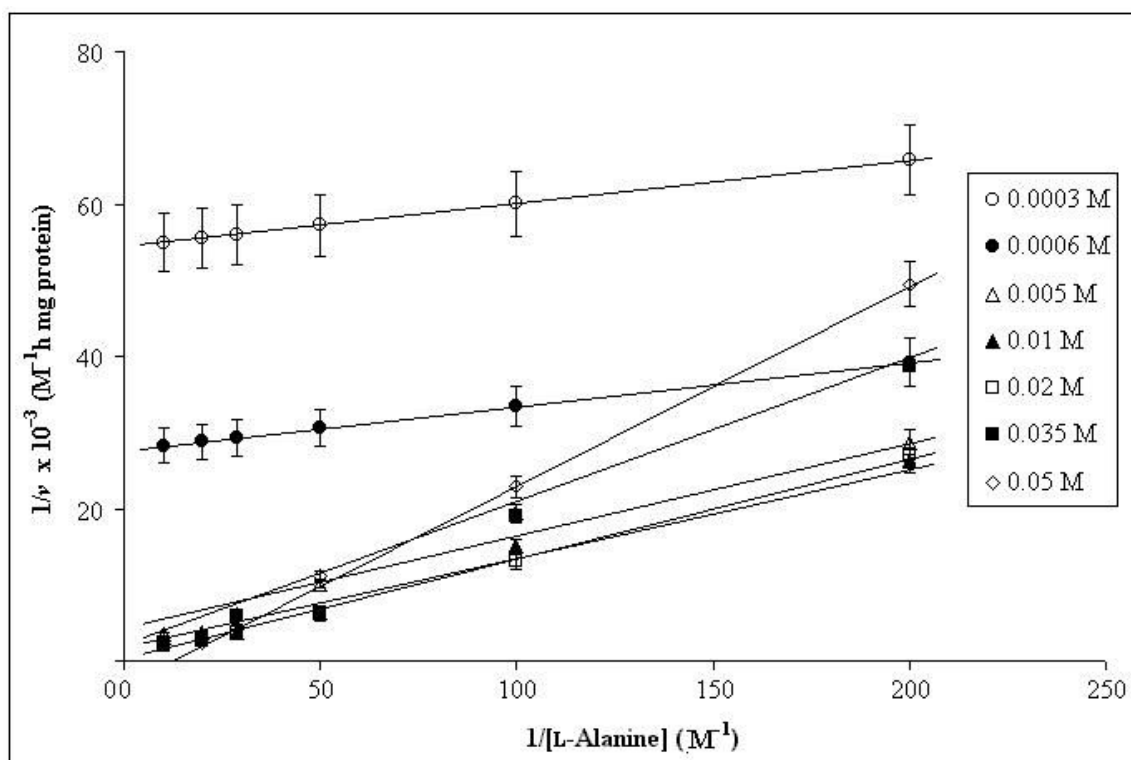


**Fig. 5.5.** Double reciprocal plots for CRL-catalyzed L-alanyl-D-glucose reaction:  $1/v$  versus  $1/[L-alanine]$ ; a series of plots show the effect of varying L-alanine concentrations at different fixed D-glucose concentrations in the range of 0.005-0.05 M. The plots shown for 0.0003 and 0.0006 M D-glucose concentrations are from the computer simulation.

**Table 5.2. Experimental and predicted initial rate values for the synthesis of L-alanyl-D-glucose by RML**

L-Alanine (M)	D-Glucose (M)	$v_{\text{experimental}} \times 10^6$ (M h <sup>-1</sup> mg <sup>-1</sup> ) <sup>a</sup>	$v_{\text{predictive}} \times 10^6$ (M h <sup>-1</sup> mg <sup>-1</sup> ) <sup>b</sup>
0.005	0.005	30	51
0.005	0.01	37	45
0.005	0.015	28	37
0.005	0.02	25	31
0.005	0.025	15	27
0.01	0.005	38	73
0.01	0.01	51	72
0.01	0.015	55	64
0.01	0.02	49	56
0.01	0.025	55	49
0.015	0.005	48	84
0.015	0.01	46	91
0.015	0.015	72	84
0.015	0.02	91	75
0.015	0.025	88	67
0.02	0.005	65	92
0.02	0.01	97	104
0.02	0.015	41	99
0.02	0.02	76	91
0.02	0.025	127	83
0.025	0.005	71	97
0.025	0.01	146	114
0.025	0.015	116	112
0.025	0.02	132	104
0.025	0.025	111	96
0.05	0.005	79	109
0.05	0.01	176	142
0.05	0.015	158	149
0.05	0.02	176	147
0.05	0.025	176	141

<sup>a</sup> Graphical method.<sup>b</sup> Curve-fitted values.

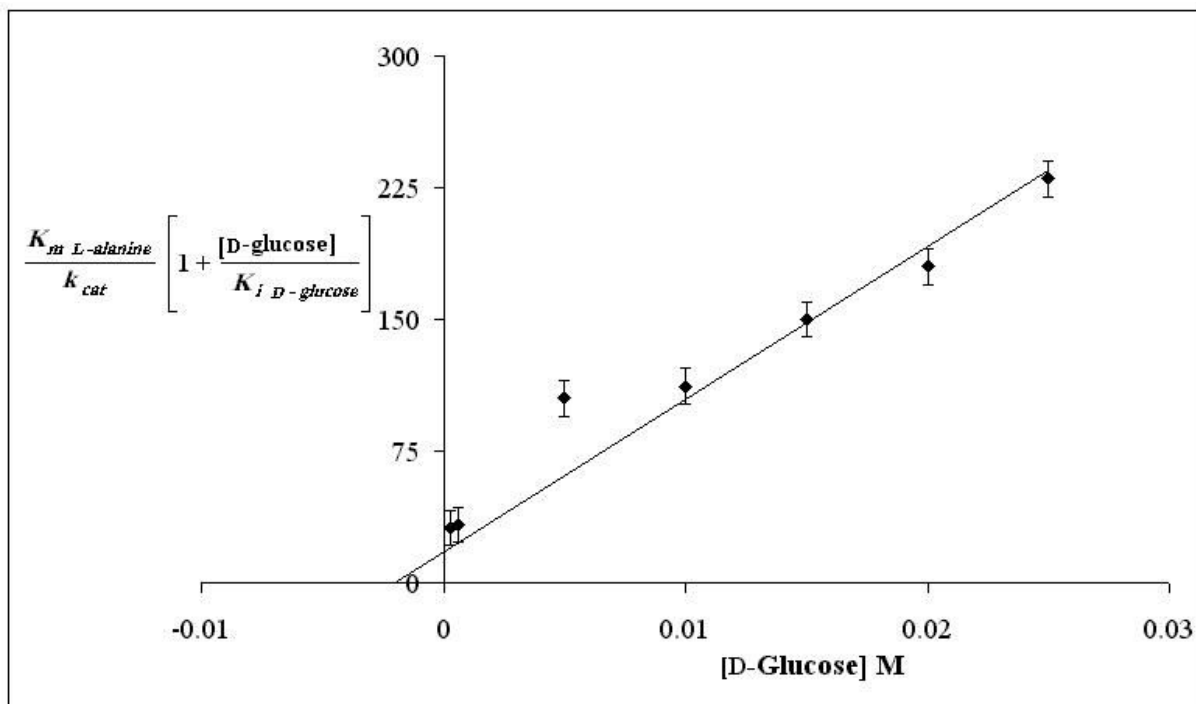


Fig. 5.6. Replot of slopes obtained from Fig. 5.3 versus [D -glucose] (RML).

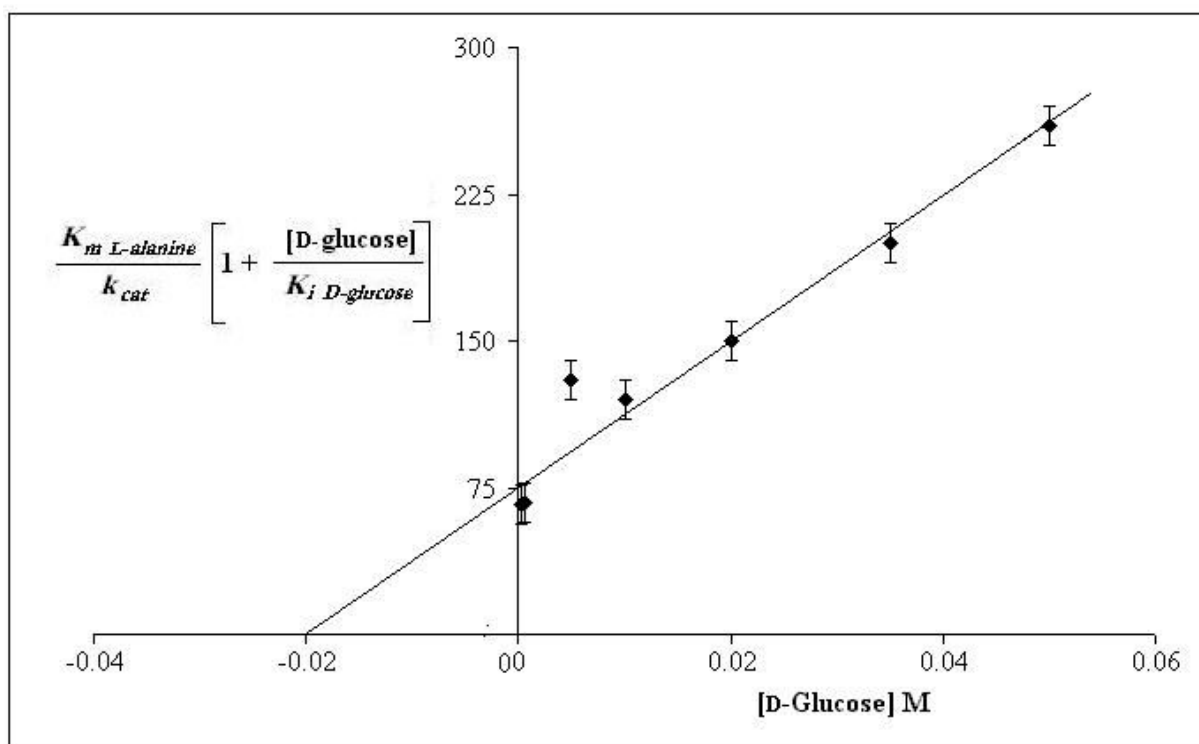


Fig. 5.7. Replot of slopes obtained from Fig. 5.5 versus [D-glucose] (CRL).

**Table 5.3. Experimental and predicted initial rate values for the synthesis of L-alanyl-D-glucose by CRL**

L-Alanine (M)	D-Glucose (M)	$v_{\text{experimental}}^{\text{a}} \times 10^6$ (M h <sup>-1</sup> mg <sup>-1</sup> )	$v_{\text{predictive}}^{\text{b}} \times 10^6$ (M h <sup>-1</sup> mg <sup>-1</sup> )
0.005	0.005	35	55
0.005	0.01	38	52
0.005	0.02	37	42
0.005	0.035	26	32
0.005	0.05	20	25
0.01	0.005	52	89
0.01	0.01	66	92
0.01	0.02	76	78
0.01	0.035	53	61
0.01	0.05	44	49
0.02	0.005	99	130
0.02	0.01	157	148
0.02	0.02	158	137
0.02	0.035	162	112
0.02	0.05	90	92
0.035	0.005	164	161
0.035	0.01	275	201
0.035	0.02	267	202
0.035	0.035	168	174
0.035	0.05	228	148
0.05	0.005	269	178
0.05	0.01	314	234
0.05	0.02	347	250
0.05	0.035	370	224
0.05	0.05	404	195
0.1	0.005	269	203
0.1	0.01	320	291
0.1	0.02	362	345
0.1	0.035	449	338
0.1	0.05	460	310

<sup>a</sup> Graphical method.<sup>b</sup> Curve-fitted values.

### 5.3. Discussion

This kinetic data clearly shows the inhibitory nature of D-glucose towards both RML and CRL. With increasing L-alanine concentration (Fig. 5.2 for RML and Fig. 5.4 for CRL), the initial rate increases with decreasing D-glucose concentration. With increasing D-glucose concentration up to the minimum  $1/v$ , the initial rate decreases, and the plots tend to become closer to the  $1/v$  axis (Y-axis).

Figure 5.3 (RML) and Fig. 5.5 (CRL) also show the same behavior, in which at low D-glucose concentrations, the plots appear parallel probably as long as  $K_i > K_{mB}$  concerned. However, at high fixed D-glucose concentrations, the slopes of the plots drastically vary. Thus, in these reactions, the kinetic data clearly shows the inhibitory nature of D-glucose. The competition between L-alanine and D-glucose for the active site (binding site) of lipases (RML/CRL) could result in a predominant binding of D-glucose at high concentrations, displacing L-alanine, and thus leading to the formation of the dead-end lipase-D-glucose complex.

For the RML reaction,  $K_{mA}$  ( $4.9 \pm 0.51 \times 10^{-3}$  M) is always higher than  $K_{mB}$  ( $0.21 \pm 0.018 \times 10^{-3}$  M, Table 5.1), which shows that L-alanine is bound to RML less firmly than D-glucose ( $K_{mA}/K_{mB} = 23.3$ ). A similar behavior is also observed with CRL (Table 1)  $K_{mA}$  ( $56.2 \pm 5.7 \times 10^{-3}$  M),  $K_{mB}$  ( $16.2 \pm 1.8 \times 10^{-3}$  M),  $K_{mA}/K_{mB} = 3.5$ . However, the respective values are very much higher for CRL than for RML, indicating that CRL can yield better conversions than RML. Between RML and CRL, the  $K_i$  for D-glucose is lower for RML ( $5.5 \pm 0.59 \times 10^{-3}$  M) than for CRL ( $21.0 \pm 2.3 \times 10^{-3}$  M), indicating that the RML is inhibited by D-glucose far more efficiently than CRL. This could also explain the better conversion observed with CRL than with RML.

Both RML and CRL contain amino acids in their active sites capable of forming hydrogen bonds with suitable donor molecules. The catalytic triad in RML consists of

Ser-144, His-257 and Asp-203 (Brady *et al.*, 1990). CRL contains Ser-209, Glu-341 and His-449 (Grochulski *et al.*, 1993, 1994). Brzozwski *et al.* (1991) showed in an atomic model of the inhibitor *n*-hexylchlorophosphonate ethyl ester–RML complex that in the oxyanion hole, which is directly responsible for the substrate binding, a direct covalent bond formation between the nucleophilic O<sub>γ</sub> of Ser-144 and the phosphorous atom of *n*-hexylchlorophosphonate ethyl ester is possible. In CRL, the oxyanion hole O<sub>γ</sub> (Ser-209) is formed by the amide backbones of Gly-123, Gly-124 and Ala-210 through the hydrogen bonding between the amide -CO-NH- and the hydroxyl of Ser-209, which is stabilized by the helix dipole (Grochulski *et al.*, 1994). D-Glucose possesses five hydroxyl groups and L-alanine possesses carboxyl and amino groups capable of forming hydrogen bonds with polar side chains of amino acids. Ser-144 hydroxyl and Asp-203 carboxyl groups of RML and Ser-209 and Glu-341 of CRL (Grochulski *et al.*, 1993) residues are very good candidate molecules for exhibiting hydrogen-bonding interactions.

Between D-glucose and L-alanine, the former possesses more hydrogen-bonding functional groups than the amino or carboxyl groups of L-alanine. Ser-144 in RML and Ser-209 in CRL can form hydrogen bonds with the amino N atom of L-alanine as well as the O atom of D-glucose. Because the  $K_m$  *L-alanine* values are higher than the of  $K_m$  *D-glucose* values for both enzymes, D-glucose could strongly binding to these enzymes than L-alanine.

Zaidi *et al.*, (2002) reported that the interaction between nylon-immobilized CRL and alcohol through hydrogen-bonding could block the nucleophilic site of the enzyme engaged in acylation, leading to inhibition. A similar behavior can also be envisaged between D-glucose hydroxyl groups and the above-mentioned oxygen of serine and the carboxylate groups of glutamic acids. Hence, this kinetic study could clearly explain the

inhibition of both RML and CRL by D-glucose. Also, for the first time, it has been found that D-glucose could be inhibitor to both the lipases at higher concentrations.

## 5.4. Experimental section

### 5.4.1. Kinetic experiments

Kinetic experiments were conducted by refluxing L-alanine and D-glucose along with 90 mg of RML or CRL in 100 ml of dichloromethane and dimethylformamide (v/v 90:10) solvent mixture (Somashekar and Divakar, 2007; Somashekar *et al.*, 2007) containing 0.1 mM (0.1 ml of 0.1 M) sodium acetate buffer (pH 4.0) for RML or 0.1 mM (0.1 ml of 0.1 M) sodium phosphate buffer (pH 7.0) for CRL. Unprotected and unactivated molecules of L-alanine and D-glucose were employed as substrates. The temperature of the reaction mixture was maintained at the reflux temperature of dichloromethane (40 °C). Experiments with RML were conducted by maintaining the concentration of one of the substrates constant in the range of 0.005 - 0.05 M and varying the concentration of the other in the same concentration range and *vice versa*. With CRL, the concentration range employed was 0.005 - 0.1 M. Product workout involved distilling off the solvent, heating to denature the enzyme, stirring and filtering to remove the lipase. The filtrate was then evaporated to obtain a residue containing L-alanine, D-glucose and the ester. The residue was subjected to high performance liquid chromatography. The retention times of L-alanine and L-alanyl-D-glucose were found to be 2.6 min and 3.4 min, respectively. No D-glucose was detected at 210 nm. The molar concentrations of the ester products formed were determined from the L-alanyl-D-glucose peak area with reference to that of free unreacted L-alanine in the reaction mixture. The error in yield measurement was within  $\pm 10\%$ .



**5.4.2. High Performance Liquid Chromatography (HPLC)**

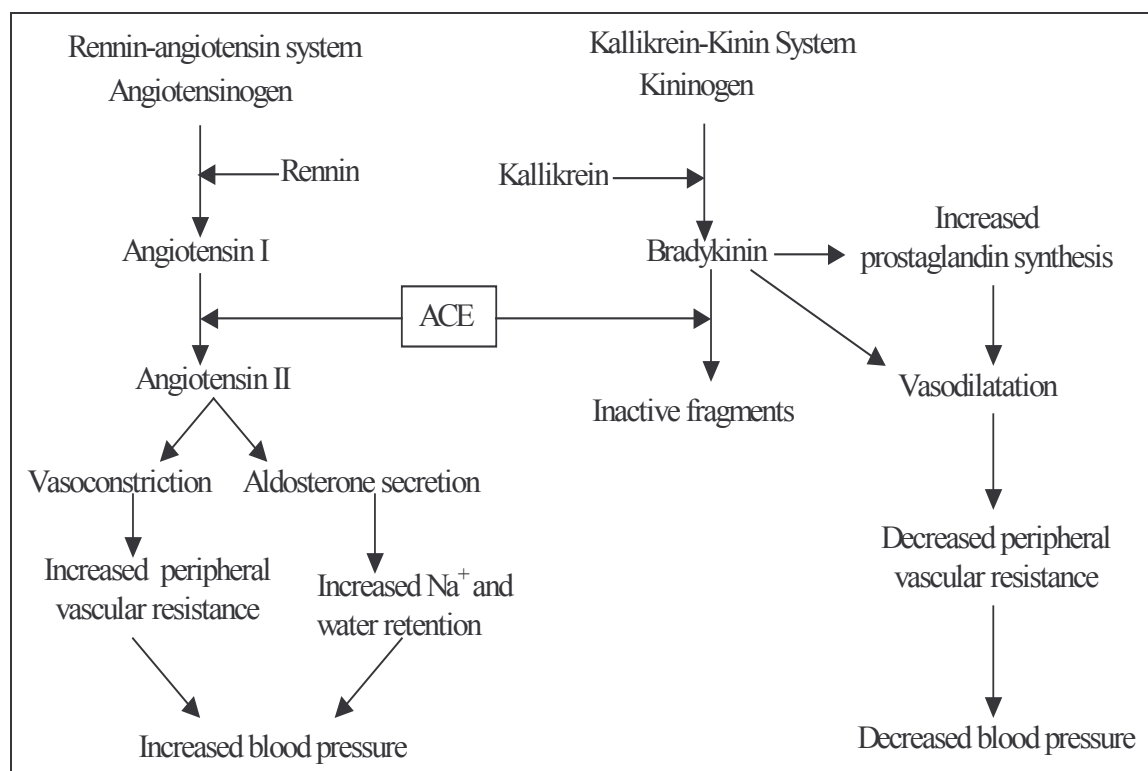
A Shimadzu LC 10AT HPLC instrument connected to a LiChrosorb RP-18 column (5  $\mu\text{m}$  particle size, 4.6 x 150 mm length) was employed for analyzing the reaction mixture. Acetonitrile: water (v/v 20:80) as a mobile phase at a flow rate of 1ml/min was used with an UV detector at 210 nm. The retention times of L-alanine and L-alanyl-D-glucose were found to be 2.6 min and 3.4 min, respectively. No D-glucose was detected at 210 nm.

## *Chapter 6*

*Angiotensin Converting Enzyme inhibition activity  
of L-alanyl, L-valyl, L-leucyl and L-isoleucyl esters of  
carbohydrates*

## 6.1. Introduction

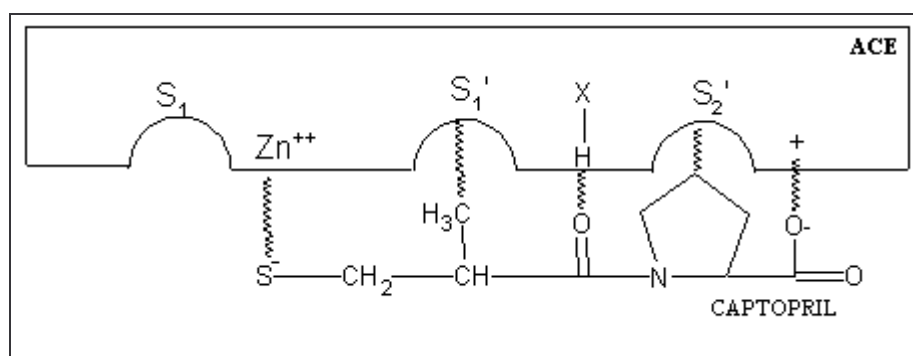
Angiotensin Converting Enzyme (dipeptidyl carboxypeptidase, EC 3.4.15.1) is a zinc containing nonspecific dipeptidyl carboxypeptidase widely distributed in mammalian tissues (Li *et al.*, 2004). Angiotensin-converting enzyme (ACE) regulates the blood pressure by modulating renin-angiotensin system as shown in **Scheme 6.1** (Vermeirssen *et al.*, 2002). This enzyme increases the blood pressure by converting the decapeptide angiotensin I into the potent vaso-constricting octapeptide, angiotensin II. Angiotensin II brings about several central effects, all leading to a further increase in blood pressure. ACE is a multifunctional enzyme that also catalyses the degradation of bradykinin (blood pressure-lowering napeptide) and therefore inhibition of ACE results in an overall antihypertensive effect (Li *et al.*, 2004; Johnston, 1992).



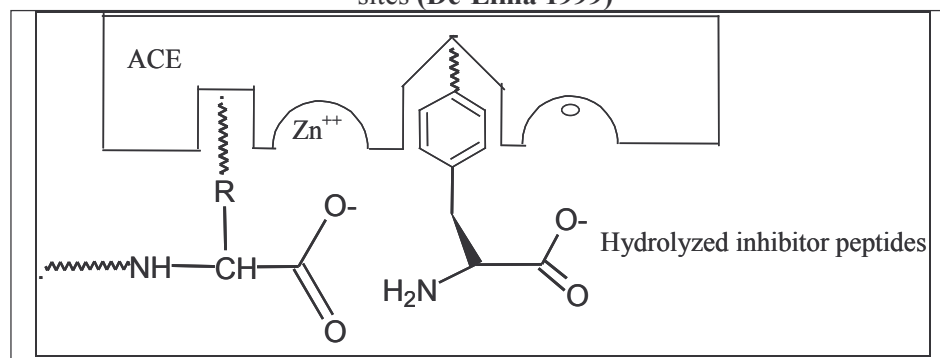
**Scheme 6.1** Role of angiotensin converting enzyme (ACE) in regulating blood pressure (Li *et al.*, 2004)

Several synthetic drugs and bio-molecules are available for ACE inhibition. Captopril is a successful synthetic anti-hypertensive drug and similar such molecules like

enalapril, perindopril, ceranopril, ramipril, quinapril and fosinopril also show ACE inhibitory activities (Hyuncheol *et al.*, 2003; Dae-Gill *et al.*, 2003; Chong-Qian *et al.*, 2004). The mechanism of ACE inhibition by captopril is shown in **Scheme 6.2** (De-Lima, 1999). The hypothetical representation of inhibitors (hydrolyzed products of peptides) binding to the ACE is shown in **Scheme 6.3** and also reported that glycine, valine and leucine at the carboxyl terminus of the peptide inhibitor are the potent inhibitors (De-Lima, 1999; Wu *et al.*, 2002; Kim *et al.*, 2001).



Scheme 6.2. Hypothetical representation of ACE inhibition by captopril binding to the active sites (De-Lima 1999)



**Scheme 6.3. Hypothetical representation of ACE active sites and binding of inhibitors** (De-Lima 1999)

Some naturally occurring 'biologically active peptides' also act as ACE inhibitors. Deloffre *et al.*, (2004) reported that a neuro-peptide from leach brain showed ACE inhibition with an  $IC_{50}$  value of 19.8  $\mu$ M. The N-terminal dipeptide (Tyr-Leu) of  $\beta$ -lactorphin was found to be the most potent inhibitor (Mullally *et al.*, 1996). Many peptide inhibitors are derived from different food proteins like Asp-Leu-Pro and Asp-Gly

from soy protein hydrolysis (Wu *et al.*, 2002) and Gly-Pro-Leu and Gly-Pro-Val from bovine skin gelatin hydrolysis (Kim *et al.*, 2001). Cooke *et al.*, (2003) prepared 4-substituted phenylalanyl esters of alkyl or benzyl derivatives, which exhibited ACE inhibitory activity.

Amino acyl esters of carbohydrates find wide variety of applications in food and pharmaceutical industries. Amino acyl esters have not been shown so far to exhibit ACE inhibition activity. Since most of the ACE inhibitory drugs are peptides, it was envisaged that the amino acyl esters of carbohydrates also could possess ACE inhibition activities as they contain amino acyl groups as part of their structure. Hence, this chapter deals with exploration of ACE inhibition activities for some enzymatically synthesized L-alanyl **1**, L-valyl **2**, L-leucyl **3** and L-isoleucyl **4** esters of carbohydrates **16a-e** to **53a,b** using lipases in organic media.

## **6.2. Present investigation**

Some selective synthesized esters (each one from aldohexoses **5,6**, ketose **8**, pentose **10**, disaccharide **11, 12** and carbohydrate alcohol **14, 15** esters of L-alanine **1**, L-valine **2**, L-leucine **3** and L-isoleucine **4**) were tested for the inhibitory activities of ACE isolated from porcine lung (Section 6.4.1). Thus amino acyl esters - L-alanine **1**, L-valine **2**, L-leucine **3** and L-isoleucine **4** esters of D-glucose **5**, D-galactose **6**, D-fructose **8**, D-ribose **10**, lactose **11** maltose **12**, D-mannitol **14** and D-sorbitol **15** were subjected to ACE inhibition activities studies. The enzymatic reactions were carried out under optimized conditions worked out for these reactions (Section 6.4.2). ACE inhibition activity of the above mentioned amino acyl esters of carbohydrates were carried out by the Cushman and Cheung method (1984). Since hippuryl-L-histidyl-L-leucine (HHL) mimics the carboxyl dipeptide of angiotensin I and is resistant to angiotensinase, it has been

routinely used as the substrate for screening ACE inhibitors (Cushman and Cheung, 1969).

Underivatized L-amino acids and carbohydrates were also tested for ACE inhibition as such as controls and they did not show any ACE inhibitory activities. Only esters showed activities. Isolated ACE inhibitor tested for lipase and protease activity (Table 6.1) showed a small extent of protease activity (13.3 %) compared to ACE activity but no lipase activity. In presence of L-isoleucyl-D-glucose prepared, the isolated ACE showed 8.9 % protease activity (Table 6.1) compared to the ACE activity. This confirmed that the ACE inhibition observed in the presence of amino acyl esters prepared is more due to ACE inhibition rather than protease inhibition.

**Table 6.1. Protease inhibition assay for D-glucose ester <sup>a</sup>**

System	Protease activity Unit min <sup>-1</sup> mg <sup>-1</sup> enzyme protein <sup>b</sup>	Percentage of protease activity with respect to ACE activity <sup>c</sup>
Control		
ACE- 0.5 ml + 0.5 ml of 0.6% hemoglobin + 0.5 ml Buffer	0.0436	13.3
L-Isoleucyl-D-glucose - 0.5 ml ester + ACE -0.5 ml + 0.5 ml of 0.6% hemoglobin	0.0267	8.9

<sup>a</sup> Conditions: ACE – 0.5 ml (0.5mg), All the solutions were prepared in 0.1 M Tris-HCl (pH 7.5), incubation period – 30 min, temperature – 37 °C, 0.5 ml of 10 % trichloro acetic acid added to arrest the reaction; Blank performed without enzyme and ester; Absorbance measured at 440 nm; ester – 0.5 ml of 0.8 mM; <sup>b</sup>Average absorbance values from three individual experiments; <sup>c</sup>Percentage protease activity with respect to an ACE activity of 0.327 µmol/(min.mg protein).

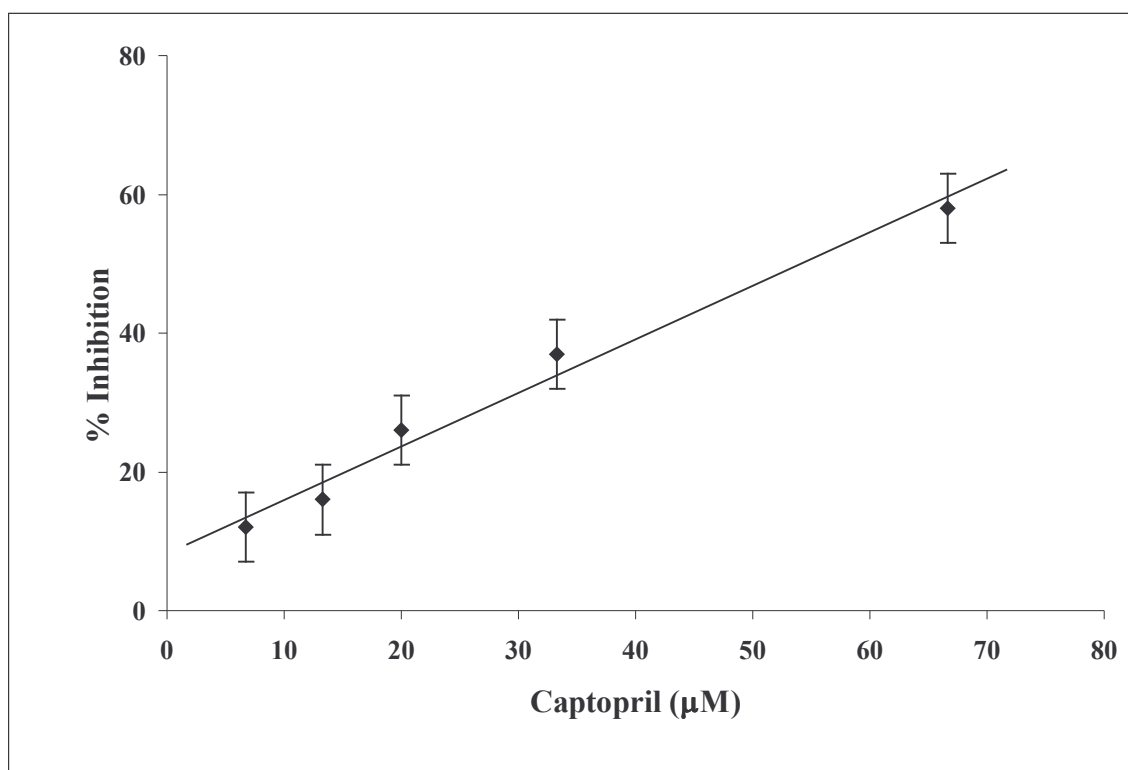


**Fig. 6.1.** A typical ACE inhibition plot for captopril. Concentration range – 6.7 - 66.7 µM  
Substrate – 0.1 ml hippuryl-histidyl-leucine (5 mM), Buffer – 100 mM phosphate buffer (pH 8.3) containing 300 mM NaCl, Incubation period – 30 min, temperature - 37 °C.  $IC_{50}$  value -  $0.060 \pm 0.006$  mM.

**Table 6.2. IC<sub>50</sub> values for ACE inhibition by amino acyl esters of carbohydrates<sup>a</sup>**

Amino acyl ester of carbohydrates	Conversion Yield (%) <sup>b</sup>	Products (% Proportion) <sup>c</sup>	IC <sub>50</sub> value (mM) <sup>d</sup>
L-Alanyl-β-D-glucose	30	<b>16a</b> 2- <i>O</i> -L-alanyl-β-D-glucose (47) <b>16b</b> 3- <i>O</i> -L-alanyl-β-D-glucose (12) <b>16c</b> 6- <i>O</i> -L-alanyl-β-D-glucose (20) <b>16d</b> 2,6-di- <i>O</i> -L-alanyl-β-D-glucose (15) <b>16e</b> 3,6-di- <i>O</i> -L-alanyl-β-D-glucose (6)	3.1±0.30
L-Alanyl-D-ribose	48	<b>21a</b> 3- <i>O</i> -L-alanyl-D-ribose (16) <b>21b</b> 5- <i>O</i> -L-alanyl-D-ribose (32) <b>21c</b> 3,5-di- <i>O</i> -L-alanyl-D-ribose (52)	2.7±0.25
L-Alanyl-lactose	20	<b>22a</b> 6- <i>O</i> -L-alanyl-lactose (34) <b>22b</b> 6'- <i>O</i> -L-alanyl-lactose (34) <b>22c</b> 6,6'-di- <i>O</i> -L-alanyl-lactose (32)	2.0±0.20
L-Valyl-D-glucose	68	<b>25a</b> 2- <i>O</i> -L-valyl-D-glucose (10) <b>25b</b> 3- <i>O</i> -L-valyl-D-glucose (12) <b>25c</b> 6- <i>O</i> -L-valyl-D-glucose (31) <b>25d</b> 2,6-di- <i>O</i> -L-valyl-D-glucose ( <b>23</b> ) <b>25e</b> 3,6-di- <i>O</i> -L-valyl-D-glucose ( <b>24</b> )	6.0±0.59
L-Valyl-D-fructose	34	<b>28a</b> 1- <i>O</i> -L-valyl-D-fructose (29) <b>28b</b> 6- <i>O</i> -L-valyl-D-fructose (34) <b>28c</b> 1,6-di- <i>O</i> -L-valyl-D-fructose (37)	2.8±0.28
L-Valyl-maltose	42	<b>31a</b> 6- <i>O</i> -L-valyl-maltose (49) <b>31b</b> 6'- <i>O</i> -L-valyl-maltose (51)	3.1±0.30
L-Valyl-D-mannitol	56	<b>33</b> 1- <i>O</i> -L-valyl-D-mannitol	1.0±0.09
L-Leucyl-D-glucose	43	<b>34a</b> 2- <i>O</i> -L-leucyl-D-glucose (17) <b>34b</b> 3- <i>O</i> -L-leucyl-D-glucose (20) <b>34c</b> 6- <i>O</i> -L-leucyl-D-glucose (48) <b>34d</b> 2,6-di- <i>O</i> -L-leucyl-D-glucose ( <b>8</b> ) <b>34e</b> 3,6-di- <i>O</i> -L-leucyl-D-glucose (7)	2.8±0.27
L-Leucyl-D-fructose	48	<b>37</b> 6- <i>O</i> -L-leucyl-D-fructose	0.9±0.08
L-Leucyl-D-ribose	38	<b>39a</b> 3- <i>O</i> -L-leucyl-D-ribose ( <b>16</b> ) <b>39b</b> 5- <i>O</i> -L-leucyl-D-ribose ( <b>32</b> ) <b>39c</b> 3,5-di- <i>O</i> -L-leucyl-D-ribose (52)	1.5±0.14
L-Leucyl-D-sorbitol	60	<b>43</b> 1- <i>O</i> -L-leucyl-D-sorbitol	2.7±0.25
L-Isoleucyl-D-glucose	47	<b>44a</b> 3- <i>O</i> -L-isoleucyl -D-glucose (42) <b>44b</b> 6- <i>O</i> -L-isoleucyl -D-glucose (58)	0.7±0.07
L-Isoleucyl-D-fructose	42	<b>47a</b> 1- <i>O</i> -L-isoleucyl-D-fructose ( <b>36</b> ) <b>47b</b> 6- <i>O</i> -L-isoleucyl-D-fructose ( <b>30</b> ) <b>47c</b> 1,6-di- <i>O</i> -L-isoleucyl-D-fructose (34)	0.9±0.09
L-Isoleucyl-D-ribose	53	<b>49a</b> 3- <i>O</i> -L-isoleucyl-D-ribose (52) <b>49b</b> 5- <i>O</i> -L-isoleucyl-D-ribose (20) <b>49c</b> 3,5-di- <i>O</i> -L-isoleucyl-D-ribose (28)	3.8±0.37
L-Isoleucyl-maltose	54	<b>51a</b> 2- <i>O</i> -L-isoleucyl- maltose (38) <b>51b</b> 6- <i>O</i> -L-isoleucyl -maltose (40) <b>51c</b> 6'- <i>O</i> -L-isoleucyl -maltose (22)	0.9±0.09

<sup>a</sup> Respective amino acids and carbohydrates as controls showed no ACE inhibition activity; <sup>b</sup> Conversion yields were from HPLC within ± 10 % errors in HPLC yield measurements; <sup>c</sup> Product proportions determined from <sup>13</sup>C, 2D HSQCT NMR C6 peak areas (C5 cross peaks in case of ribose) or their cross peaks; <sup>d</sup> IC<sub>50</sub> values compared to that of captopril 0.060 ± 0.006 mM determined by Cushman and Cheung method.



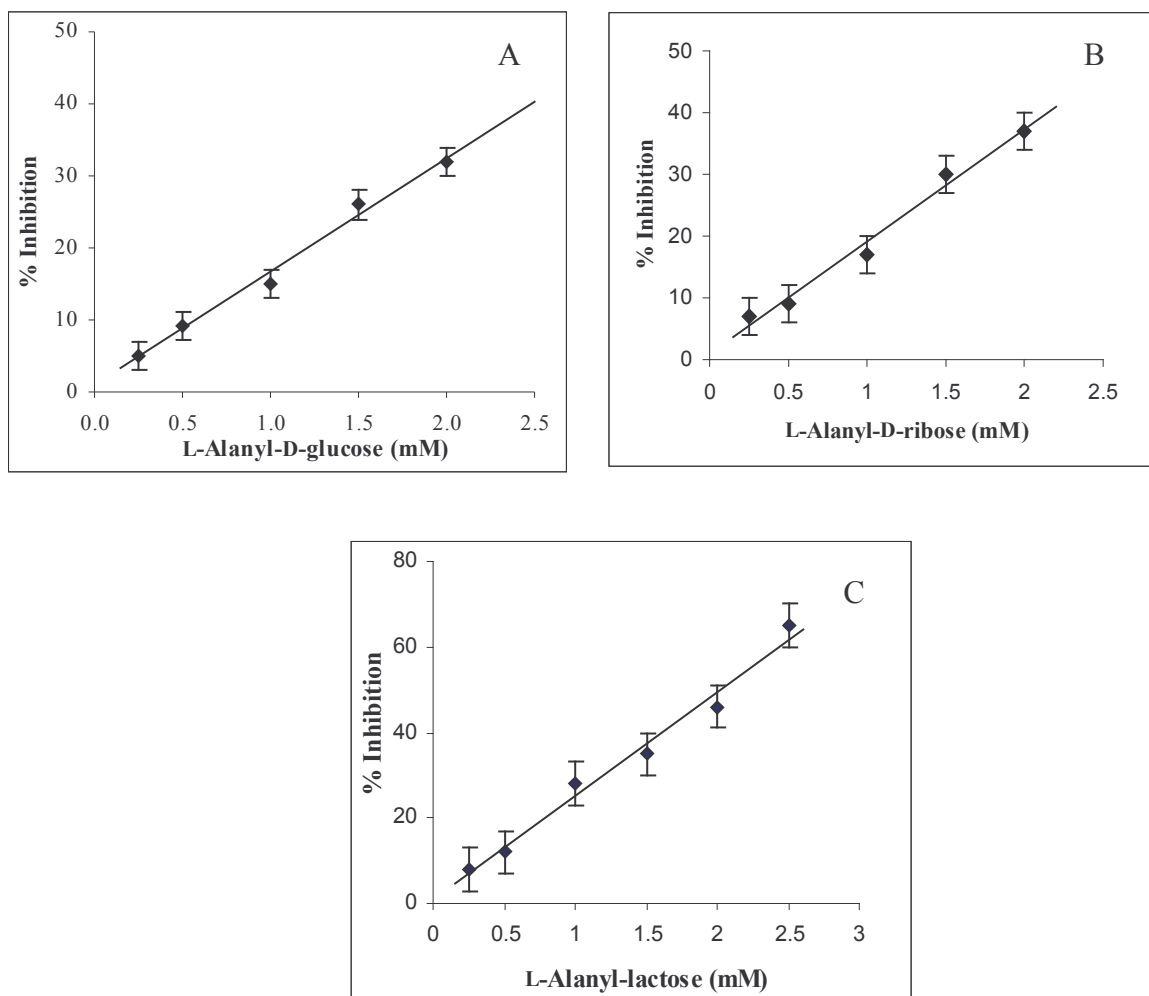


**Fig. 6.2.** ACE inhibition plots for L-alanyl esters of carbohydrates, (A) L-alanyl-D-glucose **16a-e**, concentration range – 0.25 – 2.0 mM, substrate – 0.1 ml hippuryl-histidyl-leucine (5 mM), Buffer – 100 mM phosphate buffer (pH 8.3) containing 300 mM NaCl, Incubation period – 30 min, Temperature-37 °C, (B) L-alanyl-D-ribose **21a-c**, concentration range – 0.25 - 2.0 mM. (C) L-alanyl-D-lactose **22a-c**, concentration range – 0.25 – 2.5 mM.

Figure 6.1 shows a typical ACE inhibition plot for captopril which showed an  $IC_{50}$  value of  $0.060 \pm 0.006$  mM. ACE inhibition plots for all the tested esters, such as carbohydrate esters of L-alanine (Fig. 6.2), L-valine (Fig. 6.3), L-leucine (Fig. 6.4) and L-isoleucine (Fig. 6.5) are shown. Table 6.2 shows the compounds tested, their conversion yields from the respective enzymatic reactions, proportions and nature of the esters formed and ACE inhibitory activities for these compounds.

The compounds were characterized by two-dimensional Heteronuclear Single Quantum Coherence Transfer (2D-HSQCT) NMR spectra recorded for the samples (Chapter 4). From NMR it was confirmed that mono and di esters, in different proportions were detected (Table 6.2). In some cases like L-valyl-maltose **31a,b**, L-valyl-D-mannitol **33**, L-leucyl-D-fructose **37**, L-leucyl-D-mannitol **42** and L-isoleucyl-D-glucose **44a,b** only monoesters were found to be formed. A 1-*O*- monoester was formed in case of L-valyl-D-fructose **28a**, L-valyl-D-mannitol **33**, L-leucyl-D-sorbitol **43** and L-isoleucyl-D-fructose **47a**. A 2-*O*- monoester was found to be formed in case of L-alanyl- $\beta$ -D-glucose **16a**, L-valyl-D-glucose **25a**, L-leucyl-D-glucose **34a** and L-isoleucyl-maltose **51a**. A 3-*O*- monoester was found to be formed in case of L-alanyl- $\beta$ -D-glucose **16b**, L-valyl-D-glucose **25b** and L-leucyl-D-glucose **34b** and L-isoleucyl-D-glucose **44a**. A 6'-*O*- monoester was found to be formed in case of L-alanyl-lactose **22b**, L-valyl-maltose **31b** and L-isoleucyl-maltose **51c**. All the esters invariably showed formation of 6-*O*- monoester (**16c**, **22a**, **25c**, **28b**, **31a**, **34c**, **37**, **44b**, **47b** and **51b**) except L-alanyl-D-ribose **21a-c**, L-leucyl-D-ribose **39a-c** and L-isoleucyl-D-ribose **49a-c** where the primary C-5 hydroxyl group reacted to form 5-*O*- ester (**21b**, **39b** and **49b**). Diesters such as 1,6-di-*O*-, 2,6-di-*O*-, 3,6-di-*O*-, 3,5-di-*O*- and 6,6'-di-*O*- were found to be formed in case of L-alanyl- $\beta$ -D-glucose **16d,e**, L-alanyl-D-ribose **21c**, L-alanyl-lactose **22c**, L-valyl-D-glucose

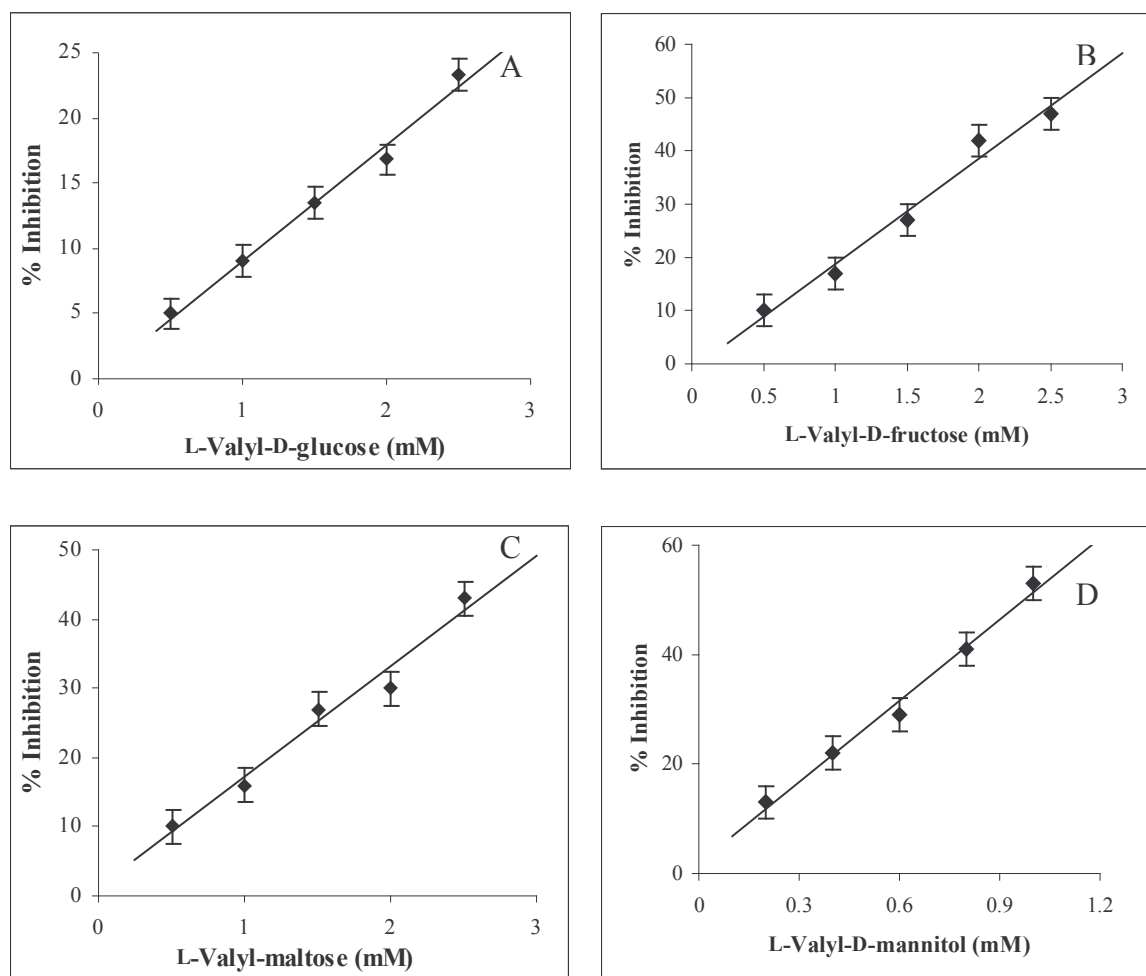


**Fig. 6.3.** ACE inhibition plots for L-valyl esters of carbohydrates (A) L-valyl-D-glucose **25a-e**, concentration range – 0.5 – 2.5 mM, substrate – 0.1 ml hippuryl-histidyl-leucine (5 mM), Buffer – 100 mM phosphate buffer (pH 8.3) containing 300 mM NaCl, Incubation period – 30 min, Temperature-37 °C. (B) L-valyl-D-fructose **28a-c**, concentration range – 0.5 – 2.5 mM. (C) L-valyl-maltose **31a,b**, concentration range – 0.5 – 2.5 mM. (D) L-valyl-D-mannitol **33**, concentration range – 0.2 – 1.0 mM.

**25d,e**, L-valyl-D-fructose **28c**, L-leucyl-D-glucose **34d,e**, L-leucyl-D-ribose **39c**, L-isoleucyl-D-fructose **47c** and L-isoleucyl-D-ribose **49c**. It was not possible to separate the individual esters from their reaction mixtures even through chromatography on Sephadex G-10 or Bio Gel P2. Thus the activities described are for the mixtures of these mono and diesters.

### **6.3. Discussion**

Among the esters, L-isoleucyl-D-glucose ( $0.7 \pm 0.07$  mM) was found to exhibit the best inhibitory activity. With increase in alkyl side chain branching, D-glucose esters of L-alanine ( $3.1 \pm 0.30$  mM), L-valine ( $6.0 \pm 0.59$  mM), L-leucine ( $2.8 \pm 0.27$  mM) and L-isoleucine ( $0.7 \pm 0.07$  mM) showed better inhibition (lesser  $IC_{50}$  values), than the other esters, which could be directly correlated to increase in hydrophobicity (Table 6.2).  $IC_{50}$  values  $\leq 1.0$  mM were detected for L-valyl-D-mannitol ( $1.0 \pm 0.09$  mM), L-isoleucyl-D-glucose ( $0.7 \pm 0.07$  mM), L-isoleucyl-D-fructose ( $0.9 \pm 0.09$  mM), L-isoleucyl-maltose ( $0.9 \pm 0.09$  mM) and L-leucyl-D-fructose ( $0.9 \pm 0.08$  mM). Although, amino acyl esters were separated from the reaction mixture by column chromatography, it was difficult to separate the individual esters. Hence, the actual potency of the individual esters could not be unequivocally established in the present work.

The present work for the first time has shown the ACE inhibitory potency of the above mentioned amino acyl esters prepared enzymatically. Since milder reaction conditions were employed, the products formation did not suffer due to side reactions. Captopril is N-[(S)-3-mercapto-2-methylpropionyl]-L-proline containing prolyl unit as essential for ACE inhibition (De-Lima 1999). Some naturally occurring 'biologically active peptides' such as N-terminal dipeptide (Tyr-Leu) of  $\beta$ -lactorphin, Asp-Leu-Pro and Asp-Gly from soy protein and Gly-Pro-Leu and Gly-Pro-Val from bovine skin gelatin

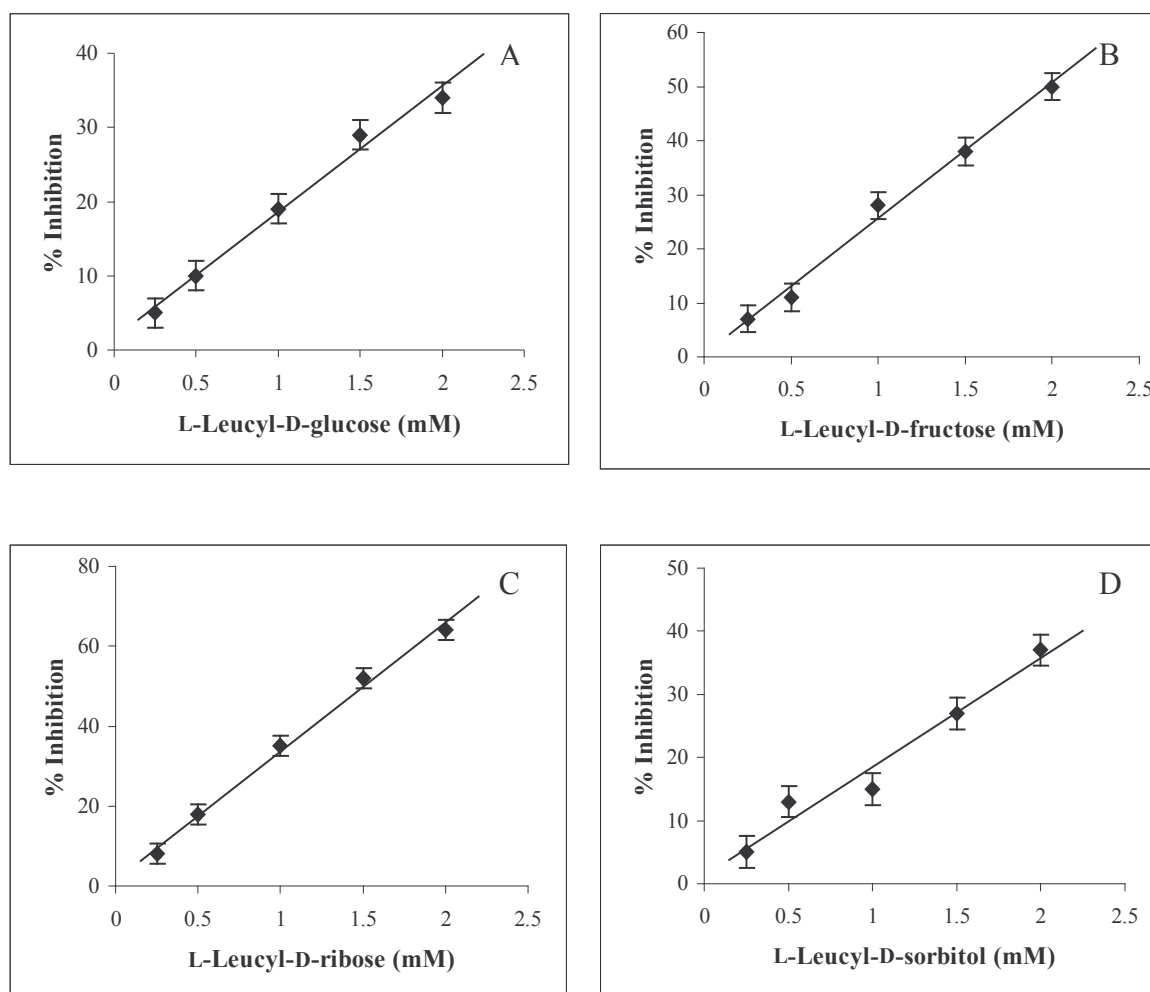


**Fig. 6.4.** ACE inhibition plots for L-leucyl esters of carbohydrates. (A) L-leucyl-D-glucose **34a-c**, concentration range – 0.25 – 2.0 mM, substrate – 0.1 ml hippuryl-histidyl-leucine (5 mM), Buffer – 100 mM phosphate buffer (pH 8.3) containing 300 mM NaCl, Incubation period –30 min, Temperature-37 °C. (B) L-leucyl-D-fructose **37**, concentration range – 0.25 – 2.0 mM, (C) L-leucyl-D-ribose **39a-c**, concentration range – 0.25 – 2.0 mM, (D) L-leucyl-D-sorbitol **41**, concentration range – 0.25 – 2.0 mM.

hydrolysis also act as ACE inhibitors (Deloffre *et al.*, 2004; Mullally *et al.*, 1996; Wu *et al.* 2002; Kim *et al.*, 2001). Although, the aliphatic amino acyl esters of D-glucose, D-fructose, D-ribose and lactose were prepared and tested, mere presence of a alkyl unit does not give rise to a high level of ACE inhibition. Overall it was clear that alkyl side chains can be accommodated in the hydrophobic S<sub>1</sub> and S<sub>2</sub> subsites of angiotensin I converting enzyme (Michaud *et al.*, 1997; De-Lima, 1999). The free amino group in the amino acid esters can also serve as good ligands for Zn<sup>2+</sup> in the ACE active site. Carbohydrates in esters could also bind to the hydrophobic and/or hydrophilic subsites of angiotensin I converting enzyme, as they possess both hydrophobic and hydrophilic groups in their structure. Although the ACE preparation in the present work from pig lung is ACE I (Andujar-Sanchez *et al.*, 2003), it showed a low protease inhibitory activity but no lipase activity. This indicates that the amino acyl esters of carbohydrates inhibit ACE rather than the proteases as protease inhibition activity can be construed some times to be ACE inhibition. The results indicate that the esters hold promise as the potential inhibitors for ACE.

## 6.4. Experimental

### 6.4.1. Extraction of ACE from pig lung

ACE was extracted from pig lung (Section 2.2.15) using the method described by Andujar-Sanchez *et al.*, (2003). A 100 g of pig lung was minced and homogenized using a blender with 10 mM HEPES buffer (pH 7.0) containing 0.4 M NaCl at a volume ratio of 5:1 (v/w of pig lung) at 4 °C. The homogenate was centrifuged at 9000 g for 60 min. The supernatant was discarded and the precipitate was washed twice with 200 ml of 10 mM HEPES buffer (pH 7.0) containing 0.4 M NaCl. The final precipitate was resuspended in 200 ml of 10 mM HEPES buffer pH 7.0 containing, 0.4 M NaCl, 10 µM

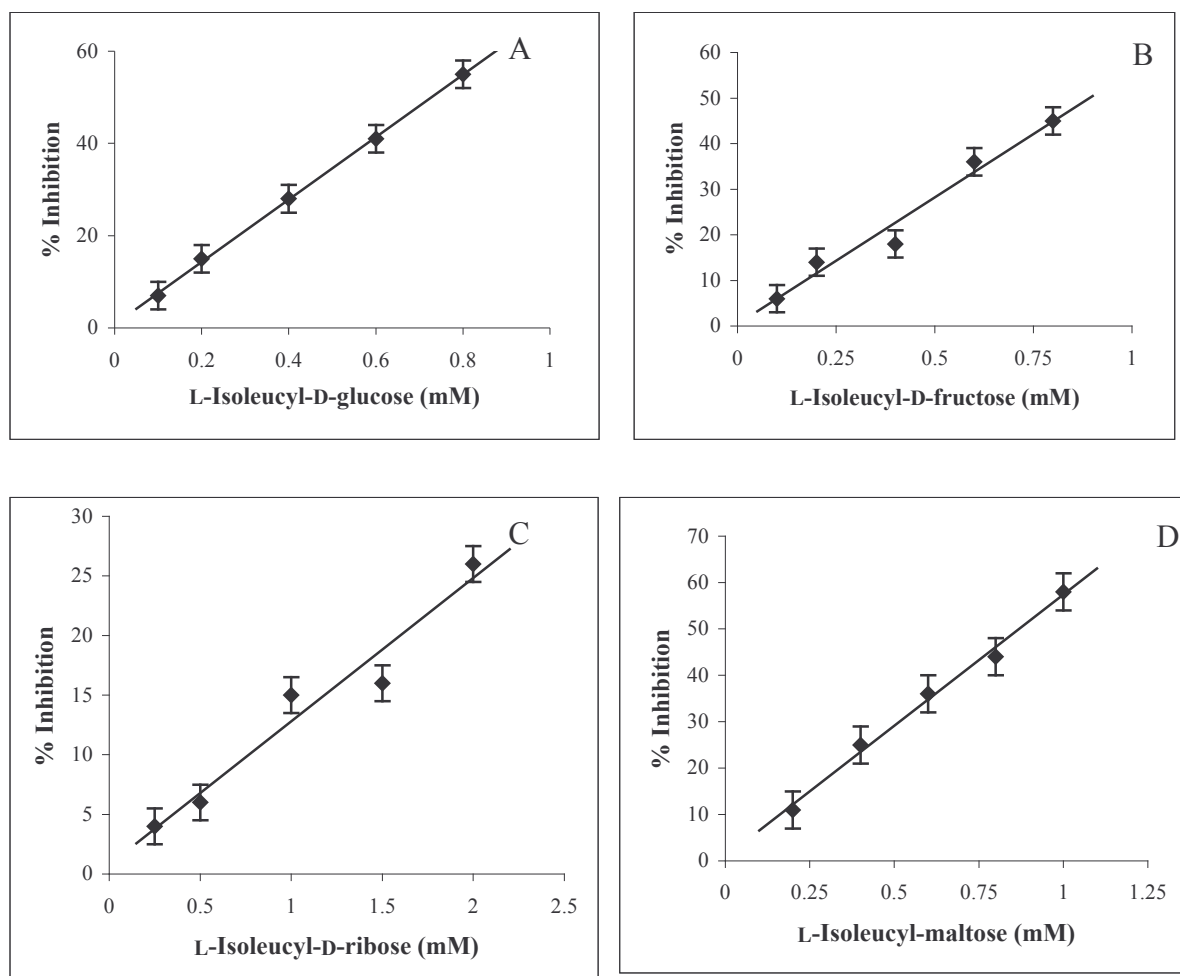


**Fig. 6.5.** ACE inhibition plots for L-isooleucyl esters of carbohydrates (A) L- isooleucyl-D-glucose **44a,b**, concentration range – 0.2 – 0.8 mM, substrate – 0.1 ml HHL (5 mM), Buffer – 100 mM phosphate buffer (pH 8.3) containing 300 mM NaCl, Incubation period –30 min, Temperature-37 °C. (B) L-isooleucyl-D-fructose **47a-c**, concentration range – 0.2 – 0.8 mM, (C) L-isooleucyl-D-ribose **48-c**, Concentration range 0.25 – 2.0 mM, (D) L-isooleucyl-maltose **51a-c**, concentration range – 0.2 – 1.0 mM.

ZnCl<sub>2</sub>, 0.5 % (w/v) Triton-X-100 and stirred over night at 4 °C. The solution was centrifuged to remove the pellets. The supernatant was dialyzed against water and later lyophilized. The protein content of ACE determined by Lowry's method was found to be 8.3 %. The specific activity of the enzyme was found to be 0.243 μmol/min/mg of enzyme protein.

#### 6.4.2. Esterification Procedure

A general procedure employed for the esterification reaction is as follows. Esterification was carried out in a flat bottom two necked flask by reacting 0.001- 0.008 mol unprotected L-amino acid (L-alanine, L-valine, L-leucine and L- isoleucine) and 0.001 – 0.002 mol of carbohydrate (D-glucose, D-galactose, D-fructose, D-ribose, lactose and D-mannitol) along with 100 ml CH<sub>2</sub>Cl<sub>2</sub>:DMF (v/v 90:10, 40 °C) or hexane:CHCl<sub>3</sub>:DMF (v/v/v 45:45:10, 61 °C) in presence of 0.60 - 0.180 g of lipases (40 to 50 % w/w carbohydrate employed) under reflux for a period of three days. *Rhizomucor miehei* lipase in presence of 0.1 mM (0.1ml of 0.1 M) acetate buffer (pH 4.0) towards L-alanyl esters of carbohydrates syntheses and *Candida rugosa* lipase (CRL) in presence of 0.1 mM (0.1 ml of 0.1 M) phosphate buffer (pH 7.0) towards L-valyl, L-leucyl and L-isoleucyl esters of carbohydrates syntheses were employed. The condensed vapour of solvents which formed an azeotrope with water was passed through a desiccant before being returned into the reaction mixture, thereby facilitating complete removal of water of reaction (Lohith and Divakar, 2005). This set up maintained a very low water activity of  $a_w = 0.0054$  throughout the reaction period. After completion of the reaction, the solvent was distilled off 20 - 30 ml of warm water was added, stirred and filtered to remove the lipase. The filtrate was evaporated to get a mixture of the unreacted carbohydrate, unreacted L-amino acids and the product esters, which were then analyzed by HPLC. A Shimadzu LC10AT HPLC connected to LiChrosorb RP-18



column (5  $\mu\text{m}$  particle size, 4.6 x 150 mm length) with acetonitrile: water (v/v 20:80) as a mobile phase at a flow rate of 1 ml/min was employed using an UV detector at 210 nm. The conversion yields were determined with respect to peak areas of the L-amino acid and that of the esters. The esters formed were separated by size exclusion chromatography using Sephadex G-10 and Bio Gel P-2 as column materials and eluted with water. The product esters separated were subjected to spectral characterization by UV, IR, mass, specific rotation and 2D-NMR.

#### **6.4.3. Angiotensin Converting Enzyme (ACE) inhibition assay**

ACE inhibition assay for the esters prepared were performed by the Cushman and Cheung method (Cushman and Cheung, 1971). Aliquots of ester solutions in the concentration range 0.2 to 2.5 mM (0.1 ml to 1.0 ml of 5.0 mM stock solution) were taken and to this 0.1 ml of ACE solution (0.1% in 0.1 M phosphate buffer, pH 8.3 containing 300 mM NaCl) was added. To this solution, 0.1 ml of 5.0 mM hippuryl-L-histidyl-L-leucine (HHL) was also added and the total volume made upto 1.25 ml by adding phosphate buffer (1.05 ml to 0.15 ml of 0.1 M, pH 8.3 containing 300 mM NaCl). The solution was incubated on a Heto-Holten shaking water bath for 30 min at 37 °C. Blanks were performed without the enzyme by taking only the ester solution (0.1 to 1.0 ml) along with 0.1 ml of 5.0 mM HHL. The total volume was made upto to 1.25 ml by adding same buffer (1.15 ml to 0.25 ml). The reaction was terminated by adding 0.25 ml of 1M HCl. Hippuric acid formed in the reaction was extracted with 1.5 ml of ethyl acetate. One ml of the ethyl acetate layer was evaporated to dryness and treated with equal amount of distilled water and absorbance was measured at 228 nm for hippuric acid. The hippuric acid formed in 1.5 ml of ethyl acetate was determined from a calibration plot prepared by using a standard hippuric acid in 1 ml of distilled water in the concentration range 0-400 nmol and measuring its absorbance at 228 nm. Specific

activity was expressed as millimoles of hippuric acid formed per min per mg of enzyme protein.

$$\text{Specific activity} = \frac{A_{\text{ts}} - A_{\text{blank}}}{T \times S \times E}$$

$A_{\text{ts}}$  = absorbance of test solution,

$A_{\text{blank}}$  = absorbance of blank solution,

T = incubation period in min,

S = slope value of the calibration plot ( $1.006 \times 10^{-2}$  Abs units/nmol of hippuric acid),

E = amount of the enzyme in mg protein.

Percentage inhibition was expressed as the ratio of the specific activity of ACE in the presence of the inhibitor to that in the absence of the inhibitor, the latter being considered as 100 %.  $IC_{50}$  value was expressed as the concentration of the inhibitor required for 50 % reduction in ACE specific activity. Molecular weights of the esters employed in the calculations are weighted averages of molecular weights of esters detected by NMR spectroscopy.

A Shimadzu UV-1601 spectrophotometer was employed for the measurement of absorbance readings at 228nm.

#### 6.4.4. Protease and lipase assay

Protease activity for the ACE inhibitor (Section 2.2.2) was determined by the method described by Dubey and Jagannadham (2003) and lipase activity (Section 2.2.1.1) by the tributyrin method (Vorderwulbecke *et al.*, 1992) in presence of L-isoleucyl-D-glucose (0.8 mM in 0.1M Tris-HCl buffer, pH 7.5). Specific protease activity was expressed as the increase in absorbance at 440 nm per min per mg of the protein employed. Similarly specific lipase activity was determined as  $\mu\text{mol}$  of butyric acid formed per min per mg of the protein employed.

*Conclusions*

**The important findings of the present investigation are:**

1. The esterification potentialities of lipases from *Rhizomucor miehei* (RML), *Candida rugosa* (CRL) and porcine pancreas (PPL) were explored in detail in the syntheses of L-alanyl **1**, L-valyl **2**, L-leucyl **3** and L-isoleucyl **4** esters of carbohydrates - D-glucose **5**, D-galactose **6**, D-mannose **7**, D-fructose **8**, D-arabinose **9**, D-ribose **10**, lactose **11**, maltose **12**, sucrose **13**, D-mannitol **14** and D-sorbitol **15**, using unprotected and unactivated amino acids and carbohydrates.
2. An experimental set-up was employed which maintained a very low water activity ( $a_w = 0.005$ ) throughout the reaction. The set-up involved refluxing an appropriate amount of L-amino acid and carbohydrate in presence of buffer salts and lipases in the specified low boiling solvent mixture. The condensed vapors of the solvent was passed through a desiccant before being returned into the reaction mixture, which facilitated complete removal of water of reaction. This set-up facilitated use of larger concentrations of substrates and lesser amounts of the enzymes which resulted in higher conversions.
3. The present study investigated the effect of buffer salts on this esterification reaction which rendered 'pH tuning' of the enzyme, besides providing optimum water activity necessary for the better performance of the enzyme. All the three lipases RML, CRL and PPL showed higher conversions when a small amount of buffer salt was employed.
4. Two dimensional HSQCT NMR confirmed the formation of 1-*O*-, 2-*O*-, 3-*O*-, 4-*O*-, 5-*O*-, 6-*O*- and 6'-*O*- mono esters and 1,6-di-*O*-, 2,5-di-*O*-, 2,6-di-*O*-, 3,5-di-*O*-, 3,6-di-*O*-, 4,6-di-*O*- and 6,6'-di-*O*- diesters to varying extents depending on the carbohydrate employed. Nature of the products clearly indicated that primary

hydroxyl groups of the carbohydrates (1-*O*-, 5-*O*-, 6-*O*- and 6'-*O*-) esterified predominantly over the secondary hydroxyl groups (2-*O*-, 3-*O*- and 4-*O*-). Among the secondary hydroxyl groups, 4-*O*- ester was formed only in case of D-mannose (**18b**, **36b** and **46b**). Carbohydrates containing axial hydroxyl groups in axial position like C2 in D-mannose and D-ribose and C4 in D-galactose have not reacted, indicating that esterification with axial secondary hydroxyl groups are difficult, especially with alkyl amino acyl donors. In case of L-alanyl-D-glucose **16a-e**, only  $\beta$ -anomer of D-glucose reacted, the D-glucose employed being a 40:60 mixture of  $\alpha$  and  $\beta$  anomers respectively. Lesser incubation periods gave rise to only monoesters. The anomeric hydroxyl groups of carbohydrate molecules did not react because of rapid glycosidic ring opening and closing process.

5. Aldohexoses (D-glucose, D-mannose and D-galactose), ketohexose (D-fructose), pentose (D-ribose) and the disaccharides (maltose) showed better conversions with all the four amino acids employed. Least conversions were observed for carbohydrate alcohols and sucrose esters. L-Valyl esters (25 - 78 %) as well as L-leucyl esters (21 - 65 %) showed better conversion than L-alanyl esters (3 - 78 %) and L-isoleucyl esters (9 - 55 %). Among the lipases employed, *Candida rugosa* lipase and porcine pancreas lipase have shown better conversions than *Rhizomucor miehei* lipase. L-Alanine **1**, L-valine **2** and L-leucine **3** with D-glucose **5** and L-alanine **1** and L-isoleucine **4** with D-mannose **7** gave five diastereomeric esters. Both D-arabinose **9** and D-ribose **10** have shown three diastereomeric esters with all the amino acids (**1-4**) employed. Lactose **11** did not react with L-valine and L-leucine and D-sorbitol **15** with L-alanine, L-valine and L-isoleucine. L-Alanyl-sucrose **24**, L-valyl-D-mannose **27**, L-valyl-sucrose **32**, L-leucyl-maltose **40**, L-leucyl- sucrose **41** and L-isoleucyl-sucrose **52** formed only 6-*O*-ester. Carbohydrates like lactose **11**, D-mannitol **14** and

D-sorbitol **15** reacted selectively depending on the amino acid indicating that they may not be good nucleophiles, probably could be due to more hydrogen bonding propensity for D-mannitol and D-sorbitol and more steric hindrance in case of lactose. Loss of specificity could be due to use of larger amount of enzymes (about 40 % w/w carbohydrate), which gave a large number of esters. In the present esterification no maillard reaction product was found to be formed. Although underivatized amino acids were employed, less than 3 % peptide formation was detected and that too in few cases only.

6. About 99 L-amino acyl esters of carbohydrates (**16a-e** – **53a,b**) have been synthesized in the present work of which 97 esters are reported for the first time. The new esters reported are: L-alanyl-D-glucose **16a,d,e**, L-alanyl-D-galactose **17a-c**, L-alanyl-D-mannose **18a-e**, L-alanyl-D-fructose **19a-c**, L-alanyl-D-arabinose **20a-c**, L-alanyl-D-ribose **21a-c**, L-alanyl-lactose **22a-c**, L-alanyl-maltose **23a-c**, L-alanyl-sucrose **24**, L-valyl-D-glucose **25a-e**, L-valyl-D-galactose **26a-c**, L-valyl-D-mannose **27**, L-valyl-D-fructose **28a-c**, L-valyl-D-arabinose **29a-c**, L-valyl-D-ribose **30a-c**, L-valyl-maltose **31a, b**, L-valyl-sucrose **32**, L-valyl-D-mannitol **33**, L-leucyl-D-glucose **34a-e**, L-leucyl-D-galactose **35a,b**, L-leucyl-D-mannose **36a-c**, L-leucyl-D-fructose **37**, L-leucyl-D-arabinose **38a-c**, L-leucyl-D-ribose **39a-c**, L-leucyl-maltose **40**, L-leucyl-sucrose **41**, L-leucyl-D-mannitol **42a,b**, L-leucyl-D-sorbitol **43**, L-isoleucyl-D-glucose **44a,b**, L-isoleucyl-D-galactose **45a-c**, L-isoleucyl-D-mannose **46a-e**, L-isoleucyl-D-fructose **47a-c**, L-isoleucyl-D-arabinose **48a-c**, L-isoleucyl-D-ribose **49a-c**, L-isoleucyl-lactose **50a-c**, L-isoleucyl-maltose **51a-c**, L-isoleucyl-sucrose **52** and L-isoleucyl-D-mannitol **53a,b**.
7. A kinetic study on the esterification of D-glucose with L-alanine catalyzed by lipases from *Rhizomucor miehei* (RML) and *Candida rugosa* (CRL) investigated in detail

showed that both the lipases followed Ping-Pong Bi-Bi mechanism wherein L-alanine and D-glucose bind in subsequent steps releasing water and L-alanyl-D-glucose also in subsequent steps, with competitive substrate inhibition by D-glucose at higher concentrations leading to the formation of dead-end lipase-D-glucose complexes.

8. Among the amino acyl esters synthesized, about 15 amino acyl esters of carbohydrates were tested for angiotensin converting enzyme (ACE) inhibition activity. Among them, L-isoleucyl-D-glucose **44a,b** ( $IC_{50}$ :  $0.7 \pm 0.067$  mM), L-leucyl-D-fructose **37** ( $IC_{50}$ :  $0.9 \pm 0.08$  mM), L-isoleucyl-maltose **51a-c** ( $IC_{50}$ :  $0.9 \pm 0.09$  mM) and L-valyl-D-mannitol **33** ( $IC_{50}$ :  $1.0 \pm 0.092$  mM) showed the best ACE inhibitory activities. Other esters showed  $IC_{50}$  values in the range 1.5 mM – 6.0 mM.

*Summary*



Amino acyl esters of carbohydrates are used as sweetening agents, surfactants, microcapsules in pharmaceutical preparations, active nucleoside amino acid esters, antibiotics and in the delivery of biological active agents. Chemical acylation of carbohydrates regio-selectively is complex due to the presence of multiple hydroxyl groups, which require protection and deprotection. However enzymatic reactions can overcome this drawback. Hitherto, very few references are available on the lipase catalyzed esterification of amino acyl esters of sugars. Most of the earlier workers used proteases and N-protected and carboxyl group activated amino acids for synthesizing aminoacyl esters of carbohydrates. All these reactions were conducted in shake flasks using lesser quantity of substrates and larger quantity of enzymes. The present work deals with lipases catalyzed preparation of amino acyl esters of carbohydrates using unprotected and unactivated amino acids and carbohydrates.

Chapter **ONE** deals with literature survey on mainly lipase catalysed synthesis in organic media. Biotechnological applications of lipase catalysis in different food and pharmaceutical industries are discussed. A brief description on the lipase structure and catalytic mechanism on esterification is made. Parameters regulating lipase activity in organic media like nature of substrates, nature of solvents, effect of salt, thermal stability of lipases, water activity and immobilization are discussed. Diverse application of lipases like esterification using reverse micelles, supercritical carbon dioxide, micro oven, ionic liquids assisted reactions, kinetic studies and resolution of racemic mixture are presented. The chapter ends with a brief description on the scope of the present investigation.

Chapter **TWO** deals with materials and methods. Chemicals employed and their sources are listed. Methods of preparation of L-amino acyl esters of carbohydrates and the other related appropriate aspects of the same are discussed in detail.

Chapter **THREE** describes results from optimization of reaction parameters for the lipase catalyzed synthesis of L-alanyl **16a-e**, L-valyl **25a-e** and L-leucyl **34a-e** esters of D-glucose. Lipases from *Rhizomucor miehei* (RML), porcine pancreas (PPL) and *Candida rugosa* (CRL) were employed. The reaction conditions were optimized in terms of incubation period, solvent, enzyme concentrations, substrate concentrations, buffer (pH and concentration) and enzyme reusability. Under the experimental conditions employed, all the three lipases exhibited good esterification potentialities. Both RML and PPL showed maximum conversion yields of L-alanyl-D-glucose **16a-e** (30 % and 18 % respectively) at 40 % (w/w D-glucose) of enzyme, L-valyl-D-glucose **25a-e** (59 % and 62 % respectively) at 10 % (w/w D-glucose) of enzyme and L-leucyl-D-glucose **34a-e** (85 % and 18 % of respectively) at 40 % (w/w D-glucose) of enzyme employed. CRL showed a maximum conversion of 84 % of L-valyl-D-glucose **25a-e** at 30 % (w/w D-glucose) enzyme concentration. The present work showed enhanced activity of RML and CRL in presence of buffer salts. Optimum pH was found to be pH 4.0 for RML and pH 5.0 for PPL in case of L-alanyl-D-glucose, pH 7.0 for CRL in case of L-valyl-D-glucose and pH 5.0 for RML in case of L-leucyl-D-glucose reactions. Higher equivalents of D-glucose were found to inhibit RML in case of L-alanyl-D-glucose reaction. However, in case of L-valyl-D-glucose and L-leucyl-D-glucose reactions, free amino acids and D-glucose were not found to be inhibitors of RML and CRL. In the synthesis of L-alanyl-D-glucose **16a-e**, RML could be reused upto four cycles where as PPL could be used only upto two cycles.

Chapter **FOUR** describes the syntheses and characterization of L-alanyl **1**, L-valyl **2**, L-leucyl **3** and L-isoleucyl **4** esters of carbohydrates - D-glucose **5**, D-galactose **6**, D-mannose **7**, D-fructose **8**, D-arabinose **9**, D-ribose **10**, lactose **11**, maltose **12**, sucrose **13**, D-mannitol **14** and D-sorbitol **15**. Esterification was carried out by reacting 0.002 mol

unprotected L-amino acid (**1-4**) and 0.001 mol of carbohydrate (**5-15**) along with 100 ml CH<sub>2</sub>Cl<sub>2</sub>: DMF (90:10 v/v, 40 °C) in presence of 40 % (w/w carbohydrate employed) of lipases under reflux for a period of three days. *Rhizomucor miehei* lipase (RML) in presence of 0.1 mM (0.1 ml of 0.1 M) of pH 4.0 acetate buffer, *Candida rugosa* lipase (CRL) in presence of 0.1 mM (0.1 ml of 0.1 M) of pH 7.0 phosphate buffer and crude porcine pancreas lipase in presence of 0.1 mM (0.1 ml of 0.1 M) of pH 5.0 acetate buffer were employed to impart 'pH tuning' to the enzyme. All the three lipases employed showed broad substrate specificity towards amino acids as well as carbohydrates. Esterification yields were obtained in the range of 3 – 78 %. Two dimensional HSQCT NMR confirmed the formation of 1-*O*-, 2-*O*-, 3-*O*-, 4-*O*-, 5-*O*-, 6-*O*- and 6'-*O*- mono esters and 1,6-di-*O*-, 2,5-di-*O*-, 2,6-di-*O*-, 3,5-di-*O*-, 3,6-di-*O*-, 4,6-di-*O*- and 6,6'-di-*O*- diesters to varying extents depending on the carbohydrate employed. Nature of the products clearly indicated that primary hydroxyl groups of the carbohydrates (1-*O*-, 5-*O*-, 6-*O*- and 6'-*O*-) esterified predominantly over the secondary hydroxyl groups (2-*O*-, 3-*O*- and 4-*O*-). Among the secondary hydroxyl groups, 4-*O*- ester was formed only in case of D-mannose (**18b**, **36b** and **46b**). Carbohydrates containing hydroxyl groups in axial position like C2 in D-mannose and D-ribose and C4 in D-galactose have not reacted, indicating that esterification with axial secondary hydroxyl groups are difficult, especially with alkyl amino acyl donors. In case of L-alanyl-D-glucose **16a-e**, only β-anomer of D-glucose reacted, the D-glucose employed being a 40: 60 mixture of α and β anomers respectively. Lesser incubation periods gave rise to only monoesters. The anomeric hydroxyl groups of carbohydrate molecules did not react because of rapid glycosidic ring opening and closing process. Aldohexoses (D-glucose, D-mannose and D-galactose), ketohexose (D-fructose), pentose (D-ribose) and the disaccharides (maltose) showed better conversions with all the four amino acids. Least conversions were

observed for carbohydrate alcohols and sucrose esters. L-Valyl esters (25 – 78 %) as well as L-leucyl esters (21 – 65 %) showed better conversion than L-alanyl esters (3 – 78 %) and L-isoleucyl esters (9 – 55 %). Among the lipases employed, *Candida rugosa* lipase and porcine pancreas lipase have shown better conversions than *Rhizomucor miehei* lipase. L-Alanine **1**, L-valine **2** and L-leucine **3** with D-glucose **5** and L-alanine **1** and L-isoleucine **4** with D-mannose **7** gave five diastereomeric esters. Both D-arabinose **9** and D-ribose **10** showed three diastereomeric esters with all the amino acids (**1-4**) employed. Lactose **11** did not react with L-valine and L-leucine and D-sorbitol **15** did not react with L-alanine, L-valine and L-isoleucine. L-Alanyl-sucrose **24**, L-valyl-D-mannose **27**, L-valyl-sucrose **32**, L-leucyl-maltose **40**, L-leucyl-sucrose **41** and L-isoleucyl-sucrose **52**, formed only 6-*O*- esters. Carbohydrates like lactose **11**, D-mannitol **14** and D-sorbitol **15** reacted selectively depending on the amino acid indicating that they may not be good nucleophiles, probably due to more hydrogen bonding propensity for D-mannitol and D-sorbitol and steric hindrance in case of lactose. About 99 L-amino acyl esters of carbohydrates were prepared out of which 97 esters have not been reported before. So far unreported esters are L-alanyl-D-glucose **16a,d,e**, L-alanyl-D-galactose **17a-c**, L-alanyl-D-mannose **18a-e**, L-alanyl-D-fructose **19a-c**, L-alanyl-D-arabinose **20a-c**, L-alanyl-D-ribose **21a-c**, L-alanyl-lactose **22a-c**, L-alanyl-maltose **23a-c**, L-alanyl-sucrose **24**, L-valyl-D-glucose **25a-e**, L-valyl-D-galactose **26a-c**, L-valyl-D-mannose **27**, L-valyl-D-fructose **28a-c**, L-valyl-D-arabinose **29a-c**, L-valyl-D-ribose **30a-c**, L-valyl-maltose **31a,b**, L-valyl-sucrose **32**, L-valyl-D-mannitol **33**, L-leucyl-D-glucose **34a-e**, L-leucyl-D-galactose **35a,b**, L-leucyl-D-mannose **36a-c**, L-leucyl-D-fructose **37**, L-leucyl-D-arabinose **38a-c**, L-leucyl-D-ribose **39a-c**, L-leucyl-maltose **40**, L-leucyl-sucrose **41**, L-leucyl-D-mannitol **42a,b**, L-leucyl-D-sorbitol **43**, L-isoleucyl-D-glucose **44a,b**, L-isoleucyl-D-galactose **45a-c**, L-isoleucyl-D-mannose **46a-e**, L-isoleucyl-D-fructose **47a-c**, L-isoleucyl-D-arabinose

**48a-c**, L-isoleucyl-D-ribose **49a-c**, L-isoleucyl-lactose **50a-c**, L-isoleucyl-maltose **51a-c**, L-isoleucyl-sucrose **52** and L-leucyl-D-mannitol **53a,b**.

Chapter **FIVE** describes kinetic study on the esterification of D-glucose **5** with L-alanine **1** catalyzed by lipases from *Rhizomucor miehei* (RML) and *Candida rugosa* (CRL). A detailed investigation showed that both the lipases followed Ping-Pong Bi-Bi mechanism wherein L-alanine and D-glucose bind in subsequent steps releasing water and L-alanyl-D-glucose also in subsequent steps, with competitive substrate inhibition by D-glucose at higher concentrations leading to the formation of dead-end lipase-D-glucose complexes. An attempt to obtain the best fit of this kinetic model through curve fitting yielded in good approximation, the apparent values of four important kinetic parameters, RML:  $k_{cat} = 0.29 \pm 0.028 \times 10^{-3} \text{ M h}^{-1} \text{ mg}^{-1}$ ,  $K_m \text{ L-alanine} = 4.9 \pm 0.51 \times 10^{-3} \text{ M}$ ,  $K_m \text{ D-glucose} = 0.21 \pm 0.018 \times 10^{-3} \text{ M}$ ,  $K_i \text{ D-glucose} = 1.76 \pm 0.19 \times 10^{-3} \text{ M}$ ; CRL:  $k_{cat} = 0.75 \pm 0.08 \times 10^{-3} \text{ M h}^{-1} \text{ mg}^{-1}$ ,  $K_m \text{ L-alanine} = 56.2 \pm 5.7 \times 10^{-3} \text{ M}$ ,  $K_m \text{ D-glucose} = 16.2 \pm 1.8 \times 10^{-3} \text{ M}$ ,  $K_i \text{ D-glucose} = 21.0 \pm 1.9 \times 10^{-3} \text{ M}$ .

Chapter **SIX** describes potentiality of some of the amino acyl esters of carbohydrates as inhibitors towards Angiotensin Converting enzyme (ACE) activity. The esters tested are: L-alanyl-D-glucose **16a-e**, L-alanyl-lactose **22a-c**, L-valyl-D-glucose **25a-e**, L-valyl-D-fructose **28a-c**, L-valyl-D-arabinose **29a-c**, L-valyl-D-ribose **30a-c**, L-valyl-maltose **31a,b**, L-valyl-D-mannitol **33**, L-leucyl-D-glucose **34a-e**, L-leucyl-D-fructose **37**, L-leucyl-D-ribose **39a-c**, L-leucyl-D-sorbitol **43**, L-isoleucyl-D-glucose **44a,b**, L-isoleucyl-D-fructose **47a-c**, L-isoleucyl-D-ribose **49a-c** and L-isoleucyl-maltose **51a-c**. Amino acyl esters of carbohydrates tested for ACE inhibition activity showed  $IC_{50}$  values for ACE inhibition in the 0.7 mM to 6.0 mM range. Among them, L-isoleucyl-D-glucose **44a,b** ( $IC_{50}$ :  $0.7 \pm 0.067 \text{ mM}$ ), L-leucyl-D-fructose **37** ( $IC_{50}$ :  $0.9 \pm 0.08 \text{ mM}$ ), L-

isoleucyl-maltose **51a-c** ( $IC_{50}$ :  $0.9 \pm 0.09$  mM) and L-valyl-D-mannitol **33** ( $IC_{50}$ :  $1.0 \pm 0.092$  mM) showed the best ACE inhibitory activities.

## *References*

- Adachi S, Kobayashi T. Synthesis of esters by immobilized-lipase-catalyzed condensation reaction of sugars and fatty acids in water-miscible organic solvent. **J Biosci Bioeng** 2005; 99:87-94.
- Adlerhorst K, Björking F, Godtfredsen SE, Kirk O. Enzyme catalyzed preparation of 6-*O*-acylglucopyranosides. **Synthesis** 1990; 1: 112-115.
- Aires-Barros MR, Cabral JMS, Willson RC, Hamel JFP, Cooney CL. Esterification-coupled extraction of organic acids. Partition enhancement and underlying reaction and distribution equilibria. **Biotechnol Bioeng** 1989; 34: 909-915.
- Akoh CC, Copper C, Nwosu CV. Lipase-G catalyzed synthesis of monoglycerides in organic solvent and analysis by HPLC. **J Am Oil Chem Soc** 1992; 69: 257-260.
- Alhir S, Markajis S, Chandan R. Lipase of *Penicillium caseicolum*. **J Agri Food Chem** 1990; 38: 598-601.
- Andujar-Sanchez M, Camara-Artigas A, Jara-Perez V. Purification of angiotensin-I converting enzyme from pig lung using concanavalin-A sepharose chromatography. **J Chromatogr B. Analyt Technol Biomed Life Sci** 2003; 783: 247-52.
- Arcos JA, Hill-Jr CG, Otero C. Kinetics of the lipase catalyzed synthesis of glucose esters in acetone. **Biotech Bioeng** 2001; 73: 104-110.
- Arroyo M, Sanchez-Monter JM, Sinisterra JV. Thermal stabilization of immobilized lipase B from *Candida antarctica* on different supports: Effect of water activity on enzymatic activity in organic media. **Enzyme Microb Technol** 1999; 24: 3-12.
- Athawale V, Manjrekar N, Athawale M. Lipase-catalyzed synthesis of geranyl methacrylate by transesterification: study of reaction parameters. **Tetrahedron Lett** 2002; 43: 4797-4800.
- Ayala G, Gomez-Puyou T, Gomez-Puyou A, Darzon A. Thermostability of membrane enzymes in organic solvents. **FEBS Lett** 1986; 20: 41- 43.
- Bacola M, Stubbs MJ, Sotriffer C, Hauer B, Fiendrich T, Dittrich K, Klebe G. Structural and energetic determinants for enantio-preferences in kinetic resolutions of lipases. **Protein Eng** 2003; 16: 122-128.
- Belarbi EH, Molina E, Chisti Y. A process for high yield and scaleable recovery of high purity eicosapentaenoic acid esters from micro algae and fish oil. **Enzyme Microb Technol** 2000; 26: 516-529.
- Berger RG. In: *Aroma Biotechnology*. New York, USA: Springer, Berlin Heidelberg; 1955.
- Berglund P, Hutt K. Biocatalytic synthesis of enantiopure compounds using lipases. In: Patel RN, editor. *Stereoselective biocatalysis*. New York: Marcel Dekker; 2000.



- Beuge JA, Aust SD. Microsomal lipid peroxidation. **Methods Enzymol** 1978; 52: 302-309.
- Bevinakatti H, Banerjee A. Lipase catalysis: factors governing transesterification. **Biotechnol Lett** 1988; 10: 397-398.
- Birner-Grunberger R, Scholze H, Faber K, Hermetter A. Identification of various lipolytic enzymes in crude porcine pancreatic lipase preparations using covalent fluorescent inhibitors. **Biotechnol Bioeng** 2004; 85: 147-154.
- Blanchard LA, Gu Z, Brennecke JF. High-pressure phase behavior of ionic liquids/carbon di-oxide systems. **J Phys Chem B** 2001; 105: 2437-2444.
- Blanco RM, Guisan J, Halling PJ. Agarose chymotrypsin as a catalyst for peptide and amino acid ester synthesis. **Biotechnol Lett** 1989; 11: 811-816.
- Blanco RM, Terreros P, Fernandez-Perez M, Otero C, Díaz-González G. Functionalization of mesoporous silica for lipase immobilization Characterization of the support and the catalysts. **J Mol Catal B: Enzym** 2004; 30: 83-93.
- Bloomer S, Adlercreutz P, Mattiasson B. Facile synthesis of fatty acid esters in higher yields. **Enzyme Microb Technol** 1992; 14: 89-97.
- Bloomer S. Lipase-catalyzed lipase modifications in non-aqueous media, Lund, Sweden: Doctoral Dissertation, Lund University; 1992.
- Bock K, Pedersen C. Carbon-13 nuclear magnetic resonance data for monosaccharides. **Adv Carbohydr Chem Biochem** 1983; 41: 27-66.
- Bock K, Pedersen C, Pedersen H. Carbon-13 nuclear magnetic resonance data for oligosaccharides. **Adv Carbohydr Chem Biochem** 1984; 42: 193-225.
- Bornscheuer UT. Enzymes in lipid modification. Weinheim. Berlin: Wiley-VCH; 2000.
- Borzeix F, Monot F, Vandecasteele JP. Strategies for enzymatic esterification in organic solvents: Comparison of microaqueous, biphasic and micellar systems. **Enzyme Microb Technol** 1992; 14: 791-797.
- Bosley JA, Clayton JC. Blueprint for a lipase support: Use of hydrophobic controlled-pore glasses as model system. **Biotechnol Bioeng** 1994; 43: 934-938.
- Bousquet M, Willemot R, Monsan P, Boures E. Enzymatic synthesis of unsaturated fatty acid glucoside esters for dermo-cosmetic applications. **Biotechnol Bioeng** 1999; 63: 730-736.
- Boyer V, Stanchev M, Fairbanks AJ, Davis BG. Ready protease catalysed synthesis of carbohydrate-amino acid conjugates. **Chem Commun** 2001; 19: 1908-1909.
- Brady L, Brzozowski AM, Derewenda U, Derewenda. ZS, Dodson GG, Tolley S, Turkenburg JP, Christiansen L, Huge-Jensen B, Nashkov L, Thim L, Menge U. A

- serine protease triad forms the catalytic center of triglycerol lipase. **Nature** 1990; 343: 767-770.
- Brink LES, Tramper J. Optimization of organic solvent in multiple biocatalysis. **Biotechnol Bioeng** 1985; 27: 1259-1269.
- Brzozowski AM, Derewenda U, Derewenda ZS, Dodson GG, Lawson DM, Turkenburg JP, Bjorkling F, Hugel-Jensen B, Patkar SA, Thim L. A model for interfacial activation in lipases from the structure of a fungal lipase-inhibitor complex. **Nature** 1991; 351: 491-494.
- Brzozowski AM, Derewenda U, Derewenda ZS. A model for interfacial activation in lipases from the structure of a fungal lipase-inhibitor complex. **Nature** 1990; 351: 491-494.
- Bullock C. Immobilised enzymes. **Sci Progress** 1995; 78:119-34.
- Burdock. In: Fenaroli's Handbook of flavor ingredients. 3rd ed. Volume II: CRC press; 1994.
- Camacho Paez B, Robles Medina A, Camacho Rubio F, Gonzalez Moreno P, Molina Grim E. Modeling the effect of free water on enzyme activity in immobilized lipase-catalyzed reactions in organic solvents. **Enzyme Microb Technol** 2003; 33: 845-853.
- Cambou B, Klibanov AM. Lipase-catalyzed production of optically active acids via asymmetric hydrolysis of esters. Effect of the alcohol moiety. **Appl Biochem Biotechnol** 1984a; 9: 255-260.
- Cambou B, Klibanov AM. Comparison of different strategies for the lipase-catalyzed preparative resolution of racemic acids and alcohols: Asymmetric hydrolysis, esterification and transesterification. **Biotechnol Bioeng** 1984b; 9: 1449-1454.
- Cameron PA, Davison BH, Frymier PD, Barton JW. Direct transesterification of gases by dry immobilized lipase. **Biotechnol. Bioeng** 2002; 78: 251-256.
- Camp JV, Huyghebaert A, Goeman P. In: Christophe AB, editor. Structural modified food fats: Synthesis Biochemistry and use. Champaign: AOCS press; 1998.
- Cardenas F, de-Castro MS, Sanchez-Montero JM, Sinisterra JV, Valmaseda M, Elson SW, Alvarez E. Novel microbial lipases: catalytic activity in reactions in organic media. **Enzyme Microb Technol** 2001; 28: 2-3.
- Carrea G, Ottolina G, Riva S. Role of solvents in the control of enzyme selectivity in organic media. **Trends Biotechnol** 1995; 13: 63-70.
- Carrillo-Munoz JR, Bouvet D, Guibe-Jampel E, Loupy A, Petit A. Microwave-promoted lipase-catalyzed reactions. Resolution of ( $\pm$ )-1-phenylethanol. **J Org Chem** 1996; 61: 7746-49.

- Chand S, Adlercreutz P, Mattiasson B. Lipase-catalysed esterification of ethylene glycol to mono and diesters. The effect of process parameters on reaction rate and production. **Enzyme Microb Technol** 1997; 20: 102-106.
- Chiang WD, Chang SW, Shieh CJ. Studies on the optimized lipase-catalyzed biosynthesis of cis-3-hexen-1-yl acetate in *n*-hexane. **Process Biochem** 2003; 38: 1193-1199.
- Chong-Qian L, Bo-Gang L, Hua-Yi Q, Qi-Lin L, Feng-Peng W, Guo-Lin Z. Three cyclooctapeptides and one glycoside from *Microtoena prainiana*. **J Natur Prod** 2003; 67, 978-982.
- Chowdary GV, Divakar S, Prafulla SG. Modeling on isoamyl isovalerate synthesis from *Rhizomucor miehei* lipase in organic media: optimization studies. **World J Microbiol Biotechnol** 2002; 18: 179-185.
- Chulalaksananukul W, Condoret JS, Combes D. Geranyl acetate synthesis by lipase catalysed transesterification in supercritical carbon dioxide. **Enzyme Microb Technol** 1993; 15: 691-698.
- Chulalaksananukul W, Condort JS, Combes D. Kinetics of geranyl acetate synthesis by lipase catalyzed transesterification in *n*-hexane. **Enzyme Microb Technol** 1992; 14: 293-298.
- Chulalaksananukul W, Condort JS, Delorme P, Willemot RM. Kinetic study of esterification by immobilized lipase in *n*-hexane. **FEBS Lett** 1990; 276: 181-184.
- Claon PA, Akoh CC. Effect of reaction parameters on SP435 lipase-catalyzed synthesis of citronellyl acetate in organic solvent. **Enzyme Microb Technol** 1994b; 16: 835-838.
- Claon PA, Akoh CC. Lipase catalyzed synthesis of terpene esters by trans esterification in *n*-hexane. **Biotechnol Lett** 1994a; 16: 235-240.
- Clifford AA. In: Kiran E, Levelt-Sengers JMH, editors. *Supercritical Fluids: Fundamentals and applications*. Dordrecht: Kluwer Academic Publishers; 1994. p. 449-464.
- Crespo JS, Queiroz N, Nascimento MG, Soldi V. The use of lipases immobilized on poly (ethylene oxide) for the preparation of alkyl esters. **Process Biochem** 2005; 40: 401-409.
- Cushman DW, Cheung HS. A simple substrate for assay for dog lung Angiotensin Converting enzyme. **Federation Proc** 1969; 28; 3019.
- Cushman D.W, Cheung HS. Spectrophotometric assay and properties of the Angiotensin-Converting Enzyme of rabbit lung. **Biochem Pharmacol** 1971; 20: 1637-1648.

- Cygler M, Grochulski P, Kazlauskas RS, Schrag JD, Bouthillier F, Rubin B, Serreqi AN, Gupta AK. A structural basis for the chiral preferences of lipases. **J Am Chem Soc** 1994; 116: 3180-3186.
- Dabulis K, Klibanov AM. Dramatic enhancement of enzymatic activity in organic solvents. **Biotechnol Bioeng** 1993; 41: 566 – 571.
- Dae-Gill K, Yong-Sup L, Hyoung-Ja K, Yun-Mi L, Ho-Sub L. Angiotensin converting enzyme inhibitory phenylpropanoid glycosides from *Clerodendron trichotomum*. **J Ethnopharmacol** 2003; 89: 151-154.
- Deloffre L, Sautiere PE, Huybrechts R, Hens K, Vieau D, Salzet M. Angiotensin converting enzyme inhibition studies by natural leech inhibitors by capillary electrophoresis and competition assay. **Eur J Biochem** 2004; 271: 2101-2106.
- Deng H-T, Xu Z-K, Liu Z-M, Wu J, Ye P. Adsorption immobilization of *Candida rugosa* lipases on polypropylene hollow fiber micro filtration membranes modified by hydrophobic polypeptides. **Enzyme Microb Technol** 2004; 35: 437-443
- De-Lima DP. Synthesis of Angiotensin-Converting Enzyme (ACE) inhibitors: An important class of antihypertensive drugs. **Quim Nova** 1999; 22: 375-381.
- Derewenda U, Brzozowski AM, Lawson D.M, Derewenda ZS. Catalysis at the interface: The anatomy of a conformational change in a triglyceride lipase. **Biochemistry** 1992; 31: 1532-1541.
- Derewenda ZS, Sharp AM. News from the interface: the molecular structure of triacyl glyceride lipases. **Trends Biochem Sci** 1993; 18: 20-25.
- Divakar S, Kiran KR, Harikrishna S, Karanth NG. An improved process for the preparation of esters of organic acids and alcohols. Indian Patent, 1243/DEL/99 No. 191078, 1999.
- Divakar S. Lipase catalysed regioselective esterification of protocatechuic aldehyde. **Indian J Chem Section B** 2003; 42B: 1119-1122.
- Dixon M, Webb EC. Enzymes. Orlando, FL, USA: Academic Press; 1979.
- Donner. Preparation of porcine pancreatic lipase free of co-lipase activity. **Acta Chem Scand B** 1976; 30: 430-434.
- Dordick JS. Enzymatic catalysis in monophasic organic solvents. **Enzyme Microb Technol** 1989; 11: 194 –211.
- Dorm N, Belafi-Bak K, Bartha L, Ehrenstein U, Gubicza L. Manufacture of an environmental-safe bio-lubricant from fusel oil by enzymatic esterification in solvent-free system. **Biochem Eng J** 2004; 21: 229-234.

- Duan G, Ching CB, Lim E, Ang CH. Kinetic study of enantioselective esterification of ketoprofen with *n*-propanol catalysed by an lipase in an organic medium **Biotechnol Lett** 1997; 19: 1051-1055.
- Dubey VK, Jagannadham MB. Procerain, a stable cysteine protease from the latex of *Calotropis procera*. **Phytochem** 2003; 62: 1057-1071.
- Eigtved P. Immobilization of *Humicola* lipase on a particulate macroporous resin. US Patent, 4,798,793, 1989.
- Engel KH, Bohnen M, Dobe M. Lipase catalyzed reaction of chiral hydroxyacid esters. Competition of esterification and transesterification. **Enzyme Microb Technol** 1991; 13: 655-660.
- Feichte C, Faber K, Griengl H. Biocatalytic resolution of long-chain 3-hydroxyalkanoic esters. **Tetrahedron Lett** 1989; 30: 551-552.
- Ferrer M, Cruces MA, Bernable M, Ballesteros A, Plou FJ. Lipase catalysed regio selective acylation of sucrose in two solvent mixtures. **Biotechnol Bioeng** 1999; 65: 10-16.
- Ferrer M, Soliveri J, Plou FJ, Cortes NL, Duarte DR, Christensenc M, Patinob JLC, Ballesterosa A. Synthesis of sugar esters in solvent mixtures by lipases from *Thermomyces lanuginosus* and *Candida antarctica* B, and their antimicrobial properties. **Enzyme Microb Technol** 2005; 36:391-398.
- Fonte N, Harger N, Halling PJ, Barrieros S. Salt hydrates for *In situ* water activity control have acid-base effects on enzymes in non-aqueous media. **Biotechnol Bioeng** 2003; 82: 802-808.
- From M, Adlercreutz P, Mattiasson B. Lipase catalyzed esterification of lactic acid. **Biotechnol Lett** 1997; 19: 315 - 317.
- Gargouri M, Drouet P, Legoy MD. Synthesis of a novel macrolactone by lipase-catalyzed intra-esterification of hydroxy-fatty acid in organic media. **J Biotechnol** 2002; 92: 259-266.
- Gayot S, Santarelli X, Coulon D. Modification of flavonoid using lipase in non-conventional media: effect of the water content. **J Biotechnol** 2003; 101: 29-36.
- Gelo-Pujic M, Guibe-Jampel E, Loupy A, Galema SA, Mathe D. Lipase catalysed esterification of some  $\alpha$ -D-glucopyranosides in dry media under focused microwave irradiation. **J Chem Soc Perkin Trans** 1996; 1: 2777-2780.
- Ghamgui H, Karra-Chabouni M, Gargouri Y. 1-Butyl oleate synthesis by immobilized lipase from *Rhizopus oryzae*: a comparative study between *n*-hexane and solvent-free system. **Enzyme Microb Technol** 2004; 35: 355-363.
- Gill I, Valivety R. Polyunsaturated fatty acids: Part 1. Occurrence, biological activities and applications. **Trends Biotechnol** 1997; 15: 401-409.

- Gillies B, Yamazaki H, Armstrong DW. Production of flavor esters by immobilized lipase. **Biotechnol Lett** 1987; 9: 709-714.
- Glinskii, Guennadi V. Preparation of amino acid-linked glycoamine as antitumor agents that alter cell adhesion. US patent, PCT Int. Appl. WO 98 23, 625 (Cl. C07H5/04), 1998.
- Gordon CM. New developments in catalysis using ionic liquids. **Appl Catal A** 2001; 222: 101-117.
- Gorman LAS, Dordick JS. Organic solvents strip water off enzymes. **Biotechnol Bioeng** 1992; 39: 392-397.
- Goto M, Hatanaka C, Masahiro G. Immobilization of surfactant-lipase complexes and their high heat resistance in organic media. **Biochem Eng J** 2005; 24: 91-94.
- Grochulski P, Bouthillier F, Kazlauskas RJ, Serreqi AN, Schrag JD, Ziomek E, Cygler M. Analogs of reaction intermediates identify a unique substrate binding site in *Candida rugosa* lipase. **Biochem** 1994; 33: 3494-3500.
- Grochulski P, Li Y, Schrag JD, Bouthillier F, Smith P, Harrison D, Rubin B, Cygler M. Insight into interfacial activation from an open structure of *Candida rugosa* lipase. **J Biol Chem** 1993; 268: 12843-12847.
- Grünke S. The influence of conductivity on the Karl Fischer titration. **Food Chem** 2003; 82: 99-105.
- Gubicza L, Kabiri-Badr A, Keoves E., Belafi-Bako. Large-scale enzymatic production of natural flavour esters in organic solvent with continuous water removal. **J Biotechnol** 2000; 84:193-196.
- Gunnlaugsdottir B, Jaremo M, Sivik B. Process parameters influencing ethanolysis of cod liver oil in supercritical carbon dioxide. **J Super Fluids** 1998; 12: 85-93.
- Gutman AL, Shapira. Effect of water on enzymatic activity and stereoselectivity in organic solvents. Trans esterification of a disubstituted malonate diester. **J Chem Soc Chem Commun** 1991; 1467-1468.
- Guvenc A, Kapucu N, Mehmetoglu I. The production of isoamyl acetate using immobilized lipases in a solvent-free system. **Process Biochem** 2002; 38: 379-386.
- Hahn-Hagerdal B. Water activity: a possible external regulator in biotechnical processes. **Enzyme Microb Technol** 1986; 8: 322-327.
- Haines AH. Selective removal of protecting groups in carbohydrate chemistry. **Adv Carbohydrate Chem Biochem** 1981; 39: 13 –70.
- Halling PJ. Lipase catalyzed modification of fats in organic two-phase systems. **Fat Sci Technol** 1990; 92: 74-79.

- Halling PJ. Organic liquids and biocatalysts: theory and practice. **Trends Biotechnol** 1989; 7: 50-52.
- Halling PJ. Salt hydrates for water activity control with biocatalysis in organic media. **Biotechnol Tech** 1992; 6: 271-276.
- Halling PJ. Thermodynamic predictions for biocatalysis in non-conventional media: theory, dynamics predictions and recommendations for experimental design and analysis. **Enzyme Microb Technol** 1994; 16:178-206.
- Hamsaveni DR, Prafulla SG, Divakar S. Optimization of isobutyl butyrate synthesis using central composite rotatable design. **Process Biochem** 2001; 36: 1103-1109.
- Han Y, Chu Y. The catalytic properties and mechanism of cyclohexane/DBSA/water microemulsion system for esterification. **J Mol Cat A: Chemical** 2005; 237: 232-237.
- Harikrishna S, Divakar S, Karanth NG. Enzymatic synthesis of isoamyl acetate using immobilized lipase from *Rhizomucor miehei*. **J Biotechnol** 2001; 87: 193-201.
- Harikrishna S, Karanth NG. Lipase-catalyzed synthesis of isoamyl butyrate. A kinetic study. **Biochim Biophys Acta** 2001; 1547: 262–267.
- Harikrishna S, Manohar B, Divakar S, Prapulla SG, Karanth NG. Optimization of isoamyl acetate production using immobilized lipase from *Mucor miehei* by response surface methodology. **Enzyme Microb Technol** 2000; 26: 132-138.
- Hartmann T, Meyerb HH, Scheper T. The enantioselective hydrolysis of 3-hydroxy-5-phenyl-4-pentenoicacid ethylester in supercritical carbon dioxide using lipases. **Enzyme Microb Technol** 2001; 28: 653-660.
- Hawkin Cl, Davis MJ. Generation and propagation of radical reactions on proteins. **Biochim Biophys Acta** 2001; 1504: 196-219.
- Hermosa J, Pignol D, Kerfelec B, Crenon I, Chapus C, Fontecilla-camps JC. Lipase activation by non-ionic detergents: The crystal structure of the porcine lipase co-lipase-tetraethylene glycol monoctyl ether complex. **J Biol Chem** 1996; 270: 18007-18016.
- Hirakawa H, Kamiya N, Kawarabayashi Y, Nagamune T. Log P effect of organic solvents on a thermophilic alcohol dehydrogenase. **Biochim Biophys Acta** 2005; 1748: 94-99.
- Holmberg K, Lassen B, Stark MB. Enzymatic glycerolysis of a triglyceride in aqueous and non-aqueous emulsions. **J Am Oil Chem Soc** 1989; 66: 1796-1800.
- Hooper NM, Turner AJ. Isolation of two differentially glycosylated forms of peptidyl-dipeptidase A (angiotensin converting enzyme) from pig brain: a re-evaluation of their role in neuropeptide metabolism. **Biochem J** 1987; 241: 625-633.

- Huang SY, Chang HL, Goto M. Preparation of surfactant-coated lipase for the esterification of geraniol and acetic acid in organic solvents. **Enzyme Microb Technol** 1998; 22: 552-557.
- Hult K, Norin T. Enantioselectivity of some lipases: control and prediction. **Ind J Chem** 1993; 32B: 123-126.
- Humeau M, Girardin B, Rovel AM. Effect of the thermodynamic water activity and the reaction medium hydrophobicity on the enzymatic synthesis of ascorbyl palmitate. **J Biotechnol** 1998; 63: 1-8.
- Hyuncheol O, Dae-Gill KC, Hun-Taeg L, Ho-Sub. Four glycosides from the leaves of *Abeliophyllum distichum* with inhibitory effects on angiotensin converting enzyme. **Phytother Res** 2003; 17, 811-813.
- Ide N, Lau BHS, Ryu K, Matsuura H, Itakura Y. Antioxidant effects of fructosyl arginine, a maillard reaction product in aged garlic extract. **J Nutr Biochem** 1999; 10: 372-376.
- Iso M, Chen B, Eguchi M, Kudo T, Shrestha S. Production of biodiesel fuel from triglycerides and alcohol using immobilized lipase. **J Mol Cat B: Enzym** 2001; 16: 53-58
- Ison AP, Dunill P, Lilly M, Macrae AR, Smith C. Enzymic interesterification of fats: immobilization and immuno-gold localization of lipase on ion-exchange resins. **Biocatalysis** 1990; 3: 329-342.
- Iwai M, Okumura S, Tsujisaka Y. Synthesis of terpene alcohol esters by lipase. **Agri Biol Chem** 1980; 44: 2731-2732.
- Jackson MA, King JW. Lipase catalyzed glycerolysis of soybean oil in super critical carbon dioxide. **J Am Oil Chem Soc** 1997; 74: 103-106.
- Jaeger KE, Reetz TM. Microbial lipases from versatile tools for biotechnology. **Trends Biotechnol** 1998; 16: 396-403.
- Jensen RG, de-Jong FA, Clark RM. Determination of lipase specificity. **Lipid** 1983; 18: 239-252.
- Janssen AEM, Sijnsnes BJ, Vakurov AV, Halling PJ. Kinetics of lipase catalyzed esterification in organic media: correct model and solvent effects on parameters. **Enzyme Microb Technol** 1999; 24: 463-470.
- Jeon GJ, Park OJ, Hur BK, Yang JW. Enzymatic synthesis of amino acid-sugar alcohol conjugates in organic media. **Biotechnol Lett** 2001; 23: 929-934.
- Jeric I, Horvat S. Novel ester-linked carbohydrate-peptide adducts: Effect of the peptide substituent on the pathways of intramolecular reactions. **Eur J Org Chem** 2001; 8: 1533 - 1539.



- Johnston CI. Renin-angiotensin system: A dual tissue and hormonal system for cardiovascular control. **J Hypertens** 1992; 10: 13-26.
- Kanwar L, Goswami P. Isolation of a *Pseudomonas* lipase produced in pure hydrocarbon substrate and its application in the synthesis of isoamyl acetate using membrane-immobilised lipase. **Enzyme Microb Technol** 2002; 31:727-735.
- Kawaguchi V, Honda H, Toniguchi-Morimura J, Iwasaki S. The codon CUG is read as serine in an asporogenic yeast *Candida cylindracea*. **Nature** 1989; 341: 164-166.
- Khaled N, Montet D, Pina M, Graille J. Fructose oleate synthesis in a fixed catalyst bed reactor. **Biotechnol Lett** 1991; 13: 167-172.
- Kim KW, Song B, Choi MY, Kim MJ. Biocatalysis in ionic liquids: Markedly enhanced enantioselectivity of lipase. **Org Lett** 2001; 3: 1507-1509.
- Kim J, Haam S, Park DW, Ahn IS, Lee TG, Kim HS, Kim WS. Biocatalytic esterification of  $\beta$ -methylglucoside for synthesis of biocompatible sugar-containing vinyl esters. **Chem Eng J** 2004; 99: 15-22.
- Kim SK, Byun HG, Park PJ, Shahidi F. Angiotensin I converting enzyme inhibitory peptides purified from bovine skin gelatin hydrolysate. **J Agri Food Chem** 2001; 49: 2992-2997.
- Kiran KR, Divakar S. Enzyme inhibition by *p*-cresol and lactic acid in lipase mediated syntheses of *p*-cresyl acetate and stearoyl lactic acid: A kinetic study. **World J Microbiol Biotechnol** 2002; 18: 707 - 712.
- Kiran KR, Divakar S. Lipase catalysed esterification of organic acids with lactic acid. **J Biotechnol** 2001; 87: 109-121.
- Kiran KR, Harikrishna H, Suresh Babu CV, Karanth NG, Divakar S. An esterification method for determining lipase activity. **Biotechnol Lett** 2000; 22: 1511-1514.
- Kiran KR, Karanth N. G, Divakar S. An improved enzymatic process for the preparation of fatty acid hydroxyacid ester. Indian Patent, 1978/DEL/98:187313, 1998
- Kiran KR, Manohar B, Divakar S. A central composite rotatable design analysis of lipase catalysed synthesis of lauroyl lactic acid at bench-scale level. **Enzyme Microb Technol** 2001a; 29: 122-128.
- Kiran KR, Suresh-Babu CV, Divakar S. Thermostability of porcine pancreas lipase in non-aqueous media. **Process Biochem** 2001b; 36: 885-892.
- Kirk O, Bjorkling F, Godfredsen SE, Larsen TS. Fatty acid specificity in lipase catalysed synthesis of glucoside esters. **Biocatalysis** 1992; 6:127-134.
- Kittleson JR, Pantaleone. Enzymic biphasic process for the synthesis of aromatic esters flavoring agents from corresponding carboxylic acid and alcohol by esterification mediated by a lipase from *Candida cylindracea*. US. Patent, 5,437,991, 1994.

- Klibanov AM. Enzymes that work in organic solvents. **Chem Technol** 1986; 16: 354-359.
- Klnc A, Teke M, Onal S, Telefoncu A. Immobilization of pancreatic lipase on chitin and chitosan. **Preparative Biochem Biotechnol** 2006; 36: 153-163.
- Knez Z, Leitgeb M, Završnik D, Lavrie B. Synthesis of oleic acid esters with immobilized lipase. **Fat Sci Technol** 1990; 4: 169-172.
- Krieger N, Bhatnagar T, Baratti JC, Baron AM, De-Lima VM, Mitchell D. Non-aqueous biocatalysis in heterogeneous solvent systems. **Food Technol Biotechnol** 2004; 42: 279-286.
- Kuhl P, Halling PJ, Jakubke H-D. Chymotrypsin suspended in organic solvents with salt hydrates is a good catalyst for peptide synthesis from mainly undissolved reactants. **Tetrahedron Lett** 1990; 31: 5213 –5216.
- Kumar R, Modak J, Madras G. Effect of the chain length of the acid on the enzymatic synthesis of flavors in supercritical carbon dioxide. **Biochem Eng J** 2005; 23: 199-202.
- Kumura H, Mikawa K, Saito Z. Influence of milk proteins on the thermostability of the lipase *Pseudomonas fluorescens*. **J Dairy Sci** 1993; 76: 2164-2167.
- Kung S, Rhee J. Effect of solvents on hydrolysis of olive oil by immobilized lipase in reverse phase system. **Biotechnol Lett** 1989; 11: 37-42.
- Kvittingen L. Some aspects of biocatalysis in organic solvents. **Tetrahedron** 1994; 50: 8253-8274.
- Kvittingen L, Sjørsnes B, Anthonsen T, Halling PJ. Use of salt hydrate pairs to buffer optimal water level during lipase catalyzed synthesis in organic media. A practical procedure for organic chemists. **Tetrahedron** 1992; 48: 2793-2802.
- Laane C, Boeren S, Vos K, Veeger C. Rules for optimization of biocatalysis in organic solvents. **Biotechnol Bioeng** 1987; 30: 81-87.
- Laemmli UK. Cleavage of structural proteins during assembly of the head bacteriophage T4. **Nature** 1970; 227: 680-685.
- Langrand G, Rondot N, Triantaphylides C, Baratti J. Short-chain flavor esters synthesis by microbial lipases. **Biotechnol Lett** 1990; 12: 581-586.
- Langrand G, Triantaphylides C, Baratti J. Lipase catalysed formation of flavor esters. **Biotechnol Lett** 1988; 10: 549-554.
- Lau RM, Rantwijk FV, Seddon K R, Sheldon RA. Lipase catalyzed reactions in ionic liquids. **Org Lett** 2000; 2: 4189-91.

- Lee SB. Enzyme reaction kinetics in organic solvents: A theoretical kinetic model and comparison with experimental observations. **J Ferm Bioeng** 1995; 79: 479-484.
- Leszczak JP, Tran-Minh C. Optimized enzymatic synthesis of methyl benzoate in organic medium. Operating conditions and impact of different factors on kinetics. **Biotechnol Bioeng** 1998; 60: 556-561.
- Li GH, Le GW, Yong-Hui S, Shrestha S. Angiotensin I-converting enzyme inhibitory peptides derived from food proteins and their physiological and pharmacological effects. **Nutr Res** 2004; 24: 469-486.
- Liese A, Seelbach K, Wandrey C. Industrial biotransformations. Weinheim: Wiley-VCH; 2000.
- Lindsay JP, Clark DS, Dordick JS. *Penicillin* amidase is activated for use in non-aqueous media by lyophilizing in the presence of KCl. **Enzyme Microb Technol** 2002; 31: 193-197.
- Lohith K, Divakar S. *Candida rugosa* catalyzed preparation of L-prolyl, L-phenylalanyl, L-tryptophanyl and L-histidyl esters of carbohydrates. **Biochem Eng J** 2007; 34: 28-43.
- Lohith K, Divakar S. Lipase catalysed synthesis of L-phenylalanine esters of D-glucose. **J Biotechnol** 2005; 117: 49-56.
- Lohith K, Somashekar BR, Manohar B, Divakar S. An improved enzymatic process for the preparation of amino acyl esters of disaccharides. Indian patent, 285/NF/2006, 2006.
- Lohith K, Vijaya-kumar GR, Manohar B, Divakar S. An improved enzymatic process for the preparation of amino acyl esters of mono and disaccharides. Indian Patent, NF-492/03, PCT/03/00466, 2003.
- Longhi S, Fasetti F, Grandori R, Lotti M, Vanoni M, Alberghina L. Cloning and nucleotide sequences of two lipase genes from *Candida cylindracea*. **Biochim Biophys Acta** 1992; 1131: 227-23
- Lortie R, Trani M, Ergon F. Kinetic study of the lipase catalysed synthesis of triolein. **Biotechnol Bioeng** 1993; 41: 1021-1026.
- Loupy A, Petit A, Hamelin J, Texier-Boullet F, Jacquault P, Mathe D. New solvent free organic synthesis using focused microwaves. **Synthesis** 1998; 2: 1213-1234.
- Lowry OH, Rosenbrough NJ, Farr AL, Randal RJ. Protein measurement with Folin-Phenol reagent. **J Biol Chem** 1951; 193: 265-275.
- Ma L, Persson M, Adlercreutz P. Water activity dependence of lipase catalysis in organic media explains successful transesterification reactions. **Enzyme Microb Technol** 2002; 31: 1024-1029.

- Macedo AC, Tavares TG, Malcata FX. Esterase activities of intracellular extracts of wild strains of lactic acid bacteria isolated from Serra da Estrela cheese **Food Chem** 2003; 81: 379-381.
- Macedo GA, Pastore GM, Rodrigues MI. Optimising the synthesis of isoamyl butyrate using *Rhizopus* sp. lipase with a central composite rotatable design. **Process Biochem** 2004; 39: 687-692.
- Macrea AR. Biocatalyst in organic synthesis. In: Tramper J, Vander-Plas HC, Linko P, editors. Amsterdam: Elsevier; 1985. p. 195-208.
- Malcata FX, Reyes HR, Garcia HS, Hill JCG. Immobilized lipase reactors for modifications of fats and oils. **J Am Oil Chem Soc** 1990; 67: 890-910.
- Mancheno JM, Pernas MA, Martinez MJ, Ochoa B, Ruo ML, Hermosa JA. Structural insights into the lipase/esterase behavior in the *Candida rugosa* family: crystal structure of the lipase 2 isozyme at 1.97 Å resolution. **J Mol Biol** 2003; 332: 1059-1069.
- Manini P, Napolitano A, d'Ischia M. Reaction of D-glucose with phenolic amino acids: further insights into competition between Maillard and Pictet-Spengler condensation pathways. **Carbohydr Res** 2005; 340: 2719 – 2727.
- Manjon A, Iborra JL, Arocas A. Short-chain flavor ester synthesis by immobilized lipase in organic media. **Biotechnol Lett** 1991; 13: 339-334.
- Manohar B, Divakar S. Application of surface plots and statistical designs to selected lipase catalysed esterification reactions. **Process Biochem** 2004a; 39: 847-851.
- Manohar B, Divakar S. Porcine pancreas lipase acetylation of beta-cyclodextrin anchored 4-t-butylcyclohexanol. **Indian J Chem Section B** 2004b; 43B: 2661-2665.
- Manohar B, Divakar S. Application of central composite rotatable design to lipase catalyzed syntheses of *m*-cresyl acetate. **World J Microbiol Biotechnol** 2002; 18: 745-751.
- Marlot C, Langrand G, Triantaphylides C, Baratti J. Ester synthesis in organic solvent catalyzed by lipase immobilized on hydrophilic supports. **Biotechnol Lett** 1985; 7: 647-650.
- Martinelle M, Holmquist M, Hult K. On the interfacial activation of *Candida antarctica* lipase A and B as compared with *Humicola lanuginosa* lipase. **Biochim Biophys Acta** 1995; 1258: 272-276.
- Marty A, Chulalaksunakul W, Willemot RM, Condoret JS. Kinetics of lipase-catalyzed esterification in supercritical carbon dioxide. **Biotechnol Bioeng** 1992; 39: 273-76.
- Maruyama T, Nagasawa SI, Goto M. Enzymatic synthesis of sugar esters in organic solvents. **J Biosci Bioeng** 2002; 94: 357-361.

- Mestri S, Pai JS. Effect of moisture on lipase catalyzed esterification of geraniol palmrosa oil in non-aqueous system. **Biotechnol Lett** 1994a; 17: 459-461.
- Mestri S, Pai JS. Synthesis of isoamyl butyrate by lipase by lipase of *Mucor miehei*. **PAFAI J** 1994b. 2: 24-26.
- Michal G. Biochemical Pathways. New York: John Wiley and Sons; 1999.
- Michaud A, Williams TA, Chauvet MT, Corvol P. Substrate dependence of angiotensin I-converting enzyme inhibition: captopril displays a partial selectivity for inhibition of N-acetyl-seryl-aspartyl-lysyl-proline hydrolysis compared with that of angiotensin I. **Mol Pharmacol** 1997; 51: 1070-1076.
- Miller C, Austin H, Posorske L, Gonzelez J. Characteristics of an immobilized lipase for the commercial synthesis of esters. **J Am Oil Chem Soc** 1988; 65: 927-931.
- Mishio T, Takahashi K, Yoshimoto T, Kodera Y, Saito Y, Inada Y. Terpene alcohol ester synthesis by polyethylene glycol modified lipase in benzene. **Biotechnol Lett** 1987; 9: 187-190.
- Mullally MM, Meisel H, Fitz-Gerald RJ. Synthetic peptides corresponding to  $\alpha$ -lactalbumin and  $\beta$ -lactoglobulin sequences with angiotensin-I-converting enzyme inhibitory activity. **Biol Chem** 1996; 377: 259-260.
- Murakata T, Yusa K, Yada M, Kato Y, Sato S. Esterification activity of lipase entrapped in reverse micelles formed in liquefied gas. **J Chem Eng Japan** 1996; 29: 277-281.
- Nagayama K, Yamasaki N, Imai M. Fatty acid esterification catalyzed by *Candida rugosa* lipase in lecithin microemulsion-based organogels. **Biochem Eng J** 2002.12: 231-236.
- Nakamura K, Takobe Y, Kitayama T, Ohno A. Effect of solvent structure on enantioselectivity of lipase-catalyzed transesterification. **Tetrahedron Lett** 1991; 32: 4941-4944.
- Naoe K, Ohsa T, Kawagoe M, Imai M. Esterification by *Rhizopus delemar* lipase in organic solvent using sugar ester reverse micelles. **Biochem Eng J** 2001; 9: 67-72.
- Nara SJ, Harjani JR, Salunkhe MM. Lipase-catalysed transesterification in ionic liquids and organic solvents: a comparative study. **Tetrahedron Lett** 2002; 43: 2979-2982.
- Nara SJ, Mohile SS, Harjani JR, Naik PU, Salunkhe MM. Influence of ionic liquids on the rates and regioselectivity of lipase-mediated biotransformations on 3,4,6-tri-O-acetyl-D-glucal. **J Mol Cat B: Enzym** 2004; 28: 39-43.
- Ngrek S. Synthesizing power of liver lipase. **Acta Biol Exptl** 1947; 14: 157-174.

- Noel M, Combes D. Effects of temperature and pressure on *Rhizomucor miehei* lipase stability. **J Biotechnol** 2003; 102: 23-32.
- Noureddini H, Gao X, Philkana RS. Immobilized *Pseudomonas cepacia* lipase for biodiesel fuel production from soybean oil. **Biores Technol** 2005; 96: 769-777.
- Ongino H, Miyamoto K, Yasuda M, Ishimik, Ishikawa H. Growth of organic solvent - tolerant *Pseudomonas aeruginosa* LST-03 in the presence of various organic solvents and production of lipolytic enzyme in the presence of cyclohexane. **Biochem Eng J** 1999; 4: 1-6.
- Orrenius C, Norin T, Hult K, Carrea G. The *Candida antarctica* lipase B catalysed kinetic resolution of seudenol in non-aqueous media of controlled water activity. **Tetrahedron Asym** 1995; 12: 3023-3030.
- Osorio NM, Ferreira-Dias S, Gusmao JH, Da-Fonseca MMR. Response surface modelling of the production of  $\omega$ -3 polyunsaturated fatty acids-enriched fats by a commercial immobilized lipase **J Mol Cat B: Enzym** 2001; 11: 677-686.
- Pabai F, Kermasha S, Morin A. Interesterification of butter fat by partially purified extracellular lipases from *Pseudomonas putida*, *Aspergillus niger* and *Rhizopus oryzae*. **World J Microbiol Biotechnol** 1995a; 11:669-77.
- Pabai F, Kermasha S, Morin A. Lipase from *Pseudomonas fragi* CRDA 323: partial purification, characterization and interesterification of butter fat. **Appl Microbiol Biotechnol** 1995b; 43:42-51.
- Paiva AL, Balcao FVM, Malcata X. Kinetics and mechanisms of reactions catalyzed by immobilized lipases. **Enzyme Microb Technol** 2000; 27: 187-204.
- Palomo JM, Segura RL, Mateo C, Terreni M, Guisan JM, Fernandez-Lafuente R. Synthesis of enantiomerically pure glycidol via a fully enantioselective lipase-catalyzed resolution. **Enzyme Microb Technol** 2003; 33: 97-103.
- Parida S, Dordick JS. Substrate structure and solvent hydrophobicity control: lipase catalysis and enantioselectivity in organic media. **J Am Chem Soc** 1991; 113: 2253-2259.
- Parida S, Dordick JS. Tailoring lipase specificity by solvent substrate chemistries. **J Org Chem** 1993; 58: 3238-3244.
- Park OJ, Jeon G. J, Yang JW. Protease catalysed synthesis of disaccharide amino acid esters in organic media. **Enzyme Microb Technol** 1999; 25: 455-462.
- Park OJ, Park HG, Yang JW. Enzymatic transesterification of monosaccharides and amino acid esters in organic solvents. **Biotechnol Lett** 1996; 18: 473-478.
- Park S, Kazlauskas RJ. Improved preparation and use of room temperature ionic liquids in lipase-catalyzed enantio- and regioselective acylation. **J Org Chem** 2001; 66: 8395-8401.

- Parke M-C, Besson T, Lamare S, Legoy M-D. Microwave radiation can increase the rate of enzyme-catalyzed reactions in organic media. **Tetrahedron Lett** 1996; 37: 8383-8386.
- Partridge J, Harper N, Moore B, Halling PJ. Enzymes in Nonaqueous Solvents Methods and Protocols In Series: Methods in Biotechnology 2001 p. 227-234.
- Partridge J, Dennison PR, Moore BD, Halling PJ. Activity and mobility of subtilisin in low water organic media: hydration is more important than solvent dielectric. **Biochim Biophys Acta** 1998; 1386: 79-89.
- Patel Y, Seddon KR, Dutta L, Fleet A. Green Industrial Application of Ionic Liquids. In Rogers RD, Seddon KR, Volkov S, editors. NATO Science Series II: Mathematics, Physics and Chemistry; 2002. p 492-499
- Pernas M, Lopez C, Prada A, Hermoso J, Rua ML. Structural basis for the kinetics of *Candida rugosa* Lip1 and Lip3 isoenzymes. **Colloids Surfaces B: Biointerfaces** 2002; 26: 67-74.
- Perng CH, Kearney AS, Patel K, Palepu NR, Zuber G. Investigation of formulation approaches to improve the dissolution of SD-210661, a poorly water soluble 5-lipoxygenase inhibitor. *Int J Pharmacol* 1998; 176: 31-38.
- Perraud R, Laboret F. Optimization of methyl propionate production catalyzed by *Mucor miehei* lipase. **Appl Microbiol Biotechnol** 1989; 44: 321-326.
- Peschke G. Active components and galenic aspects of enzyme preparations. In: Lankisch PG, editor. Pancreatic enzymes in health and disease. Berlin: Springer; 1991. p. 55-64
- Pleiss J, Fisher M, Schmid RD. Anatomy of lipase binding site. **Chem Phys Lipids** 1998; 93: 67-80.
- Plou FJ, Cruces MA, Pastor E, Ferrer M, Bernabe M, Ballesterose A. Acylation of sucrose with vinyl esters using immobilized hydrolysis: demonstration that chemical catalysis may interfere with enzymatic catalysis. **Biotechnol Lett** 1999; 21: 635-639.
- Quiros M, Parker MC, Turner NJ. Tuning lipase enantioselectivity in organic media using solid-state buffers. **J Org Chem** 2002; 66: 5074-5079.
- Rahman MBA, Md-Tajudin S, Hussein MZ, Rahman RNZRA, Salleh AB, Basri M. Application of natural kaolin as support for the immobilization of lipase from *Candida rugosa* as biocatalyst for effective esterification. **Appl Clay Sci** 2005; 29: 111- 116.
- Rajan A, Abraham TE. A study on enzymatic starch esterification. MACRO 2004, International Conference on Polymers for Advanced Technologies, Thiruvananthapuram, India, Dec. 15-17, 2004.

- Rantwijk F, Sheldon RA. Enantioselective acylation of chiral amines catalyzed by serine hydrolases. **Tetrahedron** 2004; 60: 501-519.
- Rao P, Divakar S. Lipase catalysed esterification of  $\alpha$ -terpineol with various organic acids application of the Plackett- Burman design. **Process Biochem** 2001; 36: 1125-1128.
- Rao P, Divakar S. Response surface methodological approach for the *Rhizomucor miehei* lipase-mediated esterification of  $\alpha$ -terpineol with propionic acid and acetic anhydride. **World J Microbiol Biotechnol** 2002; 18: 341-345.
- Razafindralambo H, Blecker C, Lognoy G, Marlier M, Wathlet JP, Severin M. Improvement of enzymatic synthesis yields of flavor acetates: the example of isoamyl acetate. **Biotechnol Lett** 1994; 16: 247-250.
- Rees GD, Robinson BH, Stephenson RG. Macrocyclic lactone synthesis by lipases in water-in-oil microemulsions. **Biochim Biophys Acta** 1995; 1257: 239-248.
- Rees GD, Robinson BH. Esterification reactions catalyzed by *Chromobacterium viscosum* lipase in CTAB-based micro-emulsion systems. **Biotechnol Bioeng** 1995; 45: 344-355.
- Reihl O, Bieme KM, Lederer MO, Schwach W. Pyridinium-carbaldehyde: active maillard reaction product from the reaction of hexose with lysine residues. **Carbohyd Res** 2004 ; 339 : 705 – 714.
- Reimann A, Robb DA, Halling PJ. Solvation of CBZ aminoacid nitrophenyl esters in organic media and the kinetics of their transesterification by subtilisin. **Biotechnol Bioeng** 1994; 43: 1081-1086.
- Riva S, Chopineau J, Kieboom APG, Klibanov AM. Protease catalysed regioselective esterification of sugars and related compounds in anhydrous dimethylformamide. **J Am Chem Soc** 1988; 110: 584-589.
- Rizzi M, Stylos P, Riek A, Reuss M. A kinetic study of immobilized lipase catalyzing the synthesis of isoamyl acetate by transesterification in n-hexane. **Enzyme Microb Technol** 1992; 14: 709-714.
- Romero MD, Calvo L, Alba C, Daneshfar A, Ghaziaskar HS. Enzymatic synthesis of isoamyl acetate with immobilized *Candida antarctica* lipase in n-hexane. **Enzyme Microb Technol** 2003; 37: 42-48.
- Romero MD, Calvo L, Alba C, Habulin M, Primozić M, Knez Z. Enzymatic synthesis of isoamyl acetate with immobilized *Candida antarctica* lipase in supercritical carbon dioxide. **J Supercrit Fluids** 2005b; 33: 77-84.
- Rosenthal K, Loussale F. Critical micelle concentration determination of non-ionic detergent with Coomassie Brilliant Blue – G 250. **Anal Chem** 1983; 55: 1115-1117.



- Ru MT, Dordick JS, Reimer JA, Clark DS. Optimizing the salt-induced activation of enzymes in organic solvents: effect of lyophilization time and water content. **Biotechnol Bioeng** 1999; 63: 233-241.
- Ru MT, Hirokane SY, Lo AS, Dordick JS, Reimer JA, Clark DS. On the salt-induced activation of lyophilized enzymes in organic solvents: effect of salt osmoticity on enzyme activity. **J Am Chem Soc** 2000; 122: 1565-1571.
- Ru MT, Wu KC, Lindsay JP, Dordick JS, Reimer JA, Clark DS. Towards more active biocatalysts in organic media: increasing the activity of salt-activating enzyme. **Biotechnol Bioeng** 2001; 75: 187-196.
- Rubio E, Fernandez-Mayorales A, Klivanov AM. Effect of the solvent on enzyme regioselectivity. **J Am Chem Soc** 1991; 113: 695-696.
- Sagiroglu A, Kilinc A, Telefoncu A. Preparation and properties of lipases immobilized on different supports. **Artif Cell Blood Substit Immobil Biotechnol** 2004; 32: 625-636
- Sakurai T, Margolin AL, Russell AJ, Klivanov AM. Control of enzyme enantioselectivity by the reaction medium. **J Am Chem Soc** 1988; 110: 7236-7237.
- Sarney DB, Barnard MJ, MacManus DA, Vulfson EN. Application of lipases to the regioselective synthesis of sucrose fatty acid monoesters. **J Am Oil Chem Soc** 1996; 73: 1481-1487.
- Sarney DB, Vulfson EN. Application of enzymes to the synthesis of surfactants. **Trends Biotechnol** 1995; 13: 164-172.
- Sato S, Murakata T, Suzuki T, Goto Y. Comparative study of esterification activity in organic medium between adsorptively immobilized and covalently immobilized lipase. **J Chem Eng Japan** 1999; 32: 350-353.
- Scharpe S, Uyttenbroeck W, Samyn N. Pancreatic enzyme replacement. In: Lauwers A, Scharpe S, editors. *Pharmaceutical enzymes*. New York: Marcel Dekker, INC; 1997. p 187-221.
- Schlotterbeck A, Lang S, Wray V, Wagner F. Lipase catalyzed monacylation of fructose. **Biotechnol Lett** 1993; 15: 61-64.
- Schrag JD, Crygler M. Lipase and  $\alpha/\beta$  hydrolase fold. **Methods Enzymol** 1997; 284: 85-107.
- Schrag JD, Li Y, Wu S, Cygler M. Ser-His-Glu triad forms the catalytic site of the lipase from *Geotrichum Candidum*. **Nature** 1996; 351: 761-764.
- Schreier P, Winterhalter P. In: *Progress in flavor precursor studies*. USA: Allured Carol Stream; 1993.

- Scilimati A, Ngooi TK, Sih CJ. Biocatalytic resolution of ( $\pm$ )-hydroxyalkanoic esters. A strategy for enhancing the enantiomeric specificity of lipase-catalyzed ester hydrolysis. **Tetrahedron Lett** 1988; 29: 4927-4930.
- Segel IH. Enzyme Kinetics. 2nd ed. New York, USA: John-Wiley and Sons; 1993. p 826-882.
- Segura RL, Betancor L, Palomo JM, Hidalgo, Fernandez-Lorente G, Terreni Mateo C, Cortes A, Fernandez-Lafuente R, Guisan JM. Purification and identification of different lipases contained in PPL commercial extracts: A minor contaminant is the main responsible of most esterase activity. **Enzyme Microb Technol** 2006; 39: 817-823.
- Sharma R, Chisti Y, Banerjee UC. Production, purification, characterization, and applications of lipases. **Biotechnol Adv** 2001; 19: 627-662.
- Sheih C J, Akoh CC, Yee LN. Optimized enzymatic synthesis of geranyl butyrate with lipase AY from *Candida rugosa*. **Biotechnol Bioeng** 1996; 51: 371-374.
- Sheih CJ, Akoh CC, Koehler PE. Four-factor response surface optimization of the enzymatic modification of triolein to structured lipids. **J Am Oil Chem Soc** 1995; 72: 619-623.
- Sheldon RA. Chirotechnology: Designing economic chiral syntheses. **J Chem Technol Biotechnol** 1996; 67: 1-14.
- Shiraki K, Kudou M, Nishikori S, Kitagawa H, Imanaka T, Takagi M. Arginine ethyl esters prevents thermal aggregation and inactivation of lysozyme. **Eur J Biochem** 2004; 271: 3242-3247.
- Somashekar BR, Divakar S. Lipase catalyzed synthesis of L-alanyl esters of carbohydrates. **Enzyme Microb Technol** 2007; 40: 299-309.
- Somashekar BR, Lohith K, Manohar B, Divakar S. Inhibition of *Rhizomucor miehei* and *Candida rugosa* lipases by D-glucose in esterification between L-alanine and D-glucose **J Biosci Bioeng** 2007; 103: 122-128.
- Soo E, Salleh AB, Basri M, Noor-zaliha R, Abdul-Rahman R, Kamaruddin K. Optimization of the enzyme-catalyzed synthesis of amino acid-based surfactants from palm oil fractions. **J Biosci Bioeng** 2003; 95: 361-367.
- Srivastava S, Madras S, Modak J. Esterification of myristic acid in supercritical carbon dioxide. **J Supercrit Fluids** 2003; 27: 55-64.
- Stahl M, Jeppsson – Wistrand U, Mansson MO. Induced stereoselectivity and substrate selectivity of bioimprinted  $\alpha$ -chymotrypsin in anhydrous organic solvents. **J Am Chem Soc** 1991; 113: 9366 – 9368.
- Stamatis H, Xenakis A, Kolisis FN. Bioorganic reactions in microemulsions: the case of lipases. **Biotechnol Adv** 1999; 17: 293-318.

- Stamatis H, Xenkis A, Menge V, Kolisis NF. Kinetic study of lipase catalyzed esterification in microemulsion. **Biotechnol Bioeng** 1993; 42: 931-937.
- Suresh-Babu CV, Divakar S. Selection of alcohols through Plakett-Burman design in lipase catalyzed syntheses of anthranilic acid. **J Am Oil Chem Soc** 2001; 78: 49-52.
- Suzuki Y, Shimizu T, Takeda H, Kanda K. Fermentative or enzymatic manufacture of sugar amino acid esters. Japan Patent, 03216194 A2, 1991.
- Swatloski RP, Spear SK, Holbrey JD, Rogers RD. Dissolution of cellulose with ionic liquids. **J Am Chem Soc** 2002; 124: 4974-4975.
- Takahashi K, Saito Y, Inada Y. Lipases made active in hydrophobic media. **J Am Oil Chem Soc** 1988; 65: 911-916.
- Talon R, Montel MC, Berdague JL. Production of flavor esters by lipases of *Staphylococcus warneri* and *Staphylococcus xylosus*. **Enzyme Microb Technol** 1996; 19: 620-622.
- Tamura M, Shoji M, Nakatsuka T, Kinomura K, Okai H, Fukui S. Methyl 2,3-di-(L- $\alpha$ -amimobutyryl)- $\alpha$ -D-glucopyranoside, a sweet substance and tastes of related compounds of neutral amino acids and D-glucose derivatives. **Agric Biol Chem** 1985; 49: 2579 -2586.
- Therisod M, Klibanov AM. Facile enzymatic preparation of mono acylated sugars in pyridine. **J Am Chem Soc** 1986; 108: 5638-5640.
- Tischer W, Wedekind F. Immobilized enzymes: methods and applications. **Top Curr Chem** 1999; 200: 95-126
- Torres C, Otero C. Part I. Enzymatic synthesis of lactate and glycolate esters of fatty alcohols. **Enzyme Microb Technol** 1999; 25: 745-752.
- Tramper J, Vermie MH, Beetink HH, Von-Stocker U. Biocatalysis in non-conventional media. Amsterdam: Elsevier; 1992.
- Trani M, Ergan F, Andre G. Lipase catalyzed production of wax esters. **J Am Oil Chem Soc** 1991; 68: 20-22.
- Turner NA, Duchateau DB, Vulfson EN. Effect of hydration on thermostability of serine esterases. **Biotechnol Lett** 1995; 17: 371-376.
- Ulbrich R, Golbik R, Schelleberger A. Protein adsorption and leakage in carrier-enzyme systems. **Biotechnol Bioeng** 1991; 37: 280-287.
- Undurraga D, Markovits A, Erazo S. Cocoa butter equivalent through enzymic interesterification of palm oil mid-fraction. **Process Biochem** 2001; 36: 933-9.

- Vacek M, Zarevucka M, Wimmer Z, Stransky K, De-merpva K, Legoy M-D. Selective enzymic esterification of free fatty acids with *n*-butanol under microwave irradiation and under classical heating. **Biotechnol Lett** 2000; 22: 1565-70.
- Valivety RH, Halling PJ, Macrae AR. Water as a competitive inhibitor of lipase-catalysed esterification in organic media. **Biotechnol Lett** 1993; 15: 1133-1138.
- Valiveti RH, Johnston GA, Suckling CJ, Halling PJ. Solvent effect on Biocatalysis in organic systems: equilibrium position and rates of lipase catalysed esterification. **Biotechnol Bioeng** 1991; 38: 1137-43.
- Valivety RH, Johannes LL, Rakels L, Blanco RM, Johnston RM, Brown L, Suckling CJ, Halling PJ. Measurement of pH changes in an inaccessible aqueous phase during biocatalysis in organic media. **Biotechnol Lett** 1990a; 12: 475-480.
- Valivety RH, Rakel JLL, Blanco RM, Johnston G, Brown L, Suckling CJ, Halling PJ. Water as a competitive inhibitor of lipase-catalyzed esterification in organic media. **Biotechnol Lett** 1990b; 12: 475-480.
- van-Tilbeurgh H, Sarda L, Verger R, Cambillau C. Structure of the pancreatic lipase-procolipase complex. **Nature** 1992; 359: 159-162.
- Van-Tol JBA, Odenthal JB, Jongejan JA, Duine JA. Relation of enzyme reaction rate and hydrophobicity of the solvent. In: Tramper J, Vermue MH, Beetink HH, Von-Stocker U, editors. *Biocatalysis in non-conventional media*. Amsterdam: Elsevier;1992. p. 229-235.
- Vecchia RD, Sebrao D, Nascimento MG, Soldi V. Carboxymethylcellulose and poly (vinyl alcohol) used as a film support for lipases immobilization. **Process Biochem** 2005; 40: 2677-2682.
- Verger R, De-Hass K, Sarda L, Desnuelle P. Purification from porcine pancreas of two molecular species with lipase activity. **Biochem Biophys Acta** 1969; 188: 272-282.
- Vermeirssen V, Van-Camp J, Verstraete W. Optimisation and validation of an angiotensin-converting enzyme inhibition assay for the screening of bioactive peptides. **J Biochem Biophys** 2002; 51: 75-87.
- Vermue MH, Tramper J. Biocatalysis in non-conventional media. Medium engineering aspects. **Pure Appl Chem** 1995; 67: 345-373.
- Vijayakumar GR, Lohith K, Somashekar BR, Divakar S. Lipase catalysed synthesis of L-alanyl, L-leucyl and L-phenylalanyl esters of D-glucose using unprotected amino acids. **Biotechnol Lett** 2004; 26: 1323-1328.
- Vogel I. A text book of quantitative inorganic analysis. Potentiometric titrations, 3rd edition. London: ELBS and Langman group Ltd; 1961. p. 944-948.
- Volkin DB, Staubli A, Langer R, Klibanov AM. Enzyme thermo inactivation in anhydrous organic solvents. **Biotechnol Bioeng** 1991; 37: 843-853.

- Vorderwulbecke T, Kieslich K, Erdmann H. Comparison of lipases by different assays. **Enzyme Microb Technol** 1992; 14: 631-639.
- Vulfson EN. Enzymatic synthesis of food ingredients in low water media. **Trends Food Sci Technol** 1993; 4: 209-215.
- Vulfson EN. Industrial applications of lipases In: Wolley P, Petersen SB, editors. *Lipases: Their Structure Biochemistry and Application*. New York, USA: Cambridge University Press; 1994.
- Wei Y, Schottel JL, Derewenda U, Swenson L, Patkar S, Derewenda ZS. A novel variant of the catalytic triad in the *Streptomyces scabies* esterase. **Nat Struc Biol** 1995; 2: 218 – 223.
- Welsh FW, Williams RE, Dawson KH. Lipase-mediated synthesis of low molecular weight flavor esters. **J Food Sci** 1990; 55: 1679-1682.
- Welsh FW, Williams RE. Lipase-mediated production of ethyl butyrate and butyl butyrate in nonaqueous systems. **Enzyme Microb Technol** 1990; 12: 743-748.
- Wescott CR, Klibanov AM. The solvent dependence of enzyme specificity. **Biochim Biophys Acta** 1994; 1206: 1- 9.
- West JB, Hennen WJ, Lalonde JL, Bibbs J, Zhong Z, Meyer EF, Wong CH. Enzymes as synthetic catalyst; mechanistic and active-site considerations of natural and modified chymotrypsin. **J Am Chem Soc** 1990; 112: 5313 – 5320.
- Wheeler CJ, Croteau R. Terpene cyclase catalysis in organic solvent/minimal water media: demonstration and optimization of (+)- $\alpha$ -pinene cyclase activity. **Arch Biochem Biophys** 1986; 248: 429 –434.
- Winkler F, D'Arcy A, Hunziker. Structure of human pancreatic lipase. **Nature** 1990; 343: 771-775.
- Winkler FK, Gubernator K. Structure and mechanism of human pancreatic lipase. In: Wooley, P, Peterson SB, editors. *Lipase: Their structure, Biochemistry and Applications*. Cambridge: Cambridge University Press; 1994. p. 139-157.
- Winterhalter P, Schreier, P. Biotechnology - challenge for the flavor industry. In: Acree TE, Teranishi R, editors. *Flavor science: sensible principle and techniques*. Washington, USA: American Chemical Society; 1993. p 225-258.
- Won K, Kim S, Kim K-J, Park HW, Moon S-J. Optimization of lipase entrapment in Calcium alginate gel beads. **Process Biochem** 2005; 40: 2149-2154.
- Wu J, Ding X. Characterization of inhibition and stability of soy-protein derived angiotensin-I-converting enzyme inhibitory peptides. **Food Res Int** 2002; 35: 367-375.

- Wu JC, Song BD, Xing AH, Hayashi Y, Talukder MMR, Wang SC. Esterification reactions catalyzed by surfactant-coated *Candida rugosa* lipase in organic solvents. **Process Biochem** 2002; 37: 1229-1233.
- Wu JY, Liu SW. Influence of alcohol concentration on lipase-catalyzed enantioselective esterification of racemic naproxen in isooctane: under controlled water activity. **Enzyme Microb Technol** 2000; 26: 124-130.
- Xu K, Klibanov AM. pH control of the catalytic activity of cross-linked enzyme crystals in organic solvents. **J Am Chem Soc** 1996; 118: 9815 - 9819.
- Xu Y, Wang D, Qing-Mu X, Ao-Zhao G, Zhang KC. Biosynthesis of ethyl esters of short chain fatty acids using whole-cell lipase from *Rhizopus Chinesis* CCTCCM 201021 in non aqueous phase. **J Mol Cat B: Enzym** 2002; 18: 29-37.
- Yadav GD, Devi KM. Immobilized lipase-catalysed esterification and transesterification reactions in non-aqueous media for the synthesis of tetrahydrofurfuryl butyrate: comparison and kinetic modeling. **Chem Eng Sci** 2004; 59: 373-383.
- Yadav GD, Lathi PS. Synthesis of citronellol laurate in organic media catalyzed by immobilized lipases: kinetic studies. **J Mol Cat B: Enzym** 2004; 27: 113-119.
- Yadav GD, Trivedi, A.H. Kinetic modeling of immobilized-lipase catalysed transesterification of *n*-octanol with vinyl acetate in non-aqueous media. **Enzyme Microb Technol** 2003; 32: 783-789.
- Yadav, GD, Lathi PS Kinetics and mechanism of synthesis of butyl isobutyrate over immobilised lipases. **Biochem Eng J** 2003; 16: 245-252.
- Yang Z, Russel AJ. Enzymatic reactions in organic media. In: Koskienen AMP, Klibanov AM, editors. London: Blackie; 1996. p. 43-69.
- Ye P, Xu ZK, Wang ZG, Wu J, Deng HT, Seta P.. Comparison of hydrolytic activities in aqueous and organic media for lipases immobilized on poly (acrylonitrile-co-maleic acid) ultrafiltration hollow fiber membrane. **J Mol Cat B: Enzym** 2005; 32: 115-121.
- Yuan Y, Bai S, Sun Y. Comparison of lipase-catalysed enantioselective esterification of ( $\pm$ )-menthol in ionic liquids and organic solvent. **Food Chem** 2006; 97: 324-330.
- Zacharis E, Omar IC, Patridge J, Robb DA, Halling J. Selection of salt hydrates pair for use in water control in enzyme catalysis in organic solvent. **Biotechnol Bioeng** 1997; 55: 367-371.
- Zaidi A, Gainer JL, Carta G, Mrani A, Kadiri T, Belarbi Y, Mir A. Esterification of fatty acids using nylon-immobilized lipase in *n*-hexane: kinetic parameters and chain length effects. **J Biotechnol** 2002; 93: 209-216.
- Zaks A, Dodds DR. Applications of biocatalysts and biotransformations to the synthesis of pharmaceuticals. **Drug Dev Today** 1997; 2: 513 -531.

- Zaks A, Klibanov AM. Enzyme catalysis in monophasic organic solvents. **J Biol Chem** 1988; 263: 3194-201.
- Zaks A, Klibanov AM. Substrate specificity of enzymes in organic solvents vs. water is reversed. **J Am Chem Soc** 1986; 108: 2767-2768.
- Zaks A, Klibanov AM. The effect of water on enzyme activity in organic media. **Proc Natl Acad Sci USA** 1985; 82: 3192-3196.
- Zhang T, Yang L, Zhu Z. Determination of internal diffusion limitation and its macroscopic kinetics of the transesterification of CPB alcohol catalyzed by immobilized lipase in organic media. **Enzyme Microb Technol** 2005; 36: 203-209.
- Zhou GW, Li GZ, Xu J, Sheng Q. Kinetic studies of lipase-catalyzed esterification in water-in-oil microemulsions and the catalytic behavior of immobilized lipase in MBGs. **Colloids and Surfaces A: Physicochem Eng Aspects** 2001; 194: 41-47.
- Zhu K, Jutila A, Tuominen EKJ, Patkar SA, Svendsen A, Kinnunen PK. Impact of the tryptophan residues of *Humicola lanuginosa* lipase on its thermal stability. **Biochim Biophys Acta** 2001; 1547: 329-38.

*Publications*





## Lipase catalyzed synthesis of L-alanyl, L-leucyl and L-phenylalanyl esters of D-glucose using unprotected amino acids

Giriyapura R. Vijayakumar, Kenchaiah Lohith, Bhandya R. Somashekar & Soundar Divakar\*  
Department of Fermentation Technology and Bioengineering, Central Food Technological Research Institute,  
Mysore-570020, India

\*Author for correspondence (Fax: 0821-521713; E-mail: divakar@cscftri.res.nic.in)

Received 6 May 2004; Revisions requested 27 May 2004; Revisions received 18 June 2004; Accepted 21 June 2004

**Key words:** L-alanyl-D-glucose, esterification, lipase, L-leucyl-D-glucose, L-phenylalanyl-D-glucose

### Abstract

Enzymatic synthesis of L-alanyl, L-leucyl and L-phenylalanyl esters of D-glucose was carried out in a non-polar solvent using lipases from *Rhizomucor miehei* and porcine pancreas. The unprotected amino acids at millimolar concentrations were used in presence of 10 to 50% (w/w) glucose of the lipases to give ester yields up to >99%. The reaction mixture on analysis by 2-D NMR showed that the product is a mixture of 6-*O*-, 3-*O*- and 2-*O*-monoesters and 2,6-di-*O*- and 3,6-di-*O*-esters.

### Introduction

Amino acid esters of glucose are used as detergents, as sweetening agents, as emulsifying agents, as microcapsules in pharmaceutical preparations, as bio-active nucleoside amino acid esters, as antibiotics and in the delivery of biological active agents (Margolin 1993, Zaks & Dodds 1997, Kirk *et al.* 1992). Earlier reports on the synthesis of amino acyl esters of sugars using lipases involved use of amino acids which are *N*-protected and carboxyl group activated (Suzuki *et al.* 1991, Riva *et al.* 1988, Therisod & Klivanov 1986, Park *et al.* 1999, Boyer *et al.* 2001, Maruyama *et al.* 2002).

Riva *et al.* (1988) carried out the reaction between *N*-acetyl-L-phenylalanyl chloroester and D-glucose in pyridine using subtilisin which resulted in 73% conversion to the three mono esters (80% of 6-*O*-, 15% of 3-*O*- and 5% of 2-*O*-). Park *et al.* (1999) reported that 98% of 6-*O*-*t*-Boc-L-phenylalanyl glucose was formed when the reaction was carried out between *N*-*t*-Boc-L-phenylalanyl trifluoroester and glucose in pyridine using subtilisin. They also reported that lipase from porcine pancreas and Lipozyme IM20 gave insignificant results. Reactions were conducted in shake flasks using lesser quantity of substrate and larger

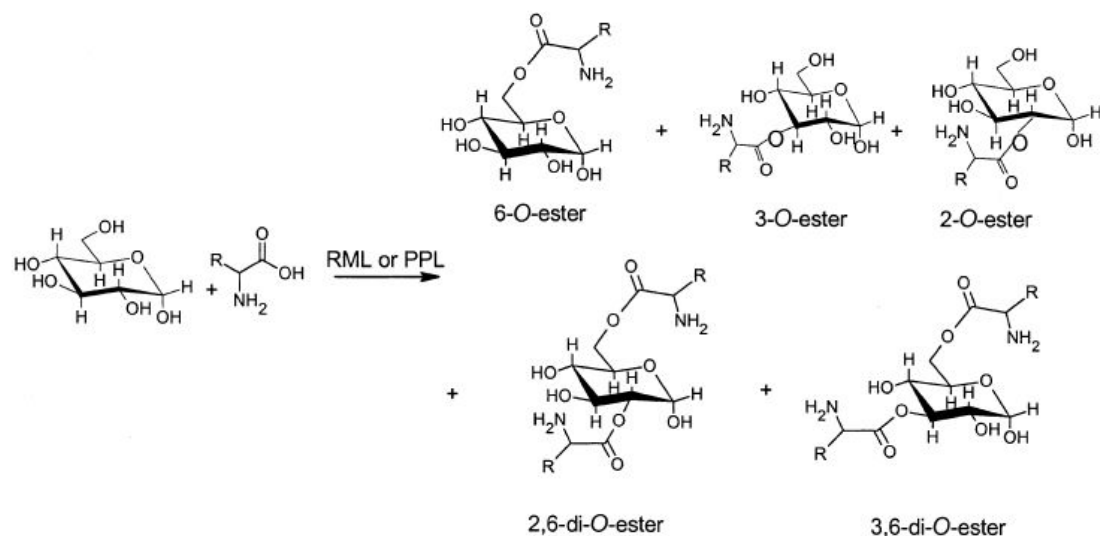
quantity of enzymes. Specific microbial enzymes like Optimase M-440 and subtilisin were employed, in some cases with longer periods of incubation up to 7 d.

We report here on an enzymatic method using *Rhizomucor miehei* lipase (RML) and porcine pancreas lipase (PPL) for the preparation of L-alanyl, L-leucyl and L-phenylalanyl esters of D-glucose (Scheme 1). This investigation employed free unprotected amino acids and the results are presented below.

### Materials and methods

#### Materials

Porcine pancreas lipase Type II, Steapsin (PPL), was from Sigma and Lipozyme IM20 (*Rhizomucor miehei*) (RML) immobilized on weak anion exchange resin was from Novo Nordisk, Denmark. L-Alanine, L-leucine and L-phenylalanine from HiMedia Ind. Ltd. were used as such. Solvents were employed after distilling once before use. Both *Rhizomucor miehei* and porcine pancreas lipases employed showed esterification activities of 0.46  $\mu\text{mol min}^{-1} \text{mg}^{-1}$  enzyme preparation and 0.06  $\mu\text{mol min}^{-1} \text{mg}^{-1}$  enzyme preparation respectively (Kiran *et al.* 2000).



Scheme 1.

#### Esterification procedure

Typically about 1–10 mmol L-amino acid (L-alanine/L-leucine/L-phenylalanine) and D-glucose (1–2.5 mmol) was refluxed with 100 ml dichloromethane/dimethylformamide (90:10 v/v) or hexane/chloroform/dimethylformamide (45:45:10 v/v) or chloroform/dimethylformamide (90:10 v/v) in presence of 0.018–0.225 g lipases (10%–50% w/w D-glucose) for 3 d. Solvents which formed an azeotrope with water were refluxed and the condensed solvent vapors were passed through a desiccant before being returned into the reaction mixture, thereby facilitating complete removal of water (Lohith *et al.* 2003, Divakar *et al.* 1999), thereby maintaining a very low water activity of  $a_w = 0.0054$  throughout the reaction. The reaction mixture after distilling off the solvent was then added to 20 ml water, stirred and filtered to remove the lipase. The filtrate was evaporated on a water bath to get the unreacted glucose, unreacted amino acid and the product esters which were analysed by HPLC. In reactions which involved use of buffer salts, buffers were added to the reaction mixture to impart 'pH memory' to the enzyme. 0.1 M acetic acid/acetate buffer at pH 4 and pH 5, 0.1 M  $\text{Na}_2\text{HPO}_4/\text{NaH}_2\text{PO}_4$  at pH 6 and pH 7 and 0.1 M  $\text{Na}_2\text{B}_4\text{O}_7/\text{HCl}$  at pH 8 buffers were employed.

#### Product monitoring and characterization

Analytical HPLC was performed using an aminopropyl column (3.9 × 300 mm length) and acetonitrile/water at 80:20 (v/v) as the mobile phase at  $1 \text{ ml min}^{-1}$  and a refractive index detector. Conversion yields were determined from HPLC peak areas of D-glucose esters and unreacted D-glucose. Error measurements in HPLC yields will be  $\pm 5\%$ . Retention times are (min): glucose 5.2, L-alanine 9.4, L-alanyl-D-glucose 11.9; L-leucine 6.4, L-leucyl-D-glucose 8.3; L-phenylalanine 6.2, L-phenylalanyl-D-glucose 9.1. L-Phenylalanyl-D-glucose esters were separated from unreacted D-glucose and L-phenylalanine by subjecting the reaction mixture to repeated HPLC.

Products were characterized by recording one-dimensional  $^1\text{H}$  and  $^{13}\text{C}$  NMR and two-dimensional NMR spectra.  $^1\text{H}$  and  $^{13}\text{C}$  NMR spectra were recorded on a Bruker DRX 500 MHz spectrometer (500.13 MHz proton and 125 MHz carbon frequencies) operating at 20 °C. Proton and carbon 90° pulse widths were 12.25 and 10.5  $\mu\text{s}$  respectively. Samples (50 mg) were dissolved in 1:1 DMSO- $d_6$  and  $\text{D}_2\text{O}$  mixture and signals were referenced to TMS to within  $\pm 0.01$ . Two dimensional Heteronuclear Single Quantum Coherence Transfer Spectra (2-D HSQCT) were recorded in magnitude mode with the sinus-

oidal shaped Z gradients of strength 25.7, 15.42 and 20.56 G cm<sup>-1</sup> in the ratio of 5:3:4 applied for a duration of 1 ms each with a gradient recovery delay of 100  $\mu$ s to defocus unwanted coherences which was incremented in 256 steps. The 2D data was accumulated on 4K size computer memory. The spectra were processed using unshifted and  $\pi/4$  shifted sine bell window function in F<sub>1</sub> and F<sub>2</sub> dimensions respectively.

NMR data for L-alanyl-D-glucose esters: 6-O-ester: <sup>1</sup>H NMR  $\delta_{\text{ppm}}$ : (500.13 MHz) 3.35 ( $\alpha$ CH), 1.54 ( $\beta$ CH<sub>3</sub>, J = 7.81), 4.8 (H-1 $\beta$ ), 3.4 (H-4 $\alpha$ ), 3.25 (H-4 $\beta$ ), 4.05 (H-6 $\alpha$ ), 3.84 (H-6 $\beta$ ); <sup>13</sup>C NMR  $\delta_{\text{ppm}}$ : (125 MHz) 53.3 ( $\alpha$ CH), 16 ( $\beta$ CH<sub>3</sub>), 175.4 (CO), 96.8 (C<sub>1</sub> $\beta$ ), 71 (C<sub>4</sub> $\alpha$ ), 65.4 (C<sub>6</sub> $\beta$ ); 3-O-ester <sup>1</sup>H  $\delta_{\text{ppm}}$ : 3.9 ( $\alpha$ CH), 4.2 (H-3 $\alpha$ ), 4.25 (H-3 $\beta$ ); <sup>13</sup>C  $\delta_{\text{ppm}}$ : 52.4 ( $\alpha$ CH), 175.2 (CO), 84 (C<sub>3</sub> $\alpha$ ), 84.1 (C<sub>3</sub> $\beta$ ); 2-O-ester <sup>1</sup>H  $\delta_{\text{ppm}}$ : 3.79 ( $\alpha$ CH), 4.05 (H-2 $\alpha$ ), 4.06 (H-2 $\beta$ ); <sup>13</sup>C  $\delta_{\text{ppm}}$ : 51.8 ( $\alpha$ CH), 76.5 (C<sub>2</sub> $\alpha$ ), 79.5 (C<sub>2</sub> $\beta$ ); 2,6-di-O-ester <sup>1</sup>H  $\delta_{\text{ppm}}$ : 3.24 (H-2 $\alpha$ ), 3.75 (H-6 $\alpha$ ) <sup>13</sup>C  $\delta_{\text{ppm}}$ : 75.7 (C<sub>2</sub> $\alpha$ ), 62.1 (C<sub>6</sub> $\alpha$ ); 3,6-di-O-ester <sup>1</sup>H  $\delta_{\text{ppm}}$ : 3.4 (H-3 $\alpha$ ), 3.76 (H-6 $\alpha$ ) <sup>13</sup>C  $\delta_{\text{ppm}}$ : 77 (C<sub>3</sub> $\alpha$ ), 59.9 (C<sub>6</sub> $\alpha$ ); NMR data for L-leucyl-D-glucose esters: 6-O-ester: <sup>1</sup>H  $\delta_{\text{ppm}}$ : 3.08 ( $\alpha$ CH), 2.51 ( $\beta$ CH<sub>2a</sub>), 1.57 ( $\gamma$ -CH), 0.81 ( $\delta$ ,  $\epsilon$ -CH<sub>3</sub>), 3.86 (H-6 $\alpha$ ); <sup>13</sup>C  $\delta_{\text{ppm}}$ : 53.5 ( $\alpha$ CH), 36 ( $\beta$ CH<sub>2</sub>), 25.3 ( $\gamma$ CH), 22.5 ( $\delta$ -CH<sub>3</sub>), 23 ( $\epsilon$ -CH<sub>3</sub>), 173.6 (CO), 102.5 (C<sub>1</sub> $\alpha$ ), 65 (C<sub>6</sub> $\alpha$ ); 3-O-ester <sup>1</sup>H  $\delta_{\text{ppm}}$ : 3.15 ( $\alpha$ CH), 1.5 ( $\gamma$ -CH), 0.77 ( $\delta$ ,  $\epsilon$ -CH<sub>3</sub>), 3.86 (H-2 $\beta$ ), 3.97 (H-3 $\alpha$ ), 3.88 (H-3 $\beta$ ); <sup>13</sup>C  $\delta_{\text{ppm}}$ : 50 ( $\alpha$ CH), 25 ( $\gamma$ CH), 23.3 ( $\delta$ -CH<sub>3</sub>), 23.1 ( $\epsilon$ -CH<sub>3</sub>), 84 (C<sub>3</sub> $\alpha$ ), 83.2 (C<sub>3</sub> $\beta$ ); 2-O-ester <sup>1</sup>H  $\delta_{\text{ppm}}$ : 2.8 ( $\alpha$ CH), 0.75 ( $\delta$ ,  $\epsilon$ -CH<sub>3</sub>), 3.79 (H-2 $\alpha$ ); <sup>13</sup>C  $\delta_{\text{ppm}}$ : 46.1 ( $\alpha$ CH), 23.4 ( $\delta$ -CH<sub>3</sub>), 23.9 ( $\epsilon$ -CH<sub>3</sub>), 76.9 (C<sub>2</sub> $\alpha$ ); 2,6-di-O-ester <sup>1</sup>H  $\delta_{\text{ppm}}$ : 3.45 (H-2 $\alpha$ ), 3.44 (H-6 $\alpha$ ); <sup>13</sup>C  $\delta_{\text{ppm}}$ : 75.5 (C<sub>2</sub> $\alpha$ ), 62.8 (C<sub>6</sub> $\alpha$ ); 3,6-di-O-ester <sup>1</sup>H  $\delta_{\text{ppm}}$ : 3.68 (H-3 $\alpha$ ), 3.45 (H-6 $\alpha$ ); <sup>13</sup>C  $\delta_{\text{ppm}}$ : 82.5 (C<sub>3</sub> $\alpha$ ), 63.1 (C<sub>6</sub> $\alpha$ ); NMR data for L-phenylalanyl-D-glucose esters: 6-O-ester <sup>1</sup>H  $\delta_{\text{ppm}}$ : 2.66 ( $\alpha$ CH, J = 6.8, 3.4), 2.89 ( $\beta$ CH<sub>2a</sub>); 2.76 ( $\beta$ CH<sub>2b</sub>), aromatic-7.2 (H<sub>2,6</sub>), 7.25 (H<sub>3,5</sub>), 7.27 (H<sub>4</sub>), 4.24 (H-1 $\alpha$ ), 3.47 (H-2 $\alpha$ ), 3.51 (H-2 $\beta$ ), 3.55 (H-4 $\alpha$ ), 3.63 (H-5 $\alpha$ ), 3.72 (H-6 $\alpha$ ); <sup>13</sup>C  $\delta_{\text{ppm}}$ : 51.85 ( $\alpha$ CH), 36.91 ( $\beta$ CH<sub>2</sub>), aromatic-137.92 (C<sub>1</sub>), 126.23 (C<sub>2</sub>, C<sub>6</sub>), 128.07 (C<sub>3</sub>, C<sub>5</sub>), 129.17 (C<sub>4</sub>), 174 (C=O), 102.46 (C<sub>1</sub> $\alpha$ ), 69.57 (C<sub>2</sub> $\alpha$ ), 69.56 (C<sub>2</sub> $\beta$ ), 69.6 (C<sub>4</sub> $\alpha$ ), 68.92 (C<sub>5</sub> $\alpha$ ), 70.2 (C<sub>5</sub> $\beta$ ), 62.97 (C<sub>6</sub> $\alpha$ , C<sub>6</sub> $\beta$ ); 3-O-ester <sup>1</sup>H  $\delta_{\text{ppm}}$ : 2.63 ( $\alpha$ CH), 3.12 ( $\beta$ CH<sub>2a</sub>), 3.69 (H-3 $\alpha$ ), 3.81 (H-3 $\beta$ ), 3.52 (H-6 $\alpha$ ); <sup>13</sup>C  $\delta_{\text{ppm}}$ : 52.3 ( $\alpha$ CH), 37.46 ( $\beta$ CH<sub>2</sub>), aromatic-137.8 (C<sub>1</sub>), 173.2 (C=O), 101.09 (C<sub>1</sub> $\alpha$ ), 81.33 (C<sub>3</sub> $\alpha$ ), 83.49 (C<sub>3</sub> $\beta$ ), 60.93 (C<sub>6</sub> $\alpha$ ); 2-O-ester <sup>1</sup>H  $\delta_{\text{ppm}}$ : 2.55 ( $\alpha$ CH), 3.02 ( $\beta$ CH<sub>2a</sub>), 3.8 (H-2 $\alpha$ ), 3.79 (H-2 $\beta$ ), 3.38 (H-6 $\alpha$ ); <sup>13</sup>C  $\delta_{\text{ppm}}$ : 52.8 ( $\alpha$ CH), 37.91 ( $\beta$ CH<sub>2</sub>), 172 (C=O), 96.72 (C<sub>1</sub> $\alpha$ ), 75.1 (C<sub>2</sub> $\alpha$ ),

Table 1. Effect of L-leucine concentration on the synthesis of L-leucyl-D-glucose<sup>a</sup>.

Amount (equiv.)	Conversion yield <sup>b</sup> (%) with:	
	PPL	RML
1	17.8	0.2
2	3.6	6.6
3	8.7	6.0
4	6.2	8.2
5	24.4	36.0

<sup>a</sup>D-Glucose (1 mmol) was employed throughout. Temperature -40 °C; time 72 h; solvent-DMF/dichloromethane mixture (10: 90 v/v).

<sup>b</sup>Conversion yields correspond to conversion of L-leucine to L-leucyl-D-glucose ester with respect to D-glucose as measured by HPLC in presence of PPL (porcine pancreas lipase) and RML (*Rhizomucor miehei* lipase).

77.32 (C<sub>2</sub> $\beta$ ), 62.8 (C<sub>6</sub> $\alpha$ ); 2,6-di-O-ester <sup>1</sup>H  $\delta_{\text{ppm}}$ : 3.42 (H-6 $\alpha$ ), 3.63 (H-2 $\alpha$ ), 3.65 (H-2 $\beta$ ); <sup>13</sup>C  $\delta_{\text{ppm}}$ : 76.21 (C<sub>2</sub> $\alpha$ , C<sub>2</sub> $\beta$ ), 63.2 (C<sub>6</sub> $\alpha$ ); 3,6-di-O-ester <sup>1</sup>H  $\delta_{\text{ppm}}$ : 3.51 (H-6 $\alpha$ ), 3.64 (H-3 $\alpha$ ), 3.54 (H-3 $\beta$ ); <sup>13</sup>C  $\delta_{\text{ppm}}$ : 81.33 (C<sub>3</sub> $\alpha$ ), 82.4 (C<sub>3</sub> $\beta$ ), 63 (C<sub>6</sub> $\alpha$ ).

## Results

### L-Leucyl-D-glucose ester

Esterification of D-glucose with L-leucine using RML and PPL was studied in detail.

### Effect of enzyme concentration

Effect of increasing enzyme concentration on the synthesis of L-leucyl-D-glucose ester was studied by employing various RML concentrations ranging from 10% to 50% (w/w) D-glucose. The results showed that the yields obtained were very low. The enzyme showed the highest yield of 10.8% at 20% enzyme concentration. With the increase in enzyme concentration from 10% (5.7% yield) to 20% (10.8% yield) there was an increase in esterification and beyond 30% there was decrease (30%–0.2% yield, 50%–0.3% yield) in esterification probably due to hydrolysis of the esters formed.

### Effect of L-leucine concentration

Effect of L-leucine concentrations at a fixed RML and PPL concentrations of 30% (w/w of D-glucose) on

Table 2. Lipase mediated synthesis of L-alanyl-D-glucose<sup>a</sup>.

Amino acid (and amount as equiv.)	Enzyme (w/w of glucose used)	Solvent mixture (% by vol.)	Buffer salt	Conversion yield (%)
L-Alanine (2 eq)	RML (40%)	Chloroform+Hexane +DMF (45:45:10)	–	14.3
L-Alanine (2 eq)	RML (50%)	Chloroform+Hexane +DMF (45:45:10)	–	32.2
L-Alanine (1 eq)	RML (30%)	Chloroform+Hexane +DMF (45:45:10)	0.1 M, pH 4 0.1 ml	48
L-Alanine (3 eq)	RML (30%)	Chloroform+Hexane +DMF (45:45:10)	0.1 M, pH 4 0.1 ml	67.1
L-Alanine (4 eq)	RML (30%)	Chloroform+Hexane +DMF (45:45:10)	0.1 M, pH 4 0.1 ml	56.2
L-Alanine (2 eq)	PPL (30%)	Dichloromethane+DMF (90:10)	–	23.6
L-Alanine (2 eq)	PPL (40%)	Dichloromethane+DMF (90:10)	–	28
L-Alanine (2 eq)	PPL (50%)	Dichloromethane+DMF (90:10)	–	23.1
L-Alanine (2 eq)	PPL (40%)	Dichloromethane+DMF (90:10)	0.1 M, pH 5 0.1 ml	28.9
L-Alanine (2 eq)	PPL (40%)	Dichloromethane+DMF (90:10)	0.1 M, pH 6 0.1 ml	22.3
L-Alanine (2 eq)	PPL (40%)	Dichloromethane+DMF (90:10)	0.1 M, pH 7 0.1 ml	16

<sup>a</sup>Conversion yields from HPLC with respect to D-glucose. D-Glucose was used at 1 mmol throughout; temperature 40–60 °C; time 72 h.

the synthesis of L-leucyl-D-glucose ester was studied by increasing the L-leucine concentration from 1 to 5 molar eq (Table 1). The results showed that better conversions could be achieved with both the enzymes at 5 equiv of L-leucine.

#### Effect of buffer salts on esterification

Depending on the method of preparation, the enzyme always possesses a micro-aqueous layer around it. Buffer salts dissolve in such a micro aqueous layer and stabilize the enzyme structure against denaturation and subsequent loss of activity in non-polar solvents. A buffer of known pH and volume was added to the reaction mixture and their effect on imparting 'pH memory' to the enzyme was studied. Like some esterification reactions (Kiran *et al.* 2001), this reaction also gave better yields in presence of buffer salts.

Effect of buffer salts in terms of pH in the range 4 to 8 with RML at 40% (w/w) of D-glucose on the synthesis of L-leucyl-D-glucose ester at 1:2 molar equiv of D-glucose and L-leucine showed that 0.2 ml pH 5

buffer gave the highest yield of 63%. The yields were: 15.7% at pH 4, 16% at pH 6, 13.7% at pH 7 and 7.3% at pH 8.

The effect of various buffer volumes in the range 0.05 to 0.6 ml by using 0.1 M pH 7 phosphate buffer showed that the esterification yields increased with increase in the buffer volumes from 0.1 ml to 0.6 ml. The yields were: with 0.05 ml 5.2%, 0.1 ml 21.2%, 0.2 ml 29.2%, 0.4 ml 31.8% and 0.6 ml 85.2%. In general, the yields were better in the presence of buffer salts than those in their absence.

#### L-Alanyl-D-glucose ester

Esterification of D-glucose and L-alanine using RML and PPL was carried out. HPLC data showed that the total ester formation was in the range 14.3% to 67.1% (Table 2). The reactions were carried out both in presence and absence of buffer salts. In case of RML, the reaction gave the best conversion at 67% in presence of 0.1 ml 0.1 M acetate buffer, pH 4, with 3 equiv L-alanine (Table 2). In case of PPL, the reaction gave a

Table 3. Lipase mediated synthesis of L-phenylalanyl-D-glucose<sup>a</sup>

Amino acid (and amount as equiv.)	Enzyme (w/w of glucose used)	Solvent mixture (% by vol.)	Buffer salt	Conversion yield (%)
L-Phenylalanine (1 eq)	RML (10%)	Dichloromethane+DMF (90:10)	–	66.6
L-Phenylalanine (1 eq)	RML (40%)	Dichloromethane+DMF (90:10)	–	97.4
L-Phenylalanine (3 eq)	RML (30%)	Dichloromethane+DMF (90:10)	–	30.1
L-Phenylalanine (5 eq)	RML (30%)	Dichloromethane+DMF (90:10)	–	>99
L-Phenylalanine (1 eq)	RML (30%)	Chloroform+Hexane+DMF (45:45:10)	0.1 M, pH 4 0.2 ml	79.6
L-Phenylalanine (1 eq)	RML (30%)	Chloroform+Hexane+DMF (45:45:10)	0.1 M, pH 7 0.2 ml	76.2
L-Phenylalanine <sup>b</sup> (1 eq)	PPL (30%)	Dichloromethane+DMF (90:10)	–	58.3
L-Phenylalanine <sup>b</sup> (1 eq)	PPL (50%)	Dichloromethane+DMF (90:10)	–	69.7
L-Phenylalanine (1 eq)	PPL (30%)	Dichloromethane+DMF (90:10)	0.1 M, pH 4, 0.2 ml	57.5
L-Phenylalanine (1 eq)	PPL (30%)	Dichloromethane+DMF (90:10)	0.1 M, pH 6, 0.2 ml	87.4

<sup>a</sup>Conversion yields were from HPLC with respect to D-glucose. D-glucose was used at 1 mmol otherwise specified; <sup>b</sup>D-glucose and L-phenylalanine 2.5 mmol each; temperature 40–60 °C; incubation period 72 h.

yield of 29% in the presence of 0.1 ml 0.1 M acetate buffer, pH 5, with 2 equiv of L-alanine.

#### L-Phenylalanyl-D-glucose

Esterification of D-glucose with L-phenylalanine was carried out by using RML and PPL. HPLC data showed that the total ester formation of L-phenylalanyl-D-glucose was in the range 10.6 to >99% (Table 3).

RML at 40% (w/w) of glucose showed better esterification (97.4%) than 50% PPL (70%). In presence of buffer salts, 10% higher yields than the control were observed. 0.2 ml 0.1 M, pH 4, acetate buffer with RML at 30% (w/w) of glucose gave the highest yield of 80% and 0.2 ml 0.1 M phosphate buffer, pH 6, with PPL at 30% (w/w) of glucose gave the highest yield of 87%.

#### Discussion

HPLC data showed that the total ester formation in case of L-alanine, L-leucine and L-phenylalanine were

14% to 67%, 0.2 to 85% and 11 to >99%, respectively. Proton and <sup>13</sup>C signals from 2D HSQCT spectra, for C6 from 6-O-, C3 from 3-O- and C2 from 2-O-monoesters and C2 and C6 from 2,6-di-O- and C3 and C6 from 3,6-di-O-esters clearly showed that as many as five esters were formed in this lipase catalyzed reaction in all the three above mentioned amino acids. Similar information could also be deduced from carbonyl and aromatic C1 signals of L-phenylalanyl-D-glucose ester. However, in case of L-alanyl-D-glucose and L-leucyl-D-glucose, the composition of monoesters and diesters were difficult to determine due to overlap of signals. In case of L-phenylalanyl-D-glucose, in an esterification yield of 81%, the composition of esters were found to be: 6-O- 24.1% (62.9 ppm), 3-O- 23.3% (60.9 ppm), 2-O- 19.2% (62.8 ppm), 2,6-di-O- 16.8% (63.2 ppm) and 3,6-di-O- 16.6% (63 ppm). Although, the D-glucose employed showed an  $\alpha$ : $\beta$  anomeric composition of 40:60, the  $\alpha$ -anomer was esterified to a greater extent than the  $\beta$ -anomer in L-leucine (26.1:14.8 in an esterification yield of 41%) and to almost equal extent in case of L-phenylalanine (32.25:32.25 in an esterifi-

fication yield of 80%). The anomeric proton signals of the L-alanyl ester could not be clearly discerned due to overlap of the solvent HDO signal. Since very mild conditions were employed, the NMR data showed <3% peptide formation. The peptide formation was still very much less (<3%) in L-alanine and L-phenylalanine. All the three amino acids gave better yields when the reactions were carried out in the presence of buffer salts.

Even though free unprotected L-amino acids were employed in the present work, comparable yields to other researchers (whose reactions were carried out in shake flasks) were observed. This could be due to the experimental set up employed in the present work which facilitated excellent conversions even with PPL and RML which were reported to be less effective catalysts in converting *N*-protected and carboxyl activated L-amino acids in shake flasks. Even with protected and activated amino acids, earlier works, have yielded only a mixture of 6-*O*-, 4-*O*-, 3-*O*- and 2-*O*-amino acyl esters (Riva *et al.* 1988, Therisod & Klivanov 1986, Park *et al.* 1999, Boyer *et al.* 2001, Maruyama *et al.* 2002). Hence, the present work has shown the effectiveness of PPL and RML in the synthesis of 6-*O*-, 3-*O*- and 2-*O*-monoesters and 2,6-*di-O*- and 3,6-*di-O*-esters from unprotected amino acids in substantial yields.

#### Acknowledgements

The department of Science and Technology, India, is acknowledged for the financial assistance rendered for this project. G.R.V. and K.L. acknowledge Council of Scientific and Industrial Research, India for the Junior Research Fellowship. NMR spectra were recorded at the Sophisticated Instruments Facility, Indian Institute of Science, Bangalore.

#### References

- Boyer V, Stanchev M, Fairbanks AJ, Davis BG (2001) Ready protease catalyzed synthesis of carbohydrate-amino acid conjugates. *Chem. Commun.* 19: 1908–1909.
- Divakar S, Kiran KR, Harikrishna S, Karanth NG (1999) An improved process for the preparation of esters of organic acids and alcohols. Indian Patent 1243/DEL/1999.
- Kiran KR, Hari Krishna S, Sureshbabu CV, Karanth NG, Divakar S (2000) An esterification method for determination of lipase activity. *Biotechnol. Lett.* 22: 1511–1514.
- Kiran KR, Manohar B, Divakar S (2001) A central composite rotatable design analysis of lipase catalysed synthesis of lauroyl lactic acid at bench-scale level. *Enzyme Microb. Technol.* 28: 122–128.
- Kirk O, Bjorkling F, Godfredsen SE, Larson TS (1992) Fatty acid specificity in lipase catalysed synthesis of glucoside esters. *Biocatalyst* 6: 127–134.
- Lohith K, Vijayakumar GR, Manohar B, Divakar S (2003) An improved enzymatic process for the preparation of amino acyl esters of monosaccharides. Indian Patent NF-492/2003.
- Margolin AL (1993) Enzymes in the synthesis of chiral drugs. *Enzyme Microb. Technol.* 15: 266–280.
- Maruyama T, Nagasawa S, Goto M (2002) Enzymatic synthesis of sugar amino acid esters in organic solvents. *J. Biosci. Bioeng.* 94: 357–361.
- Park OJ, Jeon GJ, Yong JW (1999) Protease catalyzed synthesis of disaccharide amino acid esters in organic synthesis. *Enzyme Microbial. Tech.* 25: 455–462.
- Riva S, Chopineau J, Kieboom APJ, Klivanov AM (1988) Protease catalysed regioselective esterification of sugars and related compounds in anhydrous dimethylformamide. *J. Am. Chem. Soc.* 110: 584–589.
- Suzuki Y, Shimizu T, Takeda H, Kanda K (1991) Fermentative or enzymatic manufacture of sugar amino acid esters. Jpn Kokai Tokkyo Koho Japanese Patent JP 03216194 A2 (CA 116:127007b).
- Therisod M, Klivanov AM (1986) Enzymatic preparation of monoacylated sugars in pyridine. *J. Am. Chem. Soc.* 108: 5638–5640.
- Zaks A, Dodds DR (1997) Applications of biocatalyst and and biotransformations to the synthesis of pharmaceuticals. *Drug Dev. Today* 2: 513–531.

## Angiotensin converting enzyme inhibitory activity of amino acid esters of carbohydrates

Vasudeva Kamath<sup>a</sup>, Rajini P.S.<sup>a,\*</sup>, Lohith K.<sup>b</sup>, Somashekar B.R.<sup>b</sup>, Divakar S.<sup>b</sup>

<sup>a</sup> Food Protectants and Infestation Control Department, Central Food Technological Research Institute, Mysore 570 020, India

<sup>b</sup> Fermentation Technology and Bioengineering Department, Central Food Technological Research Institute, Mysore 570 020, India

Received 8 November 2005; received in revised form 18 January 2006; accepted 19 January 2006

Available online 10 March 2006

### Abstract

L-Alanyl-D-glucose, L-valyl-D-glucose, L-phenylalanyl-D-glucose and L-phenylalanyl-lactose esters were synthesized enzymatically using two lipases viz., *Rhizomucor miehei* lipase (RML) and porcine pancreas lipase (PPL) and tested for their potential as inhibitors of angiotensin converting enzyme (ACE) in vitro. The esters exhibited concentration related ACE inhibitory activity. The potency of the various esters measured in terms of IC<sub>50</sub> values were as follows: L-phenylalanyl-D-glucose, IC<sub>50</sub>-0.121 mM (mixture of five diastereomeric esters: 6-O-24.1%; 3-O-23.3%; 2-O-19.2%; 2,6-di-O-16.6% and 3,6-di-O-16.8% from the total yield of 92.4%); L-phenylalanyl-lactose, IC<sub>50</sub>-0.229 mM (mixture of three diastereomeric esters: 6-O-42.1%; 6'-O-30.9%; and 6,6'-di-O-27.0% from the total yield of 50.58%); alanyl-D-glucose, IC<sub>50</sub>-0.23 mM (mixture of five diastereomeric esters: 6-O-46.7%; 3-O-11.5%; 2-O-19.9%; 2,6-di-O-6.6% and 3,6-di-O-15.3% from the total yield of 26.5%) and L-valyl-D-glucose, IC<sub>50</sub>-0.396 mM (mixture of five diastereomeric esters: 6-O-32.4%; 3-O-26.5%; 2-O-26.4%; 2,6-di-O-8.8% and 3,6-di-O-5.9% from the total yield of 68.2%). These in vitro data suggest a potential therapeutic role for the aminoesters of carbohydrates as inhibitors of ACE.

© 2006 Elsevier B.V. All rights reserved.

**Keywords:** Angiotensin converting enzyme inhibitor; L-Alanyl-D-glucose; L-Valyl-D-glucose; L-Phenylalanyl-D-glucose and L-phenylalanyl-lactose; Hypertension

### 1. Introduction

Hypertension is a leading cause of health concern all over the world. Renin angiotensin system (RAS) plays a major role in the development of hypertension and angiotensin converting enzyme (ACE; EC.3.4.15.1) constitutes a key component in this system. ACE raises blood pressure by converting angiotensin-I, released from angiotensinogen by renin, into the potent vasoconstrictor angiotensin-II. ACE also degrades vasodilative bradykinin in blood vessels and stimulates the release of aldosterone in the adrenal cortex. Increased ACE activity has been linked to narrowing of lumen of blood vessels, which results in increased blood pressure [1]. Inhibition of ACE is considered to be an important therapeutic approach for controlling hypertension. ACE inhibitors (viz., captopril, enalapril, fosinopril and ramepril) currently available in the market, exert antihypertensive effect by competitively binding to the active site of ACE

[2]. However, some of the currently used ACE inhibitors have certain limitations like susceptibility to proteolytic degradation leading to side effects such as bronchospasm and dry cough [3]. As a result, there have been renewed efforts in modifying available drugs or in developing new drugs with lesser side effects.

During the past decades, several fundamental studies have led to the search for ACE inhibitors from natural resources. Certain functional foods containing ACE inhibitory compounds have been found to act as alternatives for treatment of hypertension. Most of the food-derived ACE inhibitors are peptidic in nature [4]. Only a few non-peptidic compounds have been reported to possess the ACE inhibitory activity [5]. Park et al. [6] recently discussed the effectiveness of chitooligosaccharides for ACE inhibition while Huang et al. [7] have reported improved ACE inhibitory activity of chitooligosaccharides by carboxyl modification. Interestingly, the existence of carbohydrate-binding center on ACE has been proposed recently [8,9]. While many carbohydrate-peptide conjugates are reported to display a wide variety of potent biological activities of therapeutic value [10–12], use of amino acid esters of carbohydrates as inhibitors of ACE has not been reported so far. The main objective of

\* Corresponding author. Tel.: +91 821 2513210; fax: +91 821 2517233.  
E-mail address: rajini29@yahoo.com (P.S. Rajini).

the present investigation was to enzymatically synthesize amino acid esters of carbohydrates and to determine their potential as ACE inhibitors in vitro.

## 2. Experimental

### 2.1. General methods

*Rhizomucor miehei* lipase (RML) immobilized on a weak anion resin was purchased from Nova Nordisk Denmark, porcine pancreas lipase (PPL) type II, steapsin and *Candida rugosa* lipase (CRL) were purchased from Sigma Chemical Co., USA. Esterification activities for RML, PPL and CRL were found to be 0.46, 0.06 and 0.03  $\mu\text{mol}/\text{min}/\text{mg}$  of enzyme, respectively [13]. L-Amino acids were procured from Hi-Media (India), D-glucose was purchased from SD fine chemicals (India) and lactose was obtained from SISCO Research laboratories (India). Sephadex G-25 was purchased from Pharmacia, Sweden. All solvents used were of analytical grade and were procured from Qualigens Fine Chemicals (India).

### 2.2. Synthesis of amino acid esters of carbohydrates

Esterification was carried out as reported earlier [14] in presence of RML in case of L-alanyl-D-glucose and L-phenylalanyl-D-glucose, CRL in case of L-valyl-D-glucose and PPL in case of L-phenylalanyl-lactose (40% enzyme based on w/w of D-glucose/lactose) by refluxing with stirring 0.005 mol of amino acid (L-alanine, L-valine, L-phenylalanine) and 0.005 mol of D-glucose or 0.0025 mol of lactose in a 100 mL solvent mixture consisting of  $\text{CH}_2\text{Cl}_2$ :DMF (90:10 v/v) or hexane: $\text{CHCl}_3$ :DMF (45:45:10 v/v) in two necked flat bottom flask for 3 days at 40 °C (boiling point of the dichloromethane). The enzyme was imparted with 'pH memory' by employing: 0.1 mL  $\text{Na}_2\text{HPO}_4$  buffer (0.1 mM, pH 7.0) for L-valyl-D-glucose, 0.1 mL  $\text{CH}_3\text{COONa}$  buffer (0.1 mM, pH 4.0) for L-alanyl-D-glucose, 0.2 mL  $\text{CH}_3\text{COONa}$  buffer (0.2 mM, pH 4.0) for L-phenylalanyl-D-glucose and L-phenylalanyl-lactose. To facilitate complete removal of water from the reaction mixture, a very low water activity of  $a_w = 0.0054$  was achieved by condensing azeotropic solvent vapor containing small amount of water of reaction into a desiccant which was then drained back into the reaction mixture [14–17]. The same reactions were carried out in the absence of lipase, which did not show any esterification. After completion of the reaction, the solvent was distilled off and then stirred with 20 mL of water and filtered to remove the lipase. The filtrate containing unreacted substrates and product esters was evaporated to dryness on a water bath and analyzed by HPLC employing a C-18 column or an aminopropyl column [14,17]. Conversion yields were determined from HPLC peak areas of the ester and L-amino acid and expressed as percentage esterification with respect to the L-amino acid concentration. L-Alanyl-D-glucose and L-phenylalanyl-D-glucose were separated from the reaction mixture by repeated HPLC injections and L-valyl-D-glucose and L-phenylalanyl-lactose separated by size exclusion chromatography using Sephadex G-25 with water as eluant. All the esters were characterized by UV, IR and two-

dimensional Heteronuclear Single Quantum Coherence Transfer (2-D-HSQCT) NMR spectra. Two-dimensional HSQCT-NMR spectra were recorded on a Bruker DRX-500 MHz spectrometer at 40 °C by dissolving 40 mg of the sample in  $\text{DMSO-d}_6$ .

### 2.3. ACE inhibitory assay

#### 2.3.1. Preparation of ACE

ACE was prepared from porcine lung acetone powder by following the standard procedure [18]. Fresh pig lung was homogenized with 5–10 volumes of cold acetone in a waring blender. The homogenate was filtered and the residue was dried to remove the acetone. The dried lung acetone powder was stored at  $-20^\circ\text{C}$  and used for ACE extraction. ACE was extracted from the acetone powder as follows: the acetone powder was suspended in 10 volumes of Tris-HCl buffer (125 mM, pH 8.3) containing 1 M NaCl and homogenized. The homogenate was stirred overnight at 4 °C, and then centrifuged at  $30,000 \times g$ , for 20 min at 4 °C. The supernatant (the enzyme) was separated and was stored at  $-20^\circ\text{C}$ .

#### 2.3.2. Determination of ACE activity

ACE activity was determined spectrophotometrically by a modification of the method of Cushman and Cheung [19] using Hippuryl-histidyl-leucine as the substrate. Twenty-five millimole HHL and appropriate quantity of ACE inhibitor were dissolved in Tris-HCl buffer (125 mM, pH 8.3) and incubated with the purified ACE for 60 min at 37 °C. The reaction was terminated by addition of 500  $\mu\text{l}$  of 1 N HCl. The hippuric acid formed by the action of ACE was extracted into 1500  $\mu\text{l}$  of ethyl acetate. After centrifugation at  $800 \times g$  for 10 min, 1000  $\mu\text{l}$  of supernatant was transferred to a separate clean dry test tube and was evaporated to dryness at 80 °C. The residue was dissolved in 1.0 ml of distilled water and the absorbance was measured at 228 nm against distilled water. Concentration-dependent activities of inhibitors were studied and the concentration required to inhibit 50% of ACE activity was defined as the  $\text{IC}_{50}$  value.

## 3. Results and discussion

### 3.1. Chemistry

Two-dimensional heteronuclear single/multiple quantum coherence transfer (HMQCT/HSQCT) NMR data confirmed that three diastereomeric mono esters (2-O-, 3-O- and 6-O-esters) and two diastereomeric diesters (2,6-di-O- and 3,6-di-O-esters) were formed in various proportions in case of L-valyl and L-phenylalanyl esters of D-glucose and two diastereomeric mono esters (6-O- and 6'-O-esters) and one diastereomeric diester (6,6'-di-O-ester) were formed in case of L-phenylalanyl-lactose (Table 1). In case of L-alanyl-D-glucose only  $\beta$ -D-glucose was found to have reacted to give three mono and two di esters (Fig. 1). The composition of various esters were as follows: L-alanyl-D-glucose, mixture of five diastereomeric esters: 6-O-46.7%; 3-O-11.5%; 2-O-19.9%; 2,6-di-O-6.6% and 3,6-di-O-15.3% from the total yield of 26.5%; L-valyl-D-glucose, mixture of five diastereomeric



Table 1  
Composition of mono and diesters of amino acyl-D-glucose esters and their average molecular weights<sup>a</sup>

Ester	6-O-Ester (%)	3-O-Ester (%)	2-O-Ester (%)	3,6-di-O-Ester (%)	2,6-di-O-Ester (%)	6'-O-Ester (%)	6,6'-di-O-Ester (%)	Average molecular weight
L-Alanyl-D-glucose <sup>b</sup>	46.7	11.5	19.9	15.3	6.6	–	–	266.5
L-Valyl-D-glucose <sup>c</sup>	32.4	26.5	26.4	8.8	5.9	–	–	293.5
L-Phenylalanyl-D-glucose <sup>b</sup>	24.1	23.3	19.2	16.8	16.6	–	–	376.3
L-Phenylalanyl-lactose <sup>c</sup>	42.1	–	–	–	–	30.9	27.0	528.7

<sup>a</sup> Percentage compositions of all five esters as determined from <sup>13</sup>C peaks of C-6 of esters.

<sup>b</sup> L-Alanyl-D-glucose and L-phenylalanyl-D-glucose were separated from the reaction mixture by repeated HPLC injections to obtain yields of 26.5% and 92.4% respectively.

<sup>c</sup> L-Valyl-D-glucose and L-phenylalanyl-lactose were separated using sephadex G-25 to obtain yields of 68.2% and 50.58% respectively.

esters: 6-O-32.4%; 3-O-26.5%; 2-O-26.4%; 2,6-di-O-8.8% and 3,6-di-O-5.9% from the total yield of 68.2%; L-phenylalanyl-D-glucose mixture of five diastereomeric esters: 6-O-24.1%; 3-O-23.3%; 2-O-19.2%; 2,6-di-O-16.6% and 3,6-di-O-16.8% from the total yield of 92.4% and L-phenylalanyl-lactose mixture of three diastereomeric esters: 6-O-42.1%; 6'-O-30.9%; and 6,6'-di-O-27.0% from the total yield of 50.58%.

### 3.1.1. L-Alanyl-D-glucose esters

UV: 294.0 nm (log  $\epsilon$  = 2.883), 227.0 nm (log  $\epsilon$  = 3.061); IR: 3371 cm<sup>-1</sup> (NH), 3410 cm<sup>-1</sup> (OH), 2997 cm<sup>-1</sup> (CH) and 1653 cm<sup>-1</sup> (C=O); specific rotation-[ $\alpha$ ]<sub>D</sub> at 25 °C = -38.14°; CMC-2.25 mM (0.056%).

2-O-Ester: <sup>1</sup>H NMR  $\delta_{ppm}$ : (500.13 MHz): 2.95 ( $\alpha$ CH), 1.30 ( $\beta$ CH<sub>3</sub>), 3.62 (H-2 $\beta$ ), 3.83 (H-3 $\beta$ ), 3.67 (H-4 $\beta$ ), 3.44 (H-6 $\beta$ ); <sup>13</sup>C NMR  $\delta_{ppm}$  (125 MHz): 52.1 ( $\alpha$ CH), 15.7 ( $\beta$ CH<sub>3</sub>), 100.2 (C<sub>1</sub> $\beta$ ), 82.6 (C<sub>2</sub> $\beta$ ), 77.9 (C<sub>3</sub> $\beta$ ), 68.8 (C<sub>4</sub> $\beta$ ), 60.5 (C<sub>6</sub> $\beta$ ). 3-O-Ester: <sup>1</sup>H NMR  $\delta_{ppm}$ : 2.87 ( $\alpha$ CH), 3.93 (H-3 $\beta$ ), 3.58 (H-4 $\beta$ ), 3.82 (H-6 $\beta$ ); <sup>13</sup>C NMR  $\delta_{ppm}$ : 51.4 ( $\alpha$ CH), 83.3 (C<sub>3</sub> $\beta$ ), 69.3 (C<sub>4</sub> $\beta$ ), 63.5 (C<sub>3</sub> $\beta$ ). 6-O-Ester: <sup>1</sup>H NMR  $\delta_{ppm}$ : 2.95 ( $\alpha$ CH), 1.30 ( $\beta$ CH<sub>3</sub>), 3.86 (H-2 $\beta$ ), 3.4 (H-4 $\alpha$ ), 3.76 (H-5 $\beta$ ), 3.36 (H-6 $\beta$ ); <sup>13</sup>C NMR  $\delta_{ppm}$ : 50.2 ( $\alpha$ CH), 15.1 ( $\beta$ CH<sub>3</sub>), 171.4 (CO), 101.8 (C<sub>1</sub> $\beta$ ), 65.4 (C<sub>6</sub> $\beta$ ), 75.0 (C<sub>2</sub> $\beta$ ), 70.1 (C<sub>5</sub> $\beta$ ), 57.3 (C<sub>6</sub> $\beta$ ). 2,6-di-O-Ester: <sup>1</sup>H NMR  $\delta_{ppm}$ : 3.36 ( $\alpha$ CH), 1.30 ( $\beta$ CH<sub>3</sub>), 3.78 (H-2 $\beta$ ),

3.47 (H-6 $\beta$ ), <sup>13</sup>C NMR  $\delta_{ppm}$ : 49.5 ( $\alpha$ CH), 16.4 ( $\beta$ CH<sub>3</sub>), 76.5 (C<sub>2</sub> $\beta$ ), 62.7 (C<sub>6</sub> $\beta$ ). 3,6-di-O-Ester: <sup>1</sup>H NMR  $\delta_{ppm}$ : 1.30 ( $\alpha$ CH), 3.78 (H-3 $\beta$ ), 3.82 (H-6 $\beta$ ) <sup>13</sup>C  $\delta_{ppm}$ : 16.7 ( $\alpha$ CH), 81.6 (C<sub>3</sub> $\beta$ ), 63.1 (C<sub>6</sub> $\beta$ ).

### 3.1.2. L-Valyl-D-glucose esters

UV: 275.0 nm (log  $\epsilon$  = 2.4), 227.0 nm (log  $\epsilon$  = 2.65); IR: 3394 cm<sup>-1</sup> (NH), 2985 cm<sup>-1</sup> (OH), 2971 cm<sup>-1</sup> (CH) and 1638 cm<sup>-1</sup> (C=O); specific rotation-[ $\alpha$ ]<sub>D</sub> at 25 °C = +30.0°.

2-O-Ester: <sup>1</sup>H NMR  $\delta_{ppm}$  (500.13 MHz): 3.06 ( $\alpha$ CH), 2.15 ( $\beta$ CH), 1.07 ( $\gamma$ CH<sub>3</sub>), 3.89 (H-2 $\alpha$ ), 3.75 (H-2 $\beta$ ), 3.51 (H-6 $\alpha$ ); <sup>13</sup>C NMR  $\delta_{ppm}$  (125 MHz): 53.4 ( $\alpha$ CH), 20.9 ( $\beta$ CH), 9.51 ( $\gamma$ CH<sub>3</sub>), 76.1 (C<sub>2</sub> $\alpha$ ), 60.0 (C<sub>6</sub> $\alpha$ ). 3-O-Ester: <sup>1</sup>H NMR  $\delta_{ppm}$ : 3.10 ( $\alpha$ CH), 0.94 ( $\gamma$ CH<sub>3</sub>), 3.89 (H-3 $\alpha$ ), 4.01 (H-3 $\beta$ ), 3.33 (H-6 $\alpha$  $\beta$ ); <sup>13</sup>C NMR  $\delta_{ppm}$ : 52.4 ( $\alpha$ CH), 9.39 ( $\gamma$ CH<sub>3</sub>), 82.9 (C<sub>3</sub> $\alpha$ ), 83.4 (C<sub>3</sub> $\beta$ ), 60.3 (C<sub>6</sub> $\alpha$  $\beta$ ). 6-O-Ester: <sup>1</sup>H NMR  $\delta_{ppm}$ : 3.20 ( $\alpha$ CH), 2.01 ( $\beta$ CH), 0.90 ( $\gamma$ CH<sub>3</sub>), 4.95 (H-1 $\alpha$ ), 4.22 (H-1 $\beta$ ), 3.17 (H-4 $\alpha$ ), 3.0 (H-4 $\beta$ ), 3.86 (H-6 $\alpha$ ); <sup>13</sup>C NMR  $\delta_{ppm}$ : 51.9 ( $\alpha$ CH), 21.0 ( $\beta$ CH), 8.94 ( $\gamma$ CH<sub>3</sub>), 95.2 (C<sub>1</sub> $\alpha$ ), 104.5 (C<sub>1</sub> $\beta$ ), 69.5 (C<sub>4</sub> $\alpha$ ), 69.8 (C<sub>4</sub> $\beta$ ), 63.4 (C<sub>6</sub> $\alpha$ ). 2,6-di-O-Ester: <sup>1</sup>H NMR  $\delta_{ppm}$ : 3.15 ( $\alpha$ CH), 3.75 (H-2 $\alpha$ ), 3.64 (H-6 $\beta$ ), <sup>13</sup>C NMR  $\delta_{ppm}$ : 51.7 ( $\alpha$ CH), 78.7 (C<sub>2</sub> $\alpha$ ), 61.6 (C<sub>6</sub> $\alpha$ ), 3,6-di-O-Ester: <sup>1</sup>H NMR  $\delta_{ppm}$ : 3.21 ( $\alpha$ CH), 1.55 ( $\gamma$ CH<sub>3</sub>), 3.67 (H-3 $\beta$ ), 3.15 (H-6 $\alpha$  $\beta$ ); <sup>13</sup>C NMR  $\delta_{ppm}$ : 49.4 ( $\alpha$ CH), 78.6 (C<sub>3</sub> $\beta$ ), 61.3 (C<sub>6</sub> $\alpha$  $\beta$ ).

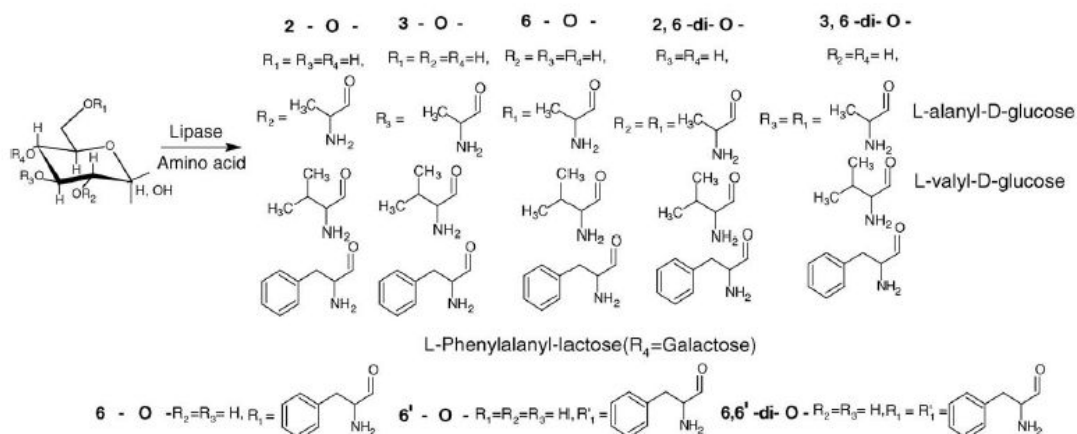


Fig. 1. Schematic representation for the lipase catalysed synthesis of L-amino acid esters of carbohydrates.

### 3.1.3. L-Phenylalanyl-D-glucose esters

UV: 308.0 nm ( $\log \varepsilon - 2.79$ ), 257.5 nm (3.08) and 237.0 nm ( $\log \varepsilon - 3.12$ ); IR: 3642  $\text{cm}^{-1}$  (NH), 3164  $\text{cm}^{-1}$  (OH), 1722  $\text{cm}^{-1}$  (C=O) and 1582  $\text{cm}^{-1}$  (aromatic); specific rotation- $[\alpha]_D$  at 25 °C = -24.2; CMC-3.25 mM (0.106%).

2-O-Ester:  $^1\text{H}$  NMR  $\delta_{\text{ppm}}$  (500.13 MHz): 2.92( $\alpha\text{CH}$ ), 2.51( $\beta\text{CH}_2\text{a}$ ), 4.6(H-1 $\alpha$ ), 3.67(H-2 $\alpha$ ), 3.4(H-6 $\alpha$ );  $^{13}\text{C}$  NMR  $\delta_{\text{ppm}}$  (125 MHz): 52.0( $\alpha\text{CH}$ ), 35.8( $\beta\text{CH}_2$ ), aromatic-136.5 ( $\text{C}_1$ ), 96.3( $\text{C}_1\alpha$ ), 77.1( $\text{C}_2\alpha$ ), 62.0( $\text{C}_6\alpha$ ). 3-O-Ester:  $^1\text{H}$  NMR  $\delta_{\text{ppm}}$ : 3.01( $\alpha\text{CH}$ ), 3.11( $\beta\text{CH}_2\text{a}$ ), 2.96( $\beta\text{CH}_2\text{b}$ ), 4.4 (H-1 $\alpha$ ), 3.61 (H-2 $\alpha$ ), 3.66(H-2 $\beta$ ), 3.82(H-3 $\alpha$ ), 3.91(H-3 $\beta$ ), 3.40(H-6 $\alpha$ );  $^{13}\text{C}$  NMR  $\delta_{\text{ppm}}$ : 53.0( $\alpha\text{CH}$ ), 36.8( $\beta\text{CH}_2$ ), aromatic-136.4 ( $\text{C}_1$ ), 97.3( $\text{C}_1\alpha$ ), 83.4( $\text{C}_3\alpha$ ), 83.9( $\text{C}_3\beta$ ), 61.9( $\text{C}_6\alpha$ ). 6-O-Ester:  $^1\text{H}$  NMR  $\delta_{\text{ppm}}$ : 3.07( $\alpha\text{CH}$ ), 3.18( $\beta\text{CH}_2\text{a}$ ,  $J = 12.1$ ); 3.06( $\beta\text{CH}_2\text{b}$ ,  $J = 12.1$ ), aromatic-7.18 (H2,6,  $J = 3.5$ ), 7.26(H3,5,  $J = 8.74$ ), 7.16(H4), 3.16(H-5 $\alpha$ ), 3.78(H-6 $\alpha$ ), 3.66(H-6 $\beta$ );  $^{13}\text{C}$  NMR  $\delta_{\text{ppm}}$ : 54.2( $\alpha\text{CH}$ ), 36.7( $\beta\text{CH}_2$ ) aromatic-136.3( $\text{C}_1$ ), 128.9( $\text{C}_2$ ,  $\text{C}_6$ ), 130.7( $\text{C}_3$ ,  $\text{C}_5$ ), 130.3( $\text{C}_4$ ), 172.5(CO), 102.2( $\text{C}_1\alpha$ ), 70.5( $\text{C}_5\alpha$ ), 65.0( $\text{C}_6\alpha$ ,  $\text{C}_6\beta$ ). 2,6-di-O-Ester:  $^1\text{H}$  NMR  $\delta_{\text{ppm}}$  3.51(H-6 $\alpha$ ), 3.61(H-6 $\beta$ ), 3.67(H-2 $\alpha$ );  $^{13}\text{C}$  NMR  $\delta_{\text{ppm}}$  77.0( $\text{C}_2\alpha$ ), 79.0( $\text{C}_2\beta$ ), 62.1( $\text{C}_6\beta$ ), 3.6-di-O-Ester:  $^1\text{H}$  NMR  $\delta_{\text{ppm}}$  3.50(H-6 $\alpha$ ), 3.61(H-3 $\alpha$ ), 3.66(H-3 $\beta$ );  $^{13}\text{C}$  NMR  $\delta_{\text{ppm}}$  82.3( $\text{C}_3\alpha$ ), 83.4( $\text{C}_3\beta$ ), 64.8( $\text{C}_6\alpha$ ).

### 3.1.4. L-Phenylalanyl-lactose

UV: 308.0 nm ( $\log \varepsilon - 2.77$ ), 258.0 nm ( $\log \varepsilon - 3.00$ ) and 237.5 nm ( $\log \varepsilon - 3.48$ ); IR: 3550  $\text{cm}^{-1}$  (NH), 3383  $\text{cm}^{-1}$  (OH), 1701  $\text{cm}^{-1}$  (C=O) and 1556  $\text{cm}^{-1}$  (aromatic).

6-O-Ester:  $^1\text{H}$  NMR  $\delta_{\text{ppm}}$  (500.13 MHz): 2.67( $\alpha\text{CH}$ ), 2.89( $\beta\text{CH}_2\text{a}$ ), aromatic-7.25 (H2,6), 7.28(H3,5), 7.2(H4), 4.32(H-1 $\alpha$ ), 4.23(H-1 $\beta$ ), 3.36(H-2 $\alpha$ ), 3.49(H-2 $\beta$ ), 3.32(H-3 $\alpha$ ), 3.80(H-3 $\beta$ ), 3.56(H-4 $\alpha$ ), 3.72(H-4 $\beta$ ), 3.90(H-5 $\alpha\beta$ ), 3.47(H-6 $\alpha\beta$ ), 4.16(H'-1 $\beta$ ), 3.14(H'-2 $\beta$ ), 3.42(H'-3 $\beta$ ), 3.62(H'-4 $\beta$ ), 3.39(H'-5 $\beta$ ), 3.54(H'-6 $\beta$ );  $^{13}\text{C}$  NMR  $\delta_{\text{ppm}}$  (125 MHz): 51.9( $\alpha\text{CH}$ ), 38.2( $\beta\text{CH}_2$ ) aromatic-138.0( $\text{C}_1$ ), 128.3( $\text{C}_2$ ,  $\text{C}_6$ ), 129.1( $\text{C}_3$ ,  $\text{C}_5$ ), 126.1( $\text{C}_4$ ), 172.5(CO), 96.6( $\text{C}_1\alpha$ ), 101.2( $\text{C}_1\beta$ ), 70.5( $\text{C}_2\alpha$ ), 73.0( $\text{C}_2\beta$ ), 74.0( $\text{C}_3\beta$ ), 82.5( $\text{C}_4\alpha$ ), 83.3( $\text{C}_4\beta$ ), 77.2( $\text{C}_5\alpha\beta$ ), 62.1( $\text{C}_6\alpha\beta$ ), 103.2( $\text{C}_1'\beta$ ), 69.9 ( $\text{C}_2'\beta$ ), 71.6( $\text{C}_3'\beta$ ), 68.2( $\text{C}_4'\beta$ ), 74.4( $\text{C}_5'\beta$ ), 60.5( $\text{C}_6'\beta$ ); 6'-O-Ester:  $^1\text{H}$  NMR  $\delta_{\text{ppm}}$ : 2.72( $\alpha\text{CH}$ ), 3.00( $\beta\text{CH}_2\text{a}$ ), 5.16(H-1 $\alpha$ ), 4.32(H-1 $\beta$ ), 3.16(H-2 $\alpha$ ), 3.45(H-2 $\beta$ ), 3.43(H-3 $\alpha$ ), 3.50 (H-3 $\beta$ ), 3.32(H-4 $\alpha$ ), 3.80(H-5 $\alpha\beta$ ), 3.49(H-6 $\alpha\beta$ ), 4.15(H'-1 $\beta$ ), 3.36(H'-2 $\beta$ ), 3.89(H'-4 $\beta$ ), 3.89 (H'-5 $\beta$ ), 3.45(H'-6 $\beta$ );  $^{13}\text{C}$  NMR  $\delta_{\text{ppm}}$ : 52.5( $\alpha\text{CH}$ ), 37.1( $\beta\text{CH}_2$ ) aromatic-137.6( $\text{C}_1$ ), 92.0( $\text{C}_1\alpha$ ), 97.1( $\text{C}_1\beta$ ), 69.7( $\text{C}_2\alpha$ ), 72.7( $\text{C}_2\beta$ ), 72.1( $\text{C}_3\alpha$ ), 74.5( $\text{C}_3\beta$ ), 79.9( $\text{C}_4\alpha$ ), 80.7( $\text{C}_4\beta$ ), 76.0( $\text{C}_5\alpha\beta$ ), 61.0( $\text{C}_6\alpha\beta$ ), 104.0( $\text{C}_1'\beta$ ), 69.3 ( $\text{C}_2'\beta$ ), 72.1( $\text{C}_3'\beta$ ), 66.3( $\text{C}_4'\beta$ ), 75.0( $\text{C}_5'\beta$ ), 63.1( $\text{C}_6\beta$ ); 6,6'-di-O-Ester:  $^1\text{H}$  NMR  $\delta_{\text{ppm}}$ : 2.55( $\alpha\text{CH}$ ), 2.89( $\beta\text{CH}_2\text{a}$ ), 4.32(H-1 $\alpha$ ), 3.23(H-2 $\alpha$ ), 3.68(H-2 $\beta$ ), 3.33(H-3 $\alpha$ ), 4.02(H-4 $\alpha$ ), 4.01(H-5 $\alpha\beta$ ), 3.45(H-6 $\alpha\beta$ ), 4.21(H'-1 $\beta$ ), 3.14(H'-2 $\beta$ ), 3.58(H'-3 $\beta$ ), 3.74(H'-4 $\beta$ ), 3.45(H'-6 $\beta$ );  $^{13}\text{C}$  NMR  $\delta_{\text{ppm}}$ : 51.7( $\alpha\text{CH}$ ), 37.9( $\beta\text{CH}_2$ ) aromatic-137.8( $\text{C}_1$ ), 95.6( $\text{C}_1\alpha$ ), 101.9( $\text{C}_1\beta$ ), 71.3( $\text{C}_2\alpha$ ), 73.2( $\text{C}_2\beta$ ), 73.3( $\text{C}_3\alpha$ ), 74.7( $\text{C}_3\beta$ ), 82.2( $\text{C}_4\alpha$ ), 84.2( $\text{C}_4\beta$ ), 77.7( $\text{C}_5\alpha\beta$ ), 62.4( $\text{C}_6\alpha\beta$ ), 103.4( $\text{C}_1'\beta$ ), 69.9 ( $\text{C}_2'\beta$ ), 72.4( $\text{C}_3'\beta$ ), 67.4( $\text{C}_4'\beta$ ), 74.7( $\text{C}_5'\beta$ ), 62.7( $\text{C}_6\beta$ ).

Riva et al. [20] reported that three different mono esters of *N*-acetyl L-phenylalanyl-D-glucose were formed when reac-

Table 2

ACE inhibitory activities of the amino acid esters of carbohydrates

Ester	ACE inhibition IC <sub>50</sub> , mM <sup>a</sup>
L-Alanyl-D-Glucose	0.230 ± 0.02
L-Valyl-D-Glucose	0.396 ± 0.03
L-Phenylalanyl-D-Glucose	0.121 ± 0.01
L-Phenylalanyl-lactose	0.229 ± 0.01

<sup>a</sup> Mean ± S.E. of three independent determinations. Respective L-alanine, L-valine, L-phenylalanine, D-glucose and lactose as controls showed no ACE inhibitory activity when tested at 0.2 mM.

tion was carried out in presence of subtilisin (2-O-, 3-O- and 6-O-mono esters). Tamura et al., [21] have reported synthesis of 2-O- and 3-O-mono esters of L-valyl-D-glucose chemically. Park et al. [22] have reported formation of three different esters of *N*-acetyl L-phenylalanyl-lactose (6-O-, 6'-O- and 6,6'-di-O-esters). The present work reports the synthesis of the 18 esters (mono and diesters) of which the following 10 esters have not been reported so far: 2-O-L-alanyl-D-glucose, 3-O-L-alanyl-D-glucose, 6-O-L-alanyl-D-glucose, 2,6-di-O-L-alanyl-D-glucose, 3,6-di-O-L-alanyl-D-glucose, 6-O-L-valyl-D-glucose, 2,6-di-O-L-valyl-D-glucose, 3,6-di-O-L-valyl-D-glucose, 2,6-di-O-L-phenylalanyl-D-glucose and 3,6-di-O-L-phenylalanyl-D-glucose. The average molecular weight of the esters in case of L-alanyl and L-phenylalanyl-D-glucose was evaluated from the percentage composition of all five esters determined from the C-6 peak area from  $^{13}\text{C}$  spectra.

### 3.2. Biological evaluation

The synthesized amino acid esters of carbohydrates were evaluated for their ability to inhibit angiotensin-converting enzyme (ACE). All the amino acid esters (in the form of mixtures) showed moderate potency as inhibitors of ACE (Table 2, Fig. 2). While L-phenylalanyl-D-glucose showed highest ACE inhibitory activity with an IC<sub>50</sub> of 0.121 mM, L-valyl-D-glucose showed lowest ACE inhibitory activity with an IC<sub>50</sub> of 0.396 mM. The other two esters showed intermediate IC<sub>50</sub> value of 0.23 mM. Although D-glucose esters of L-alanine

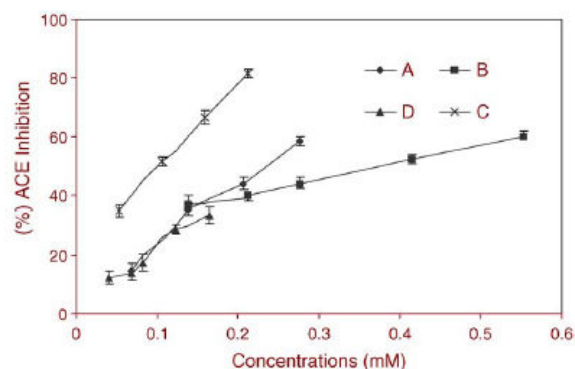


Fig. 2. ACE inhibitory patterns of L-amino acid esters of carbohydrates. Each value is a Mean ± S.E. of three determinations. ♦: L-alanyl-D-glucose; ■: L-valyl-D-glucose; ×: L-phenylalanyl-D-glucose; ▲: L-phenylalanyl-lactose.

and L-valine exhibited good in vitro inhibitory activity against ACE, L-phenylalanine esters were the most effective. Recent studies [9] have shown that monosaccharides contribute an important role in forming the supramolecular structure of ACE and also inhibit ACE dimerisation. There are reports that dipeptides containing aromatic amino acids – phenylalanyl-leucine, tryptophanyl-leucine, tyrosinyl-leucine and tryptophanyl-proline – exhibited relatively high inhibitory activity against ACE [23,24]. Non peptide prodrugs such as amino acid conjugates of acyclovir, cephalixin and bestatin were reported to be absorbed by H<sup>+</sup>-coupled peptide transporters even though they contain highly polar groups [25]. All these dipeptides and non peptide prodrugs contain free amino groups (probably charged) attached to the  $\alpha$ -CH of the amino acids with an adjacent –CO–NH– peptide linkage and aromatic or alkyl side chains which could be the probable binding groups from the drugs to the active site resulting in inhibition. The same functional portion is also present in the amino acid esters of carbohydrates reported herein, the only difference being the presence of –CO–O– linkage in the esters prepared instead of –CO–NH– from the reported drugs. This could be the reason for ACE inhibition by the esters reported in this work. Further, the amino acid residues are proposed [26] to interact through their hydrophobic side chains and block the ACE active site, thereby bestowing ACE inhibition. However, in our studies, free amino acids, D-glucose or lactose when tested at 0.2 mM did not show ACE inhibitory activity. Hence the inhibition obtained in the present study was probably due to a mixture of either all or some of the five esters in L-alanyl-D-glucose, L-valyl-D-glucose and L-phenylalanyl-D-glucose and three esters in L-phenylalanyl-lactose.

This implies that anchoring an amino group on a potent active site binding molecule like D-glucose/lactose possessing hydroxyl groups, capable of hydrogen bonding and hydrophobic interactions with some of the active site of the enzyme is essential. Since the esters in the mixtures possessed the same polarity, it was difficult to isolate the esters individually by chromatographic or other means. But, the esters were separated from the respective unreacted amino acids and D-glucose. However, potency of individual esters was not determined. But we speculate that some of the individual mono- and di-esters might possess more ACE inhibitory activity than the others.

#### 4. Conclusions

The results from the present study indicate a potential role for the amino acid esters of carbohydrates as inhibitors of

ACE. The structural approach of ACE inhibitors developed in the present work can be used with further suitable modifications in the carbohydrate moiety with the insertion of different combinations of amino acids to obtain more potent ACE inhibitors.

#### References

- [1] D. Coates, *Int. J. Biochem. Cell Biol.* 35 (2003) 769–773.
- [2] C. Verme-Gibboney, *Am. J. Health Syst. Pharm.* 54 (1997) 2603–2689.
- [3] N.M. Sharif, B.L. Evans, *Am. Pharmacother.* 28 (1994) 720–721.
- [4] Y. Ariyoshi, *Trends Food Sci. Technol.* 4 (1993) 139–144.
- [5] A. Morigiwa, A. Kitabatake, Y. Fujimoto, N. Ikekawa, *Chem. Pharm. Bull.* 34 (1998) 3025–3028.
- [6] P.J. Park, J.Y. Je, S.K. Kim, *J. Agric. Food Chem.* 51 (2003) 4930–4934.
- [7] R. Huang, E. Mendis, S.-K. Kin, *Bioorg. Med. Chem.* 13 (2005) 3649–3655.
- [8] O.A. Kost, T.A. Orth, I.I. Nikolskaya, S.N. Nametkin, A.V. Levashov, *Biochem. Mol. Biol. Int.* 44 (1998) 535–542.
- [9] O.A. Kost, N.V. Bovin, E.E. Chemodanova, V.V. Nasonov, T.A. Orth, *J. Mol. Recognit.* 13 (2000) 360–369.
- [10] C.M. Taylor, *Tetrahedron* 54 (1998) 11317–11362.
- [11] S. Horvat, J. Horvat, L. Vargadefterdarovic, K. Pavelic, N.N. Chung, P.W. Schiller, *Int. J. Pept. Res.* 41 (1993) 360–369.
- [12] R.D. Egleton, S.A. Mitchell, J.D. Huber, J. Janders, D. Stropova, R. Polt, H.I. Yamamura, V.J. Hruby, T.P. Davis, *Brain Res.* 881 (2000) 37–46.
- [13] K.R. Kiran, S. Hari Krishna, C.V. Sureshbabu, N.G. Karanth, S. Divakar, *Biotechnol. Lett.* 22 (2000) 1511–1514.
- [14] K. Lohith, S. Divakar, *J. Biotechnol.* 117 (2005) 49–56.
- [15] S. Divakar, K. R. Kiran, S. Harikrishna, N. G. Karanth, *Indian Patent* (1999) 1243/DEL/1999.
- [16] K. Lohith, G. R. Vijayakumar, B. Manohar, S. Divakar, *Indian Patent* (2003) NF-492/2003; PCT/IN03/00466.
- [17] G.R. Vijayakumar, K. Lohith, B.R. Somashekar, S. Divakar, *Biotechnol. Lett.* 26 (2004) 1323–1328.
- [18] A. Okamoto, H. Hanagata, Y. Kawamura, F. Yanagida, *Plant Foods Hum. Nutr.* 47 (1995) 39–47.
- [19] D.W. Cushman, H.S. Cheung, *Biochem. Pharmacol.* 20 (1971) 1637–1648.
- [20] S. Riva, J. Chopineau, A.P.G. Kieboom, A.M. Klibanov, *J. Am. Chem. Soc.* 110 (1988) 584–589.
- [21] M. Tamura, M. Shoji, T. Nakatsuka, K. Kinomura, H. Okai, S. Fukui, *Agric. Biol. Chem.* 49 (1985) 2579–2586.
- [22] O.J. Park, G.J. Jeon, J.W. Yang, *Enzyme Microb. Technol.* 25 (1999) 455–462.
- [23] M. Kuba, C. Tana, S. Tawata, M. Yasuda, *Process Biochem.* 40 (2005) 2191–2196.
- [24] V. Silva, M.F. Xavier, *Int. Dairy J.* 15 (2005) 1–15.
- [25] T. Terada, K. Inui, *Curr. Drug Metabol.* 5 (2004) 85–94.
- [26] M. Bala, M.A.Q. Pasha, D.K. Bhardwaj, S. Pasha, *Bioorg. Med. Chem.* 10 (2002) 3685–3691.



Original article

## Glycosides and amino acyl esters of carbohydrates as potent inhibitors of angiotensin converting enzyme

K. Lohith, G.R. Vijayakumar, B.R. Somashekar, R. Sivakumar, S. Divakar \*

*Fermentation Technology and Bioengineering, Central Food Technological Research Institute, KRS Road, 570020 Mysore, Karnataka, India*

Received in revised form 5 April 2006; accepted 20 April 2006

Available online 26 May 2006

### Abstract

About 12 glycosides prepared through amyloglucosidase catalysis and 23 amino acyl esters of carbohydrates prepared through lipase catalysis in organic solvents showed angiotensin converting enzyme (ACE) inhibition activity. Both amino acyl esters of carbohydrates and glycosides exhibited  $IC_{50}$  values for ACE inhibition in the 0.5 mM to 15.7 mM range. Eugenyl-D-glucoside ( $IC_{50}$ :  $0.5 \pm 0.04$  mM), L-isoleucyl-D-glucose ( $IC_{50}$ :  $0.7 \pm 0.067$  mM), vanillyl-D-sorbitol ( $IC_{50}$ :  $0.8 \pm 0.09$  mM), L-histidyl-D-fructose ( $IC_{50}$ :  $0.9 \pm 0.087$  mM), L-tryptophanyl-D-fructose ( $IC_{50}$ :  $0.9 \pm 0.092$  mM), octyl-D-glucoside ( $IC_{50}$ :  $1.0 \pm 0.093$  mM), vanillyl-D-mannoside ( $IC_{50}$ :  $1.0 \pm 0.089$  mM), L-valyl-D-mannitol ( $IC_{50}$ :  $1.0 \pm 0.092$  mM) and L-phenylalanyl-D-glucose ( $IC_{50}$ :  $1.0 \pm 0.089$  mM) were the compounds, which showed the best ACE inhibitory activities. © 2006 Elsevier SAS. All rights reserved.

**Keywords:** Glycosides; Amino acyl esters of carbohydrates; Enzymatic synthesis; ACE inhibition;  $IC_{50}$  values

### 1. Introduction

Angiotensin converting enzyme (dipeptidyl carboxypeptidase, EC 3.4.15.1) is a zinc containing nonspecific dipeptidyl carboxypeptidase widely distributed in mammalian tissues [1]. Angiotensin-converting enzyme (ACE) regulates the blood pressure by modulating renin-angiotensin system [2]. This enzyme increases the blood pressure by converting the decapeptide angiotensin I into the potent vaso-constricting octapeptide, angiotensin II. Angiotensin II brings about several central effects, all leading to a further increase in blood pressure. ACE is a multifunctional enzyme that also catalyses the degradation of bradykinin (blood pressure-lowering nanopeptide) and therefore inhibition of ACE results in an overall antihypertensive effect [1,3].

Several synthetic drugs and bio-molecules are available for ACE inhibition. Captopril is a successful synthetic anti-hypertensive drug and similar such molecules like enalapril, perindopril, ceranopril, ramipril, quinapril and fosinopril also show ACE inhibitory activities [4,5]. Some naturally occurring 'biologically active peptides' also act as ACE inhibitors [6–9].

Glycosides from the leaves of *Abeliophyllum distichum* like acteoside, isoacteoside, rutin, and hirsutrin moderately inhibited the Angiotensin I converting enzyme activity [10]. Glycosides like 3-O-methyl crenatoside from *Microtoena prainiana* also showed more than 30% ACE inhibitory activity [11]. Phenyl propanoid glycosides from *Clerodendron trichotomum* such as acteoside, leucosceptoside A, martynoside, acteoside isomer and isomartynoside also showed ACE inhibitory effect [12].

Certain glycosides and amino acyl esters of carbohydrates are used widely in food and pharmaceutical applications as sweeteners, surfactants, microcapsules in pharmaceutical preparations, in delivery of biologically active agents such as antibiotics, nutraceuticals and antitumor agents [13–17]. However, they have not been shown to exhibit ACE inhibition activity so far. The present work deals with detection of ACE inhibition activities for some enzymatically synthesized glycosides using amyloglucosidase and amino acyl esters of carbohydrates using lipases in organic media. The results are presented here.

### 2. Results

A total of 35 compounds were tested for the inhibitory activities of ACE isolated from pig lung. General scheme for

\* Corresponding author.

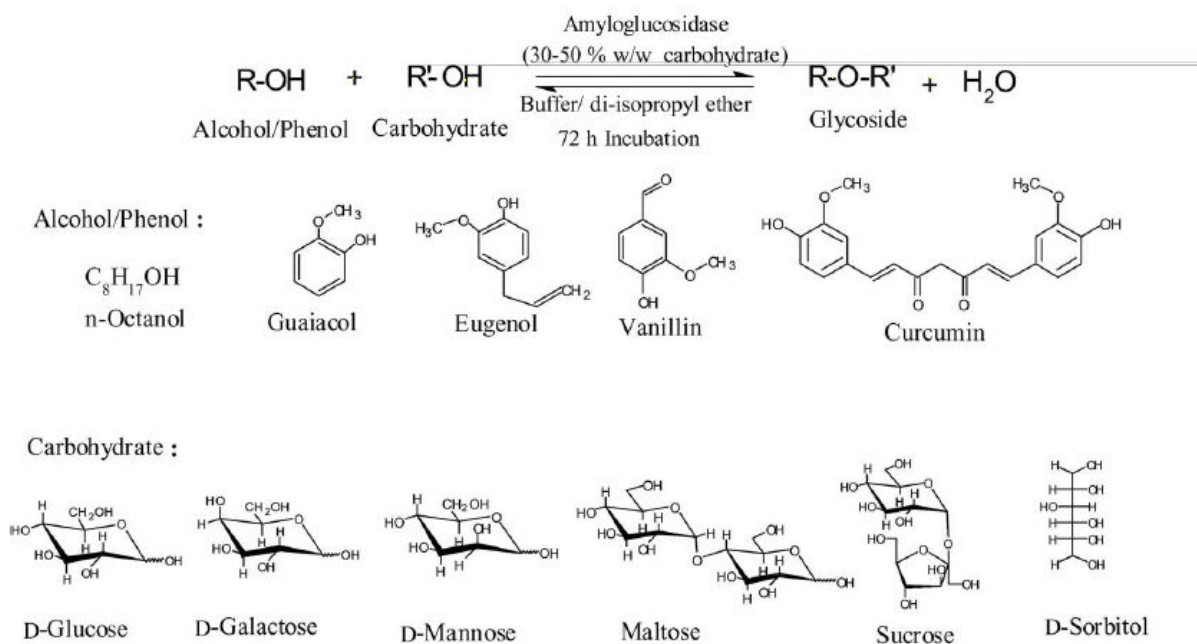
E-mail address: [divakar643@gmail.com](mailto:divakar643@gmail.com) (S. Divakar).

glycosylation and esterification are shown in Schemes 1 and 2. Enzymatic reactions were carried out under optimized conditions worked out for these reactions [18–21]. The enzymatic procedure employed unprotected and unactivated alcohols, phenols, amino acids and carbohydrates.

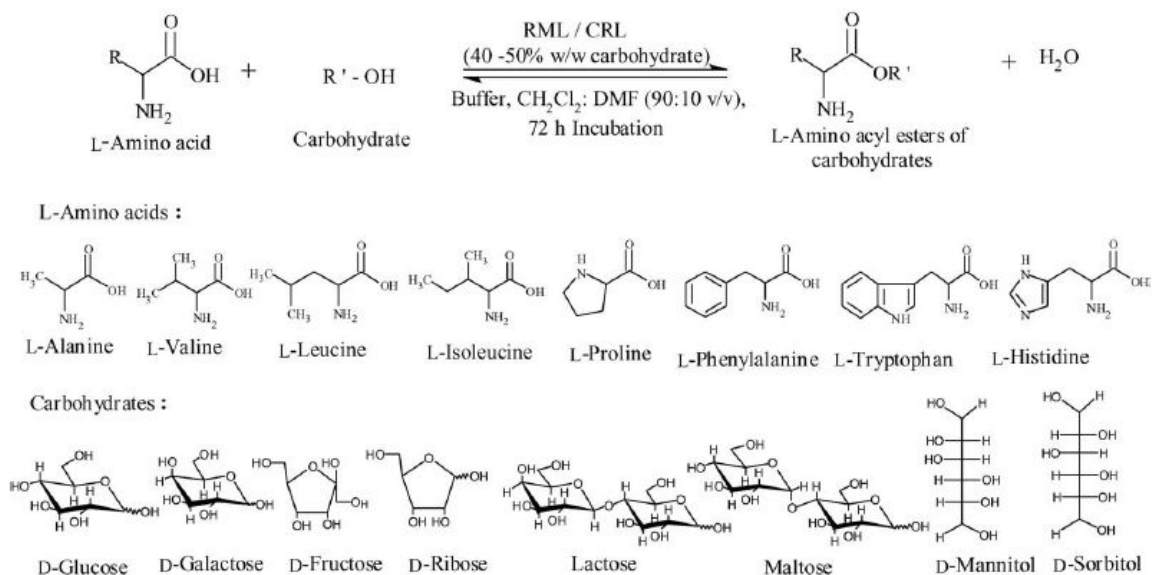
Typical ACE inhibition plots for eugenyl-D-glucoside, vanillyl-D-glucoside, L-isoleucyl-D-glucose and L-histidyl-D-fruc-

tose, are shown in Fig. 1. Tables 1 and 2, respectively, show the glycosides and amino acyl esters tested, their conversion yields from the respective enzymatic reactions, proportions of the products formed and ACE inhibitory activities for these compounds.

*n*-Octanol, guaiacol, eugenol, vanillin, curcumin and  $\alpha$ -tocopherol glycosides of different carbohydrates (D-glucose, D-ga-



Scheme 1. Amyloglucosidase catalyzed synthesis of glycosides.



Scheme 2. Lipases catalyzed synthesis of L-amino acyl esters of carbohydrates.

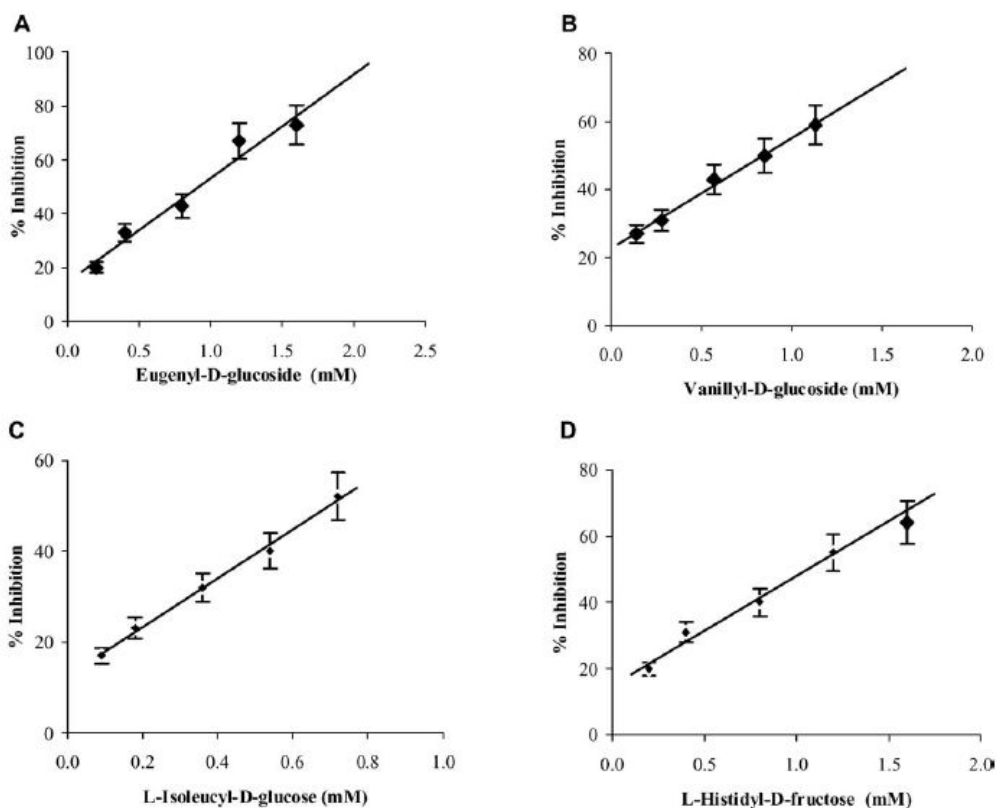


Fig. 1. **A.** Inhibition plot for eugenyl-D-glucoside, ACE: 0.1 ml (1.0 mg in 1.0 ml stock solution), Substrate: 0.1 ml hippuryl-histidyl-leucine (5 mM), Buffer: 100 mM phosphate buffer pH 8.3 contain 300 mM sodium chloride, Incubation period: 30 min, Temperature: 37 °C; **B.** Vanillyl-D-glucoside; **C.** L-Isoleucyl-D-glucose; **D.** L-Histidyl-D-fructose.

lactose, D-mannose, D-fructose, D-ribose, D-arabinose, maltose, sucrose, lactose, D-mannitol and D-sorbitol) were tested for ACE inhibition (Table 1). Among the carbohydrates employed, D-ribose, D-arabinose, D-fructose and lactose did not undergo any glycosylation.

Four amino acids containing alkyl side chains, three amino acids containing aromatic side chains and L-proline were employed for the preparation of esters. In case of aminoacyl esters, L-alanyl, L-valyl, L-leucyl, L-isoleucyl, L-prolyl, L-phenylalanyl, L-tryptophanyl and L-histidyl esters of D-glucose, D-galactose, D-fructose, D-ribose, lactose, maltose, D-sorbitol and D-mannitol were subjected to ACE inhibition activity studies (Table 2). ACE inhibition activity of the above-mentioned glycosides and amino acyl esters of carbohydrates were carried out by the Cushman and Cheung method [22]. Since hippuryl-L-histidyl-L-leucine (HHL) mimics the carboxyl dipeptide of angiotensin I, it has been routinely used as the substrate for screening ACE inhibitors.

Underivatized alcohols, phenols, L-amino acids and carbohydrates individually were also tested for ACE inhibition as controls and they did not show any ACE inhibitory activities. Only glycosides and esters showed activities. Isolated ACE inhibitor tested for lipase and protease activity (Table 3) showed

a small extent of protease activity (13.3%) compared to ACE activity but no lipase activity. In presence of glycosides and amino acids esters prepared, the isolated ACE showed 8.2% and 8.9% protease activity, respectively (Table 3) compared to the ACE activity. This confirmed that the ACE inhibition observed in the presence of glycosides and esters prepared is more due to ACE inhibition rather than protease inhibition.

The compounds were characterized by UV, IR, Mass and NMR (two-dimensional heteronuclear single quantum coherence transfer—2D-HSQC) spectroscopic techniques. In case of glycoside synthesis, the major product was the glycosylated product and relatively lesser amounts of C6-O-alkylated or C6-O-arylated products were also detected. The reaction was between the alcohol or phenolic OH groups and the anomeric and/or primary C6-OH groups of the carbohydrates.

In case of esters, mono and di esters in different proportions were detected. Individual 1-O, 2-O, 3-O, 5-O, 6-O, and 6"-O monoesters and 1,6-di-O, 2,5-di-O, 2,6-di-O, 3,6-di-O, and 6,6"-di-O esters depending on the carbohydrate employed were found to be formed. It was not possible to separate the individual glycosides and esters from their reaction mixtures even by chromatographic separation on Sephadex G-10. Thus the activities described are for the mixture of these compounds.

Table 1  
IC<sub>50</sub> values for ACE inhibition by glycosides<sup>a</sup>

Glycoside	Conversion Yield <sup>b</sup> (%)	Products formed (% proportions) <sup>c</sup>	IC <sub>50</sub> value (mM) <sup>d</sup>
<i>n</i> -Octyl- $\alpha/\beta$ -D-glucoside	46	<i>n</i> -Octyl- $\alpha$ -D-glucopyranoside (63) <i>n</i> -Octyl- $\beta$ -D-glucopyranoside (25) C6- <i>O</i> -octyl-D-glucose (12)	1.0 $\pm$ 0.093
<i>n</i> -Octyl maltoside	22	<i>n</i> -Octyl maltoside	1.5 $\pm$ 0.13
<i>n</i> -Octyl sucrose	13	C1- <i>O</i> -octyl sucrose (44) C6- <i>O</i> -octyl sucrose (56)	1.7 $\pm$ 0.15
Guaiacyl- $\alpha$ -D-glucoside	52	C1- <i>O</i> -guaiacyl- $\alpha$ -D-glucopyranoside (52) C6- <i>O</i> -guaiacyl- $\alpha$ -D-glucose (48)	3.7 $\pm$ 0.36
Eugenyl- $\alpha$ -D-glucoside	32	C1- <i>O</i> -eugenyl- $\alpha$ -D-glucopyranoside (53) C6- <i>O</i> -eugenyl-D-glucose (47)	0.5 $\pm$ 0.04
Vanillyl- $\alpha/\beta$ -D-glucoside	53	C1- <i>O</i> -vanillyl- $\alpha$ -D-glucopyranoside (52) C1- <i>O</i> -vanillyl- $\beta$ -D-glucopyranoside (17) C6- <i>O</i> -vanillyl-D-glucose (31)	1.1 $\pm$ 0.10
Vanillyl- $\alpha$ -D-galactoside	18	C1- <i>O</i> -vanillyl- $\alpha$ -D-galactopyranoside	1.1 $\pm$ 0.13
Vanillyl- $\alpha$ -D-mannoside	13	C1- <i>O</i> -vanillyl- $\alpha$ -D-mannopyranoside	1.0 $\pm$ 0.089
Vanillyl maltoside	29	C1- <i>O</i> -vanillyl- $\alpha$ -maltopyranoside (42) C6- <i>O</i> -vanillyl maltose (30) C6''- <i>O</i> -vanillyl maltose (28)	1.6 $\pm$ 0.14
Vanillyl sucrose	23	C1- <i>O</i> -vanillyl sucrose (39) C6''- <i>O</i> -vanillyl sucrose (61)	15.7 $\pm$ 1.6
Vanillyl-D-sorbitol	13	C1- <i>O</i> -vanillyl-D-sorbitol (13) C6- <i>O</i> -vanillyl-D-sorbitol (25)	0.8 $\pm$ 0.09
CurcuminyI-bis- $\alpha$ -D-glucoside	48	C1, C6 Di- <i>O</i> -vanillyl-D-sorbitol (62) C1- <i>O</i> -curcuminyI-bis- $\alpha$ -D-glucopyranoside (62) C6- <i>O</i> -curcuminyI-bis- $\alpha$ -D-glucose (38)	1.5 $\pm$ 0.13

<sup>a</sup> Respective alcohols, phenols and carbohydrates as controls for ACE inhibition activity; non reducing sugar unit carbons of disaccharide are double primed;

<sup>b</sup> Conversion yields were from HPLC with errors in yield measurements  $\pm$  10%;

<sup>c</sup> Product proportions determined from <sup>13</sup>C 2D-HSQC NMR C1/C6 peak areas or their cross peaks;

<sup>d</sup> IC<sub>50</sub> values compared to that of captopril 0.060  $\pm$  0.005 mM determined by Cushman and Cheung method [22].

### 3. Discussion

Among the glycosides tested, eugenyl-D-glucoside (0.5  $\pm$  0.04 mM), vanillyl-D-sorbitol (0.8  $\pm$  0.09 mM), vanillyl-D-mannoside (1.0  $\pm$  0.089 mM) and octyl-D-glucoside (1.0  $\pm$  0.093 mM) exhibited the best ACE inhibitory activities (IC<sub>50</sub>  $\leq$  1.0 mM; Table 1). Among the carbohydrates employed glucosides showed the best ACE inhibitory activities. Alkyl glycosides showed better inhibitory activities than the phenolic glycosides. The glycosides also showed better ACE inhibitory activities than the amino acyl esters indicating higher potency of glycosides in ACE inhibition.

With increase in alkyl side chain branching, D-glucose esters of L-alanine (3.1  $\pm$  0.30 mM), L-valine (6.0  $\pm$  0.59 mM), L-leucine (2.8  $\pm$  0.27 mM) and L-isoleucine (0.7  $\pm$  0.067 mM) showed better inhibition (lesser IC<sub>50</sub> values), than the other esters, which could be directly correlated to increase in hydrophobicity (Table 2). IC<sub>50</sub> values  $\leq$  1.0 mM were detected for L-isoleucyl-D-glucose (0.7  $\pm$  0.067 mM), L-histidyl-D-fructose (0.9  $\pm$  0.087 mM), L-tryptophanyl-D-fructose (0.9  $\pm$  0.092 mM), L-valyl-D-mannitol (1.0  $\pm$  0.092 mM) and L-phenylalanyl-D-glucose (IC<sub>50</sub>: 1.0  $\pm$  0.089 mM). Among these, L-isoleucyl-D-glucose (0.7  $\pm$  0.067 mM) was found to exhibit the best inhibitory activity. In general, aromatic amino acid esters showed comparatively higher IC<sub>50</sub> values than amino acids containing alkyl side chains, emphasizing that the latter were better inhibitors of ACE. Among the carbohydrates employed, D-mannitol esters showed better ACE inhibition (Ta-

ble 2) than the other carbohydrate esters. In case of L-prolyl esters, IC<sub>50</sub> values in the 1.6–4.4 mM range matched with those of alkyl side chain containing amino acid esters like L-alanine, L-valine, L-leucine and L-isoleucine (Table 2). Captopril is *N*-[(*S*)-3-mercapto-2-methylpropionyl]-L-proline containing prolyl unit as essential for ACE inhibition [4]. However, mere presence of a prolyl unit in the esters prepared does not give rise to a high level of ACE inhibition. Since, it was difficult to separate the individual esters, the actual potency of the individual esters could not be unequivocally established in the present work.

The present work for the first time has shown the ACE inhibitory potency of the above-mentioned glycosides and esters prepared enzymatically. Since milder reaction conditions were employed, the products formation did not suffer due to side reactions. However, the glycosides and esters tested in the present work, overall, clearly possess groups like alkyl side chains and phenolic groups which can be accommodated in the hydrophobic S<sub>1</sub> and S<sub>2</sub> subsites of angiotensin I converting enzyme [4,23]. The free amino group in the amino acid esters can also serve as good ligands for Zn<sup>2+</sup> in the ACE active site. Carbohydrates in glycosides and esters could also bind to the hydrophobic and/or hydrophilic subsites of angiotensin I converting enzyme, as they possess both hydrophobic and hydrophilic groups in their structure. Although the ACE preparation of the present work from pig lung is ACE I [24], it showed a low protease inhibitory activity but no lipase activity indicating that the glycosides and esters inhibit ACE rather than the pro-

Table 2  
 IC<sub>50</sub> values for ACE inhibition by L-aminoacyl esters of carbohydrates<sup>a</sup>

L-Amino acyl ester of carbohydrates	Conversion Yield (%) <sup>b</sup>	Products (% proportion) <sup>c</sup>	IC <sub>50</sub> value (mM) <sup>d</sup>
L-Alanyl-β-D-glucose	30	2-O-L-alanyl-β-D-glucose (47) 3-O-L-alanyl-β-D-glucose (12) 6-O-L-alanyl-β-D-glucose (20) 2,6-di-O-L-alanyl-β-D-glucose (15) 3,6-di-O-L-alanyl-β-D-glucose (6)	3.1 ± 0.30
L-Alanyl-D-ribose	48	3-O-L-alanyl-D-ribose (16) 5-O-L-alanyl-D-ribose (32) 3,5-di-O-L-alanyl-D-ribose (52)	2.7 ± 0.25
L-Alanyl-lactose	20	6-O-L-alanyl-lactose (34) 6"-O-L-alanyl-lactose (34) 6,6"-di-O-L-alanyl-lactose (32)	2.0 ± 0.21
L-Valyl-D-glucose	84	2-O-L-valyl-D-glucose (26) 3-O-L-valyl-D-glucose (26) 6-O-L-valyl-D-glucose (33) 2,6-di-O-L-valyl-D-glucose (9) 3,6-di-O-L-valyl-D-glucose (6)	6.0 ± 0.59
L-Valyl-D-fructose	34	1-O-L-valyl-D-fructose	2.8 ± 0.29
L-Valyl-maltose	42	6-O-L-valyl-maltose (35) 6"-O-L-valyl-maltose (36) 6,6"-di-O-L-valyl-maltose (29)	3.1 ± 0.33
L-Valyl-D-mannitol	56	1-O-L-valyl-D-mannitol	1.0 ± 0.092
L-Leucyl-D-glucose	43	2-O-L-leucyl-D-glucose (17) 3-O-L-leucyl-D-glucose (20) 6-O-L-leucyl-D-glucose (48) 2,6-di-O-L-leucyl-D-glucose (8) 3,6-di-O-L-leucyl-D-glucose (7)	2.8 ± 0.27
L-Isoleucyl-D-glucose	47	3-O-L-isoleucyl-D-glucose (42) 6-O-L-isoleucyl-D-glucose (58)	0.7 ± 0.067
L-Prolyl-D-glucose	62	2-O-L-prolyl-D-glucose (26) 3-O-L-prolyl-D-glucose (26) 6-O-L-prolyl-D-glucose (48)	1.7 ± 0.19
L-Prolyl-D-fructose	61	1-O-L-prolyl-D-fructose (31) 6-O-L-prolyl-D-fructose (42) 1,6-di-O-L-prolyl-D-fructose (27)	4.4 ± 0.42
L-Prolyl-D-ribose	41	3-O-L-prolyl-D-ribose (35) 5-O-L-prolyl-D-ribose (65)	2.0 ± 0.18
L-Prolyl-lactose	68	6-O-L-prolyl-lactose (58) 6"-O-L-prolyl-lactose (42)	1.6 ± 0.15
L-Phenylalanyl-D-glucose	79	2-O-L-phenylalanyl-D-glucose (19) 3-O-L-phenylalanyl-D-glucose (23) 6-O-L-phenylalanyl-D-glucose (25) 2,6-di-O-L-phenylalanyl-D-glucose (17) 3,6-di-O-L-phenylalanyl-D-glucose (16)	1.0 ± 0.089
L-Phenylalanyl-D-galactose	45	2-O-L-phenylalanyl-D-galactose (32) 3-O-L-phenylalanyl-D-galactose (20) 6-O-L-phenylalanyl-D-galactose (19) 2,6-di-O-L-phenylalanyl-D-galactose (16) 3,6-di-O-L-phenylalanyl-D-galactose (13)	4.6 ± 0.45
L-Phenylalanyl-D-fructose	50	1-O-L-phenylalanyl-D-fructose (72) 6-O-L-phenylalanyl-D-fructose (28)	13.6 ± 1.43
L-Phenylalanyl-lactose	61	6-O-L-phenylalanyl-lactose (42) 6"-O-L-phenylalanyl-lactose (31) 6,6"-di-O-L-phenylalanyl-lactose (27)	7.8 ± 0.77
L-Phenylalanyl-D-mannitol	43	1-O-L-phenylalanyl-D-mannitol (62) 1,6-di-O-L-phenylalanyl-D-mannitol (38)	2.6 ± 0.25
L-Tryptophanyl-D-glucose	42	2-O-L-tryptophanyl-D-glucose (22) 3-O-L-tryptophanyl-D-glucose (21) 6-O-L-tryptophanyl-D-glucose (38) 2,6-di-O-L-tryptophanyl-D-glucose (10) 3,6-di-O-L-tryptophanyl-D-glucose (9)	7.4 ± 0.73
L-Tryptophanyl-D-fructose	18	1-O-L-tryptophanyl-D-fructose (45) 6-O-L-tryptophanyl-D-fructose (55)	0.9 ± 0.092

(continued)



Table 2 (continued)

L-Amino acyl ester of carbohydrates	Conversion Yield (%) <sup>b</sup>	Products (% proportion) <sup>c</sup>	IC <sub>50</sub> value (mM) <sup>d</sup>
L-Histidyl-D-glucose	42	2-O-L-histidyl-D-glucose (25) 3-O-L-histidyl-D-glucose (24) 6-O-L-histidyl-D-glucose (28) 2,6-di-O-L-histidyl-D-glucose (12) 3,6-di-O-L-histidyl-D-glucose (11)	3.5 ± 0.34
L-Histidyl-D-fructose	58	6-O-L-histidyl-D-fructose	0.9 ± 0.087
L-Histidyl-D-mannitol	8	1-O-L-histidyl-D-mannitol	1.7 ± 0.16

<sup>a</sup> Respective amino acids and carbohydrates as controls for ACE inhibition activity;

<sup>b</sup> Conversion yields were from HPLC with errors in HPLC yield measurements ± 10%;

<sup>c</sup> Product proportions determined from <sup>13</sup>C 2D-HSQC NMR C6 peak areas or their cross peaks, C5 cross peaks in case of ribose;

<sup>d</sup> IC<sub>50</sub> values compared to that of captopril 0.060 ± 0.006 mM determined by Cushman and Cheung method [22].

Table 3

Protease inhibition assay for eugenyl-D-glucosides and L-isoleucyl-D-glucose<sup>a</sup>

System	Protease activity Unit min <sup>-1</sup> mg <sup>-1</sup> enzyme protein <sup>b</sup>	Percentage of protease activity with respect to ACE activity <sup>c</sup>
Control ACE- 0.5 ml + 0.5 ml of 0.6% hemoglobin + 0.5 ml Buffer	0.0436	13.3
Eugenyl-D-glucoside: 0.5 ml glycoside + ACE - 0.5 ml + 0.5 ml of 0.6% hemoglobin	0.0292	8.2
L-Isoleucyl-D-glucose: 0.5 ml ester + ACE -0.5 ml + 0.5 ml of 0.6% hemoglobin	0.0267	8.9

<sup>a</sup> Conditions: ACE: 0.5 ml (0.5 mg), All the solutions were prepared in 0.1 M pH 7.5 Tris-HCl, incubation period: 30 min, temperature: 37 °C, 0.5 ml of 10% trichloroacetic acid added to arrest the reaction; Blank performed without enzyme and glycoside or ester; Absorbance measured at 440 nm; Eugenyl-D-glucoside and isoleucyl-D-glucose: 0.5 ml of 0.8 mM;

<sup>b</sup> Average absorbance values from three individual experiments;

<sup>c</sup> Percentage protease activity with respect to an ACE activity of 0.327 μmol min<sup>-1</sup> mg<sup>-1</sup> protein.

tease activity as protease inhibition activity can be construed to be ACE inhibition. The results indicate that both the glycosides and esters bind to these enzymes and hence hold promise as potential inhibitors for the ACE.

#### 4. Experimental section

##### 4.1. Enzymes

Lipozyme IM20 *Rhizomucor miehei* (RML) immobilized on weak anion exchange resin from Novo Nordisk, Denmark, *Candida rugosa* lipase (CRL) from Sigma Chemical Co., USA, for the esterification reactions and amyloglucosidase from *Rhizopus* sp. purchased from M/S Sigma Chemical. Co., MO, USA, for the glycosylation reactions, were used in the present work. RML and CRL employed showed esterification activities of 0.46 and 0.03 μmol min<sup>-1</sup> mg<sup>-1</sup> enzyme preparation, respectively [25]. Amyloglucosidase activity determined by the Sumner and Sisler method [26] was found to be 4.7 μmol min<sup>-1</sup> mg<sup>-1</sup> protein.

ACE was extracted from pig lung using the method described by Andujar-Sanchez et al. [24]. A 100 g of pig lung was minced and homogenized using a blender with 10 mM, pH 7.0, HEPES buffer containing 0.4 M NaCl at a volume ratio of 5:1 (v/w of pig lung) at 4 °C throughout the procedure. The homogenate was centrifuged at 9000 × g for 60 min. The supernatant was discarded and the precipitate was washed twice with 200 ml of 10 mM, pH 7.0, HEPES buffer containing 0.4 M NaCl. The final precipitate was resuspended in 200 ml of 10 mM, pH 7.0, HEPES buffer containing, 0.4 M NaCl, 10 μM ZnCl<sub>2</sub>, 0.5% (w/v) Triton X100 and stirred over

night. The solution was centrifuged to remove the pellets. The supernatant was dialyzed against water and later lyophilized. The protein content of ACE determined by Lowry's method [27] was found to be 8.3%. The remaining is constituted by 17% carbohydrate, lipid and other solid tissue [5,28].

##### 4.2. Chemicals and reagents

L-Amino acids, guaiacol, D-galactose, D-fructose, gum acaia and Tris-HCl from HiMedia (Ind.) Ltd.; D-glucose, sucrose, ZnCl<sub>2</sub>, trichloroacetic acid, NaOH and NaCl from SD fine chemicals (Ind.) Ltd.; maltose, hippuryl-L-histidyl-L-leucine, bovine hemoglobin and tributyrin from Sigma Chemical Co. USA; D-mannose, D-arabinose, D-ribose, D-mannitol, eugenol, sodium dodecyl sulfate, sodium benzoate, Triton X-100 and hippuric acid from LOBA Chemie Pvt. Ltd. India; curcumin (purity > 95%) from Flavors and Essences Pvt. Ltd. India; HEPES buffer, lactose, *n*-octanol and vanillin (purity > 98%) from Sisco Research Laboratories Pvt. Ltd. India and D-sorbitol from Rolex Laboratory Reagent India Ltd., were employed as such. Sephadex G-10 from Sigma Chemical Co., USA was used. Solvents-CH<sub>2</sub>Cl<sub>2</sub>, dimethylformamide, di-isopropyl ether, petroleum ether, ethyl acetate and acetonitrile from SD Fine Chemicals (Ind.) Ltd. were employed after distilling once.

##### 4.3. Glycosylation procedure

A general procedure for the glycosylation involved reaction in a 150 ml two necked flat bottom flask by refluxing phenols (1.0 mmol) and carbohydrate (1.0 mmol) in 100 ml di-isopropyl ether in presence of buffer and appropriate quantity of amyloglucosidase (30–50% w/w carbohydrate) for 72 h. In

case of *n*-octanol and guaiacol glycosides, carbohydrate and *n*-octanol/guaiacol were taken in 1: 50 molar ratio. Buffers employed were 0.4 ml to 1.0 ml of sodium acetate for pH 4.0 and 5.0, sodium phosphate for pH 6.0 and 7.0 and sodium borate for pH 8.0. After incubation, the reaction mixture was held in a boiling water bath for 5–10 min to denature the enzyme and 15–20 ml of water was added to dissolve the unreacted carbohydrate and the product glycoside. The unreacted alcohol was separated in a separating funnel with petroleum ether or *n*-hexane and phenols were separated by extracting with chloroform. The aqueous layer was evaporated to dryness to get the unreacted carbohydrate and the product glycoside. The reaction mixtures were analyzed by HPLC using an amino-propyl column (3.9 × 300 mm length) and acetonitrile: water in 80:20 ratio (v/v) as the mobile phase at a flow rate of 1 ml/min with refractive index detector. Conversion yields were determined from HPLC peak areas of the glycoside and free carbohydrate with respect to the free carbohydrate employed. Error in HPLC measurements will be ± 10%. The glycosides formed were separated through size exclusion chromatography using Sephadex G-10 eluting with water.

The isolated glycosides and esters were characterized by UV, IR, MS, 2D-NMR (HSQCT) and optical rotation, which provided good information on the nature and proportions of the products formed. A Shimadzu UV-1601 spectrophotometer was used for recording UV spectra of the isolated glycosides and esters in aqueous solutions at 0.2–1.0 mM concentration. A Nicolet 5700 FTIR instrument was used for recording the IR spectra with 1.0–3.0 mg of glycosides and ester samples as KBr pellet. Specific rotations of the isolated glycosides and esters were measured at 25 °C using Perkin-Elmer 243 polarimeter with 0.5% aqueous solution of the esters. Mass spectra of the isolated glycosides and esters were recorded using a Q-ToF Waters Ultima instrument (No. Q-ToF GAA 082, Waters corporation, Manchester, UK) fitted with an electron spray ionization (ESI) source.

<sup>1</sup>H and <sup>13</sup>C NMR spectra were recorded on a Bruker DRX-500 MHz spectrometer (500.13 MHz for <sup>1</sup>H and 125 MHz <sup>13</sup>C).

Proton and carbon 90° pulse widths were 10.5 and 12.25 μs, respectively. About 40 mg of the sample dissolved in DMSO-d<sub>6</sub> and D<sub>2</sub>O was used for recording the spectra at 35 °C. Chemical shift values were expressed in ppm relative to internal tetramethylsilane standard to within ± 0.01 ppm. 2D-HSQCT spectra were recorded for the glycosides and esters. In the NMR data, only resolvable signals are shown. Some assignments are interchangeable. *n*-Octanol/phenol signals are primed and signals from non reducing end units in maltose, lactose and sucrose are double primed. Since, the compounds are surfactant molecules, they appear to aggregate in the solvent and usually give broad signals, thus, making it difficult to resolve the coupling constant values accurately.

#### 4.3.1. Glycosides

4.3.1.1. *n*-Octyl- $\alpha/\beta$ -D-glucoside. Solid; UV (H<sub>2</sub>O,  $\lambda_{\max}$ ): 206 nm ( $\sigma \rightarrow \sigma^*$ ,  $\epsilon_{206}$ –1230 M<sup>-1</sup>), 278 nm ( $n \rightarrow \pi^*$ ,

$\epsilon_{278}$ –72 M<sup>-1</sup>). IR (KBr): 1053 cm<sup>-1</sup> (glycosidic C-O-C symmetrical), 3605 cm<sup>-1</sup> (OH). Optical rotation (*c* 1, H<sub>2</sub>O) [ $\alpha$ ]<sub>D</sub> at 25 °C = +45.8°. MS (*m/z*) 294 [M + 2]<sup>+</sup>, 317 [M + 2 + Na]<sup>+</sup>. 2D-HSQCT (DMSO-d<sub>6</sub>) *n*-Octyl- $\alpha$ -D-glucopyranoside: <sup>1</sup>H NMR  $\delta_{\text{ppm}}$ : (500.13 MHz) 4.62 (H-1 $\alpha$ ), 3.18 (H-2 $\alpha$ ), 3.42 (H-3 $\alpha$ ), 3.74 (H-4 $\alpha$ ), 3.18 (H-5 $\alpha$ ), 3.42 (H-6 $\alpha$ ), 3.1 (CH<sub>2</sub>-1'), 1.51 (CH<sub>2</sub>-2'), 1.23 (CH<sub>2</sub>-3'-7'), 0.85 (CH<sub>2</sub>-8'); <sup>13</sup>C NMR  $\delta_{\text{ppm}}$ : (125 MHz) 98.5 (C1 $\alpha$ ), 72.0 (C2 $\alpha$ ), 72.4 (C3 $\alpha$ ), 70.2 (C4 $\alpha$ ), 72.1 (C5 $\alpha$ ), 60.8 (C6  $\alpha$ ), 14.0 (C8'), 23.0 (C7'), 31.2 (C6'), 29.8 (C3'), 30.0 (C5'), 70.2 (C1'). *n*-Octyl- $\beta$ -D-glucopyranoside: <sup>1</sup>H NMR  $\delta_{\text{ppm}}$ : 4.17 (H-1 $\beta$ ), 2.88 (H-2 $\beta$ ), 3.12 (H-5 $\beta$ ), 3.60 (H-6 $\beta$ ), 3.1 (CH<sub>2</sub>-1'), 1.51 (CH<sub>2</sub>-2'), 1.23 (CH<sub>2</sub>-3'-7'), 0.85 (CH<sub>2</sub>-8'); <sup>13</sup>C NMR  $\delta_{\text{ppm}}$ : 103.2 (C1 $\beta$ ), 74.7 (C2 $\beta$ ), 77.1 (C3 $\beta$ ), 71.0 (C4 $\beta$ ), 77.1 (C5 $\beta$ ), 61.5 (C6  $\beta$ ), 14.0 (C8'), 23.0 (C7'), 31.2 (C6'), 30.0 (C5'), 70.5 (C1'). *C6*-O-octyl-D-glucose: <sup>1</sup>H NMR  $\delta_{\text{ppm}}$ : 4.90 (H-1 $\alpha$ ), 3.20 (H-2 $\alpha$ ), 3.10 (H-5 $\alpha$ ), 3.64 (H-6 $\alpha$ ), 3.1 (CH<sub>2</sub>-1'), 1.51 (CH<sub>2</sub>-2'), 1.21 (CH<sub>2</sub>-3'-7'), 0.85 (CH<sub>2</sub>-8'); <sup>13</sup>C NMR  $\delta_{\text{ppm}}$ : 92.2 (C1 $\alpha$ ), 72.5 (C2 $\alpha$ ), 72.1 (C5 $\alpha$ ), 67.2 (C6  $\alpha$ ), 14.0 (C8'), 29.5 (C3'), 30.0 (C5'), 70.5 (C1').

4.3.1.2. *n*-Octyl maltoside. Solid; UV (H<sub>2</sub>O,  $\lambda_{\max}$ ): 194 nm ( $\sigma \rightarrow \sigma^*$ ,  $\epsilon_{194}$ –1479 M<sup>-1</sup>), 278.5 nm ( $n \rightarrow \pi^*$ ,  $\epsilon_{278.5}$ –95 M<sup>-1</sup>). IR (KBr): 1033 cm<sup>-1</sup> (glycosidic C-O-C symmetrical), 1255 cm<sup>-1</sup> (glycosidic C-O-C asymmetrical), 3415 cm<sup>-1</sup> (OH). Optical rotation (*c* 1, H<sub>2</sub>O), [ $\alpha$ ]<sub>D</sub> at 25 °C = +91.1°. MS (*m/z*) 455 [M + 1]<sup>+</sup>. 2D-HSQCT (DMSO-d<sub>6</sub>) <sup>1</sup>H NMR  $\delta_{\text{ppm}}$ : (500.13 MHz) 4.63 (H-1 $\alpha$ ), 3.30 (H-5 $\alpha$ ), 3.66 (H-6 $\alpha$ ), 4.99 (H-1' $\alpha$ ), 3.46 (H-2''), 3.20 (H-3''), 3.08 (H-4''), 3.44 (H-6''), 2.9 (CH<sub>2</sub>-1'), 1.11–1.25 (CH<sub>2</sub>-2'-7'), 0.85 (CH<sub>2</sub>-8'); <sup>13</sup>C NMR  $\delta_{\text{ppm}}$ : (125 MHz) 98.8 (C1 $\alpha$ ), 75.0 (C5 $\alpha$ ), 60.5 (C6 $\alpha$ ), 100.8 (C1' $\alpha$ ), 71.8 (C2''), 72.1 (C3''), 70.2 (C4''), 61.0 (C6''), 14.1 (C8'), 23.0 (C7'), 31.5 (C6'), 29.8 (C3'), 29.0 (C2'), 70.3 (C1').

4.3.1.3. *n*-Octyl sucrose. Solid; UV (H<sub>2</sub>O,  $\lambda_{\max}$ ): 205 nm ( $\sigma \rightarrow \sigma^*$ ,  $\epsilon_{205}$ –2570 M<sup>-1</sup>), 276 nm ( $n \rightarrow \pi^*$ ,  $\epsilon_{276}$ –257 M<sup>-1</sup>). IR (KBr): 1054 cm<sup>-1</sup> (glycosidic C-O-C symmetrical), 1259 cm<sup>-1</sup> (glycosidic C-O-C asymmetrical), 3357 cm<sup>-1</sup> (OH). Optical rotation (*c* 1, H<sub>2</sub>O), [ $\alpha$ ]<sub>D</sub> at 25 °C = +13.3°. MS (*m/z*) 455 [M + 1]<sup>+</sup>. 2D-HSQCT (DMSO-d<sub>6</sub>) *C1*-O-octyl sucrose: <sup>1</sup>H NMR  $\delta_{\text{ppm}}$  (500.13 MHz): 3.76 (H-1), 3.81 (H-4), 3.79 (H-5), 3.40 (H-6), 5.18 (H-1' $\alpha$ ), 3.10 (H-3''), 3.03 (H-4''), 3.54 (H-5''), 3.62 (H-6''), 3.01 (H-1'), 1.01–1.23 (H-2-7'), 0.84 (H-8'); <sup>13</sup>C NMR  $\delta_{\text{ppm}}$  (125 MHz): 62.8 (C1), 104.0 (C2), 75.4 (C4), 83.0 (C5), 62.0 (C6), 91.5 (C1' $\alpha$ ), 72.2 (C3''), 70.5 (C4''), 72.0 (C5''), 61.0 (C6''), 14.4 (C8'), 23.2 (C7'), 31.5 (C6'), 29.2 (C5'), 29.6 (C2'), 70.2 (C1'). *C6*-O-octyl sucrose: <sup>1</sup>H NMR  $\delta_{\text{ppm}}$ : 3.54 (H-1), 3.87 (H-3), 3.72 (H-4), 3.72 (H-5), 3.25 (H-6), 4.90 (H-1' $\alpha$ ), 3.17 (H-3''), 3.11 (H-4''), 3.44 (H-5''), 3.48 (H-6''), 3.01 (H-1'), 1.0–1.25 (H-2-7'), 0.85 (H-8'); <sup>13</sup>C NMR  $\delta_{\text{ppm}}$ : 61.8 (C1), 104.04 (C2), 77.4 (C3), 76.0 (C4), 82.0 (C5), 63.0 (C6), 92.1 (C1' $\alpha$ ), 72.2 (C3''), 70.2 (C4''), 72.0 (C5''), 61.2 (C6''), 14.6 (C8'), 23.3 (C7'), 31.3 (C6'), 29.6 (C4'), 29.7 (C2'), 70.0 (C1').

4.3.1.4. Guaiacyl- $\alpha$ -D-glucoside. Solid; UV (H<sub>2</sub>O,  $\lambda_{\max}$ ): 210 nm ( $\sigma \rightarrow \sigma^*$ ,  $\epsilon_{210}$ –398 M<sup>-1</sup>), 270 nm ( $\pi \rightarrow \pi^*$ ,

$\epsilon_{270-69} \text{ M}^{-1}$ ). IR (KBr): 1030  $\text{cm}^{-1}$  (glycosidic aryl alkyl C–O–C symmetrical), 1236  $\text{cm}^{-1}$  (glycosidic aryl alkyl C–O–C asymmetrical). Optical rotation ( $c$  1,  $\text{H}_2\text{O}$ ):  $[\alpha]_{\text{D}}^{25} = +92.3^\circ$ . MS ( $m/z$ ) 286  $[\text{M}]^+$ . *CI-O-guaiacyl- $\alpha$ -D-glucopyranoside*:  $^1\text{H}$  NMR  $\delta_{\text{ppm}}$  (500.13 MHz): 4.65 (H-1 $\alpha$ ), 3.3 (H-2 $\alpha$ ), 3.72 (H-3 $\alpha$ ), 3.75 (H-4 $\alpha$ ), 3.10 (H-5 $\alpha$ ), 3.43 (H-6 $\alpha$ ), 7.08 (H-6'), 6.98 (H-5'), 6.94 (H-4'), 7.09 (H-3');  $^{13}\text{C}$  NMR  $\delta_{\text{ppm}}$  (125 MHz): 98.7 (C1 $\alpha$ ), 74.9 (C2 $\alpha$ ), 72.0 (C3 $\alpha$ ), 70.1 (C4 $\alpha$ ), 74.9 (C5 $\alpha$ ), 60.9 (C6 $\alpha$ ), 113.4 (C6'), 118.5 (C5'), 121.9 (C4'), 110.5 (C3'). *C6-O-guaiacyl- $\alpha$ -D-glucose*:  $^1\text{H}$  NMR  $\delta_{\text{ppm}}$ : 4.97 (H-1 $\alpha$ ), 3.06 (H-2 $\alpha$ ), 3.16 (H-3 $\alpha$ ), 3.63 (H-4 $\alpha$ ), 3.14 (H-5 $\alpha$ ), 3.60 (H-6 $\alpha$ ), 6.80 (H-5'), 6.84 (H-4'), 6.88 (H-3');  $^{13}\text{C}$  NMR  $\delta_{\text{ppm}}$ : 100.0 (C1 $\alpha$ ), 74.9 (C2 $\alpha$ ), 74.0 (C3 $\alpha$ ), 70.2 (C4 $\alpha$ ), 74.0 (C5 $\alpha$ ), 67.0 (C6 $\alpha$ ), 119.0 (C5'), 121.7 (C4'), 110.0 (C3').

**4.3.1.5. Eugenyl- $\alpha$ -D-glucoside.** Solid; UV ( $\text{H}_2\text{O}$ ,  $\lambda_{\text{max}}$ ): 205 nm ( $\sigma \rightarrow \sigma^*$ ,  $\epsilon_{205-1792} \text{ M}^{-1}$ ), 279 nm ( $\pi \rightarrow \pi^*$ ,  $\epsilon_{279-396} \text{ M}^{-1}$ ). IR (KBr): 1653  $\text{cm}^{-1}$  (allylic C=C), 1033  $\text{cm}^{-1}$  (glycosidic aryl alkyl C–O–C symmetrical), 1268  $\text{cm}^{-1}$  (glycosidic aryl alkyl C–O–C asymmetrical), 3330  $\text{cm}^{-1}$  (OH). Optical rotation ( $c$  1,  $\text{H}_2\text{O}$ ) at 25  $^\circ\text{C} = +59.6^\circ$ . MS ( $m/z$ ) 347  $[\text{M}+2+\text{Na}]^+$ . *CI-O-eugenyl- $\alpha$ -D-glucopyranoside*:  $^1\text{H}$  NMR  $\delta_{\text{ppm}}$  (500.13 MHz): 4.65 (H-1 $\alpha$ ), 3.55 (H-2 $\alpha$ ), 3.28 (H-3 $\alpha$ ), 3.73 (H-4 $\alpha$ ), 3.42 (H-6 $\alpha$ ), 6.86 (1H, s, H-3'), 6.70 (1H, d, H-5'), 6.85 (1H, d, H-6'), 3.28 (H-7'), 5.92 (1H, m, H-8'), 5.10 (H-9'), 3.40 (OCH<sub>3</sub>);  $^{13}\text{C}$  NMR  $\delta_{\text{ppm}}$  (125 MHz): 97.0 (C1 $\alpha$ ), 72.5 (C2 $\alpha$ ), 74.0 (C3 $\alpha$ ), 69.0 (C4 $\alpha$ ), 61.0 (C6 $\alpha$ ), 52.0 (OCH<sub>3</sub>), 113 (C3'), 120 (C5'), 115.3 (C6'), 39.0 (C7'), 137.0 (C8'), 116.0 (C9'). *C6-O-eugenyl- $\alpha$ -D-glucose*:  $^1\text{H}$  NMR  $\delta_{\text{ppm}}$ : 3.6 (H-2 $\alpha$ ), 3.50 and 3.68 (H-6 $\alpha$  a & b), 6.90 (1H, s, H-3'), 6.78 (1H, d, H-5');  $^{13}\text{C}$  NMR  $\delta_{\text{ppm}}$ : 69.0 (C2 $\alpha$ ), 66.0 (C6 $\alpha$ ), 52.0 (OCH<sub>3</sub>), 112 (C3'), 119 (C5').

**4.3.1.6. Vanillyl- $\alpha/\beta$ -D-glucoside.** Solid; UV ( $\text{H}_2\text{O}$ ,  $\lambda_{\text{max}}$ ): 195.5 nm ( $\sigma \rightarrow \sigma^*$ ,  $\epsilon_{195.5-2241} \text{ M}^{-1}$ ), 279.5 nm ( $\pi \rightarrow \pi^*$ ,  $\epsilon_{279.5-5291} \text{ M}^{-1}$ ). IR (KBr): 3358  $\text{cm}^{-1}$  (OH), 1260  $\text{cm}^{-1}$  (glycosidic aryl alkyl C–O–C asymmetric), 1030  $\text{cm}^{-1}$  (glycosidic aryl alkyl C–O–C symmetric), 1408  $\text{cm}^{-1}$  (C=C), 1636  $\text{cm}^{-1}$  (CO), 2933  $\text{cm}^{-1}$  (CH). Optical rotation ( $c$  1,  $\text{H}_2\text{O}$ ):  $[\alpha]_{\text{D}}^{25} = +62.8$ . MS ( $m/z$ ) 316  $[\text{M} + 2]^+$ . 2D-HSQCT (DMSO- $d_6$ ) *CI-O-vanillyl- $\alpha$ -D-glucopyranoside*:  $^1\text{H}$  NMR  $\delta_{\text{ppm}}$  (500.13 MHz): 4.65 (H-1 $\alpha$ , 5.5 Hz), 3.23 (H-2 $\alpha$ ), 3.42 (H-3 $\alpha$ ), 3.78 (H-4 $\alpha$ ), 3.15 (H-5 $\alpha$ ), 3.60 (H-6 $\alpha$ ), 6.59 (H-2'), 6.20 (H-5'), 3.73 (OCH<sub>3</sub>);  $^{13}\text{C}$  NMR  $\delta_{\text{ppm}}$  (125 MHz): 99.2 (C1 $\alpha$ ), 72.3 (C2 $\alpha$ ), 73.5 (C3 $\alpha$ ), 70.2 (C4 $\alpha$ ), 72.5 (C5 $\alpha$ ), 60.5 (C6 $\alpha$ ), 111.4 (C2'), 114.5 (C5'). *CI-O-vanillyl- $\beta$ -D-glucopyranoside*:  $^1\text{H}$  NMR  $\delta_{\text{ppm}}$ : 4.94 (H-1 $\beta$ , 5.3 Hz), 2.98 (H-2 $\beta$ ), 3.22 (H-3 $\beta$ ), 3.68 (H-6 $\beta$ );  $^{13}\text{C}$  NMR  $\delta_{\text{ppm}}$ : 101.5 (C1 $\beta$ ), 74.6 (C2 $\beta$ ), 76.1 (C3 $\beta$ ), 60.8 (C6 $\beta$ ). *C6-O-vanillyl- $\beta$ -D-glucose*:  $^1\text{H}$  NMR  $\delta_{\text{ppm}}$ : 4.91 (H-1 $\alpha$ ), 3.23 (H-2 $\alpha$ ), 3.20 (H-3 $\alpha$ ), 3.62 (H-4 $\alpha$ ), 3.23 (H-5 $\alpha$ ), 3.55 (H-6 $\alpha$ );  $^{13}\text{C}$  NMR  $\delta_{\text{ppm}}$ : 92.7 (C1 $\alpha$ ), 72.3 (C2 $\alpha$ ), 72.6 (C3 $\alpha$ ), 70.2 (C4 $\alpha$ ), 75.2 (C5 $\alpha$ ), 68.0 (C6 $\alpha$ ).

**4.3.1.7. Vanillyl- $\alpha$ -D-galactoside.** Solid; UV ( $\text{H}_2\text{O}$ ,  $\lambda_{\text{max}}$ ): 198.0 nm ( $\sigma \rightarrow \sigma^*$ ,  $\epsilon_{198.0-2909} \text{ M}^{-1}$ ), 281.0 nm ( $\pi \rightarrow \pi^*$ ,  $\epsilon_{281.0-519} \text{ M}^{-1}$ ). IR (KBr): 3271  $\text{cm}^{-1}$  (OH), 1261  $\text{cm}^{-1}$  (glycosidic aryl alkyl C–O–C asymmetric), 1031  $\text{cm}^{-1}$  (glycosidic

aryl alkyl C–O–C symmetric), 1406  $\text{cm}^{-1}$  (C=C), 1664  $\text{cm}^{-1}$  (CO). Optical rotation ( $c$  1,  $\text{H}_2\text{O}$ ):  $[\alpha]_{\text{D}}^{25} = +8.82$ . MS ( $m/z$ ) 314  $[\text{M}]^+$ . 2D-HSQCT (DMSO- $d_6$ ): *CI-O-vanillyl- $\alpha$ -D-galactopyranoside*:  $^1\text{H}$  NMR  $\delta_{\text{ppm}}$  (500.13 MHz): 4.22 (H-1 $\alpha$ ), 3.69 (H-2 $\alpha$ ), 3.52 (H-3 $\alpha$ ), 3.48 (H-4 $\alpha$ ), 3.43 (H-5 $\alpha$ ), 3.35 (H-6 $\alpha$ ), 7.38 (H-2'), 6.90 (H-5'), 7.33 (H-6'), 3.86 (OCH<sub>3</sub>), 9.74 (CHO);  $^{13}\text{C}$  NMR  $\delta_{\text{ppm}}$  (125 MHz): 95.8 (C1 $\alpha$ ), 69.4 (C2 $\alpha$ ), 69.9 (C3 $\alpha$ ), 70.8 (C4 $\alpha$ ), 71.1 (C5 $\alpha$ ), 62.0 (C6 $\alpha$ ), 129.2 (C1'), 111.3 (C2'), 148.6 (C3'), 153.5 (C4'), 115.9 (C5'), 126.4 (C6'), 56.1 (OCH<sub>3</sub>), 191.4 (CHO).

**4.3.1.8. Vanillyl- $\alpha$ -D-mannoside.** Solid; UV ( $\text{H}_2\text{O}$ ,  $\lambda_{\text{max}}$ ): 198.5 nm ( $\sigma \rightarrow \sigma^*$ ,  $\epsilon_{198.5-3401} \text{ M}^{-1}$ ), 278.0 nm ( $\pi \rightarrow \pi^*$ ,  $\epsilon_{278.0-284} \text{ M}^{-1}$ ). IR (KBr): 3365  $\text{cm}^{-1}$  (OH), 1249  $\text{cm}^{-1}$  (glycosidic aryl alkyl C–O–C asymmetric), 1030  $\text{cm}^{-1}$  (glycosidic aryl alkyl C–O–C symmetric), 1406  $\text{cm}^{-1}$  (C=C), 1651  $\text{cm}^{-1}$  (CO), 2940  $\text{cm}^{-1}$  (CH). Optical rotation ( $c$  1,  $\text{H}_2\text{O}$ ):  $[\alpha]_{\text{D}}^{25} = -3.6$ . MS ( $m/z$ ) 314  $[\text{M}]^+$ . *CI-O-vanillyl- $\alpha$ -D-mannopyranoside*:  $^{13}\text{C}$  NMR (DMSO- $d_6$ )  $\delta_{\text{ppm}}$  (125 MHz): 100.8 (C1 $\alpha$ ), 70.5 (C2 $\alpha$ ), 71.3 (C3 $\alpha$ ), 67.1 (C4 $\alpha$ ), 73.8 (C5 $\alpha$ ), 61.3 (C6 $\alpha$ ), 109.4 (C2'), 114.72 (C5'), 121.9 (C6').

**4.3.1.9. Vanillyl maltoside.** Solid; UV ( $\text{H}_2\text{O}$ ,  $\lambda_{\text{max}}$ ): 194.5 nm ( $\sigma \rightarrow \sigma^*$ ,  $\epsilon_{194.5-4782} \text{ M}^{-1}$ ), 278.5 nm ( $\pi \rightarrow \pi^*$ ,  $\epsilon_{278.5-328} \text{ M}^{-1}$ ). IR (KBr): 3361  $\text{cm}^{-1}$  (OH), 1265  $\text{cm}^{-1}$  (glycosidic aryl alkyl C–O–C asymmetric), 1024  $\text{cm}^{-1}$  (glycosidic aryl alkyl C–O–C symmetric), 1412  $\text{cm}^{-1}$  (C=C), 1651  $\text{cm}^{-1}$  (CO), 2930  $\text{cm}^{-1}$  (CH), 1205  $\text{cm}^{-1}$  (OCH<sub>3</sub>). Optical rotation ( $c$  1,  $\text{H}_2\text{O}$ ):  $[\alpha]_{\text{D}}^{25} = +92.0$ . MS ( $m/z$ ) 478  $[\text{M} + 2]^+$ . 2D-HSQCT (DMSO- $d_6$ ) *CI-O-vanillyl- $\alpha$ -maltoside*:  $^1\text{H}$  NMR  $\delta_{\text{ppm}}$  (500.13 MHz): 4.68 (H-1 $\alpha$ ), 3.10 (H-2 $\alpha$ ), 3.20 (H-3 $\alpha$ ), 3.30 (H-4 $\alpha$ ), 3.72 (H-5 $\alpha$ ), 3.48 (H-6 $\alpha$ ), 4.94 (H-1'' $\alpha$ , 5.7 Hz), 3.25 (H-2'), 2.88 (H-3''), 3.65 (H-4''), 3.60 (H-6''), 6.26 (H-2''), 6.62 (H-5'), 7.18 (H-6'), 3.73 (OCH<sub>3</sub>);  $^{13}\text{C}$  NMR  $\delta_{\text{ppm}}$  (125 MHz): 98.2 (C1 $\alpha$ ), 70.1 (C2 $\alpha$ ), 75.1 (C3 $\alpha$ ), 79.1 (C4 $\alpha$ ), 69.8 (C5 $\alpha$ ), 60.8 (C6 $\alpha$ ), 100.3 (C1'' $\alpha$ ), 73.8 (C2''), 74.5 (C3''), 70.0 (C4''), 60.8 (C6''), 130.0 (C1'), 109.5 (C2'), 114.2 (C5'), 126.8 (C6'). *C6-O-vanillyl maltose*:  $^1\text{H}$  NMR  $\delta_{\text{ppm}}$ : 4.88 (H-1 $\alpha$ ), 3.54 (H-6 $\alpha$ ), 4.94 (H-1'' $\alpha$ );  $^{13}\text{C}$  NMR  $\delta_{\text{ppm}}$ : 92.4 (C1 $\alpha$ ), 67.2 (C6 $\alpha$ ), 100.3 (C1'' $\alpha$ ). *C6''-O-vanillyl maltose*:  $^1\text{H}$  NMR  $\delta_{\text{ppm}}$ : 4.88 (H-1 $\alpha$ ), 4.94 (H-1'' $\alpha$ ), 3.69 (H-6''),  $^{13}\text{C}$  NMR  $\delta_{\text{ppm}}$ : 92.4 (C1 $\alpha$ ), 100.3 (C1'' $\alpha$ ), 66.1 (C6'').

**4.3.1.10. Vanillyl sucrose.** Solid; UV ( $\text{H}_2\text{O}$ ,  $\lambda_{\text{max}}$ ): 194.0 nm ( $\sigma \rightarrow \sigma^*$ ,  $\epsilon_{194.0-6820} \text{ M}^{-1}$ ), 278.5 nm ( $\pi \rightarrow \pi^*$ ,  $\epsilon_{278.5-423} \text{ M}^{-1}$ ). IR (KBr): 3374  $\text{cm}^{-1}$  (OH), 1254  $\text{cm}^{-1}$  (glycosidic aryl alkyl C–O–C asymmetric), 1026  $\text{cm}^{-1}$  (glycosidic aryl alkyl C–O–C symmetric), 1412  $\text{cm}^{-1}$  (C=C), 1650  $\text{cm}^{-1}$  (CO), 2936  $\text{cm}^{-1}$  (CH), 1211  $\text{cm}^{-1}$  (OCH<sub>3</sub>). Optical rotation ( $c$  1,  $\text{H}_2\text{O}$ ):  $[\alpha]_{\text{D}}^{25} = +48.6$ . MS ( $m/z$ ) 476  $[\text{M}]^+$ . 2D-HSQCT (DMSO- $d_6$ ) *CI-O-vanillyl sucrose*:  $^1\text{H}$  NMR  $\delta_{\text{ppm}}$  (500.13 MHz): 3.49 (H-1), 3.88 (H-3), 3.89 (H-4), 3.86 (H-5), 3.4 (H-6), 4.72 (H-1'' $\alpha$ ), 3.68 (H-2''), 3.46 (H-3''), 3.62 (H-4''), 3.65 (H-5''), 3.59 (H-6''), 7.22 (H-2'), 6.60 (H-5'), 8.35 (H-6');  $^{13}\text{C}$  NMR  $\delta_{\text{ppm}}$  (125 MHz): 66.0 (C1), 76.8 (C3), 80.9 (C4), 81.5 (C5), 62.2 (C6), 98.5 (C1'' $\alpha$ ), 71.0 (C2''), 72.2 (C3''), 69.8 (C4''), 72.1 (C5''), 60.5 (C6''), 112.8 (C5'), 126.3 (C6'). *C6''-O-vanillyl*

sucrose:  $^1\text{H}$  NMR  $\delta_{\text{ppm}}$ : 3.48 (H-1), 3.67 (H-3), 3.57 (H-5), 3.46 (H-6), 4.63 (H-1' $\alpha$ ), 3.08 (H-2''), 3.42 (H-3''), 3.15 (H-4''), 3.19 (H-5''), 3.72 (H-6'');  $^{13}\text{C}$  NMR  $\delta_{\text{ppm}}$ : 62.3 (C1), 76.5 (C3), 82.2 (C5), 60.5 (C6), 98.6 (C1' $\alpha$ ), 69.9 (C2''), 72.3 (C3''), 69.8 (C4''), 71.5 (C5''), 66.1 (C6'').

4.3.1.11. *Vanillyl-D-sorbitol*. Solid; UV ( $\text{H}_2\text{O}$ ,  $\lambda_{\text{max}}$ ): 193.5 nm ( $\sigma \rightarrow \sigma^*$ ,  $\epsilon_{193.5-2940} \text{ M}^{-1}$ ), 273.0 nm ( $\pi \rightarrow \pi^*$ ,  $\epsilon_{273.0-290} \text{ M}^{-1}$ ). IR (KBr): 3386  $\text{cm}^{-1}$  (OH), 1260  $\text{cm}^{-1}$  (glycosidic aryl alkyl C–O–C asymmetric), 1038  $\text{cm}^{-1}$  (glycosidic aryl alkyl C–O–C symmetric), 1409  $\text{cm}^{-1}$  (C=C), 2943  $\text{cm}^{-1}$  (CH). Optical rotation ( $c$  1,  $\text{H}_2\text{O}$ ):  $[\alpha]_{\text{D}}^{25} = +13.9$ . MS ( $m/z$ ) mono-arylated 316  $[\text{M}]^+$ , di-arylated 451  $[\text{M} + 1]^+$ . 2D-HSQCT (DMSO- $d_6$ ): *C1-O-vanillyl-D-sorbitol*:  $^1\text{H}$  NMR  $\delta_{\text{ppm}}$  (500.13 MHz): 3.65 (H-1), 3.37 (H-2), 3.48 (H-3), 3.57 (H-4), 3.54 (H-5), 3.58 (H-6), 7.40 (H-2'), 7.20 (H-5'), 7.58 (H-6'), 3.81 (OCH<sub>3</sub>), 9.75 (CHO);  $^{13}\text{C}$  NMR  $\delta_{\text{ppm}}$  (125 MHz): 67.2 (C1), 70.5 (C2), 74.1 (C3), 71.2 (C4), 69.0 (C5), 62.9 (C6), 130.5 (C1'), 111.2 (C2'), 153.8 (C4'), 111.1 (C5'), 124.5 (C6'), 55.9 (OCH<sub>3</sub>), 191.5 (CHO). *C6-O-vanillyl-D-sorbitol*:  $^1\text{H}$  NMR  $\delta_{\text{ppm}}$ : 3.55 (H-1), 3.54 (H-2), 3.44 (H-3), 3.68 (H-4), 3.46 (H-5), 3.58 (H-6), 6.88 (H-2'), 6.85 (H-5'), 7.39 (H-6');  $^{13}\text{C}$  NMR  $\delta_{\text{ppm}}$ : 63.2 (C1), 70.8 (C2), 72.5 (C3), 73.1 (C4), 68.2 (C5), 66.2 (C6), 129.1 (C1'), 110.8 (C2'), 153.8 (C4'), 111.4 (C5'), 126.1 (C6'). *C1, C6 Di-O-vanillyl-D-sorbitol*:  $^1\text{H}$  NMR  $\delta_{\text{ppm}}$ : 3.46 (H-1), 3.35 (H-2), 3.36 (H-3), 3.54 (H-4), 3.65 (H-6), 6.65, 6.68 (H-5'), 6.69, 6.84 (H-6');  $^{13}\text{C}$  NMR  $\delta_{\text{ppm}}$ : 66.5 (C1), 67.0 (C2), 73.5 (C3), 76.1 (C4), 65.5 (C6), 129.1, 130.5 (C1'), 111.3, 111.7 (C2'), 153.5, 153.5 (C4'), 115.3, 115.9 (C5'), 119.8, 120.3 (C6').

4.3.1.12. *Curcuminyl-bis- $\alpha$ -D-glucoside*. Solid; UV ( $\text{H}_2\text{O}$ ,  $\lambda_{\text{max}}$ ): 210 nm ( $\sigma \rightarrow \sigma^*$ ,  $\epsilon_{210-1242} \text{ M}^{-1}$ ), 252 nm ( $\pi \rightarrow \pi^*$ ,  $\epsilon_{252-1537} \text{ M}^{-1}$ ), 430 nm ( $\pi \rightarrow \pi^*$  extended conjugation,  $\epsilon_{430-42} \text{ M}^{-1}$ ). IR (KBr): 1664  $\text{cm}^{-1}$  (CO), 1027  $\text{cm}^{-1}$  (aryl alkyl C–O–C symmetrical), 1254  $\text{cm}^{-1}$  (aryl alkyl C–O–C asymmetrical). Optical rotation ( $c$  1,  $\text{H}_2\text{O}$ ):  $[\alpha]_{\text{D}}^{25} = +30.3^\circ$ . MS ( $m/z$ ) 691  $[\text{M}-1]^+$ . *C1-O-curcuminyl-bis- $\alpha$ -D-glucopyranoside*:  $^1\text{H}$  NMR  $\delta_{\text{ppm}}$  (500.13 MHz): 4.66 (H-1 $\alpha$ ), 3.15 (H-2 $\alpha$ ), 3.73 (H-3 $\alpha$ ), 3.75 (H-4 $\alpha$ ), 3.53 (H-6 $\alpha$ ), 3.85 (6H, s, 2-OCH<sub>3</sub>), 6.06 (1H, s, H<sub>1</sub>), 6.71 (2H, d,  $J = 15.8 \text{ Hz}$ , H<sub>3</sub>, 3'), 7.51 (2H, d,  $J = 15.8$ , H<sub>4</sub>, 4'), 7.25 (2H, s, H<sub>6</sub>, 6'), 6.81 (2H, d,  $J = 8.2 \text{ Hz}$ , H<sub>9</sub>, 9'), 7.11 (2 H, dd,  $J = 1.45 \text{ Hz}$ , H<sub>10</sub>, 10');  $^{13}\text{C}$  NMR  $\delta_{\text{ppm}}$  (125 MHz): 99.0 (C1 $\alpha$ ), 72.2 (C2 $\alpha$ ), 73.6 (C3 $\alpha$ ), 70.6 (C4 $\alpha$ ), 61.3 (C6 $\alpha$ ), 56.1 (OCH<sub>3</sub>), 101.0 (C<sub>1'</sub>), 183.5 (C<sub>2'</sub>C<sub>2'</sub>), 121.5 (C<sub>3'</sub>C<sub>3'</sub>), 141.0 (C<sub>4'</sub>C<sub>4'</sub>), 126.8 (C<sub>5'</sub>C<sub>5'</sub>), 111.6 (C<sub>6'</sub>C<sub>6'</sub>), 148.4 (C<sub>7'</sub>C<sub>7'</sub>), 150.0 (C<sub>8'</sub>C<sub>8'</sub>), 116.1 (C<sub>9'</sub>C<sub>9'</sub>), 123.4 (C<sub>10'</sub>C<sub>10'</sub>). *C6-O-curcuminyl-bis- $\alpha$ -D-glucose*:  $^1\text{H}$  NMR  $\delta_{\text{ppm}}$ : 3.25 (H-2 $\alpha$ ), 3.65 (H-4 $\alpha$ ), 3.52, 3.70 (H-6 $\alpha$  a & b), 6.81 (H<sub>3</sub>, 3'), 7.10 (H<sub>9</sub>, 9');  $^{13}\text{C}$  NMR  $\delta_{\text{ppm}}$ : 75.0 (C2 $\alpha$ ), 70.5 (C4 $\alpha$ ), 66.5 (C6 $\alpha$ ), 123.0 (C<sub>3</sub>, C<sub>3'</sub>), 116 (C<sub>9</sub>, C<sub>9'</sub>).

#### 4.4. Esterification procedure

A general procedure employed for the esterification reaction involved reacting 0.001–0.008 mol unprotected L-amino acid

(L-alanine, L-valine, L-leucine and L-isoleucine, L-proline, L-phenylalanine, L-tryptophan and L-histidine) and 0.001–0.002 mol of carbohydrate (D-glucose, D-galactose, D-fructose, D-ribose, lactose, maltose, D-sorbitol and D-mannitol) along with 100 ml  $\text{CH}_2\text{Cl}_2/\text{DMF}$  (90:10 v/v, 40 °C) or hexane/ $\text{CHCl}_3/\text{DMF}$  (45:45:10 v/v, 61 °C) in presence of 0.60–0.180 g of lipases (40–50% w/w carbohydrate employed) under reflux for a period of three days in a flat bottom two necked flask. *Rhizomucor miehei* lipase (RML) in presence of 0.1 mM (0.1 ml), pH 4.0, acetate buffer (L-alanyl carbohydrate esters), *Candida rugosa* lipase (CRL) in presence of 0.1 mM (0.1 ml), pH 7.0, phosphate buffer (L-valyl, L-leucyl, and L-isoleucyl esters of carbohydrates) and CRL in presence of 0.2 mM (0.2 ml), pH 4.0, acetate buffer (L-prolyl, L-phenylalanyl, L-tryptophanyl and L-histidyl esters of carbohydrates) were employed. The condensed vapor of solvents which formed an azeotrope with water was passed through a desiccant before being returned into the reaction mixture, thereby facilitating complete removal of water of reaction [18] and also maintaining a very low water activity of  $a_w = 0.0054$  throughout the reaction. After completion of the reaction, the solvent was distilled off, 20–30 ml of warm water was added, stirred and filtered to remove the lipase. The filtrate was evaporated to get a mixture of the unreacted carbohydrate, unreacted L-amino acids and the product esters, which were then analyzed by HPLC. A Shimadzu LC10AT HPLC connected to LiChrosorb RP-18 column (5  $\mu\text{m}$  particle size, 4.6  $\times$  150 mm length) with acetonitrile/water (v/v 20:80) as a mobile phase at a flow rate of 1 ml  $\text{min}^{-1}$  was employed using an UV detector at 210 nm in case of L-alanyl, L-valyl, L-leucyl, L-isoleucyl and L-prolyl esters and at 254 nm in case of L-phenylalanyl, L-tryptophanyl and L-histidyl esters of carbohydrates. The conversion yields were determined with respect to peak areas of L-amino acids and those of the esters. The esters formed were separated by size exclusion chromatography using Sephadex G-10.

#### 4.4.1. Amino acyl esters of carbohydrates

4.4.1.1. *L-Alanyl- $\beta$ -D-glucose*. Solid; UV ( $\text{H}_2\text{O}$ ,  $\lambda_{\text{max}}$ ): 227.0 nm ( $\sigma \rightarrow \sigma^*$ ,  $\epsilon_{227.0-1151} \text{ M}^{-1}$ ), 294.0 nm ( $n \rightarrow \pi^*$ ,  $\epsilon_{294.0-764} \text{ M}^{-1}$ ). IR (KBr): 3371  $\text{cm}^{-1}$  (NH), 3410  $\text{cm}^{-1}$  (OH), 2297  $\text{cm}^{-1}$  (CH), 1653  $\text{cm}^{-1}$  (CO). Optical rotation ( $c$  0.5,  $\text{H}_2\text{O}$ ):  $[\alpha]_{\text{D}}^{25} = -38.1^\circ$ . MS ( $m/z$ ) 274  $[\text{M} + \text{Na}]^+$ . 2D-HSQCT (DMSO- $d_6$ ) *2-O-ester*:  $^1\text{H}$  NMR  $\delta_{\text{ppm}}$  (500.13 MHz): 2.95 ( $\alpha\text{CH}$ ), 1.07 ( $\beta\text{CH}_3$ ), 3.62 (H-2 $\beta$ ), 3.83 (H-3 $\beta$ ), 3.67 (H-4 $\beta$ ), 3.44 (H-6 $\beta$ );  $^{13}\text{C}$  NMR  $\delta_{\text{ppm}}$  (125 MHz): 52.1 ( $\alpha\text{CH}$ ), 15.7 ( $\beta\text{CH}_3$ ), 102.8 (C1 $\beta$ ), 82.6 (C2 $\beta$ ), 77.9 (C3 $\beta$ ), 68.8 (C4 $\beta$ ), 60.5 (C6 $\beta$ ). *3-O-ester*:  $^1\text{H}$  NMR  $\delta_{\text{ppm}}$ : 2.87 ( $\alpha\text{CH}$ ), 3.93 (H-3 $\beta$ ), 3.58 (H-4 $\beta$ ), 3.36 (H-6 $\beta$ );  $^{13}\text{C}$  NMR  $\delta_{\text{ppm}}$ : 51.4 ( $\alpha\text{CH}$ ), 83.3 (C3 $\beta$ ), 69.3 (C4 $\beta$ ), 57.3 (C6 $\beta$ ). *6-O-ester*:  $^1\text{H}$  NMR  $\delta_{\text{ppm}}$ : 2.95 ( $\alpha\text{CH}$ ), 1.30 ( $\beta\text{CH}_3$ ), 3.86 (H-2 $\beta$ ), 3.76 (H-5 $\beta$ ), 3.82 (H-6 $\beta$ );  $^{13}\text{C}$  NMR  $\delta_{\text{ppm}}$ : 50.2 ( $\alpha\text{CH}$ ), 15.1 ( $\beta\text{CH}_3$ ), 171.4 (CO), 101.8 (C1 $\beta$ ), 75.0 (C2 $\beta$ ), 70.1 (C5 $\beta$ ), 63.5 (C6 $\beta$ ). *2,6-di-O-ester*:  $^1\text{H}$  NMR  $\delta_{\text{ppm}}$ : 3.36 ( $\alpha\text{CH}$ ), 1.30 ( $\beta\text{CH}_3$ ), 3.78 (H-2 $\beta$ ), 3.47 (H-6 $\beta$ );  $^{13}\text{C}$  NMR  $\delta_{\text{ppm}}$ : 49.5 ( $\alpha\text{CH}$ ), 16.4 ( $\beta\text{CH}_3$ ), 100.8 (C1 $\beta$ ), 76.5 (C2 $\beta$ ), 62.7 (C6 $\beta$ ). *3,6-di-O-ester*:  $^1\text{H}$  NMR  $\delta_{\text{ppm}}$ :

1.30 ( $\beta\text{CH}_3$ ), 3.78 (H-3 $\beta$ ), 3.82 (H-6 $\beta$ );  $^{13}\text{C}$  NMR  $\delta_{\text{ppm}}$ : 51.4 ( $\alpha\text{CH}$ ), 16.7 ( $\beta\text{CH}_3$ ), 81.6 (C3 $\beta$ ), 63.1 (C6 $\beta$ ).

**4.4.1.2. L-Alanyl-D-ribose.** Solid; UV ( $\text{H}_2\text{O}$ ,  $\lambda_{\text{max}}$ ): 224.0 nm ( $\sigma \rightarrow \sigma^*$   $\epsilon_{224.0-3802} \text{ M}^{-1}$ ), 294.0 nm ( $n \rightarrow \pi^*$   $\epsilon_{294.0-1288} \text{ M}^{-1}$ ). IR (KBr): 3402  $\text{cm}^{-1}$  (NH), 3242  $\text{cm}^{-1}$  (OH), 2887  $\text{cm}^{-1}$  (CH), 1625  $\text{cm}^{-1}$  (CO). Optical rotation ( $c$  0.5,  $\text{H}_2\text{O}$ ):  $[\alpha]_{\text{D}}^{25} = +22.0^\circ$ . MS ( $m/z$ ) 221  $[\text{M}]^+$ ; 2D-HSQCT (DMSO- $d_6$ ) 2-*O*-ester:  $^1\text{H}$  NMR  $\delta_{\text{ppm}}$  (500.13 MHz): 1.25 ( $\alpha\text{CH}$ ), 3.12 ( $\beta\text{CH}_3$ ), 3.67 (H-2 $\alpha$ ), 3.50 (H-3 $\alpha$ ), 3.63 (H-4 $\alpha$ ), 3.64 (H-5 $\alpha$ );  $^{13}\text{C}$  NMR  $\delta_{\text{ppm}}$  (125 MHz): 48.2 ( $\alpha\text{CH}$ ), 15.9 ( $\beta\text{CH}_3$ ), 75.7 (C2 $\alpha$ ), 67.2 (C3 $\alpha$ ), 68.1 (C4 $\alpha$ ), 60.6 (C5 $\alpha$ ). 5-*O*-ester:  $^1\text{H}$  NMR  $\delta_{\text{ppm}}$ : 3.39 ( $\alpha\text{CH}$ ), 1.25 ( $\beta\text{CH}_3$ ), 4.95 (H-1 $\alpha$ ), 4.20 (H-1 $\beta$ ), 3.27 (H-3 $\alpha$ ), 3.88 (H-4 $\alpha$ ), 3.61(H-5 $\alpha$ );  $^{13}\text{C}$  NMR  $\delta_{\text{ppm}}$ : 53.0 ( $\alpha\text{CH}$ ), 18.5 ( $\beta\text{CH}_3$ ), 173.5 (CO), 101.6 (C1 $\alpha$ ), 103.9 (C1 $\beta$ ), 75.0 (C3 $\alpha$ ), 71.0 (C4 $\alpha$ ), 63.4 (C5 $\alpha$ ). 2,5-di-*O*-ester:  $^1\text{H}$  NMR  $\delta_{\text{ppm}}$ : 1.20 ( $\beta\text{CH}_3$ ), 3.45 (H-2 $\alpha$ ), 3.79 (H-4 $\alpha$ ), 3.52 (H-5 $\alpha$ );  $^{13}\text{C}$  NMR  $\delta_{\text{ppm}}$ : 18.5 ( $\beta\text{CH}_3$ ), 74.9 (C2 $\alpha$ ), 71.0 (C3 $\alpha$ ), 63.4 (C5 $\alpha$ ).

**4.4.1.3. L-Alanyl lactose.** Solid; UV ( $\text{H}_2\text{O}$ ,  $\lambda_{\text{max}}$ ): 220.0 nm ( $\sigma \rightarrow \sigma^*$   $\epsilon_{220.0-436} \text{ M}^{-1}$ ), 294.0 nm ( $n \rightarrow \pi^*$   $\epsilon_{294.0-240} \text{ M}^{-1}$ ). IR (KBr): 3378  $\text{cm}^{-1}$  (NH), 3378  $\text{cm}^{-1}$  (OH), 2946  $\text{cm}^{-1}$  (CH), 1624  $\text{cm}^{-1}$  (CO). Optical rotation ( $c$  0.5,  $\text{H}_2\text{O}$ ):  $[\alpha]_{\text{D}}^{25} = +7.4^\circ$ . MS ( $m/z$ ) 436  $[\text{M} + \text{Na}]^+$ . 2D-HSQCT (DMSO- $d_6$ ) 6-*O*-ester:  $^1\text{H}$  NMR  $\delta_{\text{ppm}}$  (500.13 MHz): 3.55 ( $\alpha\text{CH}$ ), 1.25 ( $\beta\text{CH}_3$ ), 4.78 (H-1 $\alpha$ ), 4.82 (H-1 $\beta$ ), 2.95 (H-2 $\alpha$ ), 3.25 (H-2 $\beta$ ), 2.95 (H-3 $\alpha$ ), 4.05 (H-4 $\alpha,\beta$ ), 3.15 (H-5 $\alpha$ ), 3.35 (H-5 $\beta$ ), 3.80 (H-6 $\alpha,\beta$ ), 4.90 (H-1 $\beta$ ), 3.90 (H-2 $\beta$ ), 2.85 (H-3 $\beta$ ), 3.70 (H-4 $\beta$ ), 3.60 (H-5 $\beta$ ), 3.40 (H-6 $\beta$ );  $^{13}\text{C}$  NMR  $\delta_{\text{ppm}}$  (125 MHz): 51.0 ( $\alpha\text{CH}$ ), 15.5 ( $\beta\text{CH}_3$ ), 173.0 (CO), 98.0 (C1 $\alpha$ ), 100.2 (C1 $\beta$ ), 70.3 (C2 $\alpha$ ), 72.4 (C2 $\beta$ ), 74.3 (C3 $\alpha$ ), 81.0 (C4 $\alpha,\beta$ ), 73.3 (C5 $\alpha$ ), 73.4 (C5 $\beta$ ), 61.2 (C6 $\alpha,\beta$ ), 100.2 (C1 $\beta$ ), 76.5 (C2 $\beta$ ), 75.1 (C3 $\beta$ ), 68.5 (C4 $\beta$ ), 78.5 (C5 $\beta$ ), 60.6 (C6 $\beta$ ). 6 $\beta$ -*O*-ester:  $^1\text{H}$  NMR  $\delta_{\text{ppm}}$ : 3.35 ( $\alpha\text{CH}$ ), 3.85 (H-4 $\alpha$ ), 3.70 (H-6 $\alpha$ );  $^{13}\text{C}$  NMR  $\delta_{\text{ppm}}$ : 53.5 ( $\alpha\text{CH}$ ), 81.5 (C4 $\alpha$ ), 64.0 (C6 $\alpha$ ). 6,6 $\beta$ -di-*O*-ester:  $^1\text{H}$  NMR  $\delta_{\text{ppm}}$  (500.13 MHz): 3.85 (H-6 $\alpha$ ),  $^{13}\text{C}$  NMR  $\delta_{\text{ppm}}$  (125 MHz): 67.5 (C6 $\beta$ ).

**4.4.1.4. L-Valyl-D-glucose.** Solid; UV ( $\text{H}_2\text{O}$ ,  $\lambda_{\text{max}}$ ): 200.0 nm ( $\sigma \rightarrow \sigma^*$   $\epsilon_{200.0-2630} \text{ M}^{-1}$ ), 295.0 nm ( $n \rightarrow \pi^*$   $\epsilon_{295.0-2089} \text{ M}^{-1}$ ). IR (KBr):  $\text{cm}^{-1}$  2889 (NH), 3407  $\text{cm}^{-1}$  (OH), 2950  $\text{cm}^{-1}$  (CH), 1622  $\text{cm}^{-1}$  (CO). Optical rotation ( $c$  0.5,  $\text{H}_2\text{O}$ ):  $[\alpha]_{\text{D}}^{25} = +8.8^\circ$ . MS ( $m/z$ ) 302  $[\text{M} + \text{Na}]^+$ . 2D-HSQCT (DMSO- $d_6$ ) 2-*O*-ester:  $^1\text{H}$  NMR  $\delta_{\text{ppm}}$  (500.13 MHz): 3.30 ( $\alpha\text{CH}$ ), 1.90 ( $\beta\text{CH}$ ), 0.98 ( $\gamma\text{CH}_3$ ), 0.98 ( $\delta\text{CH}_3$ ), 3.83 (H-2 $\alpha$ ), 3.65 (H-2 $\beta$ );  $^{13}\text{C}$  NMR  $\delta_{\text{ppm}}$  (125 MHz): 53.2 ( $\alpha\text{CH}$ ), 29.2 ( $\beta\text{CH}$ ), 18.1 ( $\gamma\text{CH}_3$ ), 18.1 ( $\delta\text{CH}_3$ ), 76.1 (C2 $\alpha$ ), 60.0 (C6 $\alpha$ ). 3-*O*-ester:  $^1\text{H}$  NMR  $\delta_{\text{ppm}}$ : 3.10 ( $\alpha\text{CH}$ ), 0.94 ( $\gamma\text{CH}_3$ ), 3.89 (H-3 $\alpha$ ), 4.01 (H-3 $\beta$ ), 3.33 (H-6 $\alpha,\beta$ );  $^{13}\text{C}$  NMR  $\delta_{\text{ppm}}$ : 52.4 ( $\alpha\text{CH}$ ), 9.39 ( $\gamma\text{CH}_3$ ), 82.9 (C3 $\alpha$ ), 83.4 (C3 $\beta$ ), 60.3 (C6 $\alpha,\beta$ ). 6-*O*-ester:  $^1\text{H}$  NMR  $\delta_{\text{ppm}}$ : 3.20 ( $\alpha\text{CH}$ ), 2.01 ( $\beta\text{CH}$ ), 0.90 ( $\gamma \text{CH}_3$ ), 4.95 (H-1 $\alpha$ ), 4.22 (H-1 $\beta$ ), 3.17 (H-4 $\alpha$ ), 3.0 (H-4 $\beta$ ), 3.86 (H-6 $\alpha$ );  $^{13}\text{C}$  NMR  $\delta_{\text{ppm}}$ : 51.9 ( $\alpha\text{CH}$ ), 21.0 ( $\beta\text{CH}$ ), 8.94 ( $\gamma \text{CH}_3$ ), 95.2 (C1 $\alpha$ ), 104.5(C1 $\beta$ ), 69.5 (C4 $\alpha$ ), 69.8 (C4 $\beta$ ), 63.4 (C6 $\alpha$ ). 2,6-di-*O*-ester:  $^1\text{H}$  NMR  $\delta_{\text{ppm}}$ : 3.15 ( $\alpha\text{CH}$ ), 3.75 (H-2 $\alpha$ ), 3.64 (H-6 $\beta$ );  $^{13}\text{C}$  NMR  $\delta_{\text{ppm}}$ : 51.7 ( $\alpha\text{CH}$ ), 78.7 (C2 $\alpha$ ), 61.6 (C6 $\alpha$ ). 3,6-di-*O*-ester:  $^1\text{H}$  NMR

$\delta_{\text{ppm}}$ : 3.21 ( $\alpha\text{CH}$ ), 1.55 ( $\gamma \text{CH}_3$ ), 3.67 (H-3 $\beta$ ), 3.15 (H-6 $\alpha,\beta$ );  $^{13}\text{C}$  NMR  $\delta_{\text{ppm}}$ : 49.4 ( $\alpha\text{CH}$ ), 78.6 (C3 $\beta$ ), 61.3 (C6 $\alpha,\beta$ ).

**4.4.1.5. L-Valyl-D-fructose.** Solid; UV ( $\text{H}_2\text{O}$ ,  $\lambda_{\text{max}}$ ): 223.0 nm ( $\sigma \rightarrow \sigma^*$   $\epsilon_{223.0-53} \text{ M}^{-1}$ ), 288.0 nm ( $n \rightarrow \pi^*$   $\epsilon_{288.0-23} \text{ M}^{-1}$ ). IR (KBr): 3352  $\text{cm}^{-1}$ (NH), 3290  $\text{cm}^{-1}$ (OH), 2946  $\text{cm}^{-1}$ (CH), 1623  $\text{cm}^{-1}$ (CO). Optical rotation ( $c$  0.5,  $\text{H}_2\text{O}$ ):  $[\alpha]_{\text{D}}^{25} = -6.7^\circ$ . MS ( $m/z$ ) 304  $[\text{M} + 2 + \text{Na}]^+$ . 2D-HSQCT (DMSO- $d_6$ ) 1-*O*-ester:  $^1\text{H}$  NMR  $\delta_{\text{ppm}}$  (500.13 MHz): 3.30 ( $\alpha\text{CH}$ ), 1.90 ( $\beta\text{CH}$ ), 0.98 ( $\gamma\text{CH}_3$ ), 0.98 ( $\delta\text{CH}_3$ ), 3.80 (H-1 $\alpha$ ), 4.85 (H-2 $\beta$ ), 3.85 (H-3 $\alpha$ ), 3.30 (H-6 $\alpha$ );  $^{13}\text{C}$  NMR  $\delta_{\text{ppm}}$  (125 MHz): 3.30 ( $\alpha\text{CH}$ ), 1.90 ( $\beta\text{CH}$ ), 0.98 ( $\gamma\text{CH}_3$ ), 0.98 ( $\delta\text{CH}_3$ ), 175.0 (CO), 63.5 (C1 $\alpha$ ), 102.4 (C2 $\beta$ ), 70.8 (C3 $\alpha$ ), 62.8 (C6 $\alpha$ ).

**4.4.1.6. L-Valyl-maltose.** Solid; UV ( $\text{H}_2\text{O}$ ,  $\lambda_{\text{max}}$ ): 221.0 nm ( $\sigma \rightarrow \sigma^*$   $\epsilon_{221.0-1622} \text{ M}^{-1}$ ), 291.0 nm ( $n \rightarrow \pi^*$   $\epsilon_{291.0-776} \text{ M}^{-1}$ ). IR (stretching frequency): 3419  $\text{cm}^{-1}$  (NH), 3267  $\text{cm}^{-1}$  (OH), 2936  $\text{cm}^{-1}$  (CH), 1634  $\text{cm}^{-1}$  (CO). Optical rotation ( $c$  0.5,  $\text{H}_2\text{O}$ ):  $[\alpha]_{\text{D}}^{25} = +341.7^\circ$ . MS ( $m/z$ ) 464  $[\text{M} + \text{Na}]^+$ . 2D-HSQCT (DMSO- $d_6$ ) 6-*O*-ester:  $^1\text{H}$  NMR  $\delta_{\text{ppm}}$  (500.13 MHz): 3.05 ( $\alpha\text{CH}$ ), 2.25 ( $\beta\text{CH}$ ), 0.99 ( $\gamma,\delta\text{CH}_3$ ), 4.80 (H-1 $\alpha$ ), 4.20 (H-1 $\beta$ ), 4.05 (H-2 $\alpha,\beta$ ), 3.30 (H-3 $\alpha$ ), 3.85 (H-4 $\alpha,\beta$ ), 3.65 (H-5 $\alpha,\beta$ ), 3.94 (H-6 $\alpha,\beta$ ), 4.90 (H-1 $\alpha$ ), 2.95 (H-2 $\alpha$ ), 3.10 (H-3 $\alpha$ ), 3.50 (H-4 $\alpha$ ), 3.60 (H-5 $\alpha$ ), 3.60 (H-6 $\alpha$ );  $^{13}\text{C}$  NMR  $\delta_{\text{ppm}}$  (125 MHz): 51.0 ( $\alpha\text{CH}$ ), 28.9 ( $\beta\text{CH}$ ), 18.9 ( $\gamma,\delta\text{CH}_3$ ), 175.5 (CO), 97.0 (C1 $\alpha$ ), 100.5 (C1 $\beta$ ), 79.7 (C2 $\alpha,\beta$ ), 76.4 (C3 $\alpha$ ), 81.5 (C4 $\alpha,\beta$ ), 77.2 (C5 $\alpha,\beta$ ), 67.2 (C6 $\alpha,\beta$ ), 100.7 (C1 $\alpha$ ), 70.3 (C2 $\alpha$ ), 71.8 (C3 $\alpha$ ), 69.9 (C4 $\alpha$ ), 72.4 (C5 $\alpha$ ), 60.6 (C6 $\alpha$ ); 6 $\beta$ -*O*-ester:  $^1\text{H}$  NMR  $\delta_{\text{ppm}}$ : 2.99 ( $\alpha\text{CH}$ ), 3.81 (H-6 $\alpha$ );  $^{13}\text{C}$  NMR  $\delta_{\text{ppm}}$  (125 MHz): 52.5 ( $\alpha\text{CH}$ ), 68.0 (C6 $\alpha$ ). 6,6 $\beta$ -di-*O*-ester:  $^1\text{H}$  NMR  $\delta_{\text{ppm}}$  (500.13 MHz): 3.81 (H-6 $\alpha$ );  $^{13}\text{C}$  NMR  $\delta_{\text{ppm}}$  (125 MHz): 64.0 (C6 $\beta$ ).

**4.4.1.7. L-Valyl-D-mannitol.** Solid; UV ( $\text{H}_2\text{O}$ ,  $\lambda_{\text{max}}$ ): 225.0 nm ( $\sigma \rightarrow \sigma^*$   $\epsilon_{225.0-372} \text{ M}^{-1}$ ), 270.0 nm ( $n \rightarrow \pi^*$   $\epsilon_{270.0-178} \text{ M}^{-1}$ ). IR (KBr): 3294  $\text{cm}^{-1}$  (OH), 2957  $\text{cm}^{-1}$  (CH), 1630  $\text{cm}^{-1}$  (CO). Optical rotation ( $c$  0.5,  $\text{H}_2\text{O}$ ):  $[\alpha]_{\text{D}}^{25} = +6.6^\circ$ . MS ( $m/z$ ) 464  $[\text{M} + \text{Na}]^+$ . 2D-HSQCT (DMSO- $d_6$ ) 1-*O*-ester:  $^1\text{H}$  NMR  $\delta_{\text{ppm}}$  (500.13 MHz): 3.42 ( $\alpha\text{CH}$ ), 2.05 ( $\beta\text{CH}$ ), 0.85 ( $\gamma\text{CH}_3$ ), 3.52 (H-1), 3.46(H-2), 3.53 (H-3), 3.56 (H-4), 3.41 (H-5), 3.46(H-6);  $^{13}\text{C}$  NMR  $\delta_{\text{ppm}}$  (125 MHz): 55.8( $\alpha\text{CH}$ ), 29.8( $\beta\text{CH}_2$ ), 19.8 ( $\gamma\text{CH}_3$ ), 60.6(C1), 69.6(C2), 68.2(C3), 71.3 (C4), 71.2(C5) 63.6(C6).

**4.4.1.8. L-Leucyl-D-glucose.** Solid; UV ( $\text{H}_2\text{O}$ ,  $\lambda_{\text{max}}$ ): 221.0 nm ( $\sigma \rightarrow \sigma^*$   $\epsilon_{221.0-1622} \text{ M}^{-1}$ ), 291.0 nm ( $n \rightarrow \pi^*$   $\epsilon_{291.0-776.2} \text{ M}^{-1}$ ). IR (KBr): 3419  $\text{cm}^{-1}$  (NH), 3267  $\text{cm}^{-1}$  (OH), 2936  $\text{cm}^{-1}$  (CH), 1634  $\text{cm}^{-1}$  (CO). Optical rotation ( $c$  0.5,  $\text{H}_2\text{O}$ ):  $[\alpha]_{\text{D}}^{25} = +34.7^\circ$ . MS ( $m/z$ ) 464  $[\text{M} + \text{Na}]^+$ . 2D-HSQCT (DMSO- $d_6$ ) 2-*O*-ester:  $^1\text{H}$   $\delta_{\text{ppm}}$  (500.13 MHz): 2.8 ( $\alpha\text{CH}$ ), 0.75 ( $\delta, \epsilon \text{CH}_3$ ), 3.79 (H-2 $\alpha$ );  $^{13}\text{C}$   $\delta_{\text{ppm}}$  (125 MHz): 46.1 ( $\alpha\text{CH}$ ), 23.4 ( $\delta\text{CH}_3$ ), 23.9 ( $\epsilon\text{CH}_3$ ), 76.9 (C2 $\alpha$ ). 3-*O*-ester:  $^1\text{H}$   $\delta_{\text{ppm}}$ : 3.15 ( $\alpha\text{CH}$ ), 1.5 ( $\gamma\text{CH}$ ), 0.77 ( $\delta,\epsilon\text{CH}_3$ ), 3.86 (H-2 $\beta$ ), 3.97 (H-3 $\alpha$ ), 3.88 (H-3 $\beta$ );  $^{13}\text{C}$   $\delta_{\text{ppm}}$ : 50.0 ( $\alpha\text{CH}$ ), 25.0 ( $\gamma\text{CH}$ ), 23.3 ( $\delta\text{CH}_3$ ), 23.1 ( $\epsilon\text{CH}_3$ ), 84.0 (C3 $\alpha$ ), 83.2 (C3 $\beta$ ). 6-*O*-ester:  $^1\text{H}$   $\delta_{\text{ppm}}$ : 3.08 ( $\alpha\text{CH}$ ), 2.51 ( $\beta\text{CH}_2$ ), 1.57 ( $\gamma\text{CH}$ ), 0.81 ( $\delta, \epsilon \text{CH}_3$ ), 3.86 (H-6 $\alpha$ );  $^{13}\text{C}$   $\delta_{\text{ppm}}$ :

53.5 ( $\alpha$ CH), 36.0 ( $\beta$ CH<sub>2</sub>), 25.3 ( $\gamma$ CH), 22.5 ( $\delta$ -CH<sub>3</sub>), 23.0 ( $\epsilon$ CH<sub>3</sub>), 173.6 (CO), 102.5 (C1 $\alpha$ ), 65.0 (C6 $\alpha$ ). 2,6-di-O-ester: <sup>1</sup>H  $\delta_{\text{ppm}}$ : 3.45 (H-6 $\alpha$ ), 3.44 (H-6 $\alpha$ ); <sup>13</sup>C  $\delta_{\text{ppm}}$ : 75.5 (C2 $\alpha$ ), 62.8 (C6 $\alpha$ ). 3,6-di-O-ester: <sup>1</sup>H  $\delta_{\text{ppm}}$ : 3.68 (H-3 $\alpha$ ), 3.45 (H-6 $\alpha$ ); <sup>13</sup>C  $\delta_{\text{ppm}}$ : 82.5 (C3 $\alpha$ ), 63.1 (C6 $\alpha$ ).

4.4.1.9. *L-Isoleucyl-D-glucose*. Solid; UV (H<sub>2</sub>O,  $\lambda_{\text{max}}$ ): 230.0 nm ( $\sigma \rightarrow \sigma^*$   $\epsilon_{230.0-724}$  M<sup>-1</sup>), 297.0 nm ( $n \rightarrow \pi^*$   $\epsilon_{297.0-363}$  M<sup>-1</sup>). IR (KBr): 3383 cm<sup>-1</sup> (NH), 3360 cm<sup>-1</sup> (OH), 2240 cm<sup>-1</sup> (CH), 1657 cm<sup>-1</sup> (CO). Optical rotation (*c* 0.5, H<sub>2</sub>O):  $[\alpha]_{\text{D}}$  at 25 °C = -3.1°. MS (*m/z*) 316 [M + Na]<sup>+</sup>. 2D-HSQCT (DMSO-d<sub>6</sub>): 3-O-ester: <sup>1</sup>H  $\delta_{\text{ppm}}$ : 3.13 ( $\alpha$ CH), 1.61 ( $\beta$ CH), 1.08 ( $\gamma$ CH<sub>2</sub>), 0.59 ( $\delta$  CH<sub>3</sub>), 0.61 ( $\epsilon$  CH<sub>3</sub>), 5.0 (H-1 $\alpha$ ), 4.4 (H-1 $\beta$ ), 4.01 (H-3 $\alpha$ ), 3.88 (H-3 $\beta$ ), 3.46 (H-4 $\alpha$ ), 3.58 (H-6 $\alpha$ , $\beta$ ); <sup>13</sup>C  $\delta_{\text{ppm}}$ : 51.0 ( $\alpha$ CH), 35.4 ( $\beta$ CH), 25.6 ( $\gamma$ CH<sub>2</sub>), 11.2 ( $\delta$  CH<sub>3</sub>), 14.0 ( $\epsilon$  CH<sub>3</sub>), 171.4 (CO), 91.8 (C1 $\alpha$ ), 95.8 (C1 $\beta$ ), 82.0 (C3 $\alpha$ ), 81.9 (C3 $\beta$ ), 67.5 (C4 $\alpha$ ), 63.0 (C6 $\alpha$ , $\beta$ ). 6-O-ester: <sup>1</sup>H  $\delta_{\text{ppm}}$ : 3.11 ( $\alpha$ CH), 1.61 ( $\beta$ CH), 1.08 ( $\gamma$ CH<sub>2</sub>), 0.59 ( $\delta$  CH<sub>3</sub>), 0.61 ( $\epsilon$  CH<sub>3</sub>), 3.59 (H-2 $\alpha$ ), 3.48 (H-3 $\alpha$ ), 3.64 (H-4 $\alpha$ ), 3.63 (H-5 $\alpha$ ), 3.82 (H-6 $\alpha$ , $\beta$ ); <sup>13</sup>C  $\delta_{\text{ppm}}$ : 53.1 ( $\alpha$ CH), 35.3 ( $\beta$ CH), 25.2 ( $\gamma$ CH<sub>2</sub>), 11.2 ( $\delta$  CH<sub>3</sub>), 14.0 ( $\epsilon$  CH<sub>3</sub>), 70.0 (C2 $\alpha$ ), 72.2 (C3 $\alpha$ ), 69.0 (C4 $\alpha$ ), 69.2 (C5 $\alpha$ ), 63.6 (C6 $\alpha$ , $\beta$ ).

4.4.1.10. *L-Prolyl-D-glucose*. Solid; UV(H<sub>2</sub>O,  $\lambda_{\text{max}}$ ): 200 nm ( $\sigma \rightarrow \sigma^*$   $\epsilon_{200-1862}$  M<sup>-1</sup>), 285 nm ( $n \rightarrow \pi^*$   $\epsilon_{285-512}$  M<sup>-1</sup>). IR (KBr): 3261 cm<sup>-1</sup> (OH), 1631 cm<sup>-1</sup> (CO), 1384 cm<sup>-1</sup> (CN). Optical rotation (*c* 0.6, H<sub>2</sub>O):  $[\alpha]_{\text{D}}$  at 25 °C = 19.6°. MS (*m/z*) 302 [M + 2 + Na]<sup>+</sup>. 2D-HSQCT (DMSO-d<sub>6</sub>): 2-O-ester: <sup>1</sup>H NMR  $\delta_{\text{ppm}}$  (500.13 MHz): 3.85 ( $\alpha$ CH), 2.84 ( $\beta$ CH<sub>2</sub>), 3.75 (H-2 $\alpha$ ), 3.63 (H-2 $\beta$ ), 3.55 (H-6 $\alpha$ , $\beta$ ); <sup>13</sup>C NMR  $\delta_{\text{ppm}}$  (125 MHz): 58.0 ( $\alpha$ CH), 32.0 ( $\beta$ CH<sub>2</sub>), 75.0 (C2 $\alpha$ ), 80.0 (C2 $\beta$ ), 61.5 (C6 $\alpha$ , $\beta$ ). 3-O-ester: <sup>1</sup>H NMR  $\delta_{\text{ppm}}$ : 3.46 ( $\alpha$ CH), 2.84 ( $\beta$ CH<sub>2</sub>), 2.20 ( $\delta$ CH<sub>2</sub>), 3.84 (H-3 $\alpha$ ), 3.93 (H-3 $\beta$ ), 3.46 (H-6 $\alpha$ , $\beta$ ); <sup>13</sup>C NMR  $\delta_{\text{ppm}}$ : 53.0 ( $\alpha$ CH), 32.0 ( $\beta$ -CH<sub>2</sub>), 28.0 ( $\delta$ -CH<sub>2</sub>), 98.5 (C1 $\alpha$ ), 82.4 (C3 $\alpha$ ), 84.0 (C3 $\beta$ ), 61.0 (C6 $\alpha$ , $\beta$ ). 6-O-ester: <sup>1</sup>H NMR  $\delta_{\text{ppm}}$ : 3.75 ( $\alpha$ CH), 2.85 ( $\beta$ CH<sub>2</sub>), 1.94 ( $\gamma$ CH<sub>2</sub>), 3.15 ( $\delta$ CH<sub>2</sub>), 4.38 (H-1 $\alpha$ ), 4.20 (H-1 $\beta$ ), 3.38 (H-3 $\alpha$ ), 4.20 (H-4 $\alpha$ ), 3.90 (H-4 $\beta$ ), 3.82 (H-6 $\alpha$ , $\beta$ ); <sup>13</sup>C NMR  $\delta_{\text{ppm}}$ : 56.0 ( $\alpha$ CH), 35.0 ( $\beta$ CH<sub>2</sub>), 28.0 ( $\gamma$ CH<sub>2</sub>), 46.0 ( $\delta$ CH<sub>2</sub>), 171.6 (CO), 95.2 (C1 $\alpha$ ), 101.4 (C1 $\beta$ ), 72.0 (C3 $\alpha$ ), 71.0 (C4 $\alpha$ , $\beta$ ), 63.6 (C6 $\alpha$ , $\beta$ ).

4.4.1.11. *L-Prolyl-D-fructose*. Solid; UV (H<sub>2</sub>O,  $\lambda_{\text{max}}$ ): 213 nm ( $\sigma \rightarrow \sigma^*$   $\epsilon_{213-1479}$  M<sup>-1</sup>), 280 nm ( $n \rightarrow \pi^*$   $\epsilon_{280-145}$  M<sup>-1</sup>). IR (KBr): 3070 cm<sup>-1</sup> (OH), 1604 cm<sup>-1</sup> (CO), 1402 cm<sup>-1</sup> (CN). Optical rotation (*c* 0.5, H<sub>2</sub>O):  $[\alpha]_{\text{D}}$  at 25 °C = -44.0°. MS (*m/z*) 300 [M + Na]<sup>+</sup>. 2D-HSQCT (DMSO-d<sub>6</sub>): 1-O-ester: <sup>1</sup>H NMR  $\delta_{\text{ppm}}$  (500.13 MHz): 3.15 ( $\alpha$ CH), 2.72 ( $\beta$ CH<sub>2</sub>), 2.08 ( $\gamma$ CH<sub>2</sub>), 3.12 ( $\delta$ CH<sub>2</sub>), 4.13 (H-1 $\alpha$ ), 3.13 (H-3 $\alpha$ ), 3.40 (H-3 $\beta$ ), 3.80 (H-4 $\alpha$ ), 3.62 (H-4 $\beta$ ), 3.30 (H-5 $\alpha$ ), 3.93 (H-5 $\beta$ ), 3.23 (H-6 $\alpha$ , $\beta$ ); <sup>13</sup>C NMR  $\delta_{\text{ppm}}$  (125 MHz): 60.0 ( $\alpha$ CH), 31.0 ( $\beta$ CH<sub>2</sub>), 24.0 ( $\gamma$ CH<sub>2</sub>), 48.2 ( $\delta$ CH<sub>2</sub>), 170.8 (CO), 66.1 (C1 $\alpha$ , $\beta$ ), 104.2 (C1 $\alpha$ ), 71.4 (C3 $\alpha$ ), 82.1 (C3 $\beta$ ), 69.9 (C4 $\alpha$ ), 78.2 (C4 $\beta$ ), 74.0 (C5 $\alpha$ ), 82.9 (C5 $\beta$ ), 63.7 (C6 $\alpha$ , $\beta$ ). 6-O-ester: <sup>1</sup>H NMR  $\delta_{\text{ppm}}$ : 3.32 ( $\alpha$ CH), 3.33 ( $\delta$ CH<sub>2</sub>), 3.78 (H-1 $\alpha$ ), 3.78 (H-3 $\alpha$ ), 3.29 (H-3 $\beta$ ), 3.38 (H-5 $\alpha$ ), 4.12 (H-5 $\beta$ ), 4.02 (H-6 $\alpha$ , $\beta$ ); <sup>13</sup>C NMR  $\delta_{\text{ppm}}$ : 59.2 ( $\alpha$ CH), 49.3 ( $\delta$ CH<sub>2</sub>), 64.4 (C1 $\alpha$ ), 99.1 (C2 $\alpha$ ), 71.9 (C3 $\alpha$ ), 70.7 (C4 $\alpha$ ), 75.2 (C5 $\alpha$ ), 81.9 (C5 $\beta$ ), 65.8 (C6 $\alpha$ , $\beta$ ). 1,6-di-O-

ester: <sup>1</sup>H NMR  $\delta_{\text{ppm}}$ : 2.91 ( $\alpha$ CH), 4.37 (H-1 $\alpha$ ), 3.42 (H-3 $\alpha$ ), 3.54 (H-5 $\alpha$ ), 4.28 (H-6 $\alpha$ , $\beta$ ); <sup>13</sup>C NMR  $\delta_{\text{ppm}}$ : 60.0 ( $\alpha$ CH), 66.5 (C1 $\alpha$ , $\beta$ ), 102.0 (C2 $\alpha$ ), 70.1 (C3 $\alpha$ ), 75.6 (C5 $\alpha$ ), 66.2 (C6 $\alpha$ , $\beta$ ).

4.4.1.12. *L-Prolyl-D-ribose*. Solid; UV (H<sub>2</sub>O,  $\lambda_{\text{max}}$ ): 210 nm ( $\sigma \rightarrow \sigma^*$   $\epsilon_{210-1820}$  M<sup>-1</sup>) and 280 nm ( $n \rightarrow \pi^*$   $\epsilon_{280-575}$  M<sup>-1</sup>). IR (KBr): 3307 cm<sup>-1</sup> (OH), 1621 cm<sup>-1</sup> (CO), 1403 cm<sup>-1</sup> (CN). Optical rotation (*c* 0.5, H<sub>2</sub>O):  $[\alpha]_{\text{D}}$  at 25 °C = -45.1°. MS (*m/z*) 272 [M + Na]<sup>+</sup>. 2D-HSQCT (DMSO-d<sub>6</sub>): 2-O-ester: <sup>1</sup>H NMR  $\delta_{\text{ppm}}$  (500.13 MHz): 3.52 ( $\alpha$ CH), 2.53 ( $\beta$ CH<sub>2</sub>), 1.78 ( $\gamma$ CH<sub>2</sub>), 3.30 ( $\delta$ CH<sub>2</sub>), 4.20 (H-1 $\alpha$ ), 3.55 (H-2 $\alpha$ ), 3.45 (H-4 $\alpha$ ), 3.45 (H-5 $\alpha$ , $\beta$ ); <sup>13</sup>C NMR  $\delta_{\text{ppm}}$  (125 MHz): 61.0 ( $\alpha$ CH), 34.5 ( $\beta$ CH<sub>2</sub>), 23.7 ( $\gamma$ CH<sub>2</sub>), 54.0 ( $\delta$ CH<sub>2</sub>), 170.9 (CO), 103.8 (C1 $\alpha$ ), 71.0 (C2 $\alpha$ ), 73.0 (C4 $\beta$ ), 63.0 (C5 $\alpha$ , $\beta$ ). 5-O-ester: <sup>1</sup>H NMR  $\delta_{\text{ppm}}$ : 3.62 ( $\alpha$ CH), 2.88 ( $\beta$ CH<sub>2</sub>), 1.90 ( $\gamma$ CH<sub>2</sub>), 3.08 ( $\delta$ CH<sub>2</sub>), 3.32 (H-2 $\alpha$ ), 3.42 (H-3 $\alpha$ ), 3.45 (H-4 $\alpha$ ), 3.20 (H-5 $\alpha$ , $\beta$ ); <sup>13</sup>C NMR  $\delta_{\text{ppm}}$ : 61.2 ( $\alpha$ CH), 35.8 ( $\beta$ CH<sub>2</sub>), 172.0 (CO), 97.0 (C1 $\alpha$ ), 73.2 (C2 $\alpha$ ), 66.5 (C3 $\alpha$ ), 75.0 (C4 $\alpha$ ), 65.8 (C5 $\alpha$ , $\beta$ ).

4.4.1.13. *L-Prolyl-lactose*. Solid; UV (H<sub>2</sub>O,  $\lambda_{\text{max}}$ ): 201 nm ( $\sigma \rightarrow \sigma^*$   $\epsilon_{201-2239}$  M<sup>-1</sup>) and 278 nm ( $n \rightarrow \pi^*$   $\epsilon_{278-447}$  M<sup>-1</sup>). IR (KBr): 3084 cm<sup>-1</sup> (OH), 1609 cm<sup>-1</sup> (CO), 1419 cm<sup>-1</sup> (CN). Optical rotation (*c* 0.5, H<sub>2</sub>O):  $[\alpha]_{\text{D}}$  at 25 °C = -11.4°. MS (*m/z*) 462 [M + Na]<sup>+</sup>. 2D-HSQCT (DMSO-d<sub>6</sub>): 6-O-ester: <sup>1</sup>H NMR  $\delta_{\text{ppm}}$  (500.13 MHz): 3.06 ( $\alpha$ CH), 2.72 ( $\beta$ CH<sub>2</sub>), 1.73 ( $\gamma$ CH<sub>2</sub>), 3.01 ( $\delta$ CH<sub>2</sub>), 4.12 (H-1 $\beta$ ), 3.29 (H-2 $\alpha$ ), 3.36 (H-3 $\alpha$ ), 4.10 (H-4 $\alpha$ ), 3.84 (H-5 $\alpha$ ), 3.76 (H-5 $\beta$ ), 3.85 (H-6 $\alpha$ , $\beta$ ), 4.01 (H-1'' $\beta$ ), 3.24 (H-2''), 3.33 (H-3''), 3.41 (H-4''), 3.36 (H-5''), 3.44 (H-6''); <sup>13</sup>C NMR  $\delta_{\text{ppm}}$  (125 MHz): 59.6 ( $\alpha$ CH), 30.4 ( $\beta$ CH<sub>2</sub>), 23.8 ( $\gamma$ CH<sub>2</sub>), 44.5 ( $\delta$ CH<sub>2</sub>), 101.4 (C1 $\beta$ ), 70.6 (C2 $\alpha$ ), 73.8 (C3 $\alpha$ ), 81.6 (C4 $\alpha$ ), 77.1 (C5 $\alpha$ , $\beta$ ), 64.8 (C6 $\alpha$ , $\beta$ ), 102.9 (C1'' $\beta$ ), 70.0 (C2''), 71.6 (C3''), 68.2 (C4''), 74.4 (C5''), 60.5 (C6''). 6''-O-ester: <sup>1</sup>H NMR  $\delta_{\text{ppm}}$ : 2.86 ( $\alpha$ CH), 2.48 ( $\beta$ CH<sub>2</sub>), 3.99 (H-4 $\alpha$ ), 3.78 (H-5 $\alpha$ ), 3.75 (H-6 $\alpha$ , $\beta$ ), 3.27 (H-2''), 3.58 (H-4''), 3.38 (H-5''), 3.45 (H-6''); <sup>13</sup>C NMR  $\delta_{\text{ppm}}$  (125 MHz): 60.0 ( $\alpha$ CH), 33.2 ( $\beta$ CH<sub>2</sub>), 82.4 (C4 $\alpha$ ), 77.3 (C5 $\alpha$ , $\beta$ ), 60.8 (C6 $\alpha$ , $\beta$ ), 70.2 (C2''), 68.9 (C4''), 75.0 (C5''), 62.8 (C6'').

4.4.1.14. *L-Phenylalanyl-D-glucose*. Solid; UV (H<sub>2</sub>O,  $\lambda_{\text{max}}$ ): 237.0 nm ( $\sigma \rightarrow \sigma^*$   $\epsilon_{237.0-1318}$  M<sup>-1</sup>), 257.0 nm ( $\pi \rightarrow \pi^*$   $\epsilon_{257.0-1259}$  M<sup>-1</sup>) and 308.0 nm ( $n \rightarrow \pi^*$   $\epsilon_{308.0-616}$  M<sup>-1</sup>). IR (KBr): 3186 cm<sup>-1</sup> (OH), 1722 cm<sup>-1</sup> (CO), 1582 cm<sup>-1</sup> (aromatic - C=C-). Optical rotation (*c* 0.6, H<sub>2</sub>O):  $[\alpha]_{\text{D}}$  at 25 °C = -24.2°. MS (*m/z*) 350 [M + Na]<sup>+</sup>. 2D-HSQCT (DMSO-d<sub>6</sub>): 2-O-ester: <sup>1</sup>H NMR  $\delta_{\text{ppm}}$  (500.13 MHz): 2.92 ( $\alpha$ CH), 2.51 ( $\beta$ CH<sub>2</sub>), 4.6 (H-1 $\alpha$ ), 3.79 (H-2 $\alpha$ ), 3.80 (H-2 $\beta$ ), 3.4 (H-6 $\alpha$ ); <sup>13</sup>C NMR  $\delta_{\text{ppm}}$  (125 MHz): 52.0 ( $\alpha$ CH), 35.8 ( $\beta$ CH<sub>2</sub>), aromatic- 136.5 (C1), 96.3 (C1 $\alpha$ ), 75.1 (C2 $\alpha$ ), 77.3 (C2 $\beta$ ), 62.0 (C6 $\alpha$ ). 3-O-ester: <sup>1</sup>H NMR  $\delta_{\text{ppm}}$ : 3.01 ( $\alpha$ CH), 3.11 ( $\beta$ CH<sub>2</sub>), 2.96 ( $\beta$ CH<sub>2</sub>), 4.4 (H-1 $\alpha$ ), 3.61 (H-2 $\alpha$ ), 3.66 (H-2 $\beta$ ), 3.82 (H-3 $\alpha$ ), 3.91 (H-3 $\beta$ ), 3.40 (H-6 $\alpha$ ); <sup>13</sup>C NMR  $\delta_{\text{ppm}}$ : 53.0 ( $\alpha$ CH), 36.8 ( $\beta$ CH<sub>2</sub>), aromatic-136.4 (C1), 97.3 (C1 $\alpha$ ), 83.4 (C3 $\alpha$ ), 83.9 (C3 $\beta$ ), 61.9 (C6 $\alpha$ ). 6-O-ester: <sup>1</sup>H NMR  $\delta_{\text{ppm}}$ : 3.07 ( $\alpha$ CH), 3.18 ( $\beta$ CH<sub>2</sub>), 3.06 ( $\beta$ CH<sub>2</sub>), aromatic- 7.18 (H2, H6), 7.26 (H3, H5), 7.16 (H4), 3.16 (H-5 $\alpha$ ), 3.78 (H-6 $\alpha$ ), 3.66 (H-6 $\beta$ ); <sup>13</sup>C NMR  $\delta_{\text{ppm}}$ : 54.2 ( $\alpha$ CH), 36.7 ( $\beta$ CH<sub>2</sub>), aromatic- 136.3 (C1), 128.9 (C2, C6), 130.7 (C3, C5), 130.3 (C4), 172.5 (CO), 102.2 (C1 $\alpha$ ),

70.5 (C5 $\alpha$ ), 65.0 (C6 $\alpha\beta$ ). 2,6-di-O-ester:  $^1\text{H}$  NMR  $\delta_{\text{ppm}}$ : 3.51 (H-6 $\alpha$ ), 3.61 (H-6 $\beta$ ), 3.67 (H-2 $\alpha$ );  $^{13}\text{C}$  NMR  $\delta_{\text{ppm}}$ : 77.0 (C2 $\alpha$ ), 79.0 (C2 $\beta$ ), 62.1 (C6 $\beta$ ). 3,6-di-O-ester:  $^1\text{H}$  NMR  $\delta_{\text{ppm}}$ : 3.61 (H-3 $\alpha$ ), 3.66 (H-3 $\beta$ ), 3.50 (H-6 $\alpha$ );  $^{13}\text{C}$  NMR  $\delta_{\text{ppm}}$ : 82.3 (C3 $\alpha$ ), 83.4 (C3 $\beta$ ), 64.8 (C6 $\alpha$ ).

4.4.1.15. *L-Phenylalanyl-D-galactose*. UV ( $\text{H}_2\text{O}$ ,  $\lambda_{\text{max}}$ ): 222.0 nm ( $\sigma \rightarrow \sigma^*$   $\epsilon_{222.0} = 871 \text{ M}^{-1}$ ), 257.5 nm ( $\pi \rightarrow \pi^*$   $\epsilon_{257.5} = 437 \text{ M}^{-1}$ ) and 299.0 nm ( $n \rightarrow \pi^*$   $\epsilon_{299.0} = 331 \text{ M}^{-1}$ ). IR (KBr): 3379  $\text{cm}^{-1}$  (OH), 1761  $\text{cm}^{-1}$  (C=O), 1603  $\text{cm}^{-1}$  (aromatic,  $-\text{C}=\text{C}-$ ). Optical rotation ( $c$  0.5,  $\text{H}_2\text{O}$ ):  $[\alpha]_{\text{D}}$  at 25  $^{\circ}\text{C} = +31.1^{\circ}$ . MS ( $m/z$ ) diester - 512  $[\text{M} + \text{K}]^+$ ;  $^{13}\text{C}$  NMR DMSO- $d_6$   $\delta_{\text{ppm}}$  (125 MHz): 2-O-ester: 55.7 ( $\alpha\text{CH}$ ), 36.7 ( $\beta\text{CH}_2$ ), aromatic- 136.5 (C1), 127.4 (C2, C6), 129.6 (C3, C5), 129.1 (C4), 171.4 (CO), 97.2 (C1 $\alpha$ ) 76.3 (C2 $\alpha$ ), 75.1 (C2 $\beta$ ), 60.8 (C6 $\alpha$ ). 3-O-ester:  $^{13}\text{C}$  NMR  $\delta_{\text{ppm}}$ : 97.2 (C1 $\alpha$ ), 82.4 (C3 $\alpha$ ), 81.5 (C3 $\beta$ ), 61.0 (C6 $\alpha$ ). 6-O-ester:  $^{13}\text{C}$  NMR  $\delta_{\text{ppm}}$ : 97.2 (C1 $\alpha$ ), 70.6 (C2 $\alpha$ ), 72.2 (C3 $\alpha$ ), 73.1 (C4 $\alpha$ ), 63.0 (C6 $\alpha\beta$ ). 2,6-di-O-ester:  $^{13}\text{C}$  NMR  $\delta_{\text{ppm}}$ : 77.2 (C2 $\alpha\beta$ ), 63.1 (C6 $\beta$ ). 3,6-di-O-ester:  $^{13}\text{C}$  NMR  $\delta_{\text{ppm}}$ : 81.8 (C3 $\alpha$ ), 62.7 (C6 $\alpha\beta$ ).

4.4.1.16. *L-Phenylalanyl-D-fructose*. Solid; UV ( $\text{H}_2\text{O}$ ,  $\lambda_{\text{max}}$ ): 198.0 nm ( $\sigma \rightarrow \sigma^*$   $\epsilon_{198.0} = 4467 \text{ M}^{-1}$ ) and 257.5 nm ( $\pi \rightarrow \pi^*$   $\epsilon_{257.5} = 776 \text{ M}^{-1}$ ). IR: 3380  $\text{cm}^{-1}$  (OH), 1630  $\text{cm}^{-1}$  (CO), 1598  $\text{cm}^{-1}$  (aromatic,  $-\text{C}=\text{C}-$ ). Optical rotation ( $c$  0.4,  $\text{H}_2\text{O}$ ):  $[\alpha]_{\text{D}}$  at 25  $^{\circ}\text{C} = -14.3^{\circ}$ . MS ( $m/z$ ): 365  $[\text{M} - 1 + \text{K}]^+$ .  $^{13}\text{C}$  NMR DMSO- $d_6$   $\delta_{\text{ppm}}$  (125 MHz): 1-O-ester: 55.1 ( $\alpha\text{CH}$ ), aromatic- 138.4 (C1), 64.9 (C1 $\alpha,\beta$ ), 102.4 (C2 $\beta$ ), 76.2 (C4 $\beta$ ), 69.6 (C5 $\beta$ ), 62.3 (C6 $\alpha,\beta$ ). 6-O-ester:  $^{13}\text{C}$  NMR  $\delta_{\text{ppm}}$ : 55.0 ( $\alpha\text{CH}$ ), 63.4 (C1 $\alpha,\beta$ ), 98.1 (C2 $\beta$ ), 75.8 (C4 $\beta$ ), 81.4 (C5 $\beta$ ), 64.2 (C6 $\alpha,\beta$ ).

4.4.1.17. *L-Phenylalanyl-lactose*. Solid; UV ( $\text{H}_2\text{O}$ ,  $\lambda_{\text{max}}$ ): 214.0 nm ( $\sigma \rightarrow \sigma^*$   $\epsilon_{214.0} = 6026 \text{ M}^{-1}$ ), 257.5 nm ( $\pi \rightarrow \pi^*$   $\epsilon_{257.5} = 562 \text{ M}^{-1}$ ) and 290.0 nm ( $n \rightarrow \pi^*$   $\epsilon_{290.0} = 302 \text{ M}^{-1}$ ). IR (KBr): 3378  $\text{cm}^{-1}$  (OH), 1632  $\text{cm}^{-1}$  (CO), 1556  $\text{cm}^{-1}$  (aromatic,  $-\text{C}=\text{C}-$ ). Optical rotation ( $c$  0.2,  $\text{H}_2\text{O}$ ):  $[\alpha]_{\text{D}}$  at 25  $^{\circ}\text{C} = +31.3^{\circ}$ . MS ( $m/z$ ) 512  $[\text{M} + \text{Na}]^+$ . 2D-HSQC (DMSO- $d_6$ ): 6-O-ester:  $^1\text{H}$  NMR  $\delta_{\text{ppm}}$  (500.13 MHz): 2.67 ( $\alpha\text{CH}$ ), 2.89 ( $\beta\text{CH}_2$ ), aromatic- 7.25 (H-2,H-6), 7.28 (H-3,H-5), 7.20 (H-4), 4.32 (H-1 $\alpha$ ), 4.23 (H-1 $\beta$ ), 3.36 (H-2 $\alpha$ ), 3.49 (H-2 $\beta$ ), 3.32 (H-3 $\alpha$ ), 3.80 (H-3 $\beta$ ), 3.56 (H-4 $\alpha$ ), 3.72 (H-4 $\beta$ ), 3.90 (H-5 $\alpha,\beta$ ), 3.47 (H-6 $\alpha,\beta$ ), 4.16 (H-1'' $\beta$ ), 3.14 (H-2''), 3.42 (H-3''), 3.62 (H-4''), 3.39 (H-5''), 3.54 (H-6'');  $^{13}\text{C}$  NMR  $\delta_{\text{ppm}}$  (125 MHz): 51.9 ( $\alpha\text{CH}$ ), 38.2 ( $\beta\text{CH}_2$ ) aromatic- 138.0 (C1), 128.3 (C2, C6), 129.1 (C3, C5), 126.1 (C4), 172.5 (CO), 96.6 (C1 $\alpha$ ), 101.2 (C1 $\beta$ ), 70.5 (C2 $\alpha$ ), 73.0 (C2 $\beta$ ), 74.0 (C3 $\beta$ ), 82.5 (C4 $\alpha$ ), 83.3 (C4 $\beta$ ), 77.2 (C5 $\alpha,\beta$ ), 62.1 (C6 $\alpha\beta$ ), 103.2 (C1'' $\beta$ ), 69.9 (C2''), 71.6 (C3''), 68.2 (C4''), 74.4 (C5''), 60.5 (C6''). 6''-O-ester:  $^1\text{H}$  NMR  $\delta_{\text{ppm}}$ : 2.72 ( $\alpha\text{CH}$ ), 3.00 ( $\beta\text{CH}_2$ ), 5.16 (H-1 $\alpha$ ), 4.32 (H-1 $\beta$ ), 3.16 (H-2 $\alpha$ ), 3.45 (H-2 $\beta$ ), 3.43 (H-3 $\alpha$ ), 3.50 (H-3 $\beta$ ), 3.32 (H-4 $\alpha$ ), 3.80 (H-5 $\alpha,\beta$ ), 3.49 (H-6 $\alpha,\beta$ ), 4.15 (H-1'' $\beta$ ), 3.36 (H-2''), 3.89 (H-4''), 3.89 (H-5''), 3.45 (H-6'');  $^{13}\text{C}$  NMR  $\delta_{\text{ppm}}$ : 52.5 ( $\alpha\text{CH}$ ), 37.1 ( $\beta\text{CH}_2$ ) Aromatic- 137.6 (C1), 92.0 (C1 $\alpha$ ), 97.1 (C1 $\beta$ ), 69.7 (C2 $\alpha$ ), 72.7 (C2 $\beta$ ), 72.1 (C3 $\alpha$ ), 74.5 (C3 $\beta$ ), 79.9 (C4 $\alpha$ ), 80.7 (C4 $\beta$ ), 76.0 (C5 $\alpha,\beta$ ), 61.0 (C6 $\alpha,\beta$ ), 104.0 (C1'' $\beta$ ), 69.3 (C2''), 72.1 (C3''), 66.3 (C4''), 75.0 (C5''), 63.1

(C6''). 6,6''-di-O-ester:  $^1\text{H}$  NMR  $\delta_{\text{ppm}}$ : 2.55 ( $\alpha\text{CH}$ ), 2.89 ( $\beta\text{CH}_2$ ), 4.32 (H-1 $\alpha$ ), 3.23 (H-2 $\alpha$ ), 3.68 (H-2 $\beta$ ), 3.33 (H-3 $\alpha$ ), 4.02 (H-4 $\alpha$ ), 4.01 (H-5 $\alpha,\beta$ ), 3.45 (H-6 $\alpha,\beta$ ), 4.21 (H-1'' $\beta$ ), 3.14 (H-2''), 3.58 (H-3''), 3.74 (H-4''), 3.46 (H-6'');  $^{13}\text{C}$  NMR  $\delta_{\text{ppm}}$ : 51.7 ( $\alpha\text{CH}$ ), 37.9 ( $\beta\text{CH}_2$ ), aromatic- 137.8 (C1), 95.6 (C1 $\alpha$ ), 101.9 (C1 $\beta$ ), 71.3 (C2 $\alpha$ ), 73.2 (C2 $\beta$ ), 73.3 (C3 $\alpha$ ), 74.7 (C3 $\beta$ ), 82.2 (C4 $\alpha$ ), 84.2 (C4 $\beta$ ), 77.7 (C5 $\alpha,\beta$ ), 62.4 (C6 $\alpha,\beta$ ), 103.4 (C1'' $\beta$ ), 69.9 (C2''), 72.4 (C3''), 67.4 (C4''), 74.7 (C5''), 62.7 (C6'').

4.4.1.18. *L-Phenylalanyl-D-mannitol*. Solid; UV ( $\text{H}_2\text{O}$ ,  $\lambda_{\text{max}}$ ): 215.0 nm ( $\sigma \rightarrow \sigma^*$   $\epsilon_{215.0} = 631 \text{ M}^{-1}$ ), 257.5 nm ( $\pi \rightarrow \pi^*$   $\epsilon_{257.5} = 170 \text{ M}^{-1}$ ). IR (KBr): 3290  $\text{cm}^{-1}$  (OH), 1637  $\text{cm}^{-1}$  (CO), 1532  $\text{cm}^{-1}$  (aromatic,  $-\text{C}=\text{C}-$ ). Optical rotation ( $c$  0.6,  $\text{H}_2\text{O}$ ):  $[\alpha]_{\text{D}}$  at 25  $^{\circ}\text{C} = +1.6^{\circ}$ . MS ( $m/z$ ) 352  $[\text{M} + \text{Na}]^+$ . 2D-HSQC (DMSO- $d_6$ ): 1-O-ester:  $^1\text{H}$  NMR  $\delta_{\text{ppm}}$  (500.13 MHz): 3.48 ( $\alpha\text{CH}$ ), 2.88 ( $\beta\text{CH}_2$ ), aromatic- 7.26 (H-2, H-6), 7.26 (H-3, H-5), 7.18 (H-4), 3.38 (H-1), 3.46 (H-2), 3.70 (H-3), 3.84 (H-4), 3.52 (H-5), 3.36 (H-6);  $^{13}\text{C}$  NMR  $\delta_{\text{ppm}}$  (125 MHz): 55.8 ( $\alpha\text{CH}$ ), 37.1 ( $\beta\text{CH}_2$ ), aromatic- 137.6 (C1), 131.2 (C2, C6), 126.7 (C4), 171.0 (CO), 66.0 (C1, C6), 75.0 (C2), 70.0 (C3), 70.2 (C4), 77.8 (C5). 1,6-di-O-ester:  $^1\text{H}$  NMR  $\delta_{\text{ppm}}$ : 3.39 ( $\alpha\text{CH}$ ), 3.46 (H-1), 3.45 (H-2, H-6), 3.11 (H-3, H-4), 3.46 (H-6);  $^{13}\text{C}$  NMR  $\delta_{\text{ppm}}$ : 55.3 ( $\alpha\text{CH}$ ), 66.8 (C1), 77.0 (C2, C5), 70.4 (C3, C4), 66.8 (C6).

4.4.1.19. *L-Tryptophanyl-D-glucose*. Solid; UV ( $\text{H}_2\text{O}$ ,  $\lambda_{\text{max}}$ ): 213.0 nm ( $\sigma \rightarrow \sigma^*$   $\epsilon_{213.0} = 1479 \text{ M}^{-1}$ ), 276 nm ( $\pi \rightarrow \pi^*$   $\epsilon_{276} = 389 \text{ M}^{-1}$ ), 315 nm ( $n \rightarrow \pi^*$   $\epsilon_{315} = 118 \text{ M}^{-1}$ ). IR (KBr): 3523  $\text{cm}^{-1}$  (NH), 3336  $\text{cm}^{-1}$  (OH), 1633  $\text{cm}^{-1}$  (C=O), 1524  $\text{cm}^{-1}$  (aromatic  $-\text{C}=\text{C}-$ ). Optical rotation ( $c$  0.6,  $\text{H}_2\text{O}$ ):  $[\alpha]_{\text{D}}$  at 25  $^{\circ}\text{C} = -21.7^{\circ}$ . MS ( $m/z$ ) 366.1  $[\text{M}]^+$ . 2D-HSQC (DMSO- $d_6$ ): 2-O-ester:  $^1\text{H}$  NMR  $\delta_{\text{ppm}}$  (500.13 MHz): 2.92 ( $\alpha\text{CH}$ ), 3.06 ( $\beta\text{CH}_2$ ), Aromatic - 6.96–7.59, 4.6 (H-1 $\alpha$ ), 3.69 (H-2 $\alpha$ ), 3.72 (H-2 $\beta$ ), 3.68 (H-3 $\alpha$ ), 3.54 (H-6 $\alpha,\beta$ );  $^{13}\text{C}$  NMR  $\delta_{\text{ppm}}$  (125 MHz): 53.2 ( $\alpha\text{CH}$ ), 35.0 ( $\beta\text{CH}_2$ ), aromatic-109.4 (C1), 124.2 (C2), 136.0 (C4), 114.6 (C6), 120.8 (C7), 121.1 (C8), 100.8 (C1 $\alpha$ ), 75.9 (C2 $\alpha$ ), 76.2 (C2 $\beta$ ) 72.9 (C3 $\alpha$ ), 62.8 (C6 $\alpha,\beta$ ). 3-O-ester:  $^1\text{H}$  NMR  $\delta_{\text{ppm}}$ : 2.87 ( $\alpha\text{CH}$ ), 2.84 ( $\beta\text{CH}_2$ ), 3.82 (H-2 $\alpha$ ), 3.92 (H-3 $\alpha$ ), 3.59 (H-3 $\beta$ ), 3.58 (H-6 $\alpha,\beta$ );  $^{13}\text{C}$  NMR  $\delta_{\text{ppm}}$ : 52.3 ( $\alpha\text{CH}$ ), 35.9 ( $\beta\text{CH}_2$ ), aromatic-109.3 (C1), 124.3 (C2,C3), 136.3 (C4), 121.0 (C5), 113.0 (C6), 116.5 (C7), 120.0 (C8), 100.1 (C1 $\alpha$ ), 101.8 (C1 $\beta$ ), 74.2 (C2 $\alpha$ ), 71.2 (C2 $\beta$ ), 82.0 (C3 $\alpha,\beta$ ), 62.5 (C6 $\alpha,\beta$ ). 6-O-ester:  $^1\text{H}$  NMR  $\delta_{\text{ppm}}$ : 2.81 ( $\alpha\text{CH}$ ), 2.70 ( $\beta\text{CH}_2$ ), 3.41 (H-2 $\alpha$ ), 3.51 (H-2 $\beta$ ), 3.68 (H-3 $\alpha$ ), 3.52 (H-4 $\alpha$ ), 3.64 (H-5 $\alpha$ ), 3.70 (H-5 $\beta$ ), 3.65 (H-6 $\alpha,\beta$ );  $^{13}\text{C}$  NMR  $\delta_{\text{ppm}}$ : 51.5 ( $\alpha\text{CH}$ ), 31.0 ( $\beta\text{CH}_2$ ), aromatic- 109.2 (C1), 124.4 (C2,C3), 136.4 (C4), 121.0 (C5), 111.5 (C6), 118.2 (C7), 118.5 (C8), 172.0 (CO), 96.9 (C1 $\alpha$ ), 101.9 (C1 $\beta$ ), 71.8 (C2 $\alpha$ ), 69.5 (C2 $\beta$ ), 72.6 (C3 $\alpha$ ), 69.6 (C4 $\alpha$ ), 68.9 (C5 $\alpha$ ), 70.2 (C5 $\beta$ ), 63.0 (C6 $\alpha,\beta$ ). 2,6-di-O-ester:  $^1\text{H}$  NMR  $\delta_{\text{ppm}}$ : 2.78 ( $\beta\text{CH}_2$ ), 3.92 (H-2 $\alpha$ ), 3.82 (H-2 $\beta$ ), 3.54 (H-6 $\alpha,\beta$ ).  $^{13}\text{C}$  NMR  $\delta_{\text{ppm}}$ : 31.0 ( $\beta\text{CH}_2$ ), 77.0 (C2 $\alpha$ ), 77.3 (C2 $\beta$ ), 63.2 (C6 $\alpha,\beta$ ). 3,6-di-O-ester:  $^1\text{H}$  NMR  $\delta_{\text{ppm}}$ : 2.82 ( $\alpha\text{CH}$ ), 2.61 ( $\beta\text{CH}_2$ ), 3.74 (H-3 $\alpha$ ), 3.44 (H-6 $\alpha,\beta$ );  $^{13}\text{C}$  NMR  $\delta_{\text{ppm}}$ : 51.8 ( $\alpha\text{CH}$ ), 31.0 ( $\beta\text{CH}_2$ ), 81.2 (C3 $\alpha$ ), 63.9 (C6 $\alpha,\beta$ ).

4.4.1.20. *L-Tryptophanyl-D-fructose*. Solid; UV ( $H_2O$ ,  $\lambda_{max}$ ): 212.0 nm ( $\sigma \rightarrow \sigma^*$   $\epsilon_{212.0} = 5495 M^{-1}$ ), 265.0 nm ( $\pi \rightarrow \pi^*$   $\epsilon_{265.0} = 1862 M^{-1}$ ), 308 nm ( $n \rightarrow \pi^*$   $\epsilon_{308} = 1175 M^{-1}$ ). IR (KBr): 3284  $cm^{-1}$  (OH), 1631  $cm^{-1}$  (C=O), 1364  $cm^{-1}$  (CN) and 1492  $cm^{-1}$  (aromatic,  $-C=C-$ ). Optical rotation ( $c$  0.7,  $H_2O$ ):  $[\alpha]_D$  at 25 °C =  $-10.8^\circ$ . MS ( $m/z$ ) 165  $[M - 1]^+$ . 2D-HSQCT (DMSO- $d_6$ ): 1-*O-ester*:  $^1H$  NMR  $\delta_{ppm}$  (500.13 MHz): 3.44 ( $\alpha CH$ ), 2.59 ( $\beta CH_2$ ), aromatic - 7.1 (H-2), 8.18 (H-3), 7.32 (H-7), 7.74 (H-8), 4.32 (H-1 $\alpha$ ), 3.78 (H-3 $\alpha$ ), 3.48 (H-4 $\alpha$ ), 3.42 (H-6 $\alpha,\beta$ );  $^{13}C$  NMR  $\delta_{ppm}$  (125 MHz): 58.2 ( $\alpha CH$ ), 30.2 ( $\beta CH_2$ ), aromatic-109.5 (C<sub>1</sub>), 124.0 (C<sub>2</sub>), 122.0 (C<sub>3</sub>), 111.5 (C<sub>6</sub>), 120.6 (C<sub>7</sub>), 119.0 (C<sub>8</sub>), 66.4 (C1 $\alpha$ ), 104.2 (C2 $\alpha$ ), 71.6 (C3 $\alpha$ ), 70.6 (C4 $\alpha$ ), 63.1 (C6 $\alpha,\beta$ ). 6-*O-ester*:  $^1H$  NMR  $\delta_{ppm}$ : 3.32 ( $\alpha CH$ ), 2.50 ( $\beta CH_2$ ), 3.27 (H-1 $\alpha$ ), 3.78 (H-4 $\alpha$ ), 4.38 (H-6 $\alpha,\beta$ );  $^{13}C$  NMR  $\delta_{ppm}$ : 59.0 ( $\alpha CH$ ), 29.8 ( $\beta CH_2$ ), 63.9 (C1 $\alpha$ ), 102.0 (C2 $\alpha$ ), 72.5 (C4 $\alpha,\beta$ ), 66.4 (C6 $\alpha,\beta$ ).

4.4.1.21. *L-Histidyl-D-glucose*. Solid; UV ( $H_2O$ ,  $\lambda_{max}$ ): 210.0 nm ( $\sigma \rightarrow \sigma^*$   $\epsilon_{210.0} = 1072 M^{-1}$ ), 264.0 nm ( $\pi \rightarrow \pi^*$   $\epsilon_{264.0} = 933 M^{-1}$ ). IR (KBr): 3126  $cm^{-1}$  (OH), 1720  $cm^{-1}$  (C=O), 1343  $cm^{-1}$  (NH), 1588  $cm^{-1}$  (aromatic,  $-C=C-$ ). Optical rotation ( $c$  1.0,  $H_2O$ ):  $[\alpha]_D$  at 25 °C =  $-33.3^\circ$ . MS ( $m/z$ ) 318  $[M + 1]^+$ . 2D-HSQCT (DMSO- $d_6$ ): 2-*O-ester*:  $^1H$  NMR  $\delta_{ppm}$  (500.13 MHz): 3.08 ( $\alpha CH$ ), 2.70 ( $\beta CH_2$ ), Aromatic - 6.93 (H2), 7.69 (H3), 4.78 (H-1 $\alpha$ ), 3.86 (H-2 $\alpha$ ), 3.76 (H-2 $\beta$ ), 3.19 (H-3 $\alpha$ ), 3.12 (H-3 $\beta$ ), 3.62 (H-4 $\alpha$ ), 3.58 (H-6 $\alpha,\beta$ );  $^{13}C$  NMR  $\delta_{ppm}$  (125 MHz): 52.0 ( $\alpha CH$ ), 30.8 ( $\beta CH_2$ ), aromatic-115.6 (C1), 134.2 (C2), 134.8 (C3), 171.5 (CO), 96.2 (C1 $\alpha$ ), 75.0 (C2 $\alpha$ ), 76.7 (C2 $\beta$ ), 70.0 (C3 $\alpha$ ), 80.0 (C3 $\beta$ ), 69.3 (C4 $\alpha$ ), 62.2 (C6 $\alpha,\beta$ ). 3-*O-ester*:  $^1H$  NMR  $\delta_{ppm}$ : 3.00 ( $\alpha CH$ ), 2.82 ( $\beta CH_2$ ), aromatic- 6.93 (H2), 7.71 (H3), 4.75 (H-1 $\alpha$ ), 3.60 (H-2 $\alpha$ ), 3.32 (H-2 $\beta$ ), 3.77 (H-3 $\alpha$ ), 3.93 (H-3 $\beta$ ), 3.67 (H-4 $\alpha$ ), 3.42 (H-6 $\alpha,\beta$ );  $^{13}C$  NMR  $\delta_{ppm}$ : 52.8 ( $\alpha CH$ ), 27.7 ( $\beta CH_2$ ), aromatic-116.2 (C1), 134.4 (C2), 134.8 (C3), 171.0 (CO), 95.5 (C1 $\alpha$ ), 72.2 (C2 $\alpha$ ), 74.9 (C2 $\beta$ ), 81.7 (C3 $\alpha$ ), 83.2 (C3 $\beta$ ), 68.9 (C4 $\alpha$ ), 61.3 (C6 $\alpha,\beta$ ). 6-*O-ester*:  $^1H$  NMR  $\delta_{ppm}$ : 2.84 ( $\alpha CH$ ), 3.06 ( $\beta CH_2$ ), aromatic - 6.93 (H2), 7.72 (H3), 4.72 (H-1 $\alpha$ ), 3.59 (H-2 $\alpha$ ), 3.12 (H3- $\alpha$ ), 3.80 (H-4 $\alpha$ ), 2.90 (H-5 $\alpha$ ), 3.80 (H-6 $\alpha,\beta$ );  $^{13}C$  NMR  $\delta_{ppm}$ : 51.2 ( $\alpha CH$ ), 26.8 ( $\beta CH_2$ ), aromatic-115.6 (C1), 134.4 (C2), 134.9 (C3), 170.3 (CO), 95.0 (C1 $\alpha$ ), 100.2 (C1 $\beta$ ), 72.5 (C2 $\alpha$ ), 73.1 (C3 $\alpha$ ), 70.6 (C4 $\alpha$ ), 75.0 (C5 $\alpha$ ), 63.6 (C6 $\alpha,\beta$ ). 2,6-*di-O-ester*:  $^1H$  NMR  $\delta_{ppm}$ : 2.90 ( $\alpha CH$ ), 2.78 ( $\beta CH_2$ ), 3.73 (H-2 $\alpha$ ), 3.75 (H-2 $\beta$ ), 3.47 (H-6 $\alpha,\beta$ );  $^{13}C$  NMR  $\delta_{ppm}$ : 52.5 ( $\alpha CH$ ), 30.8 ( $\beta CH_2$ ), 102.1 (C1 $\beta$ ), 76.7 (C2 $\alpha$ ), 78.0 (C2 $\beta$ ), 70.5 (C4 $\alpha$ ), 62.7 (C6 $\alpha,\beta$ ). 3,6-*di-O-ester*:  $^1H$  NMR  $\delta_{ppm}$ : 2.80 ( $\beta CH_2$ ), 3.73 (H-3 $\alpha$ ), 3.60 (H-3 $\beta$ ), 3.26 (H-6 $\alpha,\beta$ );  $^{13}C$  NMR  $\delta_{ppm}$ : 30.0 ( $\beta CH_2$ ), 81.7 (C3 $\alpha$ ), 82.3 (C3 $\beta$ ), 70.2 (C4 $\alpha$ ), 62.4 (C6 $\alpha,\beta$ ).

4.4.1.22. *L-Histidyl-D-fructose*. Solid; UV ( $H_2O$ ,  $\lambda_{max}$ ): 210.0 nm ( $\sigma \rightarrow \sigma^*$   $\epsilon_{210.0} = 617 M^{-1}$ ), 267.0 nm ( $\pi \rightarrow \pi^*$   $\epsilon_{267.0} = 240 M^{-1}$ ), 321.0 nm ( $n \rightarrow \pi^*$   $\epsilon_{321.0} = 170 M^{-1}$ ). IR (KBr): 3136  $cm^{-1}$  (OH), 1605  $cm^{-1}$  (C=O), 1393  $cm^{-1}$  (CN), 1592  $cm^{-1}$  (aromatic,  $-C=C-$ ). Optical rotation ( $c$  0.6,  $H_2O$ ):  $[\alpha]_D$  at 25 °C =  $-20.0^\circ$ . MS ( $m/z$ ) 340  $[M + Na]^+$ . 2D-HSQCT NMR: 6-*O-ester*:  $^1H$  NMR  $\delta_{ppm}$  (500.13 MHz): 3.45 ( $\alpha CH$ ),

3.21 ( $\beta CH_2$ ), aromatic - 6.85 (H2), 7.42 (H3), 3.67 (H-3 $\alpha$ ), 3.52 (H-4 $\alpha$ ), 3.24 (H-6 $\alpha,\beta$ );  $^{13}C$  NMR  $\delta_{ppm}$  (125 MHz): aromatic-116.5 (C1), 134.2 (C2), 124.5 (C3), 170.5 (CO), 62.8 (C1 $\alpha$ ), 102.1 (C2 $\alpha$ ), 69.2 (C3 $\alpha$ ), 70.0 (C4 $\alpha$ ) 70.6 (C4 $\alpha$ ), 64.2 (C6 $\alpha,\beta$ ).

4.4.1.23. *L-Histidyl-D-mannitol*. Solid; UV ( $H_2O$ ,  $\lambda_{max}$ ): 210.0 nm ( $\sigma \rightarrow \sigma^*$   $\epsilon_{210.0} = 3802 M^{-1}$ ), 267.0 nm ( $\pi \rightarrow \pi^*$   $\epsilon_{267.0} = 1349 M^{-1}$ ), 324.0 nm ( $n \rightarrow \pi^*$   $\epsilon_{324.0} = 776 M^{-1}$ ). IR (KBr): 3344  $cm^{-1}$  (OH), 1631  $cm^{-1}$  (C=O), 1319  $cm^{-1}$  (CN), 1511  $cm^{-1}$  (aromatic). Optical rotation ( $c$  0.2,  $H_2O$ ):  $[\alpha]_D$  at 25 °C =  $+17.4^\circ$ . 2D-HSQCT NMR: 1-*O- ester*:  $^1H$  NMR  $\delta_{ppm}$  (500.13 MHz): 3.46 ( $\alpha CH$ ), 3.32 ( $\beta CH_2$ ), aromatic 7.38 (H3), 3.44 (H-1), 3.39 (H-2), 3.47 (H-3), 3.54 (H-4), 3.57 (H-5), 3.38 (H-6);  $^{13}C$  NMR  $\delta_{ppm}$  (125 MHz): 54.3 ( $\alpha CH$ ), aromatic- 128.2 (C2), 123.4 (C3), 63.8 (C1, C6), 71.4 (C2, C5), 69.8 (C3, C4).

#### 4.5. Angiotensin converting enzyme (ACE) inhibition assay

ACE inhibition assay for the esters prepared were performed by the Cushman and Cheung method [23]. Aliquots of glycoside or ester solutions in the concentration range 0.12 to 1.60 mM (0.1–0.8 ml of 2.0 mM stock solution) were taken and to this 0.1 ml of ACE solution (0.1% in 0.1 M phosphate buffer, pH 8.3 containing 300 mM NaCl) was added. To this solution, 0.1 ml of 5.0 mM hippuryl-L-histidyl-L-leucine (HHL) was also added and the total volume made up to 1.25 ml by adding phosphate buffer (0.95–0.25 ml of 0.1 M pH 8.3 containing 300 mM NaCl). The solution was incubated on a Heto-Holten shaking water bath for 30 min at 37 °C. Blanks were performed without the enzyme by taking only the glycoside or ester solutions (0.1 to 0.8 ml) along with 0.1 ml of 5.0 mM HHL. The total volume was made up to 1.25 ml by adding same buffer (1.05–0.35 ml). The reaction was terminated by adding 0.25 ml of 1 M HCl. Hippuric acid formed in the reaction was extracted with 1.5 ml of ethyl acetate. One ml of the ethyl acetate layer was evaporated to dryness and treated with equal amount of distilled water and absorbance was measured at 228 nm for hippuric acid. The hippuric acid formed in 1.5 ml of ethyl acetate was determined from a calibration plot prepared by using a standard hippuric acid in 1 ml of distilled water in the concentration range 0–400 nmol and measuring its absorbance at 228 nm.

Specific activity was expressed as hippuric acid formed (mM) per min, per mg of enzyme protein.

$$\text{Specific activity} = \frac{A_{ts} - A_{blank}}{T \times S \times E}$$

$A_{ts}$  = absorbance of test solution,  $A_{blank}$  = absorbance of blank solution,  $T$  = incubation period in min,  $S$  = slope value of the calibration plot ( $1.00 \times 10^{-2}$  Abs units/nmol of hippuric acid),  $E$  = amount of the enzyme in mg protein. The specific activity value for each glycoside and ester is an average from two independent measurements. Percentage inhibition was expressed as the ratio of the specific activity of ACE in the pre-



sence of the inhibitor to that in the absence of the inhibitor, the latter being considered as 100%. IC<sub>50</sub> value was expressed as the concentration of the inhibitor required for 50% reduction in ACE specific activity. Molecular weights of the glycosides and esters employed in the calculations are weighted averages of molecular weights of glycosides and esters detected by NMR and Mass spectroscopy. In case of samples where NMR spectra were not recorded, molecular weights of the mono glycosides and mono esters were considered for the calculations.

#### 4.6. Protease and lipase assay

Protease activity for the ACE inhibitor was determined by the method described by Dubey and Jagannadham [29] and lipase activity by the tributyrin method [30] in presence of eugenyl-D-glucoside (0.8 mM in 0.1 M, pH 7.5, Tris-HCl buffer) and L-isoleucyl-D-glucose (0.8 mM in the same buffer) individually. Specific protease activity was expressed as the increase in absorbance at 440 nm min<sup>-1</sup> mg<sup>-1</sup> of the protein employed. Similarly specific lipase activity was determined as μmol of butyric acid formed per min per mg of the protein employed.

#### Acknowledgements

Authors acknowledge the Department of Science and Technology, India for financial support to this work. K.L., G.R.V. and R.S. acknowledge Council of Scientific and Industrial Research, India for providing Senior Research Fellowships and B. R.S. acknowledges Department of Science and Technology, India for providing Junior Research Fellowship.

#### References

- [1] G.H. Li, G.W. Le, S. Yong-Hui, S. Shrestha, *Nutr. Res.* 24 (2004) 469–486.
- [2] V. Vermeirssen, J. Van-Camp, W. Verstraete, *J. Biochem. Biophys. Methods* 51 (2002) 75–87.
- [3] I. Johnston, *J. Hypertens.* 10 (1992) 13–26.
- [4] A. Michaud, T.A. Williams, M.T. Chauvet, P. Corvol, *Mol. Pharmacol.* 51 (1997) 1070–1076.
- [5] N.M. Hooper, A.J. Turner, *Biochem. J.* 241 (1987) 625–633.
- [6] L. Deloffre, P.E. Sautiere, R. Huybrechts, K. Hens, D. Vieau, M. Salzet, *Eur. J. Biochem.* 271 (2004) 2101–2106.
- [7] M.M. Mullally, H. Meisel, R.J. Fitz-Gerald, *Biol. Chem.* 377 (1996) 259–260.
- [8] J. Wu, X. Ding, *Food Res. Int.* 35 (2002) 367–375.
- [9] S.K. Kim, H.G. Byun, P.J. Park, F. Shahidi, *J. Agric. Food Chem.* 49 (2001) 2992–2997.
- [10] O. Hyuncheol, K.C. Dae-Gill, L. Hun-Taeg, Ho-Sub, *Phytotherapy Res.* 17 (2003) 811–813.
- [11] L. Chong-Qian, L. Bo-Gang, Q. Hua-Yi, L. Qi-Lin, W. Feng-Peng, Z. Guo-Lin, *J. Natur. Prod.* 67 (2004) 978–982.
- [12] K. Dae-Gill, L. Yong-Sup, K. Hyoung-Ja, L. Yun-Mi, L. Ho-Sub, *J. Ethnopharmacol.* 89 (2003) 151–154.
- [13] O.J. Park, G.J. Jeon, J.W. Yang, *Enzyme Microb. Technol.* 25 (1999) 455–462.
- [14] O. Kirk, F. Bjorkling, S.E. Godfredsen, T.S. Larsen, *Biocatalysis* 6 (1992) 127–134.
- [15] A. Zaks, D.R. Dodds, *Drug Dev. Today* 2 (1997) 513–531.
- [16] D. Ikeda, S. Umezawa, in: R. Ikan (Ed.), *Naturally Occurring Glycosides*, John Wiley & Sons Ltd., New York, 1999, pp. 1–42.
- [17] V. Kren, L. Martinkova, *Curr. Med. Chem.* 8 (2001) 1313–1318.
- [18] K. Lohith, S. Divakar, *J. Biotechnol.* 117 (2005) 49–56.
- [19] G.R. Vijayakumar, B. Manohar, S. Divakar, *Eur. Food Res. Technol.* 220 (2005) 272–277.
- [20] G.R. Vijayakumar, S. Divakar, *Biotechnol. Lett.* 27 (2005) 1411–1415.
- [21] R. Sivakumar, S. Divakar, *Tetrahedron Lett.* 47 (2006) 695–699.
- [22] D.W. Cushman, H.S. Cheung, *Biochem. Pharmacol.* 20 (1971) 1637–1638.
- [23] D.P. De-Lima, *Quim. Nova* 22 (1999) 375–381.
- [24] M. Andujar-Sanchez, A. Camara-Artigas, V. Jara-Perez, *J. Chromatogr. B* 783 (2003) 247–252.
- [25] K.R. Kiran, S. Harikrishna, C.V. Sureshbabu, N.G. Karanth, S. Divakar, *Biotechnol. Lett.* 22 (2000) 1511–1514.
- [26] J.B. Sumner, E.B. Sisler, *Arch. Biochem.* 4 (1944) 333–336.
- [27] O.H. Lowry, N.J. Rosenbrough, A.L. Farr, R.J. Randal, *J. Biol. Chem.* 193 (1951) 265–275.
- [28] R.K. Merkle, R.D. Cummings, in: V. Ginsburg (Ed.), *Methods in Enzymology*, 1987, pp. 232–259.
- [29] V.K. Dubey, M.B. Jagannadham, *Phytochem.* 62 (2003) 1057–1071.
- [30] T. Vorderwulbecke, K. Kieslich, H. Erdmann, *Enzyme Microb. Technol.* 14 (1992) 631–639.



## Lipase catalyzed synthesis of L-alanyl esters of carbohydrates

Bhandya R. Somashekar, Soundar Divakar\*

*Fermentation Technology and Bioengineering, Central Food Technological Research Institute, Mysore 570020, India*

Received 5 January 2006; received in revised form 13 April 2006; accepted 21 April 2006

### Abstract

Synthesis of L-alanyl esters of carbohydrates like aldohexoses (D-glucose, D-galactose and D-mannose), ketohexose (D-fructose), pentoses (D-arabinose and D-ribose) and disaccharides (lactose, maltose and sucrose) were carried out using *Rhizomucor miehei* lipase (RML) in organic solvents with conversion yields in the range 8–56%. Enzymatic esterification between L-alanine and D-glucose using RML and porcine pancreas lipase (PPL) was investigated in terms of incubation period, enzyme concentration, substrate concentration, buffer salts (pH and concentration) and enzyme reusability. RML has shown a maximum conversion yield of 28% (1.12–0.88 mmol monoesters and 0.24 mmol diesters) at 1 mmol D-glucose and 4 mmol L-alanine in presence of 30% RML (w/w, D-glucose) and 0.1 mM (0.1 ml) pH 4.0 acetate buffer in 72 h. PPL showed a maximum yield of 18% (0.36–0.28 mmol monoesters and 0.08 mmol diesters) at 1 mmol D-glucose and 2 mmol L-alanine in presence of 40% lipase (w/w, D-glucose) and 0.1 mM (0.1 ml) pH 5.0 acetate buffer in 72 h. In presence of buffer salts, RML showed 22% higher ester yield than in its absence under the same experimental conditions. However, buffer salts did not enhance esterification with PPL. Two-dimensional HSQCT NMR confirmed formation of 1-O-, 2-O-, 3-O-, 4-O-, 5-O-, 6-O- and 6'-O-monoesters and 1,6-di-O-, 2,5-di-O-, 2,6-di-O-, 3,5-di-O-, 3,6-di-O-, 4,6-di-O and 6,6'-di-O-diesters to varying extents depending on the carbohydrate employed.

© 2006 Elsevier Inc. All rights reserved.

**Keywords:** L-Alanyl esters of carbohydrates; Diesters; Enzymatic esterification; Monoesters; Porcine pancreas lipase; *Rhizomucor miehei* lipase

### 1. Introduction

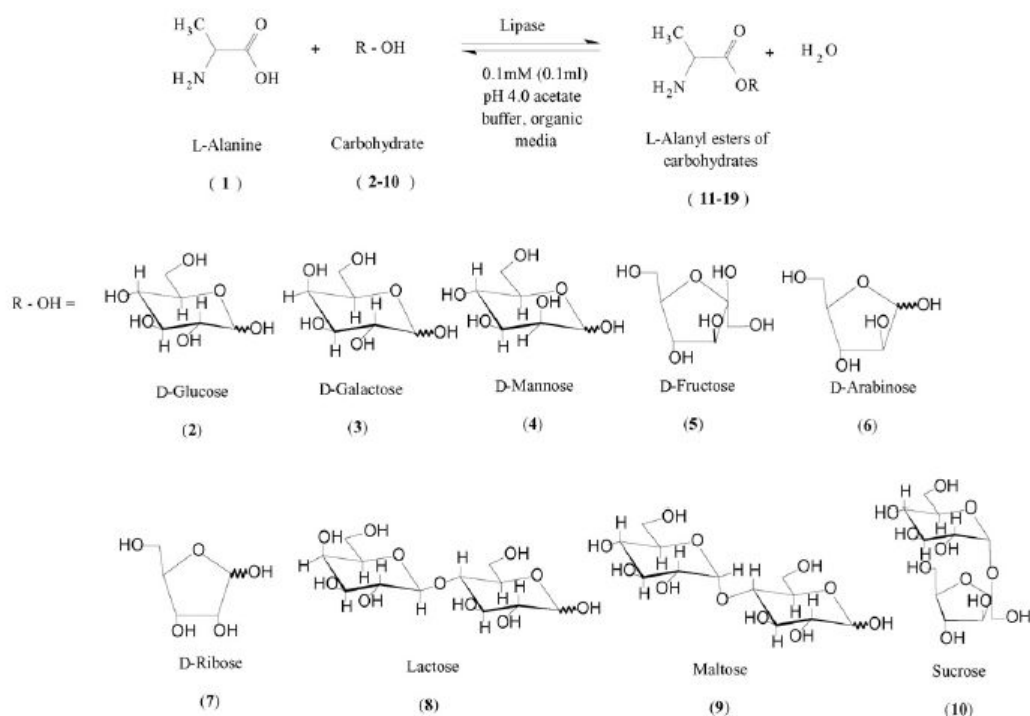
Amino acyl esters of carbohydrates are used as sweetening agents, surfactants, microcapsules in pharmaceutical preparations, active nucleoside amino acid esters, antibiotics and in the delivery of biological active agents [1–5]. Chemical acylation of carbohydrates regio-selectively is complex due to the presence of multiple hydroxyl groups, which require protection and deprotection [2,6]. When enzymes are used in organic media, they exhibit specificity [7], thermostability [8,9], molecular memory [10,11] and capacity to catalyze reverse hydrolytic reactions [12,13].

Hitherto, very few references are available on the lipase catalyzed esterification of amino acyl esters of sugars. Most of the earlier workers used proteases and N-protected and carboxyl group activated amino acids for synthesizing aminoacyl esters of carbohydrates [14–17]. Therisod and Klibanov [18] used subtilisin to acylate carbohydrates with activated carboxylic acids in anhydrous organic solvents. Riva et al. [14] carried out

subtilisin catalyzed synthesis of N-acetyl-L-alanyl-methyl-β-D-galactopyranoside in anhydrous DMF, with an yield of 70% (6-O- 84% and 4-O- 8%) and N-acetyl-D-alanyl-methyl-β-D-galactopyranoside with an yield of 35% (6-O- 68%, 4-O- 10%, 3-O- 10% and 2-O- 10%). Suzuki et al. synthesized L-alanyl-D-glucose by using D-glucose, methyl-L-alanine hydrochloride and intact cells of *Rhodotorula lactosa* [19]. Park et al. reported that lipase from porcine pancreas and Lipozyme IM20 gave very low yields (<2%), compared to proteases which gave conversion yields ranging from 15% to 98% when N-protected and carboxyl group activated amino acid was used for the acylation of D-glucose in pyridine [16]. All these reactions were conducted in shake flasks using lesser quantity of substrates and larger quantity of enzymes.

We have earlier carried out some preliminary investigation [20] on the lipase catalyzed synthesis of L-alanyl-D-glucose, L-phenylalanyl-D-glucose and L-leucyl-D-glucose. However, in the present work, a comprehensive investigation has been carried out on the lipase catalyzed synthesis of L-alanyl esters of nine carbohydrate molecules. In the present investigation, lipases from *Rhizomucor miehei* (RML) and porcine pancreas (PPL) were employed to synthesize L-alanyl esters of D-glucose. Besides, RML was also employed to synthesize L-alanyl esters of aldo-

\* Corresponding author. Tel.: +91 821 515792; fax: +91 821 517233.  
E-mail address: [divakar643@gmail.com](mailto:divakar643@gmail.com) (S. Divakar).



Scheme 1. Lipases catalyzed synthesis of L-alanyl esters of carbohydrates.

hexoses (D-glucose 2, D-galactose 3 and D-mannose 4), ketohexose (D-fructose 5), pentoses (D-arabinose 6 and D-ribose 7) and disaccharides (lactose 8, maltose 9 and sucrose 10). Attempts to synthesize the same using *N*-acetyl-L-alanine resulted in very little conversion with the above-mentioned enzymes. Hence, unprotected and unactivated L-alanine (1) and carbohydrates (2–10) were employed (Scheme 1). The results are presented below.

## 2. Materials and methods

### 2.1. Enzymes

Lipozyme IM20 (*Rhizomucor miehei* lipase, RML) immobilized on weak anion exchange resin, from Novo Nordisk, Denmark and Porcine pancreas lipase (PPL), Type II, crude Steapsin purchased from Sigma Chemical Co., USA, were used in the present work. RML and PPL employed showed esterification activities of 0.46  $\mu\text{mol}/\text{min}/\text{mg}$  enzyme preparation and 0.06  $\mu\text{mol}/\text{min}/\text{mg}$  enzyme preparation, respectively, [21].

### 2.2. Chemicals and reagents

L-Alanine, D-galactose and D-fructose from HiMedia Ltd., India; D-glucose, sucrose and Coomassie Brilliant Blue-G 250 from SD fine chemicals Ltd., India; maltose from Sigma Chemical Co., USA; D-mannose, D-arabinose, D-ribose and D-mannitol from LOBA Chemie Ltd., India; lactose from SISCO Research Laboratories Ltd., India; D-sorbitol from Rolex Laboratory Reagent Ltd., India and Karl Fischer Reagent from Qualigens Fine Chemicals Ltd., India, were employed as such. Sephadex G-10 from Sigma Chemical Co., USA, and Bio Gel P-2 from Bio-Rad Laboratories were used as such. Solvents:  $\text{CH}_2\text{Cl}_2$ ,  $\text{CHCl}_3$ , *n*-hexane, HPLC grade acetonitrile and DMF from SD fine Chemicals (Ind.) Ltd., were employed after distilling once.

### 2.3. Esterification procedure

Esterification was carried out in a flat bottomed two necked flask by reacting unprotected L-alanine 1 (0.001–0.008 mol) and 0.01–0.008 mol of carbohydrate (2–10) along with 100 ml of  $\text{CH}_2\text{Cl}_2$ :DMF (v/v, 90:10, 40 °C) or hexane: $\text{CHCl}_3$ :DMF (v/v/v, 45:45:10, 60 °C) in presence of 0.018–0.25 g of lipases (10–50% by weight of 2–10) under reflux for a period of three days. The enzymes were imparted with 'pH memory' in some experiments by adding known volumes of 0.1 M buffer solutions of specified pH value to 100 ml (solvent) of the reaction mixture [22,23]. The buffer salts thus employed were  $\text{CH}_3\text{COONa}$  for pH 4.0 and 5.0,  $\text{Na}_2\text{HPO}_4$  for pH 6.0 and 7.0 and  $\text{Na}_2\text{B}_4\text{O}_7 \cdot 10\text{H}_2\text{O}$  for pH 8.0 buffers. The condensed vapours of solvent which formed an azeotrope with water during reflux was passed through a desiccant before being returned into the reaction mixture, thereby facilitating complete removal of water of reaction [24]. This set-up maintained a very low water activity of  $a_w = 0.0054$  throughout the reaction period which was determined by Karl Fischer titration of the reaction mixture using Karl Fischer reagent by examining aliquots for the water content during the course of the reaction. After completion of the reaction, the solvent was distilled off, 20–30 ml of warm water was added, stirred and filtered to remove the lipase. The filtrate was evaporated to get a mixture of the unreacted carbohydrate, unreacted L-alanine and the product esters 11–19 which were then analyzed by HPLC. The esters formed were separated by size exclusion chromatography using Sephadex G-10 and Bio Gel P-2 as column materials and eluted with water and subjected to spectral characterization. The isolated esters were also tested for Angiotensin Converting Enzyme (ACE) inhibition activity according to the method of Cushman and Cheung [25]. Critical micellar concentration was determined for L-alanyl- $\beta$ -D-glucose by using Coomassie Brilliant Blue-G 250 reagent at 470 nm [26] and it was found to be 2.25 mM (0.056%).

### 2.4. HPLC

The reaction mixture was monitored by employing a Shimadzu LC10AT high-performance liquid chromatography instrument connected to a  $\mu$ -Bondapak aminopropyl column (10  $\mu\text{m}$  particle size, 3.9 mm  $\times$  300 mm length)

with acetonitrile:water (v/v, 80:20) as a mobile phase at a flow rate of 1 ml/min and refractive index detector. Also, a LiChrosorb RP-18 column (5  $\mu$ m particle size, 4.6 mm  $\times$  150 mm length) with acetonitrile:water (v/v, 20:80) as a mobile phase at a flow rate of 1 ml/min and UV detector at 210 nm was employed. Since different equivalents of L-alanine were employed, the conversion yields were determined based on the peak areas of L-alanine and L-alanyl ester of carbohydrate and were expressed relative to the L-alanine concentration employed. The error in HPLC yields were  $\pm$ 10–15%. In  $\mu$ -Bondapak aminopropyl column, retention times of D-glucose, L-alanine and L-alanyl-D-glucose are found to be 5.2, 9.7 and 12.3 min, respectively. In LiChrosorb RP-18 column, retention times are: L-alanine, 2.6 min; L-alanyl-D-glucose, 3.4 min; L-alanyl-D-galactose, 3.4 min; L-alanyl-D-mannose, 3.4 min; L-alanyl-D-fructose, 3.5 min; L-alanyl-D-arabinose, 3.2 min; L-alanyl-D-ribose, 3.2 min; L-alanyl-lactose, 3.3 min; L-alanyl-maltose, 3.3 min; L-alanyl-sucrose, 3.3 min. Respective carbohydrates were not detected at 210 nm.

## 2.5. Spectral characterization

A Shimadzu UV-1601 spectrophotometer was used for recording UV spectra of the isolated esters in aqueous solutions at 0.2–1.0 mM concentration. A Nicolet 5700 FTIR instrument was used for recording the IR spectra with 1.0–2.0 mg of ester sample as KBr pellet. Specific rotations of the isolated esters were measured at 25 °C using Perkin-Elmer 243 polarimeter with a 0.5% aqueous solution of the esters. Mass spectra of the isolated esters were recorded using a Q-TOF Waters Ultima instrument (No. Q-ToF GAA 082, Waters corporation, Manchester, UK) fitted with an electron spray ionization (ESI) source.

$^1\text{H}$  and  $^{13}\text{C}$  NMR spectra were recorded on a Bruker DRX-500 MHz spectrometer (500.13 MHz for  $^1\text{H}$  and 125 MHz for  $^{13}\text{C}$ ). Proton and carbon 90° pulse widths were 10.5 and 12.25  $\mu$ s, respectively. About 40 mg of the sample dissolved in DMSO- $d_6$  and D $_2$ O was used for recording the spectra at 35 °C. Chemical shift values were expressed in ppm relative to internal tetramethylsilane standard to within  $\pm$ 0.01 ppm. Two-dimensional Heteronuclear Single Quantum Coherence Transfer spectra (2D HSQCT) were recorded [21] for the esters. In the NMR data, only resolvable signals are shown. Some assignments are interchangeable. Non-reducing end carbohydrate signals are primed. Since, the esters are surfactant molecules, they appear to aggregate in the solvent and usually give broad signals, thus, making it difficult to resolve the coupling constant values accurately. Mass data for the monoesters are shown. However, although NMR data clearly indicated the presence of di-*O*-esters, they were not detected in the mass spectra which could be due to instantaneous decomposition.

### 2.5.1. L-Alanine 1

UV ( $\text{H}_2\text{O}$ ,  $\lambda_{\text{max}}$ ): 190.0 nm ( $\sigma \rightarrow \sigma^*$   $\epsilon_{190.0}$ , 111.9 M $^{-1}$ ), IR (stretching frequency): 3415 cm $^{-1}$  (OH), 2945 cm $^{-1}$  (CH), 1715 cm $^{-1}$  (CO); optical rotation ( $c$  1.0, H $_2$ O):  $[\alpha]_D$  at 25 °C = +3.33°; 2D HSQCT (DMSO- $d_6$ ):  $^1\text{H}$  NMR  $\delta_{\text{ppm}}$  (500.13 MHz): 3.35 ( $\alpha$ -CH), 1.25 ( $\beta$ -CH $_3$ );  $^{13}\text{C}$  NMR  $\delta_{\text{ppm}}$  (125 MHz): 53.0 ( $\alpha$ -CH), 15.5 ( $\beta$ -CH $_3$ ), 170.5 (CO).

### 2.5.2. L-Alanyl- $\beta$ -D-glucose 11

UV ( $\text{H}_2\text{O}$ ,  $\lambda_{\text{max}}$ ): 227.0 nm ( $\sigma \rightarrow \sigma^*$   $\epsilon_{227.0}$ , 1150.8 M $^{-1}$ ), 294.0 nm ( $n \rightarrow \pi^*$   $\epsilon_{294.0}$ , 763.8 M $^{-1}$ ); IR (stretching frequency): 3371 cm $^{-1}$  (NH), 3410 cm $^{-1}$  (OH), 2297 cm $^{-1}$  (CH), 1653 cm $^{-1}$  (CO); optical rotation ( $c$  0.5, H $_2$ O):  $[\alpha]_D$  at 25 °C = -38.1°; mass, 274 [M + Na] $^+$ ; ACE activity: IC $_{50}$  value = 3.1  $\pm$  0.3 mM; 2D HSQCT (DMSO- $d_6$ ) 2-*O*-ester 11a:  $^1\text{H}$  NMR  $\delta_{\text{ppm}}$  (500.13 MHz): 2.95 ( $\alpha$ -CH), 1.07 ( $\beta$ -CH $_3$ ), 3.62 (H-2 $\beta$ ), 3.83 (H-3 $\beta$ ), 1.30 (H-4 $\beta$ ), 3.44 (H-6 $\beta$ );  $^{13}\text{C}$  NMR  $\delta_{\text{ppm}}$  (125 MHz): 52.1 ( $\alpha$ -CH), 15.7 ( $\beta$ -CH $_3$ ), 102.8 (C-1 $\beta$ ), 82.6 (C-2 $\beta$ ), 77.9 (C-3 $\beta$ ), 68.8 (C-4 $\beta$ ), 60.5 (C-6 $\beta$ ); 3-*O*-ester 11b:  $^1\text{H}$  NMR  $\delta_{\text{ppm}}$  (500.13 MHz): 2.87 ( $\alpha$ -CH), 3.93 (H-3 $\beta$ ), 3.58 (H-4 $\beta$ ), 3.36 (H-6 $\beta$ );  $^{13}\text{C}$  NMR  $\delta_{\text{ppm}}$  (125 MHz): 51.4 ( $\alpha$ -CH), 83.3 (C-3 $\beta$ ), 69.3 (C-4 $\beta$ ), 57.3 (C-6 $\beta$ ); 6-*O*-ester 11c:  $^1\text{H}$  NMR  $\delta_{\text{ppm}}$  (500.13 MHz): 2.95 ( $\alpha$ -CH), 1.30 ( $\beta$ -CH $_3$ ), 3.86 (H-2 $\beta$ ), 3.76 (H-5 $\beta$ ), 3.82 (H-6 $\beta$ );  $^{13}\text{C}$  NMR  $\delta_{\text{ppm}}$  (125 MHz): 50.2 ( $\alpha$ -CH), 15.1 ( $\beta$ -CH $_3$ ), 171.4 (CO), 101.8 (C-1 $\beta$ ), 75.0 (C-2 $\beta$ ), 70.1 (C-5 $\beta$ ), 63.5 (C-6 $\beta$ ); 2,6-di-*O*-ester 11d:  $^1\text{H}$  NMR  $\delta_{\text{ppm}}$  (500.13 MHz): 3.36 ( $\alpha$ -CH), 1.30 ( $\beta$ -CH $_3$ ), 3.78 (H-2 $\beta$ ), 3.47 (H-6 $\beta$ );  $^{13}\text{C}$  NMR  $\delta_{\text{ppm}}$  (125 MHz): 49.5 ( $\alpha$ -CH), 16.4 ( $\beta$ -CH $_3$ ), 100.8 (C-1 $\beta$ ), 76.5 (C-2 $\beta$ ), 62.7 (C-6 $\beta$ ); 3,6-di-*O*-ester 11e:  $^1\text{H}$  NMR  $\delta_{\text{ppm}}$  (500.13 MHz): 1.30 ( $\beta$ -CH $_3$ ), 3.78 (H-3 $\beta$ ), 3.82 (H-6 $\beta$ );  $^{13}\text{C}$  NMR  $\delta_{\text{ppm}}$  (125 MHz): 51.4 ( $\alpha$ -CH), 16.7 ( $\beta$ -CH $_3$ ), 81.6 (C-3 $\beta$ ), 63.1 (C-6 $\beta$ ).

### 2.5.3. L-Alanyl-D-galactose 12

UV ( $\text{H}_2\text{O}$ ,  $\lambda_{\text{max}}$ ): 200.0 nm ( $\sigma \rightarrow \sigma^*$   $\epsilon_{200.0}$ , 2630.3 M $^{-1}$ ), 295.0 nm ( $n \rightarrow \pi^*$   $\epsilon_{295.0}$ , 2089.3 M $^{-1}$ ); IR (stretching frequency): 2889 cm $^{-1}$  (NH), 3407 cm $^{-1}$  (OH), 2950 cm $^{-1}$  (CH), 1622 cm $^{-1}$  (CO); optical rotation ( $c$  0.5, H $_2$ O):  $[\alpha]_D$  at 25 °C = +8.8°; mass, 274 [M + Na] $^+$ ; 2D HSQCT (DMSO- $d_6$ ) 2-*O*-ester 12a:  $^1\text{H}$  NMR  $\delta_{\text{ppm}}$  (500.13 MHz): 2.95 ( $\alpha$ -CH), 3.38 (H-2 $\alpha$ ), 3.36 (H-2 $\beta$ ), 3.55 (H-6 $\beta$ );  $^{13}\text{C}$  NMR  $\delta_{\text{ppm}}$  (125 MHz): 51.5 ( $\alpha$ -CH), 76.4 (C-2 $\alpha$ ), 76.5 (C-2 $\beta$ ), 60.7 (C-6 $\beta$ ); 3-*O*-ester 12b:  $^1\text{H}$  NMR  $\delta_{\text{ppm}}$  (500.13 MHz): 3.75 (H-3 $\alpha$ ), 3.60 (H-3 $\beta$ ), 3.35 (H-6 $\alpha$ );  $^{13}\text{C}$  NMR  $\delta_{\text{ppm}}$  (125 MHz): 81.6 (C-3 $\alpha$ ), 82.6 (C-3 $\beta$ ), 60.7 (C-6 $\alpha$ ); 6-*O*-ester 12c:  $^1\text{H}$  NMR  $\delta_{\text{ppm}}$  (500.13 MHz): 3.05 ( $\alpha$ -CH), 4.90 (H-1 $\alpha$ ), 4.85 (H-1 $\beta$ ), 3.85 (H-3 $\alpha$ ), 3.30 (H-6 $\alpha$ );  $^{13}\text{C}$  NMR  $\delta_{\text{ppm}}$  (125 MHz): 52.0 ( $\alpha$ -CH), 175.0 (CO), 95.4 (C-1 $\alpha$ ), 101.8 (C-1 $\beta$ ), 70.8 (C-3 $\alpha$ ), 63.1 (C-6 $\alpha$ ).

### 2.5.4. L-Alanyl-D-mannose 13

UV ( $\text{H}_2\text{O}$ ,  $\lambda_{\text{max}}$ ): 194.0 nm ( $\sigma \rightarrow \sigma^*$   $\epsilon_{194.0}$ , 2630.3 M $^{-1}$ ), 295.0 nm ( $n \rightarrow \pi^*$   $\epsilon_{295.0}$ , 1047.1 M $^{-1}$ ); IR (stretching frequency): 2887 cm $^{-1}$  (NH), 3387 cm $^{-1}$  (OH), 2816 cm $^{-1}$  (CH), 1626 cm $^{-1}$  (CO); optical rotation ( $c$  0.5, H $_2$ O):  $[\alpha]_D$  at 25 °C = -20.0°; mass, 274 [M + Na] $^+$ ; 2D HSQCT (DMSO- $d_6$ ) 1-*O*-ester 13a:  $^{13}\text{C}$  NMR  $\delta_{\text{ppm}}$  (125 MHz): 51.5 ( $\alpha$ -CH), 15.2 ( $\beta$ -CH $_3$ ), 74.0 (C-2 $\alpha$ ), 89.2 (C-3 $\alpha$ ), 60.1 (C-6 $\alpha$ ); 4-*O*-ester 13b:  $^{13}\text{C}$  NMR  $\delta_{\text{ppm}}$  (125 MHz): 49.7 ( $\alpha$ -CH), 14.7 ( $\beta$ -CH $_3$ ), 75.32 (C-4 $\beta$ ), 60.1 (C-6 $\alpha$ ); 6-*O*-ester 13c:  $^{13}\text{C}$  NMR (DMSO- $d_6$ )  $\delta_{\text{ppm}}$  (125 MHz): 52.1 ( $\alpha$ -CH), 15.9 ( $\beta$ -CH $_3$ ), 172.0 (CO), 95.5 (C-1 $\alpha$ ), 101.5 (C-1 $\beta$ ), 69.7 (C-2 $\alpha$ ), 69.0 (C-3 $\alpha$ ), 68.4 (C-4 $\alpha$ ), 74.9 (C-5 $\alpha$ ), 63.1 (C-6 $\alpha$ ); 3,6-di-*O*-ester 13d:  $^{13}\text{C}$  NMR  $\delta_{\text{ppm}}$  (125 MHz): 82.0 (C-3 $\alpha$ ), 82.9 (C-3 $\beta$ ), 62.8 (C-6 $\alpha$ ); 4,6-di-*O*-ester 13e:  $^{13}\text{C}$  NMR  $\delta_{\text{ppm}}$  (125 MHz): 77.2 (C-4 $\alpha$ ), 62.5 (C-6 $\alpha$ ).

### 2.5.5. L-Alanyl-D-fructose 14

UV ( $\text{H}_2\text{O}$ ,  $\lambda_{\text{max}}$ ): 200.0 nm ( $\sigma \rightarrow \sigma^*$   $\epsilon_{200.0}$ , 2630.3 M $^{-1}$ ), 295.0 nm ( $n \rightarrow \pi^*$   $\epsilon_{295.0}$ , 2089.3 M $^{-1}$ ); IR (stretching frequency): 2889 cm $^{-1}$  (NH), 3407 cm $^{-1}$  (OH), 2950 cm $^{-1}$  (CH), 1622 cm $^{-1}$  (CO); optical rotation ( $c$  0.5, H $_2$ O):  $[\alpha]_D$  at 25 °C = +8.8°; mass, 274 [M + Na] $^+$ ; 2D HSQCT (DMSO- $d_6$ ) 1-*O*-ester 14a:  $^1\text{H}$  NMR  $\delta_{\text{ppm}}$  (500.13 MHz): 3.05 ( $\alpha$ -CH), 3.40 (H-1 $\alpha$ ), 4.85 (H-2 $\beta$ ), 3.85 (H-3 $\alpha$ ), 3.30 (H-6 $\alpha$ );  $^{13}\text{C}$  NMR  $\delta_{\text{ppm}}$  (125 MHz): 52.0 ( $\alpha$ -CH), 175.0 (CO), 63.5 (C-1 $\alpha$ ), 102.4 (C-2 $\beta$ ), 70.8 (C-3 $\alpha$ ), 62.8 (C-6 $\alpha$ ); 6-*O*-ester 14b:  $^1\text{H}$  NMR  $\delta_{\text{ppm}}$  (500.13 MHz): 3.75 (H-3 $\alpha$ ), 3.60 (H-3 $\beta$ ), 3.30 (H-6 $\alpha$ );  $^{13}\text{C}$  NMR  $\delta_{\text{ppm}}$  (125 MHz): 81.6 (C-3 $\alpha$ ), 82.6 (C-3 $\beta$ ), 63.6 (C-6 $\alpha$ ); 1,6-di-*O*-ester 14c:  $^1\text{H}$  NMR  $\delta_{\text{ppm}}$  (500.13 MHz): 2.95 ( $\alpha$ -CH), 3.12 (H-1 $\alpha$ ), 3.38 (H-2 $\alpha$ ), 3.36 (H-2 $\beta$ ), 3.55 (H-6 $\beta$ );  $^{13}\text{C}$  NMR  $\delta_{\text{ppm}}$  (125 MHz): 51.5 ( $\alpha$ -CH), 63.6 (C-1 $\alpha$ ), 76.4 (C-2 $\alpha$ ), 76.5 (C-2 $\beta$ ).

### 2.5.6. L-Alanyl-D-arabinose 15

UV ( $\text{H}_2\text{O}$ ,  $\lambda_{\text{max}}$ ): 226.0 nm ( $\sigma \rightarrow \sigma^*$   $\epsilon_{226.0}$ , 1584.9 M $^{-1}$ ), 276.0 nm ( $n \rightarrow \pi^*$   $\epsilon_{276.0}$ , 933.3 M $^{-1}$ ); IR (stretching frequency): 3397 cm $^{-1}$  (NH), 3443 cm $^{-1}$  (OH), 2940 cm $^{-1}$  (CH), 1629 cm $^{-1}$  (CO); optical rotation ( $c$  0.5, H $_2$ O):  $[\alpha]_D$  at 25 °C = +34.0°; mass, 219 [M - 2] $^+$  and 293 [M + 1] $^+$ ; 2D HSQCT (DMSO- $d_6$ ) 2-*O*-ester 15a:  $^1\text{H}$  NMR  $\delta_{\text{ppm}}$  (500.13 MHz): 3.15 ( $\alpha$ -CH), 1.22 ( $\beta$ -CH $_3$ ), 5.0 (H-1 $\alpha$ ), 4.93 (H-1 $\beta$ ), 3.60 (H-2 $\alpha$ ), 3.15 (H-3 $\alpha$ ), 3.35 (H-5 $\alpha$ );  $^{13}\text{C}$  NMR  $\delta_{\text{ppm}}$  (125 MHz): 48.2 ( $\alpha$ -CH), 17.2 ( $\beta$ -CH $_3$ ), 172.5 (CO), 96.0 (C-1 $\alpha$ ), 102.0 (C-1 $\beta$ ), 77.8 (C-2 $\alpha$ ), 72.0 (C-3 $\alpha$ ), 63.5 (C-5 $\alpha$ ); 5-*O*-ester 15b:  $^1\text{H}$  NMR  $\delta_{\text{ppm}}$  (500.13 MHz): 3.92 ( $\alpha$ -CH), 1.20 ( $\beta$ -CH $_3$ ), 4.30 (H-1 $\alpha$ ), 4.18 (H-1 $\beta$ ), 3.35 (H-2 $\alpha$ ), 3.25 (H-3 $\alpha$ ), 3.60 (H-4 $\alpha$ ), 3.60 (H-5 $\alpha$ );  $^{13}\text{C}$  NMR  $\delta_{\text{ppm}}$  (125 MHz): 48.2 ( $\alpha$ -CH), 16.0 ( $\beta$ -CH $_3$ ), 97.1 (C-1 $\alpha$ ), 104.0 (C-1 $\beta$ ), 72.9 (C-2 $\alpha$ ), 72.0 (C-3 $\alpha$ ), 67.8 (C-4 $\alpha$ ), 65.1 (C-5 $\alpha$ ); 2,5-di-*O*-ester 15c:  $^1\text{H}$  NMR  $\delta_{\text{ppm}}$  (500.13 MHz): 1.30 ( $\beta$ -CH $_3$ ), 3.45 (H-2 $\alpha$ ), 3.30 (H-5 $\alpha$ );  $^{13}\text{C}$  NMR  $\delta_{\text{ppm}}$  (125 MHz): 17.2 ( $\beta$ -CH $_3$ ), 76.9 (C-2 $\alpha$ ), 65.1 (C-5 $\alpha$ ).

### 2.5.7. L-Alanyl-D-ribose 16

UV ( $\text{H}_2\text{O}$ ,  $\lambda_{\text{max}}$ ): 224.0 nm ( $\sigma \rightarrow \sigma^*$   $\epsilon_{224.0}$ , 3801.9 M $^{-1}$ ), 294.0 nm ( $n \rightarrow \pi^*$   $\epsilon_{294.0}$ , 1288.2 M $^{-1}$ ); IR (stretching frequency): 3402 cm $^{-1}$  (NH), 3242 cm $^{-1}$  (OH), 2887 cm $^{-1}$  (CH), 1625 cm $^{-1}$  (CO); optical rotation ( $c$  0.5, H $_2$ O):  $[\alpha]_D$  at 25 °C = +22.0°; mass, 221 [M] $^+$ ; ACE activity: IC $_{50}$  value = 2.7  $\pm$  0.3 mM; 2D HSQCT (DMSO- $d_6$ ) 3-*O*-ester 16a:  $^1\text{H}$  NMR  $\delta_{\text{ppm}}$  (500.13 MHz): 1.25 ( $\alpha$ -CH), 3.12 ( $\beta$ -CH $_3$ ), 3.50 (H-2 $\alpha$ ), 3.67 (H-3 $\alpha$ ), 3.63 (H-4 $\alpha$ ), 3.64 (H-5 $\alpha$ );  $^{13}\text{C}$  NMR  $\delta_{\text{ppm}}$  (125 MHz): 48.2 ( $\alpha$ -CH), 15.9 ( $\beta$ -CH $_3$ ), 67.2 (C-2 $\alpha$ ), 75.7 (C-3 $\alpha$ ), 68.1 (C-4 $\alpha$ ), 60.6 (C-5 $\alpha$ ); 5-*O*-ester 16b:  $^1\text{H}$  NMR  $\delta_{\text{ppm}}$  (500.13 MHz): 3.39 ( $\alpha$ -CH), 1.25 ( $\beta$ -CH $_3$ ), 4.95 (H-1 $\alpha$ ), 4.20 (H-1 $\beta$ ), 3.27 (H-3 $\alpha$ ), 3.88 (H-4 $\alpha$ ), 3.61 (H-5 $\alpha$ );  $^{13}\text{C}$  NMR  $\delta_{\text{ppm}}$  (125 MHz): 53.0 ( $\alpha$ -CH), 18.5 ( $\beta$ -CH $_3$ ), 173.5 (CO),

Table 1  
Effect of lipase concentration on the synthesis of L-alanyl-D-glucose<sup>a</sup>

Lipase concentration (%, w/w D-glucose)	Yield (%) (mmol)		
	<i>Rhizomucor miehei</i> lipase (RML) <sup>b</sup>	Porcine pancreas lipase (PPL) <sup>c</sup>	<i>Rhizomucor miehei</i> lipase (RML) <sup>d</sup>
10	2 (0.04)	14 (0.27)	7 (0.14)
20	1 (0.02)	15 (0.29)	10 (0.21)
30	3 (0.05)	17 (0.35)	26 (0.53)
40	9 (0.17)	18 (0.36)	30 (0.60)
50	18 (0.37)	15 (0.29)	22 (0.44)

<sup>a</sup> Conversion yields from HPLC determined with respect to L-alanine. Error in yield measurements will be  $\pm 10$ –15%. This applies to all the yields given in the subsequent tables also. D-Glucose, 1 mmol and L-alanine, 2 mmol.

<sup>b</sup> Solvent—CHCl<sub>3</sub>:hexane:DMF (v/v/v, 45:45:10) at 60 °C.

<sup>c</sup> Solvent—CH<sub>2</sub>Cl<sub>2</sub>:DMF (v/v, 90:10) at 40 °C.

<sup>d</sup> Carried out in presence of buffer with 100 ml of solvent system b containing 0.1 mM (0.1 ml) acetate buffer pH 4.0.

101.6 (C-1 $\alpha$ ), 103.9 (C-1 $\beta$ ), 75.0 (C-3 $\alpha$ ), 71.0 (C-4 $\alpha$ ), 63.4 (C-5 $\alpha$ ); 3,5-di-O-ester 16c: <sup>1</sup>H NMR  $\delta_{\text{ppm}}$  (500.13 MHz): 1.20 ( $\beta$ -CH<sub>3</sub>), 3.45 (H-3 $\alpha$ ), 3.79 (H-4 $\alpha$ ), 3.52 (H-5 $\alpha$ ); <sup>13</sup>C NMR  $\delta_{\text{ppm}}$  (125 MHz): 18.5 ( $\beta$ -CH<sub>3</sub>), 74.9 (C-3 $\alpha$ ), 63.4 (C-5 $\alpha$ ).

#### 2.5.8. L-Alanyl-lactose 17

UV (H<sub>2</sub>O,  $\lambda_{\text{max}}$ ): 220.0 nm ( $\sigma \rightarrow \sigma^*$   $\epsilon_{220.0}$ , 436.5 M<sup>-1</sup>), 294.0 nm ( $n \rightarrow \pi^*$   $\epsilon_{294.0}$ , 239.9 M<sup>-1</sup>); IR (stretching frequency): 3378 cm<sup>-1</sup> (NH), 3378 cm<sup>-1</sup> (OH), 2946 cm<sup>-1</sup> (CH), 1624 cm<sup>-1</sup> (CO); optical rotation (*c* 0.5, H<sub>2</sub>O):  $[\alpha]_{\text{D}}$  at 25 °C = +7.4°; mass, 436 [M + Na]<sup>+</sup>; ACE activity: IC<sub>50</sub> value = 2.0  $\pm$  0.2 mM; 2D HSQCT (DMSO-d<sub>6</sub>) 6-O-ester 17a: <sup>1</sup>H NMR  $\delta_{\text{ppm}}$  (500.13 MHz): 3.55 ( $\alpha$ -CH), 1.25 ( $\beta$ -CH<sub>3</sub>), 4.78 (H-1 $\alpha$ ), 4.82 (H-1 $\beta$ ), 2.95 (H-2 $\alpha$ ), 3.25 (H-2 $\beta$ ), 2.95 (H-3 $\alpha$ ), 4.05 (H-4 $\alpha,\beta$ ), 3.15 (H-5 $\alpha$ ), 3.35 (H-5 $\beta$ ), 3.80 (H-6 $\alpha,\beta$ ), 4.90 (H'-1 $\beta$ ), 3.90 (H'-2), 2.85 (H'-3), 3.70 (H'-4), 3.60 (H'-5), 3.40 (H'-6); <sup>13</sup>C NMR  $\delta_{\text{ppm}}$  (125 MHz): 51.0 ( $\alpha$ -CH), 15.5 ( $\beta$ -CH<sub>3</sub>), 173.0 (CO), 98.0 (C-1 $\alpha$ ), 100.2 (C-1 $\beta$ ), 70.3 (C-2 $\alpha$ ), 72.4 (C-2 $\beta$ ), 74.3 (C-3 $\alpha$ ), 81.0 (C-4 $\alpha,\beta$ ), 73.3 (C-5 $\alpha$ ), 73.4 (C-5 $\beta$ ), 61.2 (C-6 $\alpha,\beta$ ), 100.2 (C'-1 $\beta$ ), 76.5 (C'-2), 75.1 (C'-3), 68.5 (C'-4), 78.5 (C'-5), 60.6 (C'-6), 6'-O-ester 17b: <sup>1</sup>H NMR  $\delta_{\text{ppm}}$  (500.13 MHz): 3.35 ( $\alpha$ -CH), 3.85 (H-4 $\alpha$ ), 3.70 (H'-6); <sup>13</sup>C NMR  $\delta_{\text{ppm}}$  (125 MHz): 53.5 ( $\alpha$ -CH), 81.5 (C-4 $\alpha$ ), 64.0 (C'-6), 6,6'-di-O-ester 17c: <sup>1</sup>H NMR  $\delta_{\text{ppm}}$  (500.13 MHz): 3.85 (H'-6); <sup>13</sup>C NMR  $\delta_{\text{ppm}}$  (125 MHz): 67.5 (C'-6).

#### 2.5.9. L-Alanyl-maltose 18

UV (H<sub>2</sub>O,  $\lambda_{\text{max}}$ ): 228.0 nm ( $\sigma \rightarrow \sigma^*$   $\epsilon_{228.0}$ , 114.8 M<sup>-1</sup>), 294.0 nm ( $n \rightarrow \pi^*$   $\epsilon_{294.0}$ , 56.2 M<sup>-1</sup>); IR (stretching frequency): 3283 cm<sup>-1</sup> (NH), 3380 cm<sup>-1</sup> (OH), 2937 cm<sup>-1</sup> (CH), 1626 cm<sup>-1</sup> (CO); optical rotation (*c* 0.5, H<sub>2</sub>O):  $[\alpha]_{\text{D}}$  at 25 °C = +84.0°; mass, 436 [M + Na]<sup>+</sup>; 2D HSQCT (DMSO-d<sub>6</sub>) 6-O-ester 18a: <sup>1</sup>H NMR  $\delta_{\text{ppm}}$  (500.13 MHz): 3.55 ( $\alpha$ -CH), 1.25 ( $\beta$ -CH<sub>3</sub>), 4.80 (H-1 $\alpha$ ), 4.20 (H-1 $\beta$ ), 4.05 (H-2 $\alpha,\beta$ ), 3.30 (H-3 $\alpha$ ), 3.85 (H-4 $\alpha,\beta$ ), 3.65 (H-5 $\alpha,\beta$ ), 3.50 (H-6 $\alpha,\beta$ ), 4.90 (H'-1 $\alpha$ ), 2.95 (H'-2), 3.10 (H'-3), 3.50 (H'-4), 3.60 (H'-5), 3.60 (H'-6); <sup>13</sup>C NMR  $\delta_{\text{ppm}}$  (125 MHz): 50.0 ( $\alpha$ -CH), 175.5 (CO), 92.0 (C-1 $\alpha$ ), 96.7 (C-1 $\beta$ ), 79.7 (C-2 $\alpha,\beta$ ), 76.4 (C-3 $\alpha$ ), 81.5 (C-4 $\alpha,\beta$ ), 77.2 (C-5 $\alpha,\beta$ ), 67.5 (C-6 $\alpha,\beta$ ), 100.7 (C'-1 $\alpha$ ), 70.3 (C'-2), 71.8 (C'-3), 69.9 (C'-4), 72.4 (C'-5), 60.6 (C'-6), 6'-O-ester 18b: <sup>1</sup>H NMR  $\delta_{\text{ppm}}$  (500.13 MHz): 3.35 ( $\alpha$ -CH), 3.95 (H'-6); <sup>13</sup>C NMR  $\delta_{\text{ppm}}$  (125 MHz): 53.0 ( $\alpha$ -CH), 67.0 (C'-6 $\alpha$ ); 6,6'-di-O-ester 18c: <sup>1</sup>H NMR  $\delta_{\text{ppm}}$  (500.13 MHz): 3.75 (H'-6); <sup>13</sup>C NMR  $\delta_{\text{ppm}}$  (125 MHz): 63.0 (C'-6).

#### 2.5.10. L-Alanyl-sucrose 19

UV (H<sub>2</sub>O,  $\lambda_{\text{max}}$ ): 224.0 nm ( $\sigma \rightarrow \sigma^*$   $\epsilon_{224.0}$ , 2344.2 M<sup>-1</sup>), 294.0 nm ( $n \rightarrow \pi^*$   $\epsilon_{294.0}$ , 1288.2 M<sup>-1</sup>); IR (stretching frequency): 3100 cm<sup>-1</sup> (NH), 3319 cm<sup>-1</sup> (OH), 2958 cm<sup>-1</sup> (CH), 1625 cm<sup>-1</sup> (CO); optical rotation (*c* 0.5, H<sub>2</sub>O):  $[\alpha]_{\text{D}}$  at 25 °C = -17.4°; mass, 436 [M + Na]<sup>+</sup>; 2D HSQCT (DMSO-d<sub>6</sub>) 6-O-ester 19: <sup>1</sup>H NMR  $\delta_{\text{ppm}}$  (500.13 MHz): 3.59 ( $\alpha$ -CH), 1.30 ( $\beta$ -CH<sub>3</sub>), 3.41 (H-1 $\beta$ ), 3.79 (H-3 $\beta$ ), 3.54 (H-4 $\beta$ ), 3.47 (H-5 $\beta$ ), 3.67 (H-6 $\beta$ ), 4.35 (H'-1 $\alpha$ ), 3.31 (H'-2), 3.45 (H'-3), 3.31 (H'-4), 3.58 (H'-5), 3.54 (H'-6); <sup>13</sup>C NMR  $\delta_{\text{ppm}}$  (125 MHz): 49.5 ( $\alpha$ -CH), 18.0 ( $\beta$ -CH<sub>3</sub>), 172.0 (CO), 64.0 (C-1 $\beta$ ), 104.2 (C-2 $\beta$ ), 77.33 (C-3 $\beta$ ), 82.71 (C-4 $\beta$ ), 74.5 (C-5 $\beta$ ), 67.0 (C-6 $\beta$ ), 96.0 (C'-1 $\alpha$ ), 71.0 (C'-2), 75.5 (C'-3), 71.0 (C'-4), 74.0 (C'-5), 60.71 (C'-6).

## 3. Results

### 3.1. L-Alanyl-D-glucose

The esterification reaction between unprotected and unactivated L-alanine and D-glucose was studied in detail using RML and PPL.

#### 3.1.1. Reaction profile

In presence of RML, the conversion yields showed an increase in esterification from 15% at 24 h to 26% at 72 h and thereafter remained constant up to 120 h at 26%. From the initial slope value of the plot, the rate of esterification was found to be 0.004 mmol h<sup>-1</sup>.

#### 3.1.2. Effect of lipase concentration

In case of RML (Table 1), maximum esterification (18%) was achieved at 50% (w/w) D-glucose (1 mmol D-glucose and 2 mmol L-alanine for incubation up to 72 h). In case of PPL (Table 1), maximum yield of 18% was achieved at 40% (w/w) D-glucose (1 mmol D-glucose and 2 mmol L-alanine for a incubation period of 72 h). In presence of 0.1 mM (0.1 ml) pH 4.0 acetate buffer, RML at 40% (w/w) D-glucose showed (Table 1) a maximum esterification of 30% (for 1 mmol D-glucose and 2 mmol L-alanine for incubation up to 72 h). While lesser amounts of enzymes ( $\leq 20\%$  RML and PPL employed) could be inhibited by L-alanine (2 mmol) and D-glucose (1 mmol),  $>30\%$  RML and PPL could favour better conversion as the enzyme/substrate ratio is enhanced at  $>30\%$  enzyme concentration for the L-alanine and D-glucose employed.

#### 3.1.3. Effect of buffer salts

Carrying out this esterification reaction in presence of buffers of certain pH not only imparted 'pH memory' to the enzyme, but also provided the optimum water activity necessary for better performance of the enzyme. Besides, addition of buffer salts of certain concentration also affected ionic activities of especially the microaqueous layer around the enzyme, where the buffer salts are concentrated during the course of the reaction. All these have been found to be operative in these esterification reactions.

Table 2  
Effect of buffer salts (pH and buffer concentration) on the synthesis of L-alanyl-D-glucose<sup>a</sup>

RML				PPL			
pH <sup>b</sup>	Yield (%) (mmol)	pH 4.0 <sup>c</sup> concentration (Mm)	Yield (%) (mmol)	pH <sup>d</sup>	Yield (%) (mmol)	pH 5.0 <sup>e</sup> concentration (mM)	Yield (%) (mmol)
4.0	26 (0.53)	0.05	25 (0.49)	4.0	9 (0.18)	0.05	13 (0.25)
5.0	7 (0.13)	0.1	26 (0.53)	5.0	17 (0.33)	0.1	17 (0.33)
6.0	20 (0.39)	0.2	8 (0.16)	6.0	15 (0.31)	0.2	11 (0.23)
7.0	8 (0.16)	0.3	7 (0.15)	7.0	11 (0.23)	0.3	10 (0.21)
8.0	10 (0.19)	0.4	17 (0.34)	8.0	No yield	0.4	12 (0.24)
–	–	0.5	18 (0.35)	–	–	0.5	17 (0.34)

<sup>a</sup> D-Glucose, 1 mmol and L-alanine, 2 mmol; incubation period, 72 h; RML, 30% (w/w of D-glucose); PPL, 40% (w/w of D-glucose). One hundred millilitres of the solvent containing specified volumes, concentration and pH of the buffer.

<sup>b</sup> Solvent—100 ml CHCl<sub>3</sub>:hexane:DMF (v/v/v, 45:45:10) at 60 °C. Buffer, 0.1 mM (0.1 ml) of 0.1 M appropriate pH buffer.

<sup>c</sup> Solvent—100 ml CH<sub>2</sub>Cl<sub>2</sub>:DMF (v/v, 90:10) at 40 °C. Buffer, 0.05–0.5 ml of 0.1 M acetate pH 4.0.

<sup>d</sup> Same solvent system as c. Buffer, 0.1 mM (0.1 ml) of 0.1 M appropriate pH.

<sup>e</sup> Solvent—same solvent system as c. 0.05–0.5 ml of 0.1 M acetate pH 5.0.

In presence of buffer salts, conversion yield increased in case of RML. In presence of 0.1 mM (0.1 ml) pH 4.0 buffer, RML showed maximum esterification of 26% (at 1 mmol D-glucose and 2 mmol L-alanine for a period of 72 h, Table 2). However, PPL, in presence of 0.1 mM (0.1 ml) pH 5.0 buffer showed maximum esterification of 17% only (Table 2), similar to the conversion yield obtained in the absence of buffer salts.

The effect of buffer salt concentration was studied by using different concentrations (0.05–0.5 mM) of pH 4.0 buffer in case of RML and pH 5.0 buffer in case of PPL. In case of RML, the maximum conversion yield of 26% (at 1 mmol D-glucose and 2 mmol L-alanine for 72 h) was obtained when 0.1 mM (0.1 ml) pH 4.0 buffer was employed (Table 2). In case of PPL, 0.5 mM (0.5 ml) pH 5.0 buffer showed the maximum conversion yield (Table 2) of 17% (at 1 mmol D-glucose and 2 mmol L-alanine for 72 h incubation).

By imparting 'pH memory', the catalytic activity of the lyophilized subtilisin Carlsberg in the pH range 5–11, in organic solvents like acetonitrile and 3-pentanone was reported to be enhanced [22]. The enzymatic activity of subtilisin cross-linked crystals in anhydrous 3-pentanone was accelerated by the addition of organic soluble (a mixture of a suitable acid and sodium salt) buffers [22]. The enantioselectivity of *Candida antarctica* lipase B in organic media was increased by 'pH tuning' of the enzyme by the addition of certain buffer salts which altered the protonation state of the enzyme and selectively tuned enantioselectivity and catalytic activity [23]. Similarly, the present work also showed enhanced activity of RML in presence of buffer salts. However, buffer salts did not enhance esterification with PPL.

#### 3.1.4. Effect of substrate concentration

When L-alanine was varied from 1 to 5 mmol at a constant 1 mmol D-glucose, there was in general, an increase in esterification (Fig. 1) from 0.68 mmol (68% with respect to 1 mmol L-alanine—0.54 mmol monoesters and 0.14 mmol diesters) to 1.12 mmol (28% with respect to 4 mmol L-alanine—0.88 mmol monoesters and 0.24 mmol diesters) in presence of 0.1 mM

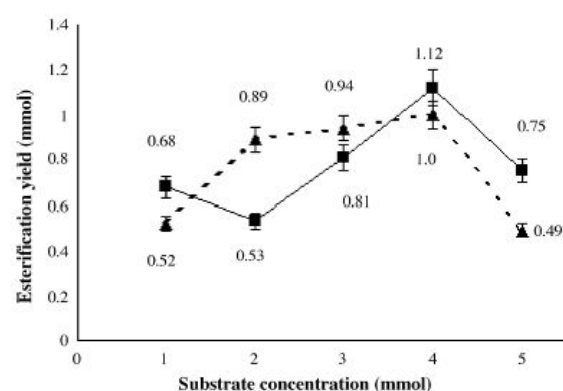


Fig. 1. Effect of substrate concentration on esterification. RML, 30% (w/w D-glucose); solvent, CH<sub>2</sub>Cl<sub>2</sub>:DMF (v/v, 90:10) at 40 °C; buffer, 0.1 mM (0.1 ml) pH 4.0 acetate buffer. L-Alanine (■) 1–5 mmol at 1 mmol D-glucose; D-glucose (▲) 1–5 mmol at 1 mmol L-alanine and a constant enzyme concentration of 54 mg.

(0.1 ml) pH 4.0 buffer for 72 h incubation. The yields were determined with respect to L-alanine concentrations which were usually greater than that of D-glucose (1 mmol). In terms of D-glucose, one D-glucose molecule forms mono as well as diesters with L-alanine. Hence, in presence of higher equivalents of L-alanine, yields >1 mmol (D-glucose concentration) are reported. Similarly, when D-glucose was varied from 1 to 5 mmol, at a constant 1 mmol L-alanine, there was a steep increase in esterification from 52% (0.52–0.41 mmol monoesters and 0.11 mmol diesters) at 1 mmol D-glucose to >99% (>0.99–0.78 mmol monoesters and 0.21 mmol diesters) at 4 mmol D-glucose. In both the cases, esterification decreased after 4 equiv. which could be due to inhibition at higher concentrations of L-alanine and D-glucose.

#### 3.1.5. Reusability of lipases

Reusability of both RML and PPL employed were studied at optimized conditions. After completion of each reaction

Table 3  
Reusability of lipase in presence and absence of buffer salts<sup>a</sup>

Number of reactions (cycles)	RML		PPL	
	Yield (%) (total enzyme activity, $\mu\text{mol}/\text{min}$ )	Yield <sup>b</sup> (%) (total enzyme activity, $\mu\text{mol}/\text{min}$ )	Yield (%) (total enzyme activity, $\mu\text{mol}/\text{min}$ )	Yield <sup>c</sup> (%) (total enzyme activity, $\mu\text{mol}/\text{min}$ )
1	24 (99.4)	17 (99.4)	19 (15)	11 (15)
2	17 (66.4)	11 (66.9)	12 (5.6)	6 (4.1)
3	10 (43.1)	8 (42.2)	10 (3.3)	–
4	8 (23.5)	5 (24.6)	3 (0.7)	–

<sup>a</sup> D-glucose, 4 mmol and L-alanine, 8 mmol; incubation period, 72 h; Solvent—100 ml  $\text{CH}_2\text{Cl}_2$ :DMF (v/v, 90:10) at 40 °C. Total enzyme activity of the recovered enzyme employed for the reaction. Percentage yields are an average from two independent experiments.

<sup>b</sup> In presence of 0.2 mM (0.2 ml) of 0.1 M acetate buffer pH 4.0 in each cycle.

<sup>c</sup> In presence of 0.2 mM (0.2 ml) of 0.1 M acetate buffer pH 5.0 in each cycle.

(cycle, 72 h), the enzyme was separated from the reaction mixture by filtration, air dried and reused in the next reaction. After each cycle, total esterification activity ( $\mu\text{mol}/\text{min}$ ) of the enzyme was determined. In case of RML, there was a steady loss of 15–22% of enzyme concentration after each cycle both in presence as well as absence of 0.2 mM (0.2 ml) buffer pH 4.0 (Table 3). In the absence of buffer salts, the esterification activity decreased from 24% (1st cycle: total enzyme activity, 99.4  $\mu\text{mol}/\text{min}$ ) to 8% (4th cycle: total enzyme activity, 23.5  $\mu\text{mol}/\text{min}$ ). The yields in 2nd and 3rd cycles were 17% (total enzyme activity, 66.4  $\mu\text{mol}/\text{min}$ ) and 10% (total enzyme activity, 43.1  $\mu\text{mol}/\text{min}$ ), respectively. In presence of buffer salts (pH 4.0), the esterification activity decreased from 17% (1st cycle: total enzyme activity, 99.4  $\mu\text{mol}/\text{min}$ ) to 5% (4th cycle: enzyme activity of 23  $\mu\text{mol}/\text{min}$ ). The yields in 2nd and 3rd cycles were 11% (total enzyme activity, 66.9  $\mu\text{mol}/\text{min}$ ) and 8% (total enzyme activity, 42.2  $\mu\text{mol}/\text{min}$ ), respectively. However, in case of PPL, there was a drastic loss of enzyme concentration from 20% to 60% after each cycle, as PPL was partially soluble in water and the reaction was stopped after the 2nd cycle due to reduction in enzyme (Table 3). In the absence of buffer salts, esterification activity of the PPL decreased from 19% (1st cycle: total enzyme activity, 15  $\mu\text{mol}/\text{min}$ ) to 3% (4th cycle: total enzyme activity, 0.7  $\mu\text{mol}/\text{min}$ ). The 2nd and 3rd cycle yields were 12% (total enzyme activity, 5.6  $\mu\text{mol}/\text{min}$ ) and 10% (total enzyme activity, 3.3  $\mu\text{mol}/\text{min}$ ), respectively. However, in presence of buffer salts (pH 5.0), the esterification activity decreased slightly from 11% (1st cycle: total enzyme activity, 15  $\mu\text{mol}/\text{min}$ ) to 6% (2nd cycle: total enzyme activity, 4.1  $\mu\text{mol}/\text{min}$ ).

### 3.2. L-Alanyl esters of carbohydrates

L-Alanyl esters of different carbohydrates like aldohexoses (D-glucose **2**, D-galactose **3** and D-mannose **4**), ketohexose (D-fructose **5**), pentoses (D-arabinose **6** and D-ribose **7**) and disaccharides (lactose **8**, maltose **9** and sucrose **10**) were synthesized by refluxing the reaction mixture consisting of 2 mmol L-alanine (**1**), 1 mmol carbohydrate at 40% RML (w/w of carbohydrate **2–10**) in presence of 0.1 mM (0.1 ml) pH 4.0 buffer in  $\text{CH}_2\text{Cl}_2$ :DMF (v/v, 90:10) for a period of 72 h. The esters were isolated and characterised as described in Section 2.3.

### 3.3. Spectral characterization of L-alanyl esters of carbohydrates

The isolated esters were characterized by UV, IR, MS and 2D NMR spectroscopic studies (data in Section 2.5). Infra red spectral data showed that the ester carbonyl stretching frequency for the prepared esters were in the range 1606–1653  $\text{cm}^{-1}$  compared to 1715  $\text{cm}^{-1}$  observed for free L-alanine indicating that L-alanine carboxylic group had been converted into its corresponding carbohydrate ester.

Two-dimensional HSQCT NMR spectroscopy of the L-alanyl esters of carbohydrates prepared by using RML gave good information on the nature and proportion of esters formed (Table 4). In case of L-alanyl-D-glucose (**11**) three monoesters (2-O-, 3-O- and 6-O-) and two diesters (2,6-di-O- and 3,6-di-O-) were found to be formed with only  $\beta$ -anomer of D-glucose, the D-glucose employed being a 40:60 mixture of  $\alpha$ - and  $\beta$ -anomers, respectively. The down field chemical shift values for C1 at 102.6 (2-O-ester), 101.8 (6-O-ester) and 100.8 (2,6-di-O-ester) clearly indicated that only  $\beta$ -D-glucose was esterified. The chemical shift values for C-2 $\beta$  at 82.6 ppm and the corresponding H-2 $\beta$  cross-peak at 3.62 ppm indicated the formation of 2-O-ester, C-3 $\beta$  at 83.3 ppm (H-3 $\beta$  at 3.93 ppm) indicated the formation of 3-O-ester, C-6 $\beta$  at 63.5 ppm (H-6 $\beta$  at 3.82 ppm) indicated the formation of 6-O-ester, C-6 $\beta$  at 62.7 ppm (H-6 $\beta$  at 3.47 ppm) and C-2 $\beta$  at 76.5 ppm (H-2 $\beta$  at 3.78 ppm) indicated the formation of 2,6-di-O-ester and the chemical shift values for C-6 $\beta$  at 63.1 ppm (H-6 $\beta$  at 3.82 ppm) and C-3 $\beta$  at 81.6 ppm (H-3 $\beta$  at 3.78 ppm) indicated the formation of 3,6-di-O-ester. In case of L-alanyl-D-galactose (**12**), three diastereomeric monoesters (2-O-, 3-O- and 6-O-) only were found to be formed. The down field chemical shift values for C-2 $\alpha$  at 76.4 ppm (H-2 $\alpha$  at 3.38 ppm) and C-2 $\beta$  at 76.5 ppm (H-2 $\beta$  at 3.36 ppm) indicated the formation of 2-O-ester, C-3 $\alpha$  at 81.6 ppm (H-3 $\alpha$  at 3.75 ppm) and C-3 $\beta$  at 82.6 ppm (H-3 $\beta$  at 3.60 ppm) indicated the formation of 3-O-ester and C-6 $\alpha$  at 63.1 ppm (H-6 $\alpha$  at 3.30 ppm) indicated the formation of 6-O-ester. In case of L-alanyl-D-mannose (**13**), five diastereomeric esters (three monoesters—3-O-, 4-O- and 6-O- and two diesters—3,6-di-O- and 4,6-di-O-) were found to be formed. The chemical shift values for C-3 $\alpha$  at 89.2 ppm indicated the formation of 3-O-ester, C-4 $\beta$  at 75.32 ppm indicated the formation of 4-O-ester, C-6 $\alpha$  at 63.1 ppm indicated the for-

Table 4  
 Synthesis of L-alanyl esters of aldohexoses, ketohexose, pentoses and disaccharides<sup>a</sup>

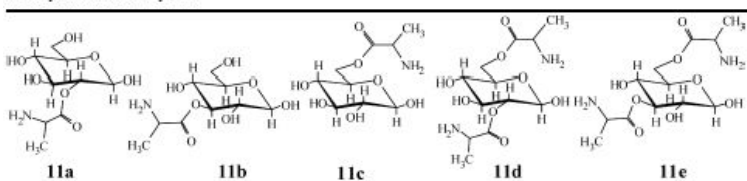
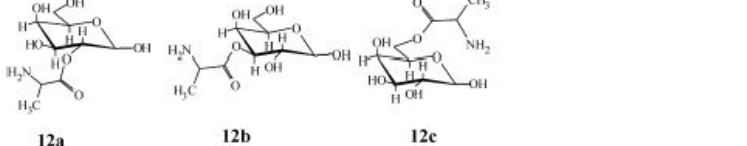
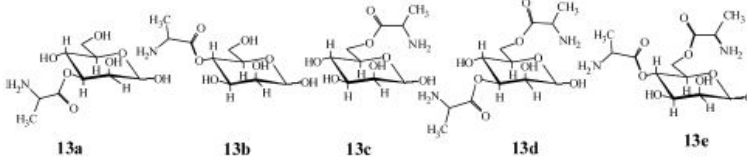
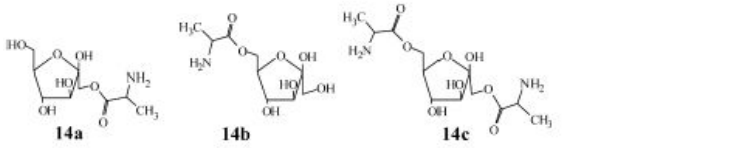
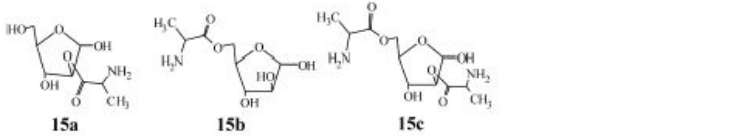
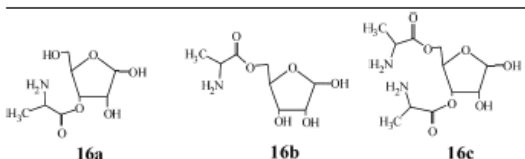
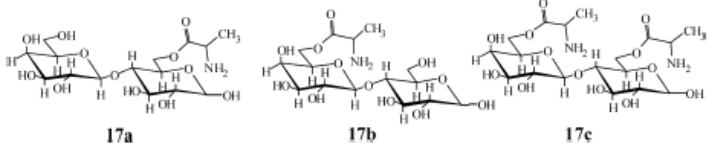
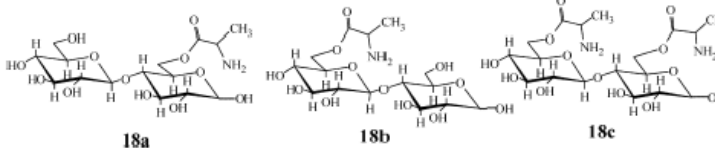
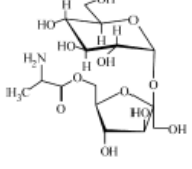
L-Alanyl esters of carbohydrates	Esterification yield (%)	Esters (% proportions) <sup>b</sup>
 <p><b>11a</b>      <b>11b</b>      <b>11c</b>      <b>11d</b>      <b>11e</b></p>	30 (monoesters, 2, diesters, 6)	11a: 2- <i>O</i> -L-alanyl-β-D-glucose (47) 11b: 3- <i>O</i> -L-alanyl-β-D-glucose (12) 11c: 6- <i>O</i> -L-alanyl-β-D-glucose (20) 11d: 2,6-di- <i>O</i> -L-alanyl-β-D-glucose (15) 11e: 3,6-di- <i>O</i> -L-alanyl-β-D-glucose (6)
 <p><b>12a</b>      <b>12b</b>      <b>12c</b></p>	21 (only monoesters)	12a: 2- <i>O</i> -L-alanyl-D-galactose (33) 12b: 3- <i>O</i> -L-alanyl-D-galactose (32) 12c: 6- <i>O</i> -L-alanyl-D-galactose (35)
 <p><b>13a</b>      <b>13b</b>      <b>13c</b>      <b>13d</b>      <b>13e</b></p>	49 (monoesters, 39, diesters, 10)	13a: 3- <i>O</i> -L-alanyl-D-mannose (25) 13b: 4- <i>O</i> -L-alanyl-D-mannose (25) 13c: 6- <i>O</i> -L-alanyl-D-mannose (30) 13d: 3,6-di- <i>O</i> -L-alanyl-D-mannose (9) 13e: 4,6-di- <i>O</i> -L-alanyl-D-mannose (11)
 <p><b>14a</b>      <b>14b</b>      <b>14c</b></p>	52 (monoesters, 35, diester, 17)	14a: 1- <i>O</i> -L-alanyl-D-fructose (34) 14b: 6- <i>O</i> -L-alanyl-D-fructose (34) 14c: 1,6-di- <i>O</i> -L-alanyl-D-fructose (32)
 <p><b>15a</b>      <b>15b</b>      <b>15c</b></p>	9 (monoesters, 6, diester, 3)	15a: 2- <i>O</i> -L-alanyl-D-arabinose (33) 15b: 5- <i>O</i> -L-alanyl-D-arabinose (34) 15c: 2,5-di- <i>O</i> -L-alanyl-D-arabinose (33)



Table 4 (Continued)

<i>L</i> -Alanyl esters of carbohydrates	Esterification yield (%)	Esters (% proportions <sup>b</sup> )
 <p><b>16a</b>                      <b>16b</b>                      <b>16c</b></p>	48 (monoesters, 23, diester, 25)	16a: 3- <i>O</i> - <i>L</i> -alanyl-D-ribose (16) 16b: 5- <i>O</i> - <i>L</i> -alanyl-D-ribose (32) 16c: 3,5-di- <i>O</i> - <i>L</i> -alanyl-D-ribose (52)
 <p><b>17a</b>                      <b>17b</b>                      <b>17c</b></p>	20 (monoesters, 14, diester, 6)	17a: 6- <i>O</i> - <i>L</i> -alanyl-lactose (34) 17b: 6'- <i>O</i> - <i>L</i> -alanyl-lactose (34) 17c: 6,6''-di- <i>O</i> - <i>L</i> -alanyl-lactose (32)
 <p><b>18a</b>                      <b>18b</b>                      <b>18c</b></p>	56 (monoesters, 38, diester, 18)	18a: 6- <i>O</i> - <i>L</i> -alanyl-maltose (34) 18b: 6'- <i>O</i> - <i>L</i> -alanyl-maltose (34) 18c: 6,6''-di- <i>O</i> - <i>L</i> -alanyl-maltose (32)
 <p><b>19</b></p>	8 (only monoester)	19: 6- <i>O</i> - <i>L</i> -alanyl-sucrose

<sup>a</sup> *L*-Alanine, 2 mmol; carbohydrates, 1 mmol; RML, 40% (w/w based on carbohydrate); buffer, 0.1 mM (0.1 ml) 0.1 M pH 4.0 acetate buffer; CH<sub>2</sub>Cl<sub>2</sub>:DMF (v/v, 90:10) at 40 °C; incubation period, 72 h. Conversion yields were from HPLC with respect to *L*-alanine concentration.

<sup>b</sup> Percentage proportions of individual esters determined from the peak areas of the <sup>13</sup>C C6, C5 (in case of pentoses) signals or from cross peaks of the 2D HSQCCT spectrum.

mation of 6-*O*-ester, and C-6 $\alpha$  at 62.8 ppm, C-3 $\alpha$  at 82.9 ppm indicated the formation of 3,6-di-*O*-ester and the chemical shift values for C-6 $\alpha$  at 62.5 ppm and C-4 $\alpha$  at 77.2 ppm indicated the formation of 4,6-di-*O*-ester. In case of L-alanyl-D-fructose (**14**), two diastereomeric monoesters (1-*O*- and 6-*O*-) and one diastereomeric diester (1,6-di-*O*-) were found to be formed. The down field chemical shift values for C-1 $\alpha$  at 63.1 ppm (H-1 $\alpha$  at 3.40 ppm) indicated the formation of 1-*O*-ester, C-6 $\alpha$  at 63.6 ppm (H-6 $\alpha$  at 3.30 ppm) indicated the formation of 6-*O*-ester and C-1, 6 $\alpha$  centered at 63.6 ppm (H-1, 6 $\alpha$  centered at 3.12 ppm) indicated the formation of 1,6-di-*O*-ester. In case of L-alanyl-D-arabinose (**15**), two diastereomeric monoesters (2-*O*- and 6-*O*-) and one diastereomeric diester (2,6-di-*O*-) were found to be formed. The chemical shift values for C-2 $\alpha$  at 77.8 ppm (H-2 $\alpha$  at 3.60 ppm) indicated the formation of 2-*O*-ester, C-5 $\alpha$  at 65.1 ppm (H-5 $\alpha$  at 3.60 ppm) indicated the formation of 5-*O*-ester and C-2 $\alpha$  at 76.9 ppm (H-2 $\alpha$  at 3.45 ppm) and C-5 $\alpha$  at 65.1 ppm (H-5 $\alpha$  at 3.30 ppm) indicated the formation of 2,5-di-*O*-ester. Both lactose and maltose showed the formation of two diastereomeric monoesters (6-*O*- and 6'-*O*-) and one diester (6,6'-di-*O*-). In case of L-alanyl-D-ribose (**16**), two diastereomeric monoesters (3-*O*- and 6-*O*-) and one diastereomeric diester (3,6-di-*O*-) were found to be formed. The chemical shift values for C-3 $\alpha$  at 75.7 ppm (H-3 $\alpha$  at 3.67 ppm) indicated the formation of 3-*O*-ester, C-5 $\alpha$  at 63.4 ppm (H-5 $\alpha$  at 3.61 ppm) indicated the formation of 5-*O*-ester and C-3 $\alpha$  at 74.9 ppm (H-3 $\alpha$  at 3.45 ppm) and C-5 $\alpha$  at 63.4 ppm (H-5 $\alpha$  at 3.52 ppm) indicated the formation of 3,5-di-*O*-ester. In case of L-alanyl-lactose (**17**), the down field chemical shift values for C-6 $\alpha,\beta$  at 61.2 ppm (H-6 $\alpha,\beta$  at 3.80 ppm) of glucose moiety indicated the formation of 6-*O*-ester, C-6' at 64.0 ppm (H-6' at 3.70 ppm) of galactose moiety indicated the formation of 6'-*O*-ester and C-6,6' centered at 67.5 ppm (H-6,6' centered at 3.85 ppm) of both galactose and glucose moieties indicated the formation of 6,6'-di-*O*-ester. In case of L-alanyl-maltose (**18**), the chemical shift values for C-6 $\alpha,\beta$  at 67.5 ppm (H-6 $\alpha,\beta$  at 3.50 ppm) of reducing end glucose moiety indicated the formation of 6-*O*-ester, C-6' at 67.0 ppm (H-6' at 3.95 ppm) of the non-reducing end glucose moiety indicated the formation of 6'-*O*-ester and C-6,6' centered at 63.0 ppm (H-6,6' centered at 3.75 ppm) of both the reducing and non-reducing end glucose moieties indicated the formation of 6,6'-di-*O*-ester. In case of L-alanyl-sucrose (**19**), only one monoester (6-*O*-) was formed. This was confirmed by the chemical shift values for C-6 $\beta$  at 67.0 ppm (H-6 $\beta$  at 3.67 ppm) of the fructose moiety. In all these esters, shifts in L-alanyl signals,  $\alpha$ -CH and  $\beta$ -CH<sub>3</sub>, also indicated esterification of L-alanine clearly.

#### 4. Discussion

The optimum conditions determined for this esterification reaction by studying the effect of variables like incubation period, enzyme and substrate concentration, pH and buffer concentration clearly explain the behaviour of the lipases. Most of the effects show that esterification increases upto a certain point, and thereafter they remain as such or decrease a little. This complex esterification reaction is not controlled by kinetic factors or thermodynamic factors or water activity alone.

Use of lower enzyme concentrations did not result in thermodynamic yields. The thermodynamic binding equilibria regulates the concentrations of the unbound substrates at different enzyme and substrate concentrations and thereby conversion as the reaction proceeds with time. At lesser enzyme concentrations, for a given amount of substrates (enzyme/substrate ratio low), rapid exchange between bound and unbound forms of both the substrates with the enzyme (on a weighted average based on binding constant values of both the substrates) leaves substantial number of unbound substrate molecules at the start of the reaction and they decrease progressively as conversion takes place [27,28]. This becomes more so, if one of them binds more firmly to the enzyme than the other (higher binding constant value) as the respective enzyme/substrate ratios keep changing (during the course of the reaction) unevenly till the conversion stops due to total predominant binding (inhibition). At intermediary enzyme concentrations, such a competitive binding results in a favourable proportions of bound and unbound substrates to effect quite a good conversion. At higher enzyme concentrations, most of the substrates would be in the bound form leading to inhibition and lesser conversion (higher enzyme/substrate ratios). Also, the esterification reaction requires larger amount of enzyme compared to hydrolysis. While this leads to lesser selectivity, they also give rise to varying bound and unbound substrate concentrations till the conversion ends. For a given amount of enzyme and substrates there is no increase in conversion beyond 72–120 h. Longer incubation periods of especially lesser enzyme concentrations could also result in partial enzyme inactivation as shown in Table 3. However, not all the enzyme are inactivated before the end of the reaction.

Besides imparting 'pH memory', added water is essential for the integrity of the three-dimensional structure of the enzyme molecule and therefore its activity [1]. Zaks and Klivanov [29] reported that at low water activities, lower the solvent polarity, the higher the enzyme activity. Beyond the critical water concentration, esterification decreases because the size of the water layer formed around the enzyme retards the transfer of acyl donor to the active site of the enzyme [30,31] and also the water layer surrounding the enzymes makes enzyme to be more flexible by forming multiple H-bonds and interacting with organic solvent causing denaturation [32]. Increase in buffer volume affected this esterification reaction significantly. It could increase the water activity of the system in the initial stages by increasing the thickness of the microaqueous layer around the enzyme. Higher volumes of the buffer in the microaqueous layer could also cause slight inactivation of the enzyme due to increase in salt concentration beyond a critical point. Partridge et al. reported that when an enzyme is suspended in a low-water organic solvent, the counter ions are in closer contact with the opposite charges on the enzyme because of the lower dielectric constant of the medium [33]. Thus, protonation of the ionizable groups on the enzyme could be controlled by the type and availability of these ions as well as hydrogen ions resulting in a 'pH memory'. The third factor is the increase in ionic strength which could play a favourable role in esterification. Optimum pH for this reaction (4.0 for RML and 5.0 for PPL) clearly indicates a slight unfavourable conformational change in the enzyme at

about pH 4.0–5.0 leading to lesser conversion beyond pH 5.0 for both the enzymes.

The experimental set-up employed in the present work is such that it maintained a low water activity ( $a_w = 0.0054$ ) due to azeotropic distillation and recycling the solvent back into the reaction system after passing through a bed of desiccant. Even the water of reaction formed could also be used to constitute the microaqueous layer around the enzyme and the excess water could be removed by azeotropic distillation. The same could occur even with the addition of added enzyme (with little water content) and buffer volume. The added carbohydrate molecule could also reduce the water content of the reaction mixture. Adachi and Koyayashi [34] have reported that the hexose which is more hydrated decreased the water activity in the system and shifts the equilibrium towards synthesis. All these factors lead to maintenance of an equilibrium concentration of water around the enzyme all the time. Hence, thermodynamic binding equilibria interplayed by inactivation and inhibition along with maintenance of an optimum water activity could be governing this reaction as reflected by the extent of conversion under different reaction conditions of added buffer, enzyme and substrate concentrations.

As monosaccharides contain five hydroxyl groups, 31 diastereomeric esters (mono, di, tri, tetra and penta) are possible for both the anomers. In case of L-alanyl-D-glucose (II) only 6-*O*- was the major ester produced (47%). While most of the carbohydrates showed 6-*O*- and 5-*O*-esters as major products, D-ribose formed 3,5-di-*O*-ester as the major product. Hence, primary hydroxyl groups invariably formed esters in major proportions. Very low conversions (<10%) were detected for D-arabinose and sucrose. However, D-ribose exhibited 48% conversion. Among the secondary hydroxyl groups of carbohydrates, 2-*O*- and 3-*O*-esters were found to be prominent than 1-*O*- or 4-*O*-esters. Among the secondary hydroxyl groups, 4-*O*-ester was formed only in case of D-mannose. Out of eleven carbohydrates employed, carbohydrate alcohols such as D-sorbitol and D-mannitol were not esterified.

Commercial crude PPL preparations contain variety of estero-/lipo-lytic enzymes with low PPL concentrations [35,36] which could also perform facile esterification. Hence, a small amount of esters formed from esterases along with those of lipases in the present reaction cannot be ruled out. Since the reactions were carried out at a low temperature of 40–60 °C, the formation of peptide was less than 3%, even though unprotected L-alanine was used for the reaction. NMR data clearly indicated that no Maillard reaction occurred. Under these reaction conditions, formation of Maillard reaction products are quite likely. For instance, Maillard and Pictet-Spengler phenolic condensation products were reported in the reaction between phenolic amino acids and D-glucose in phosphate buffer at different pH from 5.0 to 9.0 at 90 °C [37]. Similarly Maillard products from the reaction between D-glucose and *N*<sup>α</sup>-*t*-Boc-L-lysine incubated with aminoguanidine in pH 7.4 phosphate buffer at 70 °C was also reported [38]. No such Maillard reaction type products were detected by mass as well as NMR in the present investigation. RML and PPL showed significant esterification (up to 68%) when unprotected L-alanine was used. When *N*-acetyl-L-

alanine was used in the present work, both RML and PPL gave <5% yield. Riva et al. [14] have reported two monoesters (6-*O*- and 4-*O*-esters) and no diester for L-alanine, using subtilisin, a protease. Our present study has shown that comparable esterification yields to others could be achieved by employing PPL and RML instead of protease. Thus, our study clearly indicates that unprotected L-alanine could be used for esterification of carbohydrates.

## Acknowledgements

Department of Science and Technology, India, is gratefully acknowledged for funding this project. BRS acknowledge the DST, India, for providing Junior Research Fellowship.

## References

- [1] Dordick JS. Enzymatic catalysis in monophasic organic solvents. *Enzyme Microb Technol* 1989;11:194–211.
- [2] Tamura M, Shoji M, Nakatsuka T, Kinomura K, Okai H, Fukui S. Methyl 2,3-di-(L- $\alpha$ -amimobutyryl)- $\alpha$ -D-glucopyranoside, a sweet substance and tastes of related compounds of neutral amino acids and D-glucose derivatives. *Agric Biol Chem* 1985;49:2579–86.
- [3] Kirk O, Bjorkling F, Godfredsen SE, Larsen TS. Fatty acid specificity in lipase catalyzed synthesis of glucoside esters. *Biocatalysis* 1992;6:127–34.
- [4] Zaks A, Dodds DR. Applications of biocatalysts and biotransformations to the synthesis of pharmaceuticals. *Drug Dev Today* 1997;2:513–31.
- [5] Wulfson EN. Enzymatic synthesis of food ingredients in low water media. *Trends Food Sci Technol* 1993;4:209–15.
- [6] Haines AH. Selective removal of protecting groups in carbohydrate chemistry. *Adv Carbohydr Chem Biochem* 1981;39:13–70.
- [7] Wescott CR, Klivanov AM. The solvent dependence of enzyme specificity. *Biochim Biophys Acta* 1994;1206:1–9.
- [8] Ayala G, Gomez-Puyou T, Gomez-Puyou A, Darzon A. Thermostability of membrane enzymes in organic solvents. *FEBS Lett* 1986;20:41–3.
- [9] Wheeler CJ, Croteau R. Terpene cyclase catalysis in organic solvent/minimal water media: demonstration and optimization of (+)- $\alpha$ -pinene cyclase activity. *Arch Biochem Biophys* 1986;248:429–34.
- [10] Stahl M, Jeppsson-Wistrand U, Mansson MO. Induced stereoselectivity and substrate selectivity of bioimprinted  $\alpha$ -chymotrypsin in anhydrous organic solvents. *J Am Chem Soc* 1991;113:9366–8.
- [11] Dabulis K, Klivanov AM. Dramatic enhancement of enzymatic activity in organic solvents. *Biotechnol Bioeng* 1993;41:566–71.
- [12] Kuhl P, Halling PJ, Jakubke H-D. Chymotrypsin suspended in organic solvents with salt hydrates is a good catalyst for peptide synthesis from mainly undissolved reactants. *Tetrahedron Lett* 1990;31:5213–6.
- [13] West JB, Hennen WJ, Lalonde JL, Bibbs J, Zhong Z, Meyer EF, et al. Enzymes as synthetic catalyst; mechanistic and active-site considerations of natural and modified chymotrypsin. *J Am Chem Soc* 1990;112:5313–20.
- [14] Riva S, Chopineau J, Kieboom APG, Klivanov AM. Protease catalyzed regioselective esterification of sugars and related compounds in anhydrous dimethylformamide. *J Am Chem Soc* 1988;110:584–9.
- [15] Park OJ, Park HG, Yang JW. Enzymatic transesterification of monosaccharides and amino acid esters in organic solvents. *Biotechnol Lett* 1996;18:473–8.
- [16] Park OJ, Jeon GJ, Yang JW. Protease catalyzed synthesis of disaccharide amino acid esters in organic media. *Enzyme Microb Technol* 1999;25:455–62.
- [17] Jeon GY, Park OJ, Hur BK, Yang JW. Enzymatic synthesis of amino acid–sugar alcohol conjugates in organic media. *Biotechnol Lett* 2001;23:929–34.
- [18] Therisod M, Klivanov AM. Facile enzymatic preparation of mono acylated sugars in pyridine. *J Am Chem Soc* 1986;108:5638–40.
- [19] Suzuki Y, Shimizu T, Takeda H, Kanda K. Fermentative or enzymatic manufacture of sugar amino acid esters. Japan Patent, 03216194 A2, 1991.

- [20] Vijayakumar GR, Lohith K, Somashekar BR, Divakar S. Lipase catalyzed synthesis of L-alanyl, L-leucyl and L-phenylalanyl esters of D-glucose using unprotected amino acids. *Biotechnol Lett* 2004;26:1323–8.
- [21] Kiran KR, Harikrishna S, Sureshbabu CV, Karanth NG, Divakar S. An esterification method for determination of lipase activity. *Biotechnol Lett* 2000;22:1511–4.
- [22] Xu K, Klibanov AM. pH control of the catalytic activity of cross-linked enzyme crystals in organic solvents. *J Am Chem Soc* 1996;118:9815–9.
- [23] Quiros M, Parker MC, Turner NJ. Tuning lipase enantioselectivity in organic media using solid-state buffers. *J Org Chem* 2002;66:5074–9.
- [24] Lohith K, Divakar S. Lipase catalyzed synthesis of L-phenylalanyl-D-glucose. *J Biotechnol* 2004;117:49–56.
- [25] Cushman DW, Cheung HS. Spectrophotometric assay and properties of the angiotensin-converting enzyme of rabbit lung. *Chem Pharmacol* 1971;20:1637–48.
- [26] Rosenthal K, Loussale F. Critical micelle concentration determination of non-ionic detergent with Coomassie Brilliant Blue-G 250. *Anal Chem* 1983;55:1115–7.
- [27] Romero MD, Calvo L, Alba C, Daneshfar A, Ghaziaskar HS. Enzymatic synthesis of isoamyl acetate with immobilized *Candida antarctica* lipase in *n*-hexane. *Enzyme Microb Technol* 2003;37:42–8.
- [28] Marty A, Chulalaksunakul W, Willemot RM, Condoret JS. Kinetics of lipase-catalyzed esterification in supercritical carbon dioxide. *Biotechnol Bioeng* 1992;39:273–6.
- [29] Zaks A, Klibanov AM. Enzyme catalysis in monophasic organic solvents. *J Biol Chem* 1988;263:3194–201.
- [30] Humeau M, Girardin B, Rovel AM. Effect of the thermodynamic water activity and the reaction medium hydrophobicity on the enzymatic synthesis of ascorbyl palmitate. *J Biotechnol* 1998;63:1–8.
- [31] Paez BC, Medina AR, Rubio FC, Moreno PG, Grim EM. Modeling the effect of free water on enzyme activity in immobilized lipase-catalyzed reactions in organic solvents. *Enzyme Microb Technol* 2003;33:845–53.
- [32] Valiveti RH, Johnston GA, Suckling CJ, Halling PJ. Solvent effect on biocatalysis in organic systems: equilibrium position and rates of lipase catalyzed esterification. *Biotechnol Bioeng* 1991;38:1137–43.
- [33] Partridge J, Harper N, Moore B, Halling PJ. *Enzymes in Non-aqueous Solvents Methods and Protocols in Series: Methods in Biotechnology*, 2001, pp. 227–34.
- [34] Adachi S, Kobayashi T. Synthesis of esters by immobilized lipase catalyzed condensation reaction of sugar and fatty acids in water-miscible organic solvent. *J Biosci Bioeng* 2005;99:87–94.
- [35] Segura RL, Betancor L, Palomo JM, Hidalgo, Fernandez-Lorente G, Terreni Mateo C, et al. Purification and identification of different lipases contained in PPL commercial extracts: a minor contaminant is the main responsible of most esterase activity. *Enzyme Microb Technol*, in press.
- [36] Birner-Grunberger R, Scholze H, Faber K, Hermetter A. Identification of various lipolytic enzymes in crude porcine pancreatic lipase preparations using covalent fluorescent inhibitors. *Biotechnol Bioeng* 2004;85:147–54.
- [37] Manini P, Napolitano A, d'Ischia M. Reaction of D-glucose with phenolic amino acids: further insights into competition between Maillard and Pictet-Spengler condensation pathways. *Carbohydr Res* 2005;340:2719–27.
- [38] Reihl O, Bieme KM, Lederer MO, Schwach W. Pyridinium-carbaldehyde: active Maillard reaction product from the reaction of hexose with lysine residues. *Carbohydr Res* 2004;339:705–14.

## Inhibition of *Rhizomucor miehei* and *Candida rugosa* Lipases by D-Glucose in Esterification between L-Alanine and D-Glucose

Bhandya R. Somashekar,<sup>1</sup> Kenchaiah Lohith,<sup>1</sup> Balaraman Manohar,<sup>2</sup> and Soundar Divakar<sup>1\*</sup>

*Department of Fermentation Technology and Bioengineering, Central Food Technological Research Institute, Mysore-570020, India<sup>1</sup> and Department of Food Engineering, Central Food Technological Research Institute, Mysore-570020, India<sup>2</sup>*

Received 24 July 2006/Accepted 31 October 2006

**A detailed kinetic study of the esterification of D-glucose with L-alanine catalyzed by lipases from *Rhizomucor miehei* (RML) and *Candida rugosa* (CRL) showed that both lipases follow the Ping-Pong Bi-Bi mechanism, in which L-alanine and D-glucose bind in subsequent steps releasing water and L-alanyl-D-glucose, with competitive substrate inhibition by D-glucose at higher concentrations leading to the formation of dead-end lipase · D-glucose complexes. An attempt to obtain the best fit of this kinetic model through curve fitting yielded good approximates of the apparent values of four important kinetic parameters: for RML- $k_{cat}=0.29\pm 0.028\times 10^{-3}\text{ M h}^{-1}\text{ mg}^{-1}$ ,  $K_{m\text{L-alanine}}=4.9\pm 0.51\times 10^{-3}\text{ M}$ ,  $K_{m\text{D-glucose}}=0.21\pm 0.018\times 10^{-3}\text{ M}$ , and  $K_{i\text{D-glucose}}=1.76\pm 0.19\times 10^{-3}\text{ M}$ ; for CRL- $k_{cat}=0.75\pm 0.08\times 10^{-3}\text{ M h}^{-1}\text{ mg}^{-1}$ ,  $K_{m\text{L-alanine}}=56.2\pm 5.7\times 10^{-3}\text{ M}$ ,  $K_{m\text{D-glucose}}=16.2\pm 1.8\times 10^{-3}\text{ M}$ , and  $K_{i\text{D-glucose}}=21.0\pm 1.9\times 10^{-3}\text{ M}$ .**

**[Key words:** L-alanyl-D-glucose, *Candida rugosa* lipase, *Rhizomucor miehei* lipase, Ping-Pong Bi-Bi mechanism, competitive D-glucose inhibition, dead-end lipase · D-glucose complex, hydrogen-bonding interactions]

Lipases (EC 3.1.1.3) are enzymes, that cleave ester linkages of triacylglycerides releasing glycerol and fatty acids at the water/lipid interface. Lipase is a single-domain molecule that belongs to the family of  $\alpha/\beta$ -hydrolase proteins (1, 2). Most of the lipases reported contain Ser-His-Asp/Glu catalytic triads in their active site (2) with the exception of esterases from *Streptomyces scabies*, which contain only Ser-144 and His-283 (3).

Kinetic studies of esterification (4–8), racemization (9) and hydrolysis (10) using lipases have been performed. In some esterifications, lipases follow the Ping-Pong Bi-Bi mechanism (5, 11–13). This mechanism involves binding acid with alcohol in successive steps, which is followed by the release of water and the ester products in succession. The kinetic behavior of *Candida rugosa* lipase (CRL) in the esterification of long-chain fatty acids with alcohols (12) and tetrahydrofurfuryl alcohol with butyric acid (14) follows the Ping-Pong Bi-Bi mechanism, in which the binding of an acid leads to an acyl enzyme complex followed by the release of water molecules. The subsequent binding of an alcohol leads to the transfer of the acyl group to the alcohol, which results in ester formation. Thereafter, an ester product is released. *n*-Octanol is inhibitory to *Rhizomucor miehei* lipase (RML) and CRL in the transesterification between vinyl acetate and *n*-octanol (4) following the Ternary Com-

plex Bi-Bi mechanism, in which *n*-octanol binds twice, once to bind to lipase to yield a dead-end lipase · *n*-octanol complex and a second molecule of *n*-octanol again binds to the above lipase to give another dead-end lipase · *n*-octanol complex.

For citronellyl laurate synthesis, RML follows the ordered Bi-Bi mechanism wherein  $\beta$ -citronellol binds to the enzyme to yield the  $\beta$ -citronellol-enzyme complex, which again binds to lauric acid to form the ternary enzyme- $\beta$ -citronellol-lauric acid complex. Finally, it decomposes to give  $\beta$ -citronellyl laurate and water as products in this process (13). A series of dead-end RML-lauric acid complexes were also reported in this process.

In our previous investigation, we have reported an enzymatic synthesis of L-alanyl-D-glucose and other carbohydrate esters of L-alanine (15). In this work, the kinetics of the esterification between L-alanine and D-glucose to form L-alanyl-D-glucose with RML and CRL is carried out in which both lipases follow the Ping-Pong Bi-Bi mechanism with L-alanine and D-glucose binding. In subsequent steps, water is released followed by L-alanyl-D-glucose. A competitive substrate is inhibited by D-glucose at higher concentrations that leads to the formation of dead-end lipase · D-glucose complexes.

For the first time, we have shown that D-glucose could be inhibitory to both lipases at higher concentrations. The apparent values of the important kinetic parameters  $k_{cat}$ ,  $K_{m\text{L-alanine}}$ ,  $K_{m\text{D-glucose}}$  and  $K_{i\text{D-glucose}}$  are evaluated and compared between both lipases by graphical and curve-fitting procedures.

\* Corresponding author. e-mail: [divakar643@gmail.com](mailto:divakar643@gmail.com)  
phone: +91-821-2513658 fax: +91-821-2517233

The costs of publication of this article were supported in part by Grants-in-Aid for Publication of Scientific Research Results from the Japan Society for the Promotion of Science (JSPS) (no. 183031).

## MATERIALS AND METHODS

**Enzyme and chemicals** The lipozyme IM20 (RML, immobilized on weak anion-exchange resin) was purchased from Novo Nordisk A/S (Bagsvaerd, Denmark), and CRL from Sigma Chemical (St. Louis, MO, USA). The esterification activities of RML and CRL were found to be 0.5 and 0.03  $\mu\text{mol min}^{-1}$  (mg enzyme preparation) $^{-1}$ , respectively, using 0.13 M butyric acid and 0.33 M *n*-butanol as substrates in heptane (16).

L-Alanine was purchased from Himedia Laboratories (Mumbai, India), and D-glucose from SD Fine Chemicals (Mumbai, India). HPLC-grade acetonitrile, dichloromethane and dimethylformamide were obtained from Qualigens Fine Chemicals (Mumbai, India). The other solvents employed were distilled once before use.

**Kinetic experiments** Kinetic experiments were conducted by refluxing L-alanine and D-glucose along with 90 mg of RML or CRL in 100 ml of dichloromethane and dimethylformamide (v/v, 90:10) solvent mixture (15, 17, 18) containing 0.1 ml of 0.1 M sodium acetate buffer (pH 4.0) for RML or 0.1 ml of 0.1 M sodium phosphate buffer (pH 7.0) for CRL. Unprotected and inactivated molecules of L-alanine and D-glucose were employed as substrates (Fig. 1). The temperature of the reaction mixture was maintained at the reflux temperature of dichloromethane (40°C). Experiments with RML were conducted by maintaining the concentration of one of the substrates constant in the range of 0.005–0.05 M and varying the concentration of the other in the same concentration range. With CRL, the concentration range employed was 0.005–0.1 M. Product workout involved distilling off the solvent, heating to denature the enzyme, stirring and filtering to remove the lipase. The filtrate was then evaporated to obtain a residue containing L-alanine, D-glucose and the ester. The residue was subjected to high performance liquid chromatography (HPLC) on a Shimadzu LC 10A (Shimadzu, Kyoto) using a C-18 column (LiChrosorb 100 Å, 5  $\mu\text{m}$ , 25 cm  $\times$  4.6 mm) with water/acetonitrile (80:20, v/v), as the mobile phase at a flow rate of 1 ml/min and monitored by a UV detector at 210 nm for L-alanyl-D-glucose. The retention times of L-alanine and L-alanyl-D-glucose were found to be 2.6 min and 3.4 min, respectively. No D-glucose was detected at 210 nm. The molar concentrations of the ester products formed were determined from the L-alanyl-D-glucose peak area with reference to that of free unreacted L-alanine in the reaction mixture. The error in yield measurement was within  $\pm 10\%$ . The esters formed were separated by size exclusion chromatography using a Sephadex G-10 column, eluted with water, and subjected to spectral characterization by ultraviolet (UV), infrared (IR) and 2D heteronuclear single quantum coherence transfer-nuclear magnetic resonance (HSQCT-NMR) spectroscopies.

For the concentrations of D-glucose and L-alanine, individual experiments in duplicate (30  $\times$  2 lipases) were performed for incubation periods of 3 h, 6 h, 12 h, 24 h and 36 h. Initial rate (specific reaction rate,  $\nu$ ) was determined from the initial slope of the plot of the amount of esters formed (M) versus incubation period (h) and expressed as  $\text{M h}^{-1}$  (mg protein) $^{-1}$ .  $R^2$  obtained from least-squares analysis for the initial rate in each case was found to be within

0.88–0.95. Each plot shown in this work was constructed from all experimentally determined values; a few initial rates were obtained by curve-fitting.

**Spectral characterization** A Shimadzu UV-1601 spectrophotometer was used for recording the UV spectra of isolated L-alanyl-D-glucose esters in aqueous solutions at 0.5 mM. A Nicolet 5700 FTIR instrument (Madison, WI, USA) was used for recording the IR spectra. The specific rotation of the isolated esters was measured at 25°C using a Perkin-Elmer 243 polarimeter (Überlingen, Germany) with a 0.5% aqueous solution of the esters. The mass spectra of the isolated esters were recorded using a Q-TOF Waters Ultima Instrument (Manchester, UK) fitted with an electron spray ionization (ESI) source.  $^1\text{H}$  and  $^{13}\text{C}$  NMR spectra (500.13 MHz for  $^1\text{H}$  and 125 MHz for  $^{13}\text{C}$ ) were recorded on a Bruker DRX-500 MHz spectrophotometer (Fallanden, Switzerland). The proton and carbon 90° pulse widths were 10.5 and 12.25  $\mu\text{s}$ , respectively. About 40 mg of the sample dissolved in  $\text{DMSO-}d_6$  and  $\text{D}_2\text{O}$  was used for recording the spectra at 35°C. Chemical shift value was expressed in ppm relative to an internal tetramethylsilane standard within  $\pm 0.01$  ppm.

In the NMR data, only resolvable signals are shown. Some assignments are interchangeable. Based on  $^{13}\text{C}$  NMR data, the proportions of mono- and diesters produced, detected by measuring the peak areas of the C2, C3 and C6 signals, were found to be 2-*O*-ester, 20%; 3-*O*-ester, 12%; 6-*O*-ester, 47%; 2,6-di-*O*-ester, 15%; and 3,6-di-*O*-ester, 6% (15).

Since the polarities of the five esters (2-*O*-, 3-*O*-, 6-*O*-, 2,6-di-*O*- and 3,6-di-*O*-esters) formed were identical, all the esters eluted as a single peak at 3.4 min on HPLC. Attempts to further separate these esters through HPLC and other chromatographic procedures were unsuccessful. Only  $^{13}\text{C}$  NMR gave a clear indication of the type and proportion of the esters. The down-field chemical shift values for C1 at 102.8 ppm (2-*O*-ester), 101.8 ppm (6-*O*-ester) and 100.8 ppm (2,6-di-*O*-ester) clearly indicate that only  $\beta$ -D-glucose was esterified.

L-Alanyl- $\beta$ -D-glucose UV ( $\text{H}_2\text{O}$ ,  $\lambda_{\text{max}}$ ): 227.0 nm ( $\sigma \rightarrow \sigma^*$   $\epsilon_{227.0}$  1151  $\text{M}^{-1}$ ), 294.0 nm ( $n \rightarrow \pi^*$   $\epsilon_{294.0}$  764  $\text{M}^{-1}$ ); IR (KBr, stretching frequency): 3371  $\text{cm}^{-1}$  (NH), 3410  $\text{cm}^{-1}$  (OH), 2297  $\text{cm}^{-1}$  (CH), 1653  $\text{cm}^{-1}$  (CO); optical rotation:  $[\alpha]_D = -38.1^\circ$  ( $c$  0.5,  $\text{H}_2\text{O}$ , 25°C); MS:  $m/z$  274  $[\text{M} + \text{Na}]^+$ ; 2D HSQCT ( $\text{DMSO-}d_6$ )-2-*O*-ester:  $^1\text{H-NMR}$   $\delta$ ppm: 2.95 ( $\alpha\text{CH}$ ), 1.07 ( $\beta\text{CH}_3$ ), 3.62 (H-2 $\beta$ ), 3.83 (H-3 $\beta$ ), 3.67 (H-4 $\beta$ ), 3.44 (H-6 $\beta$ ),  $^{13}\text{C-NMR}$   $\delta$ ppm: 52.1 ( $\alpha\text{CH}$ ), 15.7 ( $\beta\text{CH}_3$ ), 102.8 (C1 $\beta$ ), 82.6 (C2 $\beta$ ), 77.9 (C3 $\beta$ ), 68.8 (C4 $\beta$ ), 60.5 (C6 $\beta$ ); 3-*O*-ester:  $^1\text{H-NMR}$   $\delta$ ppm: 2.87 ( $\alpha\text{CH}$ ), 3.93 (H-3 $\beta$ ), 3.58 (H-4 $\beta$ ), 3.36 (H-6 $\beta$ ),  $^{13}\text{C-NMR}$   $\delta$ ppm: 51.4 ( $\alpha\text{CH}$ ), 83.3 (C3 $\beta$ ), 69.3 (C4 $\beta$ ), 57.3 (C6 $\beta$ ); 6-*O*-ester:  $^1\text{H-NMR}$   $\delta$ ppm: 2.95 ( $\alpha\text{CH}$ ), 1.30 ( $\beta\text{CH}_3$ ), 3.86 (H-2 $\beta$ ), 3.76 (H-5 $\beta$ ), 3.82 (H-6 $\beta$ ),  $^{13}\text{C-NMR}$   $\delta$ ppm: 50.2 ( $\alpha\text{CH}$ ), 15.1 ( $\beta\text{CH}_3$ ), 171.4 (CO), 101.8 (C1 $\beta$ ), 75.0 (C2 $\beta$ ), 70.1 (C5 $\beta$ ), 63.5 (C6 $\beta$ ); 2,6-di-*O*-ester:  $^1\text{H-NMR}$   $\delta$ ppm: 3.36 ( $\alpha\text{CH}$ ), 1.30 ( $\beta\text{CH}_3$ ), 3.78 (H-2 $\beta$ ), 3.47 (H-6 $\beta$ ),  $^{13}\text{C-NMR}$   $\delta$ ppm: 49.5 ( $\alpha\text{CH}$ ), 16.4 ( $\beta\text{CH}_3$ ), 100.8 (C1 $\beta$ ), 76.5 (C2 $\beta$ ), 62.7 (C6 $\beta$ ); 3,6-di-*O*-ester:  $^1\text{H-NMR}$   $\delta$ ppm: 1.30 ( $\beta\text{CH}_3$ ), 3.78 (H-3 $\beta$ ), 3.82 (H-6 $\beta$ ),  $^{13}\text{C-NMR}$   $\delta$ ppm: 51.4 ( $\alpha\text{CH}$ ), 16.7 ( $\beta\text{CH}_3$ ), 81.6 (C3 $\beta$ ), 63.1 (C6 $\beta$ ).

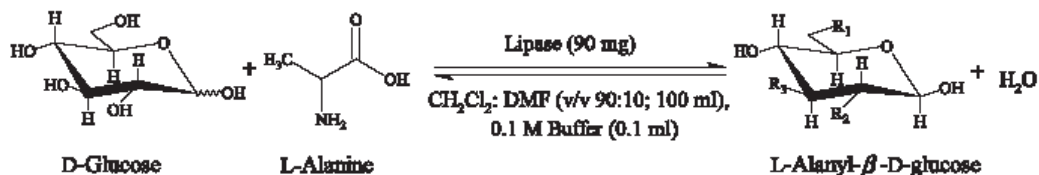


FIG. 1. Lipases-catalyzed synthesis of L-alanyl- $\beta$ -D-glucose esters. 2-*O*-Ester:  $\text{R}_2 = \text{L-CH}_2\text{CH}(\text{NH}_2)\text{COO}$ ,  $\text{R}_1 = \text{R}_3 = \text{OH}$ ; 3-*O*-ester:  $\text{R}_3 = \text{L-CH}_2\text{CH}(\text{NH}_2)\text{COO}$ ,  $\text{R}_1 = \text{R}_2 = \text{OH}$ ; 6-*O*-ester:  $\text{R}_1 = \text{L-CH}_2\text{CH}(\text{NH}_2)\text{COO}$ ,  $\text{R}_2 = \text{R}_3 = \text{OH}$ ; 2,6-di-*O*-ester:  $\text{R}_2 = \text{R}_1 = \text{L-CH}_2\text{CH}(\text{NH}_2)\text{COO}$ ,  $\text{R}_3 = \text{OH}$ ; 3,6-di-*O*-ester:  $\text{R}_3 = \text{R}_1 = \text{L-CH}_2\text{CH}(\text{NH}_2)\text{COO}$ ,  $\text{R}_2 = \text{OH}$ .

## RESULTS AND DISCUSSION

Because both RML and PPL showed good esterification potencies in L-alanyl-D-glucose synthesis, they were employed in this kinetic study to evaluate the salient features of the kinetic behavior of both these lipases in esterification.

To graphically evaluate the apparent values of the kinetic parameters, initial rate (specific reaction rate) was determined from the concentration of L-alanyl-D-glucose at different incubation periods, and typical time courses of RML and CRL-catalyzed reactions are shown in Fig. 3.

The initial rates ( $v$ ) for RML were found to be in the range of  $15\text{--}176 \times 10^{-6} \text{ M h}^{-1} (\text{mg protein})^{-1}$ . CRL experiments showed the initial rates to be in the range of  $20\text{--}460 \times 10^{-6} \text{ M h}^{-1} (\text{mg protein})^{-1}$ . At the initial periods of incubation, the reaction is relatively fast owing to the shift in equilibrium towards esterification. The process slows down at incubation periods longer than 24 h, resulting in a stable steady-state equilibrium. The effects of external mass transfer phenomena—internal and external diffusions (14, 19), if any, on the RML and CRL enzymes employed were not tested in this work.

Using initial rates, double reciprocal plots were constructed to graphically evaluate the apparent values of  $k_{\text{cat}}$ ,  $K_{\text{m L-alanine}}$ ,  $K_{\text{m D-glucose}}$  and  $K_i$ : RML, Fig. 4A ( $1/v$  versus  $1/[\text{D-glucose}]$ ) and 4B ( $1/v$  versus  $1/[\text{L-alanine}]$ ); CRL, Fig. 5A ( $1/v$  versus  $1/[\text{D-glucose}]$ ) and 5B ( $1/v$  versus  $1/[\text{L-alanine}]$ ). Figure 6A shows a replot of the slopes from Fig. 4B (RML), and Fig. 6B shows a replot of the slopes from Fig. 5B (CRL). Figure 4A from RML reactions and Fig. 5A from CRL reactions show a series of curves obtained for different fixed concentrations of L-alanine for varying D-glucose concentration, in which slight increase in initial rates are observed at lower D-glucose concentrations. At higher D-glucose concentrations, the rates markedly decrease. Also, increasing L-alanine concentration increases the initial rates at all D-glucose concentrations. Figure 4B from RML reactions and Fig. 5B from CRL reactions show a series of parallel lines for different fixed low D-glucose concentrations at varying L-alanine concentration. The slopes of these lines change at higher D-glucose concentrations.

The plots in Figs. 4A, 4B, 5A and 5B show that the kinetics could be best described by the Ping-Pong Bi-Bi model, in which L-alanine and D-glucose bind in subsequent steps that release water and L-alanyl-D-glucose. This also happens in subsequent steps (Fig. 2) with competitive substrate inhibition that leads to dead-end inhibition (20). Both RML and CRL were found to be inhibited by D-glucose. This model could be described by the rate equation

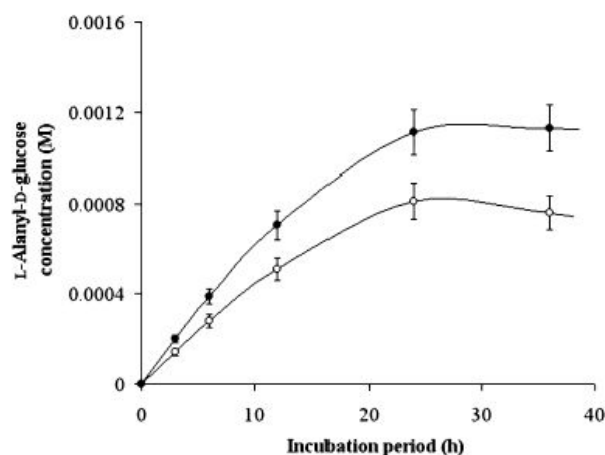


FIG. 3. Time courses of esterification reactions—concentration of L-alanyl-D-glucose versus incubation period (open circles, RML and closed circles, CRL). The RML enzyme (90 mg) or the CRL enzyme (90 mg) was reacted with 0.005 M L-alanine and 0.020 M D-glucose in 100 ml of mixture of dichloromethane/dimethylformamide (90:10, v/v) mixed with 0.1 ml of 0.1 M sodium acetate buffer (pH 4.0) for RML or 0.1 ml of 0.1 M sodium phosphate buffer (pH 7.0) for CRL.

Equation (1) is the rate equation for the Ping-Pong Bi-Bi model with competitive substrate inhibition. The parameters are defined as follows:  $v$  is initial rate,  $V_{\text{max}}$  is maximum velocity,  $[\text{A}]$  is L-alanine concentration,  $[\text{B}]$  is D-glucose concentration,  $K_{\text{mA}}$  is Michaelis-Menten constant for the lipase-L-alanine complex,  $K_i$  is dissociation constant for the lipase-inhibitor (D-glucose) complex and  $K_{\text{mB}}$  is Michaelis-Menten constant for the lipase-D-glucose complex. Because the initial rates are in  $\text{M h}^{-1} (\text{mg protein})^{-1}$ ,  $V_{\text{max}}$  is expressed as  $k_{\text{cat}} = V_{\text{max}}/\text{enzyme concentration}$ .

The apparent values of the four important kinetic parameters  $K_{\text{m D-glucose}}$ ,  $K_{\text{m L-alanine}}$ ,  $K_{\text{m D-glucose}}$  and  $k_{\text{cat}}$  were graphically evaluated. The intercepts of the positive slopes of the curves in Figs. 4A and 5A on the Y-axis, particularly, at the highest L-alanine concentration (0.05 M/0.1 M) employed, gave  $1/k_{\text{cat}}$  for RML and CRL (Table 1). Figure 6A (RML) and 6B (CRL) shows a replot of the slopes from Figs. 4B and 5B versus D-glucose, respectively, for which slope =  $K_{\text{m L-alanine}}/(k_{\text{cat}} K_i)$ , Y intercept =  $K_{\text{m L-alanine}}/k_{\text{cat}}$  and X intercept =  $-K_i$ , where  $K_i$  represents the dissociation constant for the lipase-D-glucose complex.  $K_{\text{m D-glucose}}$  was obtained using Eq. 2 derived by rearranging Eq. 1.

$$\frac{V}{V_{\text{max}}} = \frac{[\text{A}][\text{B}]}{K_{\text{mA}}[\text{B}](1 + [\text{B}]/K_i) + K_{\text{mB}}[\text{A}] + [\text{A}][\text{B}]} \quad (1)$$

Equation (2) is the rearranged rate equation. Here,  $K_{\text{mB}}$  is Michaelis-Menten constant for the lipase-D-glucose complex.

To confirm that the kinetics of the RML- and CRL-catalyzed syntheses of L-alanyl-D-glucose follow the above-mentioned model, the apparent values of the four important kinetic parameters  $k_{\text{cat}}$ ,  $K_i$ ,  $K_{\text{mA}}$  and  $K_{\text{mB}}$  were also estimated through curve fitting using Eq. 1.

The range of values tested for these parameters and the

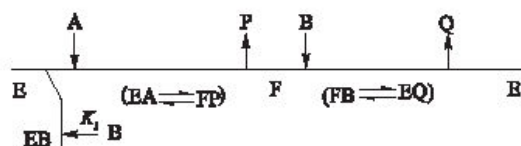


FIG. 2. Ping-Pong Bi-Bi mechanism of RML and CRL-catalyzed syntheses of L-alanyl-D-glucose. A, L-Alanine; P, H<sub>2</sub>O; B, D-glucose; E, lipase-*Rhizomucor miehei* lipase/*Candida rugosa* lipase; F, lipase-L-alanyl complex; EA, lipase-L-alanine complex; FP, lipase-L-alanyl-water complex; EB, lipase-D-glucose complex;  $K_i$ , dissociation constant of lipase-D-glucose complex; FB, lipase-L-alanyl-D-glucose complex; EQ, lipase-L-alanyl-D-glucose complex and Q, L-alanyl-D-glucose.

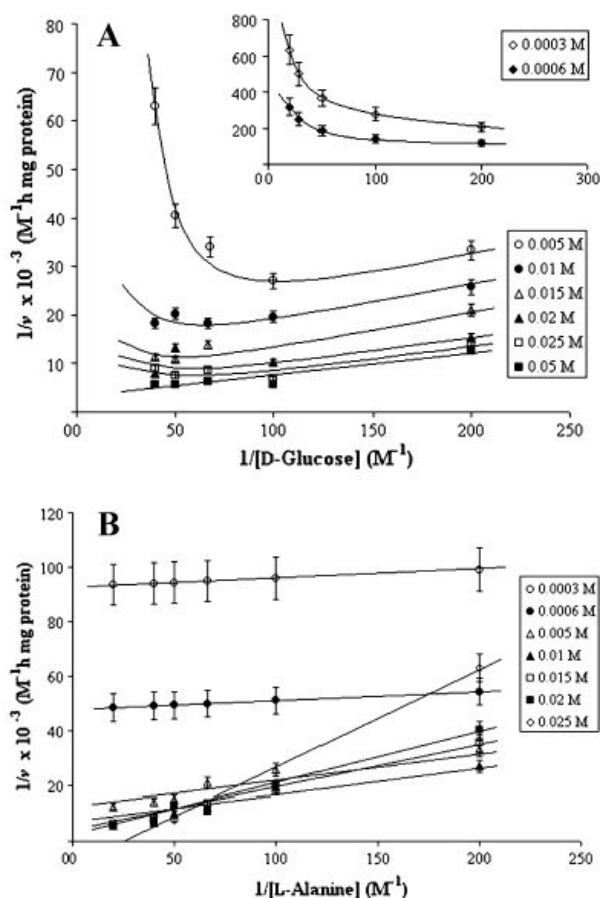


FIG. 4. Double reciprocal plots for RML-catalyzed synthesis of L-alanyl-D-glucose. (A)  $1/v$  versus  $1/[D\text{-glucose}]$  plots; a series of curves show the effect of varying D-glucose concentration at different fixed L-alanine concentrations in the range of 0.005–0.05 M. The inset shows plots obtained by computer simulation for 0.0003 M and 0.0006 M L-alanine concentrations (open trapeziums, 0.0003 M; closed trapeziums, 0.0006 M; open circles, 0.005 M; closed circles, 0.01 M; open triangles, 0.015 M; closed triangles, 0.02 M; open squares, 0.025 M; closed squares, 0.05 M). (B)  $1/v$  versus  $1/[L\text{-alanine}]$  plots, a series of lines show the effects of varying L-alanine concentration at different fixed D-glucose concentrations in the range of 0.005–0.025 M; plots shown for 0.0003 and 0.0006 M D-glucose concentrations are from computer simulation (open circles, 0.0003 M; closed circles, 0.0006 M; open triangles, 0.005 M; closed triangles, 0.01 M; open squares, 0.015 M; closed squares, 0.02 M; open trapeziums, 0.025 M).

constraints employed for the iteration procedure are:  $k_{cat} < 1 \text{ M h}^{-1} \text{ mg}^{-1}$ ,  $K_{iD\text{-glucose}} > K_{mD\text{-glucose}}$ ,  $K_{mD\text{-glucose}} < K_{mL\text{-alanine}}$ , and  $K_{mL\text{-alanine}} < 10 \text{ M}$ .

The iteration procedure for the curve fitting involved nonlinear optimization by minimizing the sum of squares of deviations between  $v_{exptl}$  and  $v_{pred}$ , such that the values of the four kinetic parameters mentioned above correspond to the best fit achieved.

Table 1 lists the graphical and curve fitted values for comparison. Table 2 shows a comparison between the experimental and predictive initial rates obtained under different reaction conditions. Although the computer-simulated  $v_{pred}$  values showed  $R^2$  values of 0.84 for RML and 0.86 for

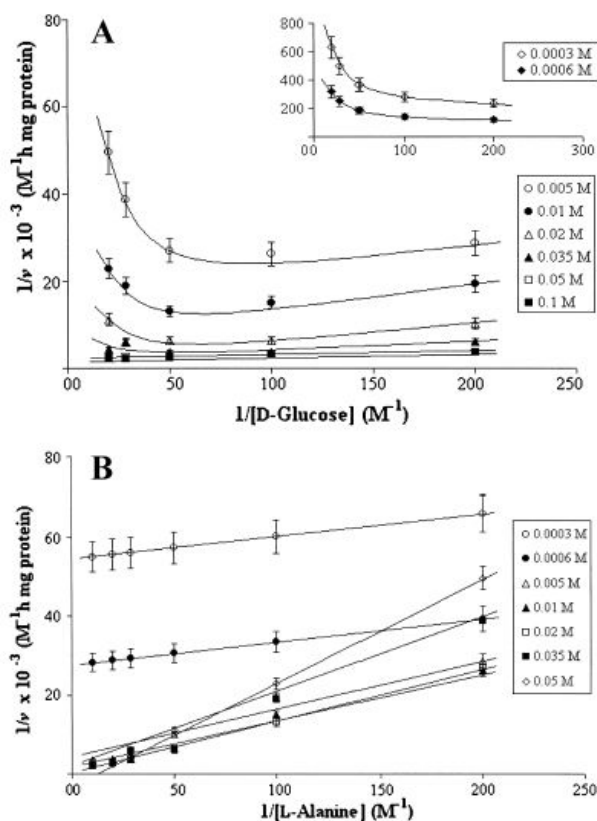


FIG. 5. Double reciprocal plots for CRL-catalyzed synthesis of L-alanyl-D-glucose. (A)  $1/v$  versus  $1/[D\text{-glucose}]$  plots; a series of plots show the effect of varying D-glucose concentration at different fixed L-alanine concentrations in the range of 0.005–0.1 M; the plots shown for 0.0003 and 0.0006 M L-alanine concentrations are from computer simulation (open trapeziums, 0.0003 M; closed trapeziums, 0.0006 M; open circles, 0.005 M; closed circles, 0.01 M; open triangles, 0.02 M; closed triangles, 0.035 M; open squares, 0.05 M; closed squares, 0.1 M). (B)  $1/v$  versus  $1/[L\text{-alanine}]$  plots, a series of plots show the effect of varying L-alanine concentrations at different fixed D-glucose concentrations in the range of 0.005–0.05 M. The plots shown for 0.0003 and 0.0006 M D-glucose concentrations are from computer simulation (open circles, 0.0003 M; closed circles, 0.0006 M; open triangles, 0.005 M; closed triangles, 0.01 M; open squares, 0.02 M; closed squares, 0.035 M; open trapeziums, 0.05 M).

CRL, the discrepancy between  $v_{exptl}$  and  $v_{pred}$  appeared to be significant at several substrate concentrations. This could be due to (i) the constraints employed in the iteration (curve fitting), which limits the flexibility required to examine a real system in solution, (ii) the error in the experimental

TABLE 1. Apparent values of kinetic parameters for RML and CRL-catalyzed syntheses of L-alanyl-D-glucose

Lipase		$k_{cat} \times 10^3$ ( $\text{M h}^{-1} \text{ mg}^{-1}$ )	$K_{mA} \times 10^3$ (M)	$K_{mB} \times 10^3$ (M)	$K_i \times 10^3$ (M)
RML	a	$0.29 \pm 0.028$	$4.9 \pm 0.51$	$0.21 \pm 0.018$	$1.76 \pm 0.19$
	b	$0.4 \pm 0.038$	$11.2 \pm 1.23$	$10.0 \pm 0.96$	$5.5 \pm 0.59$
CRL	a	$0.75 \pm 0.08$	$56.2 \pm 5.7$	$16.2 \pm 1.8$	$21.0 \pm 1.9$
	b	$1.0 \pm 0.11$	$56.2 \pm 5.4$	$16.1 \pm 1.5$	$21.0 \pm 2.3$

A, L-Alanine; B, D-glucose. a, Graphical method; b, curve-fitted values.



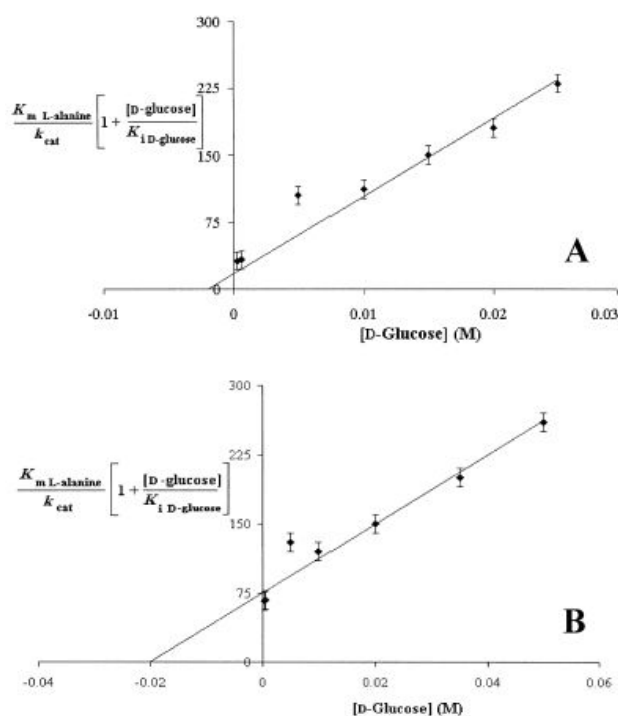


FIG. 6. Replot of slopes obtained from Fig. 4B versus [D-glucose] (RML) (A) and Fig. 5B versus [D-glucose] (CRL) (B).

graphical methods based on HPLC measurements, which itself involves errors on the order of  $\pm 10\%$  and (iii) the heterogeneous experimental conditions employed involving un-dissolved carbohydrates and enzymes, on the one hand, and, partly due to dissolved amino acids, on the other, in the mixture of dichloromethane and dimethylformamide.

With increasing L-alanine concentration (Fig. 4A for RML and Fig. 5A for CRL), the initial rate increases with decreasing D-glucose concentration. With increasing D-glucose concentration up to the minimum  $1/v$ , the initial rate decreases, and the plots tend to become closer to the  $1/v$  axis (Y-axis).

Figures 4B (RML) and 5B (CRL) also show the same behavior, in which at low D-glucose concentrations, the plots appear parallel probably as long as  $K_1 > K_{mB}$  concerned. However, at high fixed D-glucose concentration, the slopes of the plots drastically vary. Thus, in these reactions, the kinetic data clearly shows the inhibitory nature of D-glucose. The competition between L-alanine and D-glucose for the active site (binding site) of lipases (RML/CRL) could result in a predominant binding of D-glucose at high concentrations, displacing L-alanine, and thus leading to the formation of the dead-end lipase·D-glucose complex.

For the RML reaction,  $K_{mA}$  ( $4.9 \pm 0.51 \times 10^{-3}$  M) is always higher than  $K_{mB}$  ( $0.21 \pm 0.018 \times 10^{-3}$  M, Table 1), which shows that L-alanine is bound to RML less firmly than D-glucose ( $K_{mA}/K_{mB} = 23.3$ ). A similar behavior is also observed with CRL (Table 1)  $K_{mA}$  ( $56.2 \pm 5.7 \times 10^{-3}$  M),  $K_{mB}$  ( $16.2 \pm 1.8 \times 10^{-3}$  M),  $K_{mA}/K_{mB} = 3.5$ . However, the respective values are very much higher for CRL than for RML, indicating that CRL can yield better conversions than RML. Between RML and CRL, the  $K_1$  for D-glucose is lower for RML ( $5.5 \pm 0.59 \times 10^{-3}$

TABLE 2. Experimental and predicted initial rates for synthesis of L-alanyl-D-glucose by RML and CRL.

L-Alanine (M)	D-Glucose (M)	$v_{\text{experimental}}^a \times 10^6$ (M h <sup>-1</sup> mg <sup>-1</sup> )	$v_{\text{predictive}}^b \times 10^6$ (M h <sup>-1</sup> mg <sup>-1</sup> )
<b>RML</b>			
0.005	0.005	30	51
0.005	0.01	37	45
0.005	0.015	28	37
0.005	0.02	25	31
0.005	0.025	15	27
0.01	0.005	38	73
0.01	0.01	51	72
0.01	0.015	55	64
0.01	0.02	49	56
0.01	0.025	55	49
0.015	0.005	48	84
0.015	0.01	46	91
0.015	0.015	72	84
0.015	0.02	91	75
0.015	0.025	88	67
0.02	0.005	65	92
0.02	0.01	97	104
0.02	0.015	41	99
0.02	0.02	76	91
0.02	0.025	127	83
0.025	0.005	71	97
0.025	0.01	146	114
0.025	0.015	116	112
0.025	0.02	132	104
0.025	0.025	111	96
0.05	0.005	79	109
0.05	0.01	176	142
0.05	0.015	158	149
0.05	0.02	176	147
0.05	0.025	176	141
<b>CRL</b>			
0.005	0.005	35	55
0.005	0.01	38	52
0.005	0.02	37	42
0.005	0.035	26	32
0.005	0.05	20	25
0.01	0.005	52	89
0.01	0.01	66	92
0.01	0.02	76	78
0.01	0.035	53	61
0.01	0.05	44	49
0.02	0.005	99	130
0.02	0.01	157	148
0.02	0.02	158	137
0.02	0.035	162	112
0.02	0.05	90	92
0.035	0.005	164	161
0.035	0.01	275	201
0.035	0.02	267	202
0.035	0.035	168	174
0.035	0.05	228	148
0.05	0.005	269	178
0.05	0.01	314	234
0.05	0.02	347	250
0.05	0.035	370	224
0.05	0.05	404	195
0.1	0.005	269	203
0.1	0.01	320	291
0.1	0.02	362	345
0.1	0.035	449	338
0.1	0.05	460	310

<sup>a</sup> Graphical method.

<sup>b</sup> Curve-fitted values.

M) than for CRL ( $21.0 \pm 2.3 \times 10^{-3}$  M), indicating that the RML is inhibited by D-glucose far more efficiently than CRL. This could also explain the better conversion observed with CRL than with RML.

Both RML and CRL contain amino acids in their active sites capable of forming hydrogen bonds with suitable donor molecules. The catalytic triad in RML consists of Ser-144, His-257 and Asp-203 (21). CRL contains Ser-209, Glu-341 and His-449 (2, 22). Brzozowski *et al.* (23) showed in an atomic model of the inhibitor *n*-hexylchlorophosphonate ethyl ester-RML complex that in the oxyanion hole, which is directly responsible for the substrate binding, a direct covalent bond formation between the nucleophilic O<sub>y</sub> of Ser-144 and the phosphorous atom of *n*-hexylchlorophosphonate ethyl ester is possible. In CRL, the oxyanion hole O<sub>y</sub> (Ser-209) is formed by the amide backbones of Gly-123, Gly-124 and Ala-210 through the hydrogen bonding between the amide-CO-NH- and the hydroxyl of Ser-209, which is stabilized by the helix dipole (23). D-Glucose possesses five hydroxyl groups and L-alanine possesses carboxyl and amino groups capable of forming hydrogen bonds with polar side chains of amino acids. Ser-144 hydroxyl and Asp-203 carboxyl groups of RML and Ser-209 and Glu-341 of CRL (2) residues are very good candidate molecules for exhibiting hydrogen-bonding interactions.

Between D-glucose and L-alanine, the former possesses more hydrogen-bonding functional groups than the amino or carboxyl groups of L-alanine. Ser-144 in RML and Ser-209 in CRL can form hydrogen bonds with the amino N atom of L-alanine as well as the O atom of D-glucose. Because the  $K_{m \text{ L-alanine}}$  values are higher than the  $K_{m \text{ D-glucose}}$  values for both enzymes, D-glucose could strongly bind to these enzymes than L-alanine.

Zaidi *et al.* (12) reported that the interaction between nylon-immobilized CRL and alcohol through hydrogen-bonding could block the nucleophilic site of the enzyme engaged in acylation, leading to inhibition. A similar behavior can also be envisaged between D-glucose hydroxyl groups and the above-mentioned oxygen of serine and the carboxylate groups of glutamic acids. Hence, this kinetic study could clearly explain the inhibition of both RML and CRL by D-glucose.

This is the first report in which D-glucose has been unequivocally shown to inhibit both RML and CRL.

#### ACKNOWLEDGMENTS

The financial support from the Department of Science and Technology, India, is gratefully acknowledged. B.R. Somashekar thanks the Department of Science and Technology, India for providing the Junior Research Fellowship. The authors also thank Dr. Jennifer M. Bayer, CIIL, Mysore, for proof reading this manuscript.

#### NOMENCLATURE

2D-HSQCT:	two-dimensional heteronuclear single quantum coherence transfer
[ $\alpha$ ]	: optical rotation
A	: reactant A, L-alanine
B	: reactant B, D-glucose

CRL	: <i>Candida rugosa</i> lipase
DMSO	: dimethyl sulfoxide
E	: lipase: <i>Rhizomucor miehei</i> lipase/ <i>Candida rugosa</i> lipase
EA	: lipase·L-alanine complex
EB	: lipase·D-glucose complex
EQ	: lipase·L-alanyl-D-glucose complex
F	: lipase·L-alanyl complex
FB	: lipase·L-alanyl·D-glucose complex
FP	: lipase·L-alanyl·water complex
HPLC	: high-performance liquid chromatography
IR	: infrared
$k_{cat}$	: catalytic efficiency of enzyme
$K_{i \text{ D-glucose}}$	: dissociation constant for lipase·inhibitor (D-glucose) complex
$K_i$	: dissociation constant for lipase·inhibitor (D-glucose) complex
$K_{m \text{ A}}$	: Michaelis–Menten constant for lipase·L-alanine complex
$K_{m \text{ B}}$	: Michaelis–Menten constant for lipase·D-glucose complex
$K_{m \text{ D-glucose}}$	: Michaelis–Menten constant for lipase·D-glucose complex
$K_{m \text{ L-alanine}}$	: Michaelis–Menten constant for lipase·L-alanine complex
MS	: mass spectrometry
NMR	: nuclear magnetic resonance
P	: H <sub>2</sub> O
Q	: L-alanyl-D-glucose
R	: regression coefficient
RML	: <i>Rhizomucor miehei</i> lipase
UV	: ultraviolet
$v$	: initial rate
$V_{max}$	: maximum velocity

#### REFERENCES

1. Derewenda, U., Brzozowski, A.M., Lawson, D.M., and Derewenda, Z. S.: Catalysis at the interface: the anatomy of a conformational change in a triglyceride lipase. *Biochemistry*, **31**, 1532–1541 (1992).
2. Grochulski, P., Li, Y., Schrag, J. D., Bouthillier, F., Smith, P., Harrison, D., Rubin, B., and Cygler, M.: Insight into interfacial activation from an open structure of *Candida rugosa* lipase. *J. Biol. Chem.*, **268**, 12843–12847 (1993).
3. Wei, Y., Schottel, J. L., Derewenda, U., Swenson, L., Patkar, S., and Derewenda, Z. S.: A novel variant of the catalytic triad in the *Streptomyces scabies* esterase. *Nat. Struct. Biol.*, **2**, 218–223 (1995).
4. Yadav, G. D. and Trivedi, A. H.: Kinetic modeling of immobilized-lipase catalyzed transesterification of *n*-octanol with vinyl acetate in non-aqueous media. *Enzyme Microb. Technol.*, **32**, 783–789 (2003).
5. Kiran, K. R. and Divakar, S.: Enzyme inhibition by *p*-cresol and lactic acid in lipase mediated syntheses of *p*-cresyl acetate and stearoyl lactic acid: a kinetic study. *World J. Microbiol. Biotechnol.*, **18**, 707–712 (2002).
6. Janssen, A. E. M., Sijnsnes, B. J., Vakurov, A. V., and Halling, P. J.: Kinetics of lipase catalyzed esterification in organic media: correct model and solvent effects on parameters. *Enzyme Microb. Technol.*, **24**, 463–470 (1999).
7. Lortie, R., Trani, M., and Ergon, F.: Kinetic study of the lipase catalyzed synthesis of triolein. *Biotechnol. Bioeng.*, **41**,

- 1021–1026 (1993).
8. **Rizzi, M., Stylos, P., Riek, A., and Reuss, M.:** A kinetic study of immobilized lipase catalyzing the synthesis of isoamyl acetate by transesterification in *n*-hexane. *Enzyme Microb. Technol.*, **14**, 709–714 (1992).
  9. **Duan, G., Ching, C. B., Lim, E., and Ang, C. H.:** Kinetic study of enantioselective esterification of ketoprofen with *n*-propanol catalysed by an lipase in an organic medium. *Biotechnol. Lett.*, **19**, 1051–1055 (1997).
  10. **Van-Tol, J. B. A., Odenthal, J. B., Jongejan, J. A., and Duine, J. A.:** Relation of enzyme reaction rate and hydrophobicity of the solvent, p. 229–235. *In* Tramper, J., Verme, M. H., Beetink, H. H., and Von-Stocker, U. (ed.), *Biocatalysis in non-conventional media*. Elsevier, Amsterdam (1992).
  11. **Zhang, T., Yang, L., and Zhu, Z.:** Determination of internal diffusion limitation and its macroscopic kinetics of the transesterification of CPB alcohol catalyzed by immobilized lipase in organic media. *Enzyme Microb. Technol.*, **36**, 203–209 (2005).
  12. **Zaidi, A., Gainer, J. L., Carta, G., Mrani, A., Kadiri, T., Belarbi, Y., and Mir, A.:** Esterification of fatty acids using nylon-immobilized lipase in *n*-hexane: kinetic parameters and chain length effects. *J. Biotechnol.*, **93**, 209–216 (2002).
  13. **Yadav, G. D. and Lathi, P. S.:** Synthesis of citronellol laurate in organic media catalyzed by immobilized lipases: kinetic studies. *J. Mol. Catal. B: Enzym.*, **27**, 113–119 (2004).
  14. **Yadav, G. D. and Devi, K. M.:** Immobilized lipase-catalyzed esterification and transesterification reactions in non-aqueous media for the synthesis of tetrahydrofurfuryl butyrate: comparison and kinetic modeling. *Chem. Eng. Sci.*, **59**, 373–383 (2004).
  15. **Somashekar, B. R. and Divakar, S.:** Lipase catalysed synthesis of L-alanyl esters of carbohydrates. *Enzyme Microb. Technol.*, **40**, 299–309 (2007).
  16. **Kiran, K. R., Harikrishna, H., Suresh Babu, C. V., Karanth, N. G., and Divakar, S.:** An esterification method for determining lipase activity. *Biotechnol. Lett.*, **22**, 1511–1514 (2000).
  17. **Vijayakumar, G. R., Lohith, K., Somashekar, B. R., and Divakar, S.:** Lipase catalysed synthesis of L-alanyl, L-leucyl and L-phenylalanyl esters of D-glucose using unprotected amino acids. *Biotechnol. Lett.*, **26**, 1323–1328 (2004).
  18. **Lohith, K. and Divakar, S.:** Lipase catalysed synthesis of L-phenylalanine esters of D-glucose. *J. Biotechnol.*, **117**, 49–56 (2005).
  19. **Marty, A., Chulalaksananukul, W., Willemot, R. M., and Condoret, J. S.:** Kinetics of lipase catalyzed esterification in super-critical CO<sub>2</sub>. *Biotechnol. Bioeng.*, **39**, 273–280 (1992).
  20. **Segel, I. H.:** *Enzyme kinetics*, p. 826–882. Wiley, New York (1993).
  21. **Brady, L., Brzozowski, A. M., Derewenda, Z. S., Dodson, E., Dodson, G., Tolley, S., Turkenburg, J. P., Christiansen, L., Huge-Jensen, B., Norskov, L., Thim, L., and Menge, U.:** A serine protease triad forms the catalytic center of triglycerol lipase. *Nature*, **343**, 767–770 (1990).
  22. **Grochulski, P., Bouthillier, F., Kazlauskas, R. J., Serreqi, A. N., Schrag, J. D., Ziomek, E., and Cygler, M.:** Analogs of reaction intermediates identify a unique substrate binding site in *Candida rugosa* lipase. *Biochemistry*, **33**, 3494–3500 (1994).
  23. **Brzozowski, A. M., Derewenda, U., Derewenda, Z. S., Dodson, G. G., Lawson, D. M., Turkenburg, J. P., Bjorking, F., Huge-Jensen, B., Patkar, S. A., and Thim, L.:** A model for interfacial activation in lipases from the structure of a fungal lipase-inhibitor complex. *Nature*, **351**, 491–494 (1991).